

**Ing. W. Beukelman**

**Papers on Shiphydromechanics**

**Vol. II**

**Edited by P.W. de Heer**

## CONTENTS

### Reports of:

Delft University of Technology,  
Shiphydromechanics Laboratory,  
Mekelweg 2, 2628 CD Delft, the Netherlands.  
by: W. Beukelman.

### Volume I

Bepaling van het verband tussen golfhoogte, periode en pompstand van de golfopwekker.

W. Beukelman.

April 1960, Rapport No. 65.

Voortstuwing in regelmatige en onregelmatige langsscheepse golven.

J. Gerritsma, J.J. van den Bosch en W. Beukelman.

Juli 1961, Rapport No. 17-P.

IJking van golfopwekker nieuwe verlengde tank.

W. Beukelman.

Augustus 1961, Rapport No. 78.

Excitatieproef met zevendelig model no. 41.

W. Beukelman.

December 1962, Rapport No. 107.

Over de bepaling van de demping van langsscheepse bewegingen.

Yu.A. Necwetajef. Vertaling: W. Beukelman.

Februari 1963, Rapport No. 99.

Distribution of damping and added mass along the length of a shipmodel.

J. Gerritsma and W. Beukelman.

February 1963, Report No. 21-P.

The influence of a bulbous bow on the motions and the propulsion in longitudinal waves.

J. Gerritsma and W. Beukelman.

April 1963, Report No. 20-P.

Een systeem van vergelijkingen voor scheepsbewegingen, die rekening houden met de koppeling tussen de domp-, verzet- en rolbewegingen.

L.I. Pletneva-Machabeli. Vertaling: W. Beukelman.

Oktober 1963, Rapport No. 108.

De analyse van de zig-zagproef volgens Nomoto.

W. Beukelman.

Oktober 1963, Rapport No. 109.

Over de opwekkende krachten die op het schip werken in regelmatige golven.

B.E. Tosjef en W.A. Tjoetskewits. Vertaling: W. Beukelman.

Augustus 1964, Rapport No. 120-M

## Volume I (continued)

The distribution of the hydrodynamic forces on a heaving and pitching shipmodel in still water.

J. Gerritsma and W. Beukelman.

June 1964, Report No. 22-P.

Comparison of calculated and measured heaving and pitching motions of a series 60,  $C_B = .70$ , ship model in regular longitudinal waves.

J. Gerritsma and W. Beukelman.

October 1966, Report No. 139.

Bewegingen van een schip in golven (incl. dwarskracht en buigend moment).

Beschrijving van programma I-1433/Bertens-Beukelman.

W. Beukelman.

Januari 1967, Rapport No. 168-M.

Analysis of the modified strip theory for the calculation of ship motions and wave bending moments.

J. Gerritsma and W. Beukelman.

June 1967, Report No. 177.

Berekening van de bewegingen, dwarskrachten en buigende momenten van een schip in onregelmatige golven met de programma's JS-3509 en JS-4282.

W. Beukelman.

Juni 1968, Rapport No. 206-M.

Computed results of ship motions of a fast fruitcarrier.

W. Beukelman.

November 1968, Report No. 223-M.

Weerstandsmeting van twee finn-jollen.

W. Beukelman.

Juni 1969, Rapport No. 242-M.

Pitch and heave characteristics of a destroyer.

W. Beukelman.

August 1970, Report No. 257-P.

Stability of beamtrawlers in following seas.

W. Beukelman and A. Versluis.

January 1971, Report No. 295.

Resistance increase of a fast cargo ship in regular waves.

J. Gerritsma and W. Beukelman.

June 1971, Report No. 313-P.

Hydrodynamic forces on a surface piercing flat plate.

J.B. van den Brug, W. Beukelman and G.J. Prins.

August 1971, Report No. 325.

## Volume II

Zeilprestaties van drie ontwerpen van een éénheidsjacht.

W. Beukelman.

Januari 1972, Rapport No. 342.

**Volume II (continued)**

Analysis of the resistance increase in waves of a fast cargo ship.

J. Gerritsma and W. Beukelman.  
September 1972, Report No. 334-P.

Description of a program to calculate the behaviour of a ship in a seaway (named: Trial).

W. Beukelman and E.F. Bijlsma.  
August 1973, Report No. 383.

Full scale measurements and predicted seakeeping performance of the containership "Atlantic Crown".

W. Beukelman and M. Buitenhek.  
November 1974, Report No. 388-P.

Drag and sideforce measurements with a 1/6 scale model of the yacht "Antiope".

W. Beukelman and A. Huijser.  
March 1974, Report No. 395.

The effects of beam on the hydrodynamic characteristics of ship hulls.

J. Gerritsma, W. Beukelman and C.C. Glansdorp.  
June 1974, Report No. 403-P.

Zeilprestaties van de ocean cruiser 16.

W. Beukelman.  
Juni 1974, Rapport No. 404.

Comparison of seakeeping prediction methods for different ships.

W. Beukelman.  
June 1975, Report No. 420.

The influence of fin keel sweep-back on the performance of sailing yachts.

W. Beukelman and J.A. Keuning.  
November 1975, Report No. 445-P.

Variation of parameters determining seakeeping.

W. Beukelman and A. Huijser.  
December 1976, Report No. 443-P.

Handleiding voor het gebruik van het scheepsbewegingen programma voor 6 graden van vrijheid.

W. Beukelman.  
April 1977, Rapport No. 449-M.

Bottom impact pressures due to forced oscillation.

W. Beukelman.  
February 1979, Report No. 479-P.

Hydrodynamic coefficients of rectangular barges in shallow water.

J.A. Keuning and W. Beukelman.  
August 1979, Report No. 489-P.



### Volume III

Seakeeping trials with HNLMS "Tydeman".

J. Gerritsma and W. Beukelman.

March 1980, Report No. 494.

Added resistance and vertical hydrodynamic coefficients of oscillating cylinders at speed.

W. Beukelman.

September 1980, Report No. 510.

Forced oscillation experiments with a segmented model in shallow water.

J. Gerritsma and W. Beukelman.

November 1980, Report No. 513-P.

The distribution of hydrodynamic mass and damping of an oscillating shipform in shallow water.

W. Beukelman and J. Gerritsma.

March 1982, Report No. 546-P.

De verdeling van de hydrodynamische massa en demping over een in ondiep water oscillerend scheepsmodel.

W. Beukelman en J. Gerritsma.

Maart 1982, Rapport No. 546-A.

The longitudinal distribution of low frequency hydrodynamic derivatives for lateral motions in shallow water.

W. Beukelman and J. Gerritsma.

September 1983, Report No. 562-A.

Calculation methods of hydrodynamic coefficients of ships in shallow water.

W. Beukelman, R.H.M. Huijsmans and P.J. Keuning.

November 1983, Report No. 571-P.

Vertical motions and added resistance of a rectangular and triangular cylinder in waves.

W. Beukelman.

July 1983, Report No. 594.

On sway damping and added mass in shallow water.

W. Beukelman.

September 1984, Report No. 603-P.

Seakeeping calculations for high speed round bilge displacement ships sub-series 1.

W. Beukelman.

April 1984, Report No. 616-O.

Trial, a computerprogram to calculate the behaviour of a ship in regular and irregular longitudinal waves.

J.M.J. Journée and W. Beukelman.

November 1984, Report No. 451-M.

## Volume IV

The high-speed displacement ship systematic series hull forms-seakeeping characteristics.

J.J. Blok and W. Beukelman.

November 1984, Report No. 675-P.

Semi-planerende vaartuigen in zeegang, predictie van inzetbaarheid.

W. Beukelman.

Maart 1985, Rapport No. 658-O.

Ontwerp serie modellen ter bepaling van de inzetbaarheid op de Noordzee.

W. Beukelman.

April 1985, Rapport No. 664-O.

Snelle displacementsschepen in zeegang.

W. Beukelman.

April 1985, Rapport No. 754-P.

Comparison of seakeeping calculation methods for model 9 of the high speed displacement ship series.

W. Beukelman.

September 1985, Report No. 689-O.

Semi-planing vessels in a seaway, comparative prediction of operability.

A.M. van Wijngaarden and W. Beukelman.

October 1985, Report No. 755-P.

Seakeeping calculations for high speed round bilge displacement ships series of 20 models.

W. Beukelman and J.A. Keuning.

November 1985, Report No. 696-O.

## Volume V

Prediction of operability of fast semi-planing vessels in a seaway.

W. Beukelman.

January 1986, Report No. 700-P.

Bepaling van de inzetbaarheid op de Noordzee van een serie semi-planerende vaartuigen.

W. Beukelman en F. de Beer.

April 1986, Rapport No. 706-O.

Zeegangsgedrag als ontwerpparameter.

W. Beukelman en J.A. Keuning.

Mei 1986, Rapport No. 709-P.

High speed displacement hull form series.

Calculated influence of the pitch gyradius on seakeeping for the parent model.

W. Beukelman.

October 1986, Report No. 726-O.

**Volume V (continued)**

Slamdrukken op cilindervlakken bij gedwongen oscillatie.

W. Beukelman.

November 1986, Rapport No. 728.

Longitudinal distribution of drift forces for a ship model.

W. Beukelman.

December 1988, Report No. 810.

Koersstabiliteit voor een ro-ro schip als functie van waterdiepte, trim en snelheid.

W. Beukelman.

Juni 1989, Rapport No. 830-0.

Distribution of drift forces at 90 degree drift angle.

W. Beukelman.

July 1989, Report No. 839-0.

Cross flow drag on a segmented model.

W. Beukelman.

October 1989, Report No. 831-P.

De invloed van trim op de richtingsstabiliteit van een Ro-Ro schip op ondiep water.

W. Beukelman.

Januari 1990, Rapport No. 854-P.

Added resistance and vertical oscillations for cylinders at forward speed in still water and waves.

W. Beukelman.

August 1990, Report No. 873-P.

Slamming on forced oscillating wedges at forward speed.

Part I: Test results.

W. Beukelman.

May 1991, Report No. 888.

Slamming simulation on penetrating wedges at forward speed.

W. Beukelman and D. Radev.

October 1991, Report No. 888-P.

Hydromechanic aspects of marine safety.

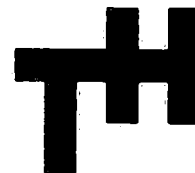
W. Beukelman.

June 1992, Report No. 921-P.

Hydrodynamic aspects of ship safety.

W. Beukelman.

August 1992, Report No. 934-P.



# LABORATORIUM VOOR SCHEEPSBOUWKUNDE

TECHNISCHE HOGESCHOOL DELFT

Zeilprestaties van drie ontwerpen van  
een éénheidsjacht

door

W. Beukelman

januari 1972

Inhoud :

blz. nr.

1. Samenvatting	2
2. De modellen	3
3. Meetresultaten en discussie	4
3.1. De vaart zonder helling en drift	4
3.2. De vaart-aan-de-wind	4
3.3. De gezeilde tijd op een standaardbaan	6
4. Verantwoording	7
5. Bibliografie	8

Tabellen

Figuren

## 1. Samenvatting

De in het Laboratorium voor Scheepsbouwkunde uitgewerkte methode voor het meten van de zeilprestaties van jachten is toegepast op drie modellen van ontwerp-eenheidsjachten [1]\*. Deze jachten zijn ontworpen door Koopmans, Maas en v.d. Stadt om te komen tot een keus voor de bouw van een eenheidsjacht. Behalve onderling zijn de prestaties van deze jachten ook vergeleken met de Halftonner [2] en de Spirit 28 [3] welke schepen qua afmetingen met de eenheidsjachten overeenkomen. De zeilprestaties van het eenheidsjacht van v.d. Stadt blijken tot een windsnelheid van 7m/sec beter te zijn dan die van de beide andere eenheidsjachten. Voor hogere windsnelheden zijn de zeilprestaties van het eenheidsjacht van Koopmans beter. De zeilprestaties van het jacht van Maas zijn vooral ongunstig beïnvloed door het aanzuigen van lucht t.p.v. de zuigzijde van de kiel bij hellingen van ongeveer 30 graden, terwijl ook de voorlijke ligging van het drukkingspunt mede verantwoordelijk geacht moet worden voor de relatief hoge weerstand. De gunstige prestaties van het eenheidsjacht van v.d. Stadt zijn vooral het gevolg van de lage weerstand van het schip rechtop, zonder helling en drift.

\* De nummers tussen de haken verwijzen naar de bibliografie op blz. 8.

## 2. De modellen

De belangrijkste karakteristieken van de modellen en de schepen zijn gegeven in tabel I<sup>a</sup> en I<sup>b</sup>, de vorm van de ontwerpwaterlijn en de kromme van spantoppervlakken in fig. 1, 2 en 3.

De kiel-roer-konfiguratie wijkt voor geen van de schepen af van de gangbare : een trapeziumvormige vinkiel en een ver naar achteren geplaatst, diepstekend, smal roer achter een korte ondiepe scheg.

Opvallend is ook de grote breedte-diepgangverhouding van de romp voor het ontwerp van Maas, terwijl uit de krommen van dwarsdoorsneden ook blijkt dat de waterverplaatsing van het voorste gedeelte van dit jacht groter is dan van de beide andere jachten, wat resulteert in een voorlijker ligging van het drukingspunt. De momenten van statische stabiliteit met betrekking tot de hellingshoek zijn voor de verschillende jachten weergegeven in fig. 4.

### 3. Resultaten en discussie

#### 3.1. De vaart zonder helling en drift

De weerstand, rechtop en zonder drift varend, is gemeten en gegeven in tabel II<sup>a</sup>, II<sup>b</sup> en II<sup>c</sup>, en in kg als functie van de scheepssnelheid, en dimensieloos als weerstand per ton waterverplaatsing van de romp als functie van het dimensieloze Froudegetal.

In tabel III zijn voor standaard Froudegetallen de waarden van de weerstand per ton waterverplaatsing van de romp onderling vergeleken, en vergeleken met de Halftonner en de Spirit 28, die qua afmetingen ongeveer overeenkomen met de eenheidsjachten, maar ook met de Staron [4] die daarbij vergeleken grotere afmetingen heeft. Omdat voor gelijke scheepsvormen bij toenemende absolute grootte (vergroting van de schaal) bij gelijk Froudegetal de weerstand per ton waterverplaatsing afneemt, is deze laatste vergelijking niet strikt eerlijk. Wordt dit in aanmerking genomen, dan blijkt uit tabel III, dat de waarden voor het eenheidsjacht van Maas betrekkelijk hoog zijn vergeleken met de andere jachten.

Van meer betekenis is de bereikbare snelheid-voor-de-wind, die te berekenen is uit de weerstandskromme na schatting van het effectief zeiloppervlak (tabel I). Fig. 5 geeft voor de verschillende jachten de snelheid-voor-de-wind,  $V_d$ , als functie van de werkelijke windsnelheid, terwijl in tabel IV deze scheepssnelheid dimensieloos is weergegeven voor enkele standaard-windsnelheden.

Uit Fig. 5 blijkt, dat de hoogste snelheid-voor-de-wind bereikt wordt door het eenheidsjacht van v.d. Stadt.

#### 3.2. De vaart-aan-de-wind

In fig. 6 is de kromme van snelheid-in-de-wind ( $V_{mg}$ ) tegen werkelijke windsnelheid ( $V_{tw}$ ) voor de drie eenheidsjachten gegeven.

Voor windsnelheden lager dan 7 m/sec blijkt de hoogste snelheid-in-de-wind bereikt te worden door het jacht van v.d. Stadt, daarboven worden door het jacht van Koopmans de hoogste snelheden-in-de-wind bereikt.

Voor standaardwindsnelheden van 3.5, 7.0 en 10.0 m/sec zijn de als Froudegetal dimensieloos gemaakte snelheid-in-de-wind en de daarbij behorende scheepssnelheid gegeven in tabel IV, tesamen met helling en drifthoek.



Ter vergelijking zijn ook de waarden van de Halftonner [2] en de Spirit 28 [3] opgenomen. De hellingshoeken van het jacht van v.d. Stadt blijken het grootst te zijn en die van Koopmans het kleinst. Dit houdt o.a. ook verband met de statische stabiliteit, zoals die weergegeven is in fig. 4. De drifthoeken blijken het hoogst te zijn voor het eenheidsjacht van Maas. Dit kan, bij hoge hellingshoeken, het gevolg zijn van het aanzuigen van lucht aan de zuigzijde van de kiel, waardoor de dwarskracht afneemt. Het bovenwater komen van de kiel is bij de hoogste hellingshoek ( $30^{\circ}$ ) voor dit jacht duidelijk geconstateerd. Fig. 7 toont een vergelijking van de dimensieloze snelheid-in-de-wind met die van andere schepen.

De metingen kunnen behalve met de opgegeven ligging van het gewichtszwaartepunt en het ontworpen zeilplan ook uitgewerkt worden met een andere, systematisch gevarieerde, ligging van gewichtszwaartepunt, effectief zeilpunt en zeiloppervlak. Hiertoe is een computerprogramma ontwikkeld, dat deze variaties snel berekent en uitwerkt. De ligging van het gewichtszwaartepunt in hoogte verandert telkens met 1% van de waterlijnlengthe.

Het zeilplan wordt gewijzigd door alleen de masthoogte te variëren. Daarmee varieert in dezelfde mate de hoogte van de voordriehoek (I) en de lengte van het voorlijk van het grootzeil (P). De variatie van de masthoogte is zo gekozen, dat de I-maat telkens met 5% van de ontwerpwaarde verandert.

Alle andere maten, zoals de basis van de voordriehoek (J), de gieklengthe (E) en de positie van de giek boven dek (BAD), worden konstant gehouden, zodat de variaties van het zeiloppervlak en de ligging van het effectief zeilpunt in hoogte gemakkelijk te berekenen zijn (tabel Va, Vb, Vc).

Voor iedere combinatie van masthoogte en ligging gewichtszwaartepunt (stabiliteit) berekent de computer de kromme van snelheid-in-de-wind ( $V_{mg}$ ) tegen windsnelheid ( $V_{tw}$ ) en bepaalt  $V_{mg}$  bij de standaardwindsnelheden 3.5, 7.0 en 10.0 m/sec. Hierna kunnen door interpolatie voor iedere windsnelheid in één figuur lijnen van gelijke snelheid-in-de-wind getekend worden, met op de horizontale as de ligging van het gewichtszwaartepunt en op de verticale as de I-maat. Voor de verschillende jachten zijn deze "stabiliteits-masthoogte velden met lijnen van konstante  $V_{mg}$ " getoond in fig. 8, 9 en 10. Bij verandering van de twee genoemde basisvariabelen is in de figuur direkt te zien hoe groot de invloed hiervan op de optimale snelheid-in-de-wind is.

In de figuur is bovendien vanuit het midden, wat het gegeven schip vertegenwoordigt, een pijl getrokken in de richting van de snelste vergroting van de snelheid-in-de-wind.

Aan de richting van deze pijlen is te zien, dat voor alle drie de jachten en windsnelheden een verlaging van het gewichtszwaartepunt, d.i. een verhoging van de stabiliteit, een verbetering van de snelheid-in-de-wind geeft.

Bij de laagste windsnelheid, 3.5 m/sec, waar normaal een overheersende invloed van het zeiloppervlak verwacht zou worden (de pijl staat dan bijna vertikaal), is verbetering door stabiliteitsvergroting voor het eenheidsjacht van v.d.Stadt en mogelijk voor dat van Koopmans van belang.

Bij een windsnelheid van 7.0 m/sec is vergroting van het zeiloppervlak van weinig belang, terwijl het bij een windsnelheid van 10 m/sec verkleind zou moeten worden (reven). Hoewel een grotere masthoogte (I-maat) een grotere spinnaker toelaat is de invloed hiervan op de snelheid-voor-de-wind niet spektakulair (zie tabel VI).

### 3.3. De gezeilde tijd op een standaardbaan

De krommen van fig. 5 en 6 kunnen gebruikt worden om de gezeilde tijd op een eenvoudige standaardbaan te vergelijken met de desbetreffende tijden van andere schepen, na toepassing van de tijdcorrectiefactor. Omdat niet het gehele polaire diagram bekend is, is het noodzakelijk voor deze baan een rechte te kiezen, evenwijdig aan de windrichting, die heen en terug gevaren wordt.

Als de lengte van een rak wordt 10 mijl vastgesteld. De op deze baan voor verschillende schepen (theoretisch) bepaalde zeiltijden zijn gegeven in tabel VII, ook weer voor standaardwindsnelheden. De meting van de drie eenheidsjachten is gelijk, zodat de berekende zeiltijden direct met elkaar vergeleken kunnen worden. Hieruit blijkt ook weer, dat voor windsnelheden onder 7.0 m/sec de gunstigste tijd gezeild wordt door het eenheidsjacht van v.d. Stadt; daarboven geeft het jacht van Koopmans de kortste zeiltijd.

Directe vergelijking met de zeiltijden van de andere jachten in tabel VII is moeilijker daar de meting niet bekend is.

Nogmaals moet opgemerkt worden dat de gezeilde tijden volgens tabel VII verkregen zijn aan de hand van modelproeven in vlak water, na gebruik van geschatte effectieve zeiloppervlakken (al is deze schatting ook steeds volgens dezelfde methode uitgevoerd). In werkelijkheid kunnen een betere bemanning de kwaliteit van de zeilen, of de zeegang belangrijke invloed uitoefenen.

#### 4. Verantwoording

De experimenten werden uitgevoerd binnen het kader van de activiteiten en afspraken in de Werkgroep Jachten.

De tekeningen voor het eenheidsjacht van Koopmans zijn vervaardigd door D. Koopmans te Lelystad en het model (121) door de jachtwerf Victoria te Alkmaar.

De tekeningen en het model (122) voor het eenheidsjacht van Maas werden vervaardigd door de jachtwerf Frans Maas N.V. te Breskens.

De tekeningen en het model (123) voor het eenheidsjacht van v.d. Stadt werden vervaardigd door E.G. v.d. Stadt, scheepswerf N.V. te Zaandam.

## 5. Bibliografie

1. G. Moeyes  
Het meten van de zeilprestaties van jachten door middel van modelproeven.  
Laboratorium voor Scheepsbouwkunde. T.H. Delft, rapport no. 286, dec. 1970.
2. G. Moeyes  
De zeilprestaties van een half-tons-jacht.  
Laboratorium voor Scheepsbouwkunde. T.H. Delft, rapport no. 291, dec. 1970.
3. G. Moeyes  
Zeilprestaties van de Spirit 28.  
Laboratorium voor Scheepsbouwkunde. T.H. Delft, rapport no. 315, juli 1971.
4. G. Moeyes  
Zeilprestaties van de Staron.  
Laboratorium voor Scheepsbouwkunde. T.H. Delft, rapport no. 326, aug. 1971.

TABEL I<sup>a</sup> :

Belangrijkste gegevens van de schepen :

Symbool	Omschrijving	eenheid	Koopmans	Maas	v.d. Stadt
L <sub>OA</sub>	lengte over alles	m	9.000	9.050	9.050
L <sub>DWL</sub>	lengte op ontwerpwaterlijn	m	7.200	7.310	7.100
B <sub>max</sub>	maximum breedte	m	2.800	3.000	2.930
B <sub>DWL</sub>	max. breedte op ontwerpwaterlijn	m	2.448	2.470	2.340
T <sub>H</sub>	diepgang van de romp	m	0.557	0.450	0.520
T	diepgang tot onderkant kiel	m	1.730*	1.700	1.700
Δ <sub>H</sub>	deplacement van de romp	1000 kg	3.661	2.949	3.237
Δ	deplacement totaal	1000 kg	3.890	3.241	3.457
LCB	ligging drukingspunt romp in lengte achter midden waterlijnlengte	m	0.311	0.019	0.249
L <sub>DWL</sub> /Δ <sub>H</sub> <sup>1/3</sup>	lengte-deplacement verhouding		4.67	5.10	4.80
B <sub>DWL</sub> /T <sub>H</sub>	breedte-diepgang verhouding		4.39	5.49	4.50
LCB/L <sub>DWL</sub>	relatieve ligging drukingspunt	%	4.32	0.26	3.51
C <sub>p</sub>	prismatische coëfficiënt van de romp		0.551	0.538	0.556
S	totaal nat oppervlak	m <sup>2</sup>	18.16	17.72	17.50
Z <sub>GS</sub>	ligging gewichtszwaartepunt onder waterlijn	m	0.135	0.080	0.055
BR	ballastverhouding		0.44 <sup>(1)</sup>	0.37 <sup>(1)</sup>	0.39 <sup>(1)</sup>
I	hoogte voordriehoek	m	10.40	11.00	11.25
J	basis voordriehoek	m	3.68	3.35	3.70
SA <sub>eb</sub>	effektief zeiloppervlak aan-de-wind	m <sup>2</sup>	30.52	29.76	31.44
SA <sub>ed</sub>	effektief zeiloppervlak voor-de-wind	m <sup>2</sup>	76.25	70.80	81.18
Z <sub>CEe</sub>	effektief zeilpunt boven ontwerp-waterlijn	m	4.68	5.05	5.06
b	kielhoogte (span)	m	1.24	1.25	1.20
c	gemiddelde koorde kiel	m	1.38	1.33	1.30
AR <sub>g</sub>	geometrisch aspektverhouding kiel		0.90	0.94	0.93
λ	pijlstelling kiel	gr	37.2	30.2	40.1

\* De diepgang tot onderkant kiel was voor dit ontwerp ook 1.700 m; de kiel van het model bleek door de wijze van bevestiging overeen te komen met een totale diepgang van 1.730 m.

TABEL I<sup>b</sup> :

Belangrijkste gegevens van de modellen (2) :

Symbool	Omschrijving	Eenheid	Koopmans model 121	Maas model 122	v.d.Stadt model 123
L <sub>OA</sub>	lengte over alles	m	2.000	2.011	2.011
L <sub>DWL</sub>	lengte op ontwerpwater- lijn	m	1.600	1.624	1.578
B <sub>max</sub>	maximum breedte	m	0.622	0.667	0.651
B <sub>DWL</sub>	maximum breedte op ontwerpwaterlijn	m	0.544	0.549	0.520
T <sub>H</sub>	diepgang van de romp	m	0.124	0.100	0.116
T	diepgang tot onderkant kiel	m	0.384	0.378	0.378
Δ	deplacement totaal	kg	42.694	35.564	37.936

(1) : als fraktie van het totaal deplacement

(2) : modelschaal 1:4.5

TABEL II<sup>a</sup>Weerstand rechtop en zonder drift voor het eenheidsjacht van Koopmans.

$V_s$ m/sec	$V_s$ kn	$R_{Ts}$ kg	$F_n^{(1)}$	$R_{TS} / \Delta H$ kg/ton
1.273	2.47	6.4	0.151	1.76
1.485	2.89	9.1	0.177	2.50
1.697	3.30	12.4	0.202	3.38
1.909	3.71	16.3	0.227	4.44
2.121	4.12	21.3	0.252	5.82
2.227	4.33	24.8	0.265	6.76
2.333	4.53	28.2	0.278	7.70
2.440	4.74	31.4	0.290	8.58
2.546	4.95	35.1	0.303	9.58
2.652	5.16	39.3	0.316	10.75
2.758	5.36	44.4	0.328	12.13
2.864	5.57	50.6	0.341	13.83
2.970	5.77	59.3	0.353	16.20
3.076	5.98	71.6	0.366	19.56
3.182	6.19	87.8	0.379	23.99
3.288	6.39	109.1	0.391	29.80
3.394	6.60	135.3	0.404	36.95
3.500	6.80	165.6	0.416	45.24
3.606	7.01	198.6	0.429	54.25
3.712	7.22	234.6	0.442	64.07
3.818	7.42	273.2	0.454	74.63

TABEL II<sup>b</sup>Weerstand rechtop en zonder drift voor het eenheidsjacht van Maas.

$V_s$ m/sec	$V_s$ kn	$R_{Ts}$ kg	$F_n^{(1)}$	$R_{Ts}/\Delta H$ kg/ton
1.061	2.06	4.9	0.125	1.64
1.273	2.47	7.0	0.150	2.38
1.485	2.89	9.7	0.175	3.27
1.697	3.30	13.0	0.200	4.41
1.909	3.71	16.9	0.225	5.73
2.121	4.12	21.8	0.250	7.39
2.227	4.33	24.5	0.263	8.31
2.333	4.53	27.5	0.275	9.33
2.440	4.74	30.9	0.288	10.48
2.546	4.95	34.6	0.301	11.73
2.652	5.16	38.7	0.313	13.12
2.758	5.36	43.9	0.326	14.89
2.864	5.57	50.2	0.338	17.02
2.970	5.77	58.0	0.351	19.67
3.076	5.98	67.8	0.363	22.99
3.182	6.19	80.4	0.376	27.26
3.288	6.39	95.7	0.388	32.45
3.394	6.60	113.1	0.401	38.35
3.500	6.80	135.1	0.413	45.81
3.606	7.01	159.1	0.426	53.95
3.712	7.22	185.8	0.438	63.00
3.818	7.42	214.5	0.451	72.74



TABEL II<sup>c</sup>

Weerstand rechtop en zonder drift voor het eenheidsjacht van v.d. Stadt.

$V_s$ m/sec	$V_s$ kn	$R_{Ts}$ kg	$F_n^{(1)}$	$R_{Ts}/\Delta H$ kg/ton
1.697	3.30	12.5	0.203	3.87
1.909	3.71	16.2	0.229	5.01
2.121	4.12	20.4	0.254	6.30
2.227	4.33	22.7	0.267	7.00
2.333	4.53	25.1	0.280	7.75
2.440	4.74	28.2	0.292	8.72
2.546	4.95	31.2	0.305	9.63
2.652	5.16	34.8	0.318	10.75
2.758	5.36	39.4	0.330	12.18
2.864	5.57	45.9	0.343	14.17
2.970	5.77	54.3	0.356	16.77
3.076	5.98	64.9	0.369	20.03
3.182	6.19	77.4	0.381	23.91
3.288	6.39	92.6	0.394	28.61
3.394	6.60	112.1	0.407	34.64
3.500	6.80	136.0	0.419	42.02
3.606	7.01	163.7	0.432	50.58
3.712	7.22	195.9	0.445	60.52
3.818	7.42	232.4	0.458	71.79

(1):  $V_s$  m/sec

$$\frac{\sqrt{gL}}{DWL}$$

TABEL III

Vergelijking van de weerstand per ton waterverplaatsing van de romp

Fn	$R_{Ts} / H$ kg/ton					
	(1)	(2)	(3)	(4)	(5)	(6)
0.10						
0.15	1.73	2.38	-	1.99	2.16	1.97
0.20	3.28	4.41	3.74	3.60	4.00	3.44
0.25	5.72	7.39	6.05	6.01	6.36	5.72
0.30	9.41	11.73	9.22	9.58	9.82	8.83
0.35	15.66	19.57	15.42	15.23	15.70	14.43
0.40	35.11	38.08	31.40	33.55	31.33	29.74

- (1) : Koopmans : model 121 :  $L_{DWL} = 7.20$  m  
(2) : Maas : model 122 :  $L_{DWL} = 7.31$  m  
(3) : v.d.Stadt: model 123 :  $L_{DWL} = 7.10$  m  
(4) : Halftonner :  $L_{DWL} = 7.00$  m  
(5) : Spirit 28 :  $L_{DWL} = 6.90$  m  
(6) : Staron :  $L_{DWL} = 9.05$  m

TABEL IV

Prestaties bij standaardwindsnelheden.

wind-snelheid m/sec	grootheid	Koopmans	Maas	v.d.Stadt	Halftonner	Spirit 28
3.5	$V_d / \sqrt{gL_{DWL}}$	0.222	0.216	0.226	0.224	0.230
	$V_{mg} / \sqrt{gL_{DWL}}$	0.178	0.186	0.192	0.176	0.191
	$V_s / \sqrt{gL_{DWL}}$	0.243	0.248	0.264	0.235	0.264
	$\phi$	6.8	7.6	9.2	8.7	9.6
	$\beta$	2.9	3.5	3.0	2.6	3.6
	7.0	$V_d / \sqrt{gL_{DWL}}$	0.376	0.376	0.389	0.383
$V_{mg} / \sqrt{gL_{DWL}}$		0.268	0.261	0.268	0.260	0.274
$V_s / \sqrt{gL_{DWL}}$		0.328	0.321	0.331	0.326	0.340
$\phi$		18.0	18.8	21.8	22.1	22.3
$\beta$		4.2	5.6	4.8	4.0	5.3
10.0		$V_d / \sqrt{gL_{DWL}}$	0.439	0.450	0.458	-
	$V_{mg} / \sqrt{gL_{DWL}}$	0.293	0.273	0.278	0.276	0.278
	$V_s / \sqrt{gL_{DWL}}$	0.355	0.338	0.333	0.336	0.351
	$\phi$	26.7	27.5	30.3	31.9	31.2
	$\beta$	5.8	8.9	7.7	6.4	8.7

 $V_d$  : snelheid-voor-de-wind in m/sec $V_{mg}$  : snelheid-in-de-wind in m/sec $V_s$  : scheepssnelheid in m/sec bij zeilen aan-de-wind $\phi$  : hellingshoek in graden $\beta$  : drifhoek in graden $g$  : versnelling van de zwaartekracht in  $m/sec^2$  $L_{DWL}$  : waterlijnlengte in m.

TABEL V :

Zeiloppervlak bij systematisch gevarieerde hoogte van de voordriehoek.

TABEL V<sup>a</sup>: Eenheidsjacht van Koopmans

I m	effektief zeiloppervlak		hoogte effectief zeilpunt boven waterlijn m
	aan-de-wind m <sup>2</sup>	voor-de-wind m <sup>2</sup>	
9.360	27.31	68.48	4.32
9.880	28.91	72.36	4.50
10.400	30.50	76.24	4.67
10.920	32.09	80.12	4.85
11.440	33.69	84.00	5.02

TABEL V<sup>b</sup>: Eenheidsjacht van Maas

I m	effektief zeiloppervlak		hoogte effectief zeilpunt boven waterlijn m
	aan-de-wind m <sup>2</sup>	voor-de-wind m <sup>2</sup>	
9.900	26.77	66.40	4.61
10.450	28.38	70.21	4.79
11.000	29.99	74.02	4.98
11.550	31.59	77.83	5.16
12.100	33.20	81.64	5.35

TABEL V<sup>c</sup>: Eenheidsjacht van v.d. Stadt

I m	effektief zeiloppervlak		hoogte effectief zeilpunt boven waterlijn m
	aan-de-wind m <sup>2</sup>	voor-de-wind m <sup>2</sup>	
10.125	28.43	73.19	4.64
10.688	30.09	77.34	4.82
11.250	31.74	81.49	5.01
11.813	33.40	85.63	5.20
12.375	35.06	89.78	5.39

TABEL VI :

Snelheid-voor-de-wind bij variabele masthoogte.

TABEL VI<sup>a</sup>: Eenheidsjacht van Koopmans.

I m	Snelheid-voor-de-wind $V_d$ in m/sec		
	$V_{tw}=3.5\text{m/sec}$	$V_{tw}=7.0\text{m/sec}$	$V_{tw}=10.0\text{m/sec}$
9.360	1.82	3.12	3.64
9.880	1.84	3.14	3.66
10.400	1.86	3.16	3.69
10.920	1.88	3.18	3.72
11.440	1.90	3.20	3.75

TABEL VI<sup>b</sup>: Eenheidsjacht van Maas

I m	Snelheid-voor-de-wind $V_d$ in m/sec		
	$V_{tw}=3.5\text{m/sec}$	$V_{tw}=7.0\text{m/sec}$	$V_{tw}=10.0\text{m/sec}$
9.900	1.79	3.14	3.75
10.450	1.81	3.16	3.78
11.000	1.83	3.19	3.81
11.550	1.85	3.21	-
12.100	1.87	3.23	-

TABEL VI<sup>c</sup>: Eenheidsjacht van v.d. Stadt

I m	Snelheid-voor-de-wind $V_d$ in m/sec		
	$V_{tw}=3.5\text{m/sec}$	$V_{tw}=7.0\text{m/sec}$	$V_{tw}=10.0\text{m/sec}$
10.125	1.84	3.20	3.76
10.688	1.87	3.22	3.79
11.250	1.89	3.25	3.82
11.813	1.91	3.27	-
12.375	1.93	3.29	-

TABEL VII :

Gezeilde tijden op een standaardbaan (1)

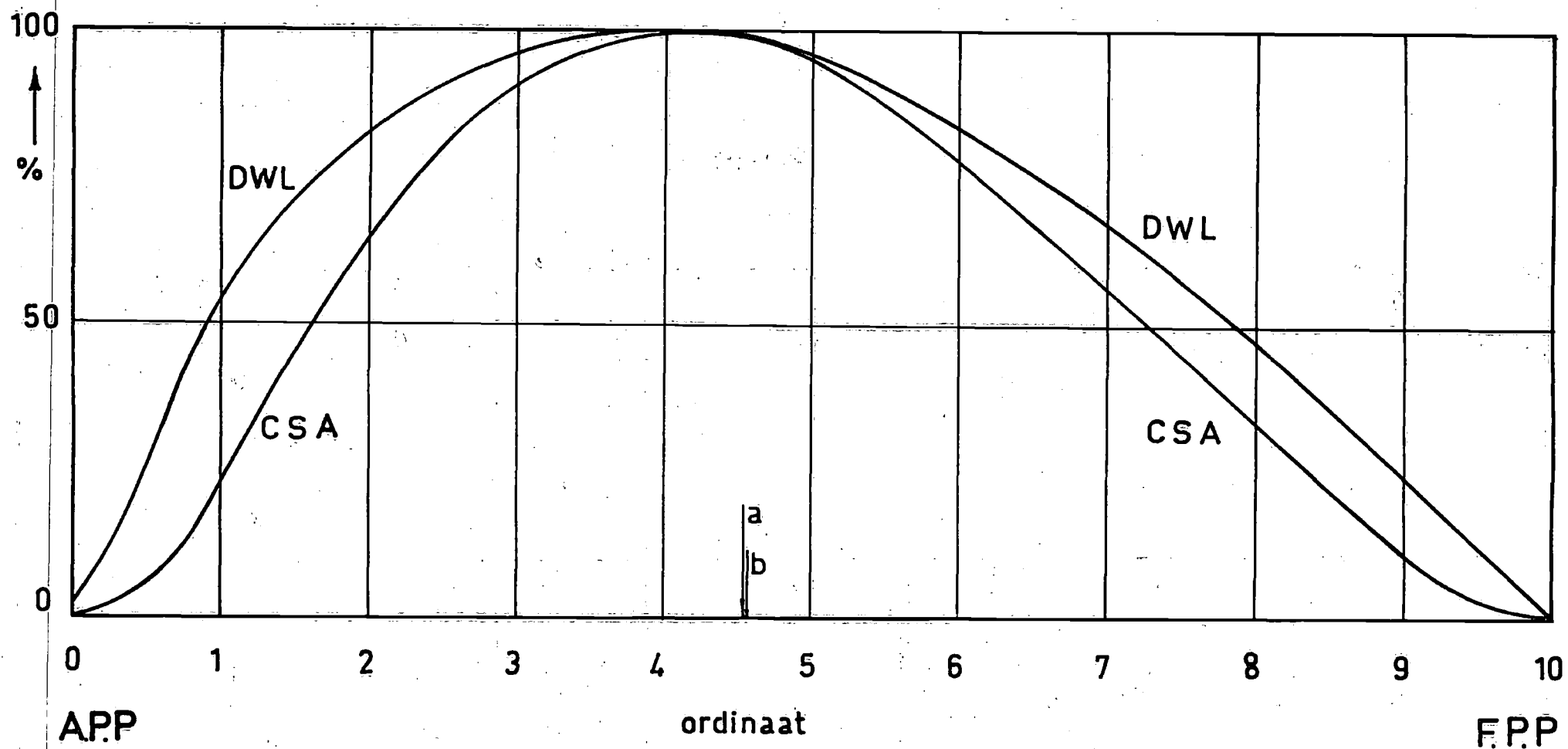
schip	gezeilde tijd (4)		
	$V_{tw}=3.5\text{m/sec}$	$V_{tw}=7.0\text{m/sec}$	$V_{tw}=10.0\text{m/sec}$
Stormy, kiel IV, verhoogd kits- tuig (2)	-	3/00/34	-
Stormy, kiel IV, laag kitstuig	-	3/02/05	-
Stormy, kiel IV, sloeptuig	4/53/20	3/04/11	-
Stormy, kiel I , laag kitstuig(3)	5/02/01	3/03/58	-
IOR-racer, model I	5/16/18	3/18/37	-
IOR-racer, model III	5/17/58	3/20/25	-
IOR-racer, model II	5/20/25	3/13/43	-
Staron	5/54/42	3/36/14	-
ALC'40, kiel I	5/37/54	3/35/12	-
ALC'40, kiel II	5/40/27	3/34/50	-
Eenheidsjacht v.d. Stadt, mod.123	5/56/19	3/52/47	3/33/34
Eenheidsjacht Koopmans, model 121	6/11/28	3/54/50	3/28/49
Eenheidsjacht Maas, model 122	6/04/22	3/56/42	3/34/37
Halftonner	6/16/32	3/59/24	-
Spirit 28	6/29/10	3/39/18	-

(1) : De baan is 10 mijl lang en wordt heen en terug gevaren. De windrichting is evenwijdig aan de baan.

(2) : Kiel IV is de nieuw aangebrachte kiel.

(3) : Kiel I is de oorspronkelijke kiel met roer.

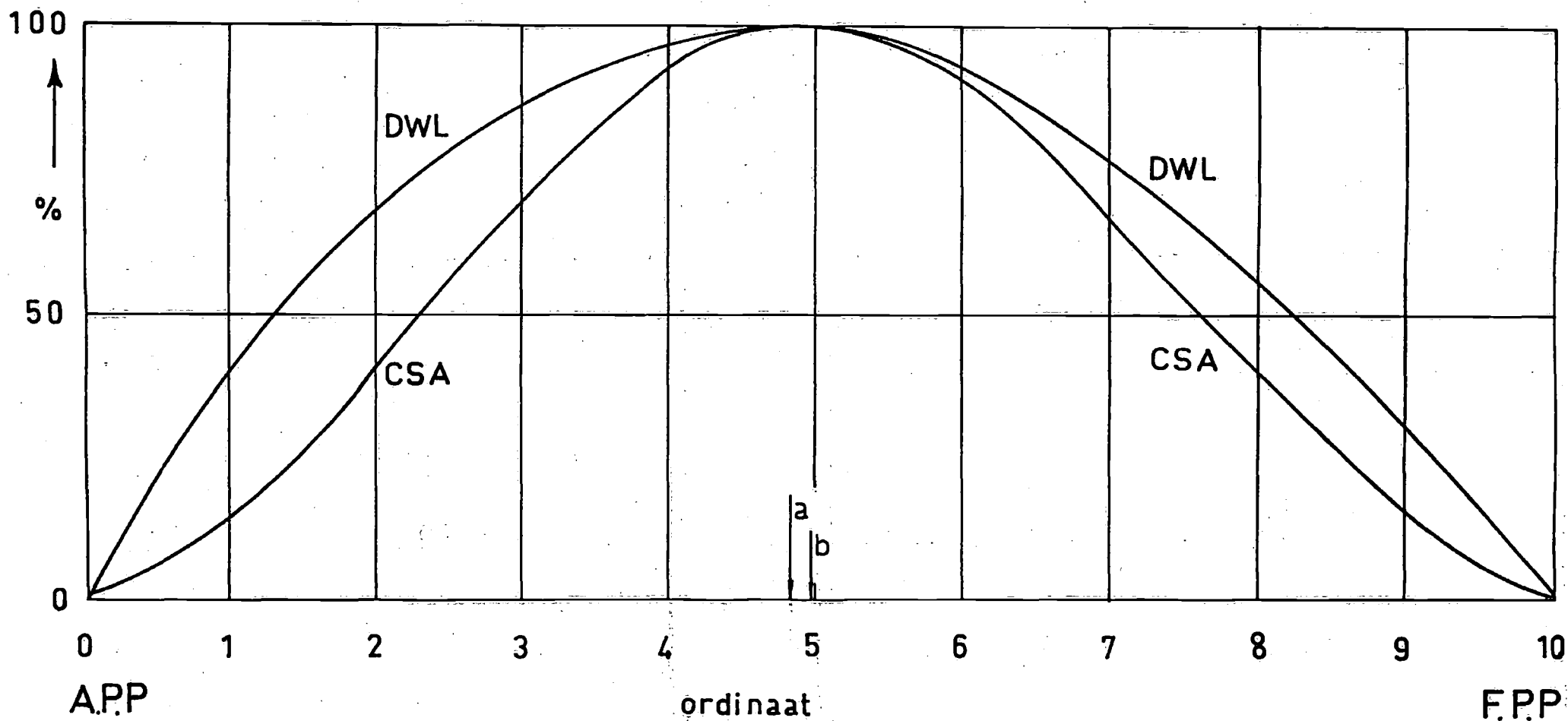
(4) : De gezeilde tijd is aangegeven in uur/min./sec.



a = waterlijnzwaartepunt in lengte

b = drukkingspunt in lengte

Fig. 1 : Vorm ontwerpwaterlijn en kromme van spantoppervlakken voor het ontwerp-eenheidsjacht van Koopmans

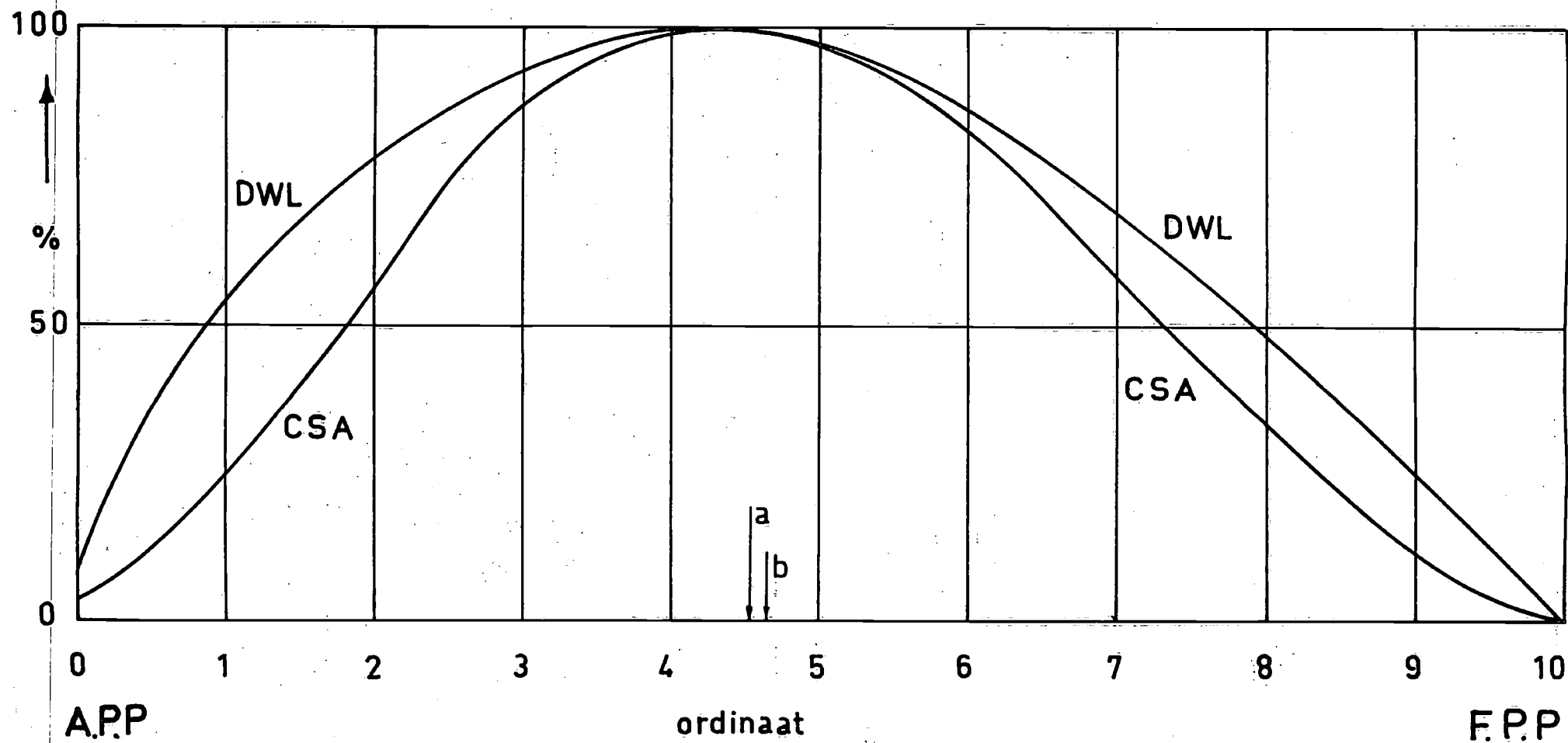


a = waterlijnzwaartepunt in lengte

b = drukkingspunt in lengte

Fig. 2 : Vorm ontwerpwaterlijn en kromme van spantoppervlakken voor het ontwerp-eenheidsjacht van Maas





a = waterlijnzwaartepunt in lengte

b = drukingspunt in lengte

Fig. 3 : Vorm ontwerpwaterlijn en kromme van spantoppervlakken voor het ontwerp-eenheidsjacht van v.d. Stadt

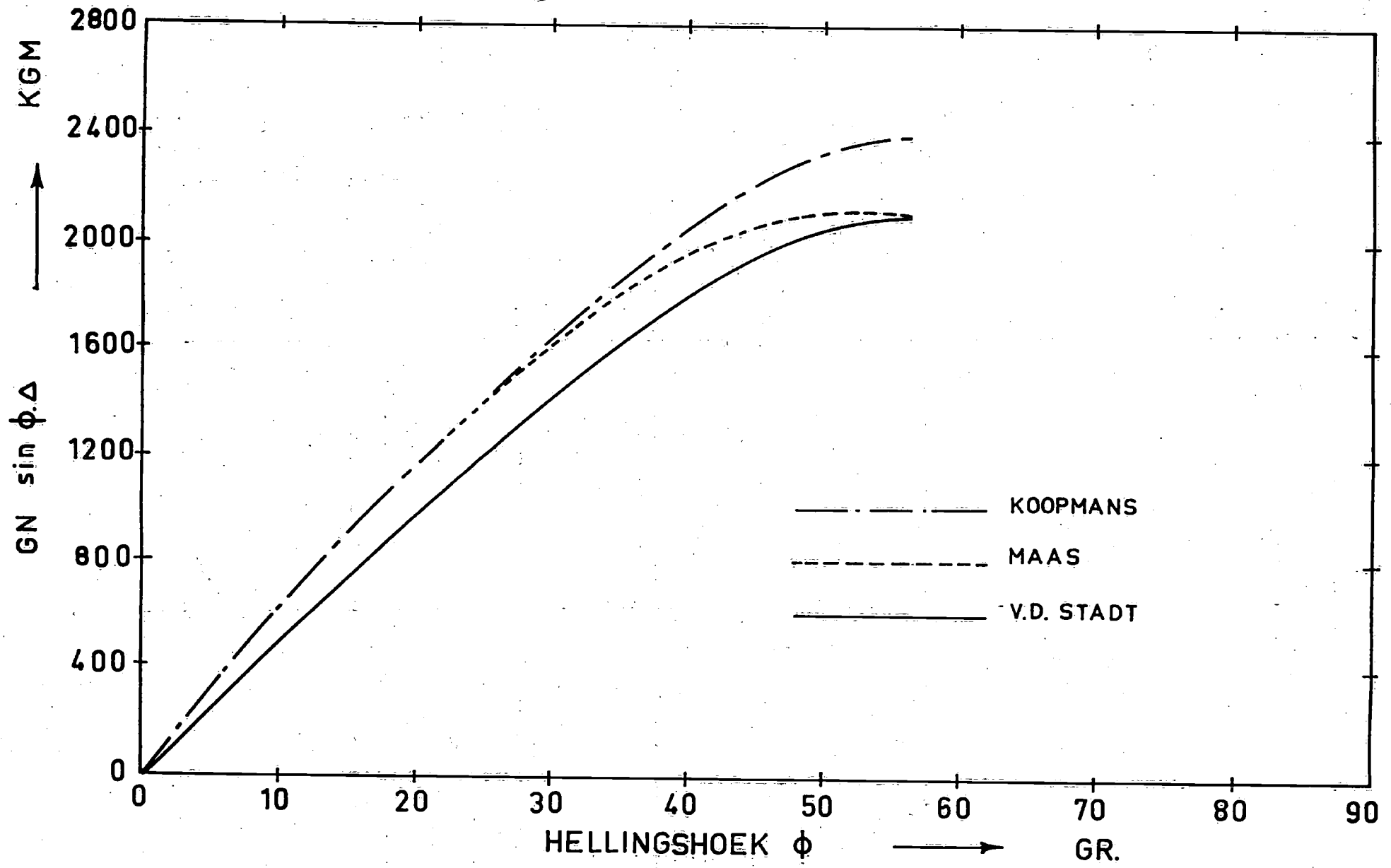


Fig. 4 : Momenten van statische stabiliteit

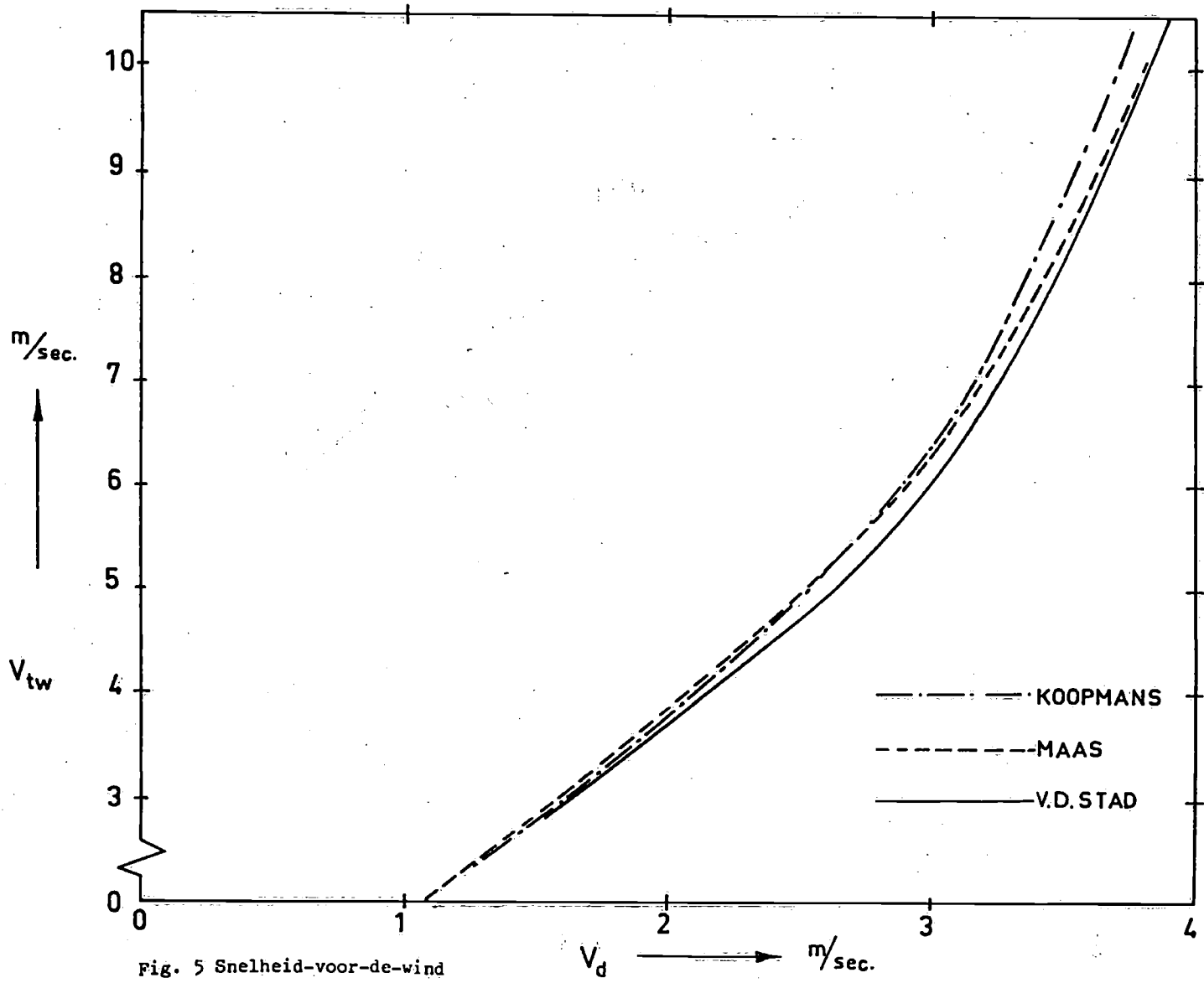


Fig. 5 Snelheid-voor-de-wind

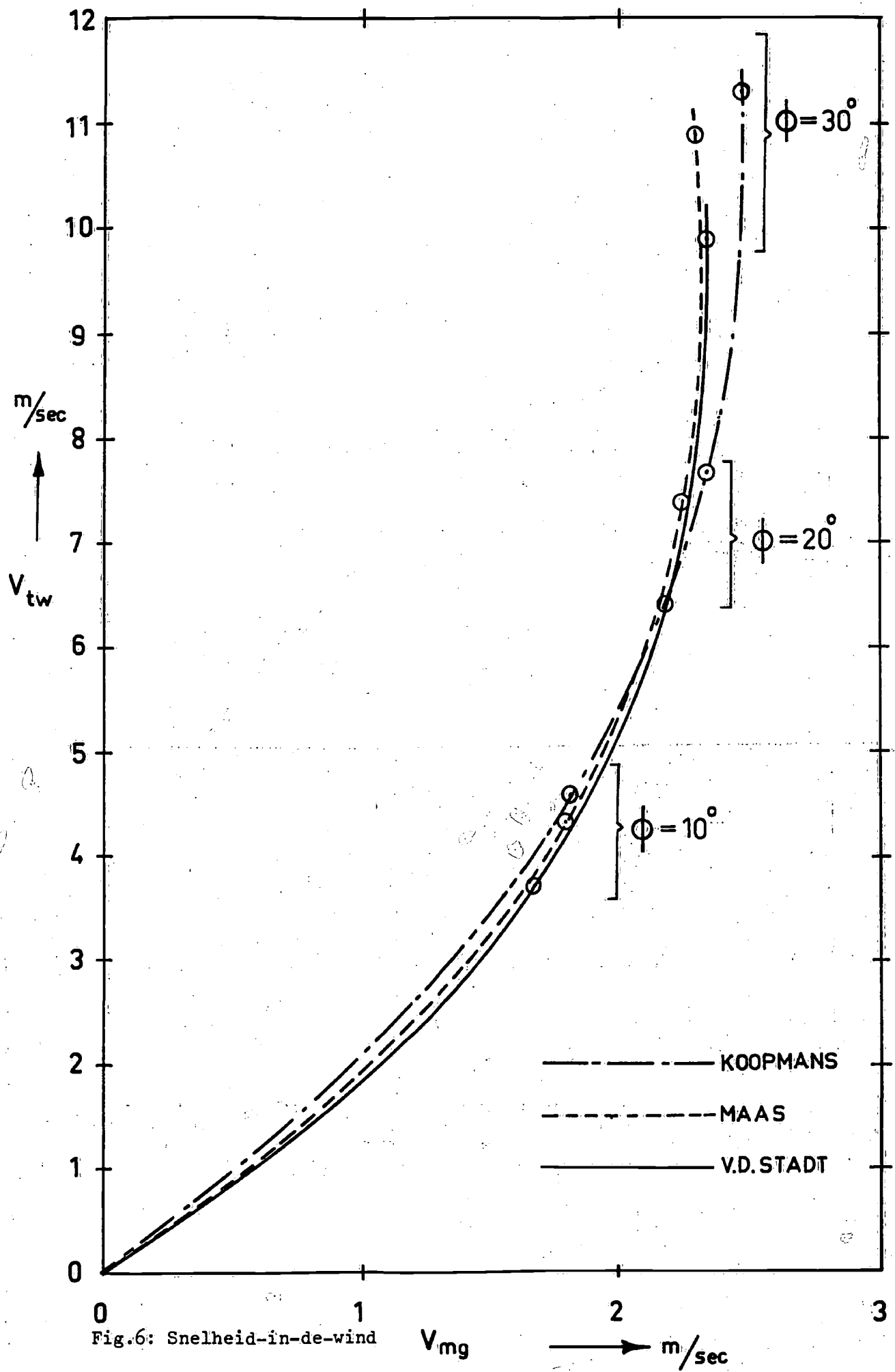


Fig.6: Snelheid-in-de-wind

$V_{mg}$

m/sec

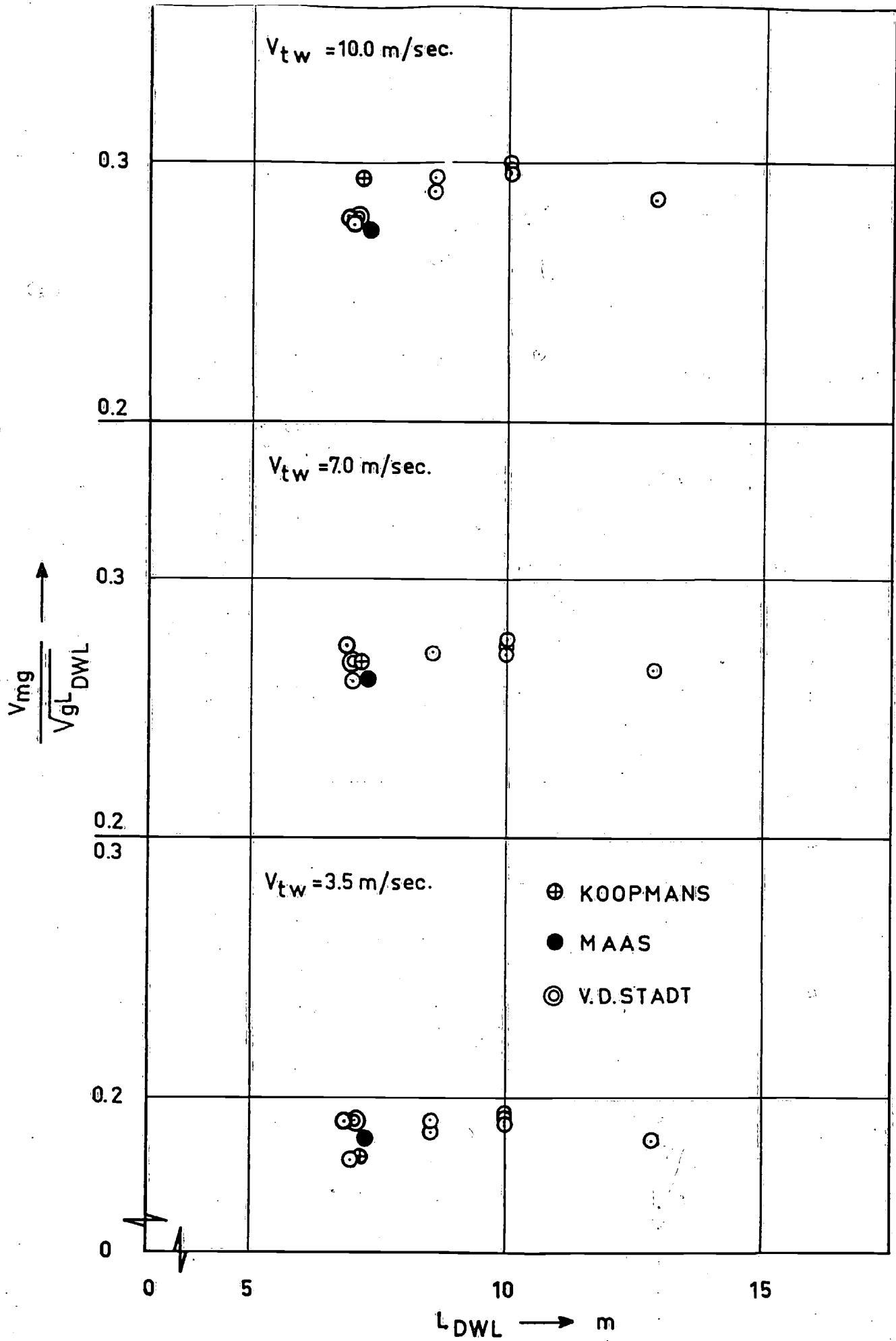


Fig. 7 Vergelijking dimensieloze snelheid - in - de - wind.

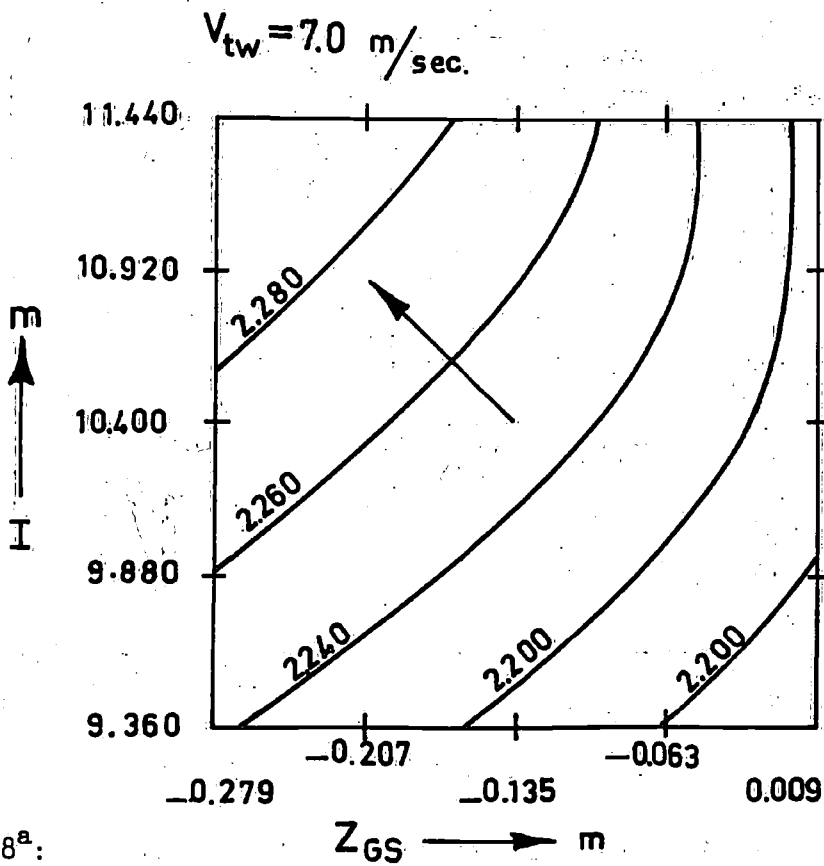
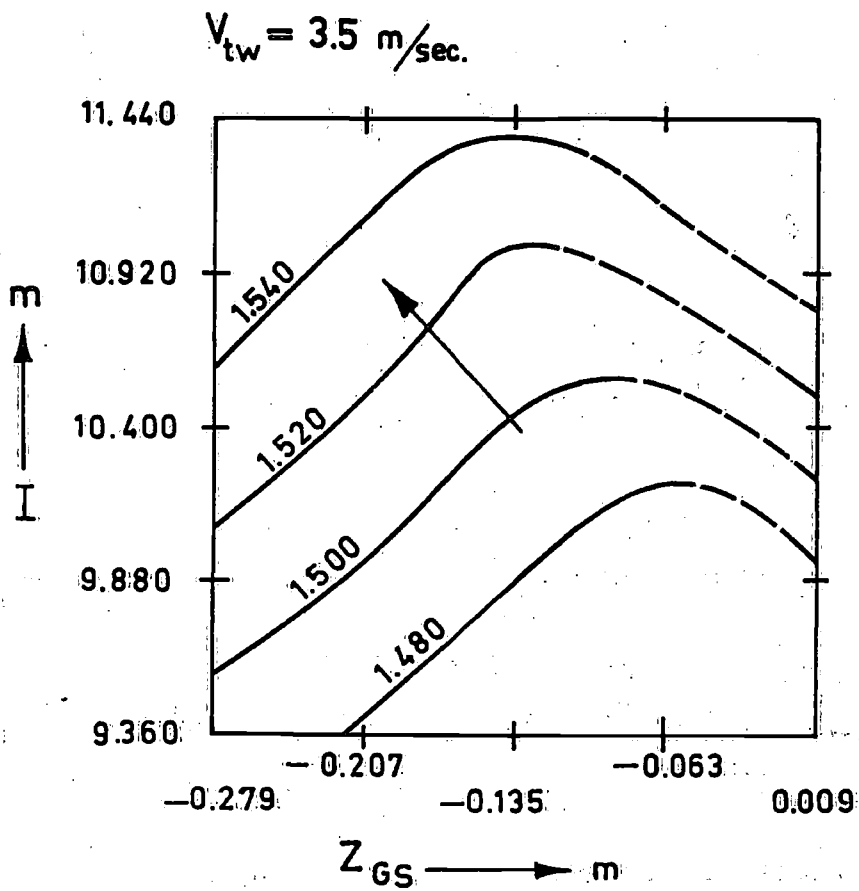


Fig. 8<sup>a</sup>:  
 $V_{mg}$  bij variabele masthoogte en stabiliteit voor het ontwerp-eenheidsjacht van Koopmans

$$V_{tw} = 10.0 \text{ m/sec}$$

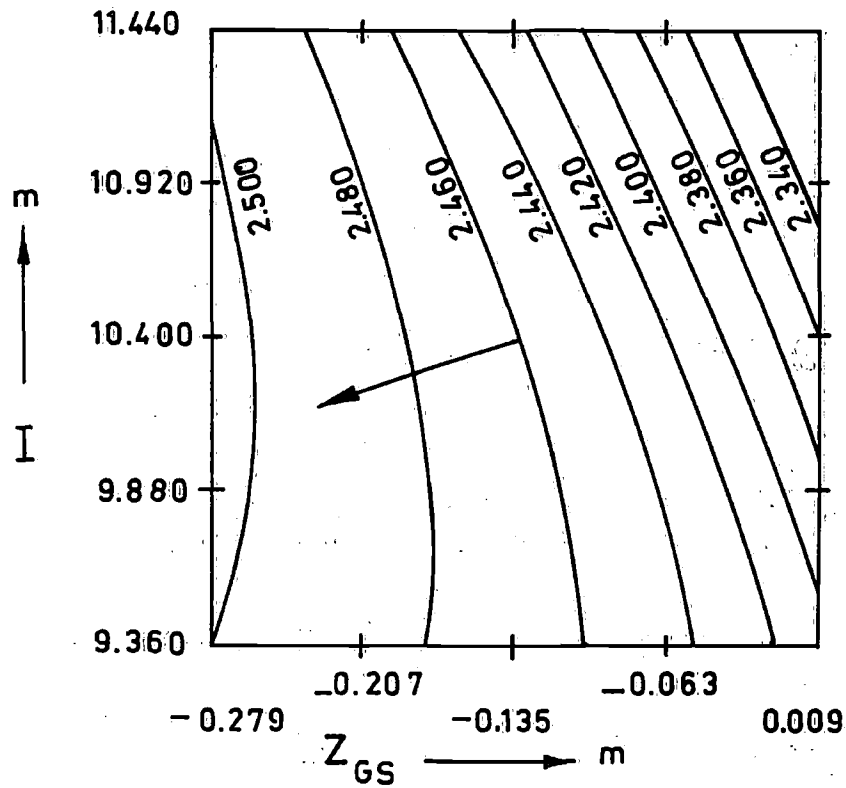
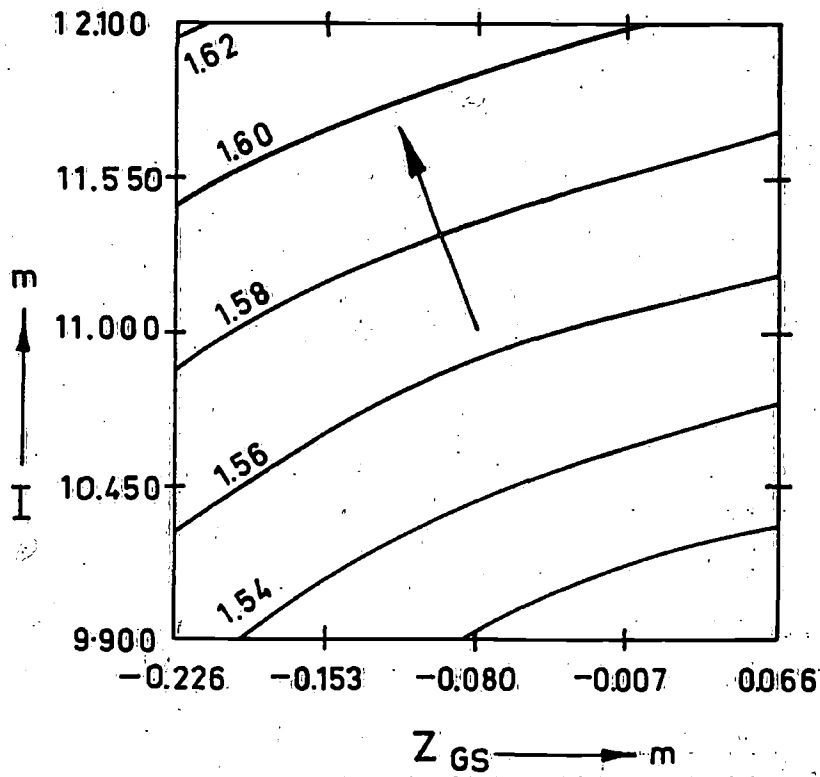


Fig. 8<sup>b</sup>:  
 $V_{mg}$  bij variabele masthoogte en stabiliteit voor het ontwerp-eenheidsjacht van Koopmans

$V_{tw} = 3.5 \text{ m/sec.}$



$V_{tw} = 7.0 \text{ m/sec.}$

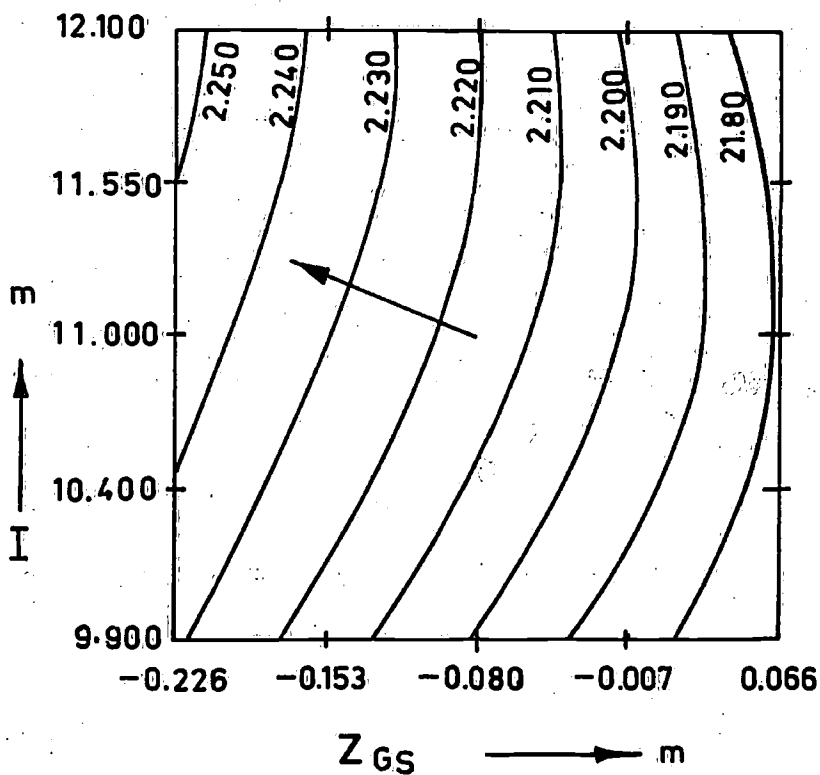


Fig. 9<sup>a</sup>:  
 $V_{mg}$  bij variabele masthoogte en stabiliteit voor het ontwerp-eenheidsjacht van Maas



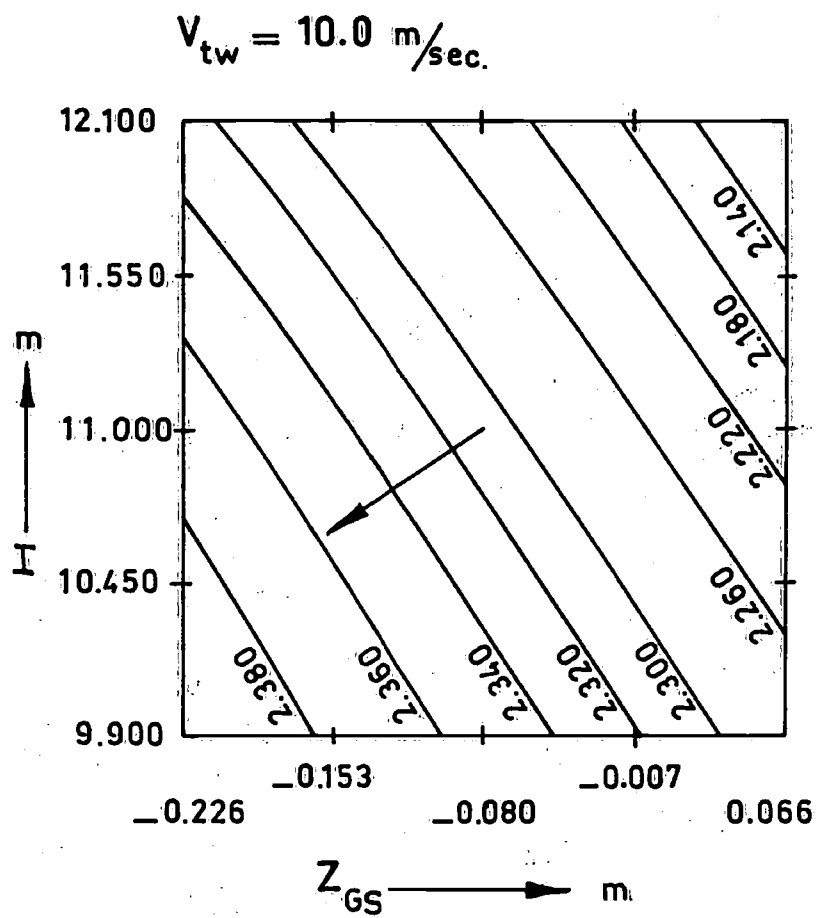


Fig. 9<sup>b</sup>:

$V_{mg}$  bij variabele masthoogte en stabiliteit voor het ontwerp-eenheidsjacht van Maas

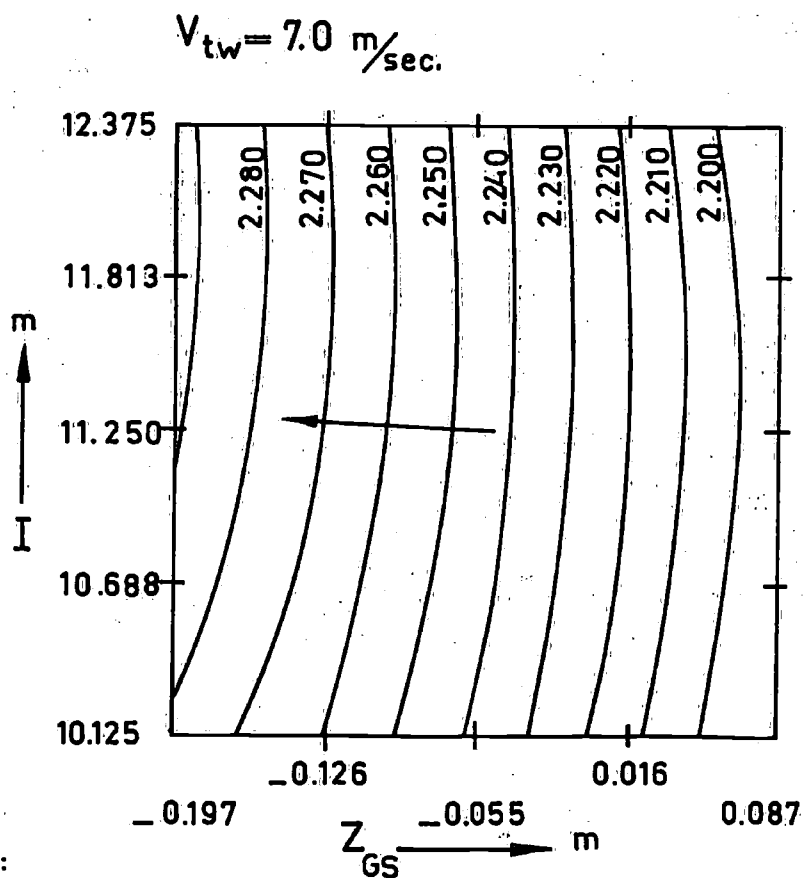
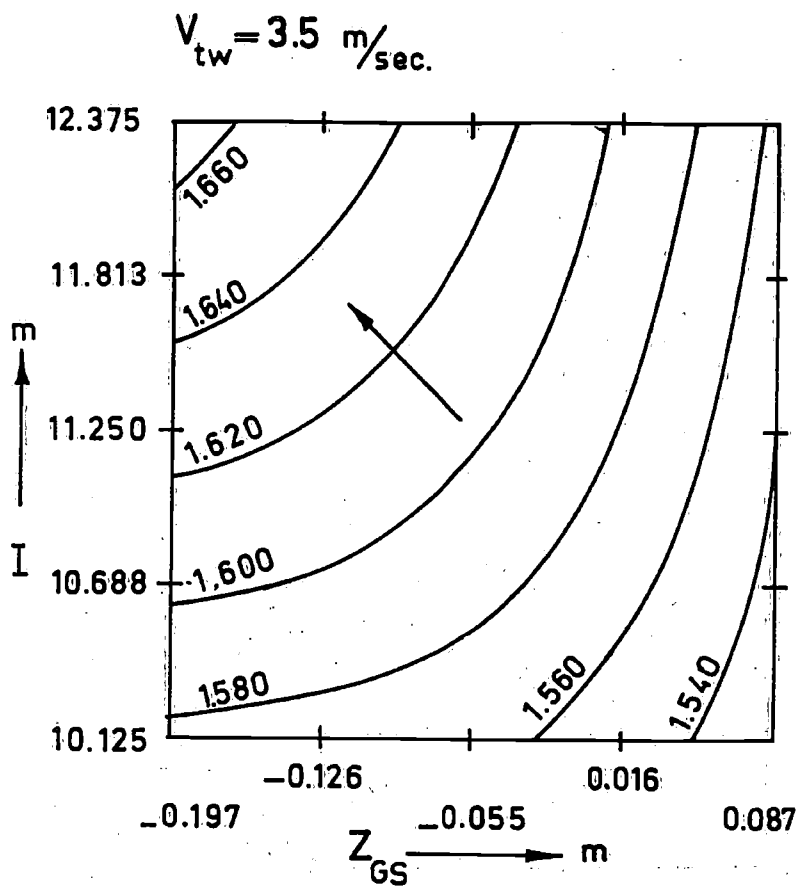


Fig. 10<sup>a</sup>:  
 $V_{mg}$  bij variabele masthoogte en stabiliteit voor het ontwerp-eenhedsjacht van van der Stadt

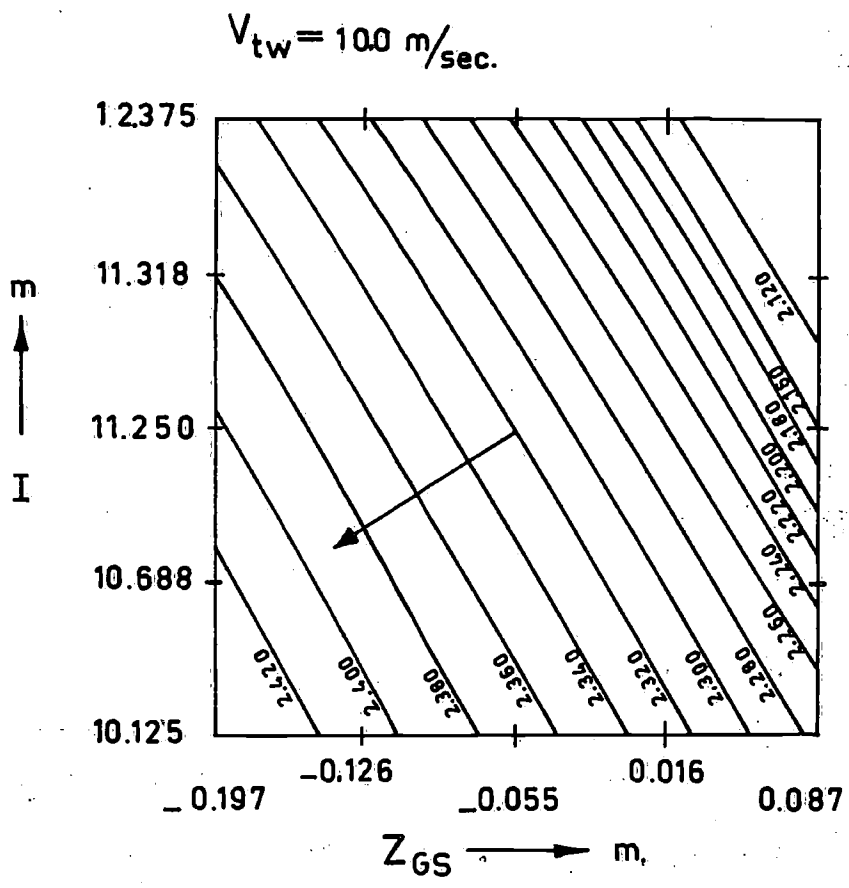
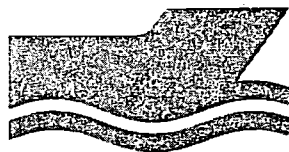


Fig. 10<sup>b</sup>:  
 $V_{mg}$  bij variabele masthoogte en stabiliteit voor het ontwerp-eenheidsjacht van v.d. Stadt



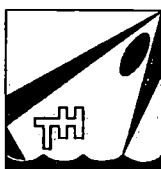
ANALYSIS OF THE RESISTANCE INCREASE  
IN WAVES OF A FAST CARGO SHIP

by Prof.ir.J.Gerritsma and  
W. Beukelman

Reportnr. 334-P

September 1972

13th ITTC - Vol.2.



Delft University of Technology  
Ship Hydromechanics Laboratory  
Mekelweg 2  
2628 CD DELFT  
The Netherlands  
Phone 015 -786882

THIRTEENTH  
INTERNATIONAL TOWING TANK  
CONFERENCE

BERLIN/HAMBURG, SEPTEMBER 1972

PROCEEDINGS

Edited by  
S. SCHUSTER and M. SCHMIECHEN

VOLUME 2

The proceedings have been printed with the financial  
contribution of the  
BUNDESMINISTER FÜR VERKEHR,  
ABTEILUNG SEEVERKEHR, HAMBURG

REPORT OF SEAKEEPING COMMITTEE  
APPENDIX 5

ANALYSIS OF THE RESISTANCE INCREASE IN WAVES OF A FAST  
CARGO SHIP

by J. Gerritsma and W. Beukelman

1. Introduction.

One of the first attempts to calculate the added resistance of a ship in waves was carried out by Havelock [1]. He determined the mean value of the longitudinal component of the pressure forces integrated over the wetted part of the oscillating ship's hull. In his treatment of the problem the water pressure was taken as the undisturbed pressure of the incident wave, which implies the use of the well-known Froude-Kryloff hypothesis. Clearly this was done to avoid the difficult problem of the evaluation of the complicated diffracted waves, which originate from the oscillating ship in the incident waves. Therefore Havelock considered his solution as a first approximation only. An interesting discussion on the use of the undisturbed wave pressure and the effect upon the calculated added resistance in waves was given by Firsoff [2]. He states that the Froude-Kryloff hypothesis is not applicable in this case. Havelock's expression for the added resistance in waves reads as follows:

$$R_{AW} = - \frac{k}{2} (F_a z_a \sin \epsilon_{zF} + M_a \theta_a \sin \epsilon_{\theta M}) \quad (1)$$

where:  $F_a$  and  $M_a$  are the amplitudes of the excitation force and moment in heave and pitch,  $z_a$  and  $\theta_a$  are the corresponding motion amplitudes with phase lags  $\epsilon_{zF}$  and  $\epsilon_{\theta M}$ .

An alternative method to find the expression (1) is to equalize the work done by the exciting force and moment to the work done by the force which is necessary to tow the ship through the given wave field [3].

According to equation (1) the added resistance is zero when the motion of the ship is vanished. The experiment shows that an added resistance force can be present in such a case.

Furthermore the Havelock values do not agree with experimental results over a large range of wave length ratio's.

In order to get a more satisfactory agreement the concept of the relative vertical motion of the ship with respect to the water has to be used, as shown in the following chapters. The method is also applicable for the

determination of the drift force on the motionless ship which corresponds to the situation of relatively small wave lengths.

To check the calculated values an accurate experiment has been carried out with a 3 meter model of a fast cargo ship "S.A. van der Stel".

Existing experimental results, as found in literature do not cover a sufficiently large speed-wave length and wave height ratio for detailed comparison purposes; also the results with standard ship forms, such as the Series Sixty, differ considerably from tank to tank. In addition there is some discussion with regard to the assumption that added resistance in waves varies as the squared wave height, particularly in the case of slender ship forms [4]. An accurate experiment with a model of a passenger-cargo ship, having a blockcoefficient  $C_B = 0.65$  confirmed the square law to a large extent. Based on this principle a prediction of the mean added resistance in a specified irregular sea was in good agreement with corresponding model test results [5]. It should be emphasized that in this case extremely low and high wave heights were excluded.

The present analysis includes an extensive series of added resistance and motion measurements in a large range of wave lengths, forward speeds and three or four wave heights. In one particular case the influence of surge was also investigated.

To a large extent the results confirm again the linear relation between added resistance and wave height squared, at constant speed and wave length, at least as a very good approximation which can be used for practical purposes.

## 2. Measurement of the added resistance and motions in waves.

In Table 1 the main particulars of the ship and the considered model are given. The model was made of glass fibre reinforced polyester on a scale of 1:50.

The bodyplan is given in Figure 1 and the test conditions are summarized in Table 2.

Four ship speeds were regarded:

$$Fn = 0.15 - 0.20 - 0.25 - 0.30.$$

For  $Fn = 0.15$  only one wave height  $\zeta_w = L/50$  has been considered.

The regular waves were measured at a distance of 4 meters in front of the model by means of a two-wire conductance wave probe. Additional measurements

Table 1. Main particulars of M.V. "S.A. van der Stel" and model.

	SHIP	MODEL
$L_{pp}$	152.5 m	3.050 m
$L_{WL}$	154.7 m	3.094 m
B	22.8 m	0.456 m
T	9.1 m	0.183 m
$\nabla$	17931 m <sup>3</sup>	0.1434 m <sup>3</sup>
$A_w$	2431 m <sup>2</sup>	0.9724 m <sup>2</sup>
$I_L$	2782993 m <sup>4</sup>	0.4453 m <sup>4</sup>
$C_B$	0.564	0.564
$C_P$	0.580	0.580
LCB	1.68 % aft $L_{pp}/2$	1.68 % aft $L_{pp}/2$
LCF	4.35 % aft $L_{pp}/2$	4.35 % aft $L_{pp}/2$
$V_{service}$	19.5 knots	1.421 m/sec
$k_{yy}/L_{pp}$	0.219	0.219

Table 2. Wave conditions

$\lambda/L$	$\zeta_w/L$		
0.6	1/50		
0.8	1/50	1/40	1/30
1.0	1/50	1/40	1/30
1.2	1/150	1/50	1/40
1.4		1/50	1/40
1.6		1/50	
1.95		1/50	

were carried out with a sonic wave probe, which showed a very satisfactory agreement with the results of the former one.

The test arrangement is given in Figure 2. The majority of the runs in waves were made with the model restrained in surge, but free to heave and pitch, as shown in Figure 2a and due care was taken to ensure a minimum of friction in the measuring part of the heave guide mechanism. The mean resistance in waves was measured by means of strain gauge dynamometers of which the output was integrated over a full number of wave periods. A comparison of the results of this resistance measurement method with results of the more conventional



system, using a dead weight as shown in Figure 2b, showed only very minor differences. The towing arrangement, given in this Figure was also used to investigate the influence of surge on the heaving and pitching motions and on the added resistance.

The oscillatory motions of the model were measured by two low-friction potentiometers. It has to be emphasized that moderate wave heights were chosen in view of the applicability of the added wave resistance operators and for comparison purposes of the results with calculations.

In Figure 3 the experimental amplitude and phase characteristics of the shipmodel are compared with the corresponding calculated values. The method of the calculation is derived from [7]. In view of the bulbous bow a close fit procedure to describe the cross-sections was used.

There is a slight indication of non-linearity in the measured motion amplitudes, and a tendency towards better agreement with the theoretical values in the case of small wave heights is observed. For  $F_n = 0.25$  the influence of surge on the heaving and pitching motions is very small, as shown in Figure 3. There is hardly any difference in the motion characteristics, whether the model is free to surge or not.

The added resistance in regular waves is shown in Figure 4 for the model which is free to pitch and heave, but restrained in surge. In addition the added resistance is given for the case where the model is restrained in heave, pitch and surge motions. The results cover the various wave height conditions as summarized in Table 2.

In view of the slight non-linearity of the vertical motions, there is surprisingly little deviation from the square wave height law. This also holds for the added resistance of the motionless model.

Figure 5 shows that the influence of surge on the added resistance in bow waves is negligible. This may not be true for following waves.

The validity of the square wave height law for this particular model with a low blockcoefficient is also clearly shown in the Figure 6, where added resistance due to waves for the pitching and heaving model and for the motionless model is plotted on a base of wave height squared. The standard deviation from the assumed quadratic law is in the order of  $3\frac{1}{2}\%$ , which includes the measurement errors both in wave height and in the added resistance.

### 5. Calculation of the added resistance in waves.

Joosen calculated the added resistance of a ship in short waves by expanding Maruo's expression into an asymptotic series with respect to the slenderness parameter [6].

Taking into account only the first order terms, he found a reasonable agreement with the experiment, although this simplified treatment results in a speed independent added resistance. In fact use is made of the strip theory to determine the resistance force. Of particular interest is the expression for the added resistance given in [6]:

$$R_{AW} = \frac{\omega^3}{2g} (N_z z_a^2 + N_\theta \theta_a^2) \quad (2)$$

which is equivalent to Havelock's equation (1).

Equation (2) shows that the added resistance can be regarded as a result from the radiated damping waves.

Although not consistent with the mathematical theory the frequency of encounter is used by Joosen when a ship with forward speed is considered. As in the case of equation (1) this expression does not take into account the relative vertical motion of the ship, with respect to the water. Therefore the following procedure is adopted for the calculation of the radiated energy  $P$  of the oscillating ship during one period of encounter. We consider longitudinal regular bow waves.

$$P = \int_0^{Te} \int_0^L b' \cdot V_z^2 dx_b dt \quad (3)$$

where:

$$b' = N' - V \frac{dm'}{dx_b}, \text{ the sectional damping coefficient for speed}$$

and  $V_z = \dot{z} - x_b \dot{\theta} + V\theta - \zeta^*$ , the vertical relative water velocity

where:  $\zeta^* = \zeta \left(1 - \frac{k}{y_w} \int_{-T}^0 y_b e^{kz_b} dx_b\right)$  is the effective vertical wave

displacement for a cross-section. For this concept reference is made to [7]. As  $V_z$  is a harmonic function with amplitude  $V_{za}$  and a frequency equal to the frequency of encounter  $\omega_e$ , we find:

$$P = \frac{\pi}{\omega_e} \int_0^L b' V_{za}^2 dx_b \quad (4)$$

Following the reasoning given in [3] the work being done by the towing force  $R_{AW}$  is also given by:

$$P = R_{AW} (V + c) T_e = R_{AW} \cdot \lambda \quad (5)$$

where:  $c$  is the wave celerity and  $\lambda$  is the wave length.

From (4) and (5) it follows that:

$$R_{AW} = \frac{k}{2\omega_e} \int_0^L b' V_{za}^2 dx_b \quad (6)$$

From (6) it is clear, that the added resistance in waves varies as the squared wave height, because  $V_{za}$  is proportional to the wave height.

We can distinguish two extreme cases:

- a. A ship without oscillatory motions in waves. This occurs when the ship sails in relatively short waves and practically no ship motion exists. The resistance increase in this case is caused by what is commonly called diffraction effects.

In this case:

$$R_{AW} = \frac{k}{2\omega_e} \int_0^L b' \dot{\zeta}^{*2} dx_b \quad (7)$$

We may write:  $\dot{\zeta}^* = \zeta e^{-kT^*}$

where:

$$T^* = -\frac{1}{k} \ln \left( 1 - \frac{k}{y_w} \int_{-T}^0 y_w e^{kz_b} dz_b \right)$$

Because  $\dot{\zeta}^* = -\zeta^* \omega$

$$\text{We find: } R_{AW} = \frac{k\omega^2}{2\omega_e} \zeta_a^2 \int_0^L b' e^{-2kT^*} dx_b \quad (8)$$

- b. Also in the case of an oscillating ship in calm water the radiated energy corresponding to the motion of the ship is the cause of resistance increase. Here the relative vertical speed of a cross-section  $x_b$  with regard to the water is given by:

$$V_z = \dot{z} - x_b \dot{\theta} + V\theta \quad (9)$$

The resistance increase follows from the equation (6) when the appropriate value of  $V_z$  is taken.

From the fact that the speed  $V_z$  appears as a quadratic form in the integrand in the expression for  $R_{AW}$ , it follows that the resistance increase in waves is not merely the sum of the resistance increase of a ship oscillating in calm water and the resistance increase of a motionless ship in waves.

The equation (6) indicates that for the motionless ship in waves a finite resistance is found which approaches zero only at increasing frequencies of encounter.

The resistance increase due to waves for the considered ship was calculated according to the equations (6) and (8).

The results are shown in the Figure 4. The comparison with the experiments shows a very satisfactory agreement for the case of a pitching and heaving ship.

For the short waves ( $\lambda/L < 0.8$ ) the experimental values are somewhat higher for speeds higher than  $F_n = 0.15$ . A possible explanation could be the influence of viscous effects, which are not included in the calculation. Because of the increasing frequency of encounter the vertical water velocities increase and consequently the viscous effects could be more important. To show the improvement with regard to Havelock's formula, the values of  $R_{AW}$  corresponding to equation (1) are given in Figures 4.

The resistance increase of the motionless ship is small but should not be neglected. There is a fair agreement with the experiment at the lower speeds, but at the highest speed, the diffraction resistance is underestimated. Here also the influence of viscous effects may be the main reason for this deviation, specially for high speeds and frequencies of encounter.

With regard to the total added resistance in waves the differences are of minor importance.

#### 4. Conclusions.

From the analysis of the experiments and the calculations of the added resistance the following conclusions may be drawn.

- a. For the considered ship form the added resistance in waves varies linearly as the squared wave height at constant wave length and constant

forward speed.

This is also valid for the resistance increase of a motionless ship in the same wave conditions: longitudinal bow waves.

- b. The added resistance in waves can be calculated by determining the radiated energy of the damping waves. To this end the strip theory is used, taking into account the relative motion of the water with respect to the ship and a close fit procedure to describe accurately the form of the cross-sections.
- c. The influence of surge on both the motions and the added resistance in waves may be neglected.

### 5. Acknowledgement.

The authors are indebted to Verolme United Shipyards who kindly provided the drawings and other data of M.V. "S.A. van der Stel".

### List of Symbols      See also [7].

$A_w$	Area of waterplane.
$B$	Breadth of ship or model.
$b'$	Sectional damping coefficient for speed.
$C_B$	Block coefficient.
$C_p$	Longitudinal prismatic coefficient.
$c$	Wave celerity.
$F_a$	Wave force amplitude. (Amplitude of excitation force in heave)
$F_n$	Froude number.
$g$	Acceleration of gravity.
$I_L$	Longitudinal moment of inertia of waterplane with respect to the $y_b$ axis.
$k=2\pi/\lambda$	Wave number.
$k_{yy}$	Longitudinal radius of inertia of the ship.
$L_{pp}, L$	Length between perpendiculars.
$M_a$	Wave moment amplitude. (Amplitude of excitation moment in pitch).
$m'$	Sectional added mass.
$N'$	Sectional damping coefficient for zero speed.

$N_z$	Damping coefficient for heave.
$N_\theta$	Damping coefficient for pitch.
$R_{AW}$	Added resistance in waves.
$T$	Draught of ship.
$T_e$	Period of encounter.
$t$	Time.
$V$	Forward speed of ship.
$V_z$	Vertical relative water velocity.
$V_{za}$	Amplitude of vertical relative water velocity.
$x, y, z$ $x_b, y_b, z_b$ }	Right hand coordinate system fixed to the ship.
$y_w$	Half width of designed waterline.
$z$	Heave displacement.
$z_a$	Heave amplitude.
$\epsilon$	Phase angles.
$\zeta$	Instantaneous wave elevation.
$\zeta_a$	Wave amplitude.
$\zeta_w$	Wave height (double amplitude).
$\theta$	Pitch angle.
$\theta_a$	Pitch amplitude.
$\lambda$	Wave length.
$\rho$	Density of water.
$\nabla$	Volume of displacement.
$\omega$	Circular frequency.
$\omega_e$	Circular frequency of encounter.

## 6. References.

- [1] T.H. Havelock:  
"The Resistance of a Ship among Waves".  
Proc. Roy. Soc. A, Vol. 161, 1937, p. 299.
- [2] G.A. Firsoff:  
Discussion on  
V.I. Pershin and A.I. Vosnezensky  
Study of Ship Speed Decrease in Irregular Sea.  
Proceedings Symposium on the Behaviour of Ships in a Seaway  
Wageningen, 1957.

- [3] Chapter 5, Resistance in Waves.  
Volume 8, 60th Anniversary Series  
The Society of Naval Architects of Japan 1963.
- [4] O.J. Sibul:  
"Increase of Ship Resistance in Waves"  
Report NA-67-2, 1967  
College of Engineering, University of California
- [5] J. Gerritsma, J.J. van den Bosch, W. Beukelman:  
"Propulsion in Regular and Irregular Waves"  
International Shipbuilding Progress  
Vol. 8, no. 82, 1961.
- [6] W.P.A. Joosen:  
"Added Resistance of Ships in Waves"  
Sixth Symposium  
Naval Hydrodynamics  
Washington 1966
- [7] J. Gerritsma, W. Beukelman:  
"Analysis of a Modified Strip Theory for the Calculation of Ship  
Motions and Wave Bending Moments"  
Netherlands Ship Research Center,  
Report no. 96 S, June 1967.

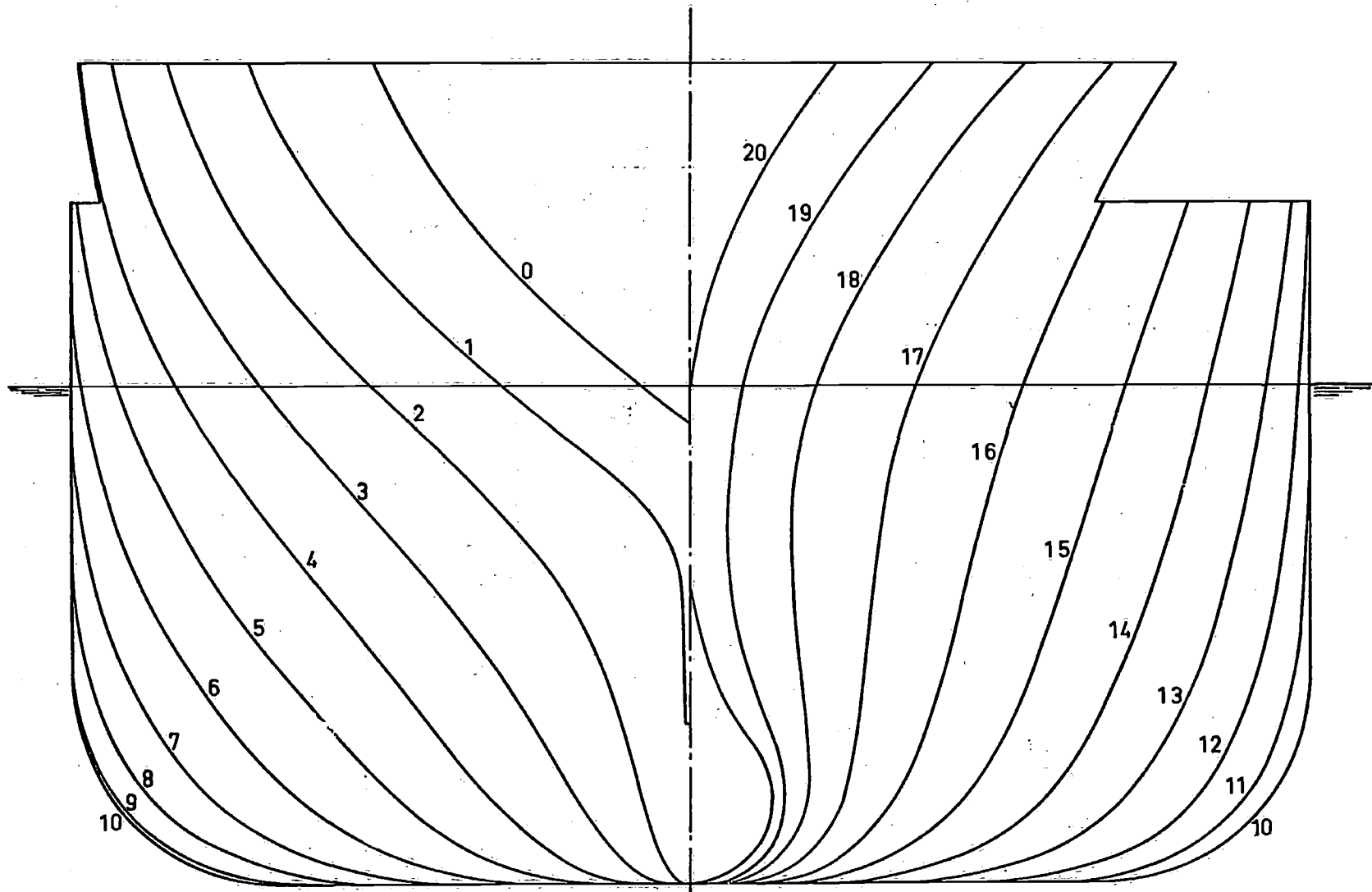


Figure 1 Body plan



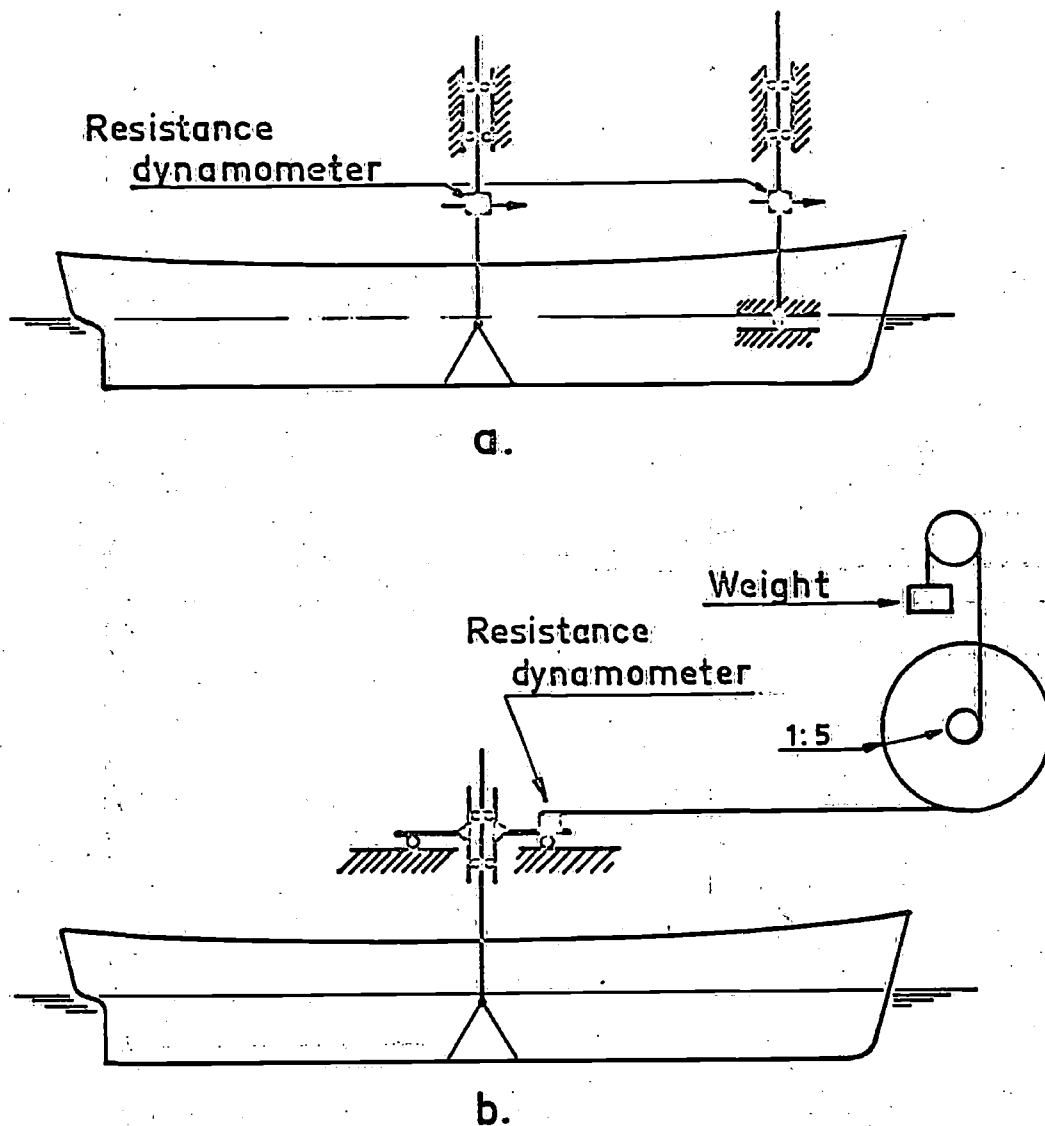


Figure 2 Arrangement for resistance tests in still water and in waves.

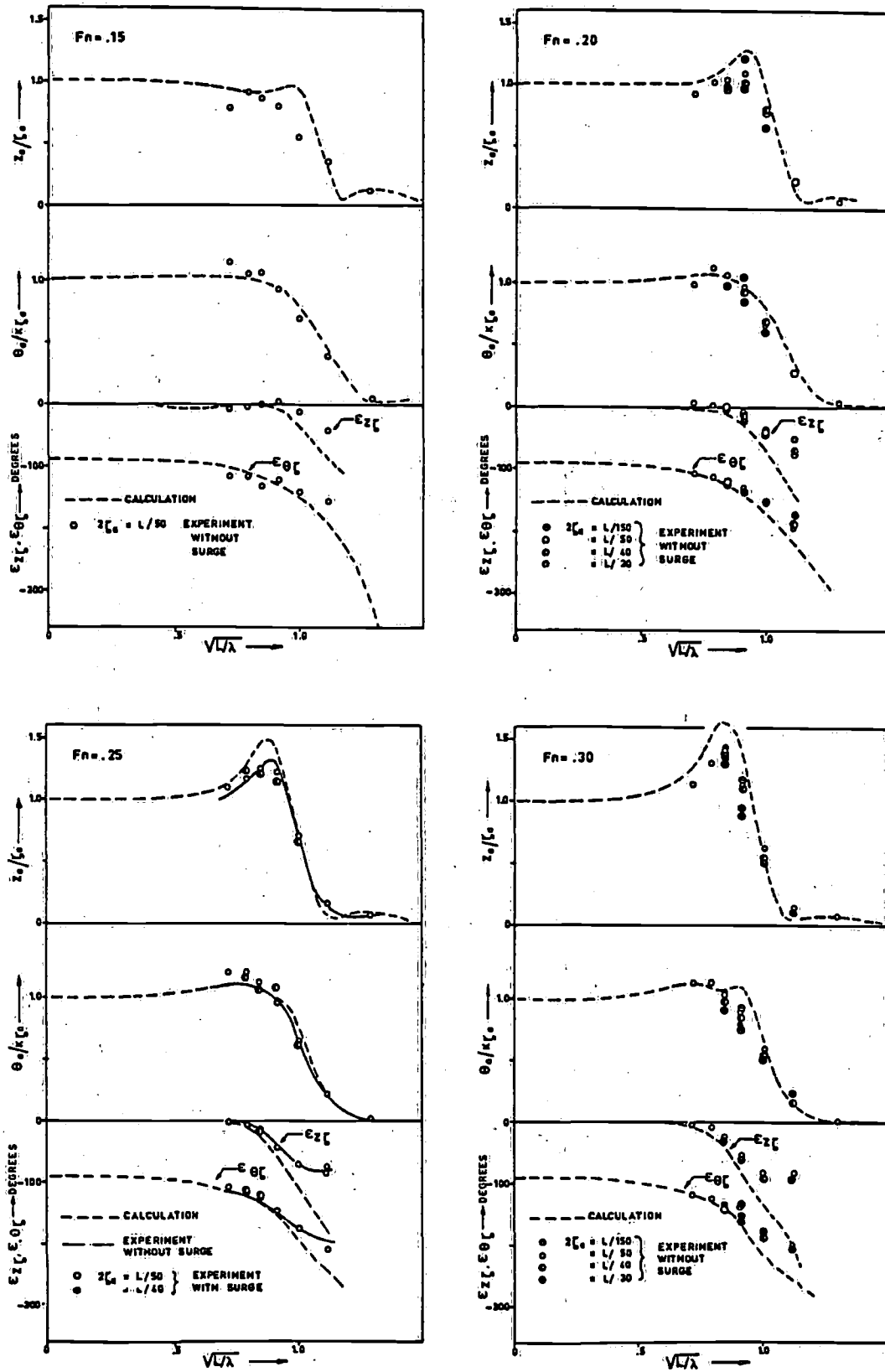


Figure 3 Experimental and calculated frequency characteristics for heave and pitch



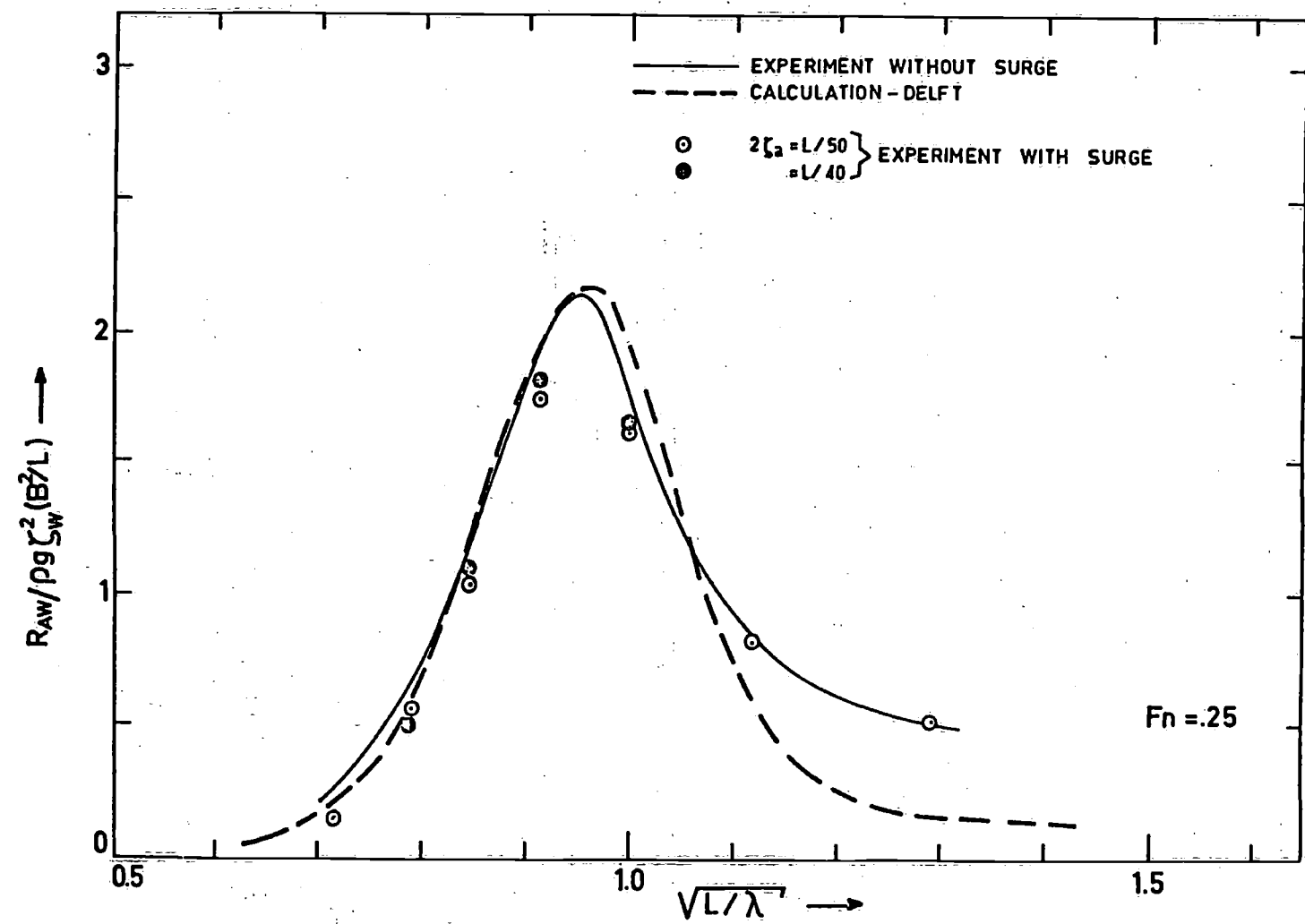


Figure 5 Influence of surge on the added resistance in waves and calculated values

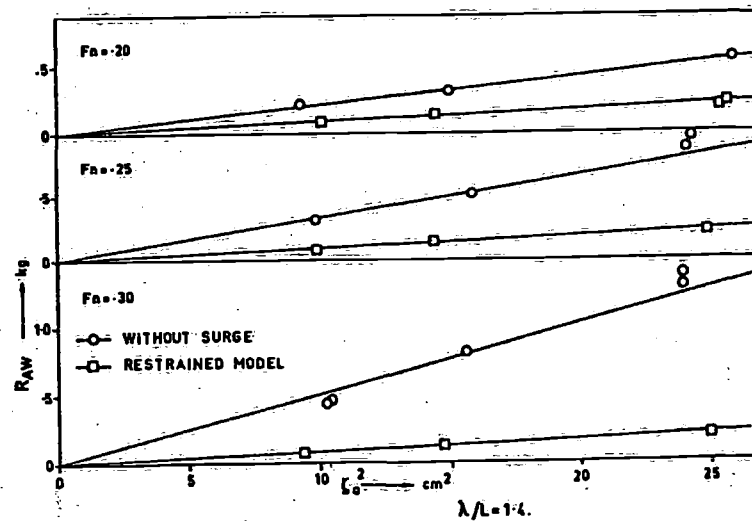
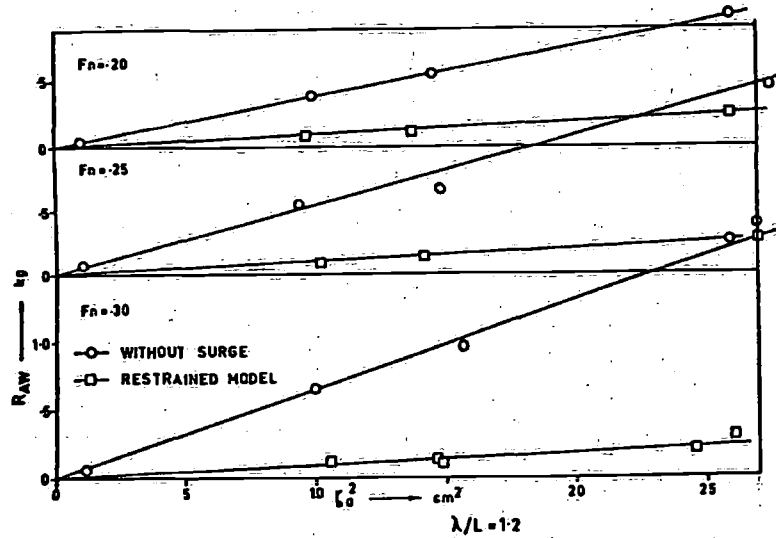
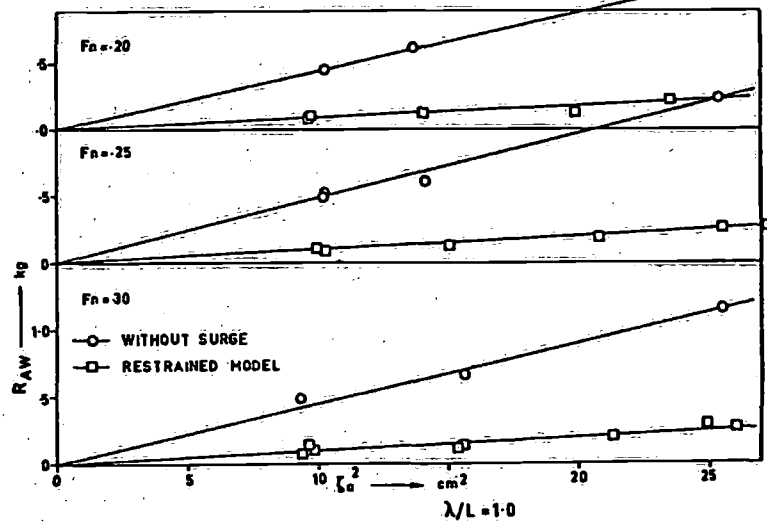
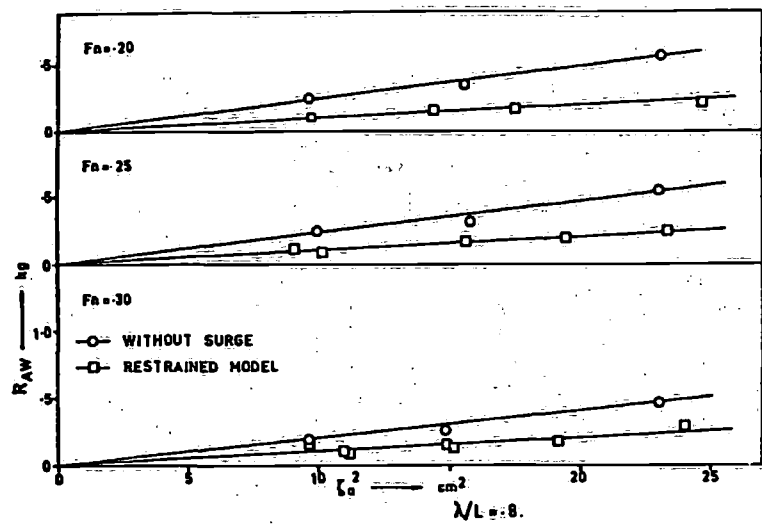
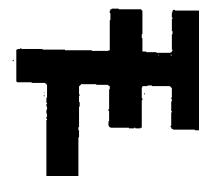


Figure 6 Added resistance in waves with respect to the square of the wave amplitude

Report No. 383



# LABORATORIUM VOOR SCHEEPSBOUWKUNDE

TECHNISCHE HOGESCHOOL DELFT

DESCRIPTION OF A PROGRAM TO CALCULATE  
THE BEHAVIOUR OF A SHIP IN A SEAWAY  
(NAMED : TRIAL)

by

W. Beukelman \*)  
Mrs. E.F. Bijlsma \*\*)

August 1973

\*) Shipbuilding Laboratory of the Delft University of Technology.  
Holland.

\*\*\*) IWIS-TNO : Institute for Mathematics, Information Processing and  
Statistics, The Hague, Holland.

## Contents

### Introduction

#### 1. General

1.1. Data for the program

1.2. Purpose

#### 2. Theoretical framework

2.1. Statical calculations

2.2. Regular waves

2.3. Irregular waves

2.3.1. General spectrum data

2.3.2. Transformation of the spectra for speed and direction of wave travel

2.3.3. Determination of the response spectra

2.4. References

#### 3. Operation

3.1. General

3.2. Description of the input data

3.3. Additional input advice

3.3.1. Section input

3.3.2. Input of frequencies of encounter

3.3.3. Introduction of the weights

3.4. Description of the output

#### 4. Example

#### 5. Structure of the program

5.1. General

5.2. Schematic flow-diagram

5.3. Job information

5.4. Listing of principal computer variables

5.5. Program listing

## Introduction

In this report a description is given of a computerprogram to calculate vertical ship motions, shearing forces, bending moments, relative motions, vertical accelerations, slamming, shipping and increased resistance in regular- and irregular waves with the well-known strip theory.

For an arbitrary direction of wave travel irregular seas are supposed to be composed of uni-directional waves. The influence of the horizontal motions has been neglected and for this reason the direction of wave travel is practically restricted.

For all sections, even bulbous ones, is made use of the Lewis-transformation. The program is developed by the Shipbuilding Laboratory of the University of Technology at Delft, Holland.

For a more detailed information the reader should consult the used literature as reflected in the references [ 1,2,3 ] .



## 1. General

The program has been suited for the IBM 360/65 computer of the Mathematical Centre of the University of Technology at Delft, Holland. For other computers some applications may be necessary.

### 1.1. Data for the program

- a. Language : Algol 60
- b. Memory : 256 K
- c. Calculation time : + 4 min. per ship
- d. Name of the program : TRIAL

### 1.2. Purpose

With the program at issue it is possible to calculate several parameters as mentioned in the introduction such as vertical motions (heave and pitch), shearing forces, bending moments, resistance increase etc.

It is the intention to obtain data, which are important to determine the significant values of vertical motions, the power increase and the chance of shipping and slamming in a wave spectrum.

These data among others are required for the routing of ships.

The significant values of shearing forces, and bending moments are of interest for the determination of the ship's strength, while a known wave-load may be important for the construction and for "springing" phenomena.

And finally it is possible to fit all these data in a ship design procedure.

## 2. Theoretical framework

In this chapter will be presented a short description of the way in which the calculations are carried out.

The calculation of ship motions in regular waves is based on the linear strip theory as presented in [1].

For the different notations see [1,2,3].

The program, essentially made for a ship model, can be used for a ship if the modelscale  $\alpha=1$  is introduced in the input. The origin of the coordinate system is assumed to be situated in the ship's centre of gravity, which is considered to be in the load waterline.

Heave and wave displacements upwards are supposed to be positive, while the pitching angle is taken positive for the bow downwards. See fig. 1.

The sections should be at equal distance, while the midship section is assumed to be at half the ship's length  $L$ . In length the ordinates of the sections are taken positive for the sections forwards of the midship section. A correction for the situation of the centre of gravity in length (LCG) with respect to the midship section will be carried out later on in the program.

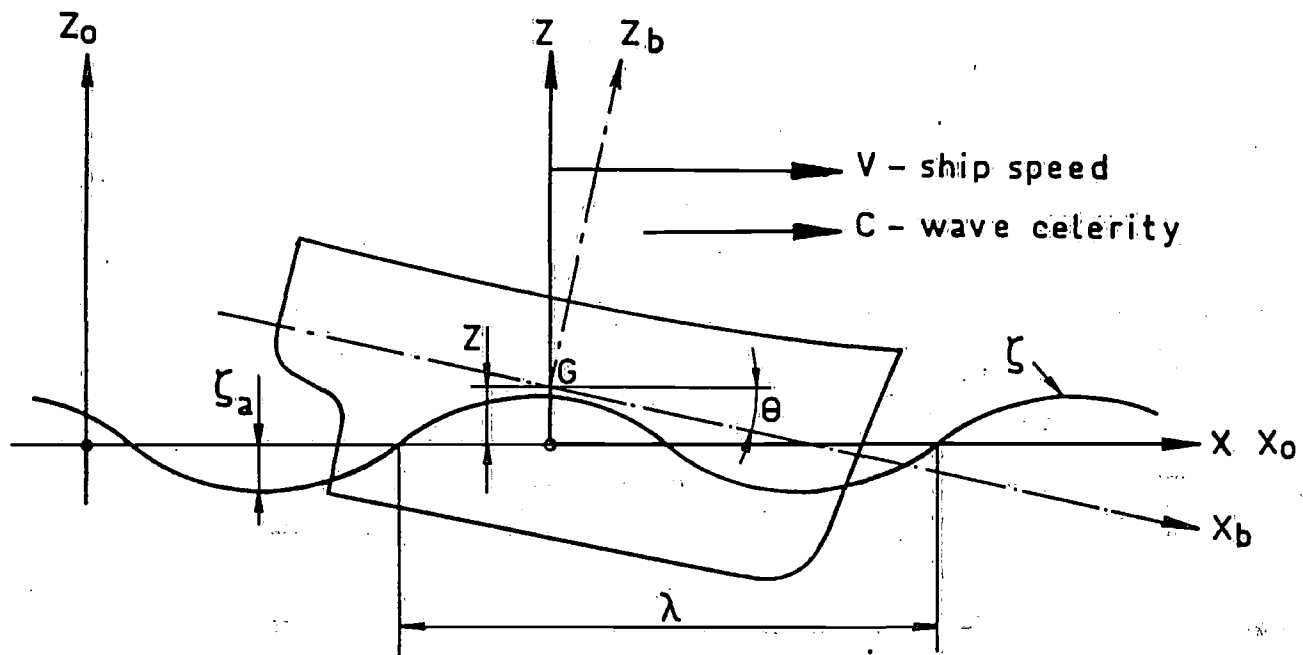
### 2.1. Statical calculations

The section offsets have to be introduced in a fixed way according to Simpson's second rule as will be described in chapter 3.3.1.

After determining of the sectional area's, the displacement and the position of the centre of buoyancy in length (LCB) with respect to the midship section are calculated. If the weight distribution is known, the integration of the weight distribution and so the ship weights from the bow to the sections can be used as an input to compute the shearing forces and bending moments in still water for the sections 0,2,4,...J. See the additional input advice 3.3.3.

### 2.2. Regular waves

After conformal mapping of the section to the unit circle according to the well known "Lewis-form" transformation the sectional added mass  $m'$  and damping  $N'$  are calculated [4]. For bulbous sections an approximation is used in such a way, that the half beam  $y_w$  of the section at the waterline is kept constant, while the draught of the section  $T_j$  is increased to such a value, that Lewis-form transformation is possible. Care had been taken, that for numerical reasons this limit is exceeded a certain value.



wave -  $\zeta = \zeta_a \cos(kx_0 \cos\mu - \omega t)$  in  $x_0 y_0 z_0$   
 $\zeta = \zeta_a \cos(\omega_e t)$  in  $x y z, x=0$   
 heave -  $z = z_a \cos(\omega_e t + \epsilon_{z\zeta})$   
 pitch -  $\theta = \theta_a \cos(\omega_e t + \epsilon_{\theta\zeta})$   
 $\omega_e = \omega + \frac{\omega^2}{g} V$

Figure:1. Definition of wave and motions

In future there will be published an extended comparison of the results for several ship types according to this adaptive "Lewis-form" transformation with the results of other procedures as close fit, MIT bulb-form [ 5 ], Frank-method. For pure head waves the direction of wave travel  $\mu$  is defined as  $\pi$  radians (180 degrees) and for pure following waves  $\mu = 0$  in radians. It is advised to deviate not more than  $\pi/6$  radians (30 degrees) from these values in the case of an actual calculation.

For the calculation of the heaving and pitching motion the next equations of motion, as presented in [ 1 ], are used :

$$(a + \rho V) \ddot{z} + b \dot{z} + cz - d \ddot{\theta} - e \dot{\theta} - g \theta = F_a \cos(\omega_e t + \epsilon_{F\zeta}) \quad (\text{heave})$$

(1)

$$(A + k_{yy} \rho V) \ddot{\theta} + B \dot{\theta} + C \theta - D \ddot{z} - E \dot{z} - G z = M_a \cos(\omega_e t + \epsilon_{M\zeta}) \quad (\text{pitch})$$

with the hydrodynamic coefficients

$a, b, c, d, e, g, A, B, C, D, E, G$  also according to [ 1 ]

$F_a$  = wave force amplitude with phase angle  $\epsilon_{F\zeta}$

$M_a$  = wave moment amplitude with phase angle  $\epsilon_{M\zeta}$

$k_{yy}$  = longitudinal radius of inertia of the model/ship

$V$  = volume of displacement

$\rho$  = density of water.

In the program it is assumed that the wave amplitude  $\zeta_a = 1$  for regular waves. The circular wave frequencies  $\omega_a$  are derived from the introduced frequencies of encounter  $\omega_e$  as denoted in 2.3.2.

After calculation of the sectional added mass  $m'$  and the damping  $H'$  the following parameters are determined for each speed  $v$ , for each frequency of encounter  $\omega_e$  and for each direction of wave travel  $\mu$  :

a. the hydrodynamic coefficients of the motion equations :

$a, b, c, d, e, g, A, B, C, D, E,$  and  $G$  [ 1 ]

b. the wave forces  $F_a$  and wave moments  $M_a$  with respectively the phase angles  $\epsilon_{F\zeta}$  and  $\epsilon_{M\zeta}$

The dimensionless wave forces and moments are reflected as :

$$F_a / \zeta g A_w \zeta_a \quad \text{and} \quad M_a / \zeta g I_1 k \zeta_a \quad [ 1 ]$$

in which  $A_w$  = area of waterplane

$g$  = acceleration of gravity

$k = 2\pi / \lambda = \omega^2 / g$  = wave number

$\lambda$  = wave length

$\omega$  = circular wave frequency

$I_1$  = longitudinal moment of inertia of waterplane.

- c. the vertical motions, heaving and pitching  $z_a$  and  $\theta_a$  with respectively the phase angles  $\epsilon_{z\zeta}$  and  $\epsilon_{\theta\zeta}$  [1].

The dimensionless transfer functions are reflected as :

$$z_a/\zeta_a \quad \text{and} \quad \theta_a/k\zeta_a$$

- d. the relative motions of locations  $x$  with respect to the water surface  $s_a(x)$  with phase angle  $\epsilon_{s\zeta}$ .

The dimensionless transfer functions are reflected as :

$$s_a(x)/\zeta_a$$

- e. the vertical accelerations of section 0,2,4,...J:

$v_{aj} \cdot \omega_e^2$  with phase angle  $\epsilon_{v\zeta}$  in which  $v_{aj}$  = amplitude of the vertical ship motion with phase angle  $\epsilon_{v\zeta}$ .

The dimensionless transfer functions are reflected as :

$$v_{aj}/\zeta_a$$

- f. The mean added resistance in waves  $R_{AW}$  [3].

The dimensionless transfer functions are reflected as :

$$R_{AW}/\rho g \zeta_w^2 (B^2/L)$$

in which  $\zeta_w = 2\zeta_a$

L = ship/model length

B = breadth of the midship section at the waterline.

- g. if the weights have been introduced (see 3.3.3) the wave shearing forces  $Q_a$  and the wave bending moments  $M_{ba}$  with respectively the phase angles  $\epsilon_{Q\zeta}$  and  $\epsilon_{M_{ba}\zeta}$  [1].

The dimensionless transferfunctions are reflected as :

$$Q_a/\rho g L B \zeta_a \quad \text{and} \quad M_{ba}/\rho g L^2 B \zeta_a$$

### 2.3. Irregular waves

If the transfer-functions are known, it is possible to calculate the behaviour of a ship or model in a wave spectrum.

For an arbitrary direction of wave travel uni-directional wave spectra will be considered. The wave spectra may be introduced in two ways viz. as:

1. standard wave spectra computed in the program
2. measured wave spectra which have to be introduced.

In the first case has been made use of the general notation for a standard spectrum with the next parameters :

the significant wave height  $\bar{H}_{1/3}$  and the average wave period  $\bar{T}$ .

This general formula for a standard spectrum reads as follows :

$$S_{\zeta}(\omega) = \frac{A}{\omega^r} \exp\left(-\frac{B}{\omega^s}\right) \quad (2)$$

$$\text{in which } A = \frac{C_1 (\bar{H}_{1/3})^h}{\bar{T}^a} \quad (3)$$

$$\text{and } B = \frac{C_2}{\bar{T}^b} \quad (4)$$

$C_1$ ,  $h$ ,  $a$ ,  $C_2$  and  $b$  are coefficients which are to be introduced.

Among others it is possible to choose the following well known spectra :

spectrum	A	r	s	$C_1$	h	a	$C_2$	b	
Pierson Moskowitz (ISSC'64)	$\frac{173\bar{H}_{1/3}^2}{\bar{T}^4}$	$\frac{691}{\bar{T}^4}$	5	4	173	2	4	69.1	4
Neumann	$\frac{3823\bar{H}_{1/3}^2}{\bar{T}^5}$	$\frac{69.8}{\bar{T}^2}$	6	2	3823	2	5	69.8	2

The wave frequencies  $\omega_m$  for which the transferfunctions have been calculated will be recalculated into frequencies for the ship (full scale) with the next relation

$$\omega_s = \omega_m / \sqrt{\alpha} \quad (5)$$

The spectra according to (2) will be computed now on the basis of these full scale wave frequencies  $\omega_s$ .

Afterwards the full scale spectra will be transformed to modelscale  $\alpha$  with the relation :

$$S_{\zeta}(\omega_m) = S_{\zeta}(\omega_s) \left(\frac{1}{\alpha}\right)^{2\frac{1}{2}} \quad (6)$$

The general spectrum data will be determined now for the case of zero ship speed (see 2.3.1)

In the second case, either spectra measured on sea or in a towing tank may be introduced, however only on full scale. So, spectra measured in towing tanks for ship models first have to be transformed into full scale spectra with (5) and the inversion of (6) :

$$S_{\zeta}(\omega_s) = S_{\zeta}(\omega_m) \alpha^{2\frac{1}{2}} \quad (7)$$

After introduction into the program these spectra will be recalculated in the program from full scale to modelscale  $\alpha$  with the inversion of (5) and with (6). Afterwards the measured spectra will be interpolated on the basis of the wave frequencies  $\omega_m$  for which the transferfunctions have been calculated.

The transformation for speed of each standard or measured wave spectrum will be calculated as shown below in 2.3.2.

### 2.3.1. General spectrum data

The area's and moments of all spectra are calculated by means of the trapezium rule.

For each wave spectrum the next parameters are determined :

- a. the variance or zero<sup>th</sup> moment of the wave spectrum :

$$m_{0\zeta} = \int_0^{\infty} S_{\zeta}(\omega) d\omega \quad (8)$$

- b. the significant wave amplitude or the average 1/3 highest value of the wave amplitudes :

$$\bar{\zeta}_{a1/3} = 2\sqrt{m_{0\zeta}} \quad (9)$$

- c. the average 1/10 highest value of the wave amplitudes :

$$\bar{\zeta}_{a1/10} = 2.55\sqrt{m_{0\zeta}} \quad (10)$$

- d. the broadness factor of the wave spectrum

$$E = \sqrt{\frac{m_{0\zeta}^m m_{4\zeta} - m_{2\zeta}^2}{m_{0\zeta}^m m_{4\zeta}}} \quad (11)$$

in which :

the second moment of the spectrum

$$m_{2\zeta} = \int_0^{\infty} \omega^2 S_{\zeta}(\omega) d\omega \quad (12)$$

and the fourth moment of the spectrum

$$m_{4\zeta} = \int_0^{\infty} \omega^4 S_{\zeta}(\omega) d\omega \quad (13)$$

- e. the average number of zero crossings of the wave per time unit :

$$N_0 = \frac{1}{2\pi} \sqrt{\frac{m_{2\zeta}}{m_{0\zeta}}} \quad (14)$$

- f. the average wave period

$$\bar{T} = 2\pi \sqrt{\frac{m_{0\zeta}}{m_{2\zeta}}} \quad (15)$$



g. the average number of wave crests and- troughs :

$$N_1 = \frac{1}{2\pi} \sqrt{\frac{m_4 \zeta}{m_2 \zeta}} \quad (16)$$

h. the ratio :

$$\frac{N_0}{N_1} = \sqrt{1-\epsilon^2} \quad (17)$$

### 2.3.2. Transformation of the spectra for speed and direction of wave travel

For each direction of wave travel  $\mu$  and for each speed and each measured or standard wave spectrum will be calculated either :

a. the transformation of the spectrum for head waves with the relation

$$S_{\zeta}(\omega_{em}) = \frac{S_{\zeta}(\omega_m)}{\sqrt{1-4v\cos\mu\omega_{em}/g}} \quad (18)$$

in which the frequency of encounter

$$\omega_{em} = \omega_m - v\cos\mu \frac{\omega_m^2}{g} \quad (19)$$

and  $v$  = model/ship speed

$\omega_m$  = wave circular frequency

$g$  = acceleration due to gravity

$\mu$  = direction of wave travel.

From (19) follows :

$$\omega_m = g / (2v\cos\mu) (1 - \sqrt{1 - 4v\cos\mu\omega_{em}/g}) \quad (20)$$

With (20) and the energy relation :

$$S_{\zeta}(\omega_{em})d\omega_{em} = S_{\zeta}(\omega_m)d\omega_m \quad (21)$$

it is possible to derive (18).

For head waves :

$$(\pi + \frac{\pi}{6} \text{ rad}) < \mu \text{ (rad)} < (\pi - \frac{\pi}{6} \text{ rad}) \quad (22)$$

The frequencies of encounter  $\omega_{em}$  should be chosen in accordance with the input advice in 3.3.2.

or :

b. the transformation of the spectrum for following waves

For this case two situations should be distinguished in relation to the ratio of the ship speed corrected for the direction of wave travel,  $v \cos \mu$ , and the wave celerity  $c$  :

b1. If the waves are overtaking the ship, so if  $c > v \cos \mu$  then  $\omega_{em}$  is determined in the same way as for head waves with (19). The wave frequency  $\omega_m$  is determined from  $\omega_{em}$  in two ways :

b1.1. if  $c > 2v \cos \mu$  then with relation (20) and afterwards the spectrum should be transformed with (18)

b1.2. if  $0 < v \cos \mu < c/2$  then  $\omega_m = g / (2v \cos \mu) (1 + \sqrt{1 - 4v \cos \mu \omega_{em} / g})$  (23)

and afterwards the spectrum should be transformed with

$$S_{\zeta}(\omega_{em}) = \frac{-S_{\zeta}(\omega_m)}{\sqrt{1 - 4v \cos \mu \omega_{em} / g}} \quad (24)$$

in the same way as for head waves (21).

The waves are overtaking the ship, so  $c > v \cos \mu$ , in the case of zero or very small speed [6].

b2. if the ship is overtaking the waves, so if  $v \cos \mu > c$  then

$$\omega_{em} = v \cos \mu \omega_m^2 / g - \omega \quad (25)$$

The frequencies of encounter  $\omega_{em}$  may be considered to be negative with respect to the preceding cases [6].

From (25) follows the wave frequency

$$\omega_m = g / (2v \cos \mu) (1 + \sqrt{1 + 4v \cos \mu \omega_{em} / g}) \quad (26)$$

The spectrum should be transformed with

$$S_{\zeta}(\omega_{em}) = \frac{S_{\zeta}(\omega_m)}{\sqrt{1 + 4v \cos \mu \omega_{em} / g}} \quad (27)$$

in the same way as for head waves (21).

It is possible to choose only the area  $c > v \cos \mu$  with a boolean for a ship with normal speed in following seas. It should be remarked, that in such a case only a part of the wave spectrum is considered.

The right choice of the frequencies of encounter is important, but also difficult for the case of a ship on normal speed in following waves. The preliminary advice is to avoid the point for which  $c = v \cos \mu$  up to a degree as reflected in the input advice 3.3.2.

In general for following waves holds :

$$((2\pi) - \frac{\pi}{6} \text{ rad}) < \mu (\text{rad}) < ((2\pi) + \frac{\pi}{6} \text{ rad}) \quad (28)$$

### 2.3.3. Determination of the response spectra

For each direction of wave travel  $\mu$  and for each modelspeed and each measured or standard wave spectrum is successively determined :

#### a. the heave spectrum

$$S_z(\omega_{em}) = |H_{z\zeta}(\omega_e)|^2 S_\zeta(\omega_{em}) \quad (29)$$

in which the dimensionless transfer-function :

$$|H_{z\zeta}(\omega_e)| = z_a / \zeta_a(\omega_e) \quad (30)$$

The variance  $m_{oz}$ ,  $\bar{z}_{a/3}$  and  $\bar{z}_{1/10}$  are reflected.

#### b. the pitch spectrum

$$S_\theta(\omega_{em}) = |H_{\theta\zeta}(\omega_e)|^2 S_\zeta(\omega_{em}) \frac{\omega_m^4}{g^2} \quad (31)$$

in which the dimensionless transfer-function :

$$|H_{\theta\zeta}(\omega_e)| = \theta_a / (k\zeta_a(\omega_e)) \quad (32)$$

and  $k = 2\pi/\lambda = \omega_m^2/g = \text{wavenumber}$ .

The variance  $m_{o\theta}$ ,  $\bar{\theta}_{a/3}$  and  $\bar{\theta}_{1/10}$  are reflected.

#### c. the spectrum of the vertical accelerations for the sections $j=0,2,4,\dots,J$ :

$$S_{A_j}(\omega_{em}) = |H_{v_j\zeta}(\omega_e)|^2 S_\zeta(\omega_{em}) \omega_{em}^2 \quad (33)$$

in which the transfer-function :

$$|H_{v_j \zeta}(\omega_e)| = v_{a_j} / \zeta_a \quad (34)$$

while  $v_{a_j}$  = the amplitude of the vertical ship motion at section j.  
The significant value of the vertical accelerations is given as :

$$\bar{A}_{a_j 1/3} = 2\sqrt{m_{oA_{a_j}}} \quad (35)$$

with the zero<sup>th</sup> moment or variance of the vertical acceleration spectrum

$$m_{oA_{a_j}} = \int_0^{\infty} S_{A_j}(\omega_{em}) d\omega_{em} \quad (36)$$

d. the added resistance spectrum

$$S_{R_{AW}}(\omega_{em}) = |H_{R_{AW} \zeta}(\omega_{em})|^2 S_{\zeta}(\omega_{em}) \quad (37)$$

in which the transfer-function :

$$|H_{R_{AW} \zeta}(\omega_{em})| = R_{AW} / \zeta_a^2(\omega_{em}) \quad (38)$$

The average resistance increase in a wave spectrum is calculated with :

$$\bar{R}_{AW} = 2 \int_0^{\infty} S_{R_{AW}}(\omega_{em}) d(\omega_{em}) \quad (39)$$

and the increased power :

$$\bar{P}_{AW} = \frac{\bar{R}_{AW} x v}{75} \text{ (EHP)} \quad (40)$$

e. the spectrum of the relative motion for location (x) :

$$S_{s(x)}(\omega_{em}) = |H_{s(x) \zeta}(\omega_{em})|^2 S_{\zeta}(\omega_{em}) \quad (41)$$

with the transfer-function :

$$|H_{s(x) \zeta}(\omega_{em})| = s_a(x) / \zeta_a \quad (42)$$

while  $s_a(x)$  = amplitude of the relative motion for (x).

With the zero<sup>th</sup> moment of this spectrum :

$$m_{os}(x) = \int_0^{\infty} S_s(x)(\omega_{em}) d\omega_{em} \quad (43)$$

will be calculated the probability, that a certain value  $f(x)$  for this location  $(x)$  will be exceeded viz:

$$P[s_a(x) \geq f(x)] = \exp[-f^2(x)/2m_{os}(x)] \quad (44)$$

The number of occurrences per hour is found with :

$$N_{s(x)} = \frac{1}{2\pi} P[s_a(x) \geq f(x)] \sqrt{\frac{m_{2s(x)}}{m_{os(x)}}} \times 3600 \quad (45)$$

in which  $m_{2s(x)}$  = the second moment of the relative motion spectrum (this moment is equal to the zero<sup>th</sup> moment of the relative velocity spectrum).

f. The spectrum of the relative motion at location  $d$  for which slamming and shipping will be calculated.

For shipping the spectrum will be :

$$S_{s'_d}(\omega_{em}) = |H_{s'_d \zeta}(\omega_e)|^2 S_{\zeta}(\omega_{em}) \quad (46)$$

with the transfer-function :

$$|H_{s'_d \zeta}(\omega_e)| = s'_{da} / \zeta_a \quad (47)$$

while  $s'_{da}$  for shipping is supposed to be the amplitude of the relative motion  $s_{da}$  amplified by a dynamic influence according to Tasaki [8] :

$$s'_{da} = s_{da} \{1 + 1/3(CB - 0.45)\omega_{em} \sqrt{L/g}\} \quad (48)$$

CB = blockcoefficient

With the zero<sup>th</sup> moment of this spectrum :

$$m_{os'_d} = \int_0^{\infty} S_{s'_d}(\omega_{em}) d\omega_{em} \quad (49)$$

the probability P will be calculated that the freeboard f, decreased by the bow wave to the effective free board  $f_e$ , will be exceeded and shipping occurs :

$$P [s'_{da} \geq f_e] = \exp \left[ -\frac{f_e^2}{2m_{os'_d}} \right] \quad (50)$$

in which

$$f_e = f - \frac{3}{4} \frac{BL}{L_e} \quad (51)$$

where  $L_e$  = the entrance length of the load waterline.

The number of occurrences of shipping or deck wetness per hour is found with

$$N_{s'_d} = \frac{1}{2\pi} P [s'_{da} \geq f_e] \sqrt{\frac{m_{2s'_d}}{m_{os'_d}}} \times 3600 \quad (52)$$

in which  $m_{2s'_d}$  = the second moment of the relative motion spectrum of location d. See also [9].

For slamming the spectrum will be :

$$S_{s'_d}(\omega_{em}) = |H_{s'_d \zeta}(\omega_e)|^2 S_{\zeta}(\omega_{em}) \quad (53)$$

with the dimensionless transfer-function :

$$|H_{s'_d \zeta}(\omega_e)| = s_{da} / \zeta_a \quad (54)$$

According to Ochi [7] slamming occurs if there is emergence of the bow from the water and if the relative velocity exceeds a threshold value

$$\dot{s}_H = 0.093 \sqrt{gL} \quad (55)$$

The formula for the probability of slamming at location d with draught T is given by :

$$P[\text{slamming}] = \exp \left[ -\frac{T^2}{2m_{os'_d}} + \frac{\dot{s}_H^2}{2m_{2s'_d}} \right] \quad (56)$$

As previously the number of occurrences per hour for slamming can be found with :

$$N_{sl.d} = \frac{1}{2\pi} P[\text{slamming}] \sqrt{\frac{m_{2s'_d}}{m_{os'_d}}} \times 3600 \quad (57)$$

If the weight distribution is known and the weights have been introduced according to 3.3.3. :

g. the spectrum of the wave shearing forces for the sections  $j=0,2,4,\dots,J-2$ :

$$S_{Q_j}(\omega_{em}) = |H_{Q_j}(\omega_e)|^2 S_{\zeta}(\omega_{em}) \{\rho g L B\}^2 \quad (58)$$

with the dimensionless transfer-function :

$$|H_{Q_j}(\omega_e)| = Q_{aj} / \rho g L B \zeta_a \quad (59)$$

while  $Q_{aj}$  = the amplitude of the wave shearing force for section  $j$ .  
 $\bar{Q}_{a1/3}$  and  $\bar{Q}_{a1/10}$  are reflected in the output for the sections  $j$ .

h. the spectrum of the wave bending moments for the sections  $j=0,2,4,\dots,J-2$ .

$$S_{M_{bj}}(\omega_{em}) = |H_{M_{bj}}(\omega_e)|^2 S_{\zeta}(\omega_{em}) \{\rho g L^2 B\}^2 \quad (60)$$

with the dimensionless transfer-function

$$|H_{M_{bj}}(\omega_e)| = M_{ba_j} / \rho g L^2 B \zeta_a \quad (61)$$

while  $M_{ba_j}$  = the amplitude of the wave bending moment for section  $j$ .

$\bar{M}_{ba1/3}$  and  $\bar{M}_{ba1/10}$  are reflected in the output for the sections  $j$ .

## 2.4. References

1. Gerritsma, J., Beukelman, W.,  
Analysis of the modified strip theory for the calculation of ship motions and wave bending moments.  
Netherlands Ship Research Centre, TNO, Report no. 96S, June 1967.
2. Gerritsma, J.,  
Behaviour of a ship in a seaway.  
Netherlands Ship Research Centre, TNO, Report no. 84S, May 1966.
3. Gerritsma, J., Beukelman, W.,  
Analysis of the resistance increase in waves of a fast cargo ship.  
Netherlands Ship Research Centre, TNO, Report no. 169S, April 1972.
4. Jong, B. de ,  
Computation of the hydrodynamic coefficients of oscillating cylinders.  
Report no. 174A, Shipbuilding Laboratory of the University of Technology, November 1969.
5. Loukakis, Theodore A.,  
Computer aided prediction of seakeeping performance in ship design,  
Massachusetts Institute of Technology (MIT), Report no. 70-3 August 1970.
6. St. Denis, M., Pierson, W.J.,  
On the motions of ships in confused seas  
SNAME, November 1953.
7. Ochi, M.K.,  
Prediction of occurrence and severity of ship slamming at sea,  
5th Symposium on Naval Hydrodynamics, Bergen, Norway, 1964.
8. Tasaki, R.,  
On shipping water,  
Monthly Report of Transportation Technical Research Institute,  
Vol. 11, No. 8, August 1961, Japan.
9. Tasai, F.,  
On the deck wetness and slamming of full ships forms,  
12th ITTC, p. 792, September 1969.



### 3. Operation

#### 3.1. General

The program operates in the technical units system (e.g. kg, m, sec). The reflection of the output has been suited for the units ton (1000kg), m, sec. Therefore it is recommended to use these units. The numbers may be introduced separated by a comma or by two or more blank places. At the end of the program calculations the used input data are shown in the same sequence as these data have been introduced. See 3.4. and 4. It is possible to run the program for several ships in one time. The necessary data sets can be introduced immediately after each other.

### 3.2. Description of the input data

The units to be used should be in accordance with the advice in 3.1. :  
ton (1000kg), m, sec. and radians.

The numbers for the input of each ship should be introduced in a sequence  
as follows in the next table :

Symbol		Description and remark
Mathematical notation	Program symbols	
I	II	i=0,1,2.....I; Number of positions of the section contour for which the potentials should be calculated. For normal ships I=4. For high frequencies I should increase up to 18.
J	JJ	j=0,1,2,....J; j=section index. Number of sections J should be even. j=0 for the sternmost section. Sections should be at equal distance. For normal ships J=20 See 3.3.1.
M	MM	m=1,2,3.....M; m=multipole index. Number of positions for which the multipole-potentials should be calculated. For normal ships M=3. For high frequencies M should increase up to 17. M=I-1,2.....
Q	QQ	Number of frequencies of encounter See 3.3.2.
	NV	Number of model/ship speeds.
	L	Length of model/ship, mostly $L_{pp}$ . In every case L should be equal to the distance between the section j=0 and the section j=J. See 2. and 3.3.1.
$\rho$	RHO	Density of water in accessory dimensions
g	G	Acceleration of gravity
	CA	Ratio of displacement of ship including and excluding appendices
	AHO	Number of directions of wave travel
	MP	Number of points along the half section contour for which the half widths have to be introduced. MP=7,10,13,.... See 3.3.1.

Symbol		Description and remark
Mathematical notation	Program symbols	
	NS	Number of locations for which the relative motion with respect to the water surface has to be calculated.
	BOOL	'TRUE' : For calculation of shearing forces and bending moments 'FALSE' : No calculation of shearing forces and bending moments is required.
	VGRC	'TRUE' : If only following waves are considered with celerity $c < v \cdot \cos \mu$ 'FALSE' : If all waves has to be taken into account and for head waves. See 3.3.2. (d).
y	B(0:JJ, 1:MP)	Half widths of the section, starting from underneath. B(0,1), B(0,2).....B(0,MP), B(1,1), B(1,2).....B(1,MP), B(JJ,1),B(JJ,2).....B(JJ,MP), $B_{j,MP} \neq 0$ , so e.g. $B_{j,MP} = 10^{-10}$ For bulbous sections : $B_{j,MP} > 0.01 B_{JJ/2,MP}$ See 3.3.1.
$T_j$	D(0:JJ)	Draught of each section
v	VV(1:NV)	Model/ship speeds in accessory dimensions
$\omega_e$	SIGMAQ(1:QQ)	Frequencies of encounter. See 3.3.2. The values should increase from 1 to QQ for head waves
	L(1:NS)	Length ordinates of locations relative to midship section for which the relative motions with respect to the water surface has to be calculated. Forwards of midship section $j = JJ/2 = +$ For location L(NS)=at FPP shipping and slamming will be calculated, $L(NS) = L/2$
w	IF BOOL='TRUE' W(0:JJ)	Weights of the ship from bow to section j, starting from section $j=0$ with $w_0$ =displacement of ship. See 3.3.3.
	IF BOOL='FALSE' FACT	Ratio of longitudinal radius of inertia and length L.
$\mu$	MUR(1:AHO)	Directions of wave travel in radians. For head waves : $\pi + \frac{\pi}{6} < \mu < \pi - \frac{\pi}{6}$ For following waves : $(2\pi) - \frac{\pi}{6} < \mu < (2\pi) + \frac{\pi}{6}$ .

Mathematical notation	Symbol	Program symbol	Description and remark
		BF	Number of standard or measured wave spectra
		GM	Number of frequencies of the measured spectra else an arbitrary number
		PIERSON	'TRUE' : Standard wave spectra are desired 'FALSE' : Measured wave spectra will be introduced
$\alpha$		ALF	Modelscale. For a ship ALF=1
CB		DELTAZ	Blockcoefficient
		FP	0.333 } Coefficients for shipping formula's 0.45 } See (48) and (52) of 2.3.3. (f) 0.75 }
		FD	
		FC	
$\dot{s}_H$		CP	0.093 Dimensionless threshold velocity for slamming. See(55) of 2.3.3. (f)
$L_e$		LE	Entrance length of the load waterline
T		DP	Draught at the location L(NS)= at FPP = at section JJ for which slamming will be calculated
f(x)		F(1:NS)	Positive distances (free board, etc) from the load waterline, for which will be calculated the chance of exceeding by the relative motion; the last distance F(NS)= at FPP= at section JJ is used for the calculation of shipping and slamming

1/3  
 F  
 C<sub>1</sub>  
 C<sub>2</sub>  
 h  
 a  
 o  
 r  
 s

```

IF PIERSON='TRUE'
  HS(1:BF)      Significant wave height of the spectra
  PM(1:BF)     Average wave period of the spectra
  CF1 }
  CF2 }         Coefficients for the calculation of the
  AH  }         standard wave spectra
  AT  }         See 2.3.
  BT  }         AH, AT, BT, RT and ST have to be integer
  RT  }
  ST  }

```

```

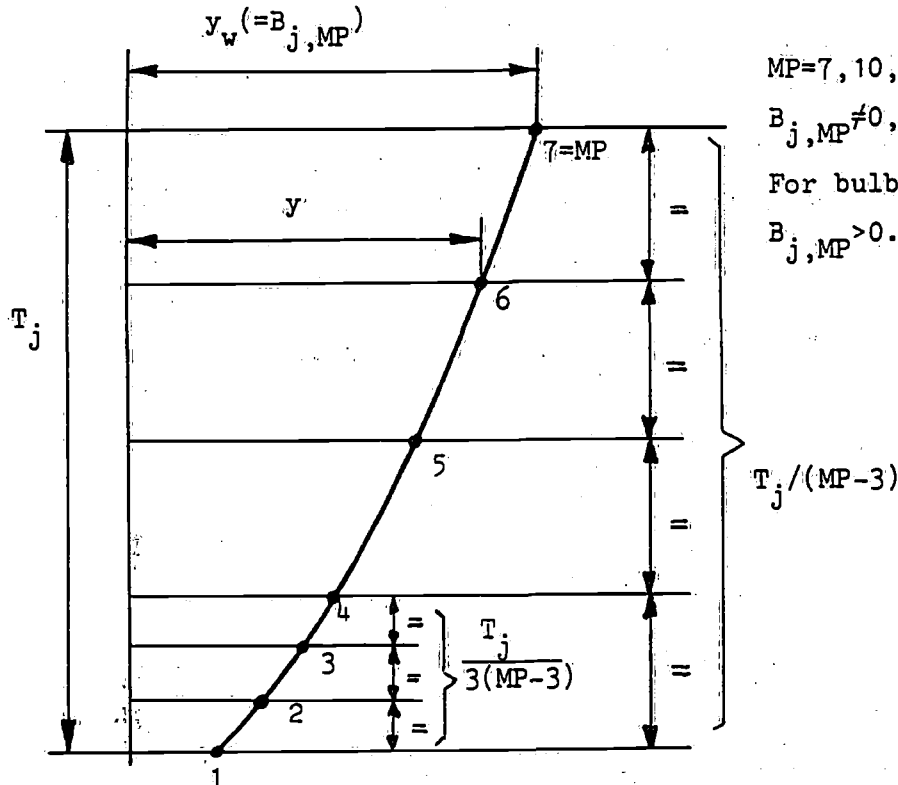
IF PIERSON='FALSE'
  GMOM(1:BF,1:GM) Circular wave frequencies of the measured
                  wave spectra
                  GMOM(1,1),GMOM(1,2).....GMOM(1,GM)
                  GMOM(2,1),GMOM(2,2).....GMOM(2,GM)
                  GMOM(BF,1),GMOM(BF,2)...GMOM(BF,GM)
  GMSP(1:BF,1:GM) Spectral values of wave amplitude for the
                  measured spectra
                  Introduction analog to GMOM(1:BF,1:GM)

```

### 3.3. Additional input advice

#### 3.3.1. Section input

For the calculation of the sectional area's etc. has been made use of Simpson's second rule. The sections have to be introduced in a way as showed in the figure with a finer subdivision for the underpart.



MP=7, 10, 13 ..... etc.  
 $B_{j,MP} \neq 0$ , so e.g.  $B_{j,MP} = 10^{-10}$   
 For bulbous sections :  
 $B_{j,MP} > 0.01 B_{JJ/2,MP}$

The sections should be equally spaced, while the midship section JJ/2 is supposed to be at half the ship's length L.

#### 3.3.2. Input of frequencies of encounter

The choice of the frequencies of encounter, which has to be introduced is very important. It is essential to obtain a wave spectrum, which delivers the same significant wave height and average wave period as has been introduced, except for the case that only following waves are taken into account, which are overtaken by the ship ( $c < v \cos \mu$ ).

For this reason the following procedure is recommended :

- a. Determine the average of the considered model/ship speeds : v

b. For head waves the circular wave frequencies  $\omega = \sqrt{kg}$  should be calculated in the same sequence (from long to short waves) for at least the next 20 wave length ratio's :

$\lambda/L = 100, 8, 4, 2.5, 2, 1.8, 1.6, 1.5, 1.4, 1.3, 1.2,$

$1.1, 1.0, 0.9, 0.8, 0.7, 0.6, 0.5, 0.4, 0.2;$

with  $k=2\pi/\lambda$  .  $\lambda$ =wave length,  $g$ = acceleration of gravity.

Afterwards the frequencies of encounter have to be computed in the same

sequence (increasing value for  $\omega_e$ ) with  $\omega_e = \omega - kv \cos \mu$  (62)

in which  $\mu$  = direction of wave travel.

c. for following waves with a wave celerity  $c > v \cos \mu$

(e.g. for small ship speeds or  $v=0$ ) the circular wave frequency  $\omega$  may be determined for the same range of wave length ratio's as has been advised for head waves (b). To check the relation between  $c$  and  $v \cos \mu$  it is remembered that  $c = \omega/k$ . The frequency of encounter may also be computed with :

$$\omega_e = \omega - k v \cos \mu$$

while

$$(2\pi) - \frac{\pi}{6} < \mu < (2\pi) + \frac{\pi}{6} \quad (\text{radians})$$

For numerical reasons take care, that  $c > 1.1 v \cos \mu$

d. for following waves with a wave celerity  $c < v \cos \mu$

the situation is quite different.

For a ship on normal speed it is preliminary advised to take into account only that part of the wave spectrum for which  $c < .95 v \cos \mu$  .

The circular wave frequency  $\omega = \sqrt{kg}$  should be calculated for the next small wave length ratio's in view of the power increase only :

$\lambda/L = 0.30, 0.28, 0.26, 0.25, 0.24, 0.23, 0.22, 0.21, 0.20$

$0.19, 0.18, 0.17, 0.16, 0.15, 0.14, 0.13, 0.12, 0.11, 0.10,$

$0.09;$

The frequency of encounter may be computed with :

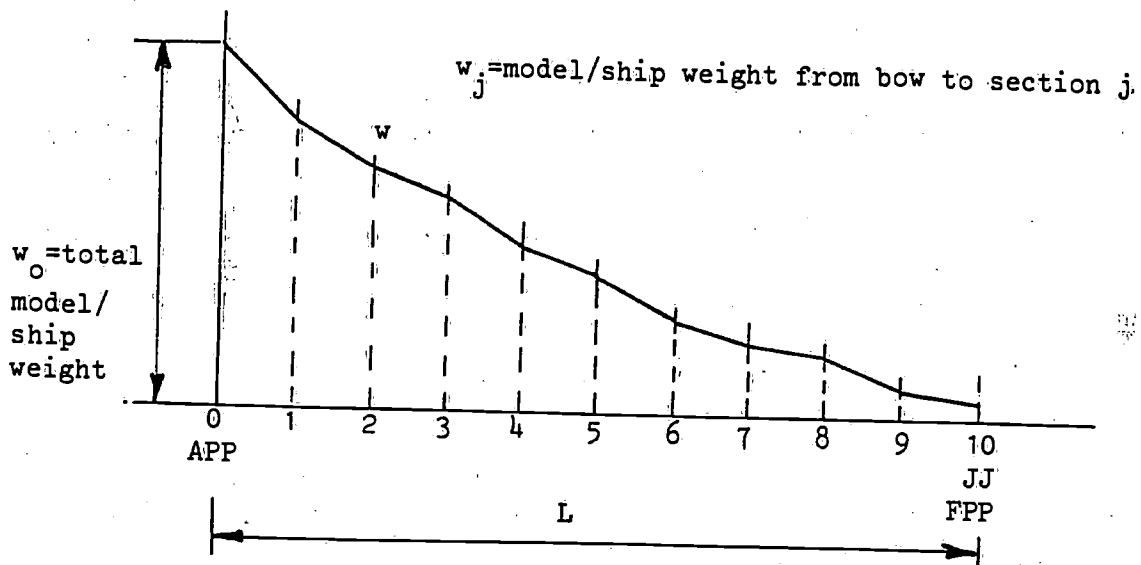
$$\omega_e = kv \cos \mu - \omega \quad (63)$$

with  $(2\pi) - \frac{\pi}{6} < \mu < (2\pi) + \frac{\pi}{6}$

Remark : For following waves with a wave celerity  $c > v \cos \mu$  (case c) the frequencies of encounter, derived from a range of waves with decreasing lengths, are not always increasing. These frequencies are for this case (c) increasing up to a value for  $\omega_e = g / (v \cos \mu)$  ( $v \cos \mu = \frac{1}{2}c$ ) and afterwards decreasing to  $\omega_e = 0$  ( $v \cos \mu = c$ ), after which the area is reached for which  $c < v \cos \mu$  (case d). Now the frequencies of encounter are again increasing with decreasing wave lengths.

### 3.3.3. Introduction of the weights

To obtain the shearing forces and bending moments it is necessary to know the weight distribution of the model or ship. The integration of the weight distribution and so the model/ship weight from the most forward point of the bow to the sections  $j$  has to be used as an input, as shown in the figure below.



To avoid wrong values for the shearing forces and bending moments, it is very important to take care that the total ship weight ( $=w_o$ ) is equal to the weight of the ship's displacement (DDPL), while the ship's centre of gravity (LCG) should be in equal position in length as the centre of buoyancy (LCB). DDPL and LCB are calculated in the program, but they have to be known in advance for adjustment of the  $w$ -curve. Therefore it is recommended to make use of the program to determine these values. A calculation time of  $\pm 1$  min. is sufficient to obtain DDPL and LCB.

Afterwards it is possible to adjust the w-curve in such a way, that the above mentioned conditions are fulfilled. For this adjustment of the weight curve w the following procedure may be useful :

The area of the weight curve w affords the total weight moment  $M_w$  with respect to section  $j=0$  (APP).

The ship's centre of gravity in length (LCG) with respect to the midship section  $JJ/2$  :

$$LCG = M_w / w_0 - L/2 \quad (64)$$

The mass moment of inertia with respect to the ship's centre of gravity can be determined in advance and is also calculated in the program with :

$$I = k_{yy}^2 \rho \nabla = 2 \int_{APP}^{FPP} w_j x_b dx_b - w_0 x_{LCG}^2 \quad (65)$$

### 3.4. Description of the output

As denoted in 3.1. the reflection of the output is according to the units ton (1000kg), m, sec.

If a number is too large to be reflected with the accessory format, first the decimal point is shifted afterwards. If this is not sufficient so many digits are omitted, that the number denoted with a \* fits in the field.

The output, shown in 4 where an example is given, may be divided into the next four parts :

#### 1. the first part (one time) with :

- the frequencies of encounter  $\omega_e$
- the ship speed v
- the sectional area  $2x_{Aj}$
- the displacement of ship or model  $\rho g \nabla$
- the centre of buoyancy in length with respect to the midship section (LCB)
- if the weights have been introduced (BOOL='TRUE'): the shearing forces and bending moments in still water for the sections  $j=0, 2, 4, \dots, J-2$
- resp.  $j, Q_s, M_{bs}$ .



2. the second part (QQ times), see 2.2., with :

a. per frequency of encounter  $\omega_e$ : the sectional damping and added mass  
resp.  $j, N', m''$

The section number is marked with a #, if the  
adaptive "Lewis-form" transformation has been applied for this  
section. See 2.2.

b. per direction of wave travel  $\mu$   
per frequency of encounter  $\omega_e$   
per model/ship speed  $v$  ( $F_n$  = number of Froude) :

the wave coefficients

wave frequency  $\omega$

wave number  $k$

wave length  $\lambda$

wave length ratio  $\lambda/L$

apparent wave length  $\lambda/|\cos\mu|$

$\text{SQRT } L/\lambda = \sqrt{L/\lambda}$

the hydrodynamic coefficients for heave and pitch

added mass  $a$ , ship mass  $\rho V$ , total mass  $a + \rho V$

$b, c, d, e, g,$

added mass moment of inertia  $A,$

mass moment of inertia of ship  $k_{yy}^2 \rho V$

total mass moment of inertia  $A + k_{yy}^2 \rho V$

$B, C, D, E, G$

the wave forces and- moments

amplitude  $F_a$ , phase (in degrees)  $\epsilon_{F\zeta}$ , coefficient  $F_a / \rho g A x_a^2$

amplitude  $M_a$ , phase (in degrees)  $\epsilon_{M\zeta}$ , coefficient  $M_a / \rho g I_1 k_a^2$

the vertical motions

heave amplitude  $z_a = z_a / \zeta_a$ , phase (in degrees)  $\epsilon_{z\zeta}$

pitch amplitude theta  $\theta_a$ , phase (in degrees)  $\epsilon_{\theta\zeta}$ , theta /

wave slope  $\theta_a / k_a \zeta_a$

the relative motions for location x

length  $x$ , amplitude  $s_a(x) = s_a(x) / \zeta_a$ , phase (in degrees)  $\epsilon_{s\zeta}$

the vertical accelerations

section number  $j$ , amplitude  $v_{aj}$ ,  $\omega_e^2$ , phase (in degrees)  $\epsilon_{v\zeta}$

the added resistance

$R_{AW}$ ,  $R_{AW}$ -non dimensional =  $R_{AW}/\rho g \zeta_w^2 (B^2/L)$

if the weights have been introduced (BOOL='TRUE') :

the wave shearing forces and the wave bending moments

even section number  $j$ , amplitude  $Q_a$ , phase (in degrees)  $\epsilon_{\theta\zeta}$   
amplitude (non dim.)  $Q_a/\rho g L B \zeta_a$   
still water (value)  $Q_s$   
amplitude  $M_{oa}$ , phase (in degrees)  $\epsilon_{M_o\zeta}$   
amplitude (non dim.)  $M_{oa}/\rho g L^2 B \zeta_a$   
still water (value)  $M_{os}$

3. the third part (AHOxNVxBF times) (see 2.3) with :

a. per direction of wave travel  $\mu$

per model/ship speed  $v$

the seaspectrum for zero speed, as introduced for the measured

spectra or calculated for the standard spectra

omega  $\omega_s$ , wave spectrum  $S_\zeta(\omega_s)$

$M_o = m_{o\zeta}$ , ampl.  $1/3 = \bar{\zeta}_{a1/3}$ , ampl.  $1/10 = \bar{\zeta}_{a1/10}$

broadnessfactor (eps) =  $\epsilon$

$N_o = N_o$

$T = \bar{T}$

$N_1 = N_1$

$N_o/N_1 = N_o/N_1$

See 2.3 and 2.3.1.

b. per direction of wave travel  $\mu$

per model/ship speed  $v$  ( $F_n$  = number of Froude)

per spectrum  $S_\zeta(\omega_m)$

the wave spectrum transformed for speed

omega  $\omega_{em}$ , wave spectrum  $S_\zeta(\omega_{em})$

with the general spectrum data as denoted in a.

the heave spectrum  $S_z(\omega_{em})$   
with  $M_0 = m_{0z}$ , ampl.  $1/3 = \bar{z}_{a1/3}$ , ampl.  $1/10 = \bar{z}_{a1/10}$

the pitch spectrum  $S_\theta(\omega_{em})$   
with  $M_0 = m_{0\theta}$ , ampl.  $1/3 = \bar{\theta}_{a1/3}$ , ampl.  $1/10 = \bar{\theta}_{a1/10}$

the added resistance spectrum  $S_{RAW}(\omega_{em})$   
with added resistance =  $\bar{R}_{AW}$   
and power increase  $\bar{P}_{AW}$  in EHP

the probability of exceeding a value  $f(x)$  by the relative motion

for location  $x$

length =  $x$ ,  $F = f(x)$ , probability =  $P[s_a(x) \geq f(x)]$

Number per hour =  $N_s(x)$

the probability of shipping and slamming

for location  $d = at$  FPP = at section JJ.

length =  $x(d)$ ,  $F = f_e$ , probability =  $P[s'_{da} \geq f_e]$

Number per hour =  $N_{sd}$ , shipping

length =  $x(d)$ ,  $F = T$ , probability =  $P[\text{slamming}]$

Number per hour =  $N_{sl.d}$ , slamming

the vertical accelerations

section number  $j$ , ampl.  $1/3 = \bar{A}_{aj1/3}$

if the weights have been introduced (BOOL='TRUE'):

the wave shearing forces and-bending moments

section number  $j$ , ampl.  $1/3 = \bar{Q}_{a1/3}$ , ampl.  $1/10 = \bar{Q}_{a1/10}$

ampl.  $1/3 = \bar{M}_{ba1/3}$ , ampl.  $1/10 = \bar{M}_{ba1/10}$

4. the fourth part (one time) with :

the input data in the same sequence as they have been introduced. See the description of the input data 3.2.

#### 4. Example

An example of the output divided into four parts has been shown on the next pages. See the description in 3.4.

The fourth part is also an example of the input.

With this example it is possible to check the program.

The example has been shown one time for each part.

DAVIDSON A DESTROYER

### OUTPUT FIRST PART (ONE TIME)

LEWIS TRANSFORM

FREQUENCY OF ENCOUNTER :	.081,	.359,	.568,	.787,	.923,	.997,	1.087,	1.140,	1.199,	1.268,	1.346,	1.438,
	1.546,	1.676,	1.837,	2.039,	2.304,	2.666,	3.197,	4.058				

SPEED : 11.945, 18.615

VERTICAL SHIP MOTIONS IN REGULAR WAVES

#### SECTIONAL AREA

SECTION AREA (42) SECTION AREA (M2)

0	4.93		
1	9.43	11	41.28
2	14.28	12	40.20
3	19.40	13	38.56
4	24.23	14	36.08
5	29.24	15	33.37
6	33.20	16	29.64
7	36.93	17	25.59
8	39.21	18	20.68
9	40.82	19	14.21
10	41.73	20	.00

DISPLACEMENT = 3429.071 TON  
 LCB = 2.013 M

WAVE AMPLITUDE ZETA = 1.0 M

#### S T I L L W A T E R

SECTION SHEARING FORCE BENDING MOMENT  
(TON) (M. TON)

0	-13.333	193.088
2	55.756	506.536
4	86.067	1367.681
6	86.001	2392.650
8	70.040	3331.981
10	16.751	3868.082
12	-42.225	3678.198
14	-75.929	2970.482
16	-101.024	1922.129
18	-94.773	734.416

# OUTPUT SECOND PART (QQ TIMES)

FREQUENCY OF ENCOUNTER  $\Omega$ MEGA(E) = 1.087

---

SECTION	DAMPING TONSEC/M2	ADDED MASS TONSEC2/M2
0	2.304	2.306
1	3.695	2.956
2	4.440	3.515
3	4.957	3.951
4	5.143	3.931
5	5.227	3.927
6	5.265	3.947
7	5.139	3.979
8	5.085	4.125
9	4.946	4.188
10	4.840	4.221
11	4.709	4.101
12	4.082	3.669
13	3.167	3.137
14	2.079	2.676
15	1.141	2.586
16*	.193	3.785
17*	.034	2.955
18*	.000	2.323
19*	.025	1.673
20	.000	.000

DIRECTION OF WAVE TRAVEL = 3.142 RAD.

## OUTPUT CONTINUATION OF THE SECOND PART (QQ TIMES)

V = 11.845 M/SEC FN = .350

WAVE FREQUENCY = .621 1/SEC WAVE NUMBER K = .039  
WAVE LENGTH = 159.753 M WAVE LENGTH RATIO = 1.368 APPARENT WAVE LENGTH = 159.7533 SQRT(L/LA) = .85494

### HYDRODYNAMIC COEFFICIENTS :

#### HEAVE

ADDED MASS A = 369.000 TONSEC<sup>2</sup>/M C = 1100.368 TON/M  
SHIP MASS = 351.418 TONSEC<sup>2</sup>/M D = -2642.095 TONSEC<sup>2</sup>  
TOTAL MASS = 740.448 TONSEC<sup>2</sup>/M E = -13446.604 TONSEC  
DAMPING B = 411.140 TONSEC/M G = -16915.054 TON

#### PITCH

ADDED MASS MOMENT OF INERTIA AA = 379158.264 MTONSEC<sup>2</sup> CC = 1026680.513 MTON  
MASS MOMENT OF SHIP = 312642.855 MTONSEC<sup>2</sup> DD = -2642.095 TONSEC<sup>2</sup>  
TOTAL MASS MOMENT = 691801.118 MTONSEC<sup>2</sup> EE = -4230.483 TONSEC  
DAMPING BB = 439169.326 MTONSEC GG = -12045.105 TON

### AMPLITUDE PHASE (IN DEGR.) COEFFICIENT

WAVE FORCES 470.829 TON -15.127 .428  
WAVE MOMENTS 17897.321 MTON -80.611 .466

### VERTICAL MOTIONS :

HEAVE : ZA = 1.831 M PHASE = -67.975 DEGR.  
PITCH : THETA = 1.387 DEGR. PHASE = 138.353 DEGR. THETA/WAVE SLOPE = .615

### RELATIVE MOTIONS :

LENGTH M	AMPLITUDE M	PHASE DEGR.
-60.340	.363	161.745
44.760	3.773	115.066
56.440	4.115	122.990

# OUTPUT CONTINUATION OF THE SECOND PART (QQ TIMES)

## ACCELERATIONS

SECTION	AMPLITUDE M/SEC <sup>2</sup>	PHASE DEGR.
0	1.032	243.369
2	1.162	259.527
4	1.363	-88.331
6	1.608	-79.573
8	1.881	-73.242
10	2.172	-68.558
12	2.473	-64.996
14	2.782	-62.215
16	3.096	-59.534
18	3.415	-58.185
20	3.734	-56.684

## ADDED RESISTANCE :

RAW = 23.352 TON  
 RAW -NON DIM. = 4.299

## S H A R I N G F O R C E S

SECTION	AMPLITUDE (TON)	PHASE	AMPLITUDE (NON DIM.)	STILL WATER
0	2.665	194.940	.002	-18.353
2	38.500	47.335	.026	55.756
4	79.879	63.628	.054	86.067
6	110.357	77.935	.074	96.001
8	117.522	93.987	.079	70.040
10	89.841	113.562	.060	16.751
12	26.272	165.629	.018	-42.225
14	85.852	-79.915	.058	-75.929
16	166.712	265.258	.112	-101.024
18	129.118	257.080	.087	-94.773

## B E N D I N G M O M E N T S

SECTION	AMPLITUDE (TON)	PHASE	AMPLITUDE (NON DIM.)	STILL WATER
0	358.300	-56.225	.002	193.089
2	380.329	-21.667	.002	506.536
4	854.572	30.730	.005	1367.631
6	1860.029	53.892	.011	2392.650
8	3092.876	67.274	.019	3331.681
10	4166.281	77.252	.024	3860.682
12	4635.538	83.635	.027	3679.199
14	4178.799	83.713	.024	2970.492
16	2676.743	77.918	.015	1922.128
18	863.482	72.805	.005	734.416



DIRECTION OF WAVE TRAVEL = 3.142 RAD.

# OUTPUT THIRD PART (AHO x NV x BF TIMES)

V = 11.845 M/SEC FN = .350

SEASPECTRUM FOR ZEPH SPEED

SPECTRUM : 1

OMEGA 1/SEC	WAVE SPECTRUM M2SEC
.074	.000
.271	.000
.387	.000
.493	.022
.553	.139
.584	.238
.621	.359
.642	.420
.665	.475
.691	.520
.720	.547
.753	.554
.791	.538
.835	.497
.887	.436
.950	.360
1.028	.276
1.128	.193
1.265	.119
1.465	.061

WAVE

MO = .26816 M2  
AMPL 1/3 = 1.0357 M  
AMPL 1/10 = 1.3205 M

BROADNESS FACTOR (EPS) = .446

NO = .144  
T = 6.768 SEC  
N1 = .160  
NO/N1 = .395

DIRECTION OF WAVE TRAVEL = 3.142 RAD.

OUTPUT

CONTINUATION OF THE THIRD PART (AHO x NV x BF TIMES)

V = 11.845 M/SEC FN = .350

SPECTRUM : 1

OMEGA(E)	WAVE SPECTRUM	HEAVE SPECTRUM	PITCH SPECTRUM	ADDED RESIST	SPECTR
.081	.000	.000	.000	.000	
.359	.000	.000	.000	.000	
.568	.000	.000	.000	.000	
.787	.010	.021	.000	.000	.036
.923	.059	.237	.000	.000	.913
.997	.099	.460	.000	.000	2.337
1.087	.144	.508	.000	.000	3.353
1.140	.165	.434	.000	.000	3.293
1.199	.182	.335	.000	.000	2.988
1.268	.195	.232	.000	.000	2.563
1.346	.200	.142	.000	.000	2.109
1.438	.197	.072	.000	.000	1.636
1.546	.185	.028	.000	.000	1.170
1.676	.165	.007	.000	.000	.770
1.837	.139	.001	.000	.000	.510
2.039	.109	.000	.000	.000	.363
2.304	.079	.000	.000	.000	.231
2.666	.052	.000	.000	.000	.120
3.197	.029	.000	.000	.000	.056
4.058	.013	.000	.000	.000	.019

WAVE

MO = .26897 M2  
 AMPL 1/3 = 1.0372 M  
 AMPL 1/10 = 1.3225 M

BROADNESS FACTOR (EPS) = .624

NO = .316  
 T = 3.165 SEC  
 N1 = .405  
 NO/N1 = .781

HEAVE

MO = .18917 M2  
 AMPL 1/3 = .8699 M  
 AMPL 1/10 = 1.1091 M

PITCH

MO = .13976 DEGR.  
 AMPL 1/3 = .7477 DEGR.  
 AMPL 1/10 = .9533 DEGR.

# OUTPUT      CONTINUATION OF THE THIRD PART (AHO x NV x BF TIMES)

## RELATIVE MOTIONS

LENGTH (M)	F	PROBABILITY	NUMBER PER HOUR
-60.340	2.170	.0000	.0
44.760	5.130	.0000	.0
56.440	5.120	.0377	31.4 SHIPPING
56.440	4.260	.0000	.0 SLAMMING

## ACCELERATIONS

SECTION	AMPL 1/3 M/SEC <sup>2</sup>
0	1.740
2	1.537
4	1.540
6	1.451
8	1.376
10	1.327
12	1.325
14	1.403
16	1.509
18	1.628
20	1.750

ADDED RESISTANCE =      4.084 TON  
 POWER INCREASE =      645.011 EHP

SECTION	SHEARING FORCE (TON)		BENDING MOMENT (M.TON)	
	AMPL 1/3	AMPL 1/10	AMPL 1/3	AMPL 1/10
0	1.7502	2.2315	177.2437	225.9857
2	59.8353	76.2900	413.8428	527.6496
4	94.8028	120.8735	1256.0072	1601.4092
6	100.9752	128.7434	2234.9364	2849.5439
8	96.1023	122.5305	3011.7106	3839.9310
10	84.1337	107.2704	3404.3772	4340.5809
12	73.6582	93.9142	3271.6727	4171.3827
14	86.8832	110.7761	2594.1995	3307.6044
16	136.6748	136.0103	1490.5993	1900.5141
18	69.2881	88.3423	443.7388	565.7670



# OUTPUT CONTINUATION OF FOURTH PART (ONE TIME)

BF = 6  
 GM = 20  
 PIERSON = TRUE  
 ALF = 1.000  
 DELTAZ = .536  
 FP = .333  
 FD = .450  
 FC = .750  
 LE = 50.390  
 DP = 4.260

F(1:NS1) :	2.17	5.13	5.13			
HS(1:BF) :	2.15	2.90	3.75	4.95	6.20	7.45
PM(1:BF1) :	6.50	7.20	7.80	8.40	9.00	9.50

CF1 = 172.800  
 CF2 = 691.200  
 AH = 2  
 AS = 4  
 BT = 4  
 RT = 5  
 ST = 4

## 5. Structure of the program

### 5.1. General

The structure of the program is according to the description in chap. 2. After the declarations of real and integer numbers the different procedures follow.

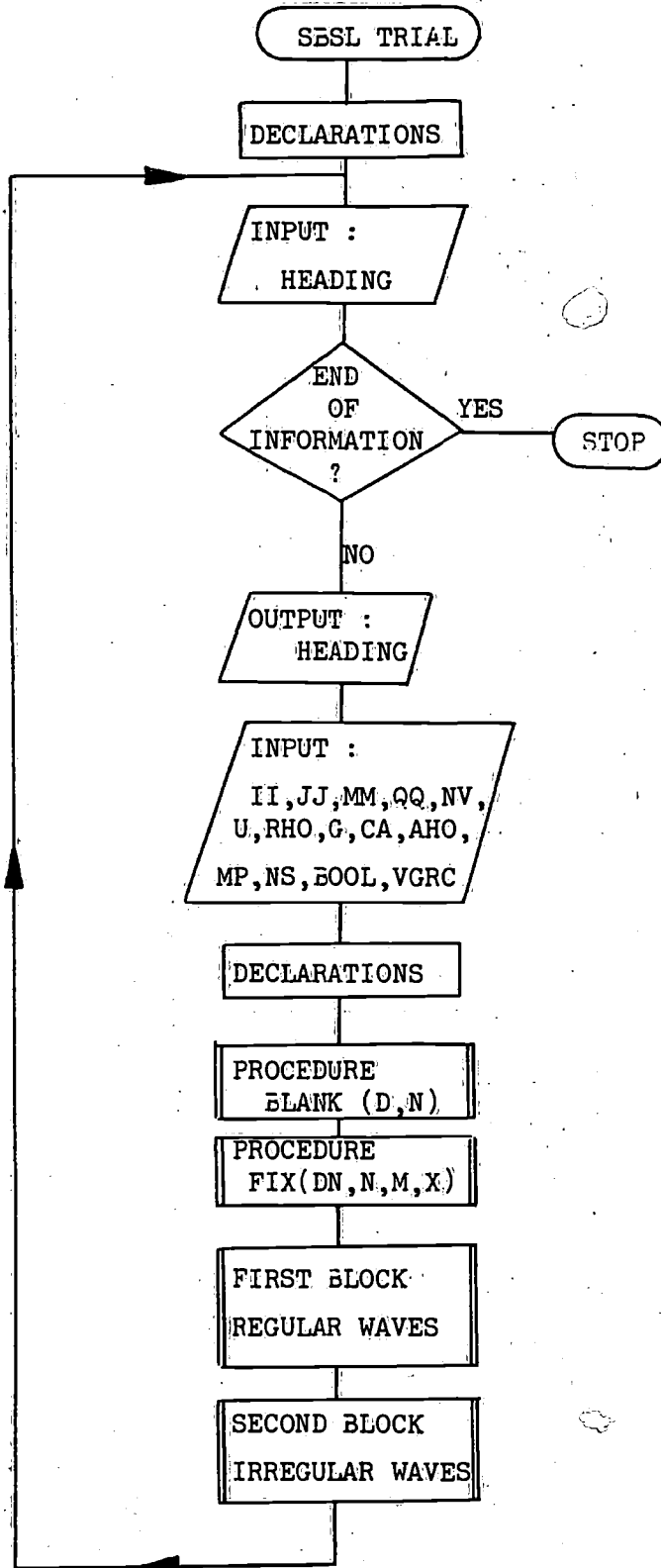
Afterwards the statical calculations are carried out and are followed by the computations of the response functions in the first block. At last the behaviour in irregular seas is calculated in the second block. See the flow diagram in 5.2.

The next part of the program, which will be carried out is clearly denoted in a star block.

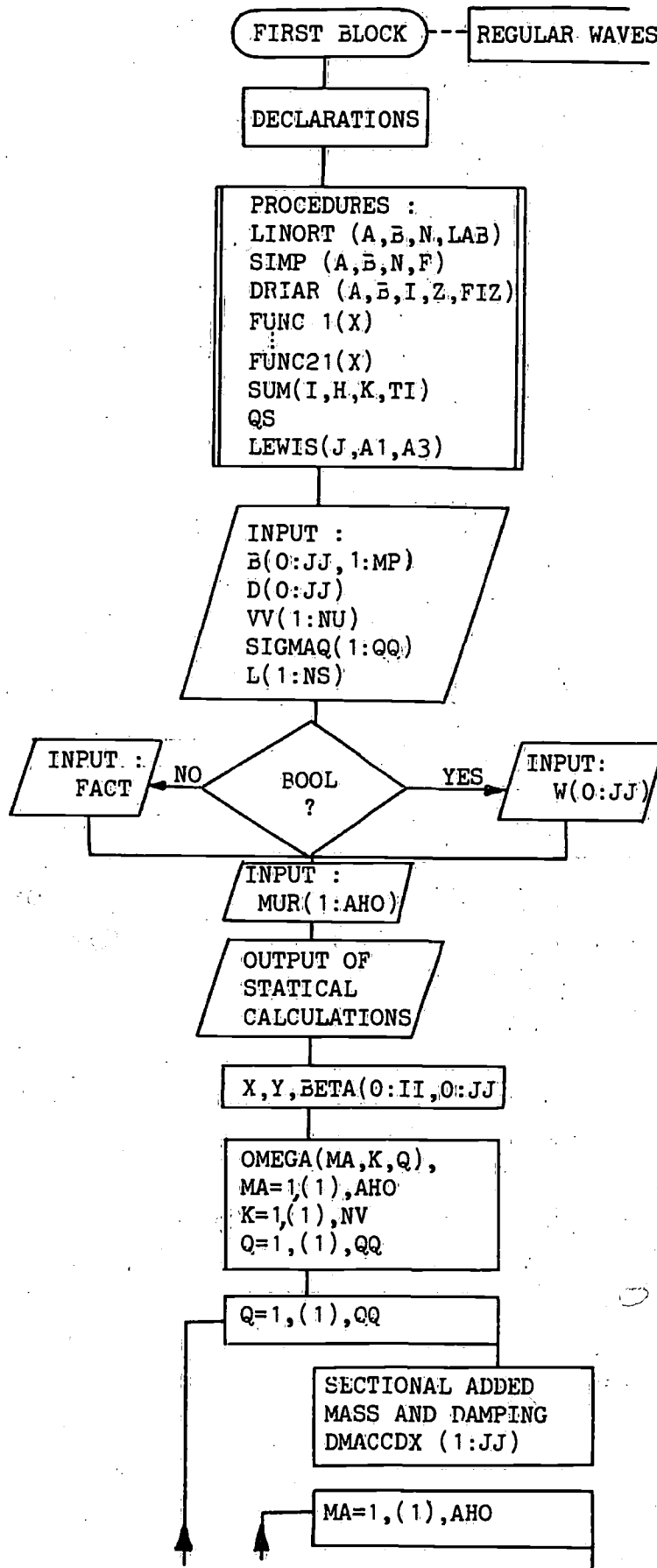
### 5.2. Schematic flow-diagram

The next pages show a schematic flow-diagram of the program "TRIAL". First a review of the total program is given. Afterwards a more detailed flow-diagram of the first and second block are shown in a schematic way too.

Schematic flow-diagram of "TRIAL"

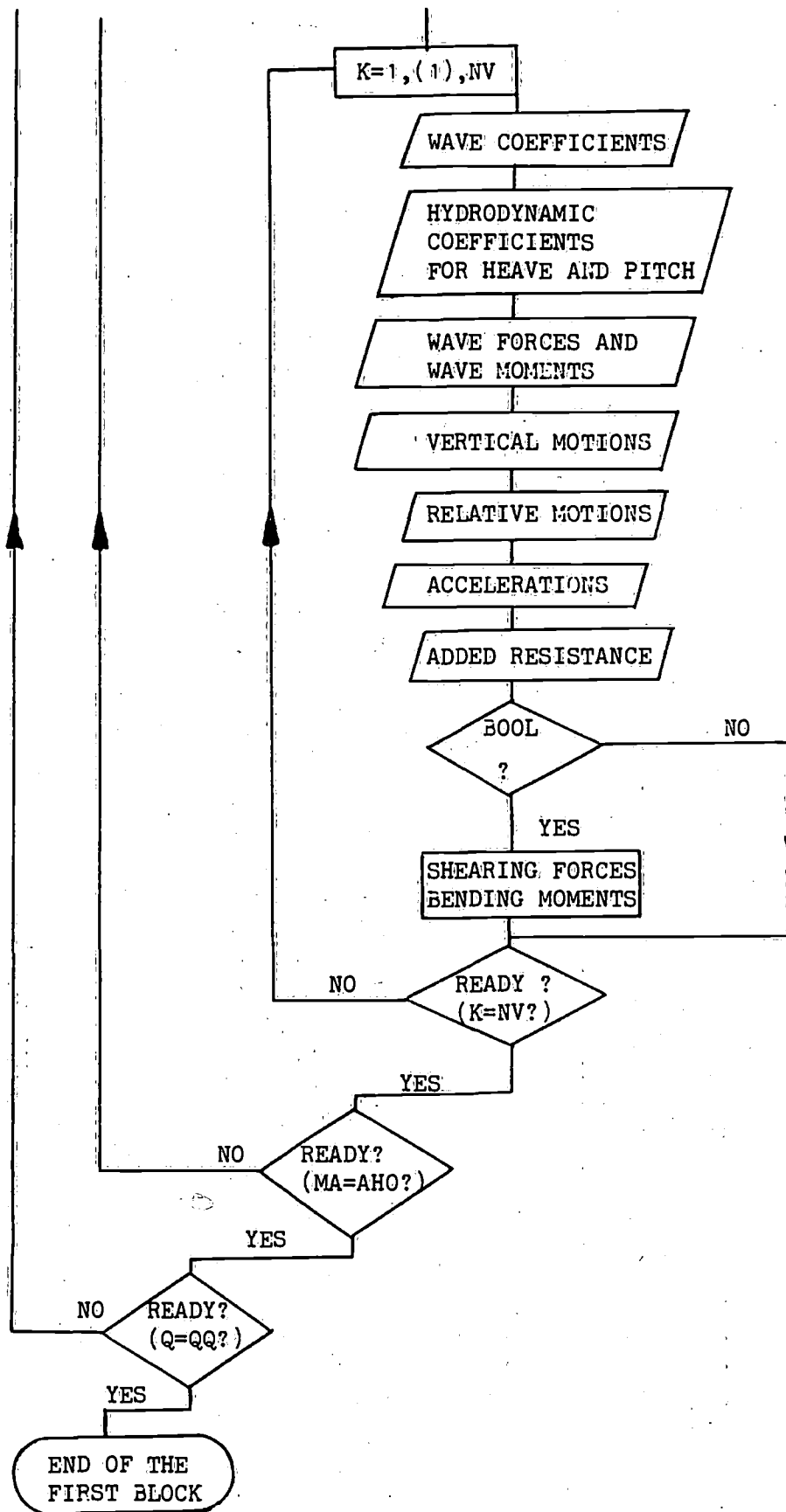


Schematic flow-diagram of the first block of "TRIAL"

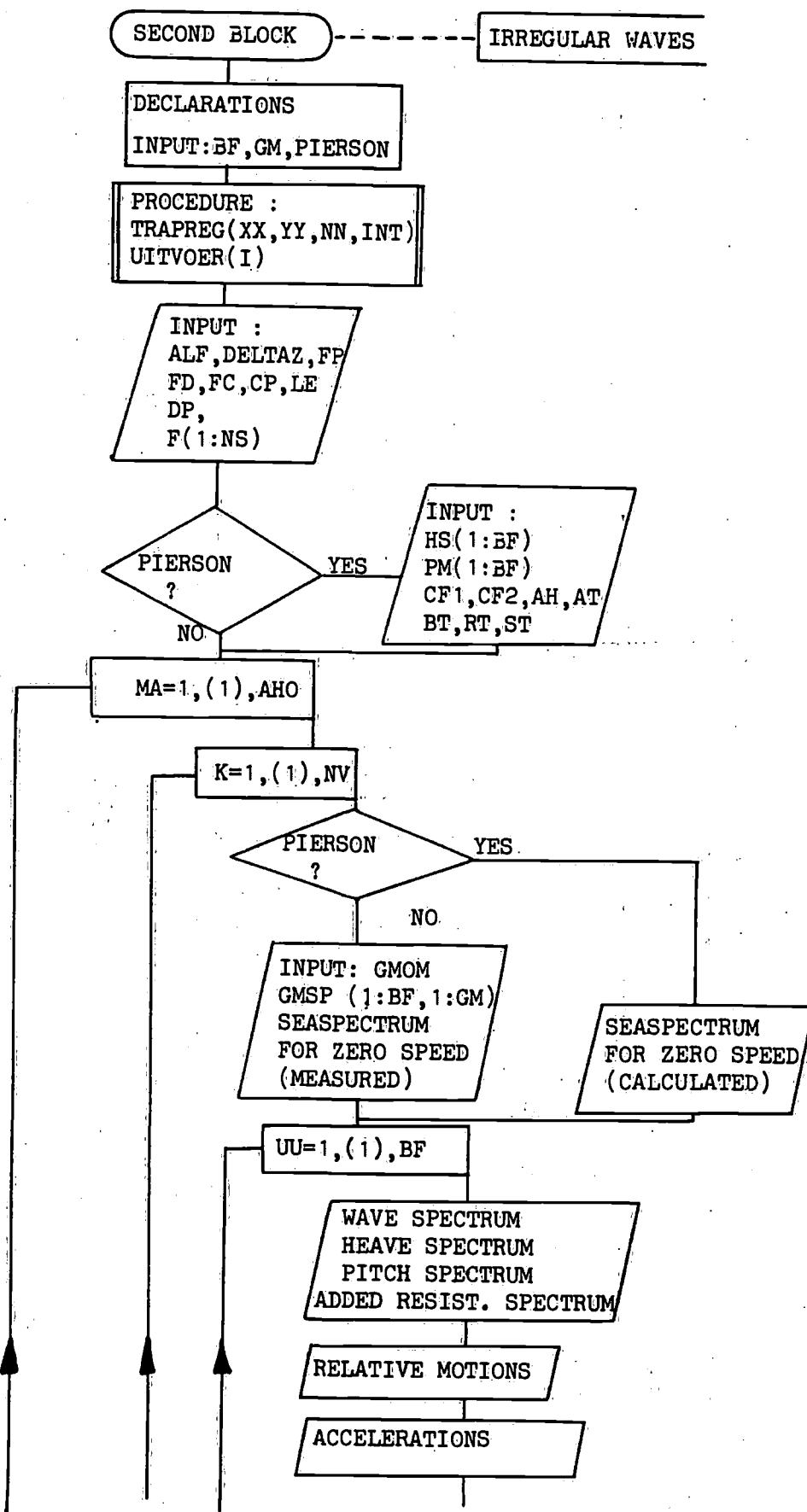




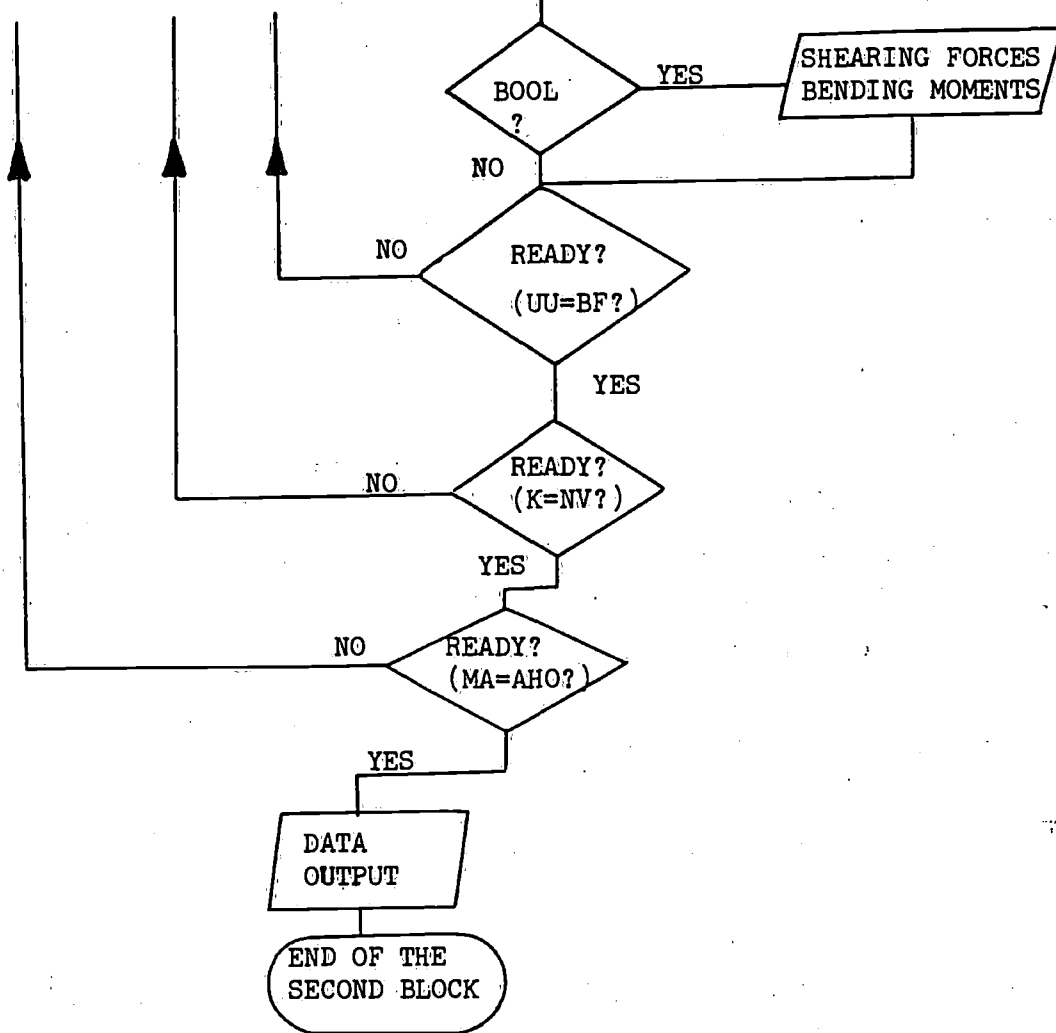
Continuation of the schematic flow-diagram of the first block of "TRIAL"



Schematic flow-diagram of the second block of "TRIAL"



Continuation of the schematic flow-diagram of the second block of "TRIAL"



### 5.3. Job information

The job information is depending on the computer type, the compiler, etc. For the IBM 360/65 computer of the Mathematical Centre of the University of Technology at Delft the job information consists of minimum 13 cards. The first card contains the jobname, the projectnumber, username, the expected calculation time and the required memory. An example of the job information for "TRIAL" looks as follows :

Before the program :

```
card 1 : //SBSL/B21UJOB(0172,A),BIJLSMA,TIME=10,REGION=256K
card 2 : //JOB LIBUDDUJDSN=SYS2.NUMLIBDA,DISP=SHR
card 3 : //UUEXECUUALGODCLG,REGION=256K,SGZ='MAX -20'
card 4 : //ALGOL.SYSLIBUDDUJDSN=SYS2.NUMLIBDA,DISP=SHR
card 5 : //ALGOL.SYSINUDDUJ*
```

The program is closed with :

```
card 6 : /*
```

followed by the card before the data set

```
card 7 : //LKED.SYSLIBUDDUJDSN=SYS2.NUMLIBDA,DISP=SHR
```

```
card 8 : //GO.ALGLDDO2UDDUJSYSOUT=A
```

```
card 9 : //GO.PRINTERUDDUSYSOUT=A,DCB=(RECFM=FA,LRECL=81,BLKSIZE=81)
```

```
card 10 : //GO.SYSINUDDUJ*
```

```
card 11 : comment (e.g. the name of the snip)
```

The data set is closed with

```
card 12 : /*
```

```
card 13 : //
```

Remark : If no comment is required card 11 should be a blank card, while on the other hand cards may be added for the comment.

The sign U denotes a blank space.

#### 5.4. Listing of principal computer variables

mathematical notation	Symbol Program symbol	Description and remark
$a_1$	A <sub>1</sub>	Coefficient of Lewis-form transformation
$a_3$	A <sub>3</sub>	Coefficient of Lewis-form transformation
a	A14	Added mass of ship or model
$A_j$	AA(0:JJ)	Half sectional area
A	AA 20	Added mass moment of inertia
$A_w$	AAW	Waterline area
$v_{a_j} / \zeta_a$	ACC(1:AHO, 1:NV, 1:QQ, 0:0.5JJ)	Transferfunction for vertical acceleration
h	AH	Coefficient for the calculation of the standard wave spectra. See 2.3. and 3.2.
	AHO	Number of directions of wave travel
$\alpha$	ALF	Modelscale
a	AT	Coefficient for the calculation of the standard wave spectra. See 2.3. and 3.2.
y	B(0:JJ, 1:MP)	Half widths of the section. See 3.2.
$A_j / (y_w xT)$	BB	The sectional area coefficient : $AA(J) / \{B(J,MP) \times D(J)\}$
b	B15	Damping coefficient for heaving
B	BB21	Damping coefficient for pitching
$\beta$	BETA(0:II, 0:JJ)	Angles of positions along the section contour with respect to vertical symmetrical ship plane for which the potentials are calculated after transformation
	BF	Number of standard or measured wave spectra See 3.2.
	BLANK	Procedure for the output of blanks; Own procedure of Mathematical Centre
	BOOL	Boolean for the calculation of shearing forces and bending moments
b	BT	Coefficient for the calculation of the standard wave spectra. See 2.3. and 3.2.

Mathematical notation	Symbol Program symbol	Description and remark
c	C16	Statical coefficient for heaving
	CA	Ratio of displacement of ship including and excluding appendices
C	CC23	Statical coefficient for pitching
$C_1$	CF1	coefficient for the calculation of the standard wave spectra. See 2.3. and 3.2.
$C_2$	CF2	coefficient for the calculation of the standard wave spectra. See 2.3. and 3.2.
$\cos \mu$	COSMUR	The cosine function of the direction of wave travel $\mu$
$\dot{s}_*$	CP	Dimensionless threshold velocity for slamming See 3.2.
$T_j$	D(0:JJ)	Draught of each section
d, D	D17	Mass coupling coefficients
LCB	DELTA X	Distance of centre of buoyancy with respect to the midship section (JJ/2)
CB	DELTA Z	Blockcoefficient. See 3.2.
$Q_a / \rho g L B \zeta_a$	DDD(1:AH0, 1:NV, 1:QQ, 0:0.5JJ)	Dimensionless transferfunction for the shearing forces. See 2.3.3. (g)
$\rho g V$	DDPL	Weight of displacement of ship or model including appendices
$Q_s$	DDS(0:0.5(JJ-1))	Shearing force in still water
	DM(1:6, 0:JJ)	Total sectional forces and moments
$\frac{dm'}{dx}$	DMACCDX(0:JJ)	Derivated mass value for a section
T	DP	Draught at the location L(NS) (=at FPP) for which slamming will be calculated
	DRIAR	Procedure to calculate the sectional area's according to Simpson's second rule

Symbol		Description and remark
Mathematical notation	Program symbol	
$e$	E18	Coupling coefficient for damping in heaving motion
$E$	EE20	Coupling coefficient for damping in pitching motion
$e^{-kTx}$ (j)	EKST(0:JJ, 1:NV)	The natural exponent for an effective draught of each section (Smith-effect)
$f(x)$	F(1:NS)	Positive distances (free board, etc) from the waterline for which will be calculated the chance of exceeding by the relative motion. F(NS)=free board at FPP.
$\epsilon_{\theta\zeta}$	FASEPSI	Phase angle of pitching motion with respect to the wave motion
$\epsilon_{z\zeta}$	FASEZ	Phase angle of heaving motion with respect to the wave motion
	FC FD	Coefficient for shipping formula See (48) and (51) of 2.3.3. and 3.2.
	FIX	Procedure for fixed point data output
$F_a \cos \epsilon_{F\zeta}$	FF1	The cosine part of the wave force
$F_a \sin \epsilon_{F\zeta}$	FF2	The sine part of the wave force
	FM(1:5,0:JJ)	The sectional wave forces and- moments
	FP	Coefficient for shipping formula. See (48) and (51) of 2.3.3. and 3.2.
	FUNC n(x) n=1,2...21	Procedures for several functions

Symbol		Description
Mathematical notation	Program symbol	
$g$	G	Acceleration of gravity
$g$	G19	Statical coupling coefficient for heaving motion
$\Gamma_c$	GAMMAC(0:II)	The cosine part of the stream function for position $i$
$\omega_e^2/g$	GAMMAQ	Ratio of the squared frequency of encounter and the acceleration of gravity
$\Gamma_s$	GAMMAS(0:II)	The sine part of the stream function for position $i$
G	GG 25	Statical coupling coefficient for pitching motion
	GM	Number of frequencies of the measured spectra. See 3.2.
	GMOM(1:BF, 1:GM)	Circular wave frequencies of the measured spectra See 3.2.
	GMSP(1:BF, 1:GM)	Spectral values of wave amplitude for the measured spectra. See 3.2.
$y_w/T$	HH	Half beam to draught ratio of each section: $B(J,MP)/D(J)$ .
$\bar{H}_{1/3}$	HS(1:BF)	Significant wave heights of the spectra
$i$	I	Positions $i$ of the section contour for which the potential should be calculated. See 3.2.
I	II	Number of positions $i$ of the section contour for which the potential should be calculated. See 3.2.
$I_L$	IIW	longitudinal moment of inertia of waterplane area with respect to $y_b$ axis
j	J	Section index. See 3.2.
J	JJ	Number of sections
	K	Step parameter in velocity loop
	KF	Working parameter in several sections
$k$	KKQ	Wave number
	L(1:NS)	Length ordinates of locations relative to the midship section for which the relative motions with respect to the water surface has to be calculated. $L(NS)=L/2$ . See 3.2.



## Symbol

## Description and remark

Mathematical notation      Program symbol

Mathematical notation	Program symbol	Description and remark
$\lambda$	LAMBDA	Wave length
$L_e$	LE	Entrance length of the waterline
	LEWIS	Procedure for Lewis-form transformation of the section
$L$ } $L$ } $L_{PP}$	LL	Length of model or ship
	LMD	Distance of aft perpendicular (section 0) to centre of buoyancy
	LINORT	Procedure for solution of matrices. Own procedure of Mathematical Centre
	LPD	Distance of fore perpendicular (section JJ) to centre of buoyancy
	MA	Step parameter in loop of directions of wave travel
$m'$	MACC(0:JJ)	Sectional added mass
$m_n$	MB	$n^{\text{th}}$ moment of a spectrum
$M_a \cos \epsilon_{M\zeta}$	MM1	The cosine part of the wave moment
$M_a \sin \epsilon_{M\zeta}$	MM2	The sine part of the wave moment
$M_{ba} / \rho g L^2 B \zeta_a$	MMB(1:AH0,1:NV, 1:QQ,0:0.5(JJ-1))	The dimensionless transferfunction for the bending moments See 2.2.
$M_{bs}$	MMBS(0:0.5(JJ-1))	Bending moment for still water
	MP	Number of points along the half section contour for which the half widths will be introduced. See 3.2.
$\mu$	MUR(1:AH0)	Directions of wave travel in radians. See 3.2.
$N'$	NNACC(0:JJ)	Sectional damping coefficient
	NS	Number of locations for which should be calculated the relative motion with respect to the water surface See 3.2.

## Symbol

## Description and remark

Mathematical notation	Program symbol	Description and remark
	NV	Number of ship/model speeds. See 3.2.
	NW	Working parameter in several spectra
$S_{A_j}(\omega_{em})$	OFA(1:QQ)	Sectional spectral values for accelerations (one dimensional array) See(33) of 2.3.3.
$S_{A_j}(\omega_{em})$	OFAC(1:QQ,0:0.5JJ)	Sectional spectral values for accelerarions (two dimensional array) See (33) of 2.3.3.
$S_{s_d}(\omega_{em})\omega_{em}^2$	OFB(1:QQ)	Spectral values for determination of the second moment of the relative motion spectrum with respect to shipping. See 2.3.3 (e)
$S_{Q_j}(\omega_{em})$	OFD(1:QQ,0.5(JJ-1))	Spectral values for shearing forces two dimensional array) See 2.3.3. (g)
$S_{Q_j}(\omega_{em})$	OFDA(1:QQ)	Spectral values for shearing forces (one dimensional array) See 2.3.3. (g)
$\omega_s$	OFF(1:A) A=QQ or GM	Circular wave frequencies (for ship) (one dimensional array) See (5) of 2.3.
$S_{s_d}(\omega_{em})$	OFK(1:QQ)	Spectral values of the relative motion with respect toshipping. See 2.3.3. (f)
$S_{\zeta}(\omega)\omega^4$	OFM(1:A) A=QQ or GM	Spectral values for determination of the fourth moment of the wave spectrum. See (13) of 2.3.1.
$S_{M_{bj}}(\omega_{em})$	OFMA(1:QQ)	Spectral values for bending moments (one dimensional array) See 2.3.3. (h)
$S_{M_{bj}}(\omega_{em})$	OFMB(1:QQ, 0.5(JJ-1))	Spectral values for bending moments (two dimensional array) See 2.3. (h)
$\omega_m$	OMEGA(1:AHO,1:NV, 1:QQ)	Circular wave frquency derived from introduced frequency of encounter. See 2.3.2.
$\omega_m$	OMMAKQ=OMEGA	Circular wave frequency derived from introduced frequency of encounter. See 2.3.2.

## Symbol

## Description and remark

Mathematical notation	Program symbol	Description and remark
$S_{\zeta}(\omega)\omega^2$	OFN(1:A)A=QQ or GM	Spectral values for the determination of the second moment of the wave spectrum. See (12) of 2.3.1.
$S_{s(x)}(\omega_{em})$	OFF(1:QQ,1:NS)	Spectral values for relative motions (two dimensional array).See (41) of 2.3.3.
$S_{s(x)}(\omega_{em})\omega_{em}^2$	OFR(1:QQ,1:NS)	Spectral values for the determination of the second moment of the relative motion spectra See 2.3.3. (e)
$S_{R_{AW}}(\omega_{em})$	OFRW(1:QQ)	Spectral values for the added resistance spectrum. See 2.3.3. (d)
$S_{\theta}(\omega_{em})$	OFS(1:QQ)	Spectral values for the pitch spectrum See (31) of 2.3.3.
$S_{s_d}(\omega_{em})$	OFV(1:QQ)	Spectral values of the relative motion with respect to slamming See (53) of 2.3.3. (f)
$S_{s_d}(\omega_{em})\omega_{em}^2$	OFY(1:QQ)	Spectral value for the determination of the second moment of the relative motion spectrum with respect to slamming. See 2.3.3. (f)
$S_z(\omega_{em})$	OFZ(1:QQ)	Spectral values for the heave spectrum See (29) of 2.3.3.
$\theta_a$	PSIA	Amplitude of pitching motion
$\phi_c$	PHIC(0:II)	The cosine part of the potential for position i.
$\phi_s$	PHIS(0:II)	The sine part of the potential for position i
$\pi$	PI	3.141597 .....

Symbol		Description and remark
Mathematical notation	Program symbol	
	PIERSON	Boolean for the calculation of standard wave spectra. See 2.3. and 3.2.
$\theta_a \cos \epsilon_{\theta \zeta}$	PIPSI	The cosine part of the pitching motion
$z_a \cos \epsilon_{z \zeta}$	PIZ	The cosine part of the heaving motion
$\bar{T}$	PM(1:BF)	Average wave period of the spectra See 3.2.
	Q	Step parameter in frequency loop
Q	QQ	Number of frequencies of encounter, which have to be introduced. See 3.2.
	QS	Procedure used in procedure "Lewis" for solution of part of stream function
$\theta_a / k \zeta_a$	RAOPSI(1:AHO, 1:NV, 1:QQ)	Transferfunction for pitch. See 2.2. (c)
$z_a / \zeta_a$	RAOZ(1:AHO, 1:NV, 1:QQ)	Transferfunction for heave. See 2.2 (c)
$R_{AW}$	RAW	Added resistance in regular waves
$R_{AW} / \rho g \zeta_w^2 (B^2/L)$	RAWZ(1:AHO, 1:NV, 1:QQ)	Dimensionless transfer-function for the added resistance in waves. See 2.2. (f)
$\rho$	RHO	Density of water
$\theta_a \sin \epsilon_{\theta \zeta}$	RHOPSI	The sine part of the pitching motion.
$z_a \sin \epsilon_{z \zeta}$	RHOZ	The sine part of the heaving motion
r	RT	Coefficient for the calculation of the standard wave spectra. See 2.3. and 3.2.
$\omega_e^2$	SIGKW	The squared frequency of encounter
$\omega_e$	SIGMAQ(1:QQ)	Frequencies of encounter. See 3.2.
	SIMP	Procedure for integration according to Simpson's first rule.

Symbol		Description and remark
Mathematical notation	Program symbol	
$S_{\zeta}(\omega)$	SPS(1:BF,1:QQ)	Spectral value of the wave according to (2) in 2.3 (two dimensional)
$S_{\zeta}(\omega)$	SPSEA(1:A) A=QQ or GM	Spectral value of the wave according to (2) in 2.3 (one dimensional)
s	ST	Coefficient for the calculation of the standard wave spectra. See 2.3. and 3.2.
	SUM	Procedure for summation
$\theta$	THETA(0:II)	Angles of positions i with respect to vertical symmetrical ship plane before transformation of the section
	TRAPREG	Procedure for integration according to trapezium rule
	UITVOER	Procedure for output of the general spectrum data. See 2.3.1.
	VGRC	Boolean to take into account only waves with celerity $c < v \cos \mu$ . See 2.3.2(b2) and 3.2 (d)
$N_{\zeta}, m_{os'd}$	VKQ	Number of zero crossings of the wave per time unit. See (14) of 2.3.1. and zero <sup>th</sup> moment of the spectrum for the relative motion with respect to shipping. See (49) in 2.3.3 (f)
	VKR	Average number of wave crests and -troughs. See (16) of 2.3.1. and second moment of the spectrum for the relative motion with respect to shipping. See 2.3.3. (f)
$N' - v \frac{dm'}{dx_b}$	VNDMX(0:JJ)	Sectional damping corrected for speed influence with the derivated mass value
$m_{4\zeta}, m_{os'd}$	VSQ	Fourth moment of wave spectrum. See 2.3.1. (d); Zero <sup>th</sup> moment of the spectrum for the relative motion with respect to slamming. See 2.3.3 (f)
$m_{2s_d}$	VSSQ	Second moment of the spectrum for the relative motion with respect to slamming. See 2.3.3. (f)

Symbol

Description and remark

Mathematical notation	Program symbol	Description and remark
$v$	VV(1:NV)	Model/ship speeds
	W(0:JJ)	Weights of the ship from bow to section j. See 3.2.
$z_i$	X(0:II,0:JJ)	Vertical ordinate of position i of the section contour after transformation
$x_b$	XB	Length ordinate of the section with respect to the centre of buoyance
$y_i$	y(0:II,0:JJ)	Horizontal ordinate of position i of the section contour after transformation
$s_a(x)/\zeta_a =$ $ H_{s(x)\zeta}(\omega_{em}) $	ZR(1:AHO,1:NV, 1:QQ,1:NS)	Transfer function for relative motion

5.5. Program listing

For a total listing of the program "TRIAL" see the next pages.

SOURCE PROGRAM

```

SC      SOURCE STATEMENT
00001  'BEGIN'
00002  'COMMENT' * * * * *
00003  *
00004  * PROGRAM TO CALCULATE THE BEHAVIOUR OF A SHIP IN REGULAR HEAD WAVES
00005  * AND IN A SEASWAY
00006  *
00007  * * * * *
00008  INTEGER I, JJ, II, IV, OV, NS, MP, MP2, I, J, K, M, N, Q, MA, PEGEL, AHD;
00009  REAL LL, LLR, RHO, G, PIZ, DELTAX, LMD, LPD, F, PI, SIGKW, FACT, S, GA,
00010  COSMUL, SINAKO, VA, VZ, VC, VD;
00011  DOUBLE BMDL, VGRG;
00012  'COMMENT' * * * * *
00013  *
00014  *          DATA INPUT
00015  *
00016  * * * * *
00017  SYSACT(1,1,60); SYSACT(1,12,1);
00018  'GOTO' FIRST;
00019  CPNIZUM: SYSACT(1,14,1);
00020  FIRST:  FPR J:=1 'STEP: 1 'UNTIL' 72 'DO'
00021  'BEGIN'
00022  INSYMBOL(1, ('QWERTYUIOPASDFGHJKLZXCVBNM, ?<- / #, / 0123456789+_])>:;
00023  ?"= ('), ());
00024  CUTSYMBOL(1, ('QWERTYUIOPASDFGHJKLZXCVBNM, ?<- / #, / 0123456789+_])>:;
00025  ?"= ('), ());
00026  'END';
00027  SYSACT(1,14,2);
00028  OUTSYMBOLS(1, ('LENS TRANSFORM')));
00029  SYSACT(1,14,2);
00030  INTEGER(0, I); ININTEGER(0, JJ); ININTEGER(0, MM); ININTEGER(0, NN);
00031  INREAL(0, LL); INREAL(0, LLR); INREAL(0, RHO); INREAL(0, G); INREAL(0, PIZ);
00032  INREAL(0, DELTAX); INREAL(0, LMD); INREAL(0, LPD); INREAL(0, F); INREAL(0, PI);
00033  INREAL(0, SIGKW); INREAL(0, FACT); INREAL(0, S); INREAL(0, GA);
00034  INDOUBLE(0, BMDL); INDOUBLE(0, VGRG); MP:=MP-2;
00035  'BEGIN'  'ARRAY' L(1:MEZ), VV(1:NVZ), R(1:OVZ), SIGMA(1:OVZ);
00036  'ARRAY' AAW, AHD, AAZ, AAPS(1:AHZ, 1:AVZ), ZP(1:AHZ, 1:AVZ);
00037  G, NS, GDD, MMF(1:AHZ, 1:AVZ), Q, W(1:JJZ);
00038  ACC(1:AHZ, 1:AVZ), QUR(1:AHZ);
00039  'COMMENT' * * * * *
00040  *
00041  *          IN-AND OUTPUT PROCEDURES
00042  *
00043  * * * * *
00044  'PROCEDURE' BLANK(D, N); 'VALUE' D, N;
00045  'INTEGER' D, N; 'CODE';
00046  'PROCEDURE' FIX(DN, N, M, X); 'VALUE' DN, N, M, X;
00047  'INTEGER' DN, N, M; 'REAL' X;

```



SC	SOURCE STATEMENT	SOURCE PROGRAM	PAGE 002
00037	- 'BEGIN'	'INTEGER' H,P,R,K,HH; 'REAL'D,DH;	00000500
00039		'BOOLEAN' T; 'SYSACT(1,12,1);	00000510
00041		'SYSACT(1,5,P); 'SYSACT(1,1,R); 'SYSACT(1,9,K);	00000520
00044		'IF' M<0 'THEN' M:=0;	00000530
00045		'IF' M<0 'THEN' N:=0;	00000540
00046		H:=H;'IF' M<1 'THEN' N 'ELSE' N+M+1;	00000550
00047		'IF' P=1 & DN=3 'THEN'	00000560
00047		'BEGIN' BLANK(1,15); R:=16; 'END';	00000570
00050		'IF' P<K 'THEN'	00000580
00050		'BEGIN' SYSACT(1,14,1); R:=1;	00000590
00052		'IF' DN=3 'THEN'	00000600
00052		'BEGIN' BLANK(1,15); R:=16;	00000610
00054		'END';	00000620
00055		'END';	00000630
00056		I:=X<0; X:=ABS(X); X:=X+.5*10**(-M)+5'-13;	00000640
00059		R:=P+4+1; D:=10**N;	00000650
00061		'IF' X>0 'THEN' 'GOTO' IIF;	00000660
00062	AA:	D:=D*.1; H:=ENTIER(X/D);	00000670
00064		'IF' H=0 & D>.5 'THEN'	00000680
00064		'BEGIN' OUTSYMBOL(1,(' '),1); 'GOTO' AA;	00000690
00064		'END';	00000700
00067		OUTSYMBOL(1,(' -0'), 'IF' D<.5 & M<1 'THEN' 3	00000710
00067		'ELSE' 'IF' T 'THEN' 2 'ELSE' 1);	00000720
00069	BB:	'IF' D<.5 'THEN'	00000730
00069		'BEGIN' 'IF' M=0 'THEN' 'GOTO' END;	00000740
00069		OUTSYMBOL(1,(' '),1);	00000750
00070		'IF' M<0 'THEN' 'GOTO' END 'ELSE' 'GOTO' CC;	00000760
00071		'END';	00000770
00072		OUTSYMBOL(1,('0123456789'),H+1);	00000780
00073	DD:	X:=X-H*D; D:=D*.1; H:=ENTIER(X/D); 'GOTO' BB;	00000790
00077	CC:	OUTSYMBOL(1,('0123456789'),H+1); M:=M-1;	00000800
00079		'IF' M<1 'THEN' 'GOTO' END;	00000810
00080		X:=X-D*M; D:=D*.1; H:=ENTIER(X/D); 'GOTO' CC;	00000820
00084	IIF:	OUTSYMBOL(1,(' -'), 'IF' T 'THEN' 2 'ELSE' 1);	00000830
00085		H:=0;	00000840
00086		'IF' M>0 'THEN' 'GOTO' GG;	00000850
00087	EE:	H:=H-1;	00000860
00088		OUTSYMBOL(1,('*'),1);	00000870
00089		'IF' HH=0 'THEN' 'GOTO' END;	00000880
00090		D:=10**N*.01;	00000890
00091	FF:	X:=X*.1;	00000900
00092		'IF' X<0 'THEN' 'GOTO' DD	00000910
00092		'ELSE' 'GOTO' FF;	00000920
00093	GG:	X:=X+.5*10**(-M);	00000930
00094	KK:	N:=N+1; M:=M-1; D:=10**N;	00000940
00097		'IF' M=0 'THEN' 'GOTO' II;	00000950
00098		'IF' X>0 'THEN' 'GOTO' KK;	00000960
00099		X:=X+.5*10**(-M);	00000970

```

00100      'GOTO' DD;                               0000990
00101      II:      'IF' X<0 'THEN' 'GOTO' JJ;      0001000
00102      N:=N+1; 'GOTO' EE;                       0001000
00104      JJ:      M:=-1; X:=X+0.5; 'GOTO' DD;     0001010
00107      END:     'IF' DN=2 'THEN' BLANK(1,6);    0001020
00108      'END'   FIX;                             0001020
00109      'COMMENT' *****                       0001040
00109      *                                           * 0001050
00109      *       THE BEGINNING OF THE FIRST BLOCK  * 0001060
00109      *                                           * 0001070
00109      * * * * *                               * 0001080
00109      'BEGIN' 'ARRAY' THETA,GAMMA,GAMMAC,PHIC,PHIS(/O:II/),DMACCOX,COF, 0001090
00109      VNOMX,HNACC,MACC,AA,A),A3(/O:JJ/),X,Y,BETA(/O:JI,O:JJ/), 0001100
00109      F(/I:MM,O:II/),MYRA(/I:MM,I:MM+1/),PJ,QJ(/I:MM+1/), 0001110
00109      BTJ(/I:MM/),DM(/I:6,O:JJ/),KST(/O:JJ,I:MM/),DMS,MMBS 0001120
00109      (/O:5*JJ-1/),FM(/I:5,O:JJ/);           0001130
00109      'REAL' E,T,U,V,GAMMA0,C1,A14,B15,C15,D17,F18,XA,PSIA, 0001140
00111      XE,Z,KQ,FF1,FF2,FM1,MM2,ALFA,G,AAN,IW,LAMBDA,HU,BS,RW, 0001150
00111      G19,AA20,BB21,CL22,CC23,GG25,FS,FQ,BPPL,MM,M,FASEPSI, 0001160
00111      ALPHA,BET,GAMMA,DELTA,EPSILON,FAEZ,MU,NU,NDEMER, 0001170
00111      KAPPAZ,LBBGAZ,KAPPAPSI,LABDAPSI,PIZ,RHOZ,PIPSI,RHOPSI,ZA: 0001180
00111      'COMMENT' *****                       * 0001190
00111      *                                           * 0001200
00111      *       MANY LITTLE PROCEDURES          * 0001210
00111      *                                           * 0001220
00111      * * * * *                               * 0001230
00111      'PROCEDURE' LINDT(A,B,H,LAE);           0001240
00112      'VALUE' N;'INTEGER' N;'ARRAY' A,B;'LABEL' LAB;'CODE'; 0001250
00117      'REAL' 'PROCEDURE' SIMP(A,B,N,F);     0001260
00118      'REAL' A,B;'INTEGER' N;              0001270
00120      'REAL' 'PROCEDURE' F;                0001280
00121      'BEGIN' 'INTEGER' K;'REAL' H,S;      0001290
00123      H:=(B-A)/N; S:=0;                   0001300
00125      'FOR' K:=1 'STEP' 2 'UNTIL' N-1 'DO' 0001310
00125      S:=S+4*F(A+K*H);                   0001320
00126      'FOR' K:=2 'STEP' 2 'UNTIL' N-2 'DO' 0001330
00126      S:=S+2*F(A+K*H);                   0001340
00127      SIMP:=(S+F(A)+F(B))*H/3           0001350
00127      'END' SIMP;                       0001360
00128      'REAL' 'PROCEDURE' DRIAR(A,B,I,Z,FIZ); 0001370
00129      'VALUE' A,B;'REAL' A,B,Z,FIZ;'INTEGER' I; 0001380
00132      'BEGIN' 'REAL' H,S;                0001390
00133      H:=(B-A)/MP; I:=0; Z:=A; S:=FIZ/3; 0001400
00137      I:=1; Z:=A+H/3; S:=S+FIZ;         0001410
00140      I:=2; Z:=A+2*H/3; S:=S+FIZ;      0001420
00143      I:=3; Z:=A+H; S:=S+4/3*FIZ;       0001430
00146      'FOR' I:=4 'STEP' 1 'UNTIL' MP+1 'DO' 0001440
00146      'BEGIN' Z:=A+(I-2)*H; S:=S+3*FIZ  0001450

```

SC	SOURCE STATEMENT	
00147	'END';	00001460
00148	'FOR' I:=6 'STEP' 3 'UNTIL' MP-1 'DO'	00001470
00148	'BEGIN' Z:=A+(I-2)*H; S:=S-FIZ;	00001480
00150	'END';	00001490
00151	I:=MP2; Z:=0; S:=S+FIZ;	00001500
00154	DRIAR:=3/8*H*S;	00001510
00155	'END'	00001520
00156	'REAL' 'PROCEDURE' FUNC1(X); 'REAL' X;	00001530
00158	FUNC1:=F(I/M,II*X/PI2 /I)*F(I/F,II*X/PI2 /I);	00001540
00159	'REAL' 'PROCEDURE' FUNC2(X);	00001550
00160	'REAL' X;	00001560
00161	'BEGIN' 'INTEGER' I;	00001570
00162	I:=II*X/PI2;	00001580
00163	FUNC2:=(GAMMA(I /I /I)-(SIN(THETA(I/I))*(1+A1(I/J))-A3(I/	00001590
00163	)*SIN(3*THETA(I/I)))/(1+A1(I/J)+A3(I/J))*GAMMA(I/	00001600
00163	I/I)*F(I/M,I/I)	00001610
00163	'END' FUNC2;	00001620
00164	'REAL' 'PROCEDURE' FUNC3(X); 'REAL' X;	00001630
00165	'BEGIN' 'INTEGER' I;	00001640
00167	I:=II*X/PI2;	00001650
00168	FUNC3:=(GAMMA(S(I /I /I)-(SIN(THETA(I/I))*(1+A1(I/J))-A3(I/	00001660
00168	)*SIN(3*THETA(I/I)))/(1+A1(I/J)+A3(I/J))*GAMMA(I/	00001670
00168	I/I)*F(I/M,I/I)	00001680
00168	'END' FUNC3;	00001690
00169	'REAL' 'PROCEDURE' FUNC4(X); 'REAL' X;	00001700
00171	'BEGIN' 'INTEGER' I; I:=II*X/PI2;	00001710
00173	FUNC4:=PHI(S(I /I /I)*(1+A1(I/J))*COS(THETA(I/I))-3*A3(I/	00001720
00173	)*COS(3*THETA(I/I))	00001730
00173	'END' FUNC4;	00001740
00174	'REAL' 'PROCEDURE' FUNC5(X); 'REAL' X;	00001750
00175	'BEGIN' 'INTEGER' I; I:=II*X/PI2;	00001760
00178	FUNC5:=PHI(C(I /I /I)*(1+A1(I/J))*COS(THETA(I/I))-3*A3(I/	00001770
00178	)*COS(3*THETA(I/I))	00001780
00178	'END' FUNC5;	00001790
00179	'REAL' 'PROCEDURE' FUNC6(X);	00001800
00180	'REAL' X;	00001810
00181	FUNC6:=MACC(I/(X+LMD)*JJ/LL/I);	00001820
00182	'REAL' 'PROCEDURE' FUNC7(X);	00001830
00183	'REAL' X;	00001840
00184	FUNC7:=VNDHX(I/(X+LMD)*JJ/LL/I);	00001850
00185	'REAL' 'PROCEDURE' FUNC8(X);	00001860
00186	'REAL' X;	00001870
00187	FUNC8:=B(I/(X+LMD)*JJ/LL,MP2/I);	00001880
00188	'REAL' 'PROCEDURE' FUNC9(X);	00001890
00189	'REAL' X;	00001900
00190	FUNC9:=MACC(I/(X+LMD)*JJ/LL/I)*X;	00001910
00191	'REAL' 'PROCEDURE' FUNC10(X);	00001920
00192	'REAL' X;	00001930

SC	SOURCE STATEMENT	SOURCE PROGRAM	PAGE 005
00193		FUNC10:=VND*(X/(X+LMD)*JJ/LL/)*X;	00001940
00194		'REAL' 'PROCEDURE' FUNC11(X);	00001950
00195		'REAL' X;	00001960
00196		FUNC11:=B/(X+LMD)*JJ/LL,*P2/)*X;	00001970
00197		'REAL' 'PROCEDURE' FUNC12(X);	00001980
00198		'REAL' X;	00001990
00199		FUNC12:=MACC/(X+LMD)*JJ/LL/)*X*X;	00002000
00200		'REAL' 'PROCEDURE' FUNC13(X);	00002010
00201		'REAL' X;	00002020
00202		FUNC13:=VND*(X/(X+LMD)*JJ/LL/)*X*X;	00002030
00203		'REAL' 'PROCEDURE' FUNC14(X);	00002040
00204		'REAL' X;	00002050
00205		FUNC14:=B/(X+LMD)*JJ/LL,*P2/)*X*X;	00002060
00206		'REAL' 'PROCEDURE' FUNC15(X);	00002070
00207		'REAL' X;	00002080
00208		FUNC15:=FM/(N*(X+LMD)*JJ/LL/);	00002090
00209		'REAL' 'PROCEDURE' FUNC16(X);	00002100
00210		'REAL' X;	00002110
00211		FUNC16:=M/(X+LMD)*JJ/LL/);	00002120
00212		'REAL' 'PROCEDURE' FUNC17(X);	00002130
00213		'REAL' X;	00002140
00214		FUNC17:=H/(X+LMD)*JJ/LL/)*X;	00002150
00215		'REAL' 'PROCEDURE' FUNC18(X); 'REAL' X;	00002160
00217		FUNC18:=OM/(N*(X-XA)*JJ/LL/);	00002170
00218		'REAL' 'PROCEDURE' FUNC19(X); 'REAL' X;	00002180
00220		FUNC19:=AA/(X+LL 2)*JJ/LL/);	00002190
00221		'REAL' 'PROCEDURE' FUNC20(X); 'REAL' X;	00002200
00223		FUNC20:=X*AA/(X+LL 2)*JJ/LL/);	00002210
00224		'REAL' 'PROCEDURE' FUNC21(X); 'REAL' X;	00002220
00225		FUNC21:=DM/(N*(X-XA)*JJ/LL/)*(XA-X);	00002230
00227		'REAL' 'PROCEDURE' SUM(I,H,K,TI);	00002240
00228		'VALUE' K; 'INTEGER' I,H,K; 'REAL' TI;	00002250
00231	'BEGIN'	'REAL' S;	00002260
00232		S:=0; 'FOR' I:=H 'STEP' 1 'UNTIL' K 'DO'	00002270
00233		S:=S+TI; SUM:=S	00002280
00234	'END';		00002290
00235		'PROCEDURE' QS;	00002300
00236	'BEGIN'	'REAL' U,AN,SN1,SN2; 'INTEGER' H;	00002310
00238		'REAL' 'PROCEDURE' NFACT(N); 'INTEGER' M;	00002320
00240	'BEGIN'	'INTEGER' I; 'REAL' W;	00002330
00242		W:=1;	00002340
00243		'FOR' I:=1 'STEP' 1 'UNTIL' H 'DO' W:=W*I;	00002350
00244		NFACT:=W	00002360
00244	'END'	NFACT;	00002370
00245		SN1:=SN2:=0;	00002380
00246		U:=GAMMA(S)*SQRT(X/(I,J))*X/(I,J)+Y/(I,J)*Y/(I,J);	00002390
00247		N:=1;	00002400
00248	REP:	AN:=U*POWER(N/(N*NFACT(N)));	00002410

SC	SOURCE STATEMENT	
00249	SN1:=SN1+AN*SIN(N*BETA(/I,J/));	00002490
00250	SN2:=SN2+AN*COS(N*BETA(/I,J/));	00002490
00251	N:=N+1;	00002490
00252	'IF' ABS(AN/SN1) 'NOTLESS' 0.001 'AND'	00002490
00252	ABS(AN/SN2) 'NOTLESS' 0.001 'THEN'	00002490
00252	'GOTO' REP; FS:=BETA(/I,J/)+SN1;	00002490
00254	FQ:=0.5772156649+LN(N)+SN2	00002490
00254	'END' JS;	00002490
00255	'COMMENT' * * * * *	00002500
00255	*	00002510
00255	* PROCEDURE FOR CALCULATION OF THE SECTIONAL ADDED MASS	00002520
00255	* AND DAMPING USING THE 'LEWIS-FORM' TRANSFORMATIONS	00002530
00255	*	00002540
00255	* * * * *	00002550
00255	'PROCEDURE' LEWIS(J,/I,A3);	00002560
00256	'INTEGER' J; 'REAL' A1,A3;	00002570
00258	'BEGIN' 'REAL' AZ,RZ,IZ,NZ,KSI;	00002580
00259	KSI:=(/J,MP2/)*GAMMAQ;	00002590
00260	'FOR' I:=0 'STEP' 1 'UNTIL' II 'DO'	00002600
00260	'BEGIN' U:=GAMMAQ*X(/I,J/);	00002610
00261	V:=EXP(-GAMMAQ*Y(/I,J/));	00002620
00262	T:=PI*V;	00002630
00263	QS;	00002640
00264	GAMMAC(/I/):=T*SIN(U);	00002650
00265	PHIC(/I/):=T*COS(U);	00002660
00266	GAMMAS(/I/):=V*(FQ*SIN(U)-FS*COS(U));	00002670
00267	PHIS(/I/):=V*(FQ*COS(U)+FS*SIN(U));	00002680
00268	'END';	00002690
00269	'FOR' M:=1 'STEP' 1 'UNTIL' MM 'DO'	00002700
00269	'FOR' I:=0 'STEP' 1 'UNTIL' II 'DO'	00002710
00269	'BEGIN' U:=1+A1+A3;	00002720
00270	V:=SIN((2*M-1)*THETA(/I/))/(2*M-1+A)	00002730
00270	SIN((2*M+1)*THETA(/I/))/(2*M+1-3*A3*SIN	00002740
00270	((2*M+3)*THETA(/I/))/(2*M+3);	00002750
00271	V:=V*KSI/;	00002760
00272	T:=1/(2*M-1)-A1/(2*M+1)-3*A3/(2*M+3);	00002770
00273	T:=T*(SIN(THETA(/I/))+A)*SIN(THETA(/I/)-	00002780
00273	A3*SIN(3*THETA(/I/)));	00002790
00274	T:=T*KSI*(-1)**M/(U*U);	00002800
00275	F(/M,I/):=-SIN(2*M*THETA(/I/))-V-T;	00002810
00275	'END';	00002820
00277	'FOR' M:=1 'STEP' 1 'UNTIL' MM 'DO'	00002830
00277	'BEGIN' 'FOR' R:=1 'STEP' 1 'UNTIL' M 'DO'	00002840
00277	MATPA(/R,M/):=MATRA(/M,P/):=SIMP(0,PI2,II,FUNC1);	00002850
00278	MATRA(/M,MM+1/):=SIMP(0,PI2,II,FUNC2);	00002860
00279	BETJ(/M/):=SIMP(0,PI2,II,FUNC3);	00002870
00280	'END';	00002880
00281	LINORT(MATRA,PJ,MM,FOUT);	00002890

SC

SOURCE STATEMENT

SOURCE PROGRAM

PAGE 007

```

00282          'FOR' M:=1 'STEP' 1 'UNTIL' M 'DO' MATRA(/M,M4+1/):= 00002900
00283          BETJ(/M/); 00002910
00284          LINCRT(MATRA,QJ,MM,FOUT); 00002920
00285          U:=1+A1+A3; 00002930
00286          AZ:=GAMMAC(/II/)+KSI/U*SUM(M,1,MM,PJ(/M/)*(-1)**(M-1)* 00002940
00287          (1/(2**M-1)-A1/(2**M+1)-3*A3/(2**4+3))) ; 00002950
00288          BZ:=GAMMAS(/II/)+KSI/U*SUM(M,1,MM,QJ(/M/)*(-1)**(M-1)* 00002960
00289          (1/(2**M-1)-A1/(2**M+1)-A3*3/(2**4+3))) ; 00002970
00290          NZ:=1/U*(SIMP(0,PI2,II,FUNC4)+SUM(M,1,MM,(-1)**(M-1)* 00002980
00291          QJ(/M/)*((1+A1)/(4**M*M-1)+9*A3/(4**M*M-9)))+PI*KSI/ 00002990
00292          4/U*((1+A1-A1*A3)*QJ(/1/)-A3*QJ(/2/)) ; 00003000
00293          MZ:=1/U*(SIMP(0,PI2,II,FUNC5)+SUM(M,1,MM,(-1)**(M-1)* 00003010
00294          PJ(/M/)*((1+A1)/(4**M*M-1)+9*A3/(4**M*M-9)))+PI*KSI/ 00003020
00295          4/U*((1+A1-A1*A3)*PJ(/1/)-A3*PJ(/2/)) ; 00003030
00296          I:=AZ*AZ+BZ*BZ; 00003040
00297          VACC(/J/):=BHO*PI*PI*B(/J,MP2/)*B(/J,MP2/)*SQ/T; 00003050
00298          M3C(/J/):=B*RHQ*B(/J,MP2/)*B(/J,MP2/)*(MZ*BZ+NZ*AZ)/ 00003060
00299          'GOTO' VER; 00003070
00300          FOUT: 00003080
00301          VER: 00003090
00302          OUTSTRING(1,('LINCRT GEFFT FOUTMELDING')) ; 00003100
00303          'END'; 00003110
00304          PI:=3.1415926536; 00003120
00305          PI2:=1.5707963263; 00003130
00306          LL2:=LL*0.5; MP2:=MP+2; 00003140
00307          'FOR' I:=1 'STEP' 1 'UNTIL' II 'DO' THETA(/I/):=I*PI2/II; 00003150
00308          THETA(/J/):=0.0000001; 00003160
00309          'COMMENT' * * * * * 00003170
00310          * 00003180
00311          *   D A T A   I N P U T 00003190
00312          * 00003200
00313          * * * * * 00003210
00314          INARRAY(0,3); INARRAY(0,4); INARRAY(0,VV); INARRAY(0,SIGMAQ); 00003220
00315          INARRAY(0,L); 00003230
00316          'IF' BOOL THEN INARRAY(0,W) 'ELSE' INREAL(0,FACT); INARRAY(0,MP); 00003240
00317          'COMMENT' * * * * * 00003250
00318          * 00003260
00319          *   S O M E   C O M M O N   Q U A N T I T I E S 00003270
00320          * * * * * 00003280
00321          OUTSTRING(1,('FREQUENCY OF ENCOUNTER :')) ; 00003290
00322          'FOR' J:=1 'STEP' 1 'UNTIL' QQ-1 'DO' 00003300
00323          'BEGIN' FIX(3,3,3,SIGMAQ(/J/)); OUTSYMBOL(1,(' '),1); 00003310
00324          'END'; FIX(3,3,3,SIGMAQ(/QJ/)); 00003320
00325          SYSACT(1,14,3); 00003330
00326          OUTSTRING(1,('SPEED :')) ; 00003340
00327          'FOR' J:=1 'STEP' 1 'UNTIL' NV-1 'DO' 00003350
00328          'BEGIN' FIX(1,3,3,VV(/J/)); OUTSYMBOL(1,(' '),1); 00003360
00329          'END'; FIX(1,3,3,VV(/M/));

```

```

SC      SOURCE STATEMENT
00319      SYSACT(1,14,2);
00320      OUTSTRING(1,('VERTICAL SHIP MOTIONS IN REGULAR WAVES'));
00321      SYSACT(1,14,3);
00322      'FOR' J:=0 'STEP' 1 'UNTIL' JJ 'DO'
00322      'BEGIN'  CCR(/J/):=1;
00323      AA(/J/):=0.147*(-D(/J/),0,1,2,B(/J,1/));
00324      BN(/J,J/):=2*RHQ*G*AA(/J/);
00325      HN:=3(/J,MP2/)/D(/J/);
00326      DB:=2A(/J/)/(B(/J,MP2/)*D(/J/));
00327      'IF' BN >= 0.03630*(10+HN+D(/J/)/B(/J,MP2/)) 'THEN'
00327      'BEGIN'  J:=-5*B(/J,MP2/)+SQRT(24*B(/J,MP2/)*3(/J,MP2/)+32*AA(/J/)/
00327      /PI);
00328      J:=1.0075*J;
00329      H:=B(/J,MP2/)/U;
00330      B3:=AA(/J/)/(B(/J,MP2/)*U);
00331      CCR(/J/):=2;
00332      'END';
00333      U:=4*RP/PI;
00334      V:=(4H-1)/(HH+1);
00335      V:=V*V;  R:=1-U;
00337      C1:=3+U+2*V;
00338      'IF' C1 > 4.5 'THEN' A3(/J/):=0 'ELSE'
00338      A3(/J/):=(-C1-C1+6+2*SQRT(9-C1-C1))/(C1+C1);
00339      A4(/J/):=(4H-1)*(A3(/J/)+1)/(HH+1);
00340      'END';
00341      SYSACT(2,14,2);
00342      OUTSTRING(1,('SECTIONAL AREA'));  SYSACT(1,14,2);
00344      OUTSTRING(1,('SECTION AREA (M2) SECTION AREA (M2)'));
00345      SYSACT(1,14,3);  OUTSTRING(1,(' 0'));
00347      FIX(1,8,2,4A(/O/)+AA(/J/));
00348      'FOR' J:=1 'STEP' 1 'UNTIL' JJ/2 'DO'
00348      'BEGIN'  SYSACT(1,14,1);
00349      FIX(1,3,0,J);  FIX(1,8,2,AA(/J/)+AA(/J/));
00351      FIX(1,6,0,J+10);  FIX(1,8,2,AA(/J+10/)+AA(/J+10/));
00353      'END';
00354      DDPL:=SIMP(-LL 2,LL 2, JJ, FUNC19);
00355      MLM:=SIMP(-LL 2,LL 2, JJ, FUNC20);
00356      DELAX:=-MLM/DDPL;
00357      CDPL:=2*RHQ*G*DDPL*CA;
00358      SYSACT(1,14,3);  OUTSTRING(1,('DISPLACEMENT ='));
00361      FIX(1,5,3,DDPL);  OUTSTRING(1,(' TON'));  SYSACT(1,14,1);
00363      OUTSTRING(1,(' LCB ='));  FIX(1,6,3,-DELTA);
00365      OUTSTRING(1,(' M'));
00366      SYSACT(1,14,4);  OUTSTRING(1,(' WAVE AMPLITUDE ZETA = 1.0 M'));
00368      SYSACT(1,14,4);
00369      LPD:=LL2+DELTA;
00370      LMD:=LL2-DELTA;
00371      'IF' = 5000 'THEN' 'GOTO' OVER;

```

SC SOURCE STATEMENT

```

00372 'COMMENT' * * * * * 00003890
00372 * * * * * 00003900
00372 * SHEARING FORCES AND BENDING MOMENTS IN STILL WATER * 00003910
00372 * * * * * 00003920
00372 * * * * * 00003930
00372 OUTSTRING(1,(' S T I L L   W A T E R ')); 00003940
00373 SYSACT(1,14,2); 00003950
00374 OUTSTRING(1,('SECTION SHEARING FORCE BENDING MOMENT')); 00003960
00375 SYSACT(1,14,1); 00003970
00376 OUTSTRING(1,(' (TON) (M-TON)')); 00003980
00377 SYSACT(1,14,1); 00003990
00378 'FOR' M:=0 'STEP' 2 'UNTIL' JJ=2 'DO' 00004000
00378 'BEGIN' X2:=LL*M/JJ-LPD; 00004010
00379 Z:=SIMP(XA,LPD,JJ-M,FUNC16); 00004020
00380 N:=3; GOS(1/M/2/1):=SIMP(XA,LPD,JJ-M,FUNC18)-X(N/M); 00004030
00382 MBS(1/M/2/1):=SIMP(XA,LPD,JJ-M,FUNC21)+Z; 00004040
00383 SYSACT(1,14,1); 00004050
00384 FIX(1,4,0,M); 00004060
00385 FIX(1,10,3,GOS(1/M/2/1)); 00004070
00386 FIX(1,11,3,MBS(1/M/2/1)); 00004080
00387 'END'; 00004090
00388 OVER: 'FOR' I:=0 'STEP' 1 'UNTIL' II 'DO' 00004100
00388 'FOR' J:=0 'STEP' 1 'UNTIL' JJ 'DO' 00004110
00388 'BEGIN' U:=R(J,MP2/1)/(1+A1(J/J)+A3(J/J)); 00004120
00389 X(I,J):=U*((1+A1(J/J))*SIN(THETA(I/J))-A3(J/J)* 00004130
00389 SIN(3*THETA(I/J))); 00004140
00390 Y(I,J):=U*((1-A1(J/J))*COS(THETA(I/J))+A3(J/J)* 00004150
00390 COS(3*THETA(I/J))); 00004160
00391 BETA(I,J):=ABS(ARCTAN(X(I,J)/Y(I,J))); 00004170
00392 'END'; 00004172
00393 'FOR' MA:=1 'STEP' 1 'UNTIL' AMO 'DO' 00004173
00393 'FOR' K:=1 'STEP' 1 'UNTIL' NV 'DO' 00004174
00393 'BEGIN' VA:=VD:=0; 00004175
00394 'FOR' Q:=1 'STEP' 1 'UNTIL' QQ 'DO' 00004176
00394 'BEGIN' 'IF' VV(K/Q)=0 'THEN' OMEGA(MA,K,Q):=SIGMAQ(Q/I) 00004177
00394 'ELSE' 00004178
00394 'BEGIN' VB:=0.5*G/(VV(K/Q))*COS(MUP(MA/Q)); 00004179
00395 VC:=4.0*VV(K/Q)*COS(MUP(MA/Q))*SIGMAQ(Q/I)/G; 00004180
00396 'IF' VC < 0.0 'THEN' 00004181
00396 OMEGA(MA,K,Q):=VB*(1.0-SQRT(1.0-VC)) 00004181
00395 'ELSE' 'IF' VGRG 'OR' VC>1.0 'THEN' 00004182
00395 OMEGA(MA,K,Q):=VB*(1.0+SQRT(1.0+VC)) 00004182
00395 'ELSE' 'IF' ABS(VC)>ABS(VA) 'AND' VD=0 'THEN' 00004183
00396 OMEGA(MA,K,Q):=VB*(1.0-SQRT(1.0-VC)) 00004184
00395 'ELSE' 'IF' ABS(VC)<ABS(VA) 'THEN' 00004185
00396 'BEGIN' VD:=1; 00004185
00397 OMEGA(MA,K,Q):=VB*(1.0+SQRT(1.0-VC)); 00004187
00398 'END'; 00004188

```



SC	SOURCE STATEMENT	SOURCE PROGRAM	PAGE 010
00398		ELSE: OMEGA (/MA, K, J) = VB * (1.0 + SQRT(1.0 + VC));	00004189
00399		VA = VC;	00004190
00400		END;	00004191
00401		END;	00004192
00402		FOR: Q=1 STEP 1 UNTIL QQ 'DO'	00004193
00402	BEGIN	SYSACT(1,15,5);	00004194
00403		OUTSTRING(1,('FREQUENCY OF ENCOUNTER OMEGA(E) ='));	00004200
00404		SQ:=SIGMAQ(/Q/); FIX(1,5,3,SQ);	00004220
00406		SYSACT(1,14,1);	00004230
00407		OUTSTRING(1,('-----'));	00004240
00407	---	);	00004250
00408		COMMENT: * * * * *;	00004260
00409		* SECTIONAL ADDED MASS AND DAMPING (PER FREQUENCY)	00004270
00409		* * * * *;	00004280
00409		* * * * *;	00004290
00409		* * * * *;	00004300
00409		SYSACT(1,14,5);	00004310
00409		OUTSTRING(1,('SECTION DAMPING ADDED MASS'));	00004320
00410		SYSACT(1,14,1);	00004330
00411		OUTSTRING(1,(' TONSEC/M2 TONSEC2/M2'));	00004340
00412		SYSACT(1,14,2);	00004350
00413		SIGMAQ:=S*SQ; GAMMAQ:=SICKW/S;	00004360
00415		FOR: J=0 STEP 1 UNTIL JJ 'DO'	00004370
00415	BEGIN	SYSACT(1,14,1); FIX(1,4,0,J);	00004380
00417		LEWIS(J,A1(/J/),A3(/J/));	00004400
00418		OUTSYMBOL(1,(' '),COP(/J/));	00004405
00419		FIX(1,7,3,HNACC(/J/));	00004410
00420		FIX(1,7,3,MACC(/J/));	00004420
00421	END	;	00004430
00422		MACCDX(/O/):=(MACC(/I/)-MACC(/O/))*I/LL;	00004440
00423		FOR: J=1 STEP 1 UNTIL JJ-1 'DO'	00004450
00423		MACCDX(/J/):=(MACC(/J+1/)-MACC(/J-1/))*JJ/(2*LL);	00004460
00424		MACCDX(/JJ/):=(MACC(/JJ/)-MACC(/JJ-1/))*JJ/LL;	00004470
00425		FOR: MA=1 STEP 1 UNTIL AHQ 'DO'	00004472
00425	BEGIN	COSHUR:=COS(HUR/MA/);	00004474
00426		FOR: K=1 STEP 1 UNTIL HV 'DO'	00004480
00426	BEGIN	SYSACT(1,15,1);	00004482
00427		OUTSTRING(1,('DIRECTION OF WAVE TRAVEL ='));	00004483
00428		FIX(1,3,3,HUR/MA/); OUTSTRING(1,(' RAD. '));	00004484
00430		SYSACT(1,14,1);	00004494
00431		OUTSTRING(1,('-----'));	00004485
00431	---	);	00004485
00432		OUTSTRING(1,('V =')); FIX(1,4,3,VV(/K/));	00004486
00435		OUTSTRING(1,(' M/SEC FH ='));	00004497
00436		FIX(1,3,3,VV(/K/)/SQRT(G*LL)); SYSACT(1,14,1);	00004498
00438		OUTSTRING(1,('-----'));	00004487

```

00439 SYSACT(1,14,3); OMKAKQ:=OMEGA/MA,K,Q/); 00004400
00441 'COMMENT' * * * * * 00004500
00441 * 00004510
00441 * WAVE COEFFICIENTS (PER FREQUENCY, PER ANGLE, PER 00004520
00441 * VELOCITY) * 00004525
00441 * 00004530
00441 * * * * * 00004540
00441 KKO:=OMKAKQ*OMAKQ/G; 00004570
00442 'ERR' J:=0 'SFFP' ) 'INFILE' JJ 'DOF' VMDMX(/J/)= 00004580
00442 'NACC(/J/)-VV(/K/)*OMACDX(/J/); 00004580
00443 A14:=SIMP(-LMD,LPD,JJ,FUNC6); 00004590
00444 'IF' DDDL 'THEN' U:=H(/O/)/G 00004610
00444 'ELSE' U:=DPL/G; 00004620
00445 OUTSTRING(1,(' WAVE FREQUENCY ='))); 00004660
00446 FIX(1,4,3,OMKAKQ); 00004670
00447 OUTSTRING(1,(' 1/SEC WAVE NUMBER K ='))); 00004680
00448 FIX(1,4,3,KKO); SYSACT(1,14,1); LAMDA:=2*PI/KKO; 00004690
00451 OUTSTRING(1,(' WAVE LENGTH ='))); 00004700
00452 FIX(1,4,3,LAMDA); LAMDA:=LAMDA/LL; 00004710
00454 OUTSTRING(1,(' M WAVE LENGTH RATIO ='))); 00004720
00455 FIX(1,4,3,LAMDA); V:=SQRT(1/LAMDA); 00004730
00457 OUTSTRING(1,(' APARENT WAVE LENGTH ='))); 00004730
00458 FIX(1,4,5,2*PI/KKO/ABS(COSMU)); 00004730
00459 OUTSTRING(1,(' SQ [ L/LA ='))); 00004735
00460 FIX(1,4,5,V); SYSACT(1,14,4); 00004735
00462 VD:=OMKAKQ*(1.0-OMKAKQ)*VV(/K/)*COSMU/R/G); 00004737
00463 'COMMENT' * * * * * 00004740
00465 * 00004750
00465 * HYDRODYNAMIC COEFFICIENTS FOR HEAVE AND PITCH * 00004760
00465 * (PER FREQUENCY, PER ANGLE, PER VELOCITY) * 00004770
00465 * 00004780
00465 * * * * * 00004790
00465 OUTSTRING(1,(' HYDRODYNAMIC COEFFICIENTS ='))); 00004800
00466 SYSACT(1,14,1); BLANK(1,32); 00004810
00466 OUTSTRING(1,(' HEAVE'))); SYSACT(1,14,2); 00004820
00468 OUTSTRING(1,(' ADDED MASS A ='))); FIX(1,7,3,A14); 00004830
00470 OUTSTRING(1,(' TONSEC2/M C ='))); 00004840
00471 B15:=SIMP(-LMD,LPD,JJ,FUNC7); 00004850
00472 AA:=2*SIMP(-LMD,LPD,JJ,FUNC8); 00004860
00473 C16:=RHO*G*AA; 00004870
00474 D17:=SIMP(-LMD,LPD,JJ,FUNC9); 00004880
00475 F18:=SIMP(-LMD,LPD,11,FUNC10)-2*VV(/K/)*A14; 00004890
00476 G19:=2*RHO*G*SIMP(-LMD,LPD,JJ,FUNC11)-VV(/K/)*B15; 00004900
00477 FIX(1,7,3,C16); OUTSTRING(1,(' TON/M'))); 00004910
00479 SYSACT(1,14,1); OUTSTRING(1,(' SHIP MASS ='))); 00004920
00481 FIX(1,7,3,U); 00004930
00482 OUTSTRING(1,(' TONSEC2/M C ='))); 00004940
00483 FIX(1,7,3,D17); OUTSTRING(1,(' TONSEC2'))); 00004950

```

SC	SOURCE STATEMENT		
00485		SYSACT(1,14,1);	OUTSTRING(1,('TOTAL MASS =')); 00004860
00487		FIX(1,7,3,A14+U);	00004870
00488		OUTSTRING(1,(' TONSEC2/M E ='));	00004880
00489		FIX(1,7,3,F18);	OUTSTRING(1,(' TONSEC')); 00004890
00491		SYSACT(1,14,1);	OUTSTRING(1,('DAMPING B =')); 00005000
00493		FIX(1,7,3,B15);	00005010
00494		OUTSTRING(1,(' TONSEC/M G ='));	00005020
00495		FIX(1,7,3,G13);	OUTSTRING(1,(' TON')); 00005030
00497		SYSACT(1,14,2);	BLANK(1,32); 00005040
00499		OUTSTRING(1,('PITCH'));	SYSACT(1,14,2); 00005050
00501		OUTSTRING(1,('ADDED MASS MOMENT OF INERTIA AA ='));	00005060
00502		AA20:=SIMP(-LMD,LPC,JJ,FUNC12);	00005070
00503		'IF' B=0L THEN	00005080
00503		V:=(2*SIMP(-LMD,LPC,JJ,FUNC17)+LMD*LMD*W/(G))/G	00005090
00503		'ELSE' V:=FACT*LL*FACT*LL*U;	00005100
00504		B21:=SIMP(-LMD,LPC,JJ,FUNC13)-2*VV/(K/)*D17;	00005110
00505		F22:=(13+2*VV/(K/)*A)4;	00005120
00506		I1W:=2*SIMP(-LMD,LPC,JJ,FUNC14);	00005130
00507		CC21:=RHO*G*I1W-VV/(K/)*E22;	00005140
00508		CC25:=G13+VV/(K/)*B15;	00005150
00509		FIX(1,9,3,AA20);	00005160
00510		OUTSTRING(1,(' MTONSEC2 CC ='));	00005170
00511		FIX(1,9,3,CC23);	OUTSTRING(1,(' MTON')); 00005180
00513		SYSACT(1,14,1);	00005190
00514		OUTSTRING(1,('MASS MOMENT OF SHIP ='));	00005200
00515		FIX(1,9,3,V);	OUTSTRING(1,(' MTONSEC2 DD =')); 00005210
00517		FIX(1,9,3,I17);	OUTSTRING(1,(' TONSEC2')); 00005220
00519		SYSACT(1,14,1);	00005230
00520		OUTSTRING(1,('TOTAL MASS MOMENT ='));	00005240
00521		FIX(1,9,3,AA20+V);	00005250
00522		OUTSTRING(1,(' MTONSEC2 EC ='));	00005260
00523		AA20:=AA20+V;	00005270
00524		FIX(1,9,3,E22);	OUTSTRING(1,(' TONSEC')); 00005280
00526		SYSACT(1,14,1);	OUTSTRING(1,('DAMPING')); 00005290
00528		BLANK(1,32);	OUTSTRING(1,('BB =')); 00005300
00530		FIX(1,9,3,B21);	00005310
00531		OUTSTRING(1,(' MTONSEC GG ='));	00005320
00532		FIX(1,9,3,GG25);	OUTSTRING(1,(' TON')); 00005330
00534		SYSACT(1,14,5);	00005340
00535		'COMMENT' * * * * *	00005350
00535		* * * * *	00005360
00535		* WAVE FORCES AND WAVE MOMENTS	* 00005370
00535		* (PER FREQUENCY, PER ANGLE, PER VELOCITY)	* 00005380
00535		* * * * *	* 00005390
00535		* * * * *	* 00005400
00535		A14:=A14+U;	00005410
00536		'FOR' J:=0 'STEP' 1 'UNTIL' JJ 'DO'	00005420
00536	'BEGIN'	XB:=-LL 2+DELTA+J*LL/JJ;	00005430

SC SOURCE STATEMENT

```

00537      U:=V:=R:=0.0;                                00005440
00538      'FOR' N:=0 'STEP' 1 'UNTIL' MP+1 'DO'        00005450
00539      'IF' B(/J,N+1/)+0.00001 < B(/J,N/)' THEN' V:=1; 00005460
00539      'IF' V=1 'THEN'                               00005470
00539      'BEGIN' Z:=-B(/J/)+D(/J/)/MP/3;              00005480
00540      T:=ABS(B(/J,1/)-B(/J,0/));                   00005490
00541      U:=U+T; R:=R+T*EXP(KKQ*Z);                   00005500
00543      Z:=-D(/J/)+2*B(/J/)/MP/3;                   00005510
00544      T:=ABS(B(/J,2/)-B(/J,1/));                   00005520
00545      U:=U+T; R:=R+T*EXP(KKQ*Z);                   00005530
00547      'FOR' N:=2 'STEP' 1 'UNTIL' MP+1 'DO'      00005540
00547      'BEGIN' Z:=-D(/J/)+(N-1)*D(/J/)/MP;          00005550
00548      T:=ABS(B(/J,N+1/)-B(/J,N/));                 00005560
00549      U:=U+T; R:=R+T*EXP(KKQ*Z);                   00005570
00551      'END';                                         00005580
00552      EKST(/J,K/):=R/U;                               00005590
00553      'END';                                         00005600
00553      'ELSE' EKST(/J,K/):=1-KKQ/B(/J,MP/1)*        00005610
00553      CFIAR(-D(/J/),0,1,Z,B(/J,1/)*EXP(KKQ*Z));  00005620
00554      R:=-KKQ*XB*CCSMUR;                             00005630
00555      V:=EKST(/J,K/)*COS(R);                       00005640
00556      U:=EKST(/J,K/)*SIN(R);                       00005650
00557      T:=2*RHQ*G*B(/J,MP/2/);                     00005660
00558      FM(/1,1/):=1*V;                               00005670
00559      FM(/2,1/):=T*U;                               00005680
00560      T:=OMMAKQ*YMMAKQ*MACC(/J/);                   00005690
00561      FM(/1,J/):=FM(/1,J/)-T*V;                     00005700
00562      FM(/2,J/):=FM(/2,J/)-T*U;                     00005710
00563      T:=OMMAKQ*YNDMX(/J/);                         00005720
00564      FM(/1,J/):=FM(/1,J/)-T*U; FM(/3,J/):=-FM(/1,J/)*XB; 00005730
00566      FM(/2,J/):=FM(/2,J/)+T*V;                     00005740
00567      'IF' 4.0*V/(K/)*CCSMUR<=0.0 'AND' VD < 0.0  00005744
00567      'THEN' FM(/2,J/):=-FM(/2,J/);                 00005745
00568      FM(/4,J/):=-FM(/2,J/)*XB;                     00005746
00569      'END';                                         00005760
00570      ALFAC:=KKQ;                                    00005770
00571      BLANK(1,14);                                   00005780
00572      OUTSTRING(1,('AMPLITUDE PHASE(IN DEGR.) COEFFICIENT 00005790
00572      SYSACT(1,14,2);                                00005800
00574      OUTSTRING(1,('WAVE FORCES'));                 00005810
00575      N:=1; FF1:=SIMP(-LMD,LPD,JJ,FUNC15);          00005820
00577      N:=2; FF2:=SIMP(-LMD,LPD,JJ,FUNC15);          00005830
00579      U:=ARCTAN(FF2/FF1);                             00005840
00580      'IF' FF1 'NOTGREATER' 0 'THEN' U:=PI+U;        00005850
00581      R:=SQRT(FF1*FF1+FF2*FF2);                     00005860
00582      V:=R/(RHQ*G*AAW);                              00005870
00583      FIX(1,6,3,R); OUTSTRING(1,('TON'));           00005880
00585      FIX(1,7,3,57.3*U); FIX(1,8,3,V); SYSACT(1,14,1); 00005890

```

SC SOURCE STATEMENT

```

00580 N1:=3; MM1:=SIMP(-LMD,LPD,JJ,FUNC15); 0000590
00590 N2:=4; MM2:=SIMP(-LMD,LPD,JJ,FUNC15); 0000591
00592 U:=ARCTAN(MM2/MM1); 0000592
00593 'IF' MM1 'NOTGREATER' 0 'THEN' U:=PI+U; 0000593
00594 R:=SQRT(MM1*MM1+MM2*MM2); 0000594
00595 V:=P/(RHF)*G*(IW*ALFAG); 0000595
00596 CUISTRING(J,'('WAVE MOMENTS')'); 0000596
00597 FIX(1,5,3,R); OUTSTRING(1,'('MTCN')'); 0000597
00599 FIX(1,6,3,57.3*U); FIX(1,8,3,V); SYSACT(1,14,5); 0000599
00602 'COMMENT' * * * * * * * * * * * * * * * * * * * * * * * * * * 0000599
00602 * * * * * * * * * * * * * * * * * * * * * * * * * * * * * * * * 0000600
00602 * VERTICAL MOTIONS 0000600
00602 * (PER FREQUENCY, PER ANGLE, PER VELOCITY) 0000601
00602 * * * * * * * * * * * * * * * * * * * * * * * * * * * * * * * * 0000602
00602 ALPHA:=A14*EA20-D17*D17; 0000603
00603 BET:=A14*SE21+B15*AA20-E17*EE22-E18*D17; 0000603
00604 GAMMA:=A; 4*CC23+B15*BE21+C16*AA20-D17*GG25- 0000604
00604 E18*EE22-G19*GG25; 0000605
00605 F1174:=B; 5*CC23+C16*BE21-F19*GG25-G19*EE22; 0000605
00606 EPSILON:=C16*CC23-G19*GG25; 0000606
00607 H1:=EPSILON-GAMMA*SIGK+ALPHA*SIGKW+SIGK; 0000607
00608 H2:=H1+H2+H3+H4; 0000608
00609 KAPPAZ:=CC23*FF1+G19*MM1-SQ*(B21*FF2+E18*MM2)-SIGKW* 0000609
00610 (AA20*FF1+D17*MM1); 0000610
00611 LABDAZ:=CC23*FF2+G19*MM2+SQ*(B21*FF1+E18*MM2)-SIGKW* 0000611
00612 (AA20*FF2+D17*MM2); 0000612
00613 KAPPAPSI:=C16*MM1+GG25*FF1-SQ*(B15*MM2+EE22*FF2)-SIGKW* 0000613
00614 (A14*MM1+D17*FF1); 0000614
00615 LABDAPSI:=C16*MM2+GG25*FF2+SQ*(B15*MM1+EE22*FF1)-SIGKW* 0000615
00616 (A14*MM2+D17*FF2); 0000616
00617 PIZ:=(KAPPAZ*MM1+LABDAZ*MM2)/HDEMER; 0000617
00618 PIPSI:=(LABDAPSI*MM1-KAPPAPSI*MM2)/HDEMER; 0000618
00619 RHOPSI:=(LABDAPSI*MM1-KAPPAPSI*MM2)/HDEMER; 0000619
00620 ZA:=SQRT(PIZ*PIZ+RHOPSI*RHOPSI); 0000620
00621 FASEZ:=ARCTAN(RHOPSI/PIZ); 0000621
00622 RAOZ(/MA,K,Q/):=ZA; 0000622
00623 PSIA:=SQRT(PIPSI*PIPSI+RHOPSI*RHOPSI); 0000623
00624 FASEPSI:=ARCTAN(RHOPSI/PIPSI); 0000624
00625 RAOPSI(/MA,K,Q/):=PSIA/KKQ; 0000625
00626 'IF' PIZ 'NOTGREATER' 0 'THEN' FASEZ:=FASEZ+PI; 0000626
00627 'IF' PIPSI 'NOTGREATER' 0 'THEN' FASEPSI:=FASEPSI+PI; 0000627
00628 OUTSTRING(1,'('VERTICAL MOTIONS :')'); SYSACT(1,14,2); 0000628
00629 OUTSTRING(1,'('WAVE : ZA =')'); FIX(1,4,3,ZZ); 0000629
00630 OUTSTRING(1,'('M PHASE =')'); 0000630
00631 FIX(1,4,3,FASEZ*57.3); 0000631

```

SC	SOURCE STATEMENT	
00632	OUTSTRING(1,(' DEGR. '));	SYSACT(1,14,1); 00006390
00634	OUTSTRING(1,(' PITCH : THETA = '));	00006400
00635	FIX(1,4,3,PSIA*57.3);	00006410
00636	OUTSTRING(1,(' DEGR. PHASE = '));	00006420
00637	FIX(1,4,3,FASEPSI*57.3);	00006430
00638	OUTSTRING(1,(' DEGR. THETA/HAVE SLOPE = '));	00006440
00639	FIX(1,4,3,RAOPSI(/MA,K,Q));	SYSACT(1,14,4); 00006450
00641	!COMMENT: * * * * *	00006460
00641	* * * * *	* 00006470
00641	* RELATIVE MOTIONS	* 00006480
00641	* (PER FREQUENCY,PER ANGLE,PER VELOCITY)	* 00006490
00641	* * * * *	* 00006500
00641	* * * * *	* 00006510
00643	OUTSTRING(1,(' RELATIVE MOTIONS : '));	SYSACT(1,14,2); 00006520
00644	OUTSTRING(1,(' LENGTH AMPLITUDE PHASE '));	00006530
00645	SYSACT(1,14,1);	00006540
00645	OUTSTRING(1,(' 4 4 DEGR. '));	00006550
00647	SYSACT(1,14,2);	00006560
00647	WJ:=Z4*COS(FASE7);	00006570
00648	VJ:=Z4*SIN(FASE7);	00006580
00649	C1:=PSIA*COS(FASEPSI);	00006590
00650	XA:=PSIA*SIN(FASEPSI);	00006600
00651	!FOR: N:=1 !STEP: 1 !UNTIL: NS !DO:	00006610
00651	!BEGIN: R:=L(/N/)+DELTA X;	00006620
00652	U:=COS(KK)*R+COSMUJ)-WJ+E*C1;	00006630
00653	V:=SIN(-KK)*R+COSVUR)-VJ+R*XA;	00006640
00654	ZR(/MA,K,Q/N/):=R:=SQRT(U*U+V*V);	00006650
00655	T:=ARCTAN(V/U);	00006660
00656	!IF: U !NOT GREATER: 0 !THEN:	00006670
00656	T:=T+PI;	00006680
00657	FIX(1,3,3,L(/N/));	FIX(1,5,3,R); 00006690
00659	FIX(1,5,3,T*57.3);	SYSACT(1,14,1); 00006700
00661	!END;	00006710
00662	!COMMENT: * * * * *	* 00006720
00662	* * * * *	* 00006730
00662	* ACCELERATIONS	* 00006740
00662	* (PER FREQUENCY,PER ANGLE,PER VELOCITY)	* 00006750
00662	* * * * *	* 00006760
00662	* * * * *	* 00006770
00662	SYSACT(1,3,REGEL);	00006780
00663	!IF: REGEL>20 !THEN: SYSACT(1,15,5)	00006790
00663	!ELSE: SYSACT(1,14,5);	00006800
00664	OUTSTRING(1,(' ACCELERATIONS: '));	SYSACT(1,14,2); 00006810
00666	OUTSTRING(1,(' SECTION AMPLITUDE PHASE '));	00006820
00667	SYSACT(1,14,1);	00006830
00668	OUTSTRING(1,(' /SEC2 DEGR. '));	00006840
00667	SYSACT(1,14,2);	00006850
00670	!FOR: J:=0 !STEP: 2 !UNTIL: JJ !DO:	00006860

```

00670          'BEGIN'      I:=J/2;                      00006840
00671          XB:=J*LL/JJ-LMD;                          00006850
00672          U:=MU-XB*CI;                               00006860
00673          V:=NU-XB*XI;                               00006870
00674          ACC(/MA,K,0,M/):=R:=SQRT(U*U+V*V);         00006880
00675          T:=ARCTAN(V/U);                            00006890
00676          'IF' UC=0 'THEN' T:=T+PI;                 00006900
00677          FIX(1,4,0,J);  FIX(1,2,3,F*SIGKW);        00006910
00679          FIX(1,4,3,57.3*T);  SYSACT(1,14,1);       00006920
00681          'END';                                       00006930
00682          'COMMENT' * * * * * * * * * * * * * * * * * 00006940
00682          * * * * * * * * * * * * * * * * * * * * * 00006950
00682          * ADDED RESISTANCE                          * 00006960
00682          * (PER FREQUENCY, PER ANGLE, PER VELOCITY) * 00006970
00682          * * * * * * * * * * * * * * * * * * * * * 00006980
00682          'FOR' J:=0 'STEP' 1 'UNTIL' JJ 'DO'       00006990
00682          'BEGIN'   XB:=-LMD+J*LL/JJ;              00007000
00683          T:=EKST(/J,K/)*OMMAKQ;  R:=KK)*XB*COSMUR; 00007010
00685          U:=-SQ*FHQZ+XB*SQ*RHQPSI+VV(/K/)*PIPSI+T*SI*(-P); 00007020
00686          V:=-SQ*PIZ+XB*SQ*PIPSI-VV(/K/)*RHQPSI+T*COS(R); 00007030
00687          FM(/5,J/):=0.5*(U*U+V*V)*VNDMX(/J/);     00007040
00689          'END';  SYSACT(1,14,1);                  00007050
00689          T:=RHQ*G*3(/JJ/2,MP2/)*R(/JJ/2,MP2/)/LL*16; 00007060
00691          N:=5;  RAW:=SIMP(-LMD,LPD,JJ,FUNC15);      00007070
00693          RAN:=-RAN*KKQ*COSMUR/SQ;                  00007075
00694          'IF' 4.0*VV(/K/)*COSMUR*SQ/G > 0.0 'AND' VD < 0.0 'THEN' 00007080
00694          RAW:=-RAN;  RAWZ(/MA,K,0/):=RAW;         00007085
00696          SYSACT(1,14,3);  OUTSTRING(1,('ADDED RESISTANCE: ')); 00007090
00698          SYSACT(1,14,1);  OUTSTRING(1,('RAW ='));   00007100
00700          FIX(1,5,3,RAW);  OUTSTRING(1,('FORM'));   00007110
00702          SYSACT(1,14,1);  OUTSTRING(1,('RAW -NON DIM. =')); 00007120
00704          FIX(1,5,3,RAW/T);SYSACT(1,14,3);         00007130
00706          'IF' 5 'BOUL' 'THEN' 'GOTO' NEG;         00007140
00707          'COMMENT' * * * * * * * * * * * * * * * * * 00007150
00707          * * * * * * * * * * * * * * * * * * * * * 00007160
00707          * SHEARING FORCES AND BENDING MOMENTS IN REGULAR WAVES* 00007170
00707          * (PER FREQUENCY, PER ANGLE, PER VELOCITY) * 00007180
00707          * * * * * * * * * * * * * * * * * * * * * 00007190
00707          * * * * * * * * * * * * * * * * * * * * * 00007200
00707          'FOR' J:=0 'STEP' 1 'UNTIL' JJ 'DO'     00007210
00707          'BEGIN'   XB:=J*LL/JJ-LMD;              00007220
00708          U:=XB*PIPSI-PIZ;                          00007230
00709          V:=XB*RHQPSI-RHQZ;                        00007240
00710          DM(/1,J/):=FM(/1,J/)+2*FHQ*G*3(/J,MP 2/)*U-VNDMX(/J/)* 00007250
00710          (V*SQ+VV(/K/)*PIPSI)-HACC(/J/)*         00007260
00710          (U*SIGKW-2*VV(/K/)*RHQPSI*SQ);          00007270
00711          DM(/2,J/):=FM(/2,J/)+2*FHQ*G*3(/J,MP 2/)*V-VNDMX(/J/)* 00007280

```

```

00711          (VV(/K/)*RHOPSI-U*SQ)-IACC(/J/)*          00007390
00711          (V*SIGKW+2*VV(/K/)*PIPSI*SQ);          00007300
00712          'END';          00007310
00713          R:=PHO*G*LL*B(/JJ/2,MP2/)*2.0;          00007320
00714          BLANK(1,16);          00007330
00715          DJFSTRING(1,('S H E A R I N G   F O R C E S'));          00007340
00716          BLANK(1,22);          00007350
00717          DJFSTRING(1,('B E N D I N G   M O M E N T S'));          00007360
00718          SYSACT(1,14,4);          00007370
00719          DJFSTRING(1,('SECTION AMPLITUDE PHASE AMPLITUDE          00007400
TILL WATER          AMPLITUDE PHASE AMPLITUDE STILL WATER'));          00007410
00720          SYSACT(1,14,1);          00007420
00721          DJFSTRING(1,('          (TON)          (NON DIM.)          00007430
          (TON)          (NON DIM.)'));          00007440
00722          SYSACT(1,14,2);          00007450
00723          'FOR' M:=0 'STEP' 2 'UNTIL' JJ-2 'DO'          00007480
00723          'BEGIN' XA=LL*M/JJ-L/D;          00007490
00724          'FOR' J:=0 'STEP' 1 'UNTIL' JJ 'DO'          00007500
00724          'BEGIN' T:=(M-J)*LL/JJ;          00007510
00725          DM(/4,J/):=DM(/1,J/)*T;          00007520
00726          DM(/5,J/):=DM(/2,J/)*T;          00007530
00727          DM(/6,J/):=DM(/J/)*T;          00007540
00728          'END';          00007550
00729          Z:=SIMP(XA,LPD,JJ-M,FUNC18);          00007560
00730          N:=1; ALPHA:=SIMP(XA,LPD,JJ-M,FUNC18)+SIGKW/G*((PIZ-00007570
00731          PIPSI*XA)*W(/(XA+L/D)*JJ/LL/)-PIPSI*Z);          00007580
00732          N:=2; BET:=SIMP(XA,LPD,JJ-M,FUNC18)+SIGKW/G*((PHOZ-00007590
00733          RHOPSI*XA)*W(/(XA+L/D)*JJ/LL/)-RHOPSI*Z);          00007600
00734          U:=SQRT(ALPHA*ALPHA+BET*BET);          00007610
00735          EPSILON:=ARCTAN(BET/ALPHA)*57.3;          00007620
00736          'IF' ALPHA <= 0 'THEN' EPSILON:= EPSILON+180;          00007630
00737          DELTA:=MMBS(/M/2/);          00007640
00738          V:=ABS(DELTA)+U;          00007650
00739          MMBS(/MA,K,Q,M/2/):=U/P;          00007660
00740          FIX(1,4,0,M);          FIX(1,3,3,U);          00007670
00742          FIX(1,4,3,EPSILON);          FIX(1,6,3,U/R);          00007680
00744          FIX(1,7,3,DELTA);          00007690
00745          N:=6; T:=SIMP(XA,LPD,JJ-M,FUNC18);          00007700
00747          N:=4; ALPHA:=SIMP(XA,LPD,JJ-M,FUNC18)-((PIZ-PIPSI*XA          00007710
00748          )+Z+2*PIPSI*T)*SIGKW/G;          00007720
00749          N:=5; BET:=SIMP(XA,LPD,JJ-M,FUNC18)-((PHOZ-RHOPSI*XA          00007730
00750          )+Z+2*RHOPSI*T)*SIGKW/G;          00007740
00751          U:=SQRT(ALPHA*ALPHA+BET*BET);          00007750
00752          EPSILON:=ARCTAN(BET/ALPHA)*57.3;          00007760
00753          'IF' ALPHA <= 0 'THEN' EPSILON:= EPSILON+180;          00007770
00754          DELTA:=MMBS(/M/2/);          00007780
00755          V:=ABS(DELTA)+U;          00007790
00756          MMBS(/MA,K,Q,M/2/):=U/(R*LL);          00007800

```



SC	SOURCE STATEMENT	SOURCE PROGRAM	PAGE 018
00757		FIX(1,14,3,U);	00007810
00759		FIX(1,4,3,EPSILON);	00007820
00761		FIX(1,6,3,U/(R=LL));	00007830
00762		FIX(1,7,3,DELTA);	00007835
00763		SYSACT(1,14,1);	00007850
00763	WEG: 'END';		00007840
00764	'END';		00007860
00765	WEG: 'END';		00007870
00766	'END';		00007880
00767	'COMMENT' * * * * *		00007900
00767	* * * * *		00007900
00767	* THE END OF THE FIRST BLOCK		00007910
00767	* * * * *		00007920
00767	* * * * *		00007930
00767	* THE BEGINNING OF THE SECOND BLOCK		00007940
00767	* * * * *		00007950
00767	* * * * *		00007960
00767	* * * * *		00007970
00767	'BEGIN' 'REAL' ALF,DP,P,PQ,DELTA2,KF,NW,LE,SP,T;		00007980
00767	VSQ,VSS,VKQ,VKR,FP,FC,CC,CP,EPS,MR,CFL,CF2;		00007990
00768	'LOGICAL' PIERSON;		00008000
00769	'INTEGER' BF,BU,M,A,QA,QM,AM,AT,RT,ST;		00008010
00770	MINILOGR(O,BF);MINILOGR(O,QM);		00008020
00772	INBDLEA(N,PIERSON);		00008030
00773	'IF' NOT PIERSON 'AND' QM 'GREATER' QO 'THEN' A:=GM;		00008040
00773	'ELSE' A:=QO;		00008050
00774	'BEGIN' 'ARRAY' OFZ,OFV,OFY,OFK,OFB,OFDA,OFMA,OFB,OFPA,OFPA/(1:QO/),		00008060
00774	OFF,OFH,OFM,SPSEA(1:A/),F(1:MS/),SPS(1:BF,1:QO/),		00008070
00774	HS,FH(1:BF/),GMDM,GMSD,OMGM,OPGM(1:BF,1:GM/),		00008080
00774	OPC,OPMG(1:QO,0:0.5*JJ/),OPP,OPR(1:QO,1:MS/),		00008090
00774	OFAC(1:QO,0:0.5*JJ/);		00008100
00775	'PROCEDURE' TRAPREG(XY,YY,NW,INT);		00008110
00776	'REAL' INT; 'INTEGER' NW; 'ARRAY' XX,YY;		00008120
00779	'BEGIN' 'INTEGER' ST; INT:=0;		00008130
00781	'FOR' ST=1 'STEP' 1 'UNTIL' NW-1 'DO' INT:=INT+		00008140
00782	ABS(XX/(ST+1/)-XX/(ST/))/2*(YY/(ST+1/)+YY/(ST/));		00008150
00782	'END' TRAPREG;		00008160
00783	'PROCEDURE' OUTYGER(I); 'INTEGER' I;		00008170
00785	'BEGIN' 'IF' I=1 'THEN' 'GOTO' THREE;		00008180
00786	TRAPREG(OFF,SPSEA,QA,KF); TRAPREG(OFF,OFH,QA,NW);		00008190
00788	TRAPREG(OFF,OFM,QA,VSQ); EPS:=SQRT((KF*VSS-NW*NW)/KF/		00008200
00789	VSQ); VKQ:=SQRT(NW/KF)/2/PI;		00008210
00791	VKR:=SQRT(VSQ/NW)/2/PI; VSSQ:=VKQ/VKR; SYSACT(1,14,3);		00008220
00794	OUTSTRING(1,('HAVE'));		00008230
00795	TWEE: SYSACT(1,14,2); OUTSTRING(1,('M' = ));		00008240
00797	'IF' I=3 'THEN'		00008250
00797	'BEGIN' FIX(1,4,5,3233.29*KF); OUTSTRING(1,(' DEGR. '));		00008255
00799	SYSACT(1,14,1); OUTSTRING(1,('AMPL /3 ='));		00008260

```

00301          KF:=SQRT(KF);                                00009270
00802          FIX(1,4,4,114.6*KF);  OUTSTRING(1,(' DEGR.')); 00009290
00804          SYSACT(1,14,1);  OUTSTRING(1,('AMPL 1/10 =')); 00009300
00806          FIX(1,4,4,146.115*KF);  OUTSTRING(1,(' DEGR.')); 00009310
00808          'GOTO' EIND;                                  00009320
00809          'ELSE'                                       00009330
00809          'BEGIN'  FIX(1,4,5,KF);  OUTSTRING(1,(' M2'));  00009332
00811          SYSACT(1,14,1);  OUTSTRING(1,('AMPL 1/3 ='));  00009334
00813          KF:=SQRT(KF);                                00009336
00814          FIX(1,4,4,KF+KF);  OUTSTRING(1,(' M'));        00009340
00816          SYSACT(1,14,1);  OUTSTRING(1,('AMPL 1/10 ='));  00009350
00818          FIX(1,4,4,2.55*KF);  OUTSTRING(1,(' M'));      00009360
00820          'IF' I=2 'THEN' 'GOTO' EIND;                 00009370
00821          'END';                                       00009380
00822          SYSACT(1,14,2);                                00009390
00823          OUTSTRING(1,('SROADNESS FACTOR (EPS) ='));      00009400
00824          FIX(1,4,3,EPS);  SYSACT(1,14,2);             00009410
00826          OUTSTRING(1,(' NO ='));  FIX(1,4,3,VKQ);      00009420
00828          SYSACT(1,14,1);  I:=1/VKQ;                  00009430
00830          OUTSTRING(1,(' I ='));  FIX(1,4,3,I);        00009440
00832          OUTSTRING(1,(' SEC'));  SYSACT(1,14,1);      00009450
00834          OUTSTRING(1,(' H1 ='));  FIX(1,4,3,VKR);      00009460
00836          SYSACT(1,14,1);                                00009470
00837          OUTSTRING(1,(' H0/H1 ='));  FIX(1,4,3,VSSQ);   00009480
00839          SYSACT(1,14,1);                                00009490
00840          'END' UIVTLE;                                  00009500
00841          'COMMENT' * * * * *                          00009510
00841          *                                             * 00009520
00841          *  D A T A  I N P U T                          * 00009530
00841          *                                             * 00009540
00841          * * * * * * * * * * * * * * * * * * * * * * * 00009550
00841          INREAL(0,ALF); INREAL(0,DELTAZ); INREAL(0,FP); 00009560
00844          INREAL(0,FD); INREAL(0,FC); INREAL(0,CP);     00009570
00847          INREAL(0,LE); INREAL(0,DP); INARRAY(0,F);     00009580
00850          'IF' = PIERSON 'THEN' 'GOTO' KORF;            00009590
00851          INARRAY(0,HS); INARRAY(0,PM); INREAL(0,CF1); INREAL(0, 00009600
00854          CF2); ININTEGER(0,AH); ININTEGER(0,AT); ININTEGER(0, 00009610
00857          I); ININTEGER(0,RT); ININTEGER(0,ST);         00009620
00860          KORF: Q4:=Q3;                                  00009630
00861          'FOR' MA=1 'STEP' 1 'UNTIL' AND 'DO'          00009632
00861          'BEGIN'  'FOR' K=1 'STEP' 1 'UNTIL' NV 'DO'  00009634
00861          'BEGIN'  P:=SQRT(ALF); V3:=VV/(K)*COS(MUR/MA); 00009636
00864          OUTSTRING(1,('DIRECTION OF WAVE TRAVEL ='));  00009638
00865          FIX(1,3,3,MUR/MA);  OUTSTRING(1,(' RAD. '));  00009640
00867          SYSACT(1,14,1);                                00009642
00868          OUTSTRING(1,('-----'))' 00009644
00868          ; SYSACT(1,14,2);  OUTSTRING(1,('V ='));      00009646
00871          FIX(1,3,3,VV/(K));  OUTSTRING(1,(' W/SFC FN =')); 00009648

```

```

00373          FIX(1,4,3,VV/(K)/SQRT(G*LL)); SYSACT(1,14,1);      00008650
00375          OUTSTRING(1,('_____'));                        00008652
00376          SYSACT(1,14,4);                                    00008654
00377          'IF' PIERSON 'THEN'                                00008660
00377 'BEGIN' 'COMMENT' * * * * *                                00008680
00377          * * * * *                                          00008690
00377          * SEASPECTRUM FOR ZERO SPEED (CALCULATED)        00008700
00377          * * * * *                                          00008710
00377          * * * * *                                          00008720
00377          OUTSTRING(1,('SEASPECTRUM FOR ZERO SPEED'));      00008730
00378          'FOR' Q:=1 'STEP' 1 'UNTIL' Q=QD;                00008740
00379          OFF(/Q/)=OMEGA(MA,K,Q)/P;                           00008750
00379          'FOR' UU:=1 'STEP' 1 'UNTIL' BF 'DO'              00008760
00379          'BEGIN' 'IF' UU=1 'THEN' SYSACT(1,14,2)            00008770
00379          'ELSE' SYSACT(1,15,9);                              00008780
00380          OUTSTRING(1,('SPECTRUM :'));                       00008790
00381          FIX(1,4,0,UU); SYSACT(1,14,3);                    00008800
00383          OUTSTRING(1,(' OMEGA WAVE SPECTRUM'));            00008810
00384          SYSACT(1,14,1);                                     00008820
00385          OUTSTRING(1,(' 1/SEC      M2SEC'));                00008830
00386          SYSACT(1,14,2);                                    00008840
00387          'FOR' Q:=1 'STEP' 1 'UNTIL' Q=QD;                  00008850
00387          'BEGIN' SPS(/UU,Q/)=((CF1*MS(/UU/)**4H/PM(/UU/)**4T/ 00008870
00387          OFF(/Q/)**RT)*EXP(-CF2/PM(/UU/)**RT/CF0)          00008880
00387          OFF(/Q/)**S1);                                     00008890
00389          FIX(1,3,3,OFF(/Q/));                               00008900
00389          SP:=SPSEA(/Q/)=SPS(/UU,Q/);                       00008900
00390          FIX(1,3,3,SP); SYSACT(1,14,1);                    00008910
00392          OFN(/Q/)=SP*OFF(/Q/)=OFF(/Q/);                   00008920
00393          OFF(/Q/)=OFN(/Q/)*OFF(/Q/)*OFF(/Q/);              00008930
00394          SPS(/UU,Q/)=SP/ALF/ALF/P;                          00008940
00395          'END';                                             00008950
00396          OUTVOER(1);                                         00008960
00397          'END';                                             00008970
00398          'END';                                             00008980
00398          'ELSE'                                           00008990
00398          'BEGIN' 'COMMENT' * * * * *                                00009010
00398          * * * * *                                          00009020
00398          * SEASPECTRUM FOR ZERO SPEED (MEASURED)          00009030
00398          * * * * *                                          00009040
00398          * * * * *                                          00009050
00398          QA:=GM;                                           00009060
00399          'IF' K>1 'OR' MA>1 'THEN' 'GOTO' MEET;           00009070
00399          OUTSTRING(1,('SEASPECTRUM FOR ZERO SPEED'));      00009080
00400          INARRAY(0,GM*MA); INARRAY(0,GM*SP);               00009090
00401          'FOR' UU:=1 'STEP' 1 'UNTIL' BF 'DO'              00009100
00403          'BEGIN' 'IF' UU=1 'THEN' SYSACT(1,14,3)            00009110
00403          'ELSE' SYSACT(1,15, 8);                             00009120

```

SC SOURCE STATEMENT

```

00904      OUTSTRING(1,('MEASURED SPECTRUM :')) ;      00009130
00905      FIX(1,4,0,U) ;      SYSACT(1,14,2) ;      00009140
00907      OUTSTRING(1,(' OMEGA WAVE SPECTRUM')) ;      00009150
00908      SYSACT(1,14,1) ;      00009160
00909      OUTSTRING(1,(' 1/SEC M2SEC')) ;      00009170
00910      SYSACT(1,14,2) ;      00009180
00911      'FOR' Q:=1 'STEP' 1 'UNTIL' GM 'DO'      00009190
00911      'BEGIN' FIX(1,3,3,GM*(/UU,Q/)) ;      00009200
00912      FIX(1,8,3,GM*(/UU,Q/)) ;      SYSACT(1,14,1) ;      00009210
00914      SPSEA(/Q/)=GMSP(/UU,Q/);      00009220
00915      OFF(/Q/)=GMOM(/UU,Q/);      00009230
00916      OFN(/Q/)=SPSEA(/Q/)*OFF(/Q/)*OFF(/Q/);      00009240
00917      OFM(/Q/)=OFN(/Q/)*OFF(/Q/)*OFF(/Q/);      00009250
00918      'GM*(/UU,Q/)=GMOM(/UU,Q/)*P;      00009260
00919      SPGM(/UU,Q/)=GMSP(/UU,Q/)/ALF/ALF/P;      00009270
00920      'END';      00009280
00921      'UTVDER(1);      00009290
00922      'END';      00009300
MEEI:      'FOR' UU:=1 'STEP' 1 'UNTIL' BF 'DO'      00009310
00923      'FOR' Q:=1 'STEP' 1 'UNTIL' QJ 'DO'      00009320
00923      'FOR' M:=1 'STEP' 1 'UNTIL' GM-1 'DO'      00009330
00923      'BEGIN' QA:=M+1; QMMAKQ:=OMEGA(/MA,K,Q/);      00009340
00925      'IF' OMEGA(/MA,K,1/) < QMMAKQ 'THEN'      00009350
00925      'BEGIN' 'IF' QMMAKQ >= QMGH(/UU,M/) &      00009360
00925      QMMAKQ <= QMGH(/UU,QA/)      00009370
00925      'THEN' 'GOTO' KAMP      00009380
00925      'ELSE' 'GOTO' KLUIS      00009390
00925      'END';      00009400
00925      'ELSE' 'IF' QMMAKQ <= QMGH(/UU,M/) &      00009410
00925      QMMAKQ >= QMGH(/UU,QA/) 'THEN'      00009420
00925      KAMP:      'BEGIN' SPS(/UU,Q/)=SPGM(/UU,M/)+(SPGM(/UU,QA/)-SPGM(/UU,      00009440
00925      M/))* (QMMAKQ-QMGH(/UU,M/)) /      00009450
00925      (QMGH(/UU,QA/)-QMGH(/UU,M/));      00009460
00926      M:=GM-1;      00009470
00927      'END';      00009480
00927      'ELSE'      00009490
00927      KLUIS:      'IF' M=GM-1 'THEN'      00009500
00927      'BEGIN' SYSACT(1,14,1);      00009510
00928      OUTSTRING(1,('GEVRAAGDE FREQUENTIE LIGT NIET IN      00009520
00928      GEMETEN SPECTRUM')) ;      SPS(/UU,Q/)=0;      00009530
00930      'END';      00009540
00931      'END';      00009550
00932      'END';      00009560
00933      P:=(R+G*LL*2*B(/JJ/2,MP2/))**2;      00009570
00934      P2:=P*LL*LL;      00009580
00935      QA:=QJ;      00009590
00936      SYSACT(1,15,1);      00009600
00937      'OUTSTRING(1,('DIRECTION OF WAVE TRAVEL =')) ;      00009620

```

SC SOURCE STATEMENT

```

00938      FIX(1,3,3,MUR(/MA/)); OUTSTRING(1,(' RAD. '));          00009622
00940      SYSACT(1,14,1);                                           00009623
00941      GJFSTRING(1,('-----')));                               00009624
00941 );
00941      SYSACT(1,14,2); OUTSTRING(1,(' V = '));                   00009625
00944      FIX(1,3,3,VV(/K/)); OUTSTRING(1,(' W/SEC FN = '));       00009626
00946      FIX(1,4,3,VV(/K/)/SQRT(G*LL)); SYSACT(1,14,1);          00009627
00948      OUTSTRING(1,('-----')));                               00009628
00949      SYSACT(1,14,2);                                           00009629
00950      'FOR' M:=1 'STEP' 1 'UNTIL' BF 'DO'
00950      'BEGIN' 'IF' M=1 'THEN' SYSACT(1,14,1)                      00009630
00950      'ELSE' SYSACT(1,15,5);                                     00009631
00951      'IF' PIERSON 'THEN' OUTSTRING(1,(' SPECTRUM : '));         00009632
00951      'ELSE' OUTSTRING(1,(' MEASURED SPECTRUM : '));           00009633
00952      FIX(1,4,0,UU); SYSACT(1,14,3);                             00009634
00954      'COMMENT' * * * * * * * * * * * * * * * * * * * * * * * * 00009635
00954      * * * * * * * * * * * * * * * * * * * * * * * * * * * * 00009636
00954      * WAVE SPECTRUM, HEAVE SPECTRUM, PITCH SPECTRUM AND      * 00009637
00954      * ADDED RESISTANCE SPECTRUM                               * 00009638
00954      * (PER ANGLE, PER VELOCITY, PER SPECTRUM)                * 00009639
00954      * * * * * * * * * * * * * * * * * * * * * * * * * * * * 00009640
00954      * * * * * * * * * * * * * * * * * * * * * * * * * * * * 00009641
00954      OUTSTRING(1,(' OMEGA (F) WAVE SPECTRUM HEAVE SPECTRUM 00009642
00954      ' PITCH SPECTRUM ADDED RESIST. SPECTRUM : ')); SYSACT(1,14,1); VA:=0; 00009643
00957      'FOR' Q:=1 'STEP' 1 'UNTIL' OQ 'DO'
00957      'BEGIN' SQ:=SIGMA(/Q/); SIGMA:=SQ*SQ;                     00009644
00959      VC:=4.0*V8*SQ/G;                                           00009645
00960      VD:=OMEGA(/MA,K,Q/)*(1.0-OMEGA(/MA,K,Q/)*V8/G);           00009646
00961      'IF' VV(/K/)=0.0 'THEN' SP:=SPS(/UU,Q/);                   00009647
00961      'ELSE' 'IF' VCG 'THEN'                                       00009648
00961      SP:=SPS(/UU,Q/)/SQRT(1.0-VC)                               00009649
00961      'ELSE' 'IF' VCG<0 'THEN'                                    00009650
00961      SP:=SPS(/UU,Q/)/SQRT(1.0+VC)                               00009651
00961      'ELSE' 'IF' VC>VA 'THEN'                                    00009652
00961      SP:=SPS(/UU,Q/)/SQRT(1.0-VC)                               00009653
00961      'ELSE' SP:=-SPS(/UU,Q/)/SQRT(1.0-VC);                     00009654
00962      VA:=VC;                                                     00009655
00963      SPS:=A(/Q/):=SP; OFF(/Q/):=SQ;                               00009656
00965      OFN(/Q/):=SP*OFF(/Q/)*OFF(/Q/);                             00009657
00966      OFM(/Q/):=OFN(/Q/)*OFF(/Q/)*OFF(/Q/);                     00009658
00967      OFZ(/Q/):=SP*RAOZ(/MA,K,Q/)**2;                             00009659
00968      OFS(/Q/):=SP*RAOSI(/MA,K,Q/)**2*OMEGA(/MA,K,Q/)**4      00009660
00968      /G/G;                                                       00009661
00969      OFRW(/Q/):=SP*RAWZ(/MA,K,Q/);                                00009662
00970      SYSACT(1,14,1); FIX(1,3,3,OFF(/Q/));                       00009663
00972      FIX(1,3,4,SP); FIX(1,10,4,OFZ(/Q/));                       00009664
00974      FIX(1,10,4,OFM(/Q/)); FIX(1,10,4,OFN(/Q/));               00009665
00976      'IF' NOT BCOL 'THEN' 'GOTO' GPROB;                          00009666
00977      'FOR' M:=0 'STEP' 2 'UNTIL' JJ-1.3 'DO'                    00009667

```

SC

SOURCE STATEMENT

SOURCE PROGRAM

PAGE 023

```

00977 'BEGIN' I:=M/2; 00009940
00978 OFD(/Q,I/):=SP*ODD(/MA,K,Q,I/)**2; 00009950
00979 OFMB(/Q,I/):=SP*MMB(/MA,K,Q,I/)**2; 00009960
00980 'END'; 00009970
00981 GADEN: 'FOR' N:=1 'STEP' 1 'UNTIL' NS 'DO' 00009980
00982 'BEGIN' OFP(/Q,N/):=SP*ZR(/MA,K,Q,N/)**2; 00009990
00983 OFR(/Q,N/):=OFP(/Q,N/)*SIGKW; 00010000
00984 'END'; 00010010
00984 'FOR' J:=0 'STEP' 2 'UNTIL' JJ 'DO' OFAC(/Q,J/):=00010020
00984 SP*FA(/Q/)*ACC(/MA,K,Q,J/2/)*SIGKW*SIGKW; 00010030
00985 OFV(/Q/):=SP*ZR(/MA,K,Q,NS/)**2; 00010040
00986 OFY(/Q/):=OFV(/Q/)*SIGKW; 00010050
00987 OFK(/Q/):=OFV(/Q/)*(1+FP*(DELTAZ-FD)*SIGMAQ(/Q/)* 00010060
00988 SQRT(LL/G))**2; 00010070
00988 OFB(/Q/):=OFK(/Q/)*SIGKW; 00010080
00989 'END'; 00010090
00990 UTIVER(1); 00010100
00991 TRAPREG(OFF,OFZ,QQ,KF); 00010110
00992 SYSACT(1,14,2); OUTSTRING(1,('HEAVE'))); 00010120
00994 UTIVER(2); 00010130
00995 TRAPREG(OFF,OF3,QQ,KF); 00010140
00996 SYSACT(1,14,2); OUTSTRING(1,('PITCH'))); 00010150
00998 UTIVER(3); SYSACT(1,3,REGEL); 00010160
01000 'IF' REGEL+9*NS>59 'THEN' SYSACT(1,15,2) 00010170
01000 'ELSE' SYSACT(1,14,2); 00010180
01001 'IF' UJ=-1 'THEN' SYSACT(1,14,2); 00010185
01002 'COMMENT' * * * * * 00010190
01002 * 00010200
01002 * RELATIVE MOTIONS 00010210
01002 * (PER ANGLE,PER VELOCITY,PER SPECTRUM) 00010215
01002 * 00010220
01002 * * * * * 00010230
01002 OUTSTRING(1,('RELATIVE MOTIONS'))); 00010240
01003 SYSACT(1,14,2); 00010250
01004 OUTSTRING(1,('LENGTH (M) F PROBABILITY NUMBER 00010260
01004 PER HOUR'))); SYSACT(1,14,2); 00010270
01006 'FOR' N:=1 'STEP' 1 'UNTIL' NS-1 'DO' 00010280
01006 'BEGIN' 'FOR' Q:=1 'STEP' 1 'UNTIL' QQ 'DO' 00010290
01006 'BEGIN' OFDA(/Q/):=OFP(/Q,N/); 00010300
01007 OFMA(/Q/):=OFR(/Q,N/); 00010310
01008 'END'; 00010320
01009 TRAPREG(OFF,OFDA,QQ,MB); MB:=MB+MB; 00010330
01011 TRAPREG(OFF,OFMA,QQ,SP); SP:=SP+SP; 00010340
01013 KF:=EXP(-F(/N/)*F(/N/)/MB); 00010350
01014 FIX(1,3,3,L(/N/)); FIX(1,7,3,F(/N/)); 00010350
01016 NI:=SQRT(SP/MB)*KF/2/PI; 00010370
01017 FIX(1,5,4,KF); FIX(1,11,1,3500*NI); 00010380
01019 SYSACT(1,14,1); 00010390

```

```

01020          'END';
01021          TRAPREG(OFF,DFV,QQ,M3);    VSQ:=MB+M3;
01023          TRAPREG(OFF,DFY,QQ,M3);    VSSQ:=MB+M3;
01025          TRAPREG(OFF,DFK,QQ,M3);    VKQ :=MB+M3;
01027          TRAPREG(OFF,DFB,QQ,M3);    VKR :=MB+M3;
01029          FIX(1,3,3,L(/S/));          FIX(1,7,3,F(/NS/));
01031          M3:=F(/NS/)-FC*2*B(/JJ/2,MP2/)*LL*VV(/K/)*VV(/K/)/G/LL
01031          /LE;
01032          KF:=EXP(-MB*M3/VKQ);        VW:=SQRT(VKR/VKQ)*KF/2/PI;
01034          FIX(1,5,4,KF);              FIX(1,11,1,3600*W);
01036          OUTSTRING(1,(' SHIPPING')));
01037          SYSACT(1,14,1);              KF:=CP*SQRT(G*LL);
01039          KF:=EXP(-DP*Q/VSQ-KF*VF/VSSQ);
01041          FIX(1,3,3,L(/S/));          FIX(1,7,3,DP);
01042          FIX(1,5,4,KF);
01044          VJ:=360*SQRT(VSSQ/VSQ)*KF/2/PI;
01044          FIX(1,11,1,W);
01045          OUTSTRING(1,(' SLAMMING')));
01046          'COMMENT' *****
01046          *
01046          * ACCELERATIONS
01046          * (PER ANGLE,PER VELOCITY,PER SPECTRUM)
01046          *
01046          * * * * *
01046          SYSACT(1,3,REGEL);
01047          'IF' REGEL>37 'THEN' SYSACT(1,15,5)
01047          'ELSE' SYSACT(1,14,4);
01048          OUTSTRING(1,('ACCELERATIONS'))); SYSACT(1,14,2);
01050          OUTSTRING(1,('SECTION AMPL )/2'))); SYSACT(1,14,1);
01052          OUTSTRING(1,(' M/SEC2'))); SYSACT(1,14,3);
01054          'FOR' J:=0 'STEP' 2 'UNTIL' JJ 'DO'
01054          'BEGIN' M:=J/2;
01055          'FOR' Q:=1 'STEP' 1 'UNTIL' Q 'DO' DFA(/Q/):=
01055          DFAC(/Q,M/);
01058          TRAPREG(OFF,DFA,QQ,M3);
01057          FIX(1,4,0,J); FIX(1,8,3,2*SQRT(M3));
01059          SYSACT(1,14,1);
01060          'END';
01061          'COMMENT' *****
01061          *
01061          * ADDED RESISTANCE AND POWER INCREASE
01061          * (PER ANGLE,PER VELOCITY,PER SPECTRUM)
01061          *
01061          * * * * *
01061          SYSACT(1,14,4);
01062          OUTSTRING(1,('ADDED RESISTANCE =')));
01063          TRAPREG(OFF,DFR4,QQ,M3);    FIX(1,8,3,M3+M3);
01065          OUTSTRING(1,(' TON')));    SYSACT(1,14,1);

```

SOURCE PROGRAM

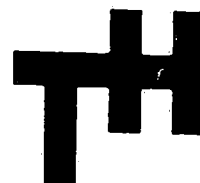
```

SC          SOURCE STATEMENT
01067      OUTSTRING(1,('POWER INCREASE =')));          00010870
01068      FIX(1,8,3,MB*VV/(K/)*1000/37.5);            00010880
01069      OUTSTRING(1,(' EHP')));                     00010890
01070      'IF' = BNDL 'THEN' 'GOTO' WATER;            00010900
01071      'COMMENT' * * * * * * * * * * * * * * * * * * 00010910
01071      *                                           * 00010920
01071      * SHEARING FORCES AND BENDING MOMENTS        * 00010930
01071      * (PER ANGLE,PER VELOCITY,PER SPECTRUM)      * 00010940
01071      *                                           * 00010950
01071      * * * * * * * * * * * * * * * * * * * * * * 00010960
01071      SYSACT(1,14,5); BLANK(1,13);                00010970
01073      OUTSTRING(1,('SHEARING FORCE (TON)')); BLANK(1,7);00010980
01075      OUTSTRING(1,('BENDING MOMENT (M.TON)'));     00010990
01076      SYSACT(1,14,2);                               00011000
01077      OUTSTRING(1,('SECTION    AMPL 1/3    AMPL 1/10  00011010
01077      AMPL 1/3    AMPL 1/10'))); SYSACT(1,14,2);    00011020
01079      'FOR' M:=0 'STEP' 2 'UNTIL' JJ=1.8 'DO'      00011030
01079      'BEGIN' J:=M/2;                               00011040
01080      'FOR' Q:=1 'STEP' 1 'UNTIL' QQ=100          00011050
01080      'BEGIN' OFDA(/Q/)=OFD(/Q,J/);               00011060
01081      OFMA(/Q/)=OFM(/Q,J/);                       00011070
01082      'DO';                                         00011080
01083      IFAPRFG(OFF,OFDA,QQ,MB);                     00011090
01084      MB:=SQRT(P*MB);                               00011100
01085      FIX(1,4,2,M);                                FIX(1,9,3,MB+MB); 00011110
01087      FIX(1,9,4,2.55*MB);                        00011120
01088      IFAPRFG(OFF,OFMA,QQ,MB);                   00011130
01089      MB:=SQRT(P*MB);                               00011140
01090      FIX(1,9,3,2*MB);                             FIX(1,9,4,2.55*MB); 00011150
01092      SYSACT(1,14,1);                             00011160
01093      'END';                                       00011170
01094      WATER:                                       00011180
01094      'END';                                       00011190
01095      'END';                                       00011200
01096      'END';                                       00011210
01097      'COMMENT' * * * * * * * * * * * * * * * * * * 00011220
01097      *                                           * 00011230
01097      *           DATA OUTPUT                     * 00011240
01097      *                                           * 00011250
01097      * * * * * * * * * * * * * * * * * * * * * * 00011250
01097      SYSACT(1,15,4); OUTSTRING(1,('INPUT'));     00011260
01099      SYSACT(1,14,3); OUTSTRING(1,('II ='));     FIX(1,4,0,II);    00011270
01102      SYSACT(1,14,1); OUTSTRING(1,('JJ ='));     FIX(1,4,0,JJ);    00011280
01105      SYSACT(1,14,1); OUTSTRING(1,('M ='));     FIX(1,4,0,MM);    00011290
01108      SYSACT(1,14,1); OUTSTRING(1,('QQ ='));     FIX(1,4,0,QQ);    00011300
01111      SYSACT(1,14,1); OUTSTRING(1,('NV ='));     FIX(1,4,0,NV);    00011310
01114      SYSACT(1,14,1); OUTSTRING(1,('LL ='));     FIX(1,4,2,LL);    00011320
01117      SYSACT(1,14,1); OUTSTRING(1,('RHQ ='));     FIX(1,4,4,RHQ);   00011330
    
```



SC	SOURCE STATEMENT	SOURCE PROGRAM		
01120	SYSACT(1,14,1);	OUTSTRING(1,('G ='));	FIX(1,4,2,G);	00011340
01123	SYSACT(1,14,1);	OUTSTRING(1,('CA ='));	FIX(1,4,4,CA);	00011350
01126	SYSACT(1,14,1);	OUTSTRING(1,('AHD ='));	FIX(1,4,0,AHD);	00011360
01129	SYSACT(1,14,1);	OUTSTRING(1,('MP ='));	FIX(1,4,0,MP+2);	00011370
01132	SYSACT(1,14,1);	OUTSTRING(1,('NS ='));	FIX(1,4,0,NS);	00011380
01135	SYSACT(1,14,1);	OUTSTRING(1,('BOOL ='));		00011390
01137	'IF' BOOL 'THEN'	OUTSTRING(1,('TRUE'));		00011400
01137	'ELSE'	OUTSTRING(1,('FALSE'));		00011410
01138	SYSACT(1,14,1);	OUTSTRING(1,('VGR ='));		00011420
01141	'IF' VGR 'THEN'	OUTSTRING(1,('TRUE'));		00011430
01141	'ELSE'	OUTSTRING(1,('FALSE'));		00011440
01141	SYSACT(1,14,3);	OUTSTRING(1,('R(0:JJ,0:MP-1)'));		00011450
01143	'FOR' J:=0 'STEP' 1 'UNTIL' JJ 'DO'			00011460
01143	'BEGIN' 'FOR' M:=0 'STEP' 1 'UNTIL' MP 'DO' FIX(3,3,3,(J,M));			00011470
01144	SYSACT(1,14,1);	BLANK(1,15);		00011480
01145	'END';			00011490
01147	SYSACT(1,14,1);	OUTSTRING(1,(' R(0:JJ) :'));		00011500
01149	'FOR' J:=0 'STEP' 1 'UNTIL' JJ 'DO' FIX(3,3,3,D(J/J));			00011510
01150	SYSACT(1,14,2);	OUTSTRING(1,(' VV(1:VV) :'));		00011520
01152	'FOR' J:=1 'STEP' 1 'UNTIL' VV 'DO' FIX(3,3,3,VV(J/J));			00011530
01153	SYSACT(1,14,2);	OUTSTRING(1,(' SIGMA(1:00) :'));		00011540
01155	'FOR' J:=1 'STEP' 1 'UNTIL' 00 'DO' FIX(3,3,3,SIGMA(J/J));			00011550
01156	SYSACT(1,14,2);	OUTSTRING(1,(' L(1:NS) :'));		00011560
01158	'FOR' J:=1 'STEP' 1 'UNTIL' NS 'DO' FIX(3,4,2,L(J/J));			00011570
01159	'IF' = BOOL 'THEN' 'GOTO' NU;			00011580
01159	SYSACT(1,14,2);	OUTSTRING(1,(' W(0:JJ) :'));		00011590
01162	'FOR' J:=0 'STEP' 1 'UNTIL' JJ 'DO' FIX(3,3,3,W(J/J));			00011600
01163	'GOTO' LZ;			00011610
01164	NU:SYSACT(1,14,2);	OUTSTRING(1,(' FACT ='));	FIX(1,4,4,FACT);	00011620
01167	LZ:SYSACT(1,14,2);	OUTSTRING(1,(' MUR(1:AHD) :'));		00011630
01169	'FOR' J:=1 'STEP' 1 'UNTIL' AHD 'DO' FIX(3,3,3,M(J/J));			00011640
01170	SYSACT(1,14,3);	OUTSTRING(1,(' BF ='));	FIX(1,4,0,BF);	00011650
01173	SYSACT(1,14,1);	OUTSTRING(1,(' GM ='));	FIX(1,4,0,GM);	00011660
01176	SYSACT(1,14,1);	OUTSTRING(1,(' PIERSON ='));		00011670
01176	'IF' PIERSON 'THEN'	OUTSTRING(1,(' TRUE'));		00011680
01178	'ELSE'	OUTSTRING(1,(' FALSE'));		00011690
01179	SYSACT(1,14,1);	OUTSTRING(1,(' ALF ='));	FIX(1,4,3,ALF);	00011700
01182	SYSACT(1,14,1);	OUTSTRING(1,(' DELTAZ ='));	FIX(1,1,3,DELTAZ);	00011710
01185	SYSACT(1,14,1);	OUTSTRING(1,(' FP ='));	FIX(1,4,3,FP);	00011720
01189	SYSACT(1,14,1);	OUTSTRING(1,(' FD ='));	FIX(1,4,3,FD);	00011730
01191	SYSACT(1,14,1);	OUTSTRING(1,(' FC ='));	FIX(1,4,3,FC);	00011740
01194	SYSACT(1,14,1);	OUTSTRING(1,(' LE ='));	FIX(1,4,3,LE);	00011750
01197	SYSACT(1,14,1);	OUTSTRING(1,(' DP ='));	FIX(1,4,3,DP);	00011760
01200	SYSACT(1,14,2);	OUTSTRING(1,(' F(1:NS) :'));		00011770
01202	'FOR' J:=1 'STEP' 1 'UNTIL' NS 'DO' FIX(3,4,2,F(J/J));			00011780
01203	'IF' = PIERSON 'THEN' 'GOTO' HU;			00011790
01204	SYSACT(1,14,2);	OUTSTRING(1,(' HS(1:BF) :'));		00011800
01206	'FOR' J:=1 'STEP' 1 'UNTIL' BF 'DO' FIX(3,4,2,HS(J/J));			00011810

SC	SOURCE STATEMENT	SOURCE PROGRAM	PAGE 027
01207	SYSACT(1,14,2);	OUTSTRING(1,(' PM(1:BF) ');	00011820
01209	'FOR' J:=1 'STEP' 1 'UNTIL' BF 'DO' FIX(3,4,2,PM(/J/));		00011830
01210	SYSACT(1,14,2);	OUTSTRING(1,('CF1 =')); FIX(1,4,3,CF1);	00011840
01213	SYSACT(1,14,1);	OUTSTRING(1,('CF2 =')); FIX(1,4,3,CF2);	00011850
01216	SYSACT(1,14,1);	OUTSTRING(1,('AH =')); FIX(1,4,0,AH);	00011860
01219	SYSACT(1,14,1);	OUTSTRING(1,('AT =')); FIX(1,4,0,AT);	00011870
01222	SYSACT(1,14,1);	OUTSTRING(1,('BT =')); FIX(1,4,0,BT);	00011880
01225	SYSACT(1,14,1);	OUTSTRING(1,('RT =')); FIX(1,4,0,RT);	00011890
01228	SYSACT(1,14,1);	OUTSTRING(1,('ST =')); FIX(1,4,0,ST);	00011900
01231	'GO TO' Z;		00011910
01232	HI: SYSACT(1,14,2);	OUTSTRING(1,('GMOM(1:BF,1:GM)'));	00011920
01234	'FOR' J:=1 'STEP' 1 'UNTIL' BF 'DO'		00011930
01234	'BEGIN' 'FOR' M:=1 'STEP' 1 'UNTIL' GM 'DO' FIX(3,3,3,GMOM(/J,M/));		00011940
01235	SYSACT(1,14,1);	BLANK(1,17);	00011950
01237	'END';		00011960
01233	SYSACT(1,14,2);	OUTSTRING(1,('GMSP(1:BF,1:GM)'));	00011970
01240	'FOR' J:=1 'STEP' 1 'UNTIL' BF 'DO'		00011980
01240	'BEGIN' 'FOR' M:=1 'STEP' 1 'UNTIL' GM 'DO' FIX(3,3,3,GMSP(/J,M/));		00011990
01241	SYSACT(1,14,1);	BLANK(1,17);	00012000
01243	'END';		00012010
01244	Z: 'END';		00012020
01245	'END';		00012030
01245	'COMMENT' * * * * *		00012040
01246	*		00012050
01246	* THE END OF THE SECOND BLOCK		00012060
01246	*		00012070
01246	* * * * *		00012080
01246	'END';		00012090
01247	SYSACT(1,15,1);		00012100
01248	'GO TO' OPNIEUW;		00012110
01249	'END'		00012120



# LABORATORIUM VOOR SCHEEPSBOUWKUNDE

TECHNISCHE HOGESCHOOL DELFT

FULL SCALE MEASUREMENTS AND PREDICTED SEA-  
KEEPING PERFORMANCE OF THE CONTAINERSHIP  
'ATLANTIC CROWN'.

W. Beukelman en M. Buitenhek

International Shipbuilding Progress,  
Volume 21, No. 243, 1974

Reportno. 388-P, Shipbuilding Laboratory  
Delft.

# FULL SCALE MEASUREMENTS AND PREDICTED SEAKEEPING PERFORMANCE OF THE CONTAINERSHIP "ATLANTIC CROWN" \*

by

W. BEUKELMAN and M. BUITENHEK

## Summary

On board the containership "Atlantic Crown" measurements have been carried out with regard to:

- a. the sea waves
- b. the heaving- and pitching motions
- c. the torque and number of revolutions of both propeller shafts
- d. the apparent wind velocity and -direction.

The measured values have been compared with predictions for power as well as for the motions and satisfactory agreement is shown

## Introduction

In April 1972 a team from the Shipbuilding Laboratory of the Delft University of Technology performed experiments on board the containership "Atlantic Crown" of the Holland Amerika Lijn (HAL). The particulars of the ship and its propellers are shown in table 1 (see page 28).

The main purpose of these experiments was to compare the actual increase in required power, as calculated from the data obtained, to values derived with the added resistance in waves as predicted by a new method based on the principle of energy balance [1].

To obtain a reliable estimation of the sea wave-motion a buoy, equipped with an accelerometer and a transmitter, was used. The vertical accelerations of the water surface were measured and transmitted to the ship. This signal, picked up by a receiver was recorded on tape together with the measured heaving- and pitching motions of the ship. During a run the torque and the number of revolutions of both turbine shafts were also measured in order to determine the power. The apparent wind velocity and -direction were measured too. These signals were recorded on paper by means of a servo recorder. Afterwards the wave accelerations and the motions were spectrally analyzed by means of both a digital method in use at the Shipbuilding Laboratory and a hybrid method, developed by the Mathematical Centre of the Delft University of Technology [2, 3].

The measured wave spectra were used as an input to calculate the heave- and pitch spectra and the mean added power in waves. Together with the measured still water resistance (from NSMB) and the results of wind resistance experiments with a ship model, it was possible to predict the total shaft power using an experimental propulsive efficiency. These predictions were compared with the final experimental results.

Since the prediction neglects horizontal motions, it may be ascertained, that with respect to power the agreement appears to be satisfactory for wave directions within 30 degrees off the bow and stern.

The agreement for the motions is satisfactory for the higher frequencies, however, less reliable for the lower frequencies. Generally these full scale tests confirm, that the present procedure for determining the added power in a seaway is useful for practical purposes.

## 1. Measurements on board

The experiments in waves on board the "Atlantic Crown" were carried out in the North Atlantic Ocean from 25 March until 3 April 1972. The ship was sailing from Southampton via Le Havre to New York.

Seven runs were accomplished for measurement in waves, some of them in following seas.

Before each run a wave-buoy was thrown overboard in order to measure the wave height.

The length of each run was limited by the power of the transmitter in the buoy. This lack of sufficient power as well as the existence of interference from the radios of surrounding ships caused some of the runs to be too short and consequently omitted.

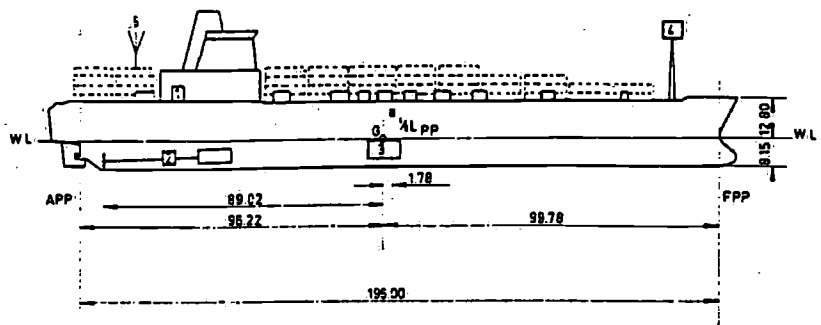
### 1.1 Execution of the experiments

A description of the wave buoy and its construction has been presented in [4] and in 1.2.1. Due to the speed of the ship it was possible to receive the signal of the buoy for about half an hour. The signal was recorded on tape as a frequency modulated pulse along with a reference signal. Tape speed variations were compensated when the demodulator is controlled by the reference signal. See [2, 3] and 2.2.1. It was necessary to wait several seconds after tossing the buoy into the

\* Report 336-P, Shipbuilding Laboratory, Delft, the Netherlands.  
Report No. 165 S, Netherlands Ship Research Centre TNO, Delft, the Netherlands.

Fig. 1. Ship's profile with denoted measuring locations.

1. Pitch
2. Torque and number of revolutions
3. Vertical acceleration (heave)
4. Relative wind velocity and - direction
5. Antenna



water to allow the wire, to which the stabilization weight was tied, to unwind from the reel.

Once the stabilization weight hung freely the buoy would float erect with its antenna upward.

The run was immediately started as soon as the antenna could be seen in the upright position.

The heaving and pitching motions were measured with the aid of a stabilized platform located as denoted in fig. 1. These signals were registered on tape too.

The relative wind velocity and - direction - meter were installed on the fore mast to avoid the influence of the bridge.

Both signals were recorded on paper by a servo-recorder (1.3.2). The torque and number of revolutions of each turbine shaft were measured about 12 m behind the turbine. The torque was determined using strain-gauges connected to the periphery of the shafts (1.2.6). In this way it was possible to measure the fluctuation of the torque in the sea. The power delivered by each turbine could be determined by the measured number of revolutions and the torque. The power could also be read from the ASEA-meter in the engine room.

The torque signal was registered on paper by a servo-recorder and the number of revolutions was recorded in a digitized form.

On the bridge the following data a.o. were observed during each run:

- the ship speed in knots
- the ship's course
- the estimated height of wind waves and swells
- the estimated direction of wave travel
- the average rudder angle
- the ship's position

During each run the ship's course was kept as constant as possible.

As soon as the signal of the wave-buoy was too weak or disturbed the run was stopped.

When the water surface was very quiet the torque and the revolutions of the turbine shafts were also measured to determine the still water power.

## 1.2 Description of the measuring instruments

The following signals had to be measured during each run:

- the wave height
- the heave amplitude
- the pitch angle
- the relative wind velocity
- the relative wind direction
- the torque of both propeller shafts
- the number of revolutions of both shafts
- the ship speed.

Fig. 1 shows the ship's profile and the places from where the above mentioned signals were measured.

### 1.2.1 The wave-buoy

Wave heights were determined with the aid of the wave-buoy. In order to perform this purpose; the buoy was equipped with an instrument which measured the linear vertical accelerations of the water surface.

The information of the vertical acceleration was continuously transmitted to the ship by means of a wireless transmitter.

The electronic part of the wave-buoy consisted of the following parts:

- the accelero-meter
- the auxiliary oscillator supplying the accelero-meter
- the demodulator
- the frequency modulator (FM)
- the transmitter with the antenna
- the stabilized power supply
- the batteries.

The mechanical part of the wave-buoy was composed of these parts:

- the spherically shaped floating body
- the stabilizer with wire
- the reel for the wire
- the stabilization weight
- the antenna.

Before launching, the wave buoy is set into action by a reed switch.

Once afloat, the wire can freely unwind from the reel. The length of the wire can be chosen according to the significant wave length.

The stabilization of the wave-buoy in vertical position is shown in fig. 2.

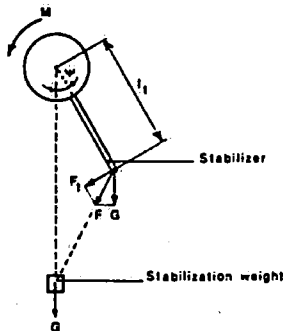


Fig. 2. Stabilization of wave-buoy.

A moment of disturbance  $M$  will cause a rotation  $\psi$  of the buoy about a horizontal axis. The righting moment may be written as:

$$F_1 l_1 = l_1 G \sin \psi \quad (1)$$

in which  $G$  is equal to the stabilization weight.

Characteristics:

Manufacture: Shipbuilding Laboratory, Delft University of Technology.

Supply	$\pm 9$ V
Frequency of modulation	2300 cps
Sensitiveness	500 cps/g
Radius of action	10-18 miles
Transmission power	250 mW
Frequency of transmission	27 mc
Buoy-diameter	.43 m
Length of antenna	1.50 m
Length of the wire	40 m
Weight of buoy	10 kg
Stabilization weight	10 kg

Remark: In the future the transmission power will be increased to 1 or 2 W in order to enlarge the radius of action.

### 1.2.2 The stabilized heave accelero-meter

This instrument may be divided into two parts:

- a. the stabilized platform
- b. the linear accelero-meter.

The stabilized platform consists of the Flux Gate Compass assembly, which is stabilized by an electrical-driven gyro.

The gyro is made to seek the vertical (with reference to the earth) by means of a rolling ball-type erection mechanism.

The erection mechanism is driven by the gyro through the medium of a magnetic drag cup. As the erection mechanism turns, a steel ball rolls around a circular track on top of the gyro housing.

The accelerometer is rigidly mounted on the bottom of the gyro assembly and is thus stabilized in a horizontal plane. This accelero-meter is a miniature self-contained servo mechanism, which automatically measures input acceleration by a null method of achieving balance between two opposing torques (fig. 3). The device is comprised of a R-F oscillator, torque mechanism, power supply and output system.

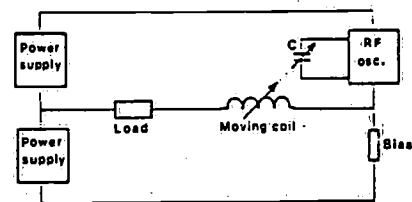


Fig. 3. Block diagram of accelero-meter.

Linear acceleration along the sensitive axis of the transducer causes an input torque on a pivoted inertial system comprised of an unbalanced moving coil and - vane assembly.

If the input torque is not completely balanced by an opposing torque due to current in the moving coil, an angular displacement of the inertial system results.

Only a minute angular deflection of the inertial system is required to produce the current through the moving coil necessary for a precise balance of torques.

Characteristics:

Manufacture:	Donner Scientific Comp.
Range:	2 g
Accuracy:	$\pm 0.1\%$ of full range
Natural frequency:	100 cps

### 1.2.3 The vertical gyro to measure the pitch angle

The vertical gyro control has an electrically driven, vertical spin axis gyro, containing two variable transformer pick-offs, which detect the angular movement of the ship about the pitch axis.

A liquid level switch mounted on the gyro serves through torque motors, to maintain the gyro in its normal upright position.

Characteristics:

Manufacture:	Sperry
Type:	A 12

### 1.2.4 The anemometer

The anemometer for measuring wind velocities consists of a cup-unit and a frequency-meter.

Eight magnets are regularly distributed around the periphery of the axis. These magnets pass a reed switch, as the axis is rotated by the wind driven cups. The pulsating output signal is transformed into an analog voltage, which is proportional to the wind velocity.

The cup-unit was fastened at the top of the fore-mast in such a position, that it received a clear wind.

Characteristics:

Manufacture: Koninklijk Nederlands Meteorologisch Instituut

Sensitiveness: 8 pulses/rev.

Calibration: 0.48 knots/cps

### 1.2.5 The wind direction-meter

The wind vane is connected to a potentiometer, the medium position of which coincides with a position of the vane parallel to the ship's longitudinal axis.

The vane unit was also mounted at the top of the fore-mast in such a way, that it received a clear wind.

### 1.2.6 The torque-meter

To measure the torque of the shafts such a system has been chosen, that the torque-tension in the axes was measured by means of strain gauges.

The FM wireless transmission system has been used to measure from the rotating axes.

The measuring system may be divided into two parts viz.: the rotating- and stationary part.

The rotating part converts the resistance change in a full-bridge strain gauge into an oscillator frequency change and radiates this frequency through a coil wound round the shaft.

The stationary part consists of a frequency signal pick-up plus a discriminator to demodulate the frequency change and provide a DC voltage whose amplitude varies directly in proportion to the original resistance change (fig. 4).

Characteristics:

Manufacture: Philips

Measurement range: 600  $\mu$ V/V

Linearity: within  $\pm 0.5\%$

Stability: zero drift not more than  $\pm 1\%$

Carrier frequency: 6750 cps

Frequency deviation:  $\pm 30\%$

Strain gauges

Type: PR 9810 S

R: 604 $\Omega$   $\pm 1\%$

k: 2.04  $\pm 1\%$

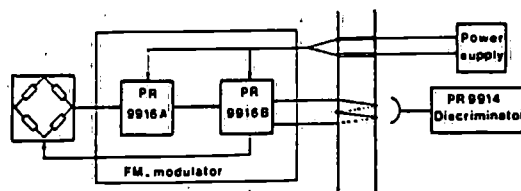


Fig. 4. Block diagram of the wireless transmission system for torque measurement.

### 1.2.7 The revolution-counter

For the measurement of the revolutions of the propeller shafts, 6 metal strips were mounted on each shaft, regularly spaced around the periphery, and located to pass a fixed magnetic pick-up as the shaft rotated.

The pulses obtained were input to a digital counter the time base of which had been adjusted to 10 sec.

The number of pulses counted during 10 sec was transmitted to a digital printer.

For a constant number of revolutions the obtained information was equal to the number of revolutions per minute.

### 1.2.8 The ship's EM-speed log

The ship speed readings were taken from the electromagnetic (EM) ship log (Sperry), while the ship's course was read directly from the ship's compass.

The equipment of the EM-log consists of the following four units:

- the flow sensor
- the master unit
- the distance-run recorder
- the speed indicator.

The flow sensor is fitted to the outside of the ship's hull below the waterline. It develops a small AC voltage proportional to the rate of flow of passing seawater. This voltage is fed to the master unit.

The master unit converts the input into a current proportional to the speed of the water passing the flow sensor.

However, boundary layers around the ship's hull cause discrepancies between the ship's speed and the speed of the water flowing past the sensor. These errors are compensated by use of a speed corrector circuit in the master unit. The speed corrector enables corrections to be applied at four points on the speed curve and can be set up by seagoing calibration trials or as a result of sea-going experience.

The ship's speed is indicated on a circular scale calibrated from 0 to 25 knots in 1 knot increments.

### 1.3 Description of the recording instruments

#### 1.3.1 The instrumentation taperecorder

The measured signals whose amplitudes and frequencies varied with time were recorded by an instrumentation taperecorder. One of two available systems may be chosen, viz.: the Direct system or the frequency modulated (FM) system. To fix low frequency phenomena on DC-level use should be made of the FM-system. In this case the analog input signal modulates the built-in carrier oscillator up to a maximum of plus or minus 40% of the used zero-frequency. This FM-signal is input to the record head. By way of the reproduce head the FM-signal is again available when playing back the tape. To record signals with higher frequencies (e.g. a reference signal) the Direct system may be utilized. The following signals have been recorded with the aid of the FM-system

- the wave acceleration
- the heave acceleration
- the pitch angle

and with the aid of the Direct system: the reference signal (derived from the crystal oscillator).

Characteristics:

Manufacture: Precision Instrument Comp.  
 Type: PS-214A  
 Tape-speed:  $3\frac{1}{2}$  inch per second  
 FM-zero-frequency: 3375 cps  
 Bandwidth (FM): 0-625 cps  
 Bandwidth (Direct): 50-7500 cps

#### 1.3.2. The servo recorder

To record stationary or quasi-stationary phenomena a servo-potentiometer recorder was used.

The advantages are:

- direct information
- satisfactory resolution (in case of sufficient deflection of the pen).

This disadvantages are that,

- the recorder is not suitable for dynamic phenomena
- it is impossible to correlate the different signals with each other.

The following signals have been recorded using the servo recorder:

- the torque of the starboard shaft
- the torque of the port shaft
- the relative wind velocity
- the relative wind direction.

Characteristics:

Manufacture: Goertz Electro  
 Type: Re 520  
 Paperwidth: 200 mm  
 Response: 130 mm within 1 sec

#### 1.4 Results of measurements

As mentioned before several runs in waves had to be cancelled because they were too short. Only three runs, numbered 4, 6 and 7, appeared to be suitable for further analysis. From these runs numbers 4 and 7 took place in head seas and number 6 in following seas. The necessary data of these runs as well as the measured results are summarized in the tables 2, 3, 4, 5, 6 and 7. Tables 2 and 3 are a.o. related to:

- the ship's position, - course and - speed
- the estimated and measured wave data
- the estimated and measured wind data.

Tables 4, 5, 6 and 7 contain results with respect to:

- the measured torque
- the measured number of revolutions per minute of both shafts
- the shaft power  $P_S$  in metric horse power (HP)

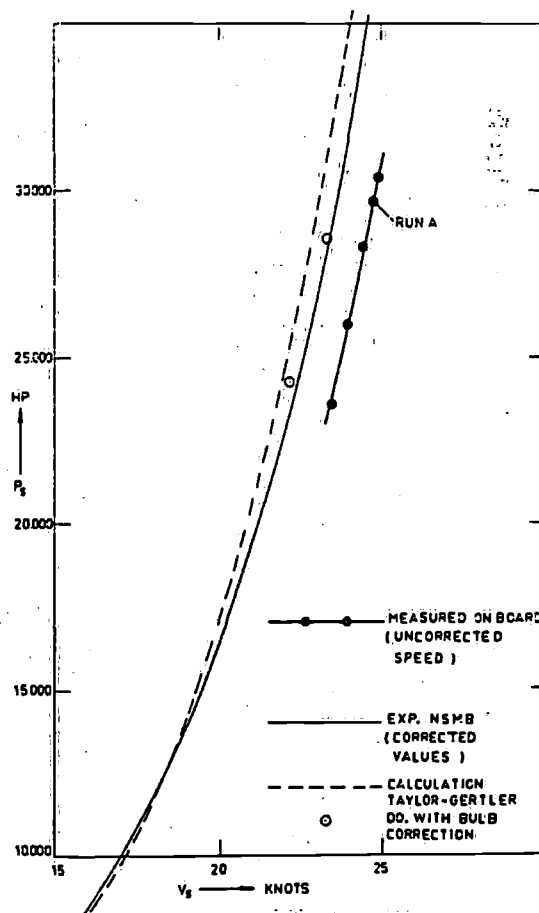


Fig. 5. Measured and predicted shaft power in still water.



One run was carried out in the English Channel as a still water test to measure ship speed, torque and number of revolutions. The measured results of this run are shown in table 7 (run A).

Other still water data pertaining to power and speed were obtained by continuously measuring the propulsion characteristics and ship speed during the initial part of the stopping manoeuvre near New York.

The results obtained from this test as well as from run A yield the relation of ship speed and shaft power  $P_{S_{sw}}$  in still water as shown in table 7 and fig. 5.

For the measured spectra, obtained after spectral analysis, reference is made to 2.2.3.

## 2 Analysis of the experiments

### 2.1 General

The analysis of the experiments has two purposes, viz.:

- to obtain the motion-spectra from the measurements and the shaft power  $P_S$  from the measured propulsion characteristics, both for comparison with calculations
- to obtain the necessary input data, such as a wave spectrum and the total propulsive efficiency,  $\eta_D$ , for the prediction of the motion-spectra and the increased shaft power, respectively.

The motion spectra as well as the wave spectra will be derived, using spectral analyses as described in 2.2.

For each run in waves the measured wave spectrum will be used to compute the spectra of the vertical motions, heave, pitch, and the increased effective power  $P_E$  in waves. The propulsive efficiency,  $\eta_D$ , derived from the propulsion analysis, is required to calculate the shaft power  $P_S$ , which will be compared with the measured values.

It is interesting to determine the wake-fraction  $w$  both in still water and in waves.

### 2.2 Spectral analysis

Data reduction of the signals recorded on magnetic tape was carried out in two ways, viz.:

- transformation of electric signals into punch tape data, which are input to a digital computer (digital method)
- direct treatment of electric signals by a hybrid computer (hybrid method).

General descriptions of the way to obtain spectrally analyzed results are presented in [3, 5, 6].

#### 2.2.1 The digital method

The analog measured signals, recorded by the instru-

mentation tape recorder are available as frequency modulated (FM) signals, when played back (see 1.3.1).

Counting equal time intervals, the frequency of the modulated signal affords information about the amplitude and the frequency of the original measured signal.

However, it is essential, that during this assimilation there is a fixed relation between the time-base and the zero frequency of the modulated signal used during the recording. A part of this relation is delivered by the tape speed.

Severe motions or vibrations on board during the measurements may result into fluctuations of the recording speed independent of the measured signal. This might cause undesirable frequency modulation in the output signal.

To prevent this error a reference signal, descended from a crystal oscillator, is simultaneously recorded with the measured signal.

During the treatment of the signal the time-base is derived from the reference signal and for this reason may be called a real time-base.

The digital information of the counter, transformed into punch tape data, was input to the digital IBM 360/65 computer of the Mathematical Centre of the University for calculation of the autocovariance function and the power spectrum as a.o. described in [3, 5, 6].

Only a slow one-channel unit was available for digitizing and punching according to the above mentioned method, which includes the total punch time equal to the product of the number of measured signals and the recording time.

With the hybrid computer the speed of treatment of the measured signal can be remarkably increased.

#### 2.2.2 The hybrid method

The hybrid computer AD 4/IBM 1800 of the Mathematical Centre of the Delft University of Technology is extremely suitable for treatment of the measured data, which are available on magnetic tape.

The analog part of the computer offers the possibility of treating various measured signals simultaneously, while the digital part provides the logic control, the memory capacity and the computation of the desired data during the play back of the magnetic tape.

The system of treatment is set up for four displacement signals and two acceleration signals. For this investigation only one displacement- and both acceleration signals have been used.

The displacement signal is obtained from the acceleration signal after two successive integrations.

To eliminate both DC-levels and to suppress undesired frequencies it is necessary to use a bandpass filter before as well as between the integration procedures.

The hybrid system of treatment consists of the following parts:

- the frequency demodulator
- the digital bandpass filter
- the integrator
- the computation unit.

#### The frequency demodulator

The frequency difference between the reference and FM-signal is determined by counting the number of zero crossings during fixed time intervals, which coincide with the sampling rate of the digital part.

The frequency difference is transformed to an analog voltage by means of monostable multivibrators, electronic switches and an integrator.

#### The digital bandpass filter

The bandpass filter function is accomplished in the digital part by calculation of instantaneous responses to samples of the input signal by means of the discretized version of the convolution integral. The response being the filter output is played back to the analog part by DA-conversion.

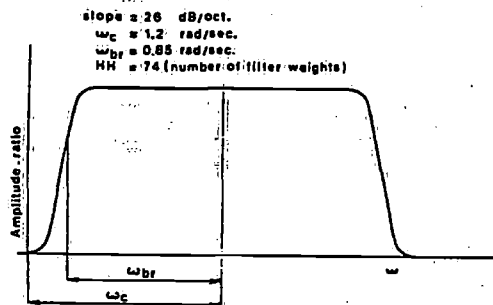


Fig. 6. Example of filter characteristic for run 4 and 7.

The resulting transfer functions of the filter used have severe oscillations in the neighbourhood of the cut-off frequency, which are explained by the Gibb's phenomenon in the theory of Fourier-transforms. If, instead of a square, a cosine bell is taken, the oscillations will almost completely disappear. In fig. 6 this phenomenon is shown for the type of bandpass used.

#### The integrator

The principle of the analog numerical integration is based upon the rectangular rule for digital numerical integration:

$$I_n = h(f_0 + f_1 + \dots + f_n) \quad (2)$$

where

$f_0, \dots, f_n$  = discrete values of the function to be integrated

$h$  = step size between two successive samples

$I_n$  = integral value after  $n$  samples

The procedure is implemented on the analog computer by a sample-hold circuit.

#### The computation unit

The autocovariance function (*acf*) is "on line" calculated with samples from analog tape at fixed time intervals. Within a fixed time interval each contribution to the autocovariance function is added to the previous contributions.

The minimum length of the time interval is determined by

- the number of lags of the *acf*
- the number of tracks, which is simultaneously processed
- the calculation time to carry out the product accumulations.

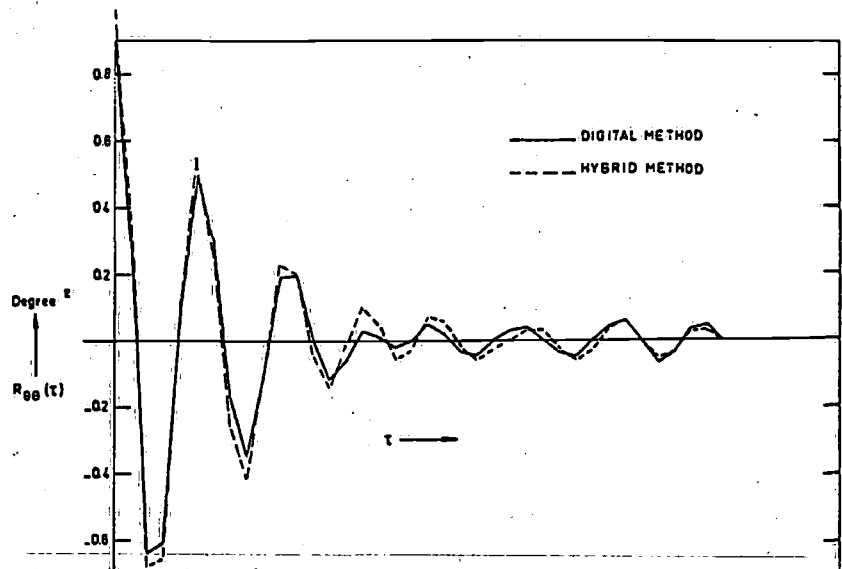


Fig. 7. Pitch autocovariance function for run 4 obtained by digital and hybrid method.

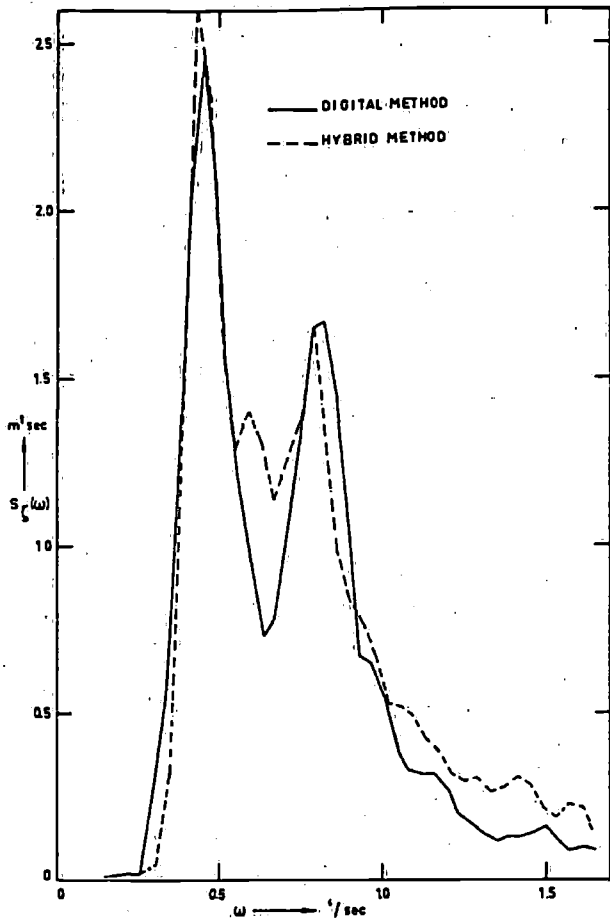


Fig. 8. Wave spectrum for run 4 obtained by digital and hybrid method.

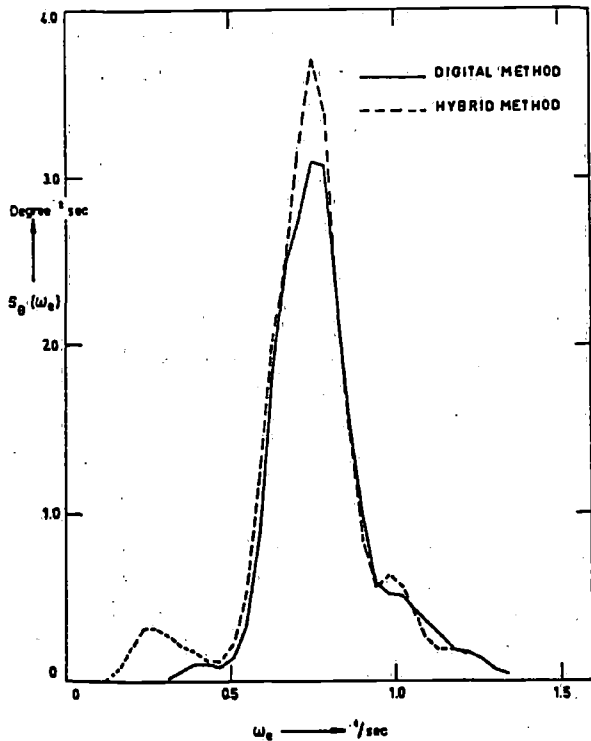


Fig. 9. Pitch spectrum for run 4 obtained by digital and hybrid method.

To reduce the computation time the power spectrum is determined in a hybrid way.

The contribution to the autopower is obtained from the available points of the *acvf* at discrete frequencies. The high speed and the capacity of the computer made it possible to accelerate the treatment by a factor of four by increasing the play-back speed of the magnetic tape recorder 4 times.

### 2.2.3 Results of the analysis

The difference between the results of the digital and hybrid method appeared to be negligible for the runs considered (4, 6 and 7). An example has been presented in the figs. 7, 8 and 9 for run 4, where the results of both methods are shown for the pitch autocovariance function  $R_{\theta\theta}(\tau)$ , the wave spectrum  $S_{\zeta}(\omega)$  and the pitch spectrum  $S_{\theta}(\omega_e)$ , respectively. It should be noted, that the wave measured by the wave-buoy with supposed zero-speed, is related to the circular wave frequency  $\omega$ , while the heaving and pitching motion, measured on board, are related to the frequency of encounter  $\omega_e$ . For convenience in the future only the results according to the digital method will be shown. The measured wave spectrum  $S_{\zeta}(\omega)$ , the heave spectrum  $S_{\zeta}(\omega_e)$  and the pitch spectrum  $S_{\theta}(\omega_e)$  for run 4 are respectively shown in the figs. 10, 11, 12 and in the figs. 14, 15, 16; for run 6 in the figs. 18, 19, 20 and for run 7 in the figs. 22, 23, 24.

For run 6 another filter had to be used because of the very low frequencies of vertical ship motions in following seas.

### 2.3 Propulsion analysis

As mentioned before, the torque and number of revolutions per minute of each shaft were measured during each run.

The average shaft power in metric HP can be calculated from the average torque and number of revolutions in the following way:

$$\begin{aligned} \bar{P}_{SP,SB} &= \frac{2\pi \cdot \bar{Q}_{P,SB} \cdot \bar{n}_{P,SB}}{60 \times 75} \\ &= \frac{\bar{Q}_{P,SB} \cdot \bar{n}_{P,SB}}{716.2} \end{aligned} \quad (3)$$

in which:

$\bar{Q}_{P,SB}$  = the average measured torque of the port- or starboard shaft respectively.

$\bar{n}_{P,SB}$  = the average number of revolutions per minute of the port- or starboard shaft respectively.

Afterwards the average total shaft power is to be determined by

$$\bar{P}_S = \bar{P}_{SP} + \bar{P}_{S_{SB}} \quad (4)$$

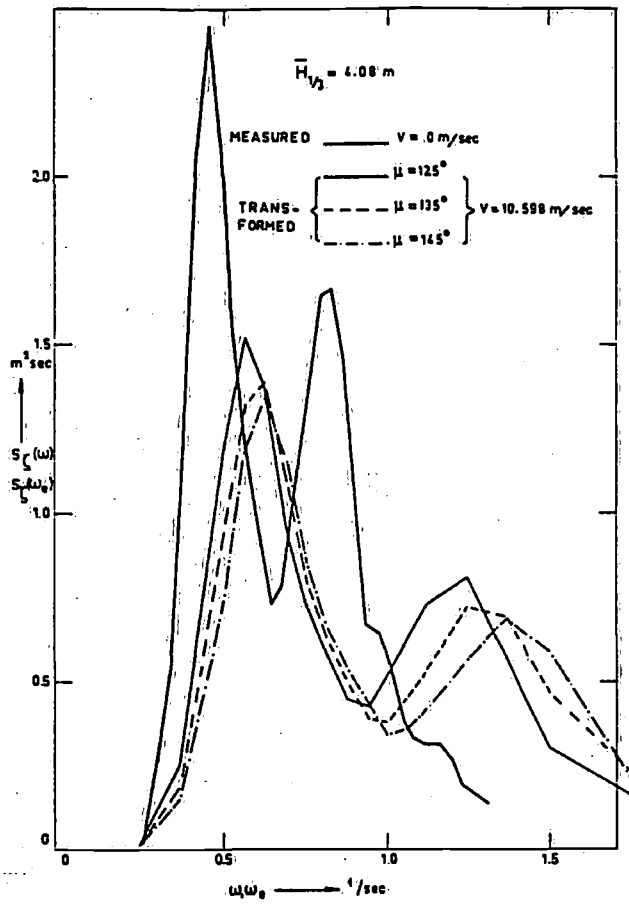


Fig. 10. Measured wave spectrum for run 4 with spectra transformed for speed and direction of wave travel  $\mu = 125^\circ, 135^\circ, 145^\circ$ .

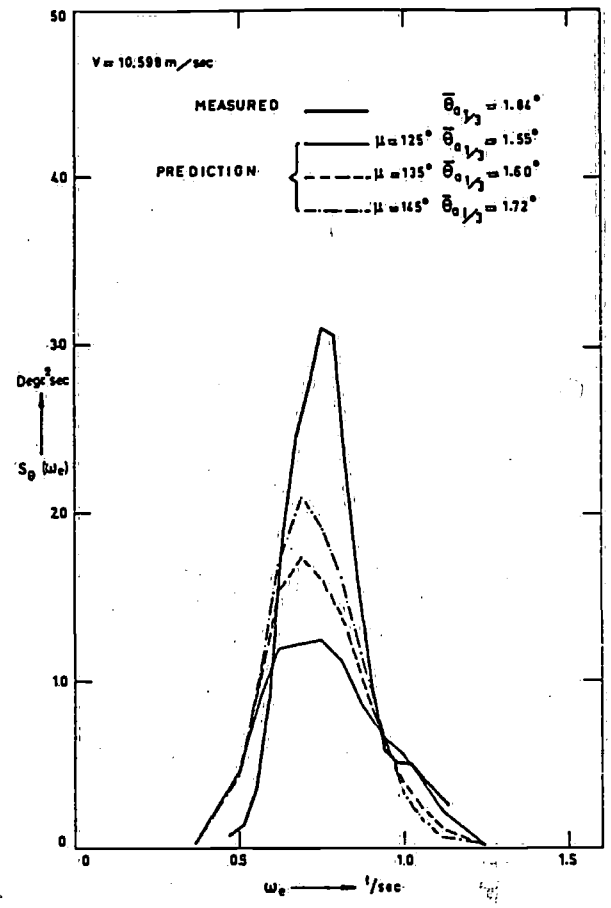


Fig. 12. Measured pitch spectrum for run 4 and predictions for direction of wave travel  $\mu = 125^\circ, 135^\circ, 145^\circ$ .

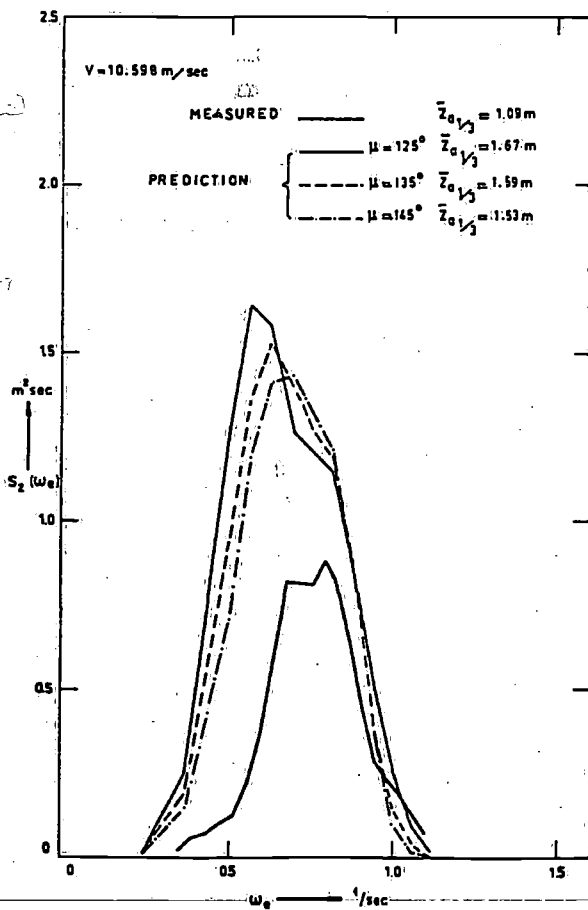


Fig. 11. Measured heave spectrum for run 4 and predictions for direction of wave travel  $\mu = 125^\circ, 135^\circ, 145^\circ$ .

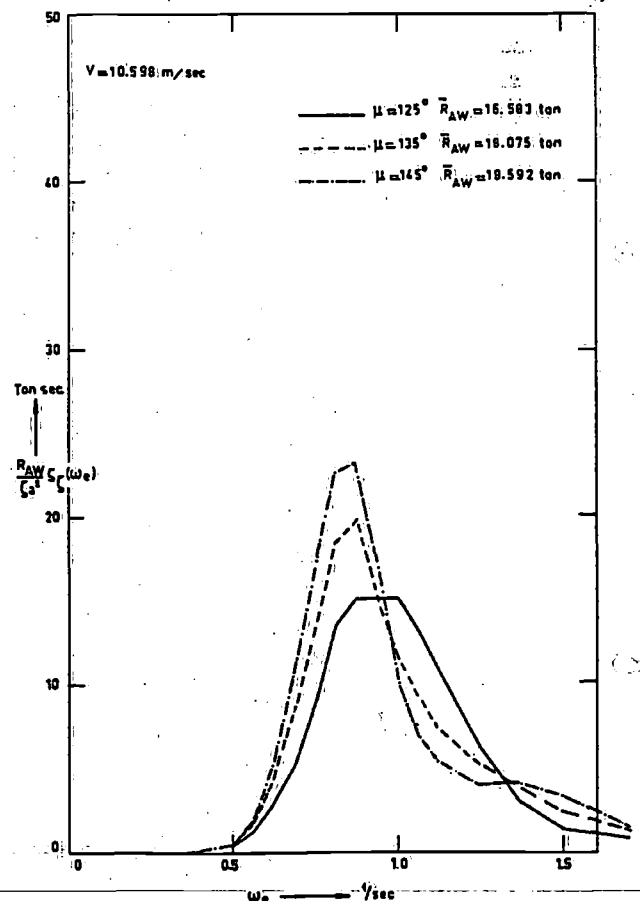


Fig. 13. Predicted added resistance spectra for run 4 and direction of wave travel  $\mu = 125^\circ, 135^\circ, 145^\circ$ .

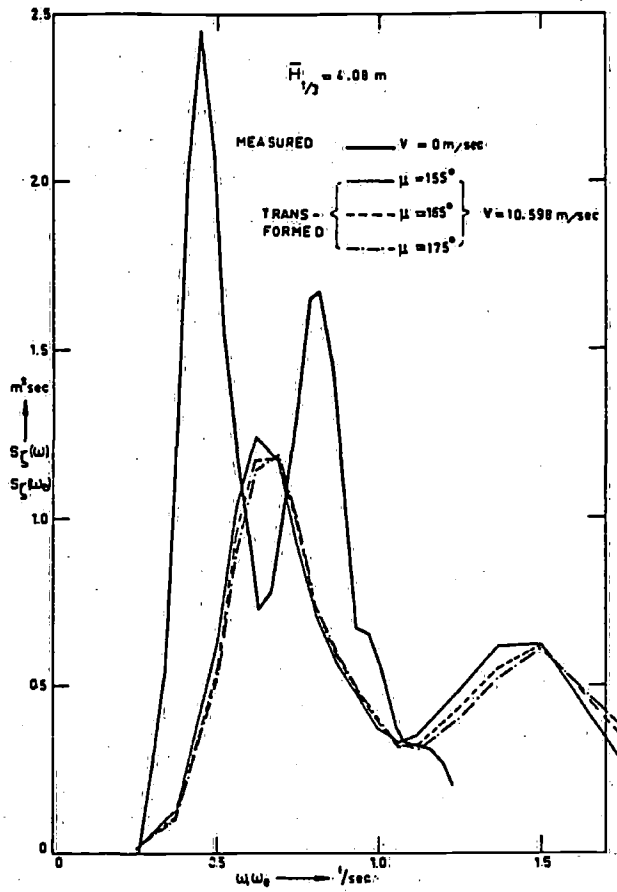


Fig. 14. Measured wave spectrum for run 4 with spectra transformed for speed and direction of wave travel  $\mu = 155^\circ, 165^\circ, 175^\circ$ .

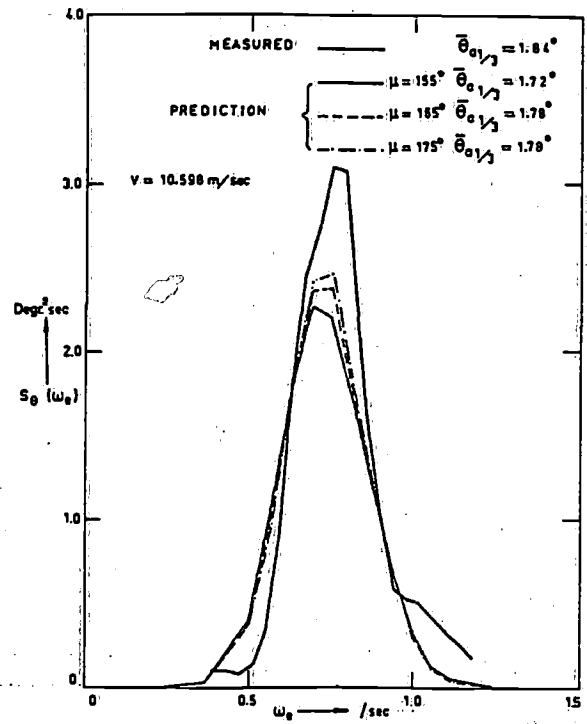


Fig. 16. Measured pitch spectrum for run 4 and predictions for direction of wave travel  $\mu = 155^\circ, 165^\circ, 175^\circ$ .

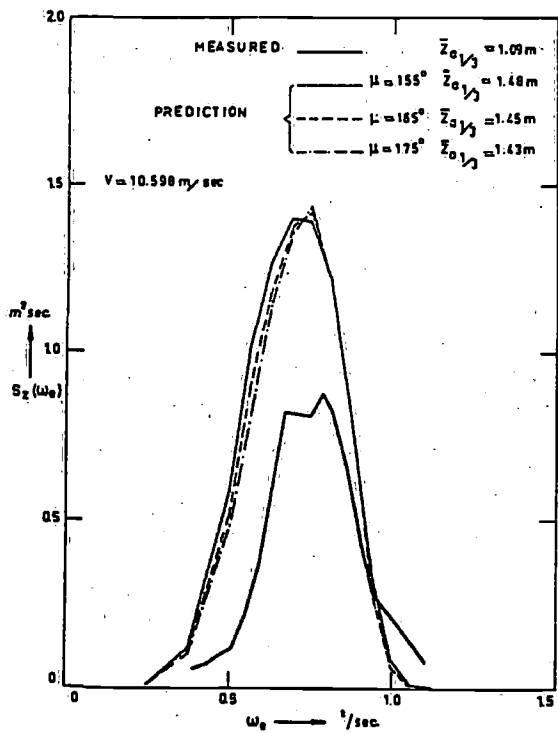


Fig. 15. Measured heave spectrum for run 4 and predictions for direction of wave travel  $\mu = 155^\circ, 165^\circ, 175^\circ$ .

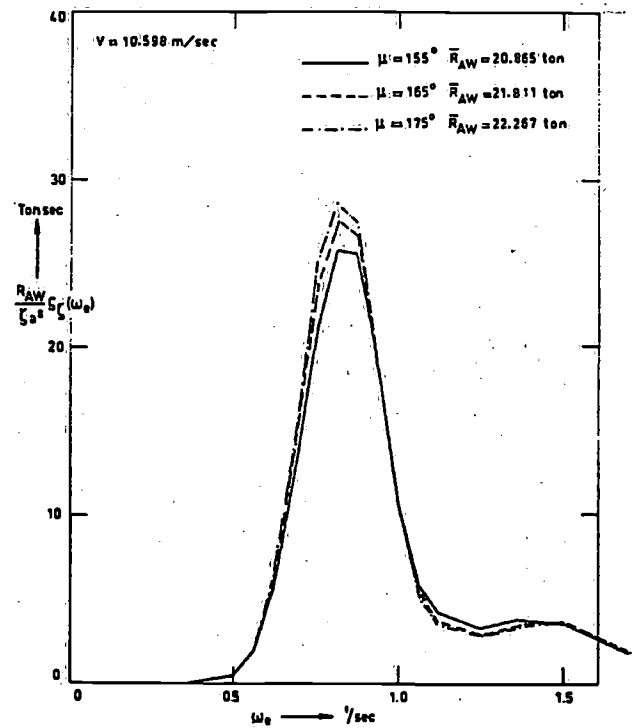


Fig. 17. Predicted added resistance spectra for run 4 and direction of wave travel  $\mu = 155^\circ, 165^\circ, 175^\circ$ .

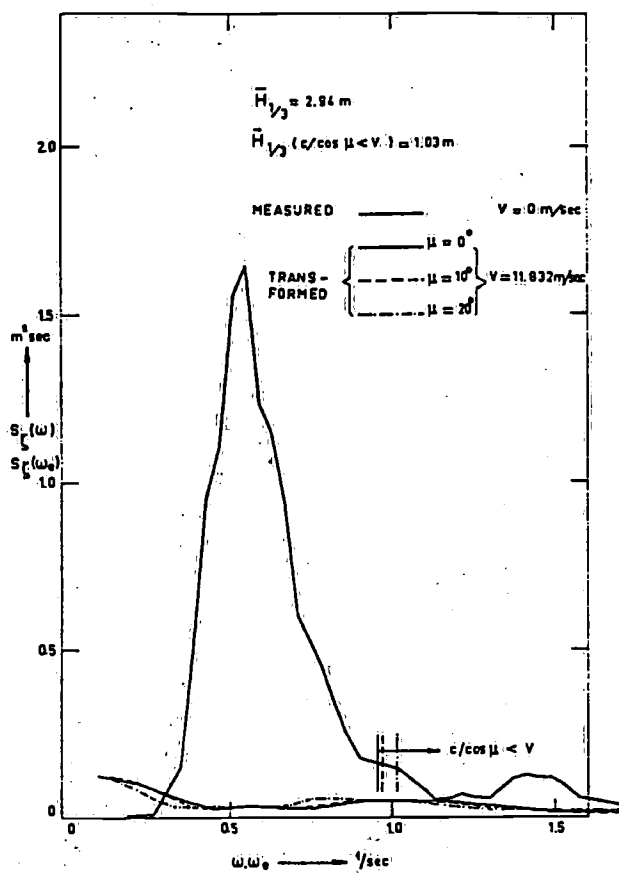


Fig. 18. Measured wave-spectrum for run 6 with spectra transformed for speed and direction of wave travel  $\mu = 0^\circ, 10^\circ, 20^\circ$ .

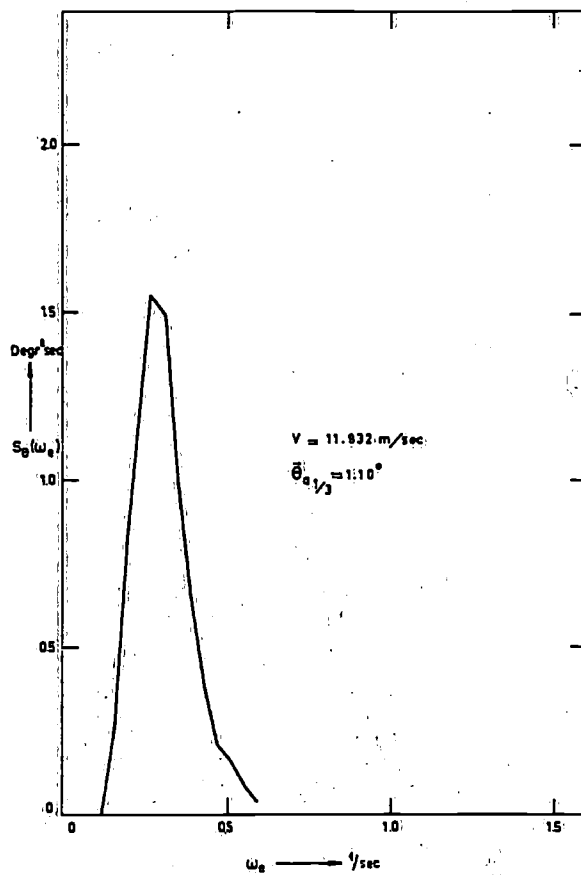


Fig. 20. Measured pitch spectrum for run 6.

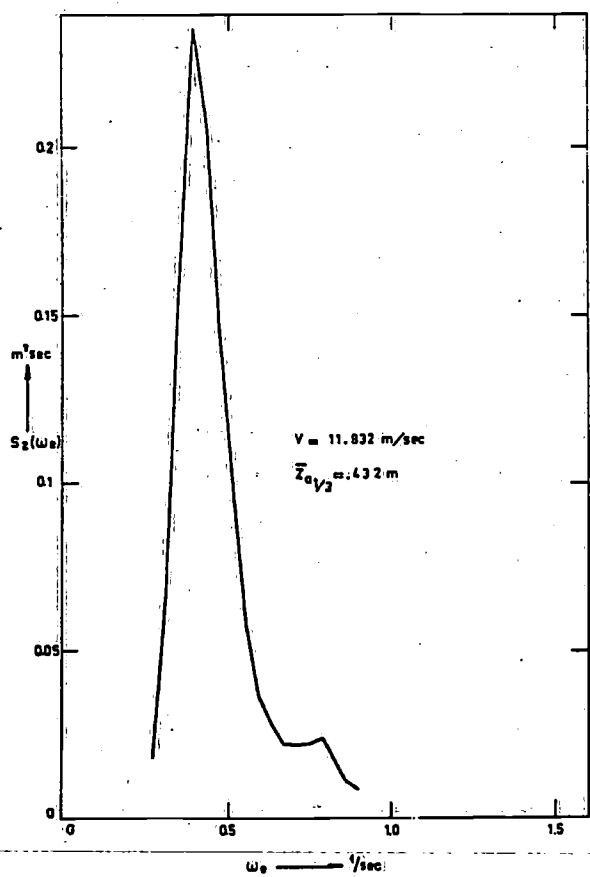


Fig. 19. Measured heave spectrum for run 6.

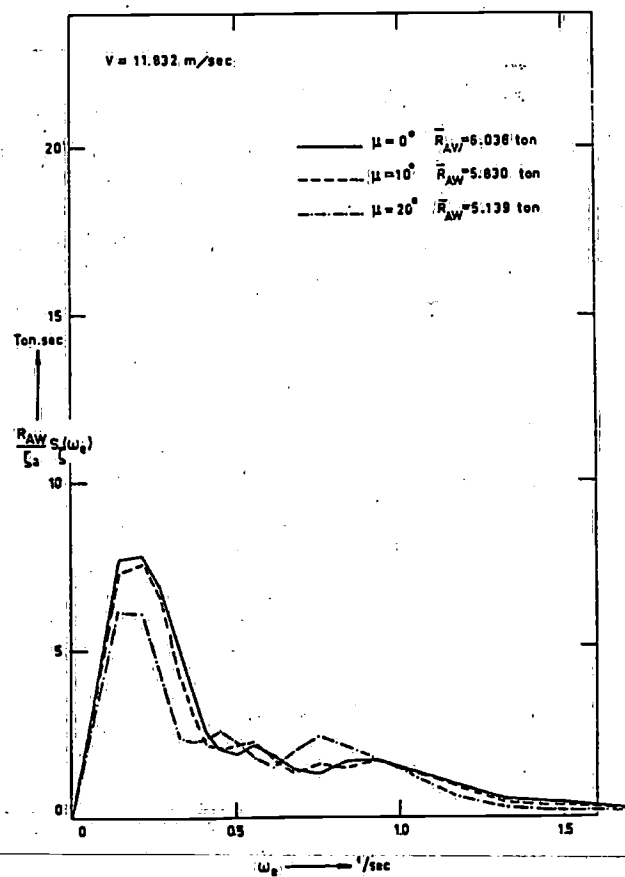


Fig. 21. Predicted added resistance spectra for run 6 and direction of wave travel  $\mu = 0^\circ, 10^\circ, 20^\circ$ .

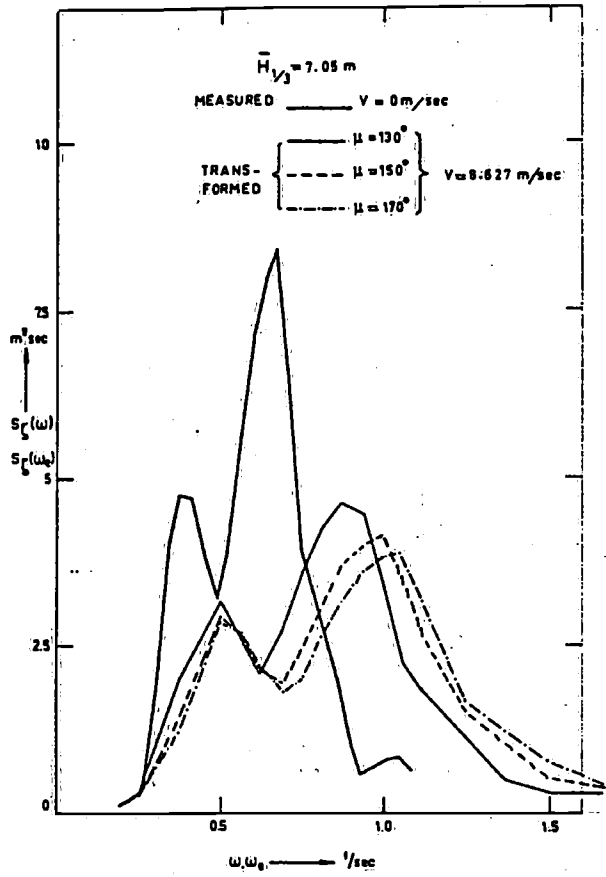


Fig. 22. Measured wave spectrum for run 7 with spectra transformed for speed and direction of wave travel  $\mu = 130^\circ, 150^\circ, 170^\circ$ .

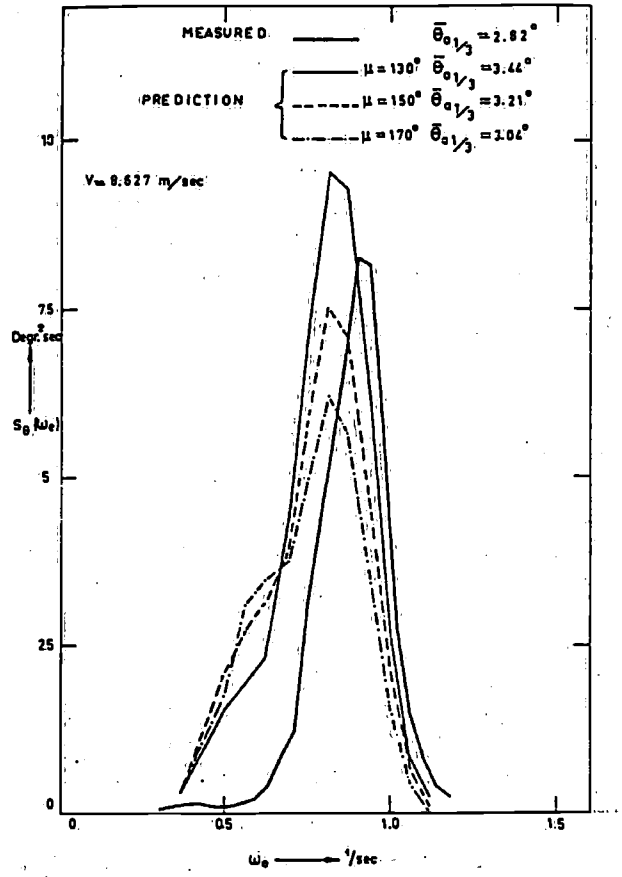


Fig. 24. Measured pitch spectrum for run 7 and predictions for direction of wave travel  $\mu = 130^\circ, 150^\circ, 170^\circ$ .

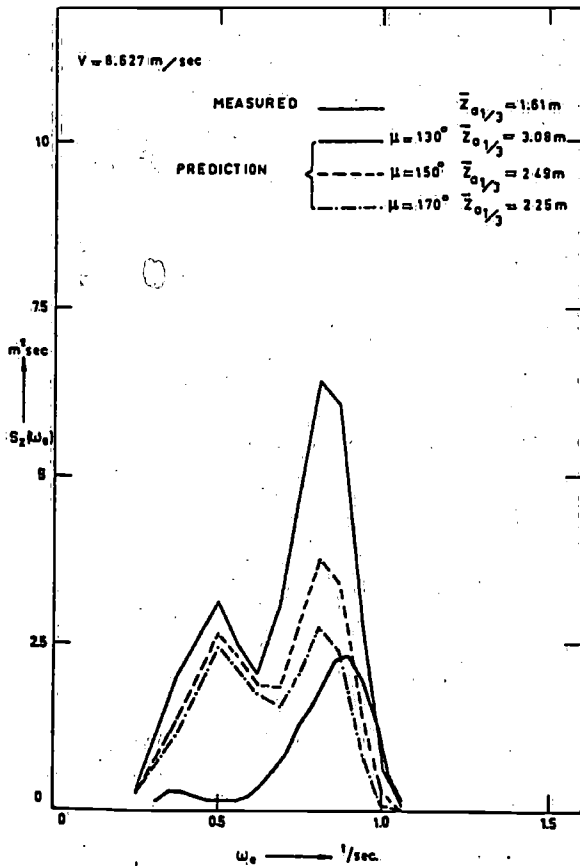


Fig. 23. Measured heave spectrum for run 7 and predictions for direction of wave travel  $\mu = 130^\circ, 150^\circ, 170^\circ$ .

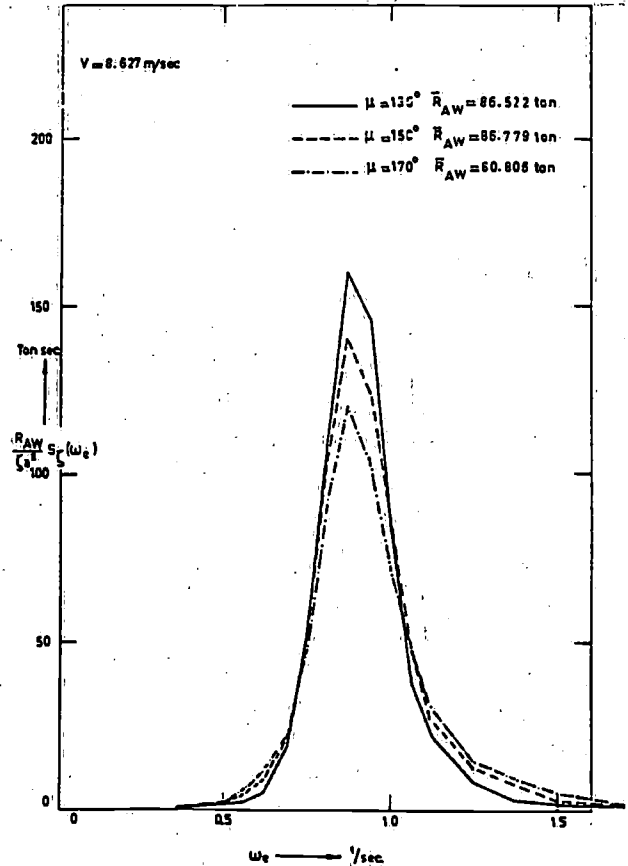


Fig. 25. Predicted added resistance spectra for run 7 and direction of wave travel  $\mu = 130^\circ, 150^\circ, 170^\circ$ .

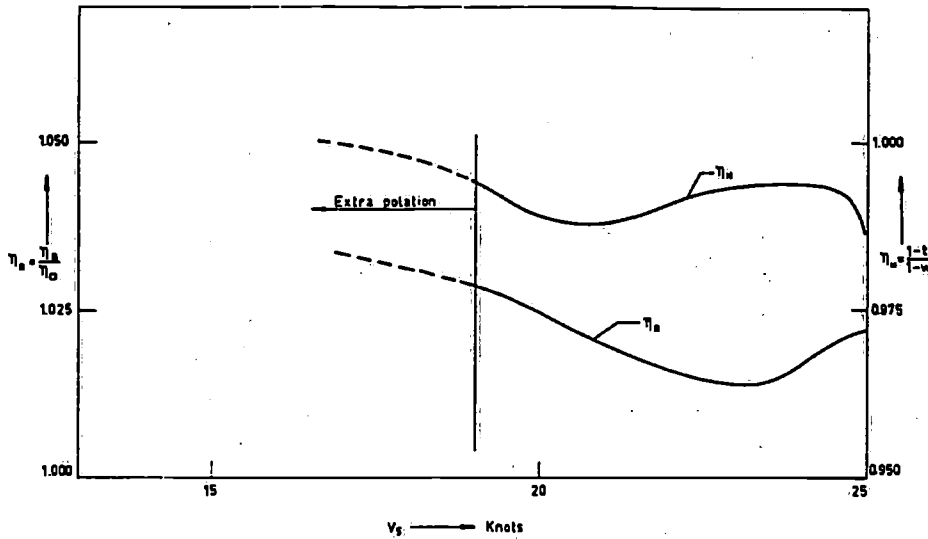


Fig. 26. The relative rotational efficiency  $\eta_R$  and the hull efficiency  $\eta_H$  as a function of ship speed.

From the torque measurements the average torque coefficient may be computed as follows:

$$K_{Q_{P,SB}} = \frac{\bar{Q}_{P,SB} \cdot \eta_S \cdot \eta_R}{\rho \cdot \bar{n}_{P,SB} \cdot D^5} \quad (5)$$

where

- $\eta_S$  = the shafting efficiency, for this case taken as .97
- $\eta_R = \eta_B/\eta_0$  = the relative rotational efficiency
- $\eta_B$  = the propeller efficiency behind the ship
- $\eta_0$  = the propeller efficiency in open water
- $D$  = propeller diameter
- $\rho$  = density of water.

The relative rotational efficiency  $\eta_R$  as well as the hull efficiency  $\eta_H$  as a function of ship speed is shown in fig. 26, which has been derived from propulsion tests of the NSMB at Wageningen [7].

With the aid of the open water diagram, shown in fig. 27, it is possible to determine the following parameters:

- $J_{P,SB}$  = the average advance coefficient
- $K_{T_{P,SB}}$  = the average thrust coefficient
- $\bar{\eta}_{0_{P,SB}}$  = the average propeller efficiency in open water.

For the average advance coefficient the following relation may be written:

$$J_{P,SB} = \frac{V_S(1 - \bar{w}_{P,SB})}{\bar{n}_{P,SB} \cdot D} \quad (6)$$

in which:

- $V_S$  = the average ship speed
- $\bar{w}_{P,SB}$  = the Taylor wake fraction
- $D$  = propeller diameter.

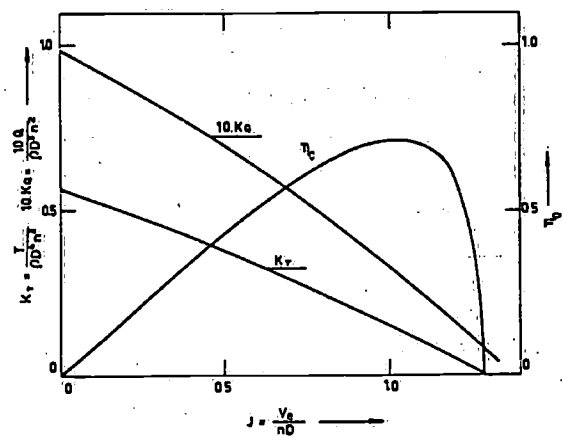


Fig. 27. Open water diagram.

The average wake fraction derived from (6) may be written as:

$$\bar{w}_{P,SB} = 1 - \frac{J_{P,SB} \cdot \bar{\eta}_{0_{P,SB}} \cdot D}{V_S} \quad (7)$$

For this case it is assumed, that the relation between the thrust deduction fraction  $t$  and the wake fraction  $w$  and consequently the hull efficiency  $\eta_H = 1 - t/1 - w$  remains constant both for still water and in waves.

The total propulsive efficiency  $\eta_{D_{P,SB}}$  may be determined in the following way:

$$\eta_{D_{P,SB}} = \eta_0 \cdot \eta_H \cdot \eta_R \cdot \eta_S \quad (8)$$

Afterwards it is possible to compute the average effective power for the port and starboard side with:

$$\bar{P}_{E_{P,SB}} = \eta_{D_{P,SB}} \cdot \bar{P}_{S_{P,SB}} \quad (9)$$

from which by addition the average total effective power for the whole ship can be obtained:

$$\bar{P}_E = \bar{P}_{E_P} + \bar{P}_{E_{SB}} \quad (10)$$



Finally the determination of the average total propulsive efficiency for the whole ship may be computed with:

$$\bar{\eta}_D = \bar{P}_E / \bar{P}_S \quad (11)$$

The results of the propulsion analysis for the runs in still water and in waves are summarized in table 11. The maximum variation in torque occurred during periods of encounter which were near the resonance period of the vertical motion ( $T_e = 6.85$  sec).

For run 7, as shown in the tables 4 and 5, this maximum variation was about 18% of the average value and occurred on the starboard shaft.

The average number of revolutions was counted each 10 seconds. The variation during this time was about 2%. The variation of the number of revolutions within a period of encounter remained unknown.

For this reason a maximum variation of power could not be established unless the number of revolutions was supposed to be almost constant. In that case the maximum variation of the power may be set equal to the maximum torque variation.

### 3 Prediction

#### 3.1 General

The total ship resistance and consequently the power may be divided into three principal parts, viz.:

- the still-water resistance  $R_{SW}$ , for a certain ship mainly depending on the ship speed  $V_S$
- the wind resistance  $R_W$  depending on wind speed  $V_W$  and -direction  $\mu$  and also on the ship speed  $V_S$
- the added resistance in waves  $R_{AW}$  for a certain ship depending on the ship speed  $V_S$ , the significant wave height  $H_3$  and the direction of wave travel  $\mu$ .

Provisionally it is supposed, that the wind direction coincides with the direction of wave travel  $\mu$ . For the predictions separate values can be used. For the total ship resistance in a seaway it is possible to write:

$$R(V_S, V_W, \mu, H_3) = R_{SW}(V_S) + R_W(V_S, V_W, \mu) + R_{AW}(V_S, H_3, \mu) \quad (12)$$

These parts of the subdivision of the total ship resistance will be treated separately in the following sections.

#### 3.2 Still water resistance

The still water resistance and consequently the effective power  $P_E$  can be determined according to several methods. For the "Atlantic Crown", the following methods have been applied:

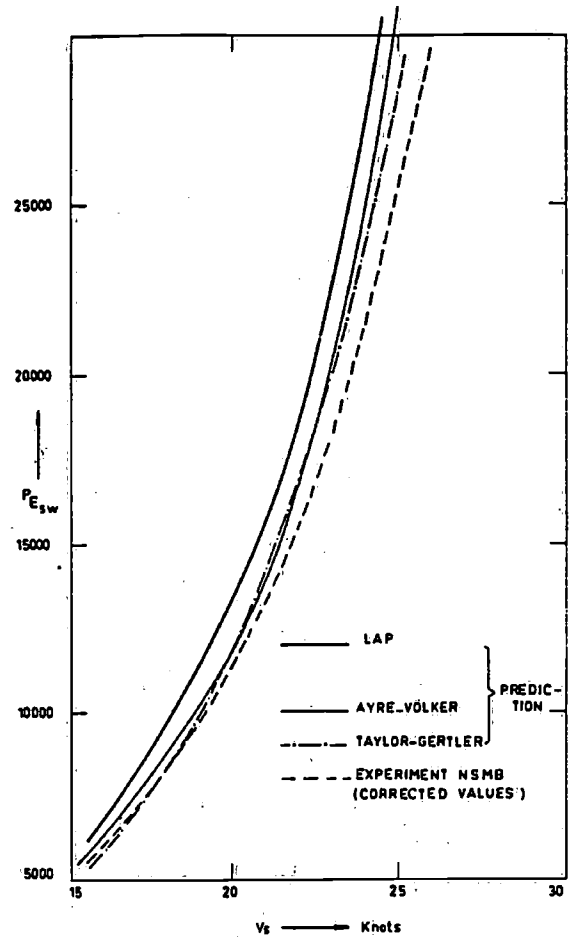


Fig. 28. Predicted and measured effective power  $P_{E_{SW}}$  in still water.

- the Taylor-Gertler method [8]
- the method according to Ayre Völker [9]
- the Lap method [10].

Extra allowances up to 15% have been taken into account because of bossings, rudder, stabilizers and bow thrusters.

The wind allowance will be treated separately in 3.3. The values of calculated effective power according to the above-mentioned methods are shown in fig. 28 together with the model measurements of NSMB [7]. For this case the measurements have been corrected for trial allowances as has been reported by De Jong in [11]. The calculated effective power as shown in fig. 28 has not yet been corrected for the influence of the bulb as e.g. mentioned in [12, 13, 14, 15, 16].

The experiments at NSMB have been carried out for a speed range of 19-26 knots. For values below 19 knots an extrapolation has been applied according to the Taylor-Gertler curve. The power has also been corrected for the difference in displacement  $\Delta$  to the ratio  $\Delta^{2/3}$ . For the determination of the shaft power  $P_S$  use has been made of the propulsion tests of NSMB. For this case too the quasi propulsive coefficient  $\eta'_D$  has

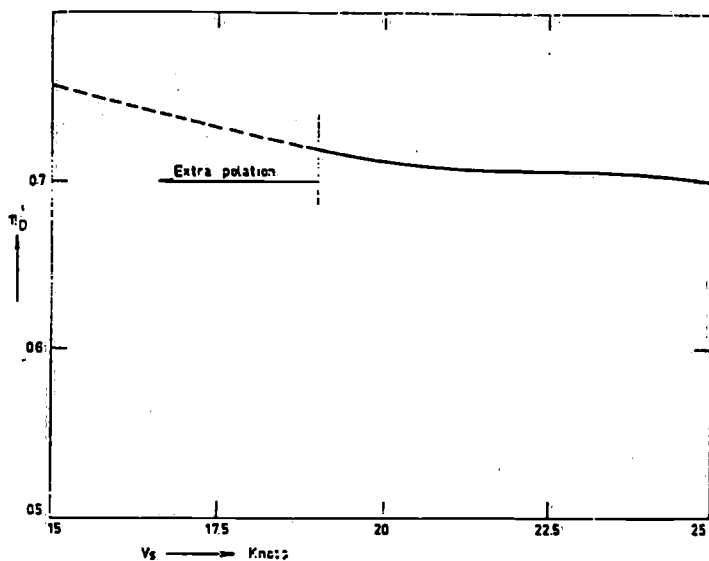


Fig. 29. The quasi propulsive coefficient  $\eta'_D$  as a function of ship speed.

been extrapolated below the speed of 19 knots as shown in fig. 29. As in the power analysis in 2.3 the shafting efficiency  $\eta_S$  will be considered to be .97. With the total propulsive efficiency  $\eta_D = \eta'_D \times \eta_S$  the shaft power  $P_S$  can be calculated as

$$P_S = P_E / \eta_D \quad (13)$$

The curves of shaft power as a function of speed for the Taylor-Gertler method and the experimental results of NSMB are shown in fig. 5.

A reduction of the shaft power on account of the influence of the bulb as mentioned before has been presented in [12, 13, 14, 15, 16] for some speeds. This reduction, which may be substantial for overpowered ships, is strongly dependent on speed. To take into account such a bulb-reduction of the shaft power for the required speed range is a risky matter. A servicable rule can hardly be derived from present literature. For the economic speed  $V_{ECO}$  in [12], defined as

$$V_{ECO} = (1.85 - 1.6C_P) \sqrt{L_f} \quad (14)$$

the reduction in shaft power may be 8.2% for the 9.5% bulb of the "Atlantic Crown". This reduction for a speed of  $0.95V_{ECO}$  has been decreased to 4.6%. A diagram of this reduction for some speeds has been presented in fig. 30 and is based on statistics of NSMB as published in [12].

The reduced values of shaft power for both above mentioned speeds are shown in fig. 5, from which it is clear, that these predicted values show a rather good agreement with the corrected NSMB measurements. In this figure is also plotted the still water shaft power

$P_S$  being a function of the speed as calculated from the measurements on board of the "Atlantic Crown". These measurements, however, showed that an indicated speed at the log of 24 knots generally appeared to be 1 knot too high.

This fact has been carefully checked with the aid of the Decca-system and stream cards.

For this reason the run speeds as indicated by the log will be corrected by the ratio  $23/24 = 0.9583$ . Looking again at fig. 5 it appears, that if this speed correction is applied to the full scale measurements in still water there is a good agreement with the corrected experimental values of NSMB.

In the future only the corrected measurements of NSMB will be used for prediction.

### 3.3. Wind resistance

It may be expected, that the influence of the wind on the total resistance will be significant for container ships, because of the large free board and the containers on deck.

The usual air resistance coefficients for normal cargo ships should yield low values for resistance forces.

Therefore a special model test has been arranged in the towing tank as described in appendix III of [17].

For this purpose a model of the "Atlantic Crown" to a scale ratio of 125 was towed through the water upside down at various angles of attack  $\mu$ .

The model was connected to an elliptical plate by force dynamometers, which restrained the model in the horizontal plane to determine the longitudinal and lateral forces and the yawing moment.

The elliptical plate was supposed to act as the free water surface. Adjustment of the angle of attack  $\mu$  was

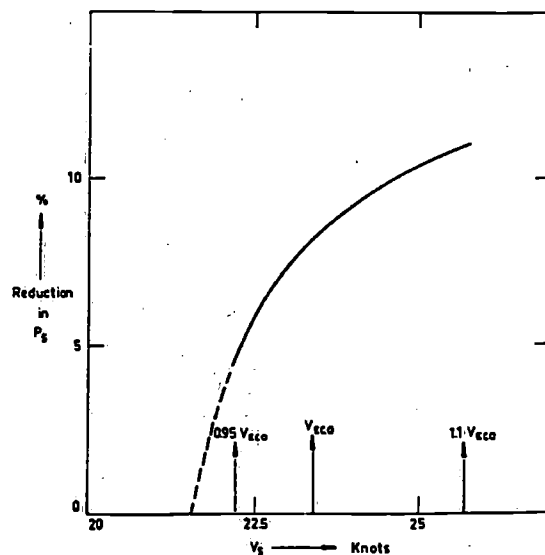


Fig. 30. Shaft power reduction related to speed on account of the bulb ( $f_{BT} = 9.5\%$ ).

achieved by rotation of the set-up round a vertical axis. For this case the longitudinal force is important. This force has been expressed in the form of a coefficient as follows:

$$C_{X_{AL}} = \frac{F_X}{\frac{1}{2} \rho_a V_R^2 A_L} \quad (15)$$

where:

- $F_X$  = the longitudinal force considered positive when directed from stern to bow
- $\rho_a$  = the density of air
- $V_R$  = the relative apparent wind speed
- $A_L$  = the lateral projected wind area of the model.

The wind force coefficient  $C_{X_{AL}}$  as a function of  $\mu$  has been shown in fig. 31 for the model speeds of .5, .75, 1, 1.5 and 2 m/sec where  $\mu$  is the angle of the relative wind off the stern.

It is important to ascertain, that air resistance coefficients determined with model tests may differ remarkably for containerhips. Analog model tests for another containerhip as described in [17] yielded air resistance coefficients with about twice the values as measured for the model of the "Atlantic Crown".

The experimental results have been compared in fig. 32 with calculations of the wind force coefficient proposed by Isherwood in [18]. In this procedure the wind force coefficient has been expressed with respect to the transverse projected wind area of the model  $A_T$ . For comparison it was necessary to transform the coefficient  $C_{X_{AT}}$  into  $C_{X_{AL}}$  while taking into account the reversed direction for  $\mu$  and  $F_X$ .

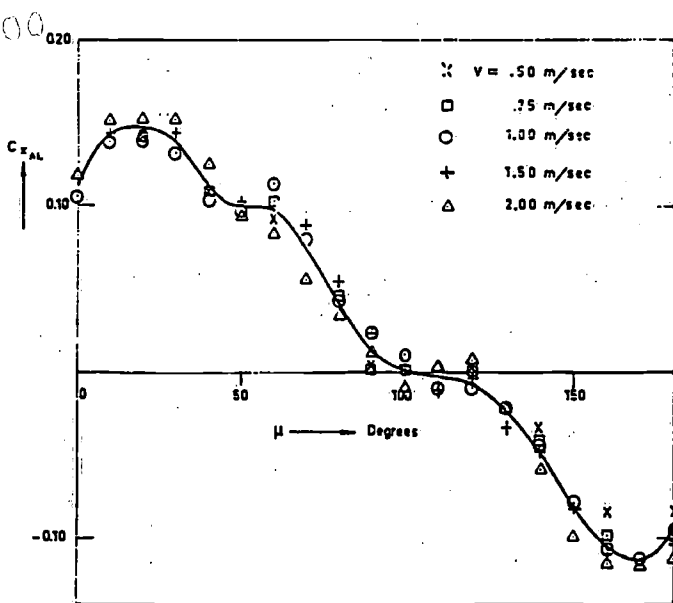


Fig. 31. The measured wind force coefficient related to wind direction  $\mu$ .

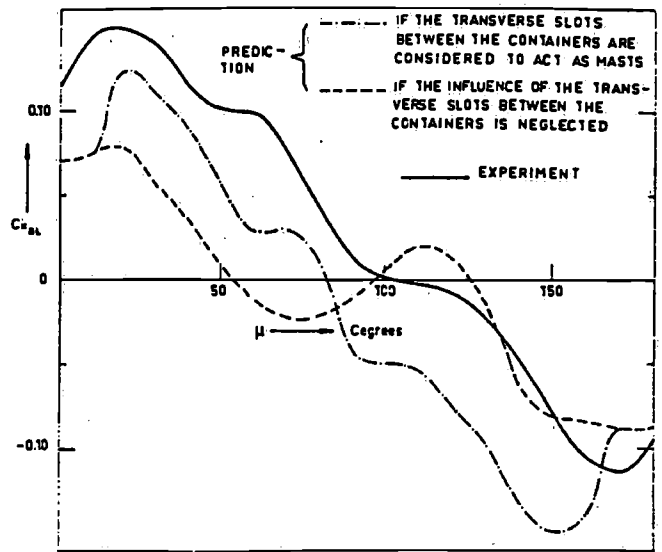


Fig. 32. Measured and predicted wind force coefficient related to wind direction  $\mu$ .

The longitudinal force coefficient as derived from experiments by Isherwood can be written as follows:

$$C_{X_{AT}} = A_0 + A_1 \frac{2A_L}{L_{OA}^2} + A_2 \frac{2A_T}{B^2} + A_3 \frac{L_{OA}}{B} + A_4 \frac{S}{L_{OA}} + A_5 \frac{C}{L_{OA}} + A_6 M \pm 1.96 S.E. \quad (16)$$

where:

- $L_{OA}$  = length overall
- $B$  = breadth of ship
- $S$  = length of perimeter of lateral projection of model excluding waterline and slender bodies such as masts and ventilators
- $C$  = distance from bow of centroid of lateral projected area
- $M$  = number of distinct groups of masts or king-posts seen in lateral projection
- $S.E.$  = standard error.

The mean value of the residual standard error for all values of  $\mu = .1$  for  $C_{X_{AT}}$ .

The calculations for the mean value of (16) have been carried out for two cases viz.:

1. if the transverse slots between the containers are considered to act as masts for the number of distinct groups of masts  $M = 10$  should be taken in (16)
2. if the influence of the transverse slots between the containers is neglected only one real mast has to be taken into account, so  $M = 1$ .

It may be observed from fig. 32, that for head winds the most satisfactory results in comparison with the

experiments are obtained for case 2 if the influence of the containers as masts is neglected.

In case 1, if the slots between the containers are considered to act as masts, the situation is somewhat reversed and for down winds better agreement is achieved than in case 2.

In fig. 33 is shown the experimental curve for  $C_{XAL}$  and the calculated mean curve with the accessory upper and lower limit following from the standard error according to [18] for the case, that the transverse slots between the containers are neglected (case 2).

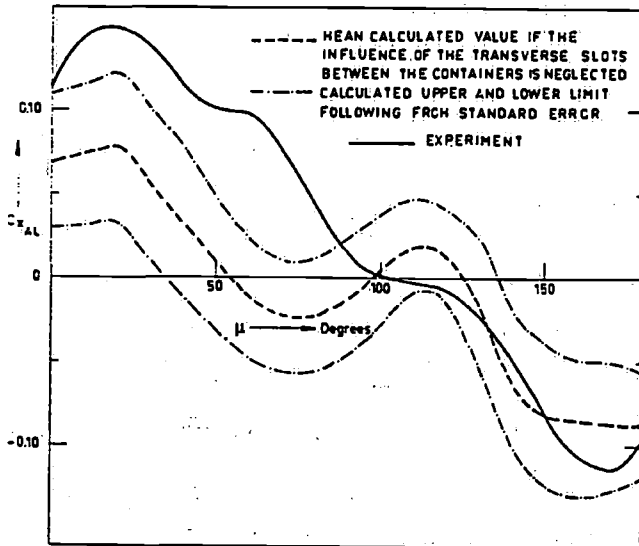


Fig. 33. Measured and predicted wind force coefficient with limit values.

It should be remarked from fig. 33, that for down winds the measured values are not within the calculated upper and lower limit at all.

For the prediction of the added power because of the wind only use will be made of the experimental results as shown in fig. 31.

In view of the calculation of the effective power because of wind a negative longitudinal force  $F_x$  and consequently the coefficient  $C_{XAL}$  will be equated to a positive resistance  $R_W$ .

With the measured wind speed  $V_R$  and the measured wind direction  $\mu$  the effective horse power due to wind can be obtained with:

$$P_{EW} = \frac{-C_{XAL} \frac{1}{2} \rho_a A_L V_R^2 V_S}{75} \quad (17)$$

From the measured wind speed  $V_R$ , the measured wind direction  $\mu$ , the ship speed  $V_S$  and the ship's course it is possible to determine the absolute wind speed and -direction. The results are shown in table 3.

### 3.4 Added resistance in waves

Following the strip theory [19], the added resistance in waves may be predicted according to the method developed in [1], where the energy of the radiated damping waves during a period of encounter is equalized to the work necessary to maintain the speed in the waves.

The regular wave surface is defined with respect to a right hand coordinate system  $xyz$ , which travels with the ship speed  $V$  relative to a system  $x_0y_0z_0$  fixed in space and shown in fig. 34. So velocities and forces are supposed to be positive when directed from stern to bow.

If a positive resistance is characterized as a negative longitudinal force, the next energy relation for oblique waves may be written:

$$-R_{AW}(c/\cos \mu - V)T_e = \int_0^L \int_0^{T_e} b' V_{za}^2 dt dx_b \quad (18)$$

in which

- $R_{AW}$  = the added resistance in waves
- $c$  = wave velocity
- $b'$  =  $N' - V(dm'/dx_b)$  = sectional damping for speed
- $N'$  = sectional damping for zero speed
- $m'$  = sectional added mass for zero speed
- $T_e$  =  $\lambda'/(c/\cos \mu - V)$  = period of encounter
- $\lambda'$  =  $\lambda/\cos \mu$  = apparent wave length
- $\lambda$  = wave length
- $\mu$  = direction of wave travel
- $V_{za}$  = amplitude of the vertical relative water velocity for each section.

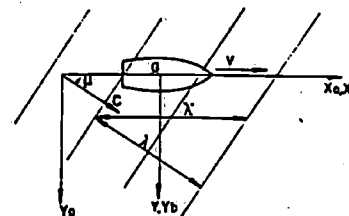
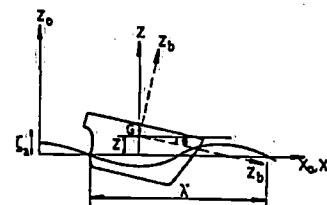


Fig. 34. Definition of wave, ship speed and motions

The added resistance for a ship in regular oblique waves follows from (18) in the same way as described in [1]:

$$R_{AW} = -\frac{k \cos \mu}{2\omega_e} \int_0^L b' V_{za}^2 dx_b \quad (19)$$

where

- $k = 2\pi/\lambda =$  wave number
- $\omega_e = 2\pi/T_e =$  circular wave frequency of encounter
- $V_{zo} =$  the amplitude of the vertical relative water velocity for each section:  $V_z = \dot{z} - x_b\dot{\theta} + V\theta - \dot{\zeta}^*$
- $z =$  heave displacement
- $\theta =$  pitch angle
- $\zeta^* = \zeta \left( 1 - \frac{k}{y_w} \int_{-T}^0 y_b e^{kz} dz_b \right) =$   
the effective vertical wave displacement for a cross section. For this conception reference is made to [19].

It may be concluded from (19), that the added resistance in waves varies as the squared wave height because  $V_{zo}$  is proportional to the wave height. This relation has also been stated in an experimental way in [1].

The dimensionless transfer function for the resistance increase  $\sigma_{AW}$  is given by

$$\sigma_{AW} = \frac{R_{AW}}{\rho g \zeta_w^2 (B^2/L)} \tag{20}$$

where

- $\rho =$  density of water
- $g =$  acceleration of gravity
- $\zeta_w =$  wave height (double amplitude)
- $B =$  breadth of ship
- $L =$  length between perpendiculars

For a known wave spectrum  $S_\zeta(\omega_e)$  the average resistance increase  $\bar{R}_{AW}$  can be calculated as described in [20] with:

$$\bar{R}_{AW} = 8\rho g \frac{B^2}{L} \int_0^\infty \sigma_{AW}(\omega_e) S_\zeta(\omega_e) d\omega_e \tag{21}$$

The effective horse power because of ship motions in a given wave spectrum  $S_\zeta(\omega_e)$  can be derived in the following way:

$$P_{EAW} = \frac{\bar{R}_{AW} \times V_S}{75} \tag{22}$$

The direction of wave travel  $\mu$  has been determined visually for the different runs. An error of 10 or even 20 degrees in this estimation is quite possible. To check the influence of such an error on the motions and the added power in a seaway the calculations have been carried out for several directions of wave travel above and below the estimated values. The dependency of the added power on the direction of wave travel and the ship speed has been demonstrated in tables 8,

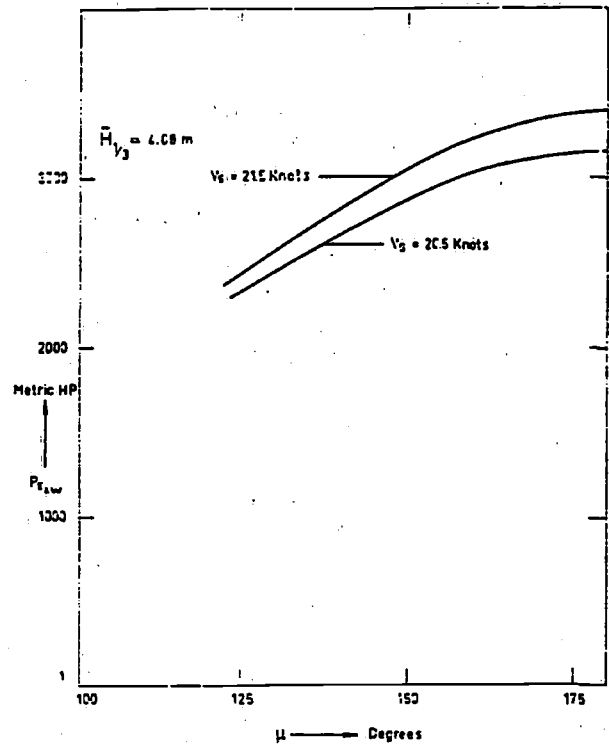


Fig. 35. The added effective power in waves  $P_{EAW}$  related to the direction of wave travel  $\mu$  for run 4.

9 and 10 for the runs considered and in fig. 35 for run 4.

The differences in ship speed are in magnitude equal to the applied ship speed correction. From tables 8-10 and fig. 35 it is obvious, that the differences in added power for a certain deviation of direction of wave travel are increasing with the approach to the beam sea condition.

Moreover one should keep in mind, that because of the neglect of the influence of the horizontal and rolling motions the differences in added power with respect to real values may also increase with the approach to the beam sea condition. For both reasons it is provisionally accepted, that the predictions of added power in waves are useful for a strip theory neglecting the horizontal and rolling motions if for following waves

$$-\frac{\pi}{6} \text{ rad } (-30 \text{ degrees}) < \mu < \frac{\pi}{6} \text{ rad } (30 \text{ degrees})$$

and for head waves if

$$\left( \pi - \frac{\pi}{6} \right) \text{ rad } (150 \text{ degrees}) < \mu < \left( \pi + \frac{\pi}{6} \right) \text{ rad } (210 \text{ degrees}) \tag{23}$$

It should be remarked, that these conditions are not satisfied in the case of run 4, so that rather large

deviations from the measured values may be expected and will be ascertained in 4.

Finally it follows from tables 8, 9 and 10, that differences in added power because of errors of 20 degrees in the estimated direction within the denoted area plus differences in ship speed of about 4% may cause deviations in the total predicted power of maximum 7%.

When considering following seas only that part of the wave spectrum which includes waves moving at a speed lower than that of the ship have been included in the added power computation. In this case the motions because of this part of the spectrum are not so important and the added power is mainly caused by wave-motion.

For the other part of the wave spectrum provisionally an equilibrium at zero between the high positive and negative values will be assumed with respect to the added resistance in waves.

It should be noted, that the pitch and heave motions in a following sea appeared to be very low in frequency as already mentioned in 2.2.3 and shown in figs. 19 and 20; therefore the added resistance may be regarded as insignificant in these cases.

### 3.5 Total power

The total effective power in a seaway can be obtained by addition of the three separate parts as mentioned in 3.1 viz.:

- the still water power
- the wind power
- the added power in waves.

In this way the total effective power will be:

$$P_E = P_{ESW} + P_{EW} + P_{EAW} \quad (24)$$

A view of these parts of the effective power for the three runs considered is given in table 12.

With the propulsive efficiency  $\eta_D$  as derived in 2.3, the total shaft power and the same subdivision as mentioned for the effective power can be predicted.

The calculated values and percentages of the different parts with respect to the total shaft power are shown in table 13 for the three runs.

The predicted values of the effective power for the port- and starboard side have been determined according to the ratio of the measured values. The shaft power for the port- and starboard side could be calculated with the respective propulsive efficiencies  $\eta_{Dp, sb}$ .

A general view of the power for the total ship and the subdivision over the port- and starboard side are presented in table 14 for both the measured and predicted values.

### 3.6 Spectra

The wave spectra derived from the buoy-signal by means of spectral analysis, as denoted in 2.2, are shown in the figs. 10, 14, 18 and 22 for the runs considered. The same spectra have been used as an input for the prediction of the pitch- and heave spectra. The required calculations have been carried out by means of the seakeeping computerprogram called "TRIAL" on the IBM 360/65 computer of the Mathematical Centre of the University [21].

First the response functions for the motions and the added resistance were calculated. Afterwards the measured wave spectra had to be transformed for the ship speed. These transformed wave spectra are also shown in the figs. 10, 14, 18 and 22 on the base of the frequency of encounter for the directions of wave travel as denoted in the tables 8, 9 and 10.

Finally the heave, pitch and added resistance spectra were computed for the different runs and the directions of wave travel and the results are shown in the figs. 11, 12, 13, 15, 16, 17, 21, 23, 24, 25 together with the measured pitch and heave spectra.

For run 6 in following waves only the transformed wave and predicted added resistance spectra have been presented. The transformed wave spectra of this run are only related to the waves with velocity lower than the ship speed in view of the added resistance in waves as had been explained under 3.4.

The part of the measured wave spectrum, that has been considered ( $c/\cos \mu < V$ ) is indicated in fig. 18 for run 6. The predicted motions appeared to be so small for this part of the spectrum, that presentation in a diagram is rather useless.

The agreement between the predicted and measured motion spectra for run 4 and run 7 is only satisfactory for the high frequency range. The difficulties with respect to the low frequency range have already been mentioned in the introduction.

It is difficult to say whether these differences in the low frequency range are caused by deviations in the analyzed wave- or motion spectra.

From figures 11-25 it is also obvious that differences in the motion spectra with respect to the wave direction are increasing with the approach to the beam sea situation. The same phenomenon has been ascertained for the added resistance in waves in 3.4.

## 4 Discussion

The differences between the predicted shaft power for the total ship and the measured values are given in percentages of the measured quantities in table 14. From this table it is obvious, that the most reasonable prediction was made for run 7 with only 4% deviation

and the worst prediction was made for run 4 with 22% deviation. For run 4 a strong difference could be expected as already had been supposed in 3.4 because of the direction of wave travel, which was 45 degrees off the bow ( $\mu = 135^\circ$ ).

The prediction of the total shaft power in a seaway depends on the accuracy of the prediction of each of the three parts mentioned before. The most influential part appears to be the still water resistance, since this part is strongly dependent on the ship speed in the higher speed range. An example of this influence is shown in table 15, where the difference of shaft power in still water for the corrected- and uncorrected speed has been expressed as a percentage of the total measured values in waves. In this way the difference between prediction and measurement of the total shaft power can partly be explained.

As stated under 3.4 the speed correction together with an error in the direction of wave travel of 20 degrees may cause a maximum difference in the total predicted shaft power of 7%, which is a good deal less than the maximum possible error of 17% in the still water part because of an unreliable ship speed measurement.

From table 13 it is clear, that for run 7 the added power in waves is 53% of the total predicted power which is notably high.

The predicted wind power as a percentage of the total predicted power has been presented in table 13 and appears to be 9, .5 and  $\approx 11\%$  for the runs 4, 6 and 7, respectively.

For head winds (runs 4 and 7) the measured test results for determination of the wind resistance coefficient agreed rather well with the results of the regression analysis of Isherwood as mentioned in [18].

More than 11% of the total power as predicted for the most reliable run 7 can hardly be expected for this ship. For other container ships the influence of the wind power may be quite different as had been mentioned in 3.3. The results of run 6 in following waves are as a first step rather satisfactory, especially if the high possible error of the still water resistance (17%) is taken into account. The ship speed in following waves is generally very high and that fact implies an increasing possible error for the part of the still water power in the total power.

## 5 Conclusions and recommendations

From the analysis of the full scale measurements of waves, wind, vertical ship motions, propulsion characteristics etc. and from model tests for the determination of wind resistance coefficients compared with predicted values, it may be stated, that

1. Prediction of added power in waves by determination of the radiated energy of the damping waves is satisfactory.
2. Restriction of the strip-theory to vertical motions only also restricts the use of such a theory to a direction of wave travel of about 30 degrees off the bow and stern.
3. The fraction of the added power in waves may be more than 50% and the wind power 11% of the total power for head seas with a significant wave height of 7 m.
4. For a satisfactory analysis of the measurements an accurate determination of the ship speed is very important, especially for the high speed range where the still water power is seriously affected by speed changes.
5. The prediction of the still water resistance in the higher speed range for ships with bulbs needs to be more accurate.
6. It is most important to note, that of the three categories of resistance previously mentioned, the still water resistance is most critical. This may be demonstrated if it is considered, that an error of 4% in the ship speed and 20 degrees in the direction of wave travel may cause a maximum error of 7% in the total power due to the added power in waves.  
However, the same error of 4% in the ship speed may cause an error of more than 10% in the total power due to the still water part.
7. Wind model tests as had been carried out for the ship considered may deliver quite different air resistance coefficients for other container ships and therefore it might be desirable to design the part of a container ship above the waterline with regard to aerodynamic considerations.
8. The procedure of Isherwood for the prediction of windpower should be adapted for container-ships.
9. A good agreement between estimated and measured significant wave height has been established.
10. While sailing in a head sea with a significant wave height of 7 m, the torque variation registered a maximum of 18% of the average value. This determination was made during periods of encounter near the resonance period of the vertical motion.
11. For a good prediction of the total shaft power in waves, it is essential to know in advance the total propulsive efficiency in overload conditions.
12. Further improvement of the measurement of the wave signal with a buoy in the future is necessary. This is especially true for the low frequency domain to obtain a better correlation between the

predicted and measured motion spectra resulting in a more reliable prediction of the added power in waves.

13. The prediction of the added power in following waves as a first step is satisfactory.
14. More investigation is necessary on the subject of added power in following seas. This may especially be said about the assumption, that the only portion of the wave spectrum to be considered is that containing waves of a speed lower than the ship speed.

## 6 Acknowledgment

The authors express their gratitude to the shipowners, the Holland-Amerika Lijn, for placing at their disposal the containership "Atlantic Crown" and all other information about the ship. They also appreciate very much the kind cooperation with the crew of the "Atlantic Crown", whose readiness contributed to the successful execution of the experiments described.

Moreover the authors are indebted to the "Netherlands Ship Research Centre TNO", who sponsored a good deal of the necessary provisions.

Special thanks are due to the various members of the staff of the Delft Shipbuilding Laboratory for their assistance in running the whole program.

Particularly the authors wish to mention two members of this staff and also participants in the measuring team viz.: Prof. Ir. J. Gerritsma, who stimulated and guided the whole project and Ir. C. C. Glansdorp, under whose superintendence the wind resistance experiments were carried out.

## References

1. GERRITSMAN, J. and W. BEUKELMAN, Analysis of the Resistance Increase in waves of a fast cargo ship. Netherlands Ship Research Centre TNO, Report no. 169 S, April 1972.
2. PASVEER, F. J., C. C. GLANSDORP and M. BUITENHEK, Data Analyses of Full Scale Measurements with a Hybrid Computer. Laboratorium voor Scheepsbouwkunde, Technische Hogeschool Delft, Report no. 352, March 1972.
3. PASVEER, F. J., Speed-corrected Demodulation and on Line Processing of Data from analog tape. Delft University of Technology Computation Centre, Proceedings of 7th AICA Congress, Praag 1973.
4. BUITENHEK, M., Een boei voor het meten van zeegolven (Dutch). Laboratorium voor Scheepsbouwkunde, Technische Hogeschool Delft, Rapport no. 340, dec. 1971.
5. GERRITSMAN, J., Shipmotions in longitudinal waves. Netherlands Ship Research Centre TNO, Report no. 35 S, February 1960. International Shipbuilding Progress 1960.
6. MARKS, W., The Application of Spectral Analysis and Statistics to Seakeeping. The Society of Naval Architects and Marine Engineers, New York, Technical and Research Bulletin no. 1-24, September 1963.
7. Netherlands Ship Model Basin (NSMB), Wageningen. Model tests with a Container Ship in regular head waves. Report no. 68-056-ZT, May 1968.
8. GERTLER, M., A Reanalysis of the original Test data for the Taylor Standard Series. NSRDC, Washington, Report 806, March 1954.
9. VAN LAMMEREN, W. P. A., L. TROOST and J. G. KONING, Resistance, propulsion and Steering of Ships. Book, 1948.
10. LAP, A. J. W., Diagrammes pour la détermination de la résistance des navires à deux hélices. Les nouveautés Techniques Maritimes.
11. DE JONG, H. J., Proeftochttoeslagen - Deel II (Dutch). Netherlands Ship Model Basin (NSMB), Wageningen, Publikatie no. 329.
12. MUNTJEWERF, J. J., Recente Onderzoekingen van modellen met extreme Bulbstevens (Dutch). Schip en Werf 1965, p. 628-637, 670-673.
13. VAN LAMMEREN, W. P. A. and R. WAHAB, Research on bulbous bow ships. Part IA. Netherlands Ship Research Centre TNO, Report no. 74 S.
14. VAN LAMMEREN, W. P. A. and F. V. A. PANGALILA, Research on bulbous bow ships. Part IB. Netherlands Ship Research Centre TNO. Report no. 76 S.
15. VAN LAMMEREN, W. P. A. and R. WAHAB, Research on bulbous bow ships. Part IIA. Netherlands Ship Research Centre TNO. Report no. 71 S.
16. VAN LAMMEREN, W. P. A. and F. V. A. PANGALILA, Research on bulbous bow ships. Part IIB. Netherlands Ship Research Centre TNO. Report no. 72 S.
17. BRUMMER, G. M. A., C. B. VAN DE VOORDE, W. R. VAN WIJK, and C. C. GLANSDORP, Simulation of the steering- and manoeuvring characteristics of a second generation container ship. Netherlands Ship Research Centre TNO. Report no. 170 S, August 1972.
18. ISHERWOOD, R. M., Wind resistance of merchant ships. Trans. RINA, 1973.
19. GERRITSMAN, J. and W. BEUKELMAN, Analysis of the Modified Strip Theory for the Calculation of Ship Motions and Wave Bending Moments. Netherlands Ship Research Centre TNO, Report no. 96 S, June 1967.
20. GERRITSMAN, J., Behaviour of a Ship in a Seaway. Netherlands Ship Research Centre TNO, Report no. 84 S, May 1966.
21. BEUKELMAN, W. and E. F. BIJLSMA, Description of a program to calculate the Behaviour of a ship in a Seaway (named: TRIAL). Laboratorium voor Scheepsbouwkunde, Technische Hogeschool Delft, Report no. 383, August 1973.



## Tables

Table 1. Main particulars and propeller data of the twin-screw containership "Atlantic-Crown"

designation	symbol	unit	dimensions
Length overall	$LOA$	m	212.42
Length between perpendiculars	$L, L_{pp}$	m	196.00
Length on the waterline	$L_{WL}$	m	203.04
Breadth	$B$	m	28.00
Draught (even keel)	$T$	m	8.153
Volume of displacement	$\nabla$	m <sup>3</sup>	26061
Weight of displacement	$\Delta$	ton	26708
Wetted surface	$S$	m <sup>2</sup>	6337
Centre of buoyancy in length with respect to section 10	$LCB$	m	-1.78
Waterline area	$A_W$	m <sup>2</sup>	3971
Height of metacentre above base	$KM$	m	12.03
Centre of flotation in length with respect to section 10	$LCF$	m	-2.16
Longitudinal radius of gyration	$k_{yy}$	m	50.12
Ratio of longitudinal radius of gyration and ship length	$k_{yy}/L_{pp}$	-	.2557
Service speed	$V_{SERV}$	knots	23.15
Taylor sectional area coefficient for bulbous bow	$f_{BT}$	-	.0949
Block coefficient	$C_B$	-	.576
Midship section coefficient	$C_M$	-	.969
Longitudinal prismatic coefficient	$C_P$	-	.580
Waterplane coefficient	$C_{WP}$	-	.724
Wind lateral area	$AL$	m <sup>2</sup>	4062.5
Transverse wind area	$AT$	m <sup>2</sup>	750.0
Length of perimeter of lateral projection excluding waterline and slender bodies such as masts and ventilators	$S$	m	265.5
Distance from bow to centroid of lateral area.	$C$	m	114.6
Propeller diameter	$D$	m	5.80
Pitch ratio of propeller	$P_{31}/D$	-	1.249
Expanded blade area ratio	$A_E/A_0$	-	.597
Number of blades	$z$	-	4

Table 2. Data about ship's position, - course, - speed; etc.

run number	date	start time GMT	stop time GMT	position	ship speed knots	corrected ship speed knots	ship's course degrees	average rudder angle degrees	stabilizers on/off	buoy number
4	30-3-'72	17.57	18.34	48.55 NB 30.00 WL	21.5	20.60	251	2-7	off	019
6	1-4-'72	13.47	14.17	42.43 NB 51.22 WL	24.0	23.00	260	2	on	008
7	1-4-'72	18.13	18.36	42.22 NB 54.06 WL	17.5	16.77	220	5	on	013

Table 3. Data about waves and wind

run number	estimated waves					measured relative wind	absolute wind for corrected ship speed					
	swell		wind waves				estimation			derived from measurements		
	direction degrees	height m	direction degrees	height m	significant wave height from measurement m		direction degrees	velocity knots	direction degrees	velocity knots	force according to Beaufort scale	direction degrees
4	-	-	205	5	4.08	224	41.5	205	-	7	202	24.0
6	30	2	70	1	2.94	206	24	160	-	4-5	145	21.7
7	190	6	180-190	2.5	7.05	198	50.9	190	30	9	188	35.7

Table 4. Measurements of torque, number of revolutions and power for the port side shaft

run number	measurement university				measurement engine room				
	average torque $\bar{Q}$ kgm	max. torque $Q_{max}$ kgm	min. torque $Q_{min}$ kgm	max. torque variation $Q_{va}$ kgm	max. torque variation percentage	number of rev./min. $n$	shaft power $P_S$ metric HP	number of rev./min. $n$	shaft power $P_S$ metric HP
4	102000	115000	91500	23500	11.5	114.5	16320	113.8	14600
6	98200	103000	92000	11000	5.6	115.0	15780	116.7	15400
7	107000	124500	93000	31500	14.70	107.0	15950	109.4	15000

Table 5. Measurements of torque, number of revolutions and power for the starboard side shaft

run number	measurement university				measurement engine room				
	average torque $\bar{Q}$ kgm	max. torque $Q_{max}$ kgm	min. torque $Q_{min}$ kgm	max. torque variation $Q_{va}$ kgm	max. torque variation percentage	number of rev./min. $n$	shaft power $P_S$ metric HP	number of rev./min. $n$	shaft power $P_S$ metric HP
4	90500	99200	80500	18700	10.3	113.0	14280	112.7	14800
6	87200	90400	84000	6400	3.7	117.0	14260	113.3	14900
7	92000	108500	75000	33500	18.2	106.0	13650	108.5	14400

Table 6. Measured power and torque variation for the total ship

run number	shaft power measured by university $P_S$ metric HP	shaft power measured by engine room $P_S$ metric HP	max. torque variation percentage
4	30600	29400	10.9
6	30040	30300	4.6
7	29600	29400	16.5

Table 7. Relation of ship speed and measured shaft power in still water

ship speed according to log knots	corrected ship speed knots	shaft power $P_{S_{SW}}$ metric HP
23.5	22.5	23600
24	23.0	26000
24.5	23.5	28300
24.8 (run A)	23.8	29650
25	24.0	30400

Table 8

Run 4.  $H_{\frac{1}{2}} = 4.08$  m

Calculated added power in waves related to direction of wave travel and ship speed

direction of wave travel $\mu$ degrees	$P_{E_{AW}}$ in metric HP	
	$V = 20.6$ knots = 10.598 m/sec	$V = 21.5$ knots = 11.060 m/sec
125	2343	2444
135 (estimation)	2554	2693
145	2768	2932
155	2948	3148
165	3082	3303
175	3146	3380

Table 9

Run 6.  $H_{\frac{1}{2}} = 2.94$  m

Calculated added power in waves related to direction of wave travel and ship speed

direction of wave travel $\mu$ degrees	$P_{E_{AW}}$ in metric HP	
	$V = 23$ knots = 11.832 m/sec	$V = 24$ knots = 12.347 m/sec
0	952	1043
10 (estimation)	920	1009
20	811	895

Table 10

Run 7.  $H_{\frac{1}{2}} = 7.05$  m

Calculated added power in waves related to direction of wave travel and ship speed

direction of wave travel $\mu$ degrees	$P_{E_{AW}}$ in metric HP		
	$V = 16.77$ knots = 8.627 m/sec	$V = 17.5$ knots = 9.003 m/sec	$V = 19.44$ knots = 10.000 m/sec
130	9953	10631	12160
150	9982	10488	11826
(estimation)			
170	9295	9757	10993

Table 11. Results of propulsion analysis for corrected ship speed

General data:

propeller diameter  $D = 5.80$  m $\bar{\eta}_S = .97$ ;  $\rho = 104.4852$  kg sec<sup>2</sup>/m<sup>4</sup>

	run 4	run 6	run 7	run A still water
port side				
$\bar{Q}$ measured in kgm	102000	98200	107000	95800
$\bar{n}$ measured in revolutions/min	114.5	115.0	107.0	116.0
$10 K_Q$	.390	.383	.489	.370
$J$	.944	.953	.810	.969
$K_T$	.181	.177	.243	.168
$\bar{w}$	.014	.105	.029	.111
$\bar{\eta}_0$	.700	.703	.643	.706
$\bar{\eta}_D$	.685	.686	.644	.692
$\bar{P}_S$ , shaft power measured in metric HP	16320	15780	15950	15517
$\bar{P}_{EP} = \bar{P}_S / \bar{\eta}_D$ , effective power in metric HP	11179	10825	10272	10738
starboard side				
$\bar{Q}$ measured in kgm	90500	87200	92000	88400
$\bar{n}$ measured in revolutions/min	113.0	117.0	106.0	114.0
$10 K_Q$	.369	.329	.430	.354
$J$	.970	1.018	.892	.988
$K_T$	.168	.145	.205	.160
$\bar{w}$	0	.027	-.059	.109
$\bar{\eta}_0$	.707	.715	.681	.711
$\bar{\eta}_D$	.692	.698	.682	.697
$\bar{P}_S$ , shaft power measured in metric HP	14280	14260	13650	14071
$\bar{P}_{ESB} = \bar{P}_S / \bar{\eta}_D$ , effective power in metric HP	9882	9953	9309	9807
total ship				
Corrected ship speed $V_S$ in knots	20.6	23.0	16.77	23.77
$\bar{\eta}_R$	1.021	1.014	1.032	1.016
$\bar{\eta}_H$	.988	.993	1.000	.994
$\bar{P}_S$ , shaft power measured in metric HP	30600	30040	29600	29588
$\bar{P}_E = \bar{P}_{EP} + \bar{P}_{ESB}$ , effective power in metric HP	21061	20778	19581	20545
$\bar{\eta}_D$	.688	.692	.662	.694

Table 12. Predicted effective power  $P_E$  in metric HP

	still water power $P_{ESW}$	wind power $P_{EW}$	added power in waves $P_{EAW}$	total effective power $P_E = P_{ESW} + P_{EW} + P_{EAW}$
Run 4 $V_S = 20.6$ kn $H_{\frac{1}{2}} = 4.08$ m $\mu = 135$ degrees	12380	1472	2554	16406
Run 6 $V_S = 23$ kn $H_{\frac{1}{2}} = 2.94$ m $\mu = 10$ degrees	18112	98	920	19130
Run 7 $V_S = 16.77$ kn $H_{\frac{1}{2}} = 7.05$ m $\mu = 150$ degrees	6800	2043	9982	18825

Table 13. Predicted shaft power  $P_S$  in metric HP and percentages of the different parts with respect to the total shaft power

	still water power $P_{Ssw}$	wind power $P_{Sw}$	added power in waves $P_{SAW}$	total shaft power $P_S = P_{Ssw} + P_{Sw} + P_{SAW}$
<b>Run 4</b> $V_S = 20.6$ kn $H_{\frac{1}{3}} = 4.08$ m $\mu = 135$ degrees $\eta_D = .688$	17987 75.4%	2139 9.0%	3710 15.6%	23836 100%
<b>Run 6</b> $V_S = 23$ kn $H_{\frac{1}{3}} = 2.94$ m $\mu = 10$ degrees $\eta_D = .692$	26186 94.7%	141 .5%	1330 4.8%	27657 100%
<b>Run 7</b> $V_S = 16.77$ kn $H_{\frac{1}{3}} = 7.05$ m $\mu = 150$ degrees $\eta_D = .662$	10279 36.1%	3089 10.9%	15089 53.0%	28457 100%

Table 14. General view of the predicted and measured effective and shaft power

	port side		starboard side		total ship		difference of prediction and measurement by university	
	prediction	measurement by university	prediction	measurement by university	prediction	measurement by university		
<b>Run 4</b> $V_S = 20.6$ knots $P_E$ $H_{\frac{1}{3}} = 4.08$ m $\mu = 135$ degrees $P_S$ $\eta_D = .688$	8708	11179	7698	9882	16406	21061	29400	-22%
<b>Run 6</b> $V_S = 23$ knots $P_E$ $H_{\frac{1}{3}} = 2.94$ m $\mu = 10$ degrees $P_S$ $\eta_D = .692$	9966	10825	9164	9953	19130	20778	30300	-8%
<b>Run 7</b> $V_S = 16.77$ knots $P_E$ $H_{\frac{1}{3}} = 7.05$ m $\mu = 150$ degrees $P_S$ $\eta_D = .662$	9875	10272	8950	9309	18825	19581	29400	-4%

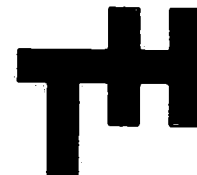
Table 15. Influence of speed correction on still water shaft power

run number	corrected speed		uncorrected speed		shaft power difference for speed correction metric HP	total shaft power in waves measured by university $P_S$ metric HP	difference of shaft power in still water and total measured value
	$V_S$ knots	still water shaft power $P_{Ssw}$ metric HP	$V_S$ knots	still water shaft power $P_{Ssw}$ metric HP			
4	20.6	18040	21.5	20777	2737	30600	-9%
6	23.0	26486	24.0	31448	4962	30040	-17%
7	16.77	9600	17.5	10900	1300	29600	-4%

## LIST OF SYMBOLS

$A_E$	expanded blade area of propeller
$A_L$	lateral projected wind area of ship or model
$A_0$	disc area of propeller
$A_T$	transverse projected wind area of ship or model
$A_W$	area of waterplane
$A_0 - A_6$	coefficients in the formula of Isherwood for the wind resistance coefficients
$B$	breadth of ship or model
$b'$	sectional damping for ship on speed
$C$	distance from bow of centroid of lateral projected wind area
$C_B$	block coefficient
$C_M$	midship section coefficient
$C_P$	longitudinal prismatic coefficient
$C_W$	waterplane coefficient
$C_{X,AL}$	longitudinal force coefficient related to the lateral projected wind area
$C_{X,AT}$	longitudinal force coefficient related to the transverse projected wind area
$c$	wave velocity
$D$	propeller diameter
$F$	force
$F_X$	longitudinal force
$f_{BT}$	Taylor sectional area coefficient for bulbous bow
$f_0 - f_n$	discrete value of a function to be integrated
$G$	stabilization weight of buoy
$g$	acceleration of gravity
$H_{\frac{1}{3}}$	significant wave height
$h$	step size between two successive values
$I_n$	integral value after $n$ samples
$J_{P,SB}$	average advance coefficient for respectively port- and starboard side
$KM$	height of metacentre above base
$K_{T,P,SB}$	average thrust coefficient for respectively port- and starboard side
$K_{Q,P,SB}$	average torque coefficient for respectively port- and starboard side
$k = 2\pi/\lambda$	wave number
$k_{yy}$	longitudinal radius of inertia of ship
$L, L_{PP}$	length between perpendiculars
$LCB$	centre of buoyancy in length with respect to midship section
$LCF$	centre of flotation in length with respect to midship section
$L_f$	length between perpendiculars in feet
$L_{OA}$	length overall
$L_{WL}$	length on the waterline
$l_1$	arm of stabilization moment of wave-buoy
$M$	moment of disturbance; number of distinct groups of masts
$m'$	sectional added mass for zero speed
$N'$	sectional damping for zero speed
$\bar{n}_{P,SB}$	average number of revolutions for respectively port- and starboard side
$P$	pitch of propeller
$P_E$	total effective power
$\bar{P}_E$	average total effective power
$P_{EAW}$	effective power because of added resistance in waves
$P_{ESW}$	effective power in still water
$P_{EW}$	effective power because of wind
$P_S$	total shaft power
$\bar{P}_S$	average total shaft power
$P_{SAW}$	shaft power because of added resistance in waves
$\bar{P}_{SP,SB}$	average shaft power for respectively port- and starboard side
$P_{SSW}$	shaft power in still water
$P_{SW}$	shaft power because of wind

$\bar{Q}_{P,SB}$	average torque for respectively port- and starboard side
$R$	total ship resistance
$R_{AW}$	added resistance in waves
$R_{SW}$	still water resistance
$R_W$	resistance because of wind
$R_{\theta\theta}$	pitch auto-covariance function
$S$	length of perimeter of lateral projection of ship or model excluding waterline and slender bodies such as masts and ventilators; wetted surface of ship
$S.E.$	standard error
$S_z$	heave spectrum
$S_\zeta$	wave spectrum
$S_\theta$	pitch spectrum
$T$	draught of ship
$T_e$	period of encounter
$t$	thrust deduction fraction; time
$V$	forward speed of ship or model
$V_{ECO}$	economical ship speed in knots
$V_R$	relative wind speed
$V_S$	ship speed
$\bar{V}_S$	average ship speed
$V_{SERV}$	service ship speed in knots
$V_W$	absolute wind speed
$V_z$	vertical relative water velocity
$V_{za}$	amplitude of the vertical relative water velocity
$w$	Taylor wake fraction in general
$\bar{w}_{P,SB}$	average Taylor wake fraction for respectively port- and starboard side
$x, y, z$ $x_b, y_b, z_b$	Right hand coordinate system fixed to ship
$y_w$	half width of designed waterline
$z$	heave displacement
$z_a$	heave amplitude
$\Delta$	weight of displacement
$\nabla$	volume of displacement
$\zeta$	instantaneous wave elevation
$\zeta_a$	wave amplitude
$\zeta_w$	wave height (double amplitude)
$\eta_B$	propeller efficiency behind the ship
$\eta_D$	total propulsive efficiency
$\bar{\eta}_D$	average total propulsive efficiency
$\eta_H$	hull efficiency
$\eta_0$	propeller efficiency in open water
$\bar{\eta}_{0,P,SB}$	average propeller efficiency in open water for respectively port- and starboard side
$\eta_R$	relative rotative efficiency
$\eta_S$	shafting efficiency
$\theta$	pitch angle
$\theta_a$	pitch amplitude
$\lambda$	wave length
$\lambda'$	apparent wave length
$\mu$	wind direction; direction of wave travel
$\rho$	density of water
$\rho_a$	density of air
$\sigma_{AW}$	dimensionless transfer function for the resistance increase
$\tau$	time lag
$\psi$	angle of rotation of wave buoy
$\omega$	circular wave frequency
$\omega_e$	circular wave frequency of encounter



# LABORATORIUM VOOR SCHEEPSBOUWKUNDE

TECHNISCHE HOGESCHOOL DELFT

DRAG AND SIDEFORCE MEASUREMENTS WITH  
A 1/6 SCALE MODEL OF THE YACHT  
"ANTIOPE"

by

W. BEUKELMAN

and

A. HUIJSER

---

March 1974

INTRODUCTION

At the instigation of the Technical and Research Panel H-13 (Sailing Yachts) of the Society of Naval Architects and Marine Engineers a program has been developed to measure in nine towing tanks the hydrodynamic drag and side force of an identical fiberglass reinforced plastic model to one-sixth scale of the 5.5 Meter Yacht ANTIOPE.

It is the specific aim of this program to improve the knowledge and test procedures in this field through intertank comparisons and by correlation with full scale tests.

Herewith the results are presented of the experiments performed at the Shipbuilding Laboratory of the Delft University of Technology. The tests have been carried out with the SNAME manufactured 1/6 - scale model.

Additional tests with a 1/3 - scale model will soon be performed and reported separately.

The reported tests with the present model have been performed in accordance with the Technical and Research Publication of the SNAME: "Antiope Yacht Model Tests Data and Recommendations", December 1971.

The main part of the reported results is devoted to the measured drag and side force for the model with a constant heel angle  $\psi$  viz.  $\psi = 0, 10, 20$  and  $30$  degrees and a fixed yaw angle  $\beta$  viz.  $\beta = 0, 2.65, 5.18$  and  $6.45$  degrees. These tests have been carried out in the small (tank 2) and large (tank 1) towing tank with speeds up to  $F_n = .50$ .

The second part of the reported results concerns the test in the large towing tank, based on the static initial angle of heel to obtain similar conditions as had been measured for the full scale tests at the Naval Ship Research and Development Center. These conditions are presented in the Technical and Research Bulletin no. 1-28 of the SNAME:

Full Scale Tank Tests of the 5.5 Meter Yacht "ANTIOPE".

Comparisons with these full scale measurements have only been made for these tests. In general the agreement is satisfactory with some comprehensible exceptions for instance in the case of very small side forces at zero yaw angle and smallest angle of heel ( $\psi = 10$  degrees). Some derivations may also be ascertained for the side force (lift) at the largest yaw angle in combination with the highest speed.

A description of the experimental set up has been presented together with the used test and extrapolation procedures.

All measuring data have been reported on sheets and the results are shown in figures.

If desired it is possible to evaluate from the data sheets the lift- and rolling moment.

It is our wish, that the reported results may contribute to useful intertank comparisons.



## 1. Technical outlift of the model and it's attachment to the towing carriage.

The correctly ballasted model (Table 1) had been attached to the carriage at the two pivot points  $P_a$  and  $P_f$  by means of two balanced guides (fig. 1), providing restraint perpendicular to the direction of motion only. Thus, at zero speed, no forces were transmitted from the guides to the model. The pivot points  $P_a$  and  $P_f$  had been positioned at equal distances (.5 m) off the center of gravity  $G_m$ .

Just above these the two dynamometers had been mounted. These measured the lift force components  $L_a$  and  $L_f$ , in the direction of the restraint. To be able to obtain a certain yaw angle  $\beta$ , the aft guide was made adjustable along a fixed scale in the horizontal side direction (lift force direction) (fig. 2).

When a run was performed the model was towed by a horizontal thread connected to the model at  $P_f$  and connected to the carriage by means of a dynamometer which measured the yacht's drag (resistance)  $D'$ . Thus restraint with respect to the carriage had been provided in surge, side motion and yaw; the model was free to heave, pitch and roll.

By moving a weight ( $p = 1.5$  kg) on top of the model in it's transverse direction over a distance  $t$  ( $t =$  moment arm) the required heel angles could be accomplished at a required fixed model speed (fig. 1 and 2). The heel angle of the model could be checked with a stepwise adjustable level (0, 10, 20 and 30 degrees).

The lift force components at the fore and aft guides,  $L_f$  respectively  $L_a$  and the model drag  $D'$  were measured electronically with strain gauge dynamometers. To filter out undesired vibratory disturbances, the following procedure was applied: after amplification, each signal was integrated over an adjustable period of time (about 20 seconds). The period of integration and the integrated signals were read off a digital voltmeter, after which division yielded the desired forces.

## 2. Turbulence stimulators on the model and model surface condition.

Location and dimensions of the applied carborundum strips on the model during the experiments are given in fig. 1.

The frictional drag (resistance) increase due to the carborundum strips was eliminated by performing two series of experiments for the upright condition without yaw: one series with strips of half nominal breadth and the other series with strips of full nominal breadth. It has been supposed that the additional half strips produced an equal drag increase as the first half strips, so that the drag without turbulence stimulators, but with turbulent flow, could be determined.

If we denote:

$D''$  = model drag (resistance) with half nominal strips

$D'$  = model drag (resistance) with full nominal strips

then the drag increase coefficient

$$C = \frac{D' - D''}{V_m^2} = \frac{\frac{1}{2}\Delta D}{V_m^2} \text{ will be only slightly dependent}$$

on the model speed  $V_m$ , since the resistance increase is due to friction. The influence of heel or waves on strip-length is neglected.

In practice  $C$  was determined as a mean value over a range of model speeds where the measurements were most accurate and no laminary flow phenomena were experienced.

The model drag  $D_m$  corrected for the frictional resistance due to the full nominal strips follows from:

$$D_m = D' - \Delta D = D' - 2 C V_m^2$$

(see columns 17, 18 and 19 of data sheets).

This procedure was applied both with the model in tank 1 and in tank 2 and the same value for  $C$  was found, viz.

$$C = 7 \times 10^{-3} \text{ kgf. sec}^2/\text{m}^2.$$

All the drag measurements with the model with heel and yaw were corrected for the strips by means of this coefficient  $C$ .

The strips consisted of carborundum grains, with a mean diameter of 1.2 mm and a density of 12 grains/cm<sup>2</sup>.

The surface of the fibreglass reinforced polyester model has been left in the condition as at arrival in Delft.

### 3. Extrapolation of the results to full scale values.

Since the keel and rudder configuration of the Antiope is relatively long and continuous and largely incorporated into the body, the characteristic length  $X$ , upon which the Reynolds number should be based, has been taken as

$$X = .7 * LDWL, \text{ where } LDWL \text{ is the length of datum waterline.}$$

To be able to approach the frictional resistance by calculation, the actual wetted surface had to be known. The Delft computer program has been used for the calculation of the hydrostatic curves, with the data input derived from the drawing "Lines of M.I.T. - Antiope model, based on templates taken off model". The output was first used to check draft and displacement relations as given in: Technical and Research Publication of the SNAME: "Antiope Yacht Model Tests Data and Recommendations", December 1971.

Since the differences were negligible a reliable value for the actual wetted surface for the model in test condition could be determined. The frictional model drag (resistance) was approached by:

$$D_{Fm} = C_{Fm} * \frac{1}{2} \rho_m V_m^2 * S_m \text{ (actual)}$$

where:

$\rho_m$  = density of water in tank

$\rho_m = 101.79 \text{ kgf. sec}^2/\text{m}^4 \text{ at } 67.1^\circ \text{ F}$

$V_m$  = model speed (m/sec)

$S_m \text{ (actual)}$  = actual wetted model surface

$S_m \text{ (actual)} = .4111 \text{ m}^2$

$$C_{Fm} = \frac{.075}{(\log R_{nm} - 2)^2}, \text{ frictional drag coefficient of model according to I.T.T.C. formula.}$$

$$R_{nm} = \frac{V_m X_m}{\nu_m}, \text{ Reynolds number of model}$$

$X_m = .7 * LDWL_m = .8079 \text{ m}$

$\nu_m$  = kinematic viscosity of water in tank

$\nu_m = 1.0188 * 10^{-6} \text{ m}^2/\text{sec} \text{ at } 67.1^\circ \text{ F}$

The residuary model drag follows from:

$$D_{Rm} = D_m - D_{Fm}$$

The full scale frictional drag of Antiope has been calculated analogous to that of the model for the full scale conditions:

$$D_{FS} = C_{FS} * \frac{1}{2} \rho_s V_s^2 * S_s \text{ (actual)}$$

where:

$\rho_s$  = density of water, full scale condition

$\rho_s = 101.69 \text{ kgf. sec}^2/\text{m}^4 \text{ at } 75^\circ \text{ F}$

$V_s$  = full scale speed (m/sec)

$S_s$  (actual) = actual full scale wetted surface

$S_s$  (actual) = 14.800 m<sup>2</sup>

$C_{FS} = \frac{.075}{(\log R_{ns} - 2)^2}$ , frictional drag coefficient of ship, according to I.T.T.C. - formula

$R_{ns} = \frac{V_s \cdot X_s}{\nu_s}$ , Reynolds number of ship

$X_s = .7 \times L_{DWL_s} = 4.847$  m

$\nu_s$  = kinematic viscosity full scale condition

$\nu_s = 9.189 \times 10^{-7}$  m<sup>2</sup>/sec at 75° F

The total drag of the Antiope full scale has been calculated from:

$D_s = D_{FS} + \alpha^3 D_{R_m}$  (column 20 of data sheets)  
 where:  $\alpha$  = model scale,  
 $\alpha = 6$

No frictional forces were supposed to be involved in the lift forces, so that the extrapolation procedure for the lift forces from model values to full scale values were calculated according to:

$L_s = \alpha^3 L_m$  (column 12 and 14 of data sheets)  
 where:  $L_m = L_a + L_f$ , lift force model (kgf)  
 $L_s$  = lift force full scale (kgf).

4. Tank dimensions and length of measured model runs.

The dimensions of the two tanks are:



	Tank 1	Tank 2
Length	140.00 m	85.00 m
Breadth	4.28 m	2.80 m
Depth	2.50 m	1.22 m

The length of each model run is defined by the model speed and period of time, over which the signals were integrated. The period of integration was for each run quite close to 20 seconds.

5. Water condition of Tank 1 and Tank 2.

The watersurface was cleaned from dust and algae in the morning, if deemed necessary. If not, an idle run was made to promote some initial turbulence.

After each run the tank was swept by means of a board floating on the water towed by the carriage on it's travel back, to suppress the waves. The time interval between the runs was up to twenty minutes, depending on the speed of the last run.

The water temperature in each tank was 67.1 degrees Fahrenheit.

## 6. Reporting of the results.

Since drag (resistance) was measured in the direction of the yacht's travel through the water and lift force (side force) in a horizontal plane perpendicular to the drag, the results are presented in this report without the need of any conversion to comply with the requirements of the intertank comparison program of Panel H-13.

### 6.1 The "Constant Heel Angle" tests.

For each value of the yaw angle  $\beta$  ( $\beta = 0, 2.65, 5.18$  and  $6.45$  degrees) a series of tests has been carried out, with the heeling ballast adjusted to obtain the required heel angle  $\psi$  over a range of model speeds:  $.125 < Fn < .44$  (.50). Four different heel angles have been tested:  $\psi = 0, 10, 20$  and  $30$  degrees.

The results of these tests are given in the data sheets:

Data sheet 1 - 5 constant heel angle tests, Tank 2

Data sheet 6 - 10 constant heel angle tests, Tank 1.

### 6.2 The "Initial Heel Angle" tests.

In addition to the constant heel angle test a few extra tests have been performed in tank 1 in order to have a direct comparison with the full scale tests as described in Technical and Research Bulletin no. 1 - 28 "Full Scale Tank Tests of the 5.5 Meter Yacht Antiope". During the full scale tests Antiope had for each series of tests a different initial heel angle at zero speed, accomplished by an adjustable weight located off-center.

So the actual heel angle varied with speed during one test series. In order to create comparable conditions for the model, the actual heel angle - speed combination at the same fixed yaw angle have been taken from the reduced data (Run no. 1274-1399, column no. 5, appendix II of T & R Bulletin no. 128) and after conversion according to the model-laws used as input data for the model tests.

The results of these tests are given in:

Data sheet no. 11 of this report.

### 6.3 The Data Sheets (appendix I).

The data sheets should be considered as the basis for any further evaluation of the test results. All calculations are made in metric units, lift force and drag are also converted to pounds, the full scale speed  $V_s$  is given in knots. The speed-length ratio

$\frac{V_s}{\sqrt{LDWL_s}}$  is given in knots/ft $^{1/2}$ .

The presented non-dimensional Froude number is based on  $LDWL_s$ , so that

$$Fn = \frac{V_m}{\sqrt{g \cdot LDWL_m}} = \frac{V_s}{\sqrt{g \cdot LDWL_s}} \quad (Fn_m = Fns)$$

where  $g = 9.81$  m/sec $^2$  (acceleration of gravity).

Both the non-dimensional lift coefficient  $C_L$  and the non-dimensional drag coefficient  $C_D$  are based on the nominal wetted surface:

$$C_L = \frac{L_m}{\frac{1}{2} \rho_m S_{mn} V_m^2} \quad \left( = \frac{L_s}{\frac{1}{2} \rho_s S_{sn} V_s^2} \right) \quad \text{Column 13 of data sheets}$$

$C_L$  has the same value for model and full scale conditions.

$$C_D = \frac{D_s}{\frac{1}{2}\rho_s S_{Sn} V_s^2} = \frac{D_s}{\frac{1}{2}\rho_s S_{mn} \alpha^3 V_m^2} \quad \text{Column 22 of data sheets}$$

$C_D$  is only applicable to full scale conditions

where:

$S_{mn}$  = nominal wetted surface of model,

$$S_{mn} = .4232 \text{ m}^2$$

$S_{Sn}$  = nominal wetted surface of ship

$$S_{Sn} = S_{mn}\alpha^2 = 15.236 \text{ m}^2$$

$$V_s^2 = V_m^2\alpha, \text{ since } F_{Ns} = F_{Nm}$$

#### 6.4 The figures (appendix II).

From the data sheets some graphs are derived to give a visualization of the test results:

fig. 3 - 15, constant heel angles	model drag versus speed model lift versus speed Tank 1 and Tank 2
fig. 16 - 45, constant heel angles	ship drag versus speed ship lift versus speed Tank 1 and Tank 2
fig. 46 - 49, constant heel angles	ship lift versus $\beta$ Tank 1
fig. 50 - 55, constant heel angles	ship - L/D versus $\phi$ Tank 1 and Tank 2
fig. 56 - 59, constant heel angles	ship - L/D versus $\beta$ Tank 1
fig. 60 - 67, constant heel angles	ship $C_D$ versus $C_L^2$ Tank 1 and Tank 2
fig. 68 - 76, initial heel angles	model drag versus speed model lift versus speed Tank 1
fig. 77 - 87, initial heel angles	ship drag versus speed ship lift versus speed Tank 1.



7. Conclusions and recommendations.

Comparison of the extrapolated measured results with measured full scale values shows a satisfactory agreement.

The influence of scale effect appears to be very small.

Further improvement may be expected from adaptation of the characteristic friction length used for extrapolation.

8. Acknowledgement.

The authors wish to acknowledge the advices and stimulation of prof.ir. J. Gerritsma and ir. M.C. Meijer in the execution of this project. Particularly the authors are indebted to mr. A. van Strien, who carried out the major part of the experiments.

Table I.Model in test condition

Displacement (F.W.)	=	11.856 kg
Draft aft station 4 (base line)	=	.239 m
Trim, down by bow, between station 0 and 8	=	.005 m
L.C.G <sub>m</sub> . (aft station 4)	=	.037 m
V.C.G <sub>m</sub> . (above keel)	=	.268 m
S <sub>m</sub> (actual)	=	.4111 m <sup>2</sup>

List of Symbols

Subscription m = model scale condition

Subscription s = full scale condition

- C = frictional drag increase coefficient,  $C = 7 \times 10^{-3} \frac{\text{kgf. sec}^2}{\text{m}^2}$
- $C_F$  = frictional drag coefficient, according to I.T.T.C. formula
- $D''$  = model drag with half nominal strips
- $D'$  = model drag with full nominal strips
- $\Delta D$  = parasitic drag of model, due to turbulence stimulators
- D = drag
- $D_F$  = frictional drag
- $D_R$  = residuary drag
- $F_n$  = Froude number,  $F_n = \frac{V}{\sqrt{g \cdot L_{DWL}}}$
- G = center of gravity
- g = acceleration of gravity,  $g = 9.81 \text{ m/sec}^2$
- $L_{DWL}$  = length of datum waterline  
 $L_{DWLm} = 1.154 \text{ m}$   
 $L_{DWLs} = 6.925 \text{ m}$
- $L_a$  = lift force component at aft guide
- $L_f$  = lift force component at fore guide
- $L_m$  = lift force model,  $L_m = L_a + L_f$
- $L_s$  = lift force full scale
- P = moment weight of the model,  $p = 1.5 \text{ kgf}$
- $P_a$  = aft pivot point of model
- $P_f$  = fore pivot point of model
- $R_n$  = Reynolds number,  $R_n = \frac{X \cdot V}{\nu}$
- S (actual) = actual wetted surface  
 $S_m \text{ (actual)} = .4111 \text{ m}^2$   
 $S_s \text{ (actual)} = 14.800 \text{ m}^2$
- $S_n$  = nominal wetted surface  
 $S_{mn} = .4232 \text{ m}^2$   
 $S_{sn} = 15.2361 \text{ m}^2$
- t = moment arm of adjustable moment weight p
- V = speed
- X = characteristic length,  $X = .7 L_{DWL}$   
 $X_m = .8079 \text{ m}$   
 $X_s = 4.847 \text{ m}$
- $\alpha$  = model scale,  $\alpha = 6$

List of symbols (cont.)

- $\beta$  = yaw angle (degrees)
- $\nu$  = kinematic viscosity of fresh water  
 $\nu_m = 1.0188 \times 10^{-6} \text{ m}^2/\text{sec}$  at  $67.1^\circ$  Fahrenheit  
 $\nu_s = 9.1890 \times 10^{-7} \text{ m}^2/\text{sec}$  at  $75.0^\circ$  Fahrenheit
- $\rho$  = density of fresh water  
 $\rho_m = 101.79 \text{ kgf}\cdot\text{sec}^2/\text{m}^4$  at  $67.1^\circ$  Fahrenheit  
 $\rho_s = 101.69 \text{ kgf}\cdot\text{sec}^2/\text{m}^4$  at  $75.0^\circ$  Fahrenheit
- $\phi$  = heel angle (degrees)

APPENDIX I

DATA SHEETS

AARD v.d. PROEF: LIFT AND DRAG MEASUREMENT															MODEL No: 127					
GEGEVENS: Model/scale d = 6; $L_{DUL}$ (nominal) = 1.154 m; $S_{m^2}$ (nominal) = 0.42322 m <sup>2</sup> ; $S_m$ (actual) = 0.4111 m <sup>2</sup> ; $X_c = 7 L_{DUL} = 8.079$ m															TYPE: ANTILOPE					
VCG (above keel) = 0.2677 m; moment weight $p = 1.5$ kg; $V_s$ (nom) = 4.7614 $V_m$ ; $F_n = 0.29721 V_m$ ; $C_L = L_m / \frac{1}{2} \rho S_{m^2} V_m^2$ ;															EXP: v. S.					
Temperature water $T = 19.8$ °C; $\rho = 101.79$ kg sec <sup>3</sup> /m <sup>4</sup> ; $\nu = 1.0188 \cdot 10^{-6}$ m <sup>2</sup> /sec; $1/16 = 0.4375$ kg; $L_{DUL} = 22.916$ ft; $C_D = D_s / \frac{1}{2} \rho S_{m^2} V_m^2$															DATUM: OKTOBER 1973					
Run no	Model speed $V_m$	$V_m^2$	Wind speed $V_s$	$V_s / \sqrt{L_{DUL}}$	$F_n$	$\beta$	Leeway/heeling angle $\varphi$	Moment arm $l$	Lift fore $L_f$	Lift after $L_a$	Lift model $L_m$	$C_L$	Lift slip $L_{s1}$	Lift slip $L_{s2}$	Drag $D'$	$\Delta D = .014 V_m^2$	Drag model $D_m = D' \cdot AD$	Drag slip $D_s$	Drag $D_s$	$C_D \cdot 10^3$
	m/sec	m <sup>2</sup> /sec	m/sec			degr.	degr.	mm	kg	kg	kg		kg	lbs	kg	kg	kg	kg	lbs	
58.	1.003	1.006	4.776	1.002	.298	0	0	0	0	0	0	0	0	0	.156	.014	.142	21.292	46.9	4.553
59	.403	.162	1.919	.402	.120	"	"	"	"	"	"	"	"	"	.023	.002	.021	2.526	5.6	3.355
60	.503	.253	2.395	.502	.149	"	"	"	"	"	"	"	"	"	.037	.004	.033	4.213	9.3	3.583
61	.603	.364	2.871	.602	.179	"	"	"	"	"	"	"	"	"	.052	.005	.047	6.195	13.7	3.662
62	.703	.494	3.347	.702	.209	"	"	"	"	"	"	"	"	"	.073	.007	.066	9.127	20.1	3.975
63	.804	.646	3.828	.803	.239	"	"	"	"	"	"	"	"	"	.097	.009	.088	12.568	27.7	4.186
64	.906	.821	4.314	.905	.269	"	"	"	"	"	"	"	"	"	.119	.011	.108	15.440	34.0	4.245
65	.957	.916	4.557	.956	.284	"	"	"	"	"	"	"	"	"	.135	.013	.122	17.693	39.0	4.156
66	.452	.209	2.152	.451	.134	"	"	"	"	"	"	"	"	"	.029	.003	.026	3.180	7.0	3.277
67	.553	.306	2.633	.552	.164	"	"	"	"	"	"	"	"	"	.044	.004	.040	5.220	11.5	3.670
68	.654	.428	3.114	.653	.194	"	"	"	"	"	"	"	"	"	.061	.006	.055	7.341	16.2	3.690
69	.755	.570	3.595	.754	.224	"	"	"	"	"	"	"	"	"	.083	.008	.075	10.412	23.0	3.930
70	.857	.734	4.081	.856	.255	"	"	"	"	"	"	"	"	"	.109	.010	.099	14.207	31.3	4.164
71	1.003	1.006	4.776	1.002	.298	"	"	"	"	"	"	"	"	"	.149	.014	.135	19.780	43.6	4.270
72	1.056	1.115	5.028	1.054	.314	"	"	"	"	"	"	"	"	"	.168	.016	.152	22.592	49.8	4.359
73	1.105	1.221	5.261	1.103	.328	"	"	"	"	"	"	"	"	"	.192	.017	.175	26.736	58.9	4.711
74	1.157	1.339	5.509	1.155	.343	"	"	"	"	"	"	"	"	"	.214	.019	.195	30.152	66.5	4.845
75	1.205	1.452	5.737	1.203	.358	"	"	"	"	"	"	"	"	"	.235	.020	.215	33.611	74.1	4.980
76	1.205	1.452	5.737	1.203	.358	"	"	"	"	"	"	"	"	"	.242	.020	.222	35.123	77.4	5.204
77	1.258	1.583	5.990	1.256	.374	"	"	"	"	"	"	"	"	"	.284	.022	.262	42.783	94.3	5.814
78	1.307	1.708	6.223	1.305	.388	"	"	"	"	"	"	"	"	"	.328	.024	.304	50.922	112.3	6.414
79	1.358	1.844	6.466	1.356	.404	"	"	"	"	"	"	"	"	"	.406	.026	.380	66.340	146.3	7.740
80	1.410	1.988	6.714	1.408	.419	"	"	"	"	"	"	"	"	"	.485	.028	.457	81.925	180.6	8.866
81	1.462	2.137	6.961	1.460	.435	"	"	"	"	"	"	"	"	"	.573	.030	.543	99.426	219.2	10.010
82	1.509	2.277	7.185	1.507	.448	"	"	"	"	"	"	"	"	"	.657	.032	.625	116.141	256.0	10.973
83	1.558	2.427	7.418	1.556	.463	"	"	"	"	"	"	"	"	"	.749	.034	.715	134.518	296.6	11.924
84	1.609	2.589	7.661	1.607	.478	"	"	"	"	"	"	"	"	"	.839	.036	.803	152.394	336.0	12.664
85	1.610	2.592	7.666	1.608	.479	"	"	"	"	"	"	"	"	"	.839	.036	.803	152.371	335.9	12.647
86	1.661	2.759	7.909	1.659	.494	"	"	"	"	"	"	"	"	"	.940	.039	.901	172.375	380.0	13.442
87	1.713	2.934	8.156	1.710	.509	"	"	"	"	"	"	"	"	"	1.060	.041	1.019	196.657	433.6	14.420
88	1.761	3.107	8.403	1.759	.524	"	"	"	"	"	"	"	"	"	.756	.039	.722	135.964	299.7	12.003
89	1.763	3.108	8.394	1.760	.524	"	"	"	"	"	"	"	"	"	1.161	.044	1.117	216.634	477.6	14.996

AARD v.d. PROEF: LIFT AND DRAG MEASUREMENT																				MODEL N.: 127		
GEGEVENS: Modelscale $\alpha = 6$ ; $L_{DUL}$ (nominal) = 1.154 m; $S_{mD}$ (nominal) = 0.42322 m <sup>2</sup> ; $S_m$ (actual) = .4111 m <sup>2</sup> ; $X = .7 L_{DUL} = 0.8079$ m																				TYPE: ANTIORSE		
VCG (above keel) = 0.2677 m; moment weight $\rho = 1.5$ kg; $V_s$ (knots) = 4.7614 $V_m$ ; $F_n = 0.2971 V_m$ ; $C_L = L_m / \frac{1}{2} \rho S_{mD} V_m^2$ ;																				EXP: v.S.		
Temperature water $T = 19.8$ °C; $\rho = 101.79$ kg sec <sup>2</sup> /m <sup>3</sup> ; $\nu = 1.0188 \cdot 10^{-6}$ m <sup>2</sup> /sec; $1/16 = \alpha^2 S_m$ kg; $L_{DUL} = 22.716/l$ ; $C_D = D_s / \frac{1}{2} \rho S_{mD} V_m^2$																				DATUM: 19-10-1975		
Run no	Model Speed $V_m$	Strip Speed $V_s$	$V_s/V_m$	$F_n$	$\beta$	heeling angle $\phi$	Moment arm $l$	Lift fore $L_f$	Lift after $L_a$	Lift model $L_m = L_f + L_a$	$C_L$	Lift $L_s = L_m \alpha^2$	Lift strip $L_s$	Drag $D'$	$\Delta D = D' / V_m$	Drag model $D_m = D' \alpha^2$	Drag strip $D_s$	Drag $D_s$	$C_D$	$L/D$	$C_L/\beta$	
	m/sec	m/sec	knots		degr.	degr.	mm	kg	kg	kg		kg	kg	kg	kg	kg	kg	kg	kg		1/rad	
91	.420	.176	3.000	.420	.125	2.65	0	9.3	.038	.018	.056	1.477	12.1	26.7	.026	.003	.024	3.030	6.7	3.704	3.988	.394
92	.631	.398	3.004	.630	.188	"	"	18.3	.084	.042	.126	1.470	27.2	60.0	.058	.006	.052	6.960	15.3	3.762	3.907	.3178
93	.841	.707	4.004	.840	.250	"	"	34.5	.150	.075	.225	1.477	48.6	107.1	.105	.010	.095	13.569	29.9	4.129	3.578	.3194
94	1.051	1.105	5.004	1.050	.312	"	"	52.7	.254	.125	.379	1.592	81.9	180.6	.178	.016	.163	25.050	55.2	4.877	3.265	.3443
95	1.262	1.593	6.009	1.261	.375	"	"	82.3	.373	.184	.557	1.623	120.3	265.2	.303	.022	.281	46.812	103.2	6.322	2.568	.3510
96	1.472	2.167	7.009	1.471	.437	"	"	117.1	.564	.269	.833	1.785	179.9	396.6	.616	.030	.586	108.504	239.2	10.772	1.657	.3859
97	1.684	2.836	8.018	1.682	.501	"	"	160.1	.714	.394	1.108	1.814	239.3	527.6	1.046	.040	1.006	194.527	418.9	14.757	1.229	.3922
98	1.684	2.836	8.018	1.682	.501	2.65	0	160.1	.728	.399	1.127	1.845	243.4	536.6	1.045	.040	1.005	194.311	428.4	14.741	1.252	.3983
99	.420	.176	3.000	.420	.125	2.65	10	-36.2	.035	.016	.051	1.345	11.0	24.3	.024	.003	.022	2.538	5.7	3.176	4.236	.2909
100	.630	.397	3.000	.629	.187	"	"	-24.8	.084	.036	.120	1.403	25.9	57.1	.059	.006	.053	7.107	15.8	3.895	3.603	.3034
101	.840	.706	4.000	.839	.250	"	"	-9.4	.164	.072	.236	1.552	51.0	112.4	.107	.010	.097	14.015	30.9	4.271	3.634	.3355
102	1.049	1.100	4.995	1.048	.312	"	"	13.7	.263	.114	.377	1.591	81.9	179.5	.178	.015	.163	25.083	55.3	4.906	3.243	.3440
103	1.260	1.588	5.999	1.259	.374	"	"	45.6	.401	.187	.588	1.719	127.0	280.0	.305	.022	.283	47.282	104.2	6.406	2.684	.3717
104	1.469	2.158	6.994	1.467	.437	"	"	79.8	.557	.256	.812	1.747	175.4	386.7	.624	.030	.594	110.295	243.2	10.996	1.589	.3777
105	1.680	2.822	7.997	1.678	.499	2.65	10	119.8	.736	.331	1.067	1.756	230.5	508.2	1.038	.040	.999	193.108	425.7	14.722	1.192	.3795
106	.639	.396	3.995	.628	.187	2.65	20	-36.5	.086	.026	.112	1.313	24.2	53.4	.057	.006	.052	6.922	15.4	3.792	3.462	.2839
107	.840	.706	4.000	.839	.250	"	"	-41.8	.149	.050	.199	1.309	43.0	94.8	.108	.010	.098	14.231	31.4	4.237	3.018	.2829
108	1.049	1.100	4.995	1.048	.312	"	"	-20.7	.244	.089	.333	1.405	71.9	158.5	.176	.015	.161	24.651	54.4	4.821	2.915	.3039
109	1.259	1.585	5.995	1.258	.374	"	"	18.3	.381	.177	.558	1.634	120.5	265.7	.314	.022	.292	49.245	108.6	6.684	2.445	.3534
110	1.468	2.155	6.990	1.467	.436	"	"	45.3	.493	.202	.695	1.497	150.1	330.9	.632	.022	.610	113.772	250.8	11.358	1.318	.3237
111	1.468	2.155	6.990	1.467	.436	"	"	47.5	.505	.208	.713	1.536	154.0	339.5	.627	.030	.592	110.964	244.6	11.078	1.387	.3321
112	1.683	2.832	8.013	1.681	.500	"	"	72.5	.662	.332	.894	1.466	193.1	425.7	1.068	.040	1.028	199.303	439.4	15.141	.968	.3169
113	1.468	2.155	6.990	1.467	.436	"	"	46.5	.510	.206	.716	1.542	154.2	341.0	.629	.030	.599	111.396	245.6	11.121	1.387	.3335
114	1.686	2.843	8.018	1.684	.501	"	"	78.2	.673	.337	.910	1.486	196.6	433.4	1.058	.040	1.018	197.073	434.5	14.913	.996	.3213
115	.421	.176	3.000	.420	.125	2.65	20	-66.4	.036	.014	.050	1.319	10.8	23.8	.026	.003	.024	3.021	6.7	3.693	3.572	.2852
116	.421	.176	3.000	.420	.125	2.65	30	-88.4	.031	.009	.040	1.055	8.6	19.0	.026	.003	.024	3.021	6.7	3.693	2.857	.2281
117	.629	.396	2.995	.628	.187	"	"	-79.9	.070	.016	.086	1.008	18.6	41.0	.059	.006	.054	7.414	16.3	4.028	2.503	.2180
118	.841	.707	4.004	.840	.250	"	"	-61.5	.132	.043	.175	1.149	37.8	83.3	.109	.010	.099	14.433	31.8	4.292	2.616	.2485
119	1.050	1.103	4.999	1.049	.312	"	"	-36.2	.229	.086	.315	1.326	68.0	150.0	.173	.015	.158	23.907	52.9	4.679	2.834	.2867
120	.839	.704	3.995	.838	.249	"	"	-61.8	.132	.041	.173	1.141	37.4	82.5	.107	.010	.097	14.029	30.9	4.287	2.661	.2467
121	1.259	1.585	5.995	1.258	.374	"	"	-2.2	.322	.154	.476	1.394	102.8	226.6	.322	.022	.300	50.973	112.4	6.919	2.015	.3014
122	1.050	1.103	4.999	1.049	.312	2.65	30	-36.4	.226	.085	.321	1.351	69.3	152.8	.178	.015	.163	25.047	55.3	4.889	2.763	.2921

\* for this speed, little water over.



AARD v.d. PROEF: LIFT AND DRAG MEASUREMENT																				MODEL N <sup>o</sup> : 127		
GEGEVENS: Model/scaled = 6; L <sub>DWL</sub> (nominal) = 1.154 m; S <sub>M</sub> (nominal) = 0.42322 m <sup>2</sup> ; S <sub>M</sub> (actual) = 0.4111 m <sup>2</sup> ; X = .7 L <sub>DWL</sub> = 0.8079 m																				TYPE: ANTIORPE		
VCG (above keel) = 0.2677 m; moment weight $\rho = 1.5$ kg; V <sub>5</sub> (nodes) = 4.7614 V <sub>m</sub> ; F <sub>n</sub> = 0.29721 V <sub>m</sub> ; C <sub>L</sub> = L <sub>m</sub> / (1/2 $\rho$ S <sub>M</sub> V <sub>m</sub> <sup>2</sup> );																				EXP: v.s.		
Temperature water T = 13.8 °C; $\rho = 101.79$ kg sec <sup>2</sup> /m <sup>4</sup> ; $\nu = 1.0188 \times 10^{-6}$ m <sup>2</sup> /sec; $\lambda = 0.4536$ kg; L <sub>DWL</sub> = 22.716 ft; C <sub>D</sub> = D <sub>s</sub> / (1/2 $\rho$ S <sub>M</sub> V <sub>m</sub> <sup>2</sup> )																				DATUM: 22-10-1975		
Run no	Model Speed V <sub>m</sub>	V <sub>m</sub> <sup>2</sup>	Ship Speed V <sub>s</sub>	V <sub>s</sub> <sup>2</sup>	F <sub>n</sub>	$\beta$	Leeway/heeling angle $\phi$	Moment arm L	Lift fore L <sub>f</sub>	Lift after L <sub>a</sub>	Lift model L <sub>m</sub> = L <sub>f</sub> + L <sub>a</sub>	C <sub>L</sub>	Lift Ship L <sub>s</sub> = L <sub>m</sub> $\lambda$	Lift ship L <sub>s</sub>	Drag D'	$\Delta D = 0.4 V_m^2$	Drag model D <sub>m</sub> = D <sub>s</sub> / D <sub>LAD</sub>	Drag ship D <sub>s</sub>	Drag ship D <sub>s</sub>	C <sub>D</sub> $\times 10^{-3}$	L/D	C <sub>L</sub> /C <sub>D</sub>
	m/sec	m <sup>2</sup> /sec <sup>2</sup>	m/sec	m <sup>2</sup> /sec <sup>2</sup>		degr.	degr.	mm	kg	kg	kg		kg	kg	kg	kg	kg	kg	kg			Year.
123	.420	.176	2.000	1.028	.125	5.18	0	20.3	.082	.047	.129	3.403	27.86	61.4	.036	.002	.034	5.190	11.4	6.344	5.364	.3764
124	.631	.398	3.004	1.544	.188	"	"	41.8	.179	.106	.285	3.324	61.56	135.7	.075	.006	.069	10.632	23.4	5.747	5.785	.3677
125	.840	.706	4.000	2.056	.250	"	"	74.0	.310	.174	.484	3.183	104.54	230.5	.121	.010	.111	17.029	37.6	5.192	6.130	.3520
126	1.049	1.100	4.995	2.567	.312	"	"	121.0	.514	.280	.794	3.351	171.50	278.1	.209	.015	.194	31.779	70.1	6.215	5.292	.3707
127	1.259	1.505	5.995	3.081	.374	"	"	176.0	.769	.413	1.182	3.462	255.31	562.9	.356	.022	.334	58.317	128.6	7.216	4.374	.3829
128	1.470	2.161	6.999	3.597	.437	5.18	0	252.7	1.106	.604	1.710	3.674	369.36	814.3	.692	.030	.662	124.252	275.5	12.441	2.953	.4063
129	.420	.176	2.000	1.028	.125	5.18	10	-26.0	.074	.033	.107	2.822	23.11	51.0	.020	.002	.018	4.734	3.8	2.120	13.216	.3122
130	.628	.394	2.990	1.537	.187	"	"	-3.7	.177	.089	.266	3.134	57.46	126.7	.054	.006	.048	6.130	13.51	3.347	9.364	.3467
131	.842	.709	4.009	2.060	.250	"	"	27.9	.319	.161	.480	3.143	102.68	228.6	.117	.010	.107	16.147	35.6	4.900	6.415	.3477
132	1.049	1.100	4.995	2.567	.312	"	"	71.8	.502	.252	.756	3.191	163.30	380.0	.201	.015	.186	30.051	66.2	5.877	5.429	.3191
133	1.260	1.588	5.999	3.083	.374	"	"	134.5	.764	.400	1.164	3.403	251.42	554.3	.354	.022	.332	57.866	127.6	7.840	4.341	.3764
134	1.468	2.155	6.990	3.592	.436	5.18	10	202.0	1.059	.568	1.627	3.505	352.43	774.8	.692	.030	.667	125.084	278.0	12.587	2.785	.3505
136	1.469	2.158	6.984	3.594	.437	5.18	20	167.1	.941	.485	1.426	3.068	308.02	679.0	.720	.030	.690	131.031	288.9	13.063	2.348	.3393
137	1.669	2.788	5.999	3.083	.374	"	"	108.3	.723	.388	1.111	3.242	239.98	529.0	.370	.022	.348	61.322	135.2	8.308	3.910	.3593
138	1.850	3.423	4.999	2.569	.312	"	"	39.4	.476	.229	.705	2.967	152.28	335.7	.207	.015	.192	31.331	69.1	6.111	4.856	.3282
139	.841	.707	4.004	2.058	.250	"	"	-3.3	.293	.136	.429	2.817	92.66	204.3	.123	.010	.113	17.457	38.5	5.312	5.303	.3116
140	.620	.392	3.000	1.542	.187	"	"	-39.1	.160	.071	.231	2.701	49.90	110.0	.064	.006	.058	8.267	18.2	4.490	6.030	.2988
141	.422	.178	2.009	1.032	.125	"	"	-60.0	.075	.031	.106	2.765	22.90	50.5	.020	.003	.017	4.501	3.3	1.814	15.239	.3058
142	1.470	2.161	6.999	3.597	.437	5.18	20	169.6	.952	.504	1.457	3.130	314.71	693.8	.728	.030	.698	132.728	292.6	13.215	2.369	.3462
143	1.474	2.173	7.008	3.607	.438	2.65	30	-6.4	.372	.168	.481	1.028	103.90	229.0	.654	.030	.624	116.670	257.2	11.551	.890	.2222
144	1.468	2.155	6.990	3.592	.436	"	"	-6.4	.373	.110	.483	1.041	104.33	230.0	.654	.030	.624	116.796	257.5	11.660	.892	.2250
145	1.260	1.588	5.999	3.083	.374	2.65	30	-8.6	.314	.144	.458	1.339	98.93	218.1	.302	.022	.280	46.634	102.8	6.318	2.119	.2895
146	1.049	1.100	4.995	2.567	.312	5.18	30	14.6	.402	.190	.593	2.503	128.09	282.4	.201	.015	.186	30.051	66.2	5.877	4.258	.2788
147	1.260	1.588	5.990	3.078	.374	"	"	73.6	.582	.313	.895	2.617	193.32	416.2	.371	.022	.349	61.538	135.7	8.337	3.138	.2894
148	1.470	2.161	6.999	3.597	.437	"	"	116.0	.743	.347	1.090	2.342	235.44	519.0	.740	.030	.710	135.330	292.3	13.473	1.738	.2590
149	.420	.176	2.000	1.028	.306	"	"	-86.6	.057	.024	.081	2.137	17.50	38.6	.025	.002	.023	2.814	6.2	3.440	6.212	.2363
150	.631	.398	3.004	1.544	.188	"	"	-26.8	.129	.053	.182	2.123	39.31	86.7	.061	.006	.055	7.608	16.8	4.113	5.162	.2348
151	.843	.711	4.004	2.063	.251	5.18	30	-35.4	.250	.112	.362	2.364	78.19	172.4	.116	.010	.106	15.917	35.1	4.816	4.908	.2615

V.1560 niet herhalen

AARD v.d. PROEF: LIFT AND DRAG MEASUREMENT

GEVEENS: Model/scale  $d = 6$ ;  $L_{DUL}$  (nominal) = 1.154 m;  $S_{m1}$  (nominal) = 0.42322 m<sup>2</sup>;  $S_m$  (actual) = 0.4111 m<sup>2</sup>;  $X_c = 7L_{DUL} = 0.8079$  m

MODEL NO: 127

TYPE: ANTILOPE

VCG (above keel) = 0.2677 m; moment weight  $p = 1.5$  kg;  $V_3$  ( knots) = 4.7614 Vm;  $F_n = 0.29721 Vm$ ;  $C_L = Lm / \frac{1}{2} \rho S_m V_m^2$ ;  $C_D = Dm / \frac{1}{2} \rho S_m V_m^2$

EXP: J.S.

Temperature water  $T = 20.0$  °C;  $\rho = 101.79$  kg sec<sup>3</sup>/m<sup>4</sup>;  $\nu = 1.0188 \times 10^{-6}$  m<sup>2</sup>/sec;  $1/b = 0.536$  kg;  $L_{owl} = 22.716/b$ ;  $C_{D0} = D_s / \frac{1}{2} \rho S_m V_m^2$

DATE: 24-10-1973

Run no	Model speed Vm	Vm <sup>2</sup>	slip speed Vs	Vs / Vm	Fm	$\beta$	Trim angle $\theta$	Moment arm L	Lift fore Lf	Lift after La	Lift model Lm = Lf + La	CL	Lift slip Ls	Lift slip Ls	Drag D'	$\Delta D = 0.4 V_m^2$	Drag model Dm = D' + $\Delta D$	Drag slip Ds	Drag slip Ds	Co	L/D	C/L
	m/sec	m <sup>2</sup> /sec <sup>2</sup>	knots			degr.	degr.	mm	kg	kg	kg		kg	kg	kg	kg	kg	kg	kg	$\times 10^{-3}$		%
152	.420	.176	3.000	1.028	.125	6.45	0	24.6	.097	.053	.150	3.957	32.4	71.4	.025	.002	.023	2.814	6.2	3.440	11.503	.3515
153	.620	.397	3.000	1.542	.187	"	"	62.6	.238	.140	.378	4.420	81.6	179.9	.075	.006	.069	10.643	23.5	5.768	7.664	.3927
154	.842	.709	4.009	2.060	.250	"	"	98.9	.410	.232	.642	4.237	139.8	308.2	.145	.010	.135	22.195	48.9	6.735	6.291	.3763
155	1.050	1.103	4.999	2.569	.312	"	"	154.5	.654	.370	1.024	4.310	221.2	487.7	.241	.015	.226	38.675	85.3	7.544	5.714	.3829
156	1.259	1.585	5.995	3.081	.374	6.45	0	225.4	.966	.539	1.505	4.408	325.1	716.7	.403	.022	.381	68.469	150.9	9.294	4.743	.3916
157	.420	.176	3.000	1.028	.125	6.45	10	-21.3	.102	.057	.159	4.194	34.3	75.6	.035	.002	.033	4.974	11.0	6.080	6.898	.3726
158	.620	.397	3.000	1.542	.187	"	"	6.0	.225	.125	.350	4.093	75.6	166.7	.079	.006	.073	11.507	25.4	6.236	6.564	.3636
159	.842	.709	4.009	2.060	.250	"	"	48.6	.404	.222	.626	4.090	135.2	298.1	.146	.010	.136	22.411	49.4	6.800	6.028	.3641
160	1.052	1.107	5.009	2.574	.313	"	"	106.9	.662	.359	1.021	4.282	220.5	486.1	.241	.015	.226	38.642	85.2	7.510	5.702	.3804
161	1.261	1.590	6.004	3.086	.375	"	"	193.0	1.005	.559	1.564	4.567	332.8	744.7	.415	.022	.393	71.023	156.6	9.610	4.752	.4057
162	1.472	2.167	7.009	3.602	.437	6.45	10	277.9	1.352	.765	2.117	4.546	459.4	1010.8	.706	.030	.676	145.224	320.2	14.418	3.153	.4038
163	1.260	1.588	5.999	3.083	.374	2.65	0	83.6	.396	.189	.585	1.710	126.4	278.7	.303	.022	.281	46.850	102.3	6.347	2.695	.3698
164	1.262	1.593	6.009	3.088	.375	"	10	52.6	.421	.192	.613	1.787	132.4	291.9	.306	.022	.284	47.460	104.6	6.410	2.787	.3863
165	1.260	1.588	5.999	3.083	.374	"	"	44.7	.409	.183	.592	1.731	127.9	282.0	.300	.022	.278	46.202	101.9	6.260	2.765	.3742
166	1.250	1.503	5.990	3.078	.374	"	10	50.2	.418	.188	.606	1.778	130.9	288.6	.296	.022	.274	45.375	100.0	6.167	2.882	.3843
167	1.259	1.505	5.985	3.081	.374	2.65	20	19.8	.385	.172	.552	1.631	120.3	265.2	.294	.022	.272	44.925	99.0	6.098	2.675	.3527
168	.419	.176	1.995	1.025	.125	6.45	20	-52.9	.089	.041	.130	3.429	28.1	61.9	.018	.002	.016	1.311	2.9	1.603	21.398	.3046
169	.620	.397	3.000	1.542	.187	"	"	-26.9	.192	.097	.294	3.438	62.5	140.0	.063	.006	.057	8.057	17.7	4.363	7.880	.3054
170	.842	.709	4.009	2.060	.250	"	"	20.4	.386	.199	.585	3.831	124.4	278.7	.130	.010	.120	18.255	41.8	5.752	6.660	.3403
171	1.051	1.105	5.004	2.572	.312	"	"	72.7	.605	.317	.922	3.874	192.2	439.2	.238	.015	.223	38.010	83.8	7.400	5.234	.3441
172	1.260	1.588	5.999	3.083	.374	"	"	157.3	.909	.521	1.430	4.181	308.9	681.0	.418	.022	.396	71.690	158.0	9.712	4.304	.3714
173	1.472	2.167	7.009	3.602	.437	6.45	20	238.9	1.215	.680	1.895	4.060	409.3	902.3	.798	.030	.768	147.816	325.9	14.675	2.766	.3606
174	1.261	1.590	6.004	3.086	.375	6.45	30	121.0	.721	.418	1.139	3.326	246.0	542.3	.424	.022	.402	72.967	160.9	9.873	3.368	.2954
175	1.051	1.105	5.004	2.572	.312	"	"	49.6	.510	.266	.776	3.260	117.6	269.5	.231	.015	.216	36.498	80.5	7.106	4.588	.2896
176	.840	.706	4.000	2.056	.250	"	"	-14.5	.307	.147	.454	2.985	98.1	216.3	.132	.010	.122	19.415	42.8	5.916	5.046	.2652
177	.620	.396	2.995	1.539	.187	"	"	-52.6	.168	.077	.245	2.872	52.9	116.6	.065	.006	.059	8.494	18.7	4.615	6.224	.2551
178	.420	.176	3.000	1.028	.125	6.45	30	-77	.074	.033	.102	2.822	23.1	50.9	.026	.002	.024	3.030	6.7	3.704	7.620	.2507
179	1.260	1.588	5.999	3.083	.374	5.18	20	107	.728	.390	1.118	3.269	241.5	532.4	.358	.022	.336	58.730	129.5	7.957	4.108	.2903

1973 10/24

AARD v.g. PROEF: LIFT AND DRAG MEASUREMENT MODEL NO: 127

GEGEVENS: Model/scaled = 6;  $L_{DWL}$  (nominal) = 1.154 m;  $S_{wp}$  (nominal) = 0.42322 m<sup>2</sup>;  $S_m$  (actual) = .4111 m<sup>2</sup>;  $X_c = .7 L_{DWL} = .8079$  m TYPE: ANTIORPE

VCG (above keel) = 0.2577 m; moment weight  $\rho = 1.5$  kg;  $V_s$  (knots) = 4.7614  $V_m$ ;  $F_n = 0.29731 V_m$ ;  $C_L = L_m / \frac{1}{2} \rho S_m V_m^2$ ; EXP: 1 S

Temperature water  $T = 19.8$  °C;  $\rho = 101.79$  kg sec<sup>2</sup>/m<sup>3</sup>;  $\nu = 1.0108 \times 10^{-6}$  m<sup>2</sup>/sec;  $l_b = 0.436$  kg;  $L_{DWL} = 22.716$  ft;  $C_D = D_s / \frac{1}{2} \rho S_m V_m^2$  DATUM: 6-11-1973

Run no	Model speed $V_m$	$V_m^2$	Ship speed $V_s$	$V_s^2$	$V_s / V_{DWL}$	$F_n$	$\beta$	Leeway/reeching angle $\rho$	Moment arm $t$	Lift fore $L_f$	Lift after $L_a$	Lift model $L_m = L_f + L_a$	$C_L$	Lift ship $L_s = L_m \cdot 6$	Lift ship $L_s$	Drag $D'$	$\Delta D = 0.14 V_m^2$	Drag model $D_m = D' \cdot \Delta D$	Drag ship $D_s$	Drag ship $D_s$	$C_D$					
	m/sec	m <sup>2</sup> /sec <sup>2</sup>	knots				degr.	degr.	mm	kg	kg	kg		kg	lbs	kg	kg	kg	kg	lbs	$\times 10^{-3}$					
230	.403	.162	1919	.403	.120	0	0	0	0	0	0	0	0	0	0	.020	.002	.018	1.878	4.1	2.494					
231	.454	.206	2.162	.454	.135	"	"	"	"	"	"	"	"	"	"	.026	.003	.023	2.514	5.5	2.626					
232	.504	.254	2.400	.503	.150	"	"	"	"	"	"	"	"	"	"	.033	.004	.029	3.339	7.4	2.828					
233	.555	.308	2.643	.554	.165	"	"	"	"	"	"	"	"	"	"	.041	.004	.037	4.551	10.0	3.179					
234	.605	.366	2.881	.604	.180	"	"	"	"	"	"	"	"	"	"	.050	.005	.045	5.741	12.7	3.375					
235	.655	.429	3.179	.654	.195	"	"	"	"	"	"	"	"	"	"	.060	.006	.054	7.113	15.7	3.567					
236	.705	.497	3.357	.704	.210	"	"	"	"	"	"	"	"	"	"	.068	.007	.061	8.022	17.7	3.473					
237	.755	.570	3.595	.754	.224	"	"	"	"	"	"	"	"	"	"	.080	.008	.072	9.764	21.5	3.685					
238	.805	.648	3.833	.804	.239	"	"	"	"	"	"	"	"	"	"	.090	.009	.081	11.043	24.3	3.666					
239	.856	.733	4.076	.855	.254	"	"	"	"	"	"	"	"	"	"	.103	.010	.093	12.925	28.5	3.794					
240	.905	.819	4.309	.904	.269	"	"	"	"	"	"	"	"	"	"	.116	.011	.105	14.806	32.6	3.890					
241	.955	.912	4.547	.954	.284	"	"	"	"	"	"	"	"	"	"	.132	.013	.119	17.076	37.6	4.028					
242	1.007	1.014	4.795	1.006	.299	"	"	"	"	"	"	"	"	"	"	.152	.014	.138	20.364	44.9	4.321					
243	1.056	1.115	5.028	1.055	.314	"	"	"	"	"	"	"	"	"	"	.170	.016	.154	23.024	50.8	4.442					
244	1.106	1.223	5.266	1.105	.329	"	"	"	"	"	"	"	"	"	"	.189	.017	.172	26.071	57.5	4.506					
245	1.158	1.341	5.514	1.157	.344	"	"	"	"	"	"	"	"	"	"	.214	.019	.195	30.134	66.4	4.834					
246	1.206	1.454	5.742	1.205	.358	"	"	"	"	"	"	"	"	"	"	.245	.020	.225	35.753	78.8	5.290					
247	1.256	1.578	5.980	1.255	.373	"	"	"	"	"	"	"	"	"	"	.281	.022	.259	42.173	93.0	5.750					
248	1.306	1.707	6.218	1.305	.388	"	"	"	"	"	"	"	"	"	"	.334	.024	.310	52.238	115.2	6.584					
249	1.356	1.839	6.456	1.355	.403	"	"	"	"	"	"	"	"	"	"	.391	.026	.365	63.139	139.2	7.386					
250	1.405	1.974	6.690	1.404	.418	"	"	"	"	"	"	"	"	"	"	.447	.028	.419	75.819	162.7	8.045					
250 <sup>A</sup>	1.405	1.974	6.690	1.404	.418	"	"	"	"	"	"	"	"	"	"	.464	.028	.436	77.491	170.8	8.445					
251	1.424	2.028	6.780	1.423	.423	"	"	"	"	"	"	"	"	"	"	.480	.028	.452	80.558	177.6	8.546					
252	1.456	2.120	6.933	1.455	.433	"	"	"	"	"	"	"	"	"	"	.530	.030	.500	90.263	199.9	9.160					
252 <sup>A</sup>	1.455	2.117	6.928	1.454	.432	"	"	"	"	"	"	"	"	"	"	.553	.030	.523	95.252	210.0	9.680					
253	1.504	2.262	7.161	1.503	.447	"	"	"	"	"	"	"	"	"	"	.642	.032	.610	113.009	249.1	10.748					
253 <sup>A</sup>	1.555	2.418	7.404	1.553	.462	"	"	"	"	"	"	"	"	"	"	.738	.034	.704	132.208	291.5	11.763					
254	1.605	2.576	7.642	1.603	.477	"	"	"	"	"	"	"	"	"	"	.813	.036	.777	146.867	323.8	12.266					
254 <sup>A</sup>	1.655	2.739	7.880	1.653	.492	"	"	"	"	"	"	"	"	"	"	.906	.038	.868	165.589	364.6	12.991					
255	1.701	2.893	8.099	1.699	.506	"	"	"	"	"	"	"	"	"	"	1.016	.041	.975	187.435	413.2	13.939					
255 <sup>A</sup>	1.747	3.052	8.318	1.745	.519	"	"	"	"	"	"	"	"	"	"	1.139	.043	1.096	212.483	468.4	14.978					
256	1.602	2.566	7.628	1.600	.476	"	"	"	"	"	"	"	"	"	"	.811	.036	.775	146.503	323.0	12.287					

TWIS 6101

AARD v.d. PROEF: LIFT AND DRAG MEASUREMENT

MODEL NO: 127

GEGEVENS: Model/scale  $\alpha = 6$ ;  $L_{DUL}$  (nominal) = 1.154 m;  $S_{mn}$  (nominal) = 0.42322 m<sup>2</sup>;  $S_m$  (actual) = .4111 m<sup>2</sup>;  $X = .7 L_{DUL} = .8079$  m

TYPE: ANTIORSE

VCG (above keel) = 0.2677 m; moment weight  $\rho = 1.5$  kg;  $V_s$  (knots) = 4.7614 Vm;  $F_n = 0.29721 Vm$ ;  $C_L = L_m / \frac{1}{2} \rho S_{mn} V_m^2$ ;

EXP: vS

Temperature water  $T = 19.8^\circ C$ ;  $\rho = 101.79$  kg sec<sup>2</sup>/m<sup>4</sup>;  $\nu = 1.0188 \times 10^{-6}$  m<sup>2</sup>/sec;  $\mu = 0.436$  kg;  $L_{DUL} = 22.716$  ft;  $C_D = D_s / \frac{1}{2} \rho S_{mn} \alpha^3 V_m^2$

DATUM: 6-11-1973

Run no	Model speed Vm	Ship speed V <sub>s</sub>	V <sub>s</sub> / V <sub>DUL</sub>	F <sub>n</sub>	$\beta$	Leeway/heeling angle $\phi$	Moment arm c	Lift fore L <sub>f</sub>	Lift after L <sub>a</sub>	Lift model L <sub>m</sub> = L <sub>f</sub> + L <sub>a</sub>	C <sub>L</sub>	Lift ship L <sub>s</sub> = L <sub>m</sub> $\alpha^3$	Lift L <sub>s</sub>	Drag D'	$\Delta D = D' / V_m^2$	Drag model D <sub>m</sub> = D' $\alpha^2$	Drag ship D <sub>s</sub>	Drag slip D <sub>s</sub>	C <sub>D</sub> * 10 <sup>-3</sup>
	m/sec	m/sec	knots		degr.	degr.	mm	kg	kg	kg		kg	lbs	kg	kg	kg	kg	lbs	
257	1.651	2.726	7.861	1.649	.491	0	0	0	0	0	0	0	0	.909	.038	.871	166.129	366.2	13.111
258	1.304	1.700	6.209	1.303	.388	"	"	"	"	"	"	"	"	.326	.024	.302	50.548	111.4	6.397
259	1.353	1.831	6.442	1.352	.402	"	"	"	"	"	"	"	"	.388	.026	.362	62.551	137.9	7.350

AARD v.d. PROEF: LIFT AND DRAG MEASUREMENT															MODEL N.: 127								
GEGEVENS: Modelscaled = 6; $L_{DUL}$ (nominal) = 1.154 m; $S_{m,n}$ (nominal) = 0.42322 m <sup>2</sup> ; $S_m$ (actual) = .4111 m <sup>2</sup> ; $X_c = .7 L_{DUL} = .8079$ m															TYPE: ANTIORP								
VCG (above keel) = 0.2677 m; moment weight $p = 1.5$ kg; $V_2$ ( knots ) = 4.7614 V <sub>m</sub> ; $F_n = 0.29721 V_m$ ; $C_L = L_m / \frac{1}{2} \rho S_m V_m^2$ ;															EXP: v.S.								
Temperature water T = 19.0 °C; $\rho = 101.79$ kg sec <sup>2</sup> /m <sup>4</sup> ; $\nu = 1.0188 \times 10^{-6}$ m <sup>2</sup> /sec; $1/6 = 0.56$ kg; $L_{0.1} = 22.716/l$ ; $C_D = D_s / \frac{1}{2} \rho S_m V_m^2 U_m^2$															DATUM: 7-11-1973								
Run no	Model speed V <sub>m</sub>	V <sub>m</sub> <sup>2</sup>	Swirl speed V <sub>s</sub>	V <sub>s</sub> / V <sub>DUL</sub>	F <sub>n</sub>	$\beta$	Leemvrijheids angle $\phi$	Moment arm L	Lift force L <sub>f</sub>	Lift after L <sub>a</sub>	Lift model L <sub>m</sub> = L <sub>f</sub> + L <sub>a</sub>	C <sub>L</sub>	Lift slip L <sub>s</sub> = L <sub>m</sub> x 10 <sup>-2</sup>	Lift slip L <sub>s</sub>	Drag D'	$\Delta D = D' - D_{MOD}$	Drag model D <sub>m</sub> = D <sub>MOD</sub>	Drag slip D <sub>s</sub>	Drag slip D <sub>s</sub>	C <sub>D</sub> x 10 <sup>-3</sup>	L/D	C <sub>L</sub> / $\beta$	
	m/sec	m <sup>2</sup> /sec <sup>2</sup>	m/sec			degr.	degr.	mm	kg	kg	kg		kg	kg	kg	kg	kg	kg	kg	kg			grad
260	.420	.176	2.000	.420	.125	2.65	0	8.6	.032	.021	.053	1.398	11.4	25.1	.022	.002	.020	2.166	4.8	2.648	5.280	.3022	
261	.421	.177	2.005	.421	.125	"	"	8.5	.034	.019	.053	1.390	11.4	25.1	.024	.002	.022	2.589	5.7	3.147	4.418	.3006	
262	.630	.397	3.000	.629	.187	"	"	19.5	.080	.046	.126	1.473	27.2	60.0	.058	.006	.052	6.971	15.4	3.778	3.900	.3186	
263	.840	.706	4.000	.839	.250	"	"	35.1	.150	.080	.230	1.512	49.7	109.6	.107	.010	.097	14.015	30.9	4.271	3.541	.3270	
264	1.052	1.107	5.009	1.051	.313	"	"	55.0	.243	.126	.369	1.548	72.7	175.7	.179	.015	.164	25.250	55.7	4.907	3.154	.3346	
265	1.261	1.590	6.004	1.260	.375	"	"	76.3	.343	.171	.514	1.501	111.0	244.7	.290	.022	.268	44.023	97.1	5.957	2.520	.3245	
266	1.469	2.158	6.994	1.467	.437	"	"	116.0	.505	.271	.776	1.670	167.6	369.5	.582	.030	.552	101.223	223.1	10.091	1.654	.3609	
267	1.693	2.832	8.013	1.681	.500	2.65	0	159.2	.710	.376	1.086	1.780	234.6	517.2	1.019	.040	.979	188.79	416.0	14.337	1.242	.3849	
268	1.423	.179	2.014	.423	.126	2.65	10	-35.5	.044	.025	.069	1.790	14.9	32.8	.024	.003	.021	2.356	5.2	2.832	6.320	.3869	
269	.630	.397	3.000	.629	.187	"	"	-24.5	.091	.045	.136	1.590	29.4	64.8	.058	.006	.052	6.971	15.4	3.778	4.210	.3479	
270	.839	.704	3.975	.838	.249	"	"	-11.3	.154	.071	.225	1.484	48.6	107.1	.104	.010	.094	13.381	29.5	4.090	3.629	.3208	
271	1.049	1.100	4.975	1.048	.312	"	"	-11.3	.266	.119	.385	1.625	83.2	183.4	.174	.015	.159	24.419	53.4	4.777	3.470	.3513	
272	1.259	1.585	5.975	1.258	.374	"	"	42.9	.397	.192	.589	1.725	127.2	280.4	.299	.022	.277	46.005	101.4	6.244	2.763	.3730	
273	1.469	2.158	6.994	1.467	.437	"	"	79.6	.544	.261	.805	1.722	173.9	383.4	.598	.030	.568	104.679	230.8	10.436	1.659	.3744	
274	1.676	2.809	7.980	1.674	.498	"	"	116.6	.734	.335	1.069	1.767	230.9	509.0	1.026	.039	.987	190.609	420.2	14.599	1.210	.3820	
275	1.051	1.105	5.004	1.050	.312	2.65	10	15.6	.266	.120	.386	1.622	83.4	183.9	.177	.015	.162	24.834	54.7	4.833	3.354	.3506	
276	.419	.176	1.975	.419	.125	2.65	20	-68.6	.035	.011	.046	1.213	9.9	21.8	.021	.002	.019	1.959	4.3	2.395	5.067	.2623	
277	.630	.397	3.000	.629	.187	"	"	-56.7	.083	.032	.115	1.345	24.8	54.7	.051	.006	.045	5.459	12.0	2.958	4.546	.2908	
278	.842	.709	4.009	.841	.250	"	"	-42.4	.150	.057	.207	1.355	44.7	98.5	.093	.010	.083	10.963	24.2	3.327	4.075	.2931	
279	1.050	1.103	4.979	1.049	.312	"	"	-18.6	.248	.099	.347	1.461	75.0	165.3	.173	.015	.158	23.987	52.9	4.679	3.122	.3158	
280	1.258	1.583	5.990	1.257	.374	"	"	-21.6	.392	.195	.587	1.722	126.8	272.5	.306	.022	.284	47.535	104.8	6.460	2.665	.3722	
281	1.471	2.164	7.004	1.470	.437	"	"	44.9	.487	.216	.703	1.508	151.8	334.7	.629	.030	.599	111.333	245.4	11.068	1.763	.3261	
282	1.680	2.822	7.979	1.678	.499	"	"	73.4	.657	.250	.907	1.499	195.9	431.9	1.016	.040	.976	188.100	414.8	14.393	1.040	.3826	
283	1.470	2.161	6.999	1.468	.437	2.65	20	41.4	.469	.206	.675	1.450	145.8	321.4	.615	.030	.585	108.330	238.8	10.785	1.345	.3175	
284	1.470	2.161	7.004	1.470	.437	2.65	30	11.9	.345	.112	.457	.982	98.7	212.6	.658	.030	.628	117.618	259.3	11.710	.838	.2123	
285	1.260	1.588	5.979	1.259	.374	"	"	-5.0	.313	.153	.466	1.362	100.7	222.0	.306	.022	.284	47.498	104.7	6.435	2.117	.2948	
286	1.049	1.100	4.975	1.048	.312	"	"	-37.2	.223	.086	.309	1.304	66.7	147.0	.175	.015	.160	24.435	53.9	4.779	2.729	.2820	
287	.841	.707	4.004	.840	.250	"	"	-60.9	.137	.051	.188	1.235	40.6	89.5	.104	.010	.094	13.353	29.4	4.063	3.038	.2669	
288	.420	.176	2.000	.420	.125	"	"	-88.6	.029	.006	.035	.993	7.6	16.8	.022	.002	.020	2.166	4.8	2.648	3.487	.1996	
289	.631	.398	3.004	.630	.188	"	"	-81.6	.066	.019	.085	.992	18.4	40.6	.053	.006	.047	5.880	13.0	3.178	3.119	.2144	
290	1.260	1.588	5.979	1.259	.374	2.65	30	-3.8	.313	.157	.470	1.374	101.5	223.8	.303	.022	.281	46.850	103.3	6.347	2.165	.2971	

1000000

AA70 v.o. PROEF: LIFT AND DRAG MEASUREMENT MODEL N: 127

GEVEENS: Model/scale  $\alpha = 6$ ;  $L_{DNL}$  (nominal) = 1.154 m;  $S_{mD}$  (nominal) = 0.42322 m<sup>2</sup>;  $S_m$  (actual) = .411 m<sup>2</sup>;  $X = .7 L_{DNL} = .8079$  m TYPE: ANTILOPE

VCG (above keel) = 0.2677 m; moment weight  $\rho = 1.5$  kg;  $V_s$  (knots) = 4.764 Vm;  $F_n = 0.29721 Vm$ ;  $C_L = L_m / \frac{1}{2} \rho S_{mD} V_m^2$ ; EXP: v.M v.S

Temperature water  $T = 19.8^\circ C$ ;  $\rho = 101.79$  kg sec<sup>3</sup>/m<sup>4</sup>;  $\nu = 1.0188 \cdot 10^{-6}$  m<sup>2</sup>/sec;  $l/b = 0.456$  kg;  $L_{DNL} = 88.716 \beta$ ;  $C_D = D_m / \frac{1}{2} \rho S_{mD} V_m^2$ ; DATUM: 9-11-1973

Run no	Model speed Vm	Vm <sup>2</sup>	Ship speed Vs	Vs <sup>2</sup>	F <sub>n</sub>	$\beta$	Leeway, veering angle $\phi$	Moment arm t	Life fore Lf	Life after La	Life model Lm = LfLa	CL	Life ship Ls = Lm $\alpha^2$	Life ship Ls	Drag D'	$\Delta D = \Delta D_m$	Drag model Dm = D' $\alpha^2$	Drag ship Ds	Drag ship Ds	CD	L/b	CL/ $\beta$
	m/sec	m <sup>2</sup> /sec <sup>2</sup>	m/sec	m <sup>2</sup> /sec <sup>2</sup>		degr.	degr.	mm	kg	kg	kg		kg	lbs	kg	kg	kg	kg	lbs	$\cdot 10^{-3}$		1/ $\beta$
291	.420	.176	2.000	.420	.125	5.18	0	17.3	.073	.040	.113	2.991	24.4	53.8	.028	.002	.026	3.462	7.6	4.232	7.044	.3297
292	.632	.399	3.009	.631	.188	"	"	39.8	.172	.103	.275	3.200	59.4	131.0	.066	.006	.060	8.676	19.1	4.678	6.840	.3540
293	.838	.702	3.990	.837	.249	"	"	73.9	.320	.185	.505	3.340	109.1	240.5	.125	.010	.115	17.931	39.5	5.495	6.077	.3694
294	1.050	1.103	4.999	1.049	.312	"	"	112.1	.498	.278	.776	3.266	167.6	369.5	.207	.015	.192	31.531	69.1	6.111	5.345	.3613
295	1.261	1.590	6.004	1.260	.375	"	"	166.8	.739	.407	1.146	3.346	247.5	545.6	.358	.022	.336	58.711	129.4	7.944	4.212	.3701
296	1.469	2.158	6.994	1.467	.437	5.18	0	243.4	1.066	.595	1.659	3.569	358.3	789.9	.683	.030	.653	96.811	213.4	9.651	3.698	.3948
297	1.677	2.812	7.985	1.675	.498	5.18	10	279.6	1.400	.770	2.170	3.593	469.7	1033.3	1.180	.039	1.141	223.850	493.5	17.126	2.092	.3963
298	1.469	2.158	6.994	1.467	.437	"	"	212.2	1.082	.595	1.677	3.609	362.2	798.5	.723	.030	.693	131.679	290.3	13.128	2.748	.3991
299	1.260	1.588	5.999	1.259	.374	"	"	132.3	.765	.412	1.177	3.441	254.2	560.4	.367	.022	.345	60.674	133.8	8.220	4.106	.3806
300	1.050	1.103	4.999	1.049	.312	"	"	72.1	.484	.249	.733	3.085	158.3	349.0	.210	.015	.195	31.979	70.5	6.237	4.946	.3413
301	1.680	2.822	7.999	1.678	.499	"	"	279.8	1.396	.768	2.164	3.560	467.4	1030.4	1.162	.040	1.122	219.676	484.3	16.747	2.126	.3938
302	.840	.706	4.000	.839	.250	"	"	27.5	.311	.167	.478	3.143	103.2	227.5	.123	.010	.113	17.471	38.5	5.324	5.904	.3477
303	.420	.176	2.000	.420	.125	"	"	-27.6	.071	.040	.111	2.928	24.0	52.9	.021	.002	.019	1.950	4.3	2.384	12.284	.3239
304	.631	.398	3.004	.630	.188	"	"	-5.7	.167	.091	.258	3.019	55.7	122.8	.062	.006	.056	7.842	17.3	4.240	7.100	.3329
305	.843	.711	4.014	.842	.251	5.18	10	28.7	.320	.170	.490	3.200	105.8	233.2	.122	.010	.112	17.213	37.9	5.202	6.143	.3539
306	.421	.177	2.005	.421	.125	5.18	20	-58.1	.073	.035	.108	2.873	23.3	51.4	.023	.002	.021	2.373	5.2	2.884	9.821	.3123
307	.630	.397	3.000	.629	.187	"	"	-35.5	.164	.082	.246	2.876	53.1	117.1	.061	.006	.055	7.619	16.8	4.129	6.967	.3182
308	.842	.709	4.009	.841	.250	"	"	-4.7	.290	.143	.433	2.835	93.5	206.1	.117	.010	.107	16.147	35.6	4.899	5.787	.3126
309	1.050	1.103	4.999	1.049	.312	"	"	42.0	.478	.242	.720	3.031	155.5	342.8	.204	.015	.189	30.683	67.3	5.985	5.064	.3352
310	1.259	1.585	5.995	1.258	.374	"	"	108.9	.713	.398	1.111	3.254	240.0	529.1	.367	.022	.345	60.693	133.8	8.238	3.950	.3599
311	1.468	2.155	6.990	1.467	.436	5.18	20	169.3	.947	.512	1.459	3.143	315.1	694.7	.717	.030	.687	130.404	287.5	13.019	2.414	.3477
312	1.260	1.588	5.999	1.259	.374	5.18	30	75.8	.577	.327	.904	2.643	195.3	430.6	.360	.022	.338	59.162	130.4	8.015	3.297	.2923
313	1.051	1.105	5.004	1.050	.312	"	"	12.3	.392	.198	.590	2.479	127.4	280.9	.196	.015	.181	28.938	63.8	5.634	4.400	.2742
314	.421	.177	2.005	.421	.125	"	"	-83.6	.055	.025	.080	2.098	17.3	38.1	.024	.002	.022	2.589	5.7	3.147	6.668	.2321
315	.629	.396	2.995	.628	.187	"	"	-62.2	.131	.061	.192	2.251	41.5	91.5	.060	.006	.054	7.414	16.3	4.028	5.588	.2490
316	.841	.707	4.004	.840	.250	"	"	-29.4	.245	.118	.363	2.384	78.4	172.8	.118	.010	.108	16.377	36.1	4.984	4.787	.2637
317	1.051	1.105	5.004	1.050	.312	5.18	30	+11.5	.391	.197	.588	2.470	127.0	280.0	.196	.015	.181	28.938	63.8	5.634	4.385	.2733

UNES BUREAU

AARD v.d. PROEF: LIFT AND DRAG MEASUREMENT																				MODEL NO: 127		
GEGEVENS: Model/scale $\alpha = 6$ ; $L_{DWL}$ (nominal) = 1.154 m; $S_{m1}$ (nominal) = 0.42322 m <sup>2</sup> ; $S_m$ (actual) = .4111 m <sup>2</sup> ; $X_c = .7 L_{DWL} = .8079$ m																				TYPE: ANTIOPS		
VCG (above keel) = 0.2677 m; moment weight $\rho = 1.5$ kg; $V_s$ (knots) = 4.7614 V <sub>m</sub> ; $F_n = 0.29721 V_m$ ; $C_L = L_m / \frac{1}{2} \rho S_m V_m^2$ ;																				EXP: J.S.		
Temperature water $T = 19.6$ °C; $\rho = 101.79$ kg sec <sup>2</sup> /m <sup>4</sup> ; $\nu = 1.0188 \times 10^{-6}$ m <sup>2</sup> /sec; $1/16 = 0.625$ ft; $L_{DWL} = 22.711$ ft; $C_D = D_m / \frac{1}{2} \rho S_m V_m^2$																				DATUM: 12-11-1973		
Run no	Model speed V <sub>m</sub>	Swirl speed V <sub>s</sub>	V <sub>0</sub> / V <sub>DWL</sub>	F <sub>n</sub>	$\beta$	Incidence angle $\phi$	Moment arm L	Life fore L <sub>f</sub>	Life after L <sub>a</sub>	Life model L <sub>m</sub> = L <sub>f</sub> + L <sub>a</sub>	C <sub>L</sub>	Life slip L <sub>s</sub> = L <sub>m</sub> $\alpha$	Life slip L <sub>s</sub>	Drag D'	$\Delta D = \frac{1}{4} V_m^2$	Drag model D <sub>m</sub> = D <sub>0</sub> D <sub>1</sub> D <sub>2</sub>	Drag ship D <sub>s</sub>	Drag slip D <sub>s</sub>	C <sub>D</sub> $\times 10^{-3}$	L <sub>y</sub> / D <sub>s</sub>	C <sub>L</sub> / $\beta$	
	m/sec	m/sec			degr.	degr.	mm	kg	kg	kg		kg	lbs	kg	kg	kg	kg	kg	kg		1/100	
318	.420	.176	2.000	.420	.125	6.45	0	22.0	.088	.055	.143	3.772	30.9	68.1	.031	.002	.029	4.110	9.1	5.024	7.508	.3351
319	.631	.398	3.004	.630	.188	"	"	52.4	.210	.132	.342	3.989	73.9	162.9	.028	.006	.072	11.180	24.9	6.097	6.543	.3543
320	.840	.706	4.000	.839	.250	"	"	93.4	.393	.240	.633	4.163	136.7	301.4	.147	.010	.137	22.655	49.9	6.904	6.029	.3698
321	1.051	1.105	5.004	1.050	.312	"	"	151.3	.654	.382	1.036	4.35	223.8	493.4	.247	.015	.232	39.954	88.1	7.779	5.595	.3867
322	1.259	1.585	5.995	1.258	.374	6.45	0	133.0	.963	.550	1.513	4.432	326.8	720.5	.408	.022	.386	69.549	153.3	9.440	4.694	.3927
323	1.469	2.158	6.994	1.467	.437	6.45	10	278.0	1.340	.770	2.112	4.554	457.3	1008.2	.778	.030	.748	143.539	316.5	14.312	3.182	.4046
324	1.259	1.585	5.995	1.258	.374	"	"	191.0	.968	.554	1.522	4.458	328.8	734.9	.410	.022	.388	69.981	154.3	9.499	4.693	.3960
325	1.047	1.096	4.985	1.046	.311	"	"	105.1	.634	.352	.986	4.177	213.0	469.6	.238	.015	.223	38.076	83.9	7.477	5.588	.3710
326	.421	.177	2.005	.421	.125	"	"	-30.0	.093	.056	.149	3.908	32.2	71.0	.032	.002	.030	4.317	9.5	5.247	7.448	.3472
327	.629	.396	2.995	.628	.187	"	"	+7.0	.215	.127	.342	4.009	73.9	162.9	.028	.006	.072	11.302	24.9	6.140	6.530	.3562
328	.841	.707	4.004	.840	.250	"	"	52.6	.400	.253	.633	4.157	136.7	301.4	.146	.010	.136	22.425	49.4	6.824	6.091	.3692
329	.421	.177	2.005	.421	.125	"	"	-22.1	.092	.052	.144	3.777	31.1	68.6	.030	.002	.028	3.885	8.6	4.722	7.977	.3355
330	1.051	1.105	5.004	1.050	.312	6.45	10	109.6	.653	.367	1.020	4.285	220.3	485.7	.240	.015	.225	38.442	84.7	7.485	5.726	.3807
331	.630	.397	3.000	.629	.187	6.45	20	-27.5	.190	.103	.293	3.426	63.3	139.6	.023	.006	.067	12.211	22.5	5.533	6.192	.3044
332	.841	.707	4.004	.840	.250	"	"	+14.7	.357	.196	.553	3.631	119.4	263.2	.139	.010	.129	20.913	46.1	6.364	5.706	.3226
333	1.049	1.100	4.995	1.048	.312	"	"	74.7	.599	.325	.924	3.900	199.6	440.0	.236	.015	.221	37.611	82.9	7.356	5.301	.3464
334	1.260	1.588	5.999	1.259	.374	"	"	149.5	.862	.510	1.372	4.011	296.4	653.4	.416	.022	.394	71.258	157.1	9.654	4.155	.3563
335	1.470	2.161	6.999	1.468	.437	"	"	225.9	.784	1.154	1.838	3.949	397.0	875.2	.669	.030	.639	119.994	264.5	11.946	3.305	.3508
336	.420	.176	2.000	.420	.125	6.45	20	-53.3	.092	.047	.139	3.666	30.0	66.1	.030	.002	.028	3.894	8.6	4.760	7.703	.3257
337	.421	.177	2.005	.421	.125	6.45	30	-77.6	.071	.034	.105	2.754	22.7	50.0	.026	.002	.024	3.021	6.7	3.672	7.500	.2446
338	.632	.399	3.009	.631	.188	"	"	-52.5	.164	.080	.244	2.839	52.7	116.2	.068	.006	.062	9.108	20.1	4.911	5.781	.2522
339	.842	.709	4.009	.841	.250	"	"	-14.8	.300	.153	.453	2.966	97.8	215.6	.130	.010	.120	18.955	41.8	5.752	5.157	.2635
340	1.051	1.105	5.004	1.050	.312	"	"	+42.6	.499	.264	.763	3.206	164.8	363.3	.221	.015	.206	34.338	75.7	6.685	4.795	.2848
341	1.259	1.585	5.995	1.258	.374	6.45	30	114.7	.700	.415	1.115	3.266	240.8	530.9	.405	.022	.383	68.901	151.9	9.352	3.492	.2901

AARD v.g. PROEF: LIFT AND DRAG MEASUREMENT

GEVEENS: Model/scale  $d = 6$ ;  $L_{DUL}$  (nominal) = 1.154 m;  $S_{MN}$  (nominal) = 0.42322 m<sup>2</sup>;  $S_M$  (actual) = .4111 m<sup>2</sup>;  $X_c = .7 L_{DUL} = .8079$  m

$VCG$  (above keel) = 0.2677 m; moment weight  $\rho = 1.5$  kg;  $V_s$  (nodes) = 4.7614  $V_m$ ;  $F_n = 0.29721 V_m$ ;  $C_L = L_m / \frac{1}{2} \rho S_{MN} V_m^2$ ;

Temperature water  $T = 19.6^\circ C$ ;  $\rho = 101.79$  kg sec<sup>2</sup>/m<sup>4</sup>;  $\nu = 1.0188 \times 10^{-6}$  m<sup>2</sup>/sec;  $1/b = 0.4336$  kg;  $L_{DUL} = 22.716$  ft;  $C_D = D_s / \frac{1}{2} \rho S_{MN} d^2 V_m^2$

MODEL NO: 127  
 TYPE: ANTIPOPE  
 EXP: v.s v.M.  
 DATUM: 15-11-73

Run no	Model speed $V_m$	$V_m^2$	Ship speed $V_s$	$V_s / \sqrt{L_{DUL}}$	$F_n$	$\beta$	Leeway angle $\phi$	Moment arm $E$	Lift fore $L_f$	Lift after $L_a$	Lift model $L_m = L_f + L_a$	$C_L$	Lift ship $L_s = L_m \cdot d$	Lift ship $L_s$	Drag $D'$	$\Delta D = 0.14 V_m$	Drag model $D_m = D \cdot d^2$	Drag ship $D_s$	Drag ship $D_s$	$C_D$	$L/D_s$	$C_L/\beta$
	m/sec	m <sup>2</sup> /sec <sup>2</sup>	nodes			degr.	degr.	mm	kg	kg	kg		kg	lbs	kg	kg	kg	kg	lbs	$\times 10^{-3}$		1/rad.
342	.420	.176	2.000	.420	.125	0	10	44.7	0	0	0	0	0	0	.020	.002	.018	1.734	3.8	2.120	0	-
343	.631	.398	3.004	.630	.188	"	"	44.7	.002	-.001	+.001	.012	.2	.4	.051	.006	.045	5.448	12.0	2.945	.040	$\infty$
344	.839	.704	3.995	.838	.249	"	"	43.8	.007	-.003	+.004	.026	.9	2.0	.099	.010	.089	12.301	27.1	3.760	.070	$\infty$
345	1.050	1.103	4.999	1.049	.312	"	"	41.6	.018	-.011	+.007	.029	1.5	3.3	.168	.015	.153	22.907	50.5	4.468	.066	$\infty$
346	1.260	1.588	5.999	1.259	.374	"	"	35.1	.033	+.009	+.042	.123	9.0	19.8	.285	.022	.263	42.962	94.7	5.820	.211	$\infty$
347	1.469	2.158	6.994	1.467	.437	"	"	34.7	.032	-.012	+.020	.047	4.3	9.5	.612	.030	.582	107.703	237.4	10.737	.040	$\infty$
348	1.679	2.819	7.994	1.677	.499	"	"	40.2	.043	-.058	-.015	-.025	-3.2	-7.1	1.033	.039	.994	192.051	423.4	14.657	.0169	$\infty$
349	1.260	1.588	5.999	1.259	.374	"	10	37.4	.031	-.004	+.027	.079	5.8	12.8	.291	.022	.269	44.258	97.6	5.996	.132	$\infty$
350	.420	.176	2.000	.420	.125	"	20	71.5	0	-.004	-.004	-.106	-.9	-2.0	.025	.002	.023	2.814	6.2	3.440	-.367	$\infty$
351	.630	.397	3.000	.629	.187	"	"	77.5	.004	-.009	-.005	-.058	-1.0	-2.2	.058	.006	.052	6.971	15.4	3.778	-.155	$\infty$
352	.842	.709	4.009	.841	.250	"	"	74.7	.012	-.011	+.001	.007	.2	.4	.105	.010	.095	13.555	29.9	4.113	.016	$\infty$
353	1.051	1.105	5.004	1.050	.312	"	"	72.5	.029	-.019	+.010	.042	2.2	4.9	.174	.015	.159	24.186	53.3	4.709	.089	$\infty$
354	1.261	1.590	6.004	1.260	.375	"	"	71.3	.052	-.014	+.066	.193	14.3	31.5	.298	.022	.276	45.751	100.9	6.190	.311	$\infty$
355	1.470	2.161	6.999	1.468	.437	"	20	66.4	.038	-.035	+.003	.006	.6	1.3	.604	.030	.574	105.954	233.6	10.548	.006	$\infty$
356	.421	.177	2.005	.421	.125	"	30	103.5	.003	-.008	-.005	-.131	-1	-2.2	.023	.002	.021	2.373	5.2	2.884	-.455	$\infty$
357	.631	.398	3.004	.630	.188	"	"	104.2	.005	-.015	-.010	-.117	-2.2	-4.9	.055	.006	.049	6.312	13.9	3.412	-.342	$\infty$
358	.844	.712	4.019	.843	.251	"	"	99.6	.016	-.010	+.006	.039	1.3	2.9	.103	.010	.093	13.095	28.9	3.957	.099	$\infty$
359	1.051	1.105	5.004	1.050	.312	"	"	96.8	.032	-.018	+.014	.059	3.0	6.6	.167	.015	.152	22.674	50.0	4.415	.133	$\infty$
360	1.262	1.593	6.009	1.261	.375	"	"	87.7	.044	+.010	.054	.157	11.7	25.8	.289	.022	.267	43.789	96.5	5.914	.266	$\infty$
361	1.470	2.161	6.999	1.468	.437	"	"	107.1	.003	-.084	-.081	-.174	-17.5	-38.6	.620	.030	.590	109.410	241.2	10.892	-.180	$\infty$
362	1.260	1.588	5.999	1.259	.374	0	30	88.3	.042	+.005	+.047	.137	10.2	22.5	.295	.022	.273	45.122	99.5	6.113	.225	$\infty$

11-55-8204



AARD v.d. PROEF: LIFT AND DRAG MEASUREMENT

GEVEGENS: Modelscale  $\alpha = 6$ ;  $L_{pvl}$  (nominal) = 1.154 m;  $S_{m1}$  (nominal) = 0.42322 m<sup>2</sup>;  $S_m$  (actual) = .4111 m<sup>2</sup>;  $X_c = .7 L_{pvl} = .8079$  m  
 VCG (above keel) = 0.2677 m; moment weight  $p = 1.5$  kg;  $V_3$  (knots) = 4.7614  $V_m$ ;  $F_n = 0.2971 V_m$ ;  $C_L = L_m / \frac{1}{2} \rho S_m V_m^2$ ;  
 Temperature water  $T = 19.9^\circ C$ ;  $\rho = 101.79$  kg/m<sup>3</sup>;  $\nu = 1.0188 \cdot 10^{-6}$  m<sup>2</sup>/sec;  $\tau = 16 = 0.456$  kg;  $L_{oul} = 22.716$  ft;  $C_D = D_s / \frac{1}{2} \rho S_m V_m^2$

MODEL NO.: 127  
 TYPE: ANTILOPE  
 EXP.: JS JH  
 DATUM: 23-11-73

Run no	Model Speed $V_m$	$V_m^2$	Ship Speed $V_s$	$V_s^2$	$V_s / V_{low}$	$F_n$	$\beta$	Leeway angle $\phi$	Moment arm $c$	Lift fore $L_f$	Lift after $L_a$	Lift model $L_m = L_f + L_a$	$C_L$	Lift ship $L_s = L_m \cdot \alpha$	Lift ship $L_s$	Drag $D'$	$\Delta D = .04 V_m^2$	Drag model $D_m = D' \cdot \alpha^2$	Drag ship $D_s$	Drag ship $D_s$	$C_D$	$L/D_s$	$C_L / \beta$
	m/sec	m <sup>2</sup> /sec	knots			degr.	degr.	mm	kg	kg	kg	$\cdot 10^{-2}$	kg	lbs	kg	kg	kg	kg	lbs	$\cdot 10^{-3}$		/rad	
363	.421	.177	2.005	.421	.125	2.65	0	8.5	.036	.021	.057	1.495	12.3	27.1	.026	.002	.024	3.021	6.7	3.672	4.072	.3232	
364	.631	.398	3.004	.630	.188	"	1.0	11.4	.074	.042	.116	1.353	25.1	55.3	.059	.006	.053	7.176	15.8	3.879	3.488	.2926	
365	.843	.711	4.014	.842	.251	"	1.0	27.7	.149	.083	.232	1.515	50.1	110.4	.109	.010	.099	14.405	31.8	4.359	3.475	.2275	
366	1.050	1.103	4.999	1.049	.312	"	3.0	43.5	.254	.123	.377	1.587	81.4	179.5	.181	.015	.166	25.715	56.7	5.016	3.164	.2431	
367	1.260	1.588	5.999	1.259	.374	"	5.0	66.4	.421	.204	.625	1.827	135.0	297.6	.303	.022	.281	46.850	103.3	6.347	2.979	.3951	
368	.421	.177	2.005	.421	.125	"	2.0	-68.2	.031	.012	.043	1.128	9.3	20.5	.022	.002	.020	2.157	4.8	2.622	4.302	.2439	
369	.632	.399	3.009	.631	.188	"	20.3	-53.9	.075	.029	.104	1.210	22.5	49.6	.053	.006	.047	5.868	12.9	3.164	3.825	.2616	
370	.842	.709	4.009	.841	.250	"	20.8	-44.0	.145	.053	.198	1.297	42.8	94.4	.101	.010	.091	12.691	28.0	3.851	3.367	.2803	
371	1.053	1.109	5.014	1.052	.313	"	20.5	-21.7	.241	.099	.340	1.423	73.4	161.8	.168	.016	.152	22.644	49.9	4.392	3.241	.3077	
372	1.262	1.593	6.009	1.261	.375	"	22.8	+14.3	.376	.188	.564	1.644	121.8	268.5	.308	.022	.286	47.892	105.6	6.468	2.541	.3554	
373	1.260	1.588	5.999	1.259	.374	2.65	5.0	60.5	.397	.194	.591	1.720	127.7	281.5	.306	.022	.284	47.498	104.7	6.435	2.685	.3736	
374	.632	.399	3.009	.631	.188	5.45	21.5	-34.0	.182	.097	.279	3.246	60.3	132.9	.073	.006	.067	10.188	22.5	5.493	5.910	.2884	
375	.421	.177	2.005	.421	.125	"	20.5	-58.9	.081	.044	.125	3.279	27.0	59.5	.036	.002	.034	5.181	11.4	6.297	5.206	.2912	
376	.842	.709	4.009	.841	.250	"	23.5	+1.2	.336	.177	.513	3.359	110.8	244.3	.140	.010	.130	21.115	46.5	6.407	5.243	.2984	
377	1.051	1.105	5.004	1.050	.312	"	25.5	62.8	.568	.311	.879	3.693	189.9	418.7	.239	.015	.224	38.228	84.3	7.442	4.962	.3281	
378	.421	.177	2.005	.421	.125	"	10.0	-21.4	.059	.059	.158	4.144	34.1	75.2	.041	.002	.039	6.261	13.7	7.610	5.446	.3681	
379	.630	.397	3.000	.629	.187	"	11.3	+6.0	.219	.128	.347	4.058	75.0	165.3	.088	.006	.082	13.451	29.7	7.289	5.567	.3605	
380	.842	.709	4.009	.841	.250	"	13.0	29.6	.364	.203	.567	3.713	122.5	270.1	.152	.010	.142	23.707	52.3	7.194	5.161	.3298	
381	1.051	1.105	5.004	1.050	.312	"	15.8	84.7	.620	.336	.956	4.017	206.5	455.2	.243	.015	.228	39.050	86.2	7.611	5.278	.3570	
382	1.261	1.590	6.004	1.260	.375	6.45	19.6	155.4	.898	.523	1.421	4.149	305.9	676.6	.403	.022	.381	68.431	150.9	9.259	4.481	.3686	
383	.421	.177	2.005	.421	.125	0	9.0	-40.9	-.002	-.007	-.009	-.236	-1.9	-4.2	.019	.002	.017	1.509	3.3	1.834	-1.287	$\infty$	
384	.630	.397	3.000	.629	.187	"	9.0	-40.8	+.003	-.005	-.002	-.023	-.4	-.9	.051	.006	.045	5.459	12.0	2.958	-.079	$\infty$	
385	.842	.709	4.009	.841	.250	"	9.2	-40.1	.018	-.005	+.013	-.085	2.8	6.2	.088	.010	.078	9.883	21.8	2.999	.284	$\infty$	
386	1.050	1.103	4.999	1.049	.312	"	9.3	-39.7	.017	-.010	.007	-.029	1.5	3.3	.168	.015	.153	22.907	50.5	4.468	.066	$\infty$	
387	1.260	1.588	5.999	1.259	.374	"	9.5	-36.2	.023	-.001	.022	-.064	4.8	10.6	.281	.022	.259	42.038	92.8	5.703	.113	$\infty$	
388	.421	.177	2.005	.421	.125	"	9.0	-40.9	.004	-.002	.002	.052	.4	.9	.022	.002	.020	2.157	4.8	2.622	.200	$\infty$	
389	.631	.398	3.004	.630	.188	0	9.0	-40.8	.005	-.004	.001	.0117	.2	.4	.054	.006	.048	6.096	13.4	3.295	.035	$\infty$	
390	.840	.706	4.000	.839	.250	0	9.2	-40.8	.012	-.006	.006	.039	1.3	2.9	.105	.010	.095	13.583	29.9	4.139	.095	$\infty$	
391	1.050	1.103	4.999	1.049	.312	2.65	20.5	-18.9	.254	.103	.357	1.503	77.1	170.0	.178	.015	.163	25.067	55.3	4.889	3.073	.3249	
392	1.258	1.583	5.990	1.257	.375	2.65	50	+59.7	.350	.190	.580	1.701	125.3	276.2	.303	.022	.281	46.887	105.4	6.372	2.669	.3678	
393	.631	.398	3.004	.630	.188	6.45	11.3	2.7	.218	.122	.340	3.966	73.4	161.8	.081	.006	.075	11.928	26.3	6.448	6.151	.3523	

APPENDIX II

FIGURES

# ANTIOPE

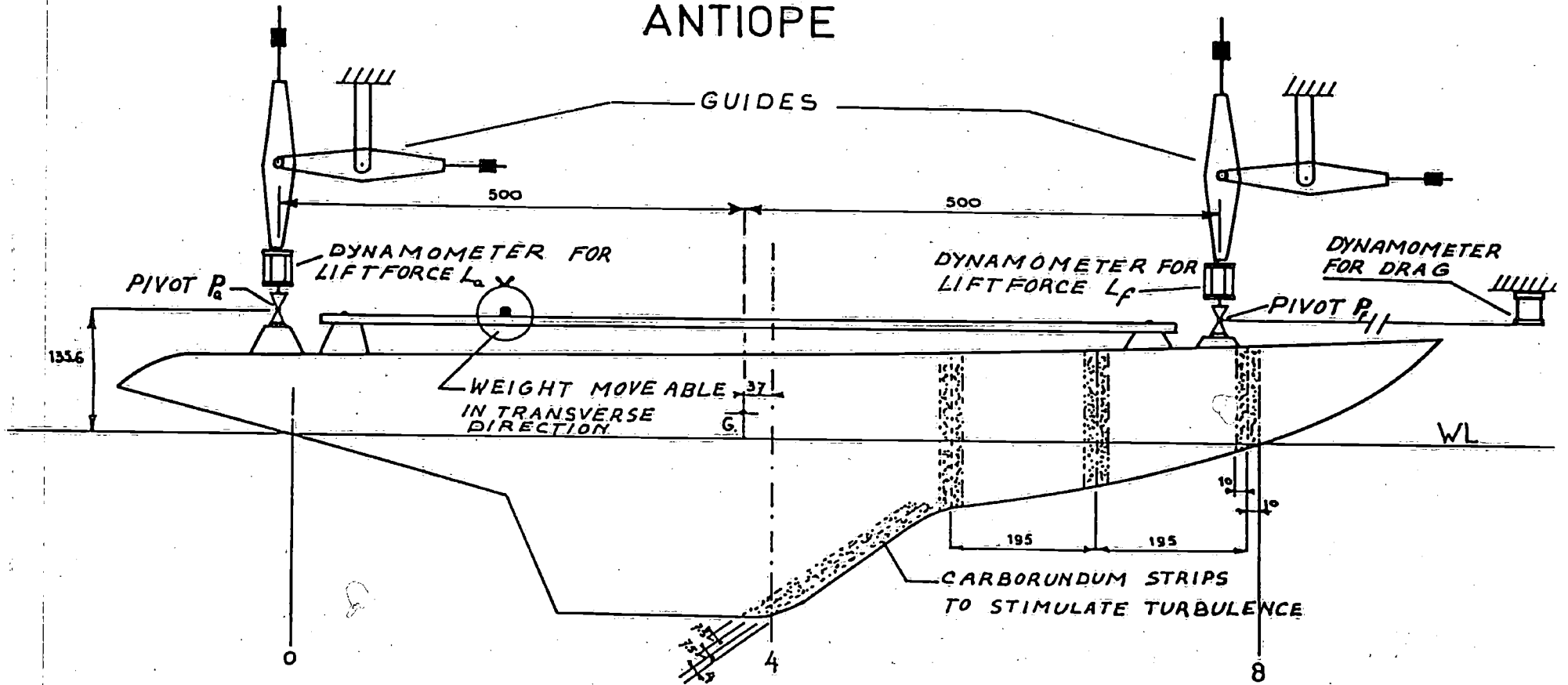


FIGURE 1.

# ANTIOPE

$\beta$  = YAW ANGLE POSITIVE FOR BOW TO STARBOARD  
 $\varphi$  = HEEL ANGLE POSITIVE FOR STARBOARD SIDE UP

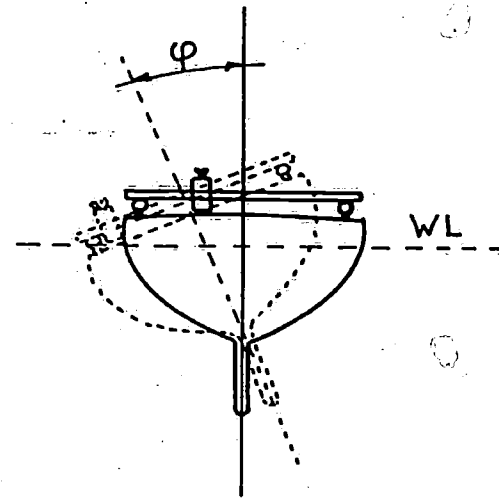
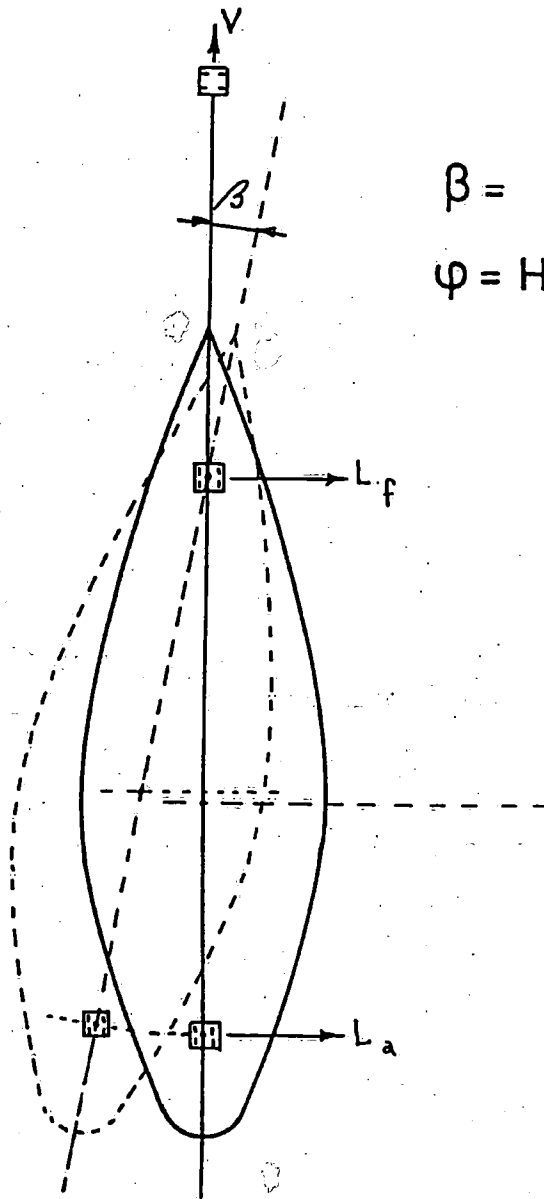


FIGURE 2.

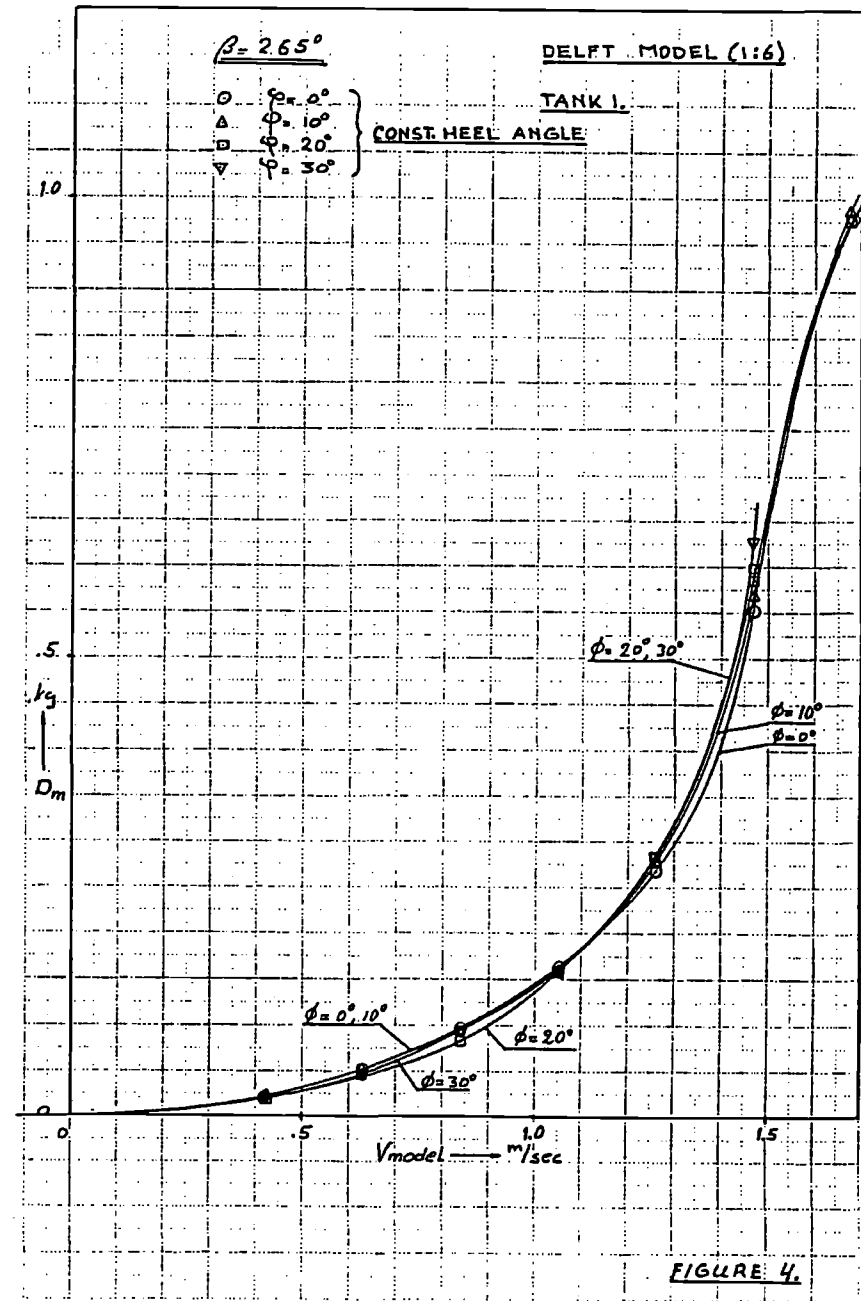
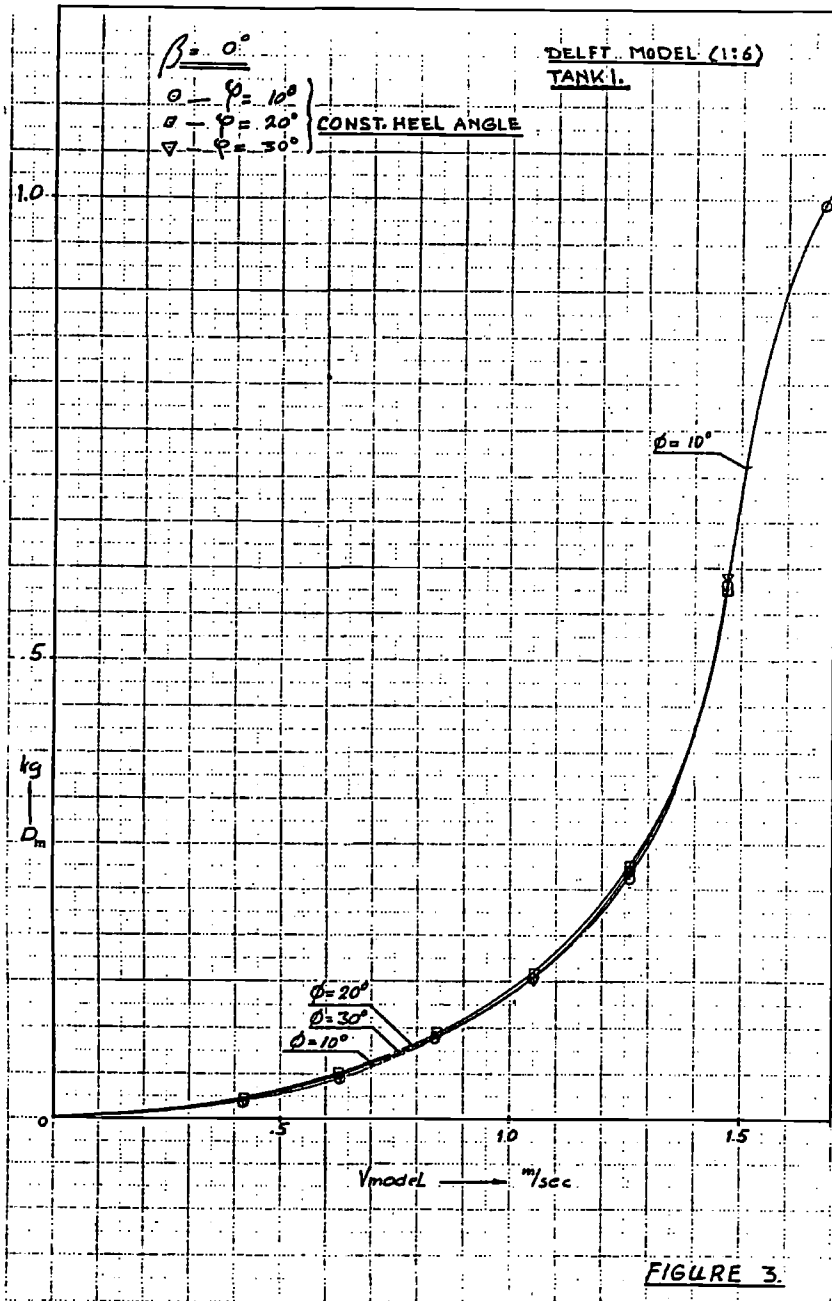
Figures 3 - 15

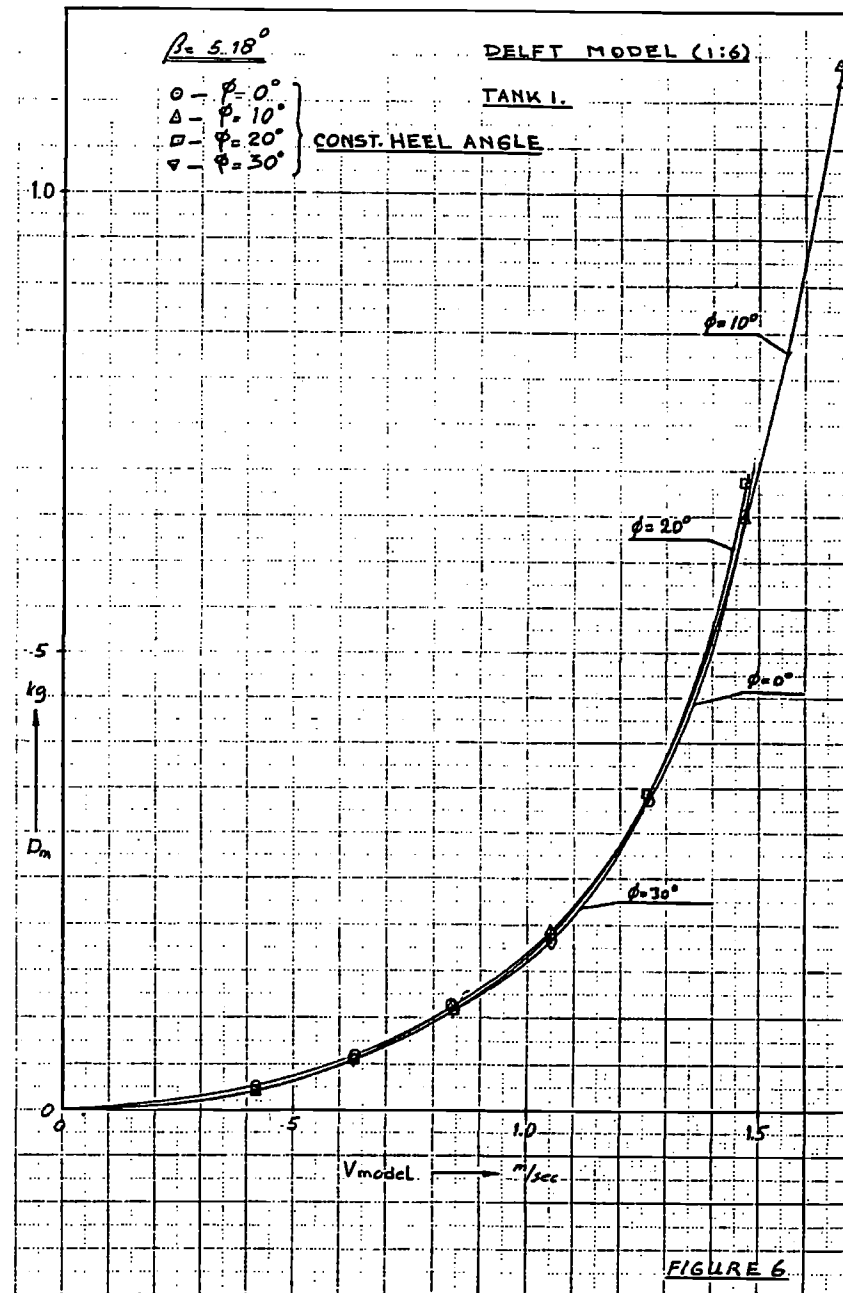
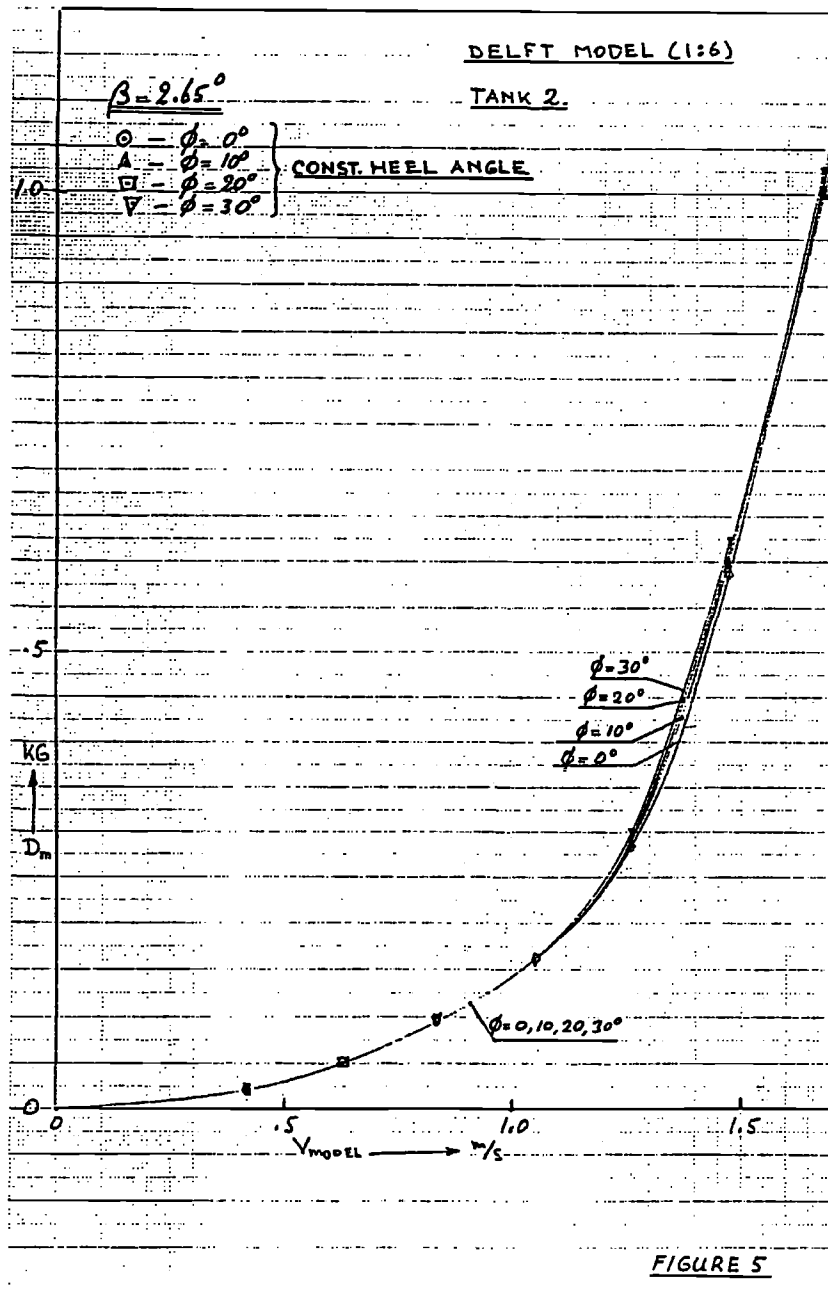
Constant Heel Angles

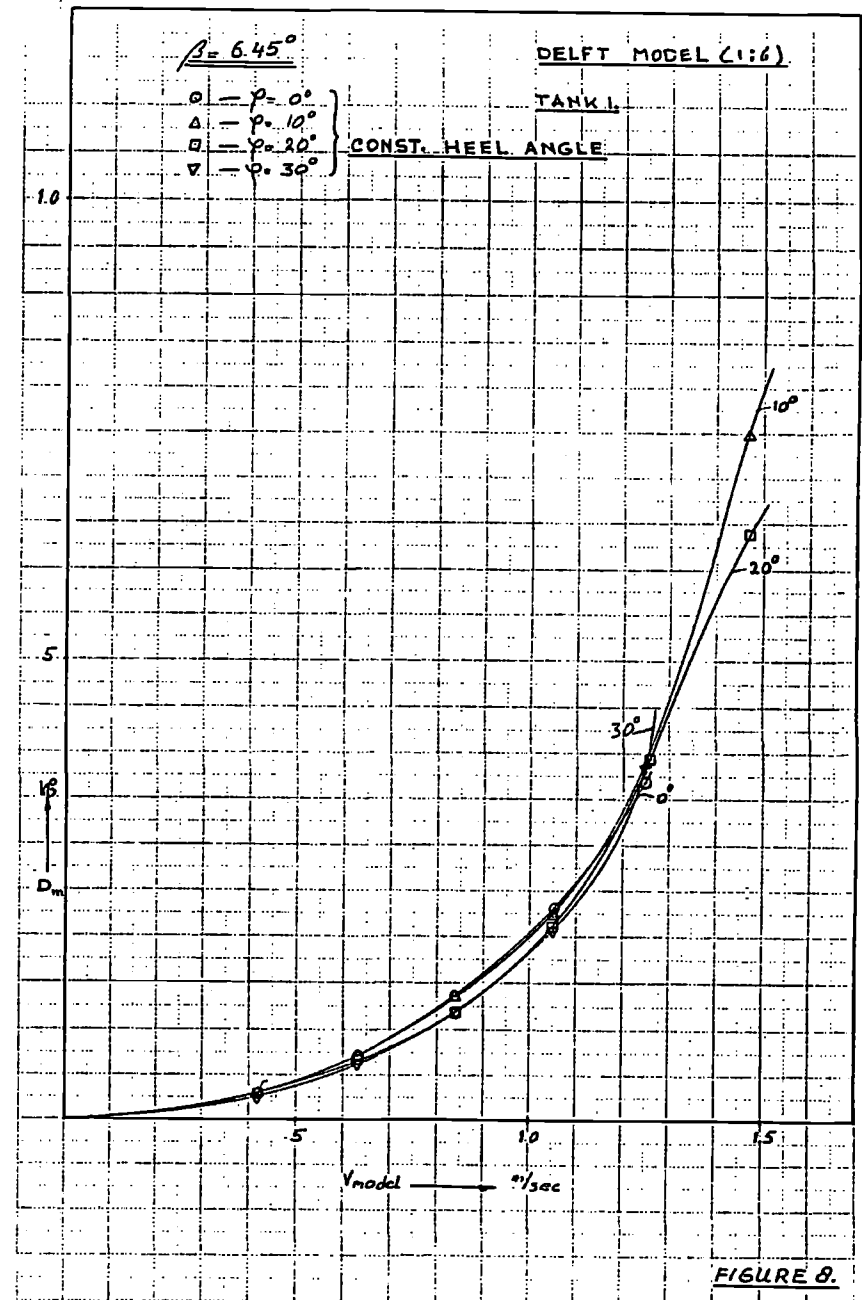
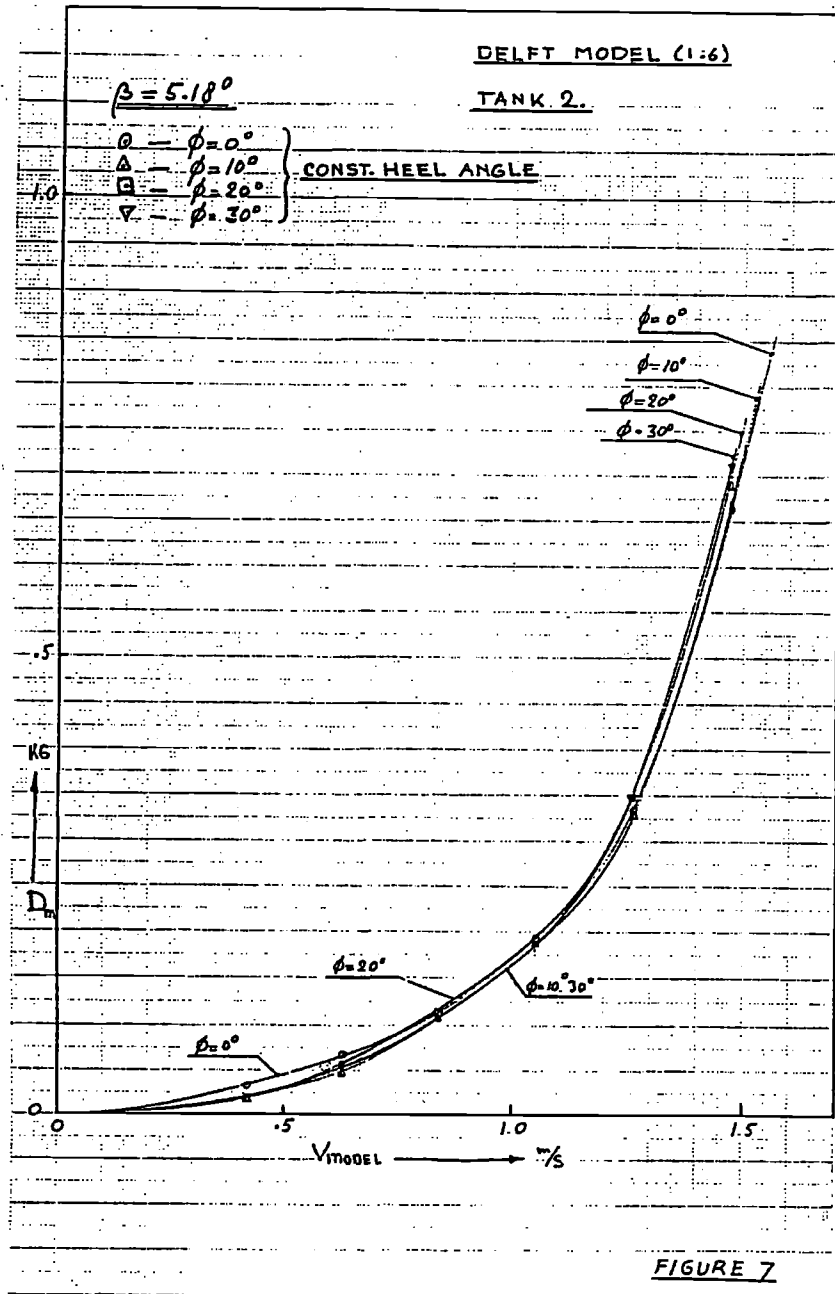
Model Drag versus Speed

Model Lift versus Speed

Tank 1 and Tank 2









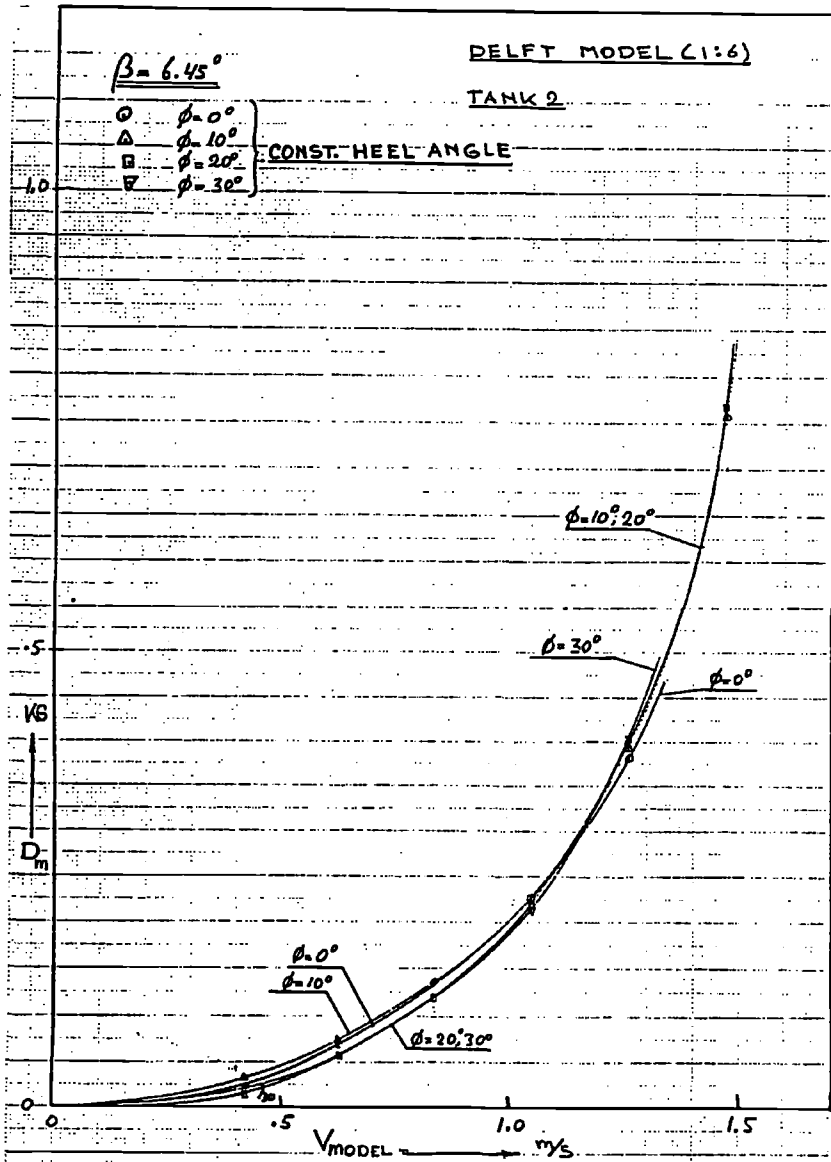


FIGURE 9

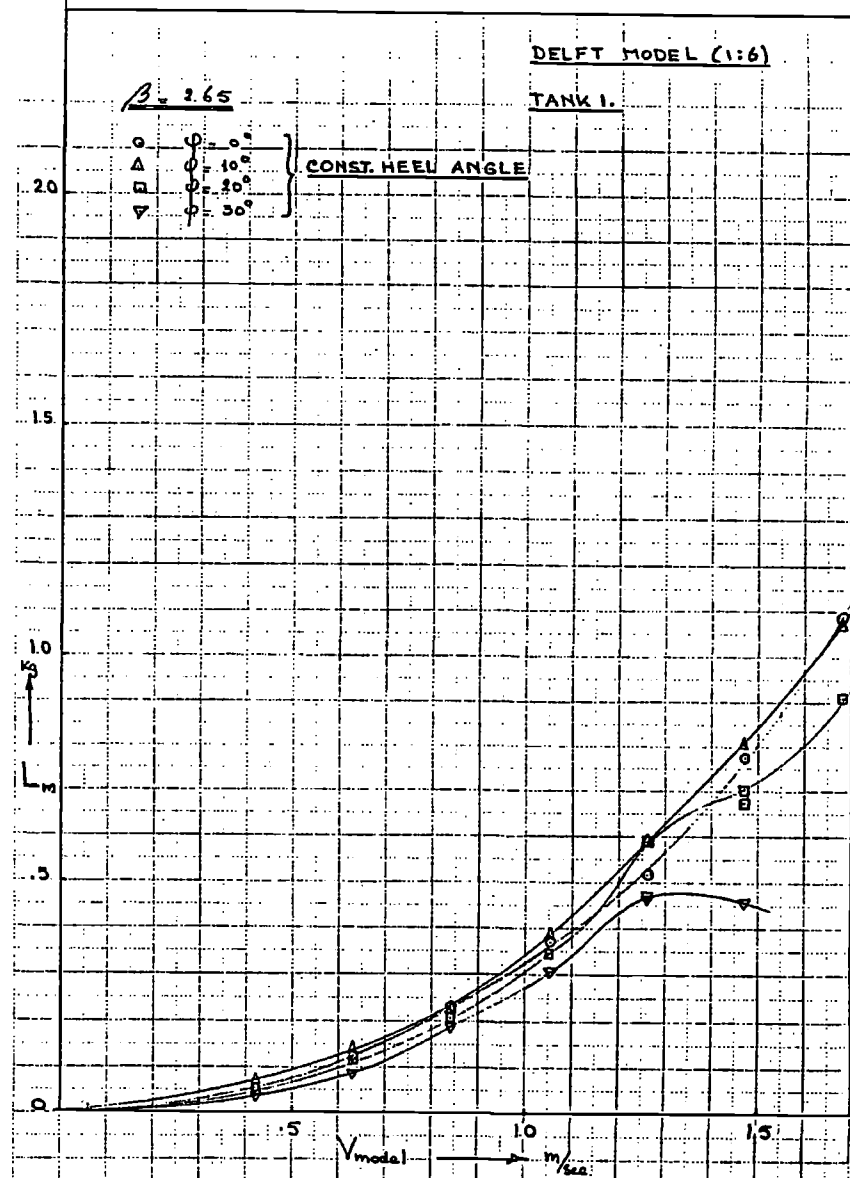


FIGURE 10

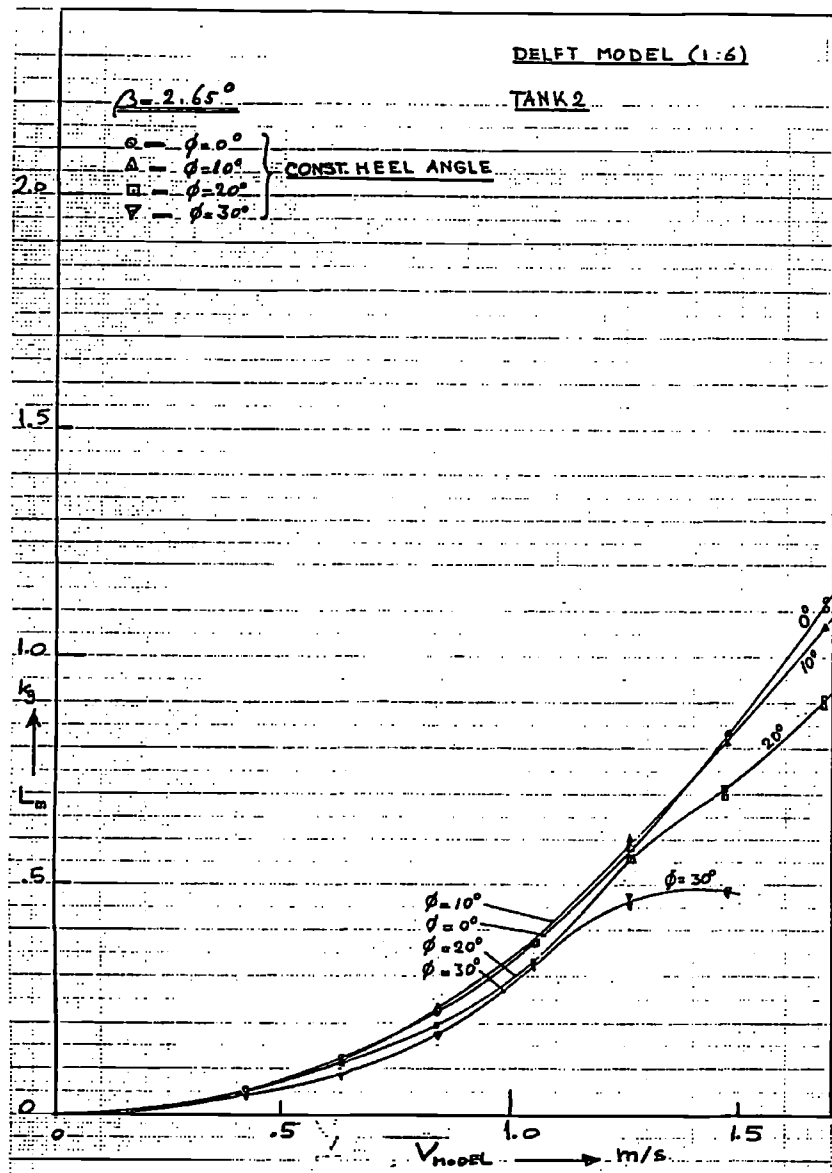


FIGURE 11

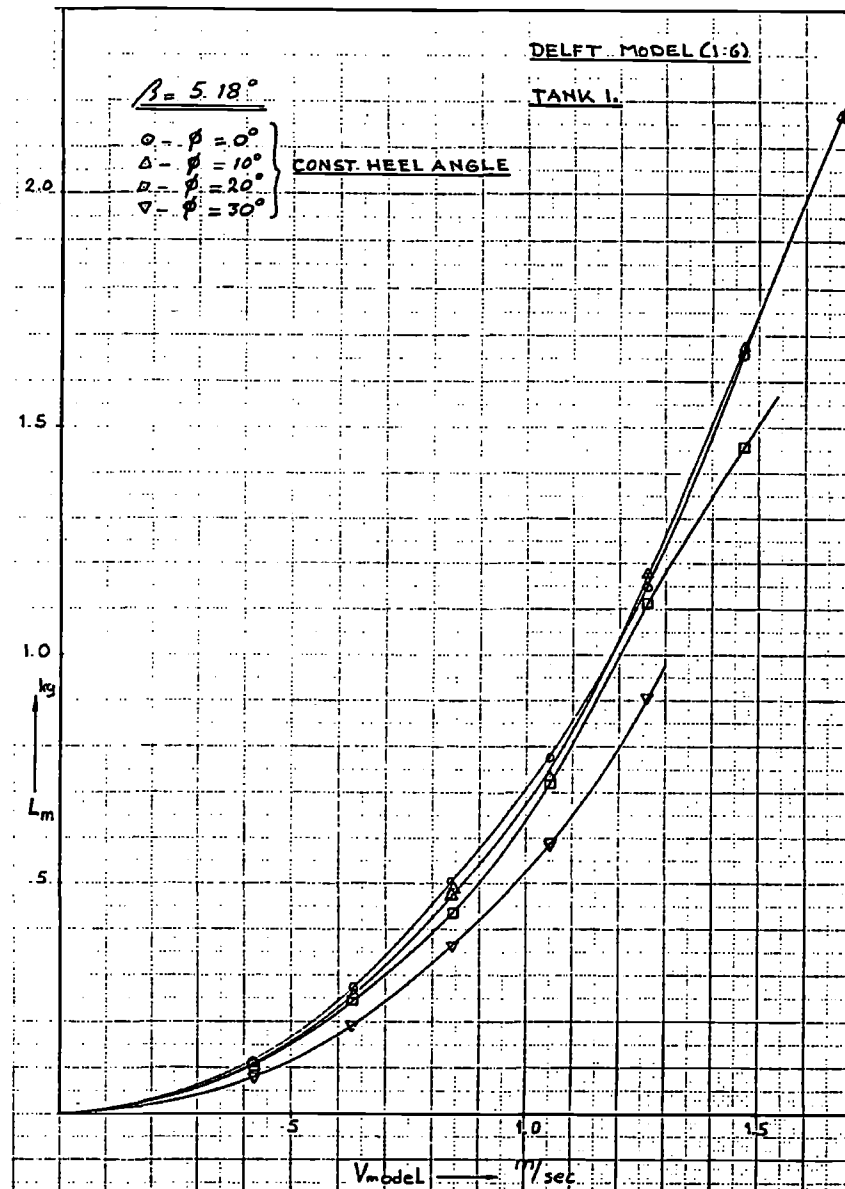


FIGURE 12

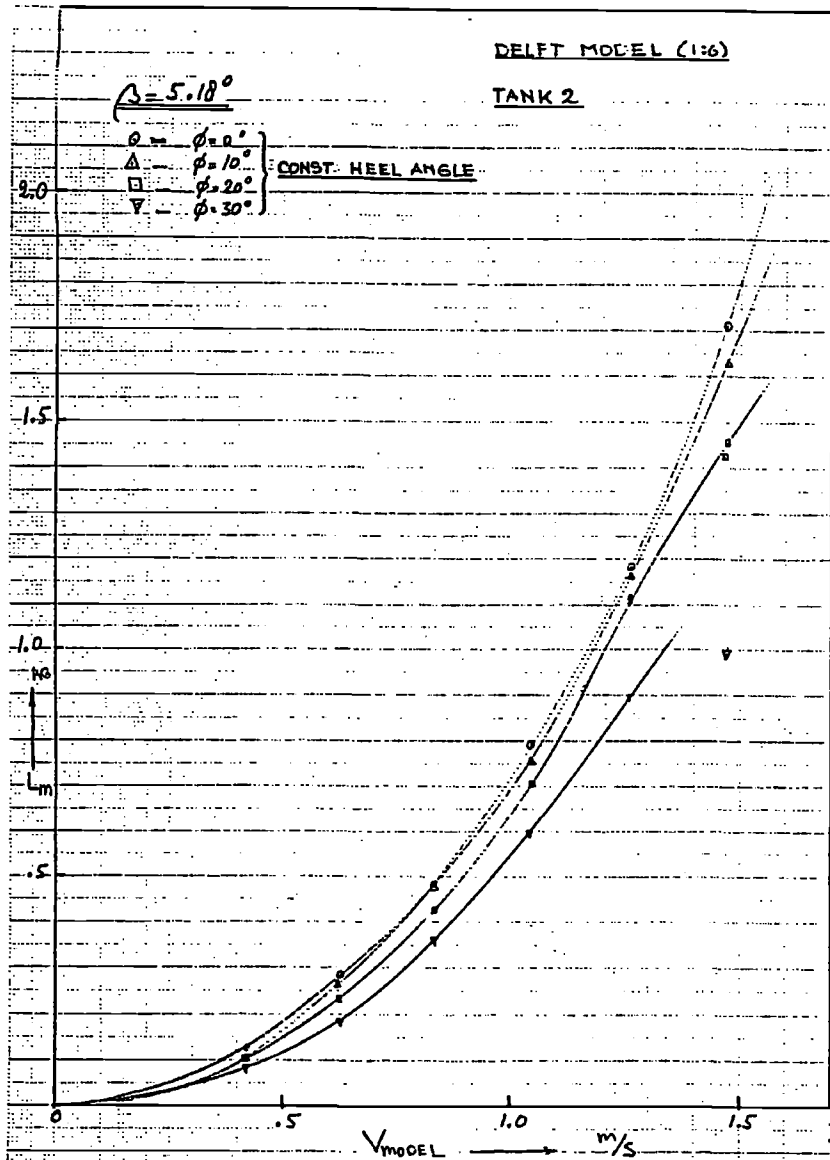


FIGURE 13.

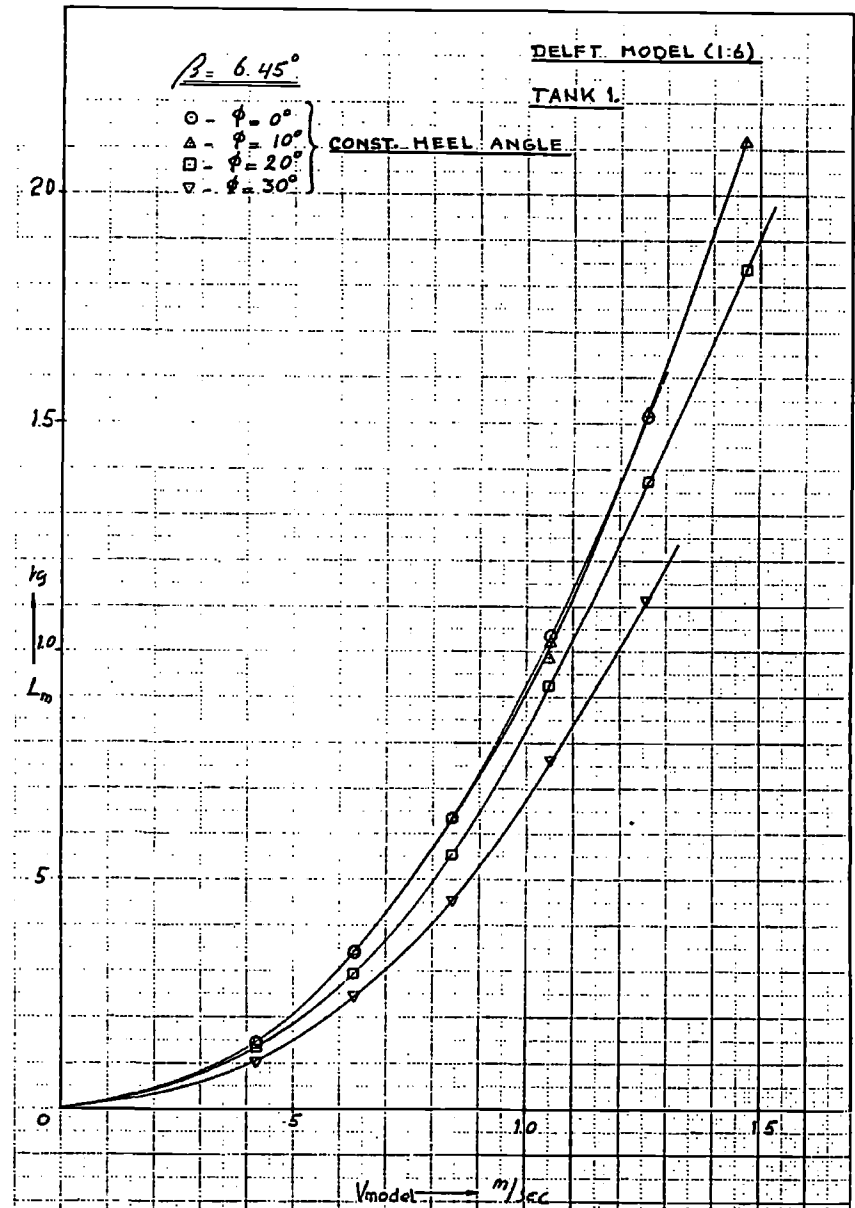


FIGURE 14.

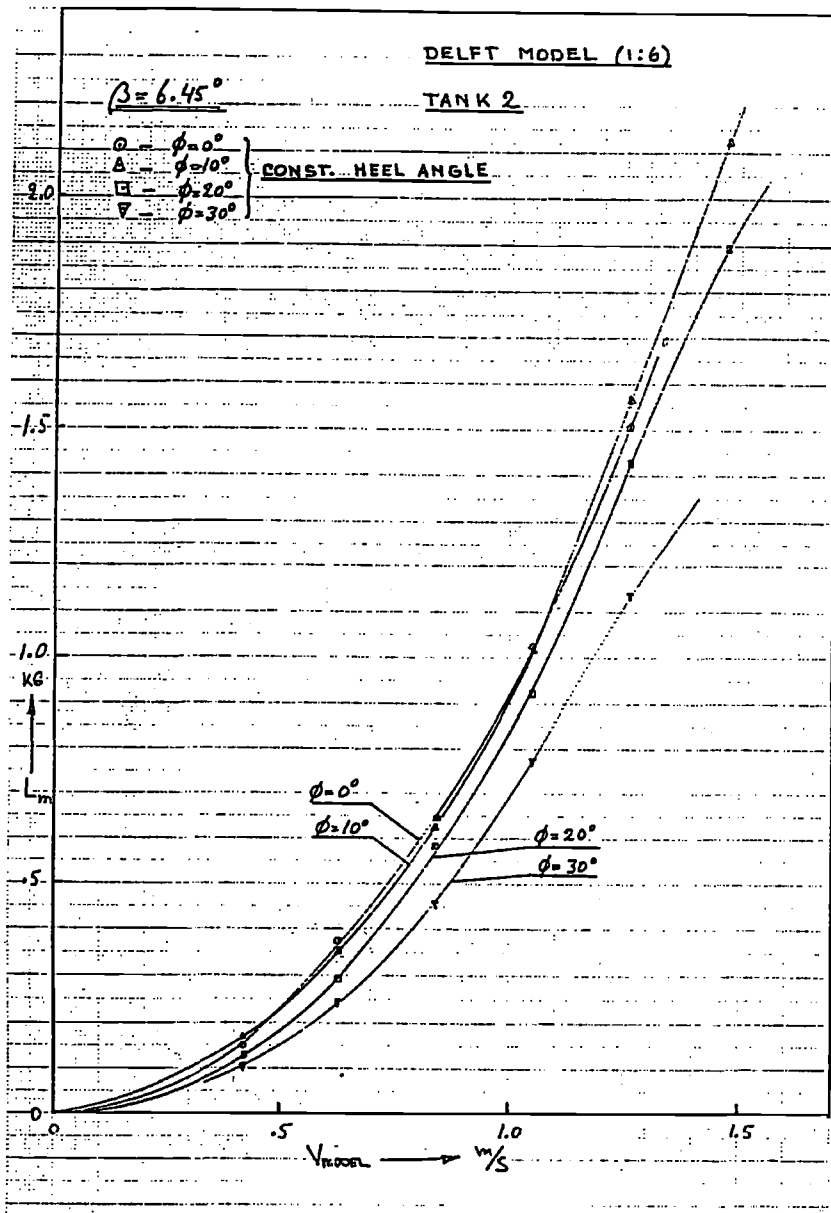


FIGURE 15.

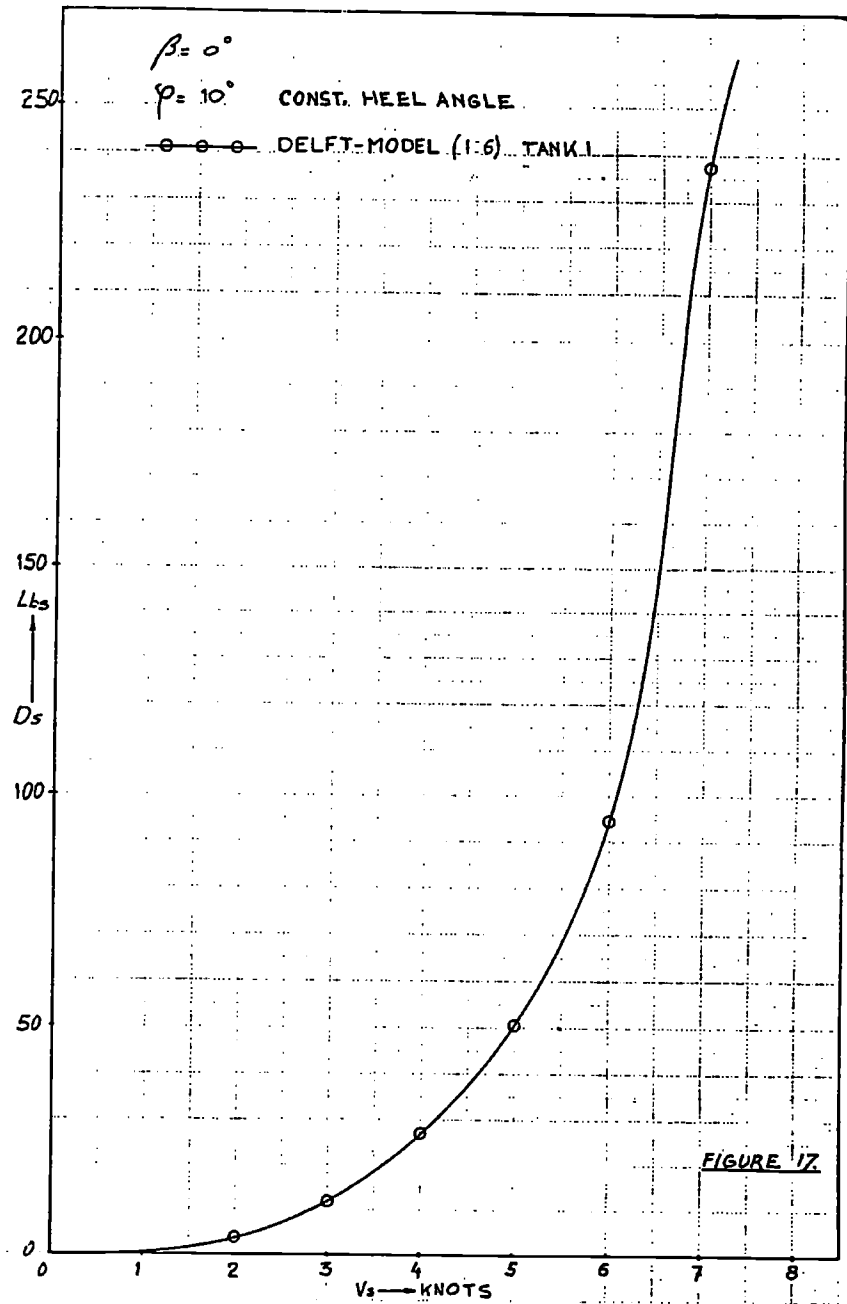
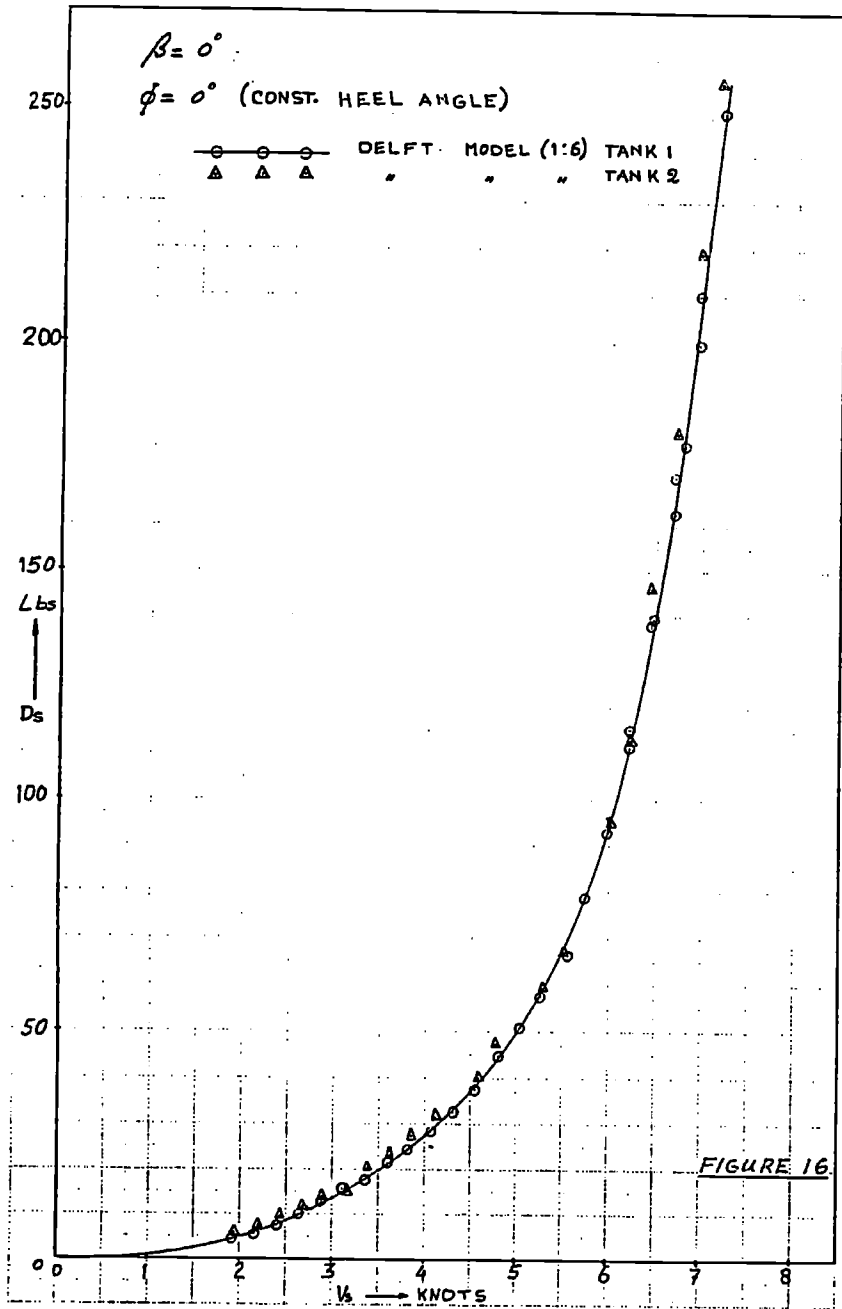
Figures 16 - 45

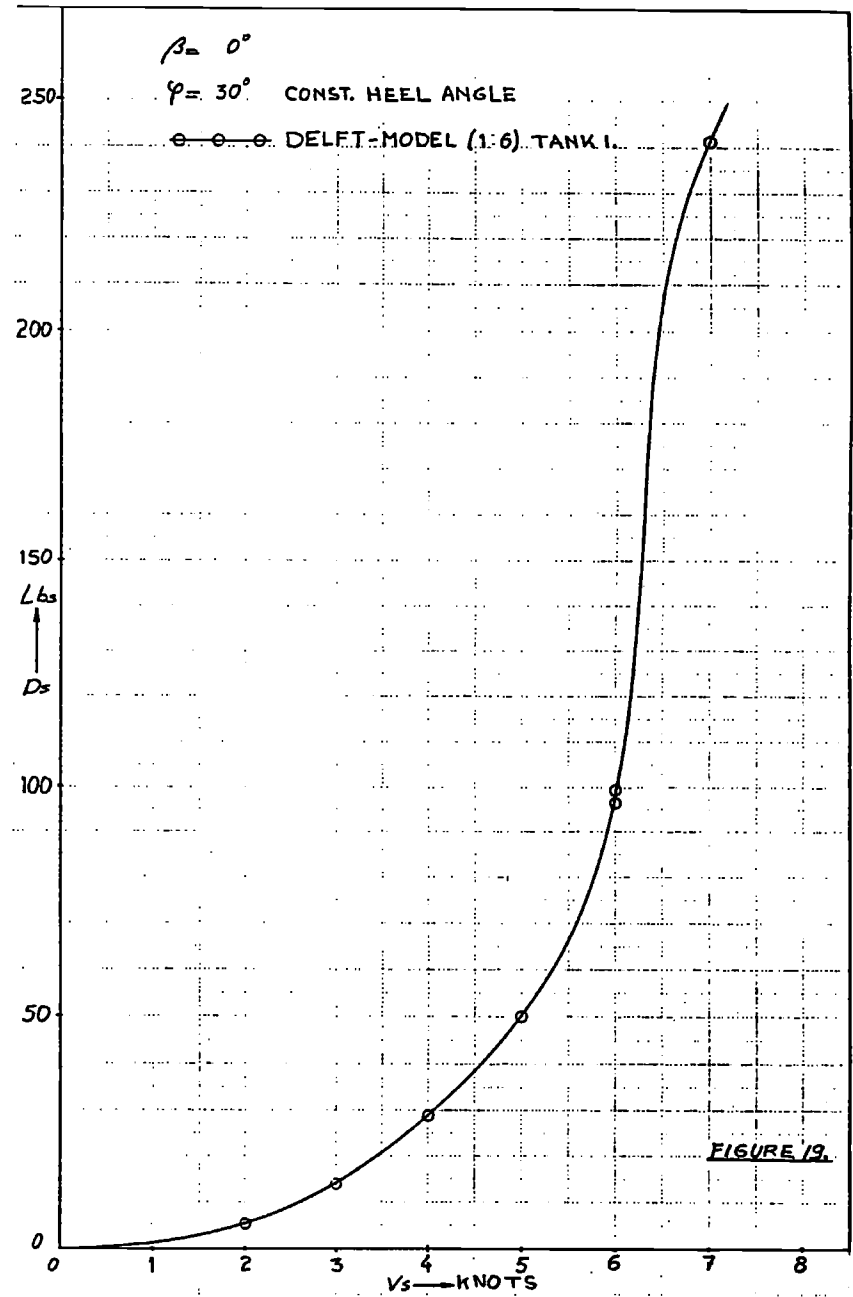
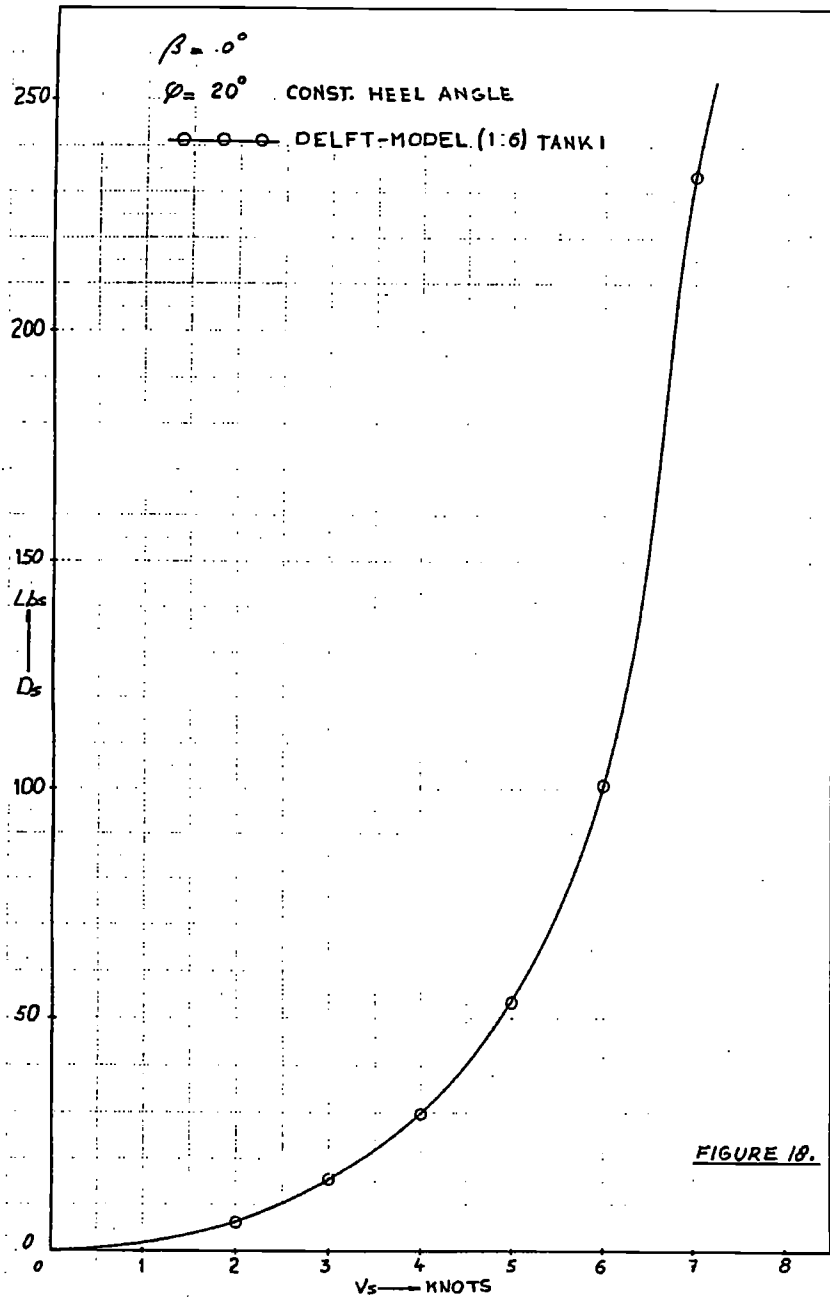
Constant Heel Angles

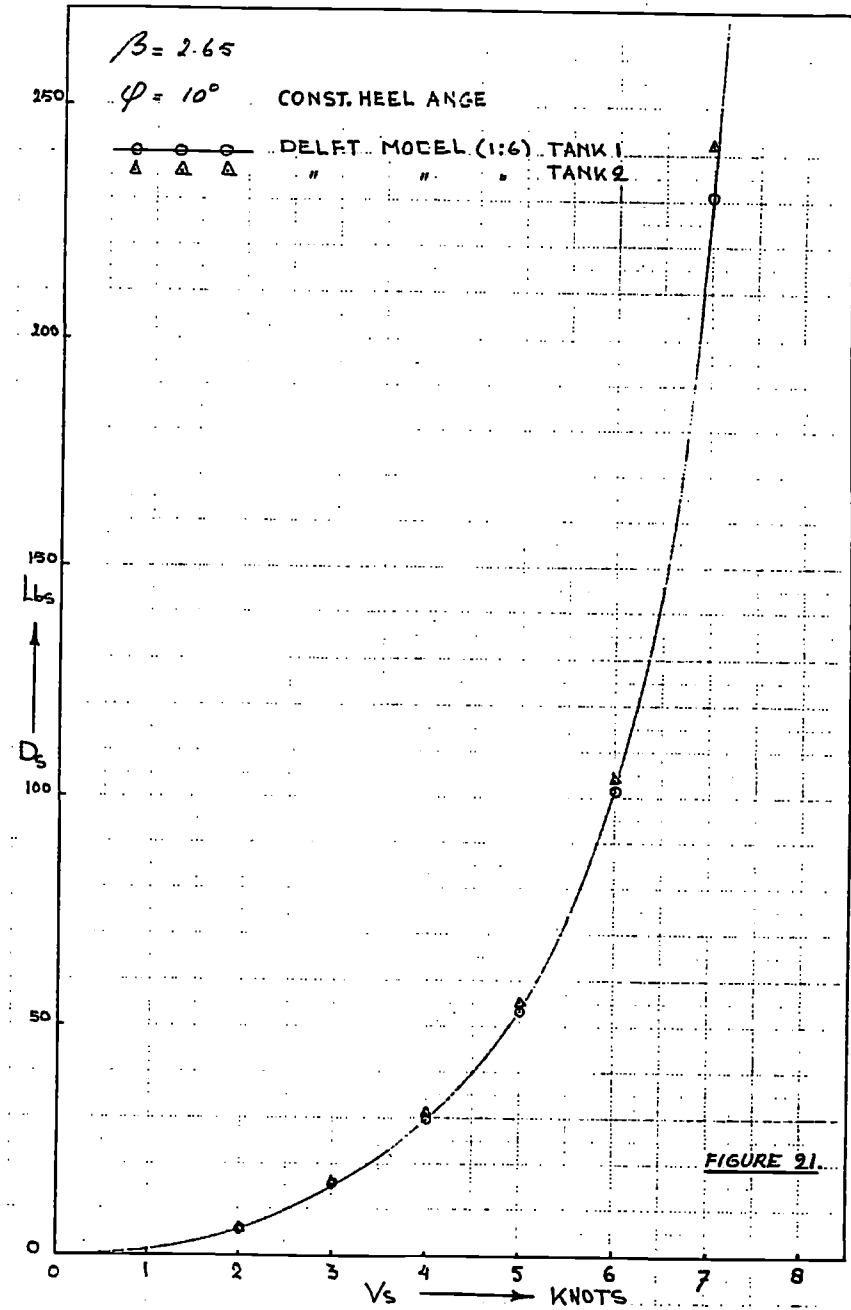
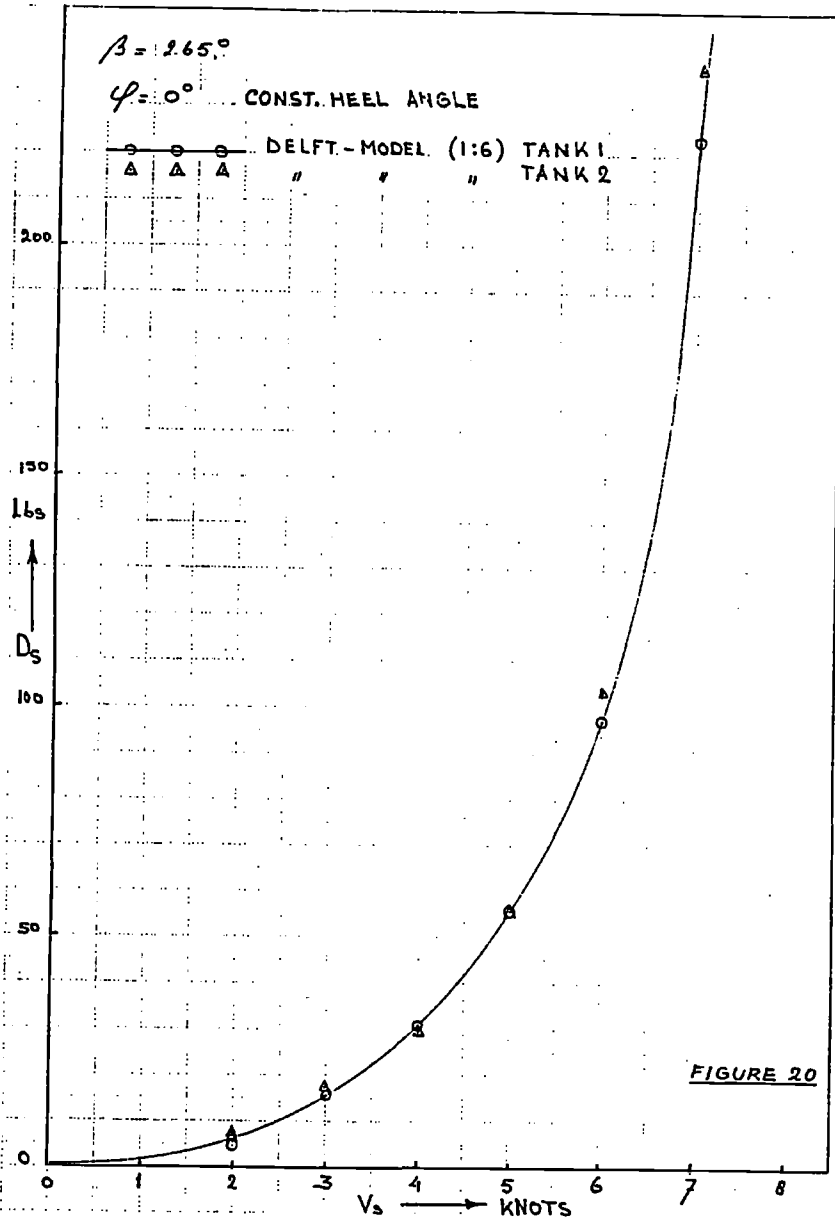
Ship Drag versus Speed

Ship Lift versus Speed

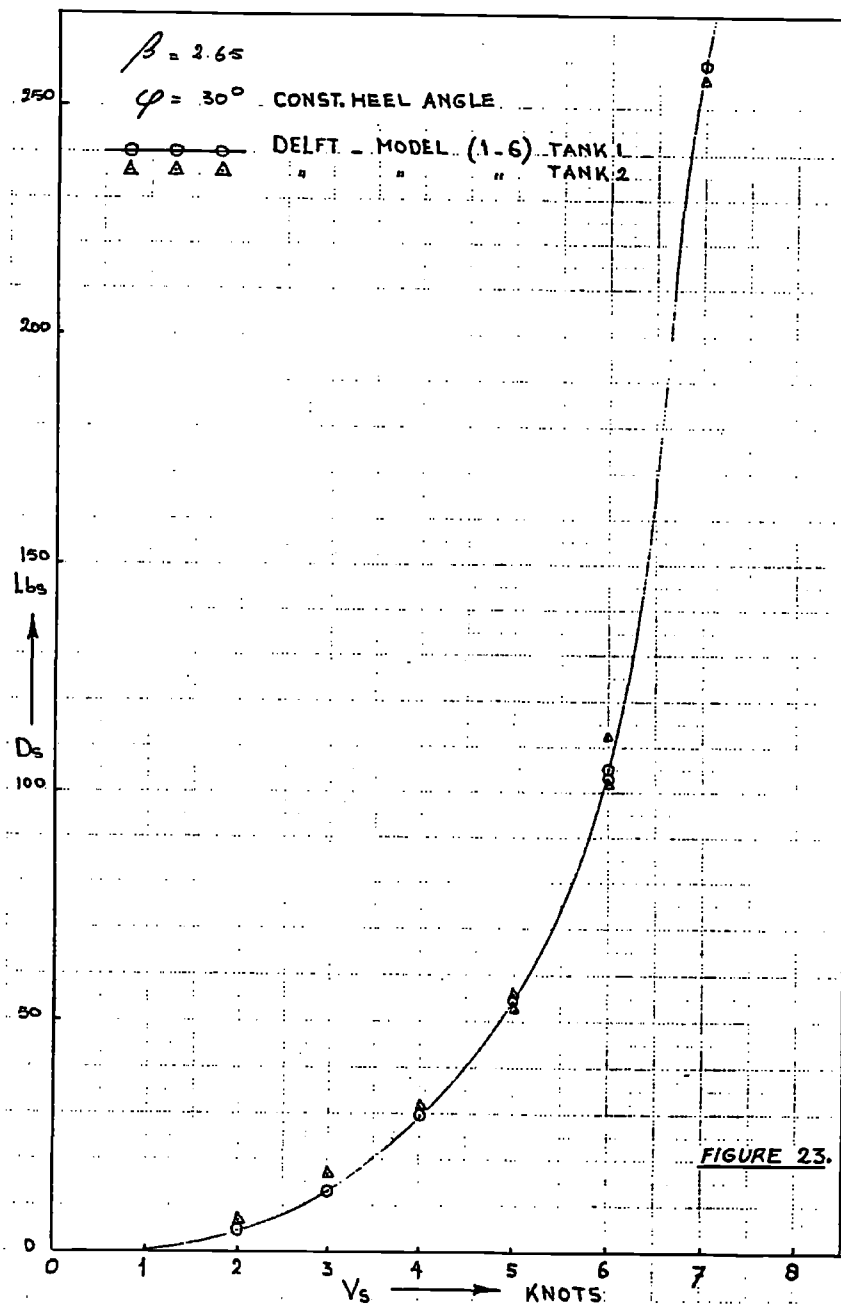
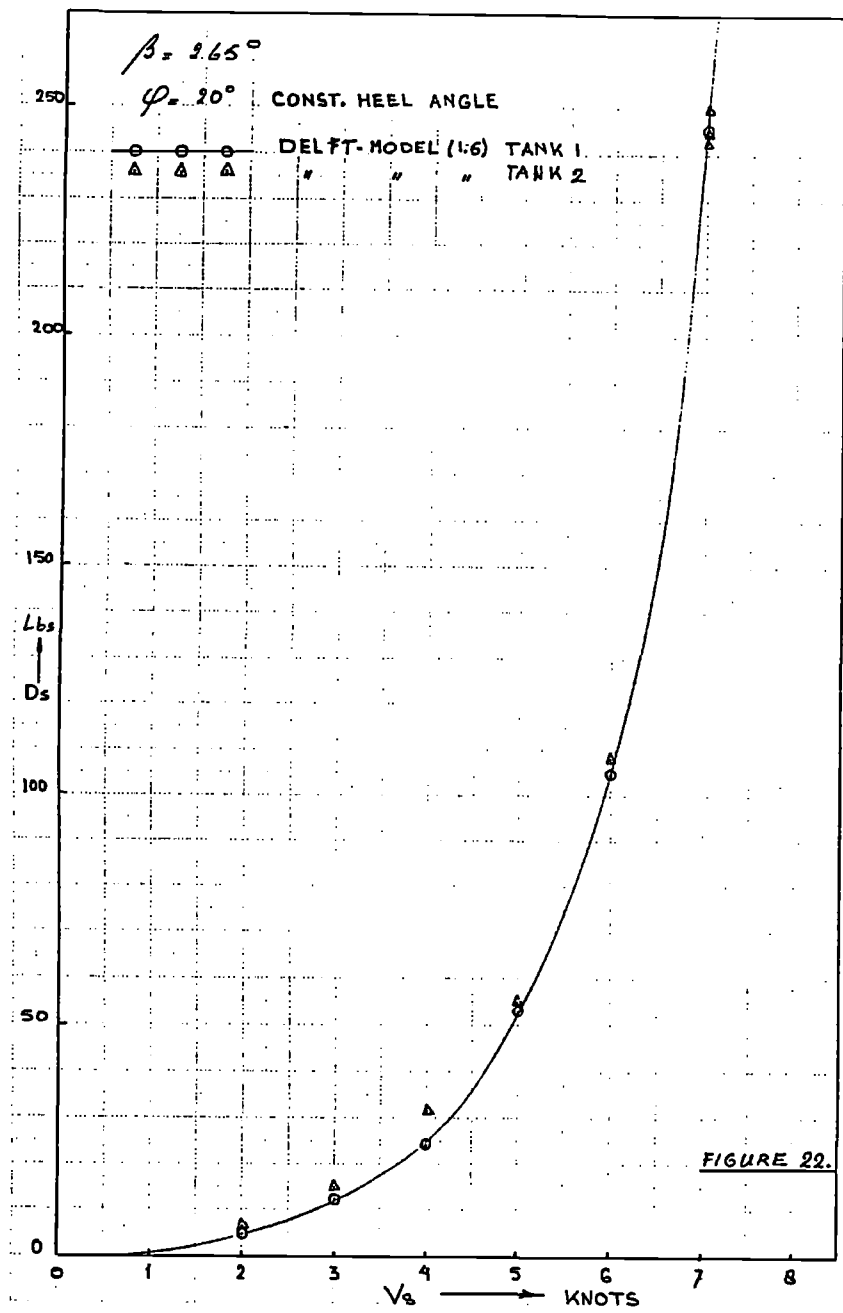
Tank 1 and Tank 2

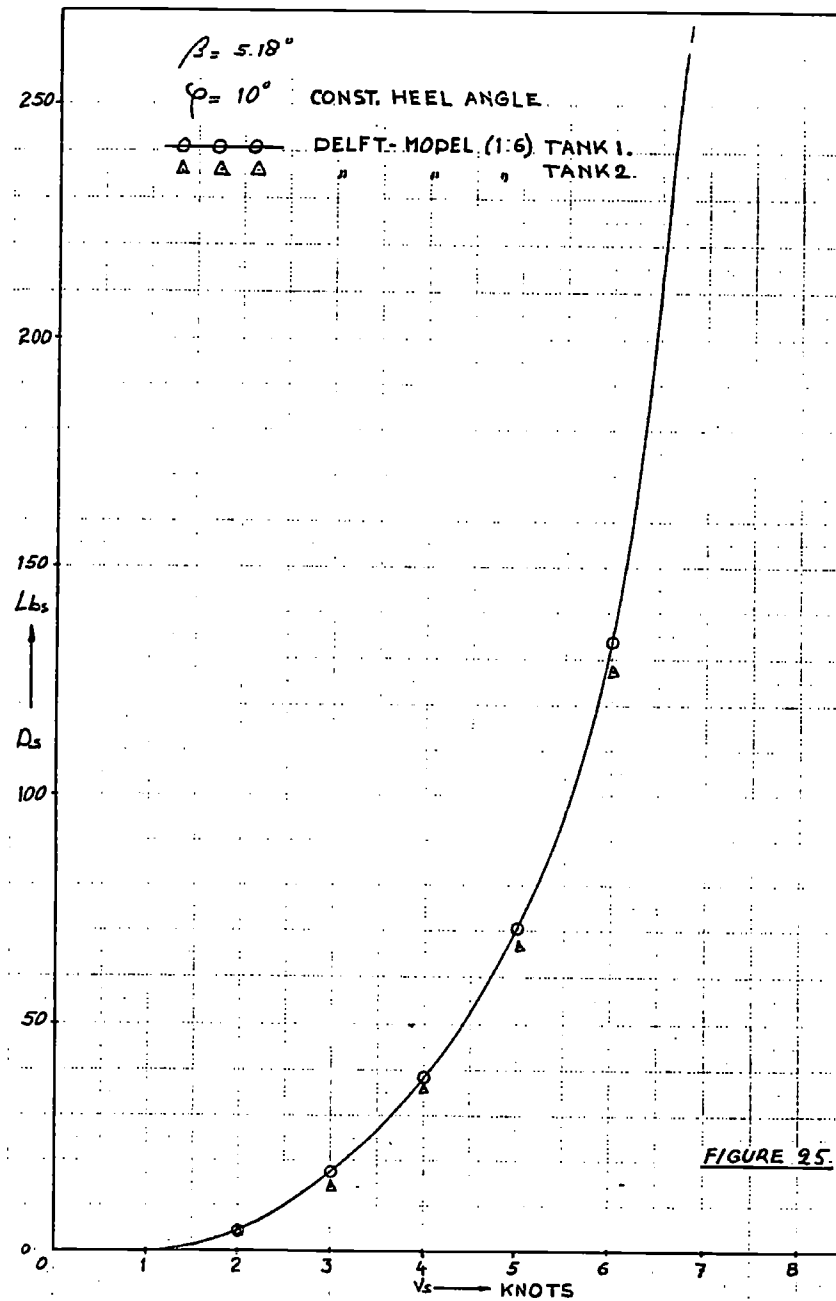
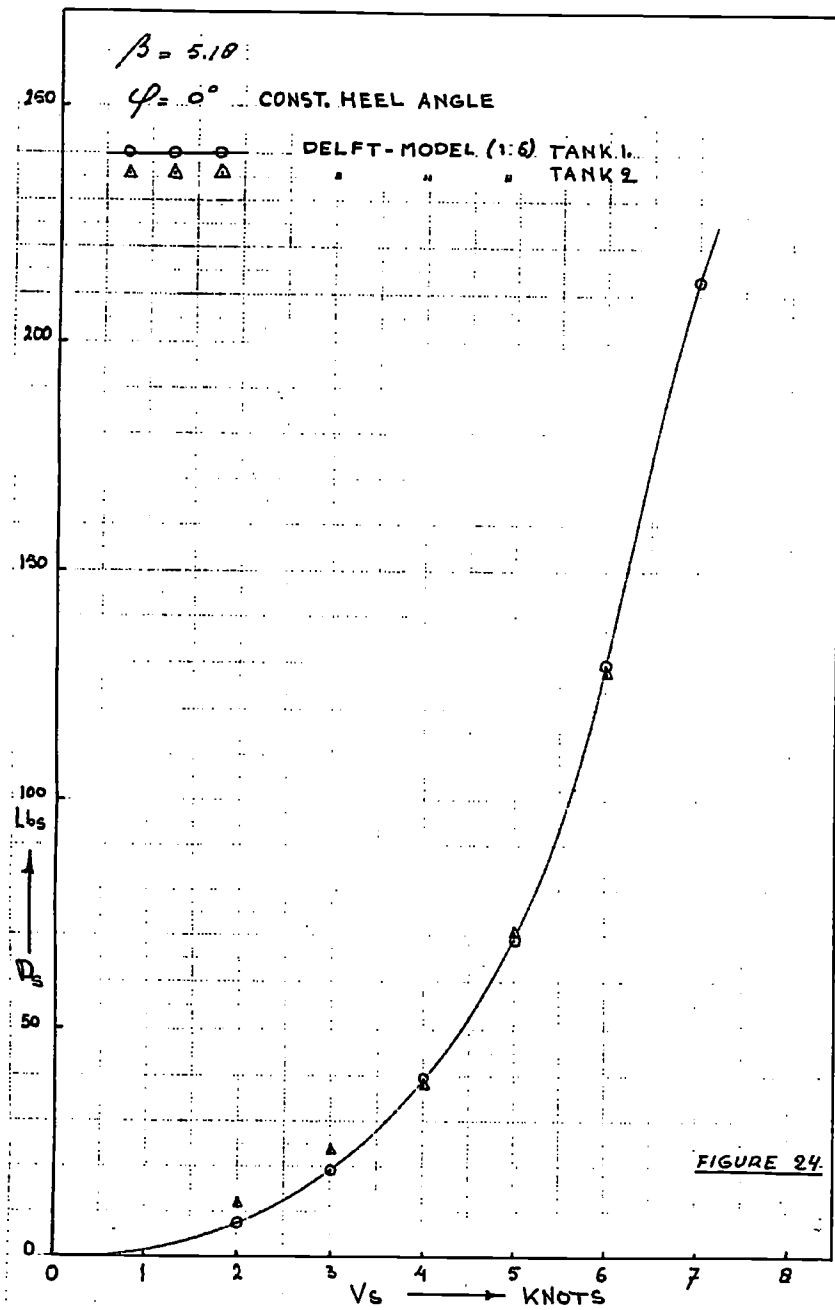


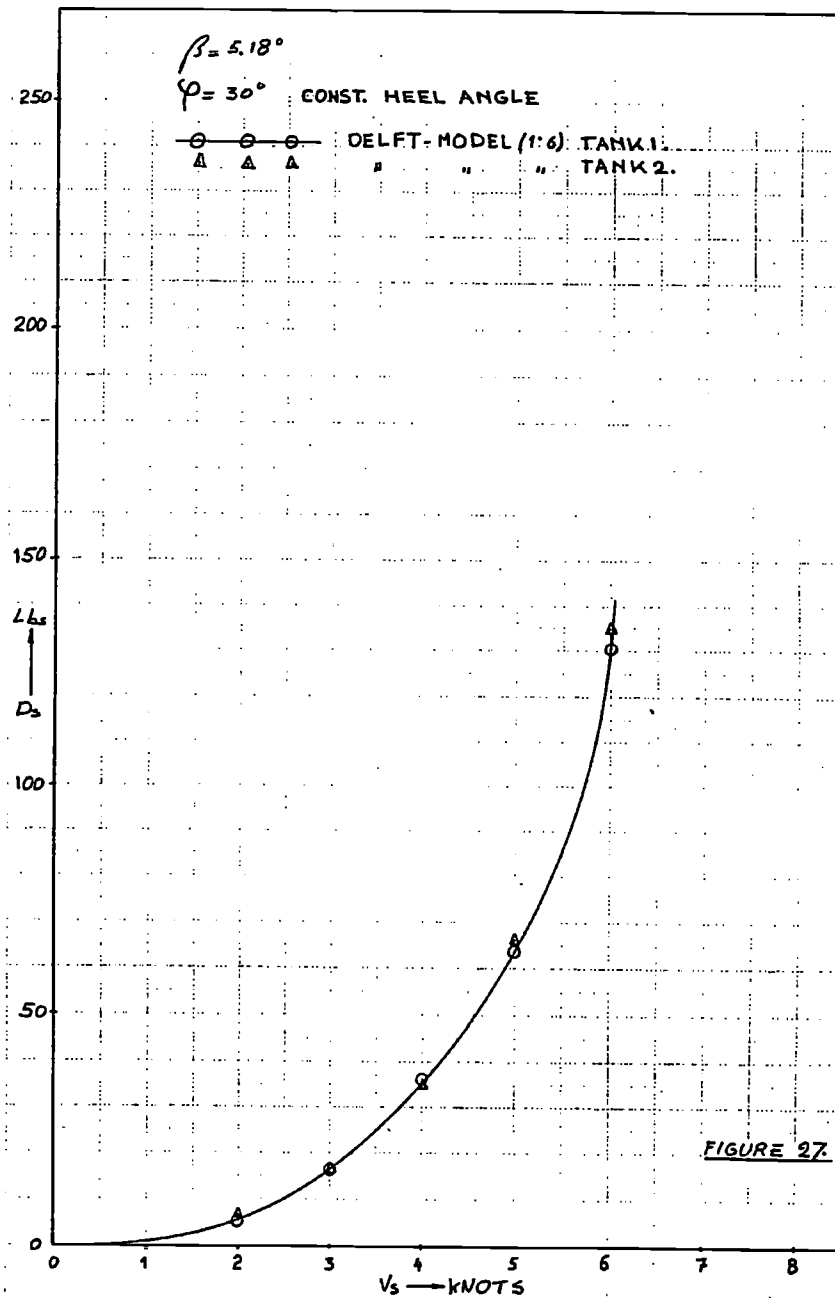
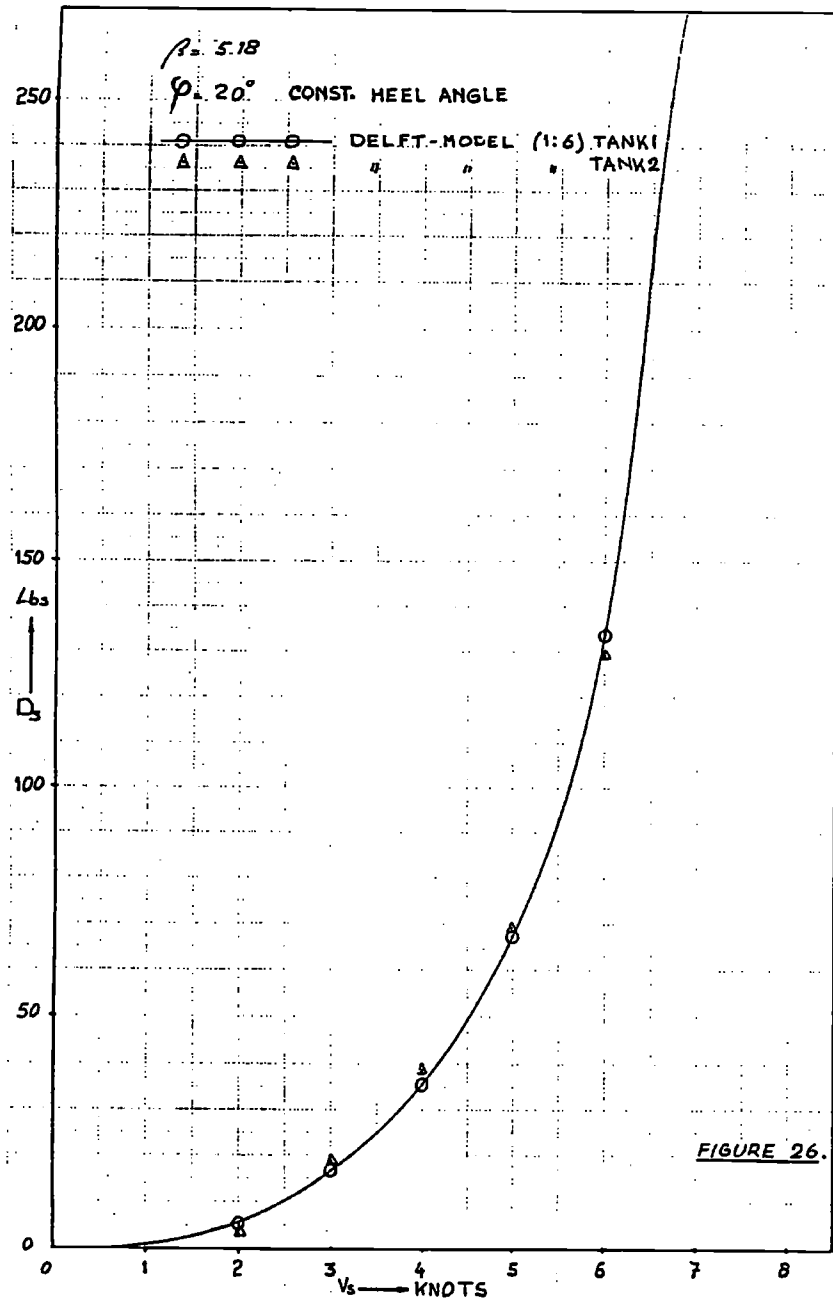


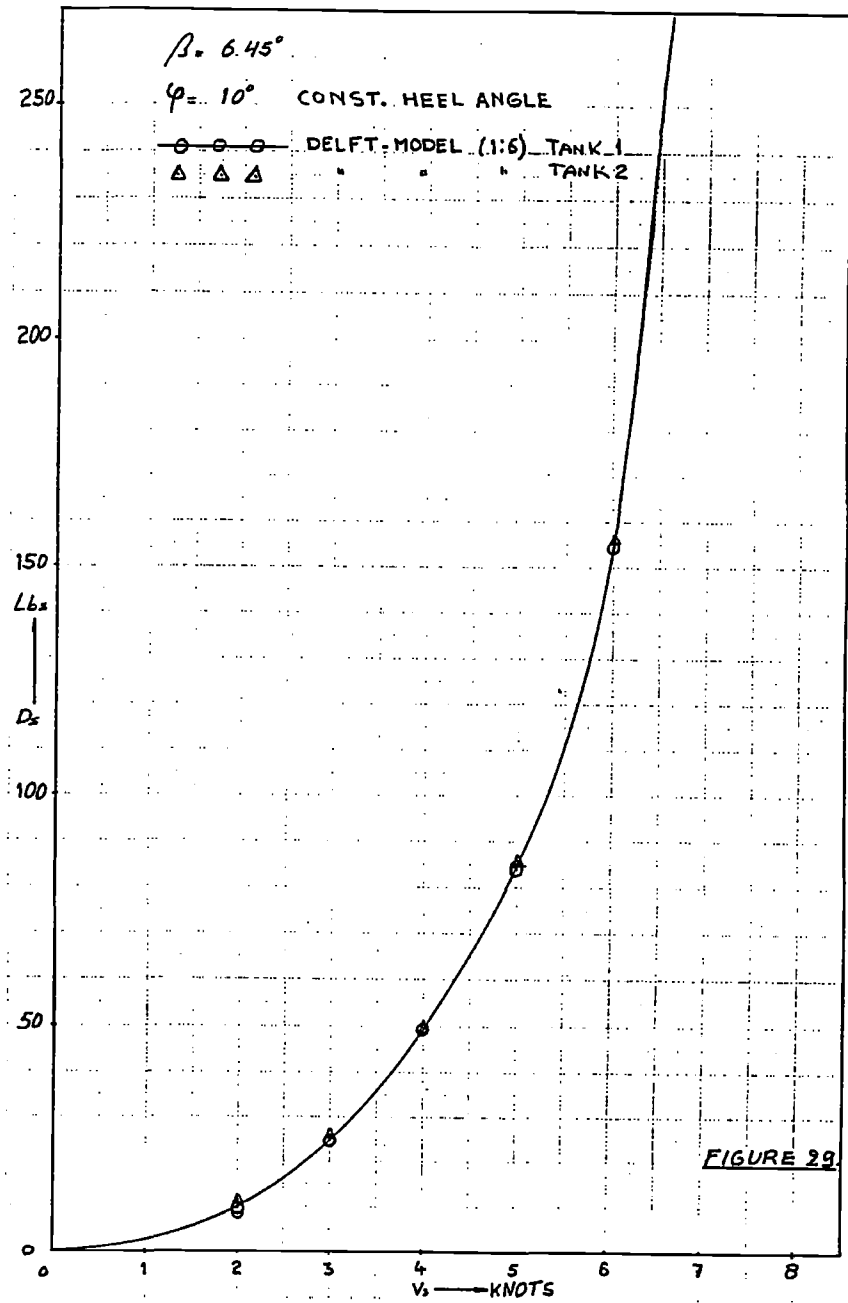
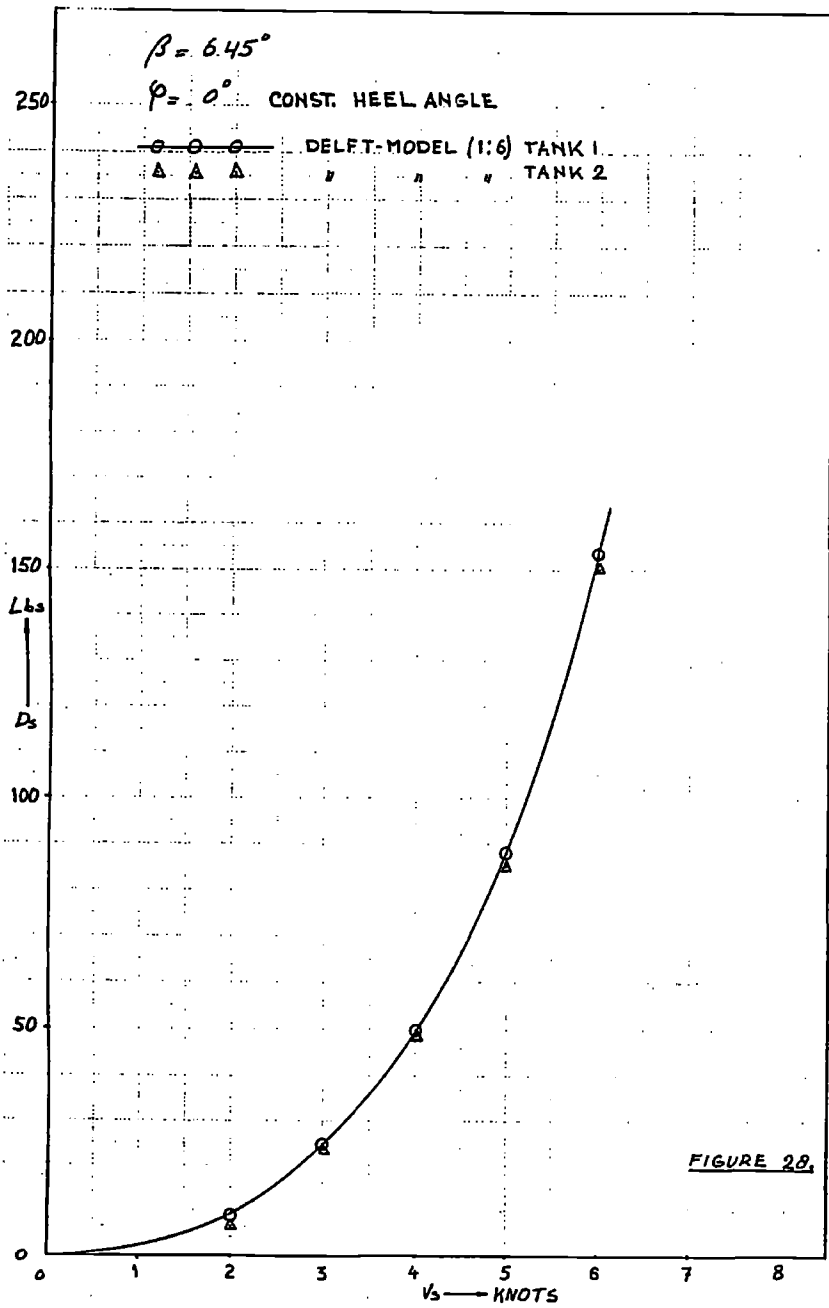


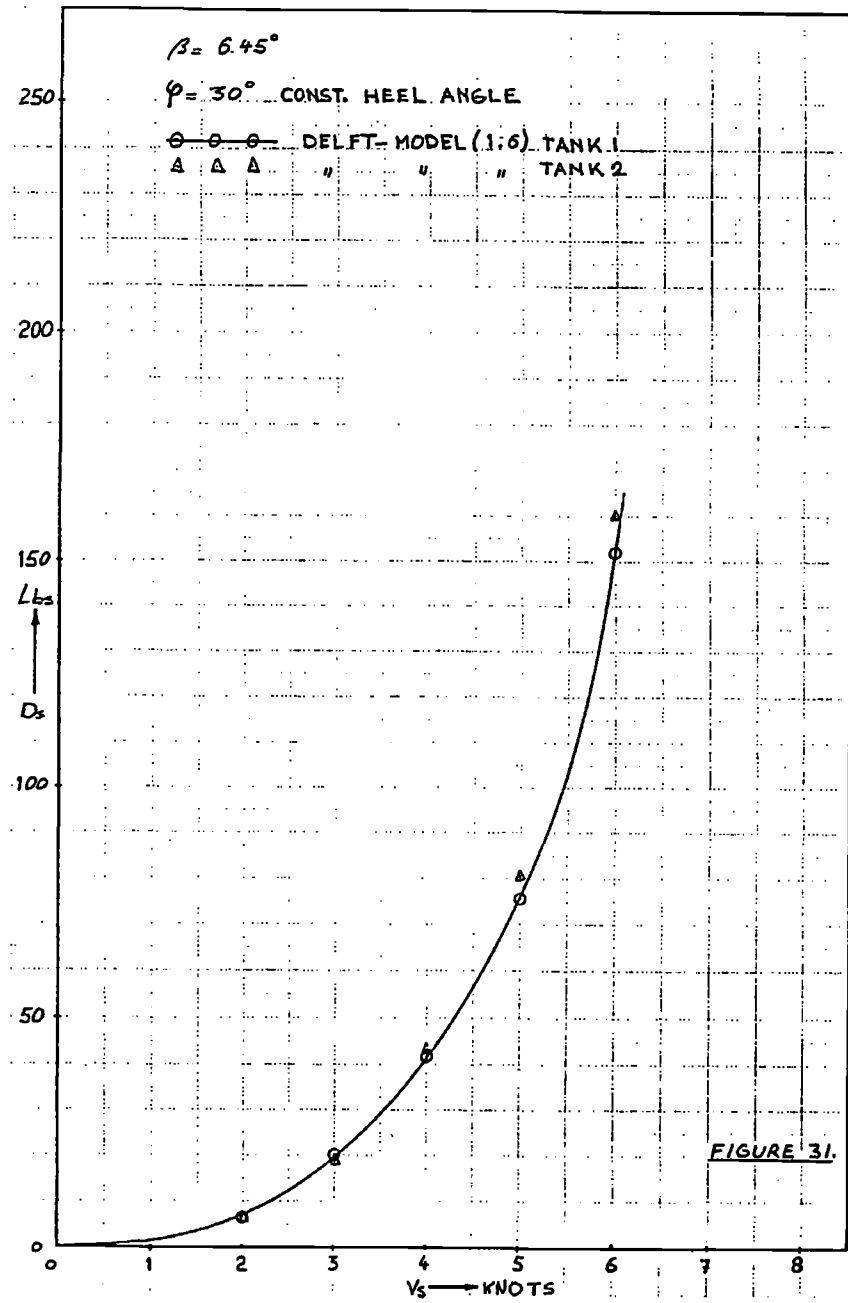
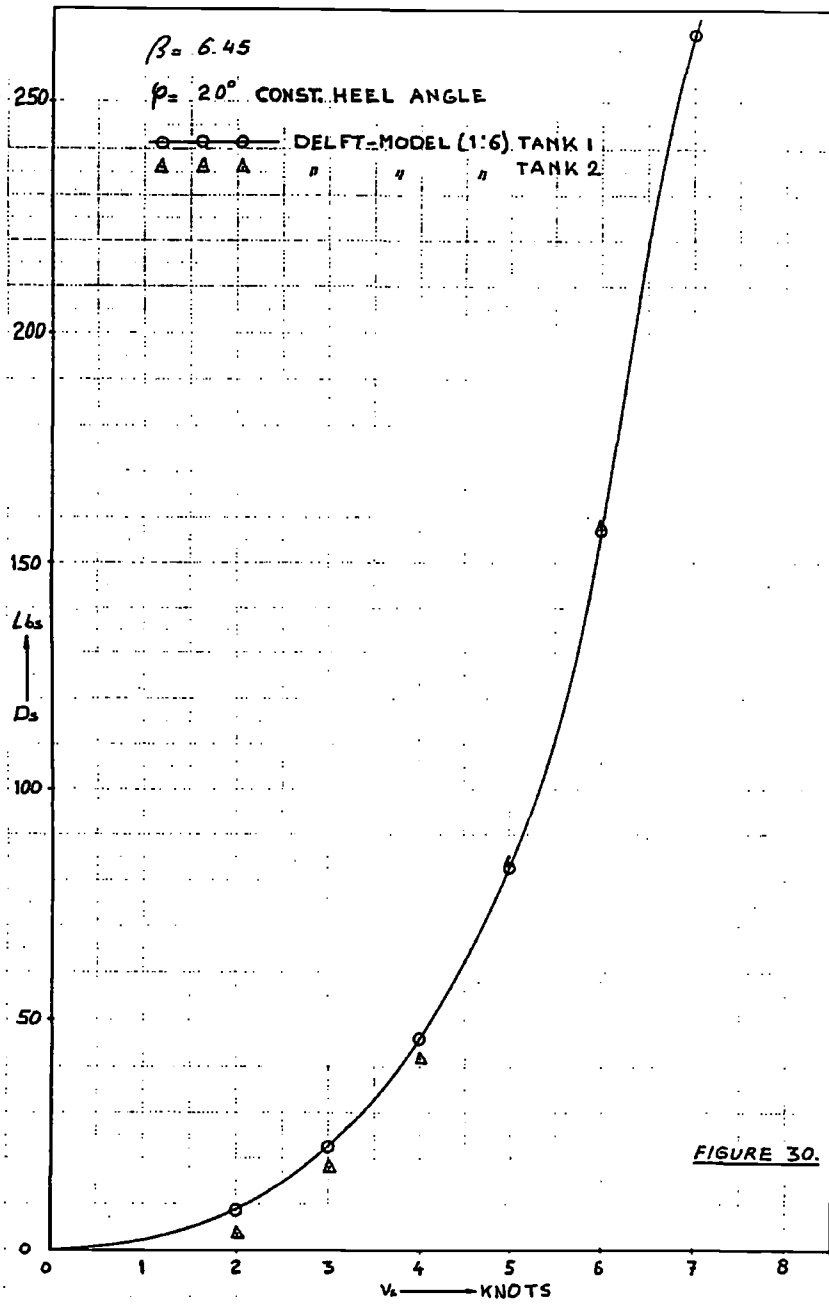


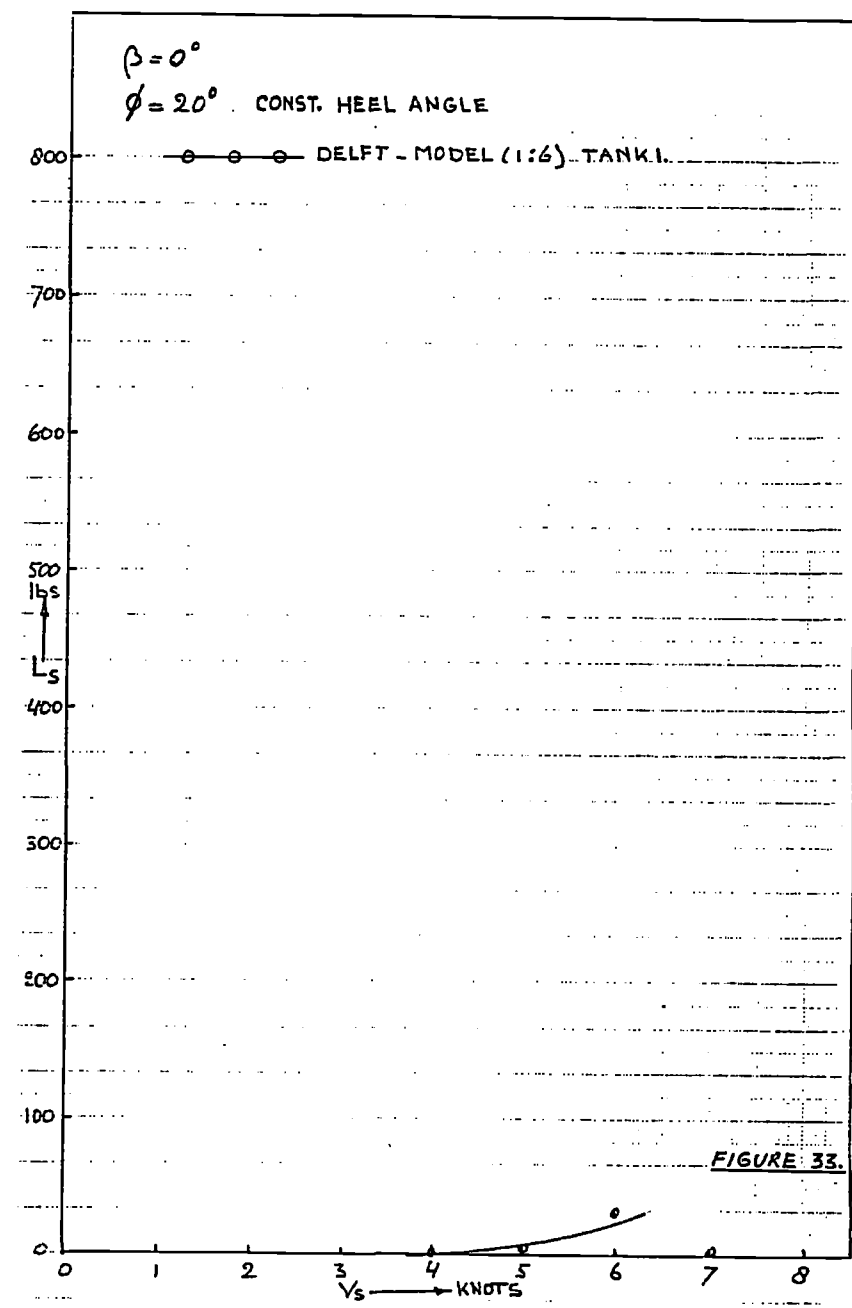
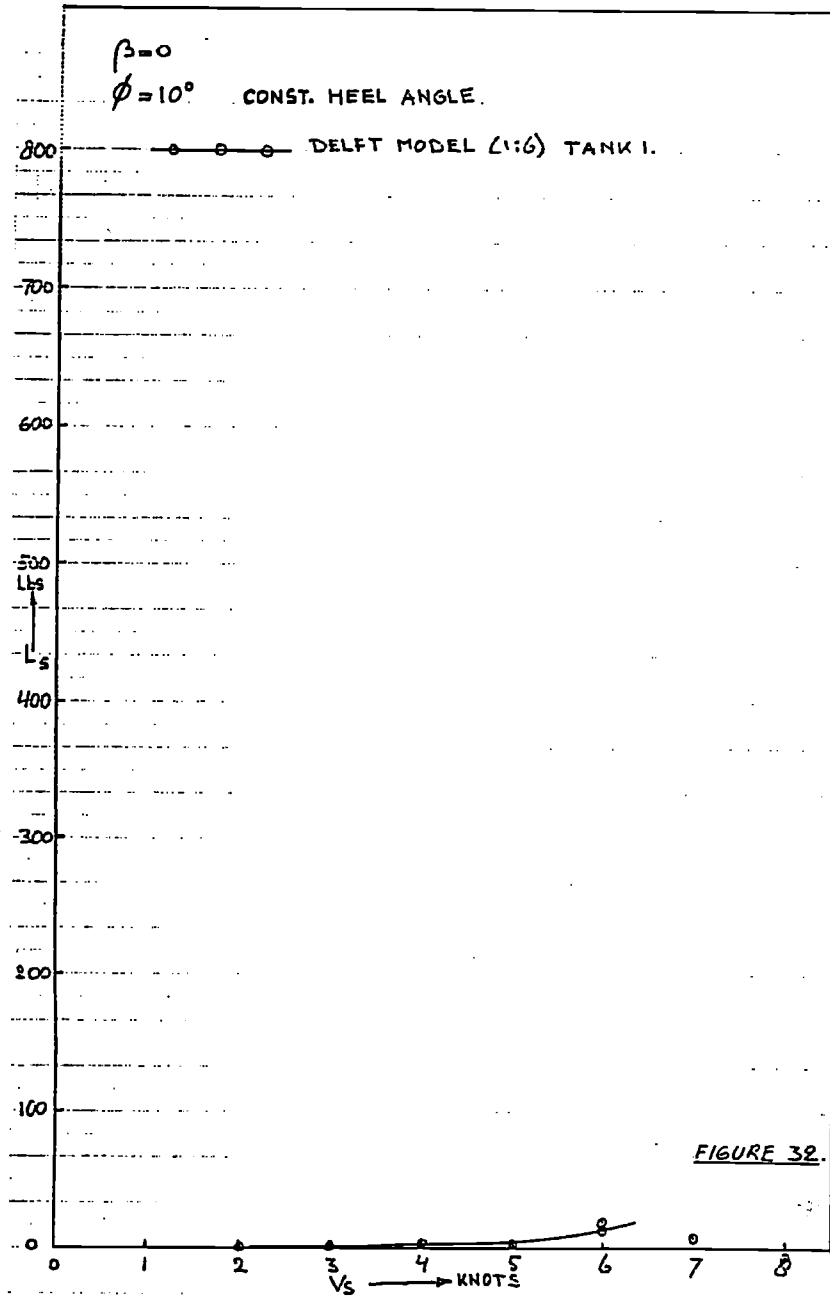


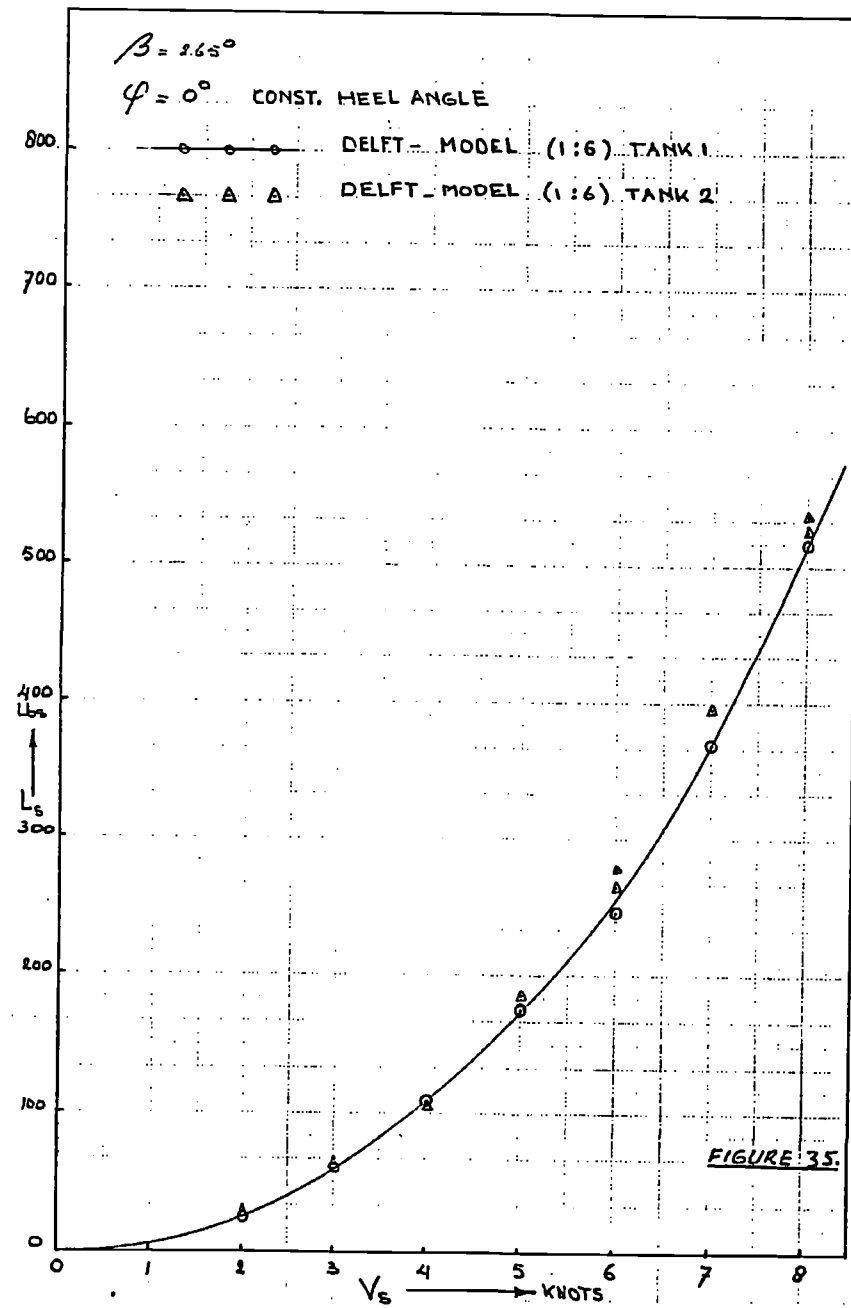
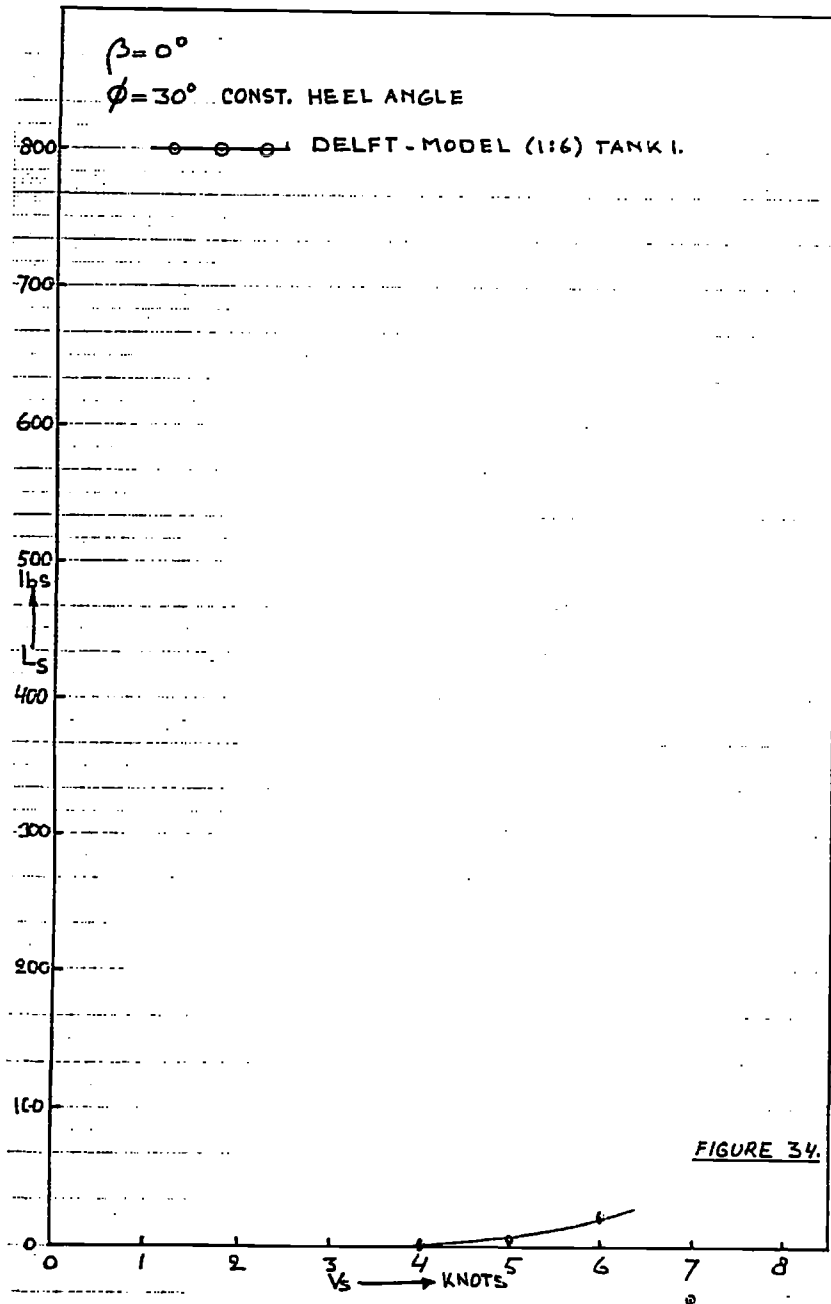


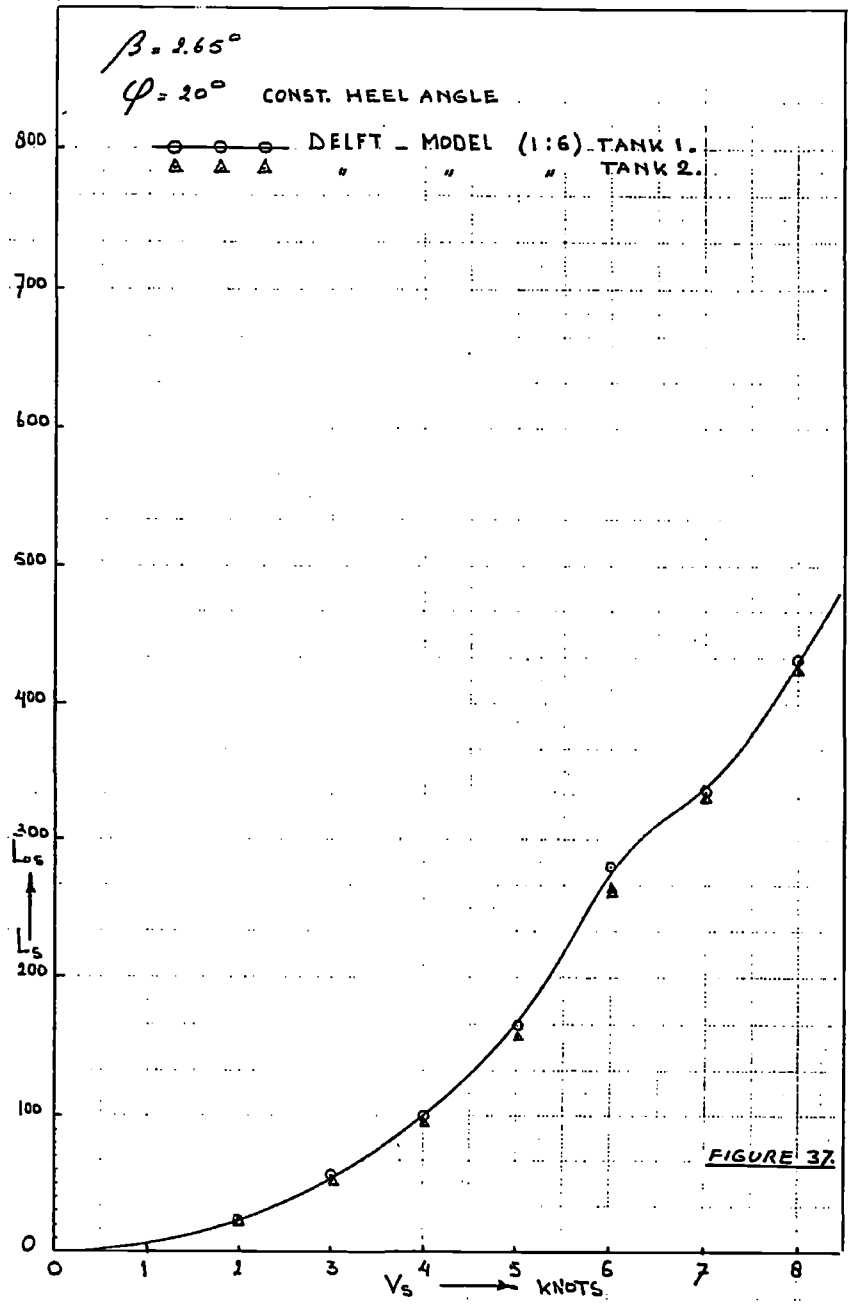
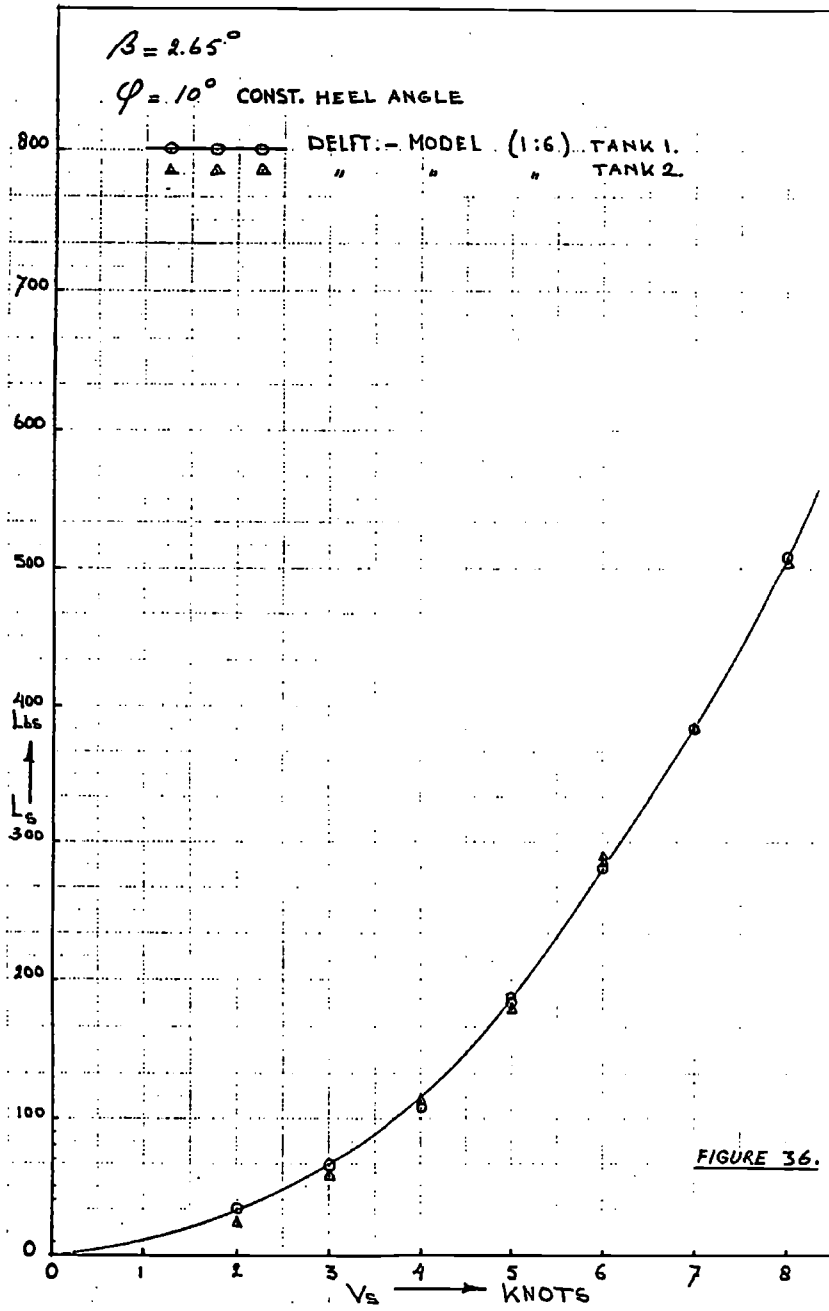




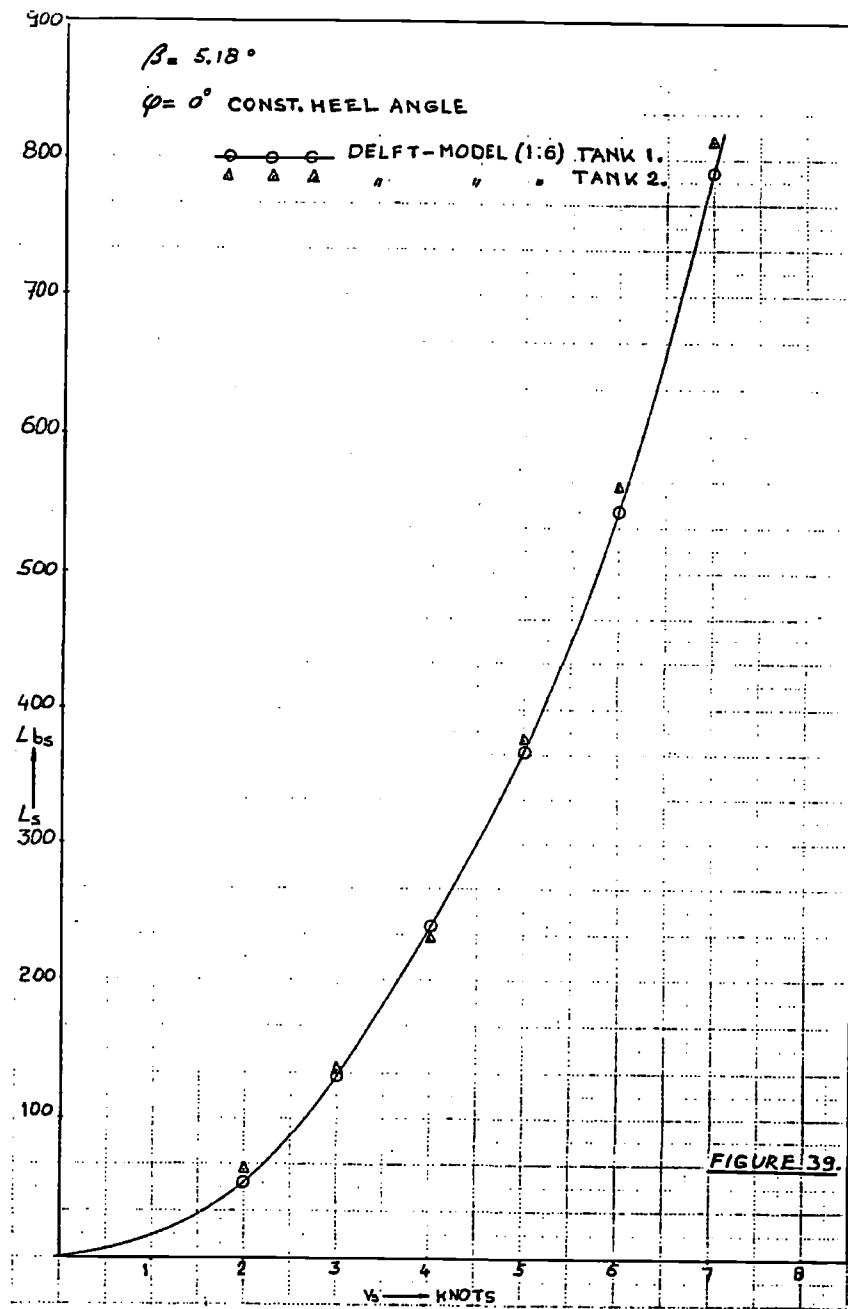
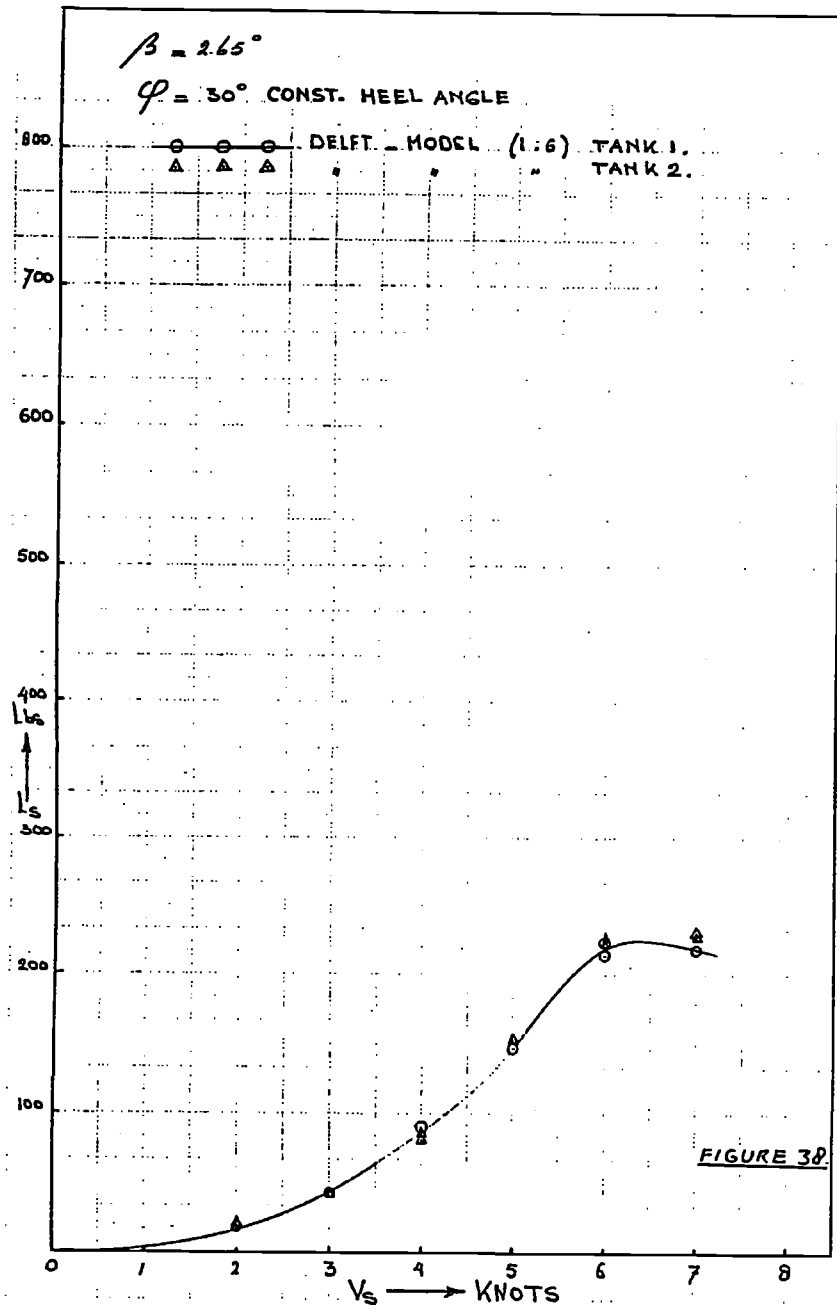


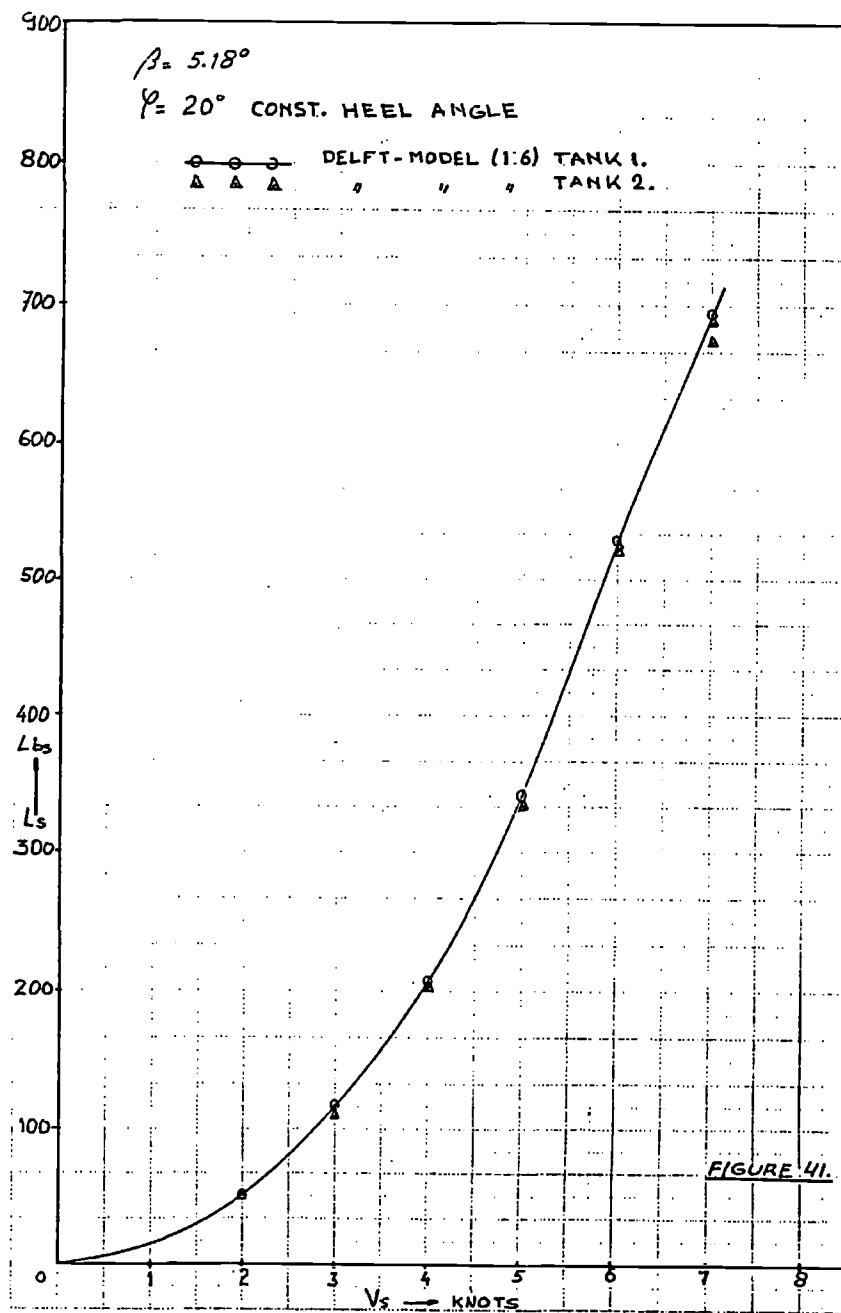
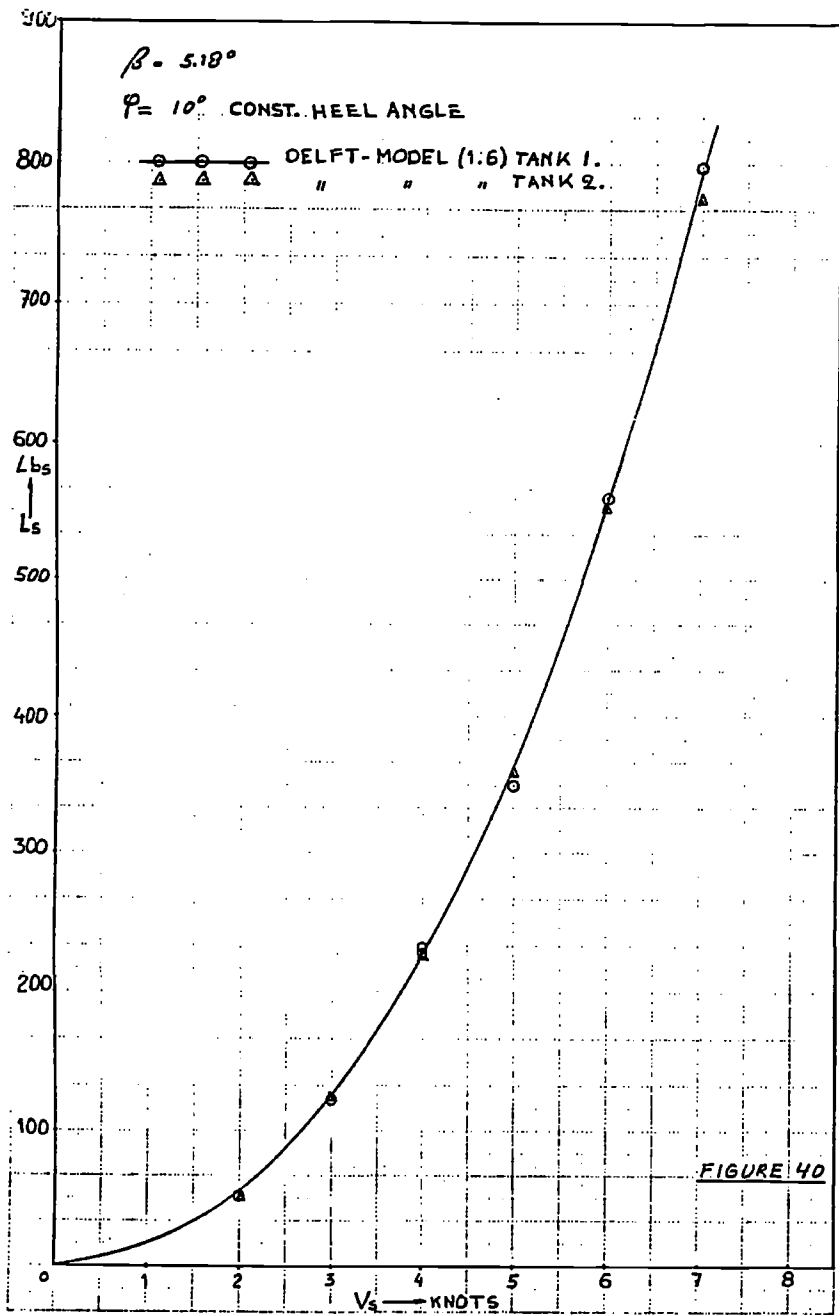


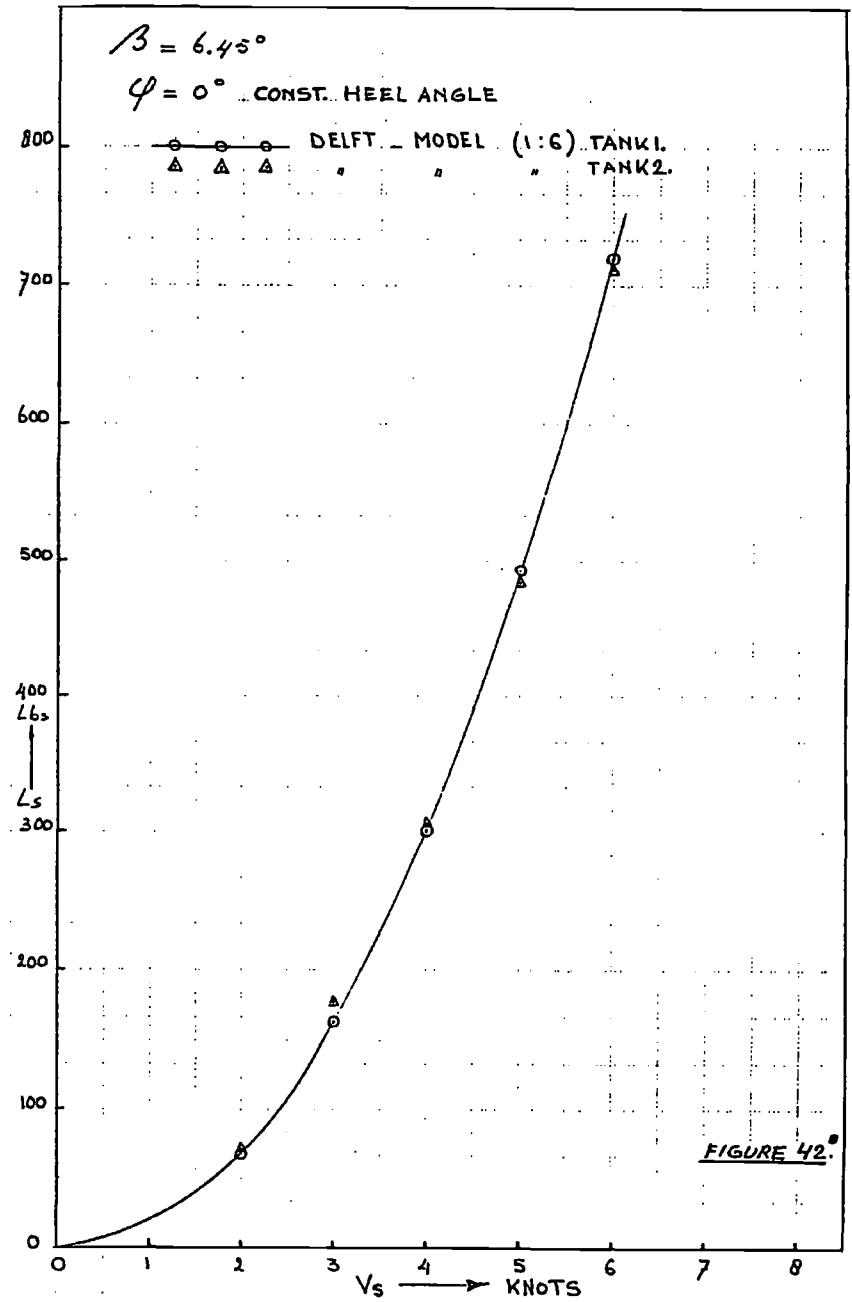
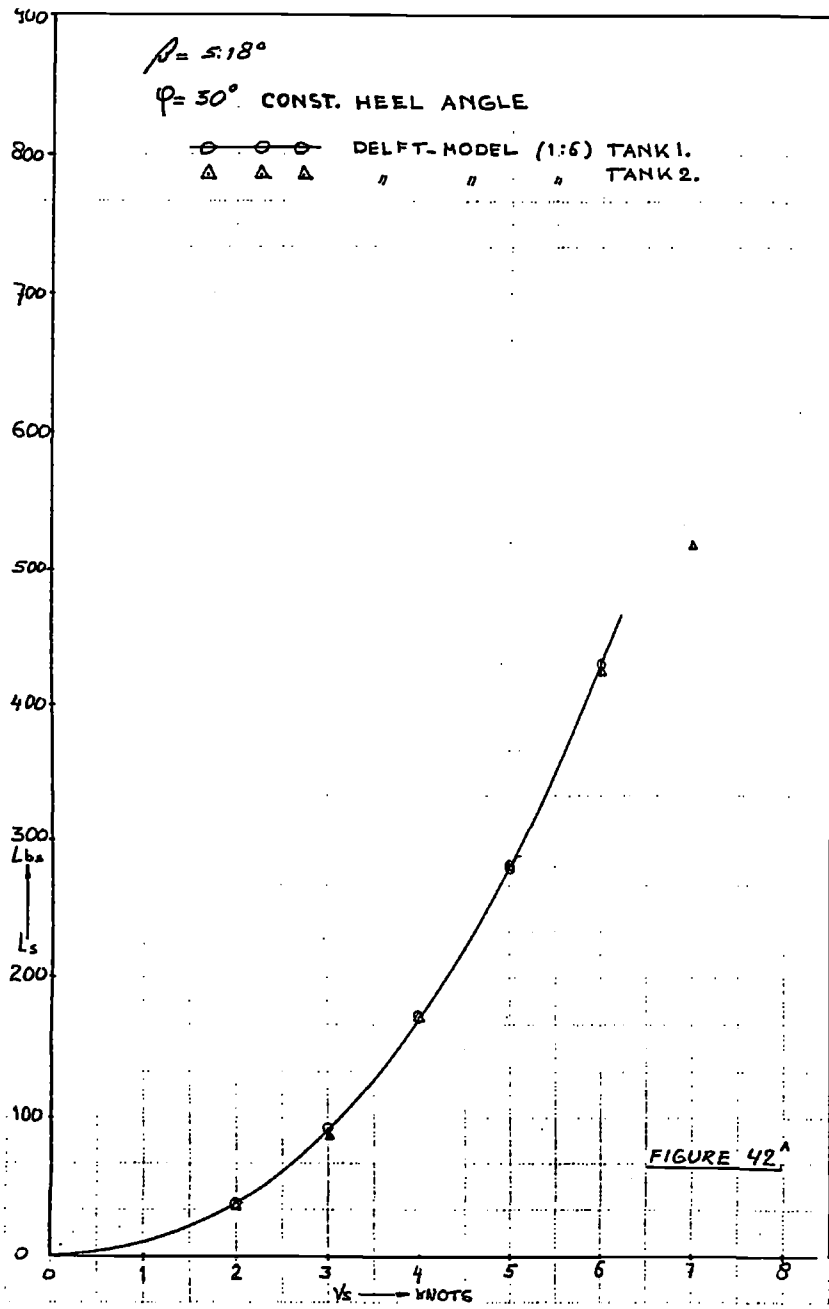


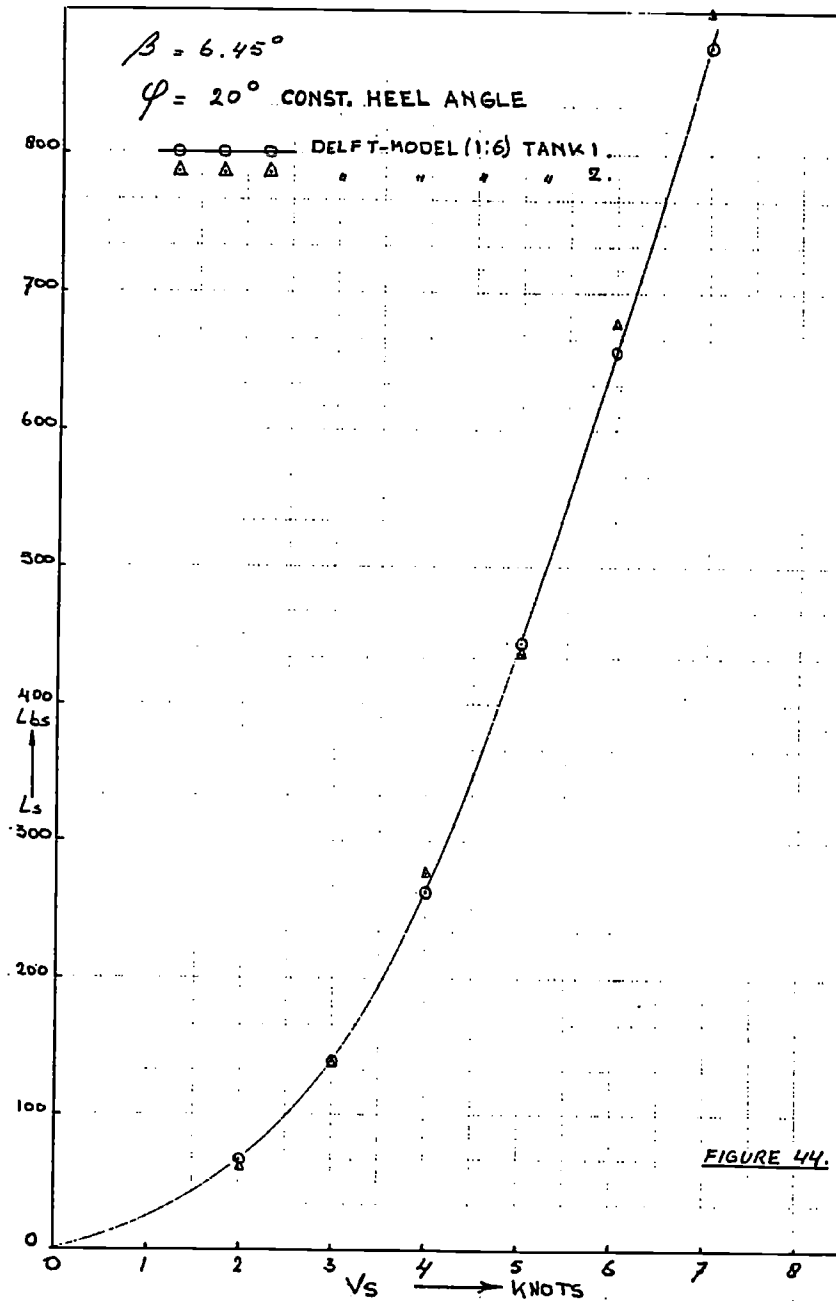
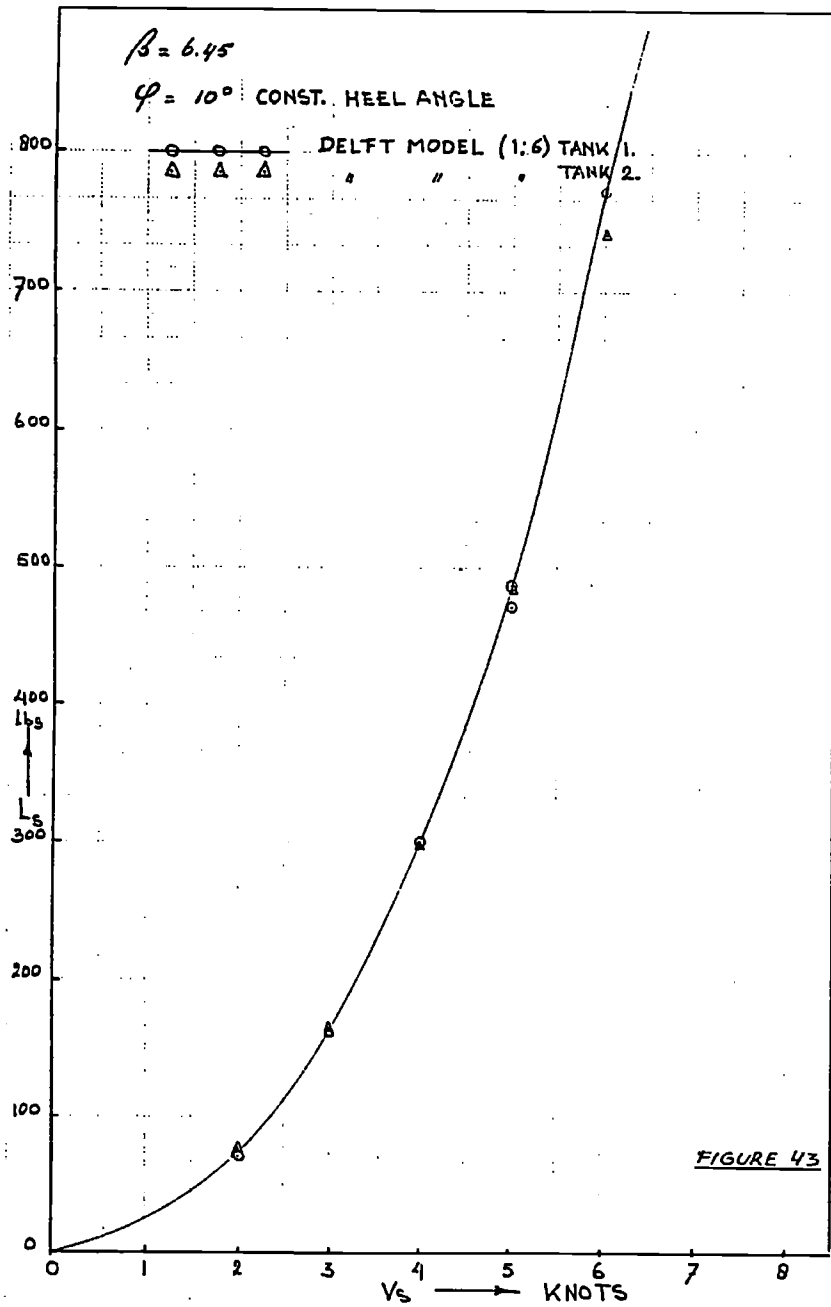












$\beta = 6.45$

$\varphi = 30^\circ$  CONST. HEEL ANGLE

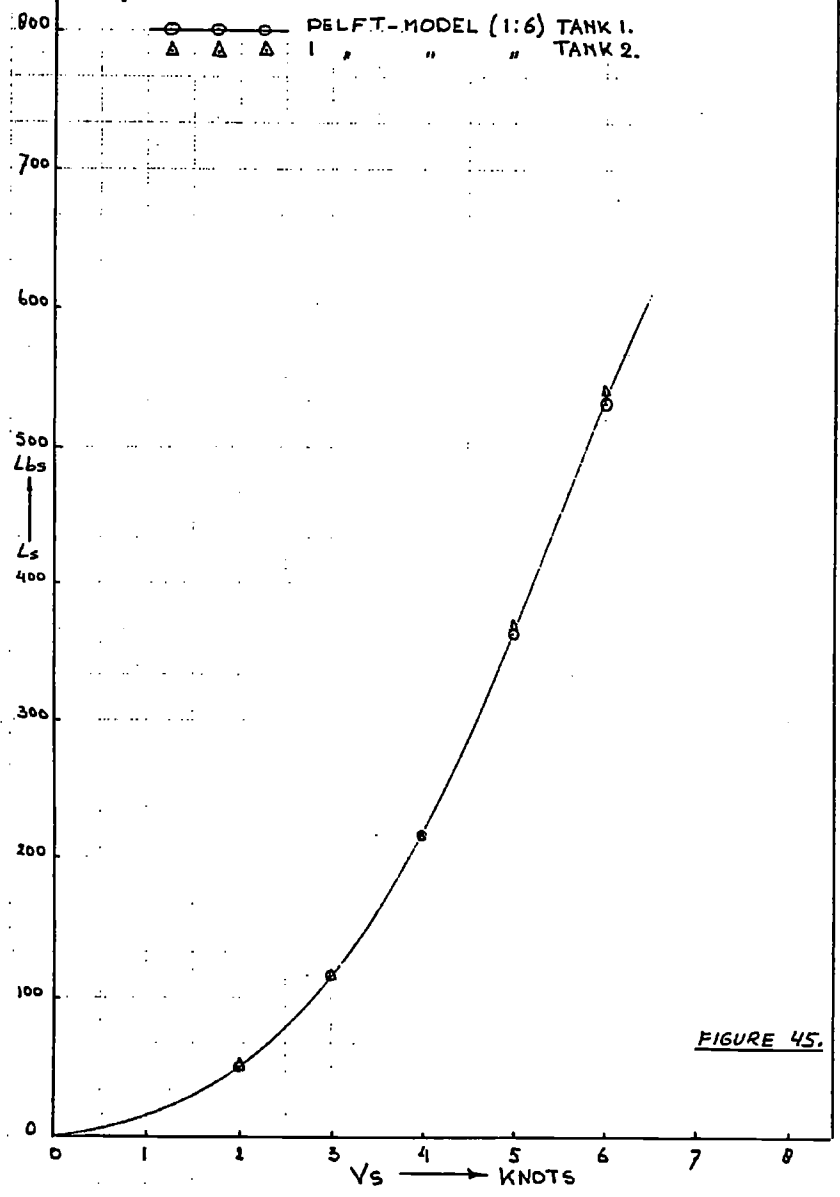


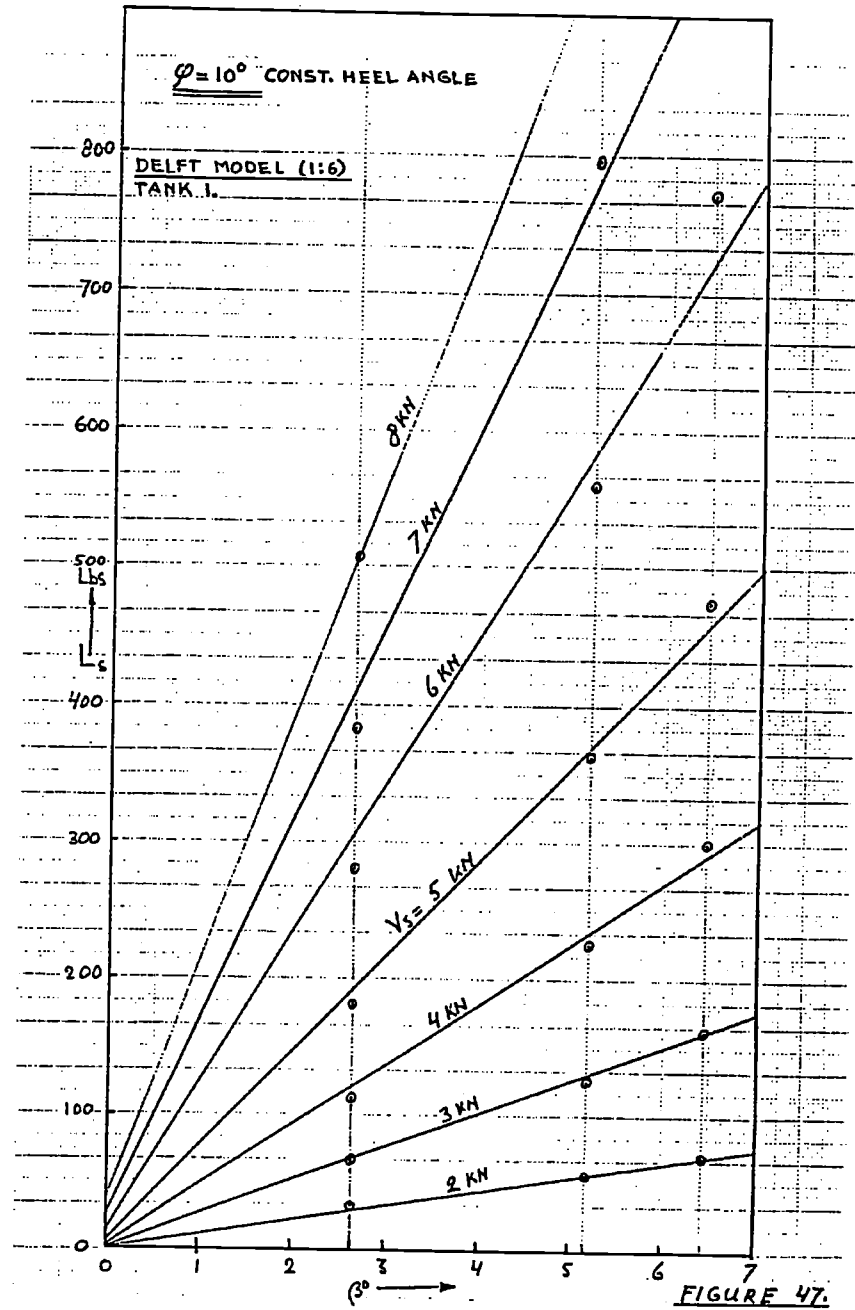
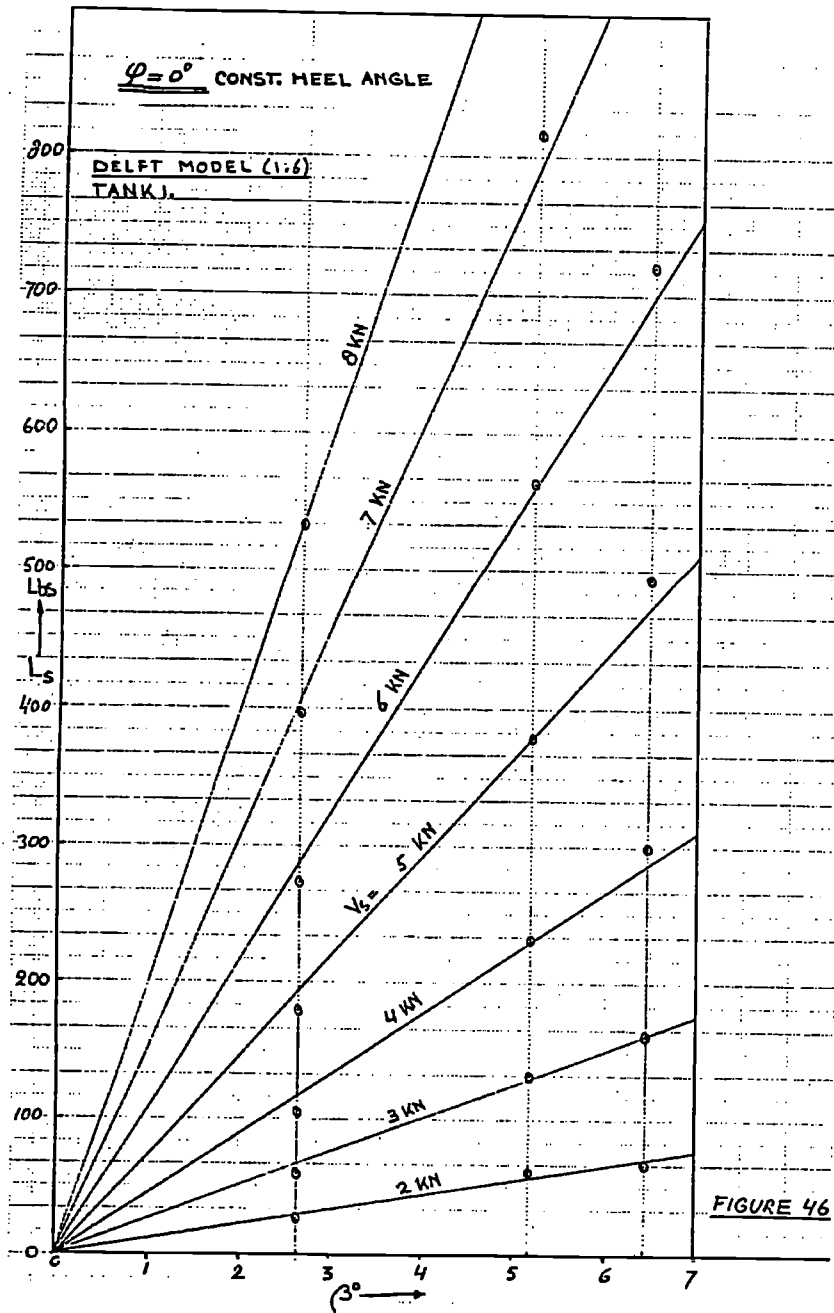
FIGURE 45.

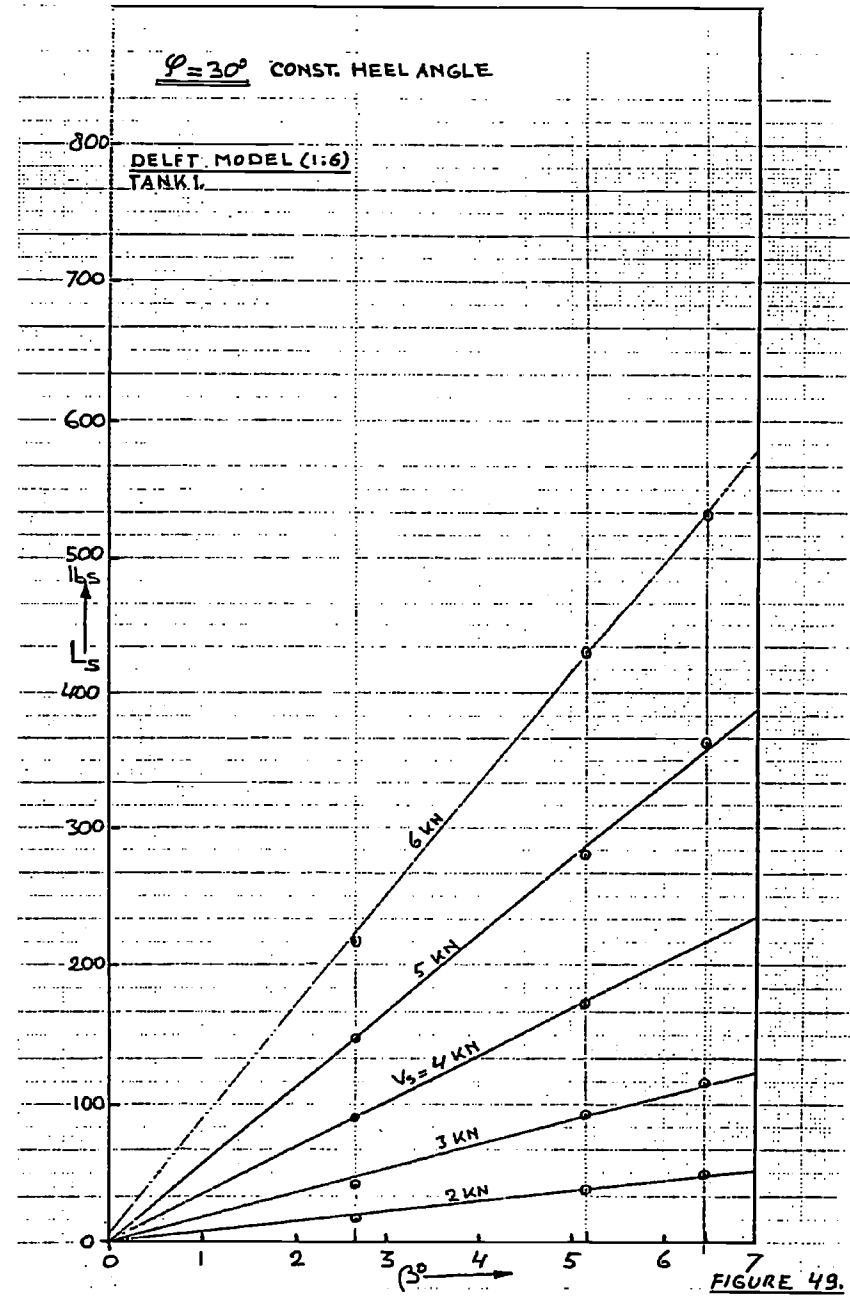
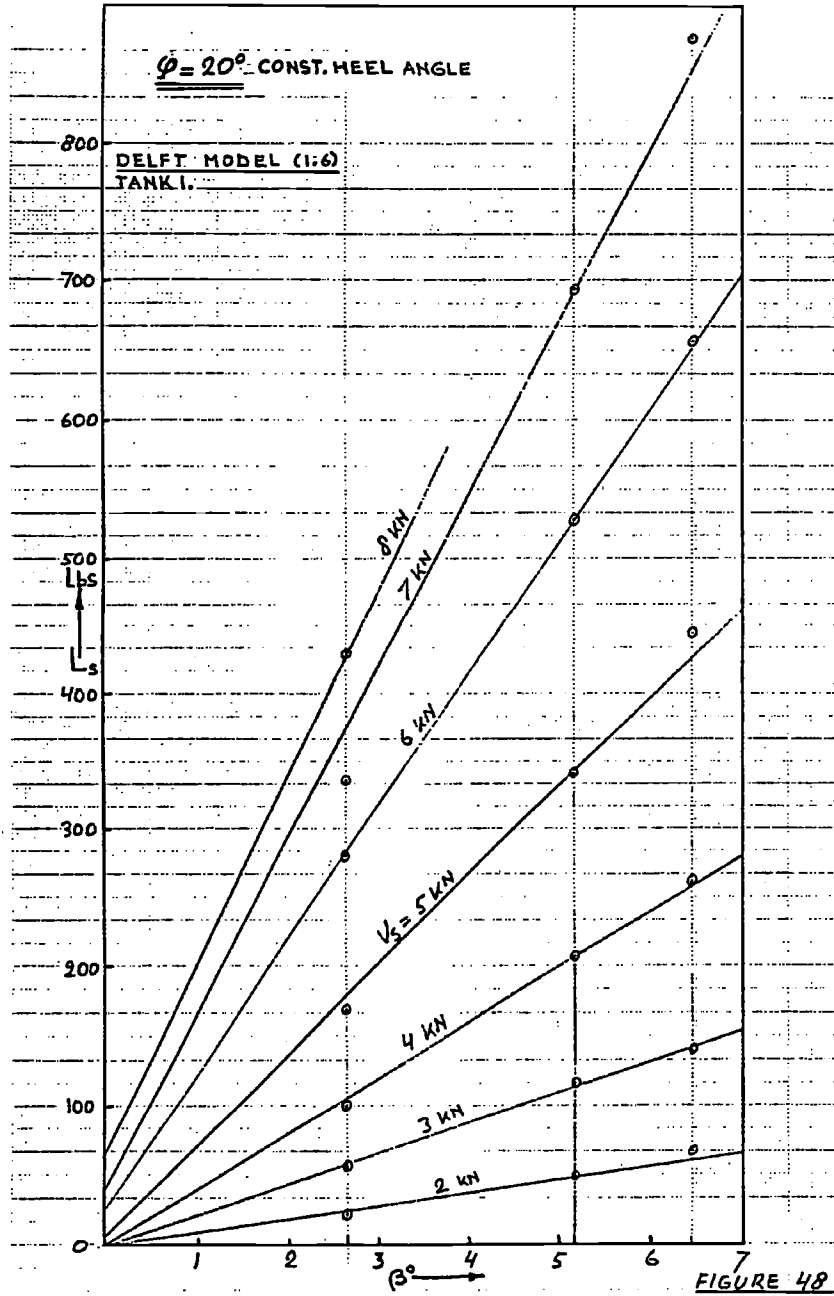
Figures 46 - 49

Constant Heel Angles

Ship Lift versus  $\beta$

Tank 1





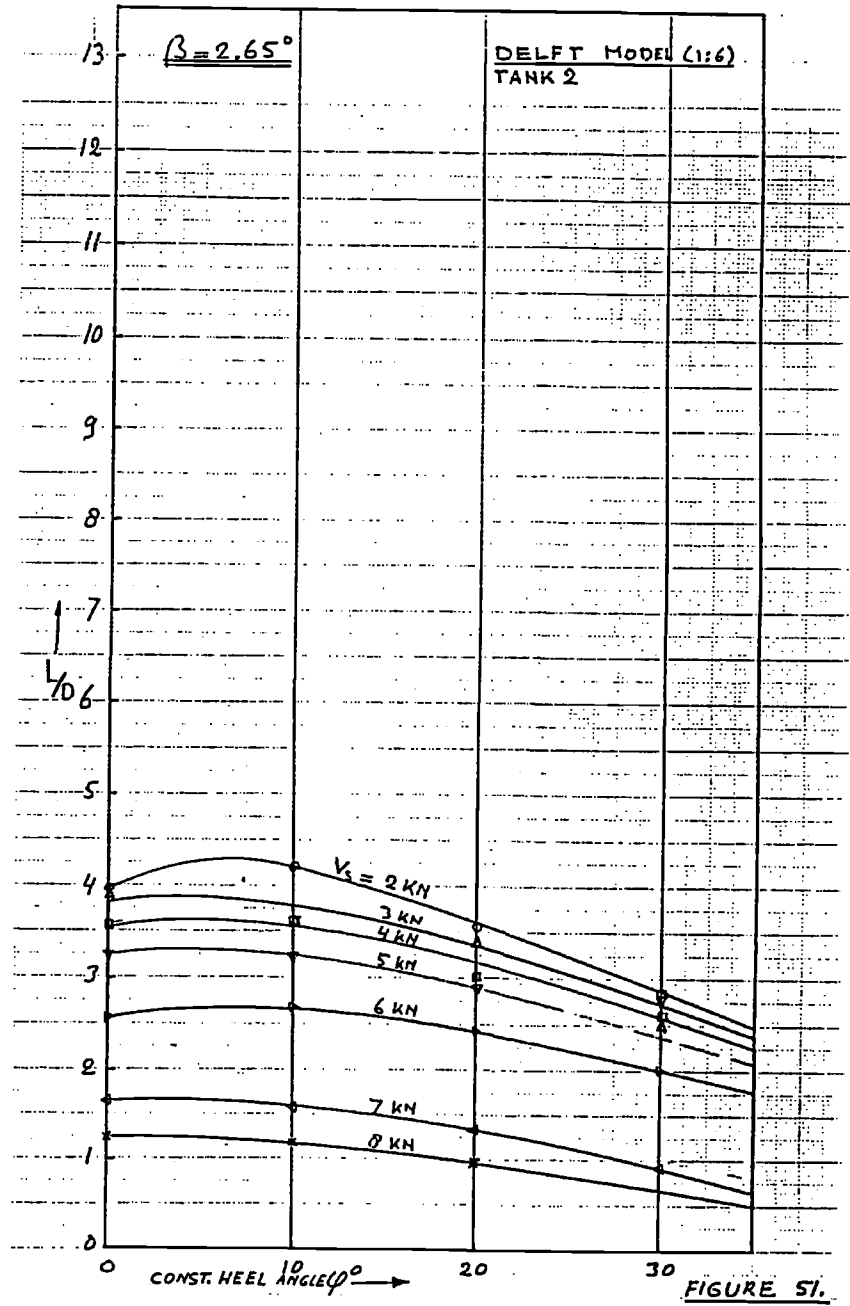
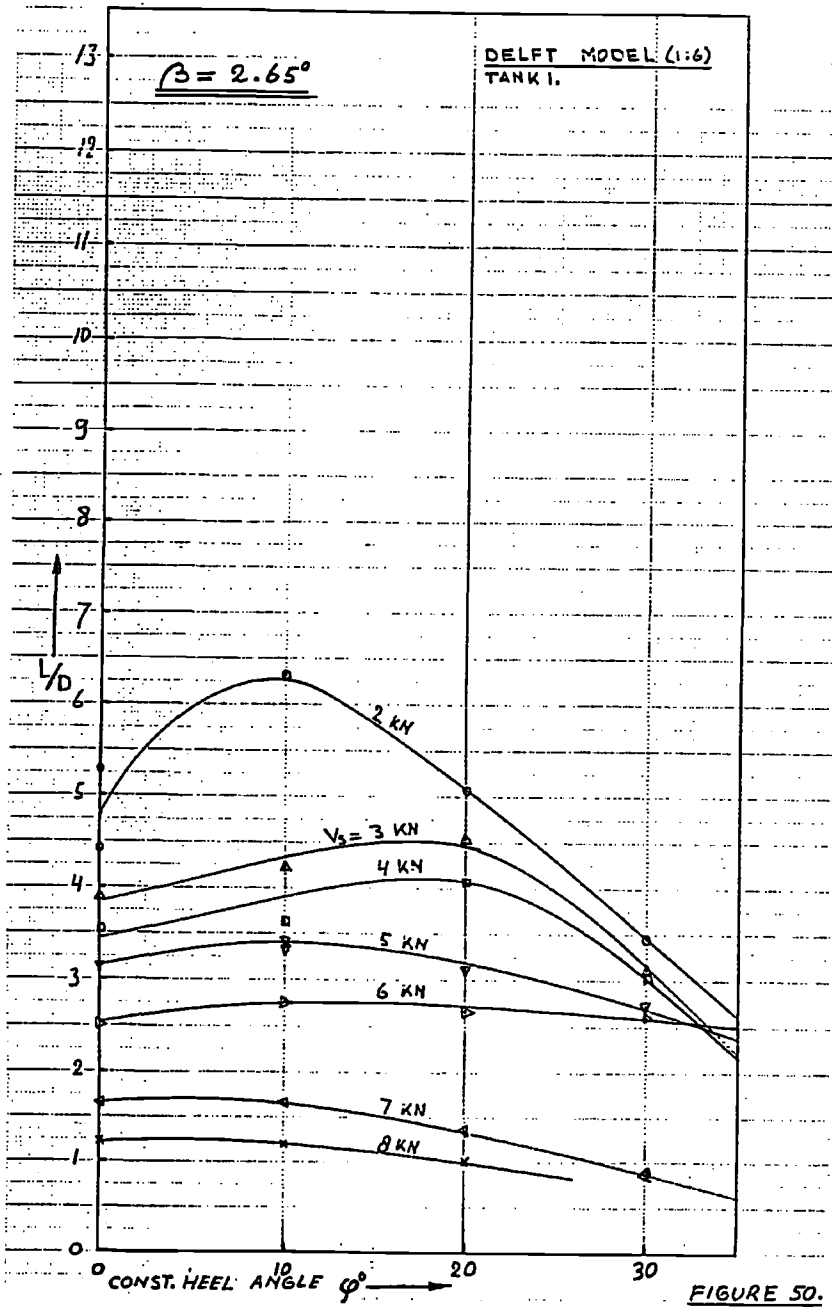


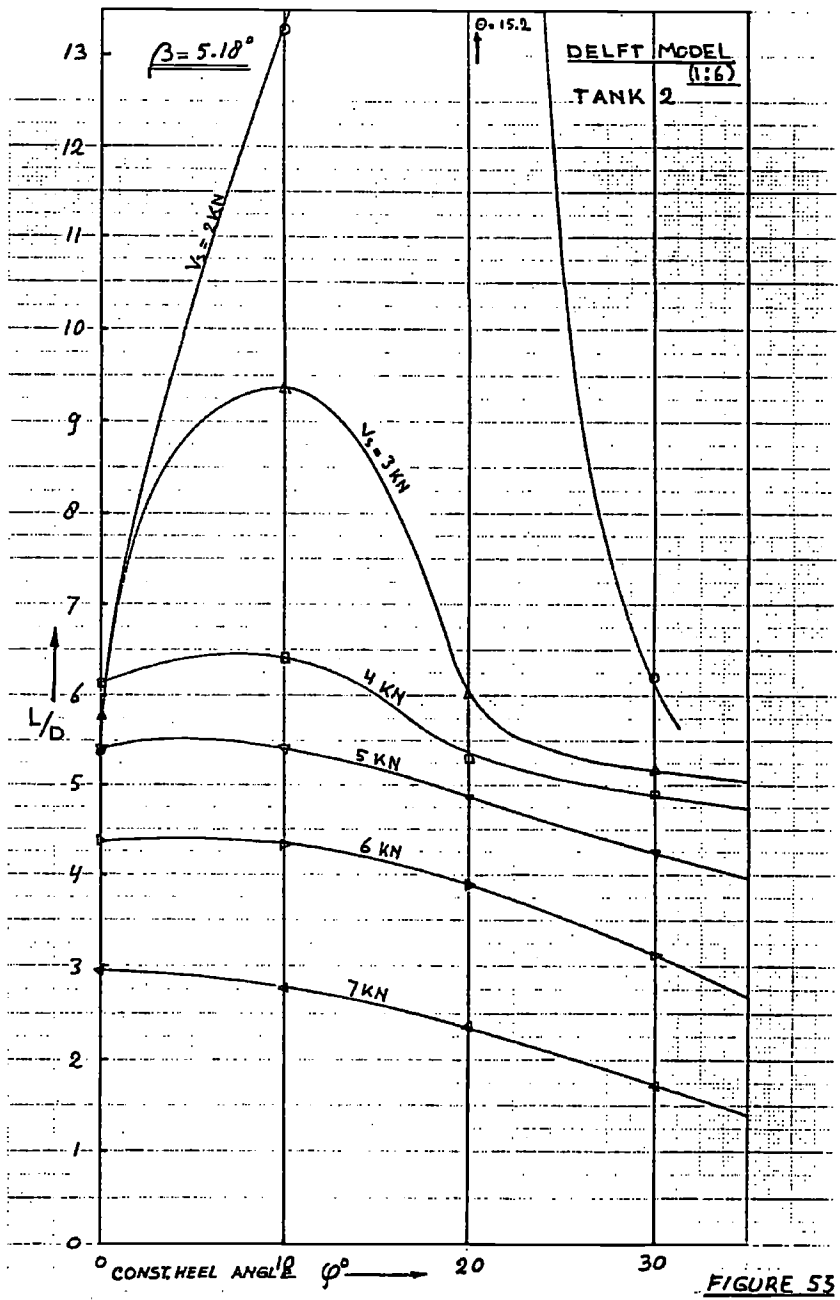
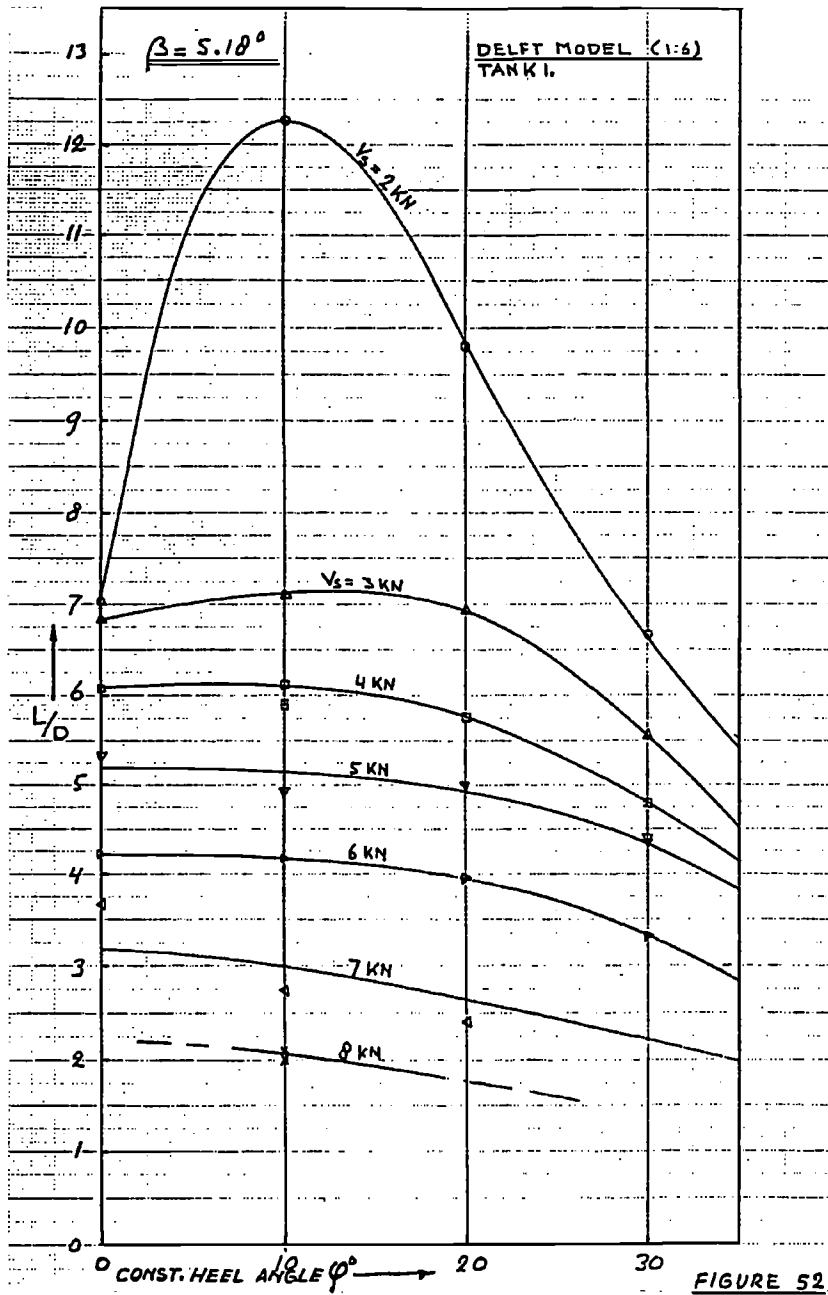
Figures 50 - 55

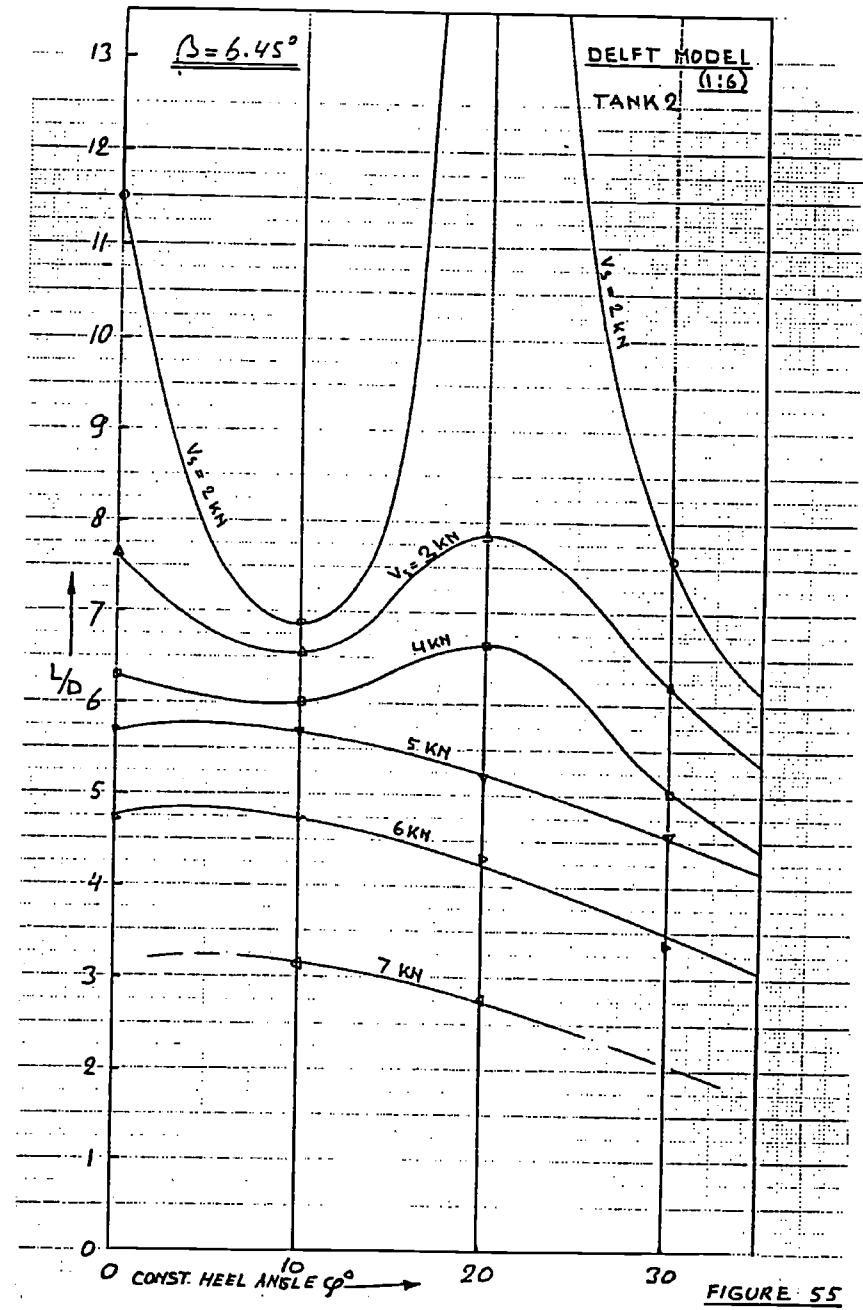
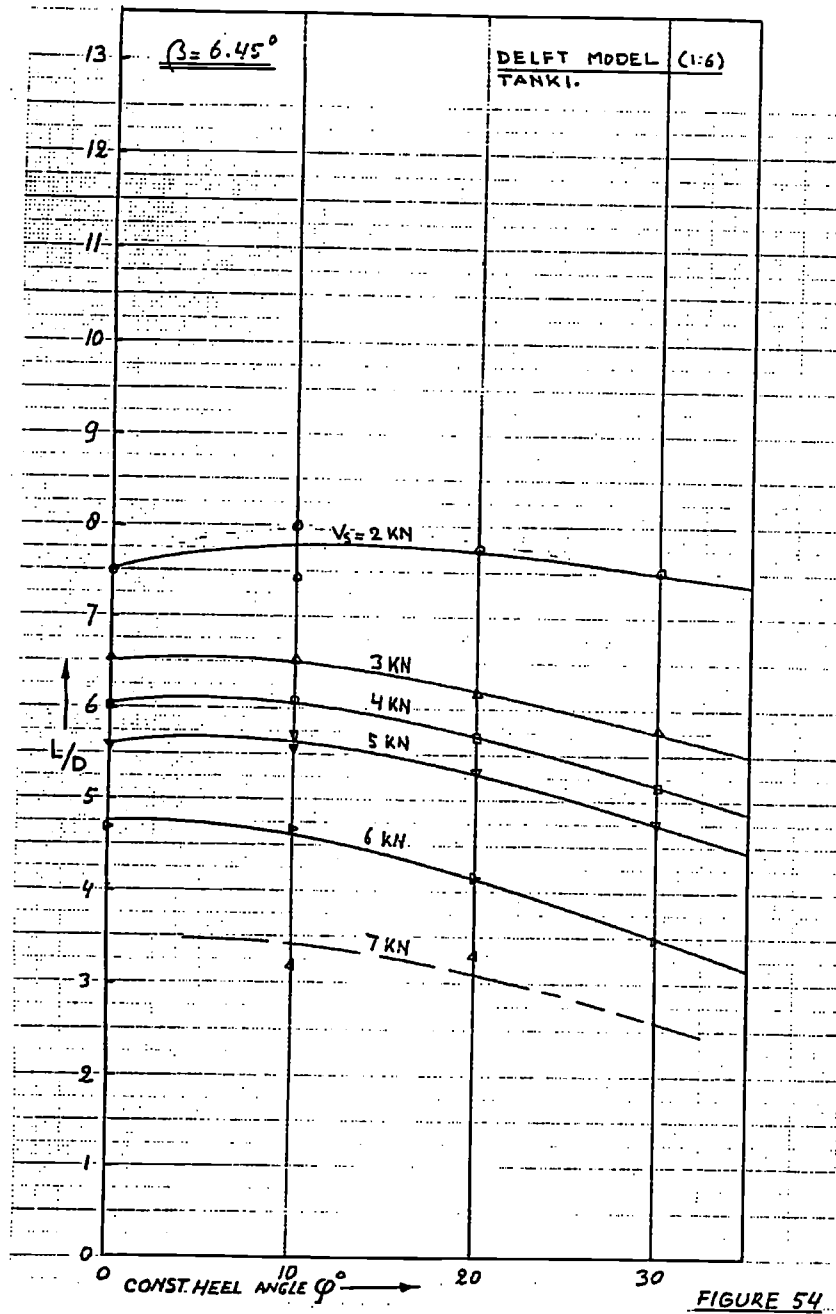
Constant Heel Angles

Ship - L/D versus  $\varphi$

Tank 1 and Tank 2





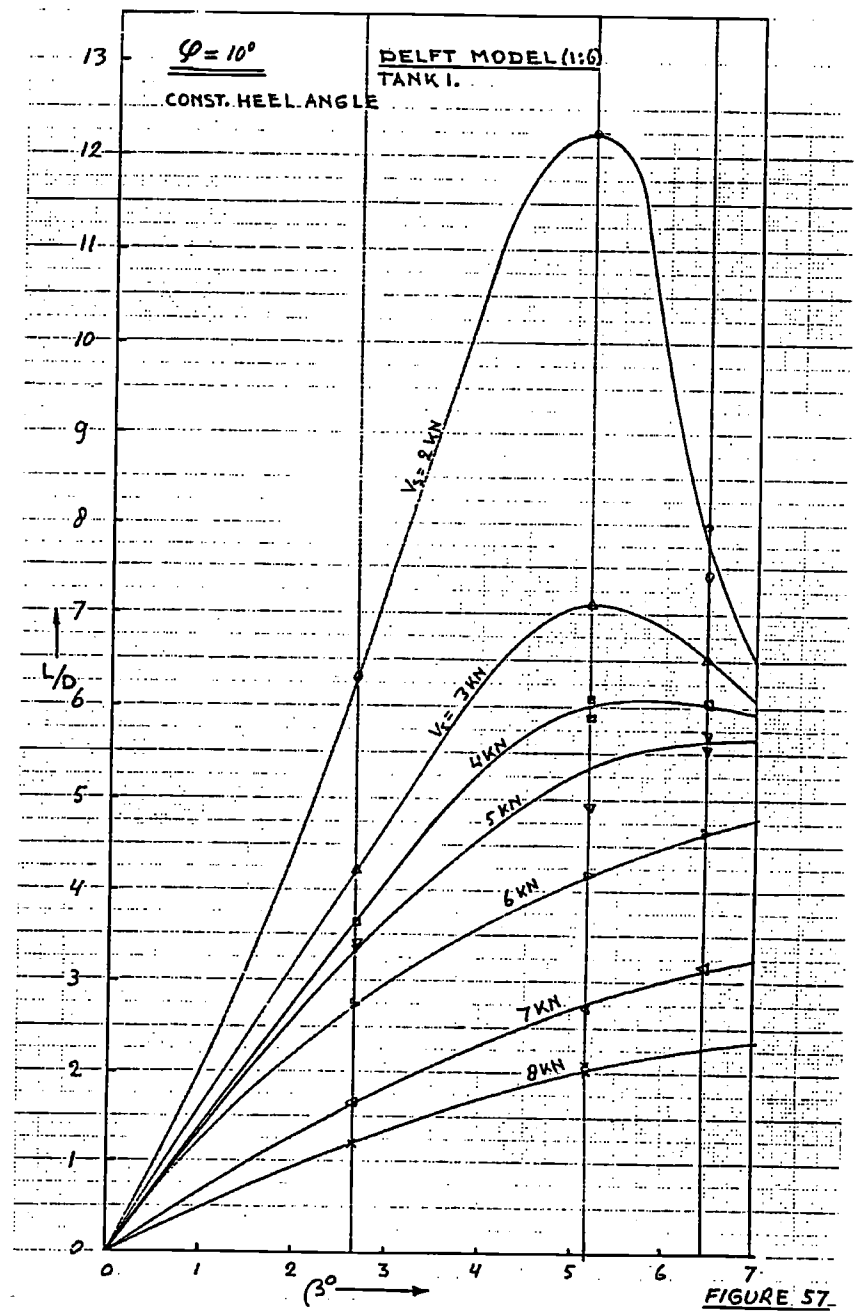
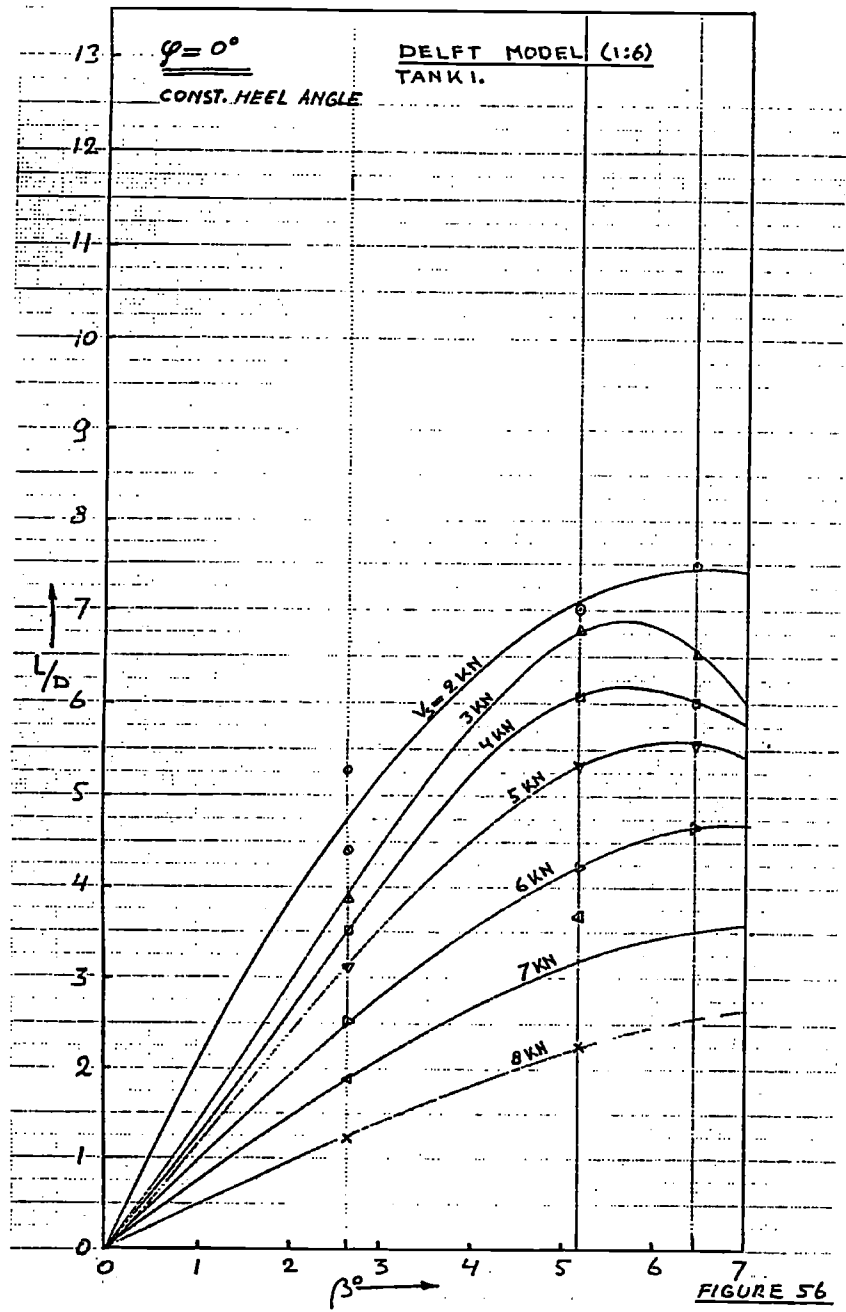


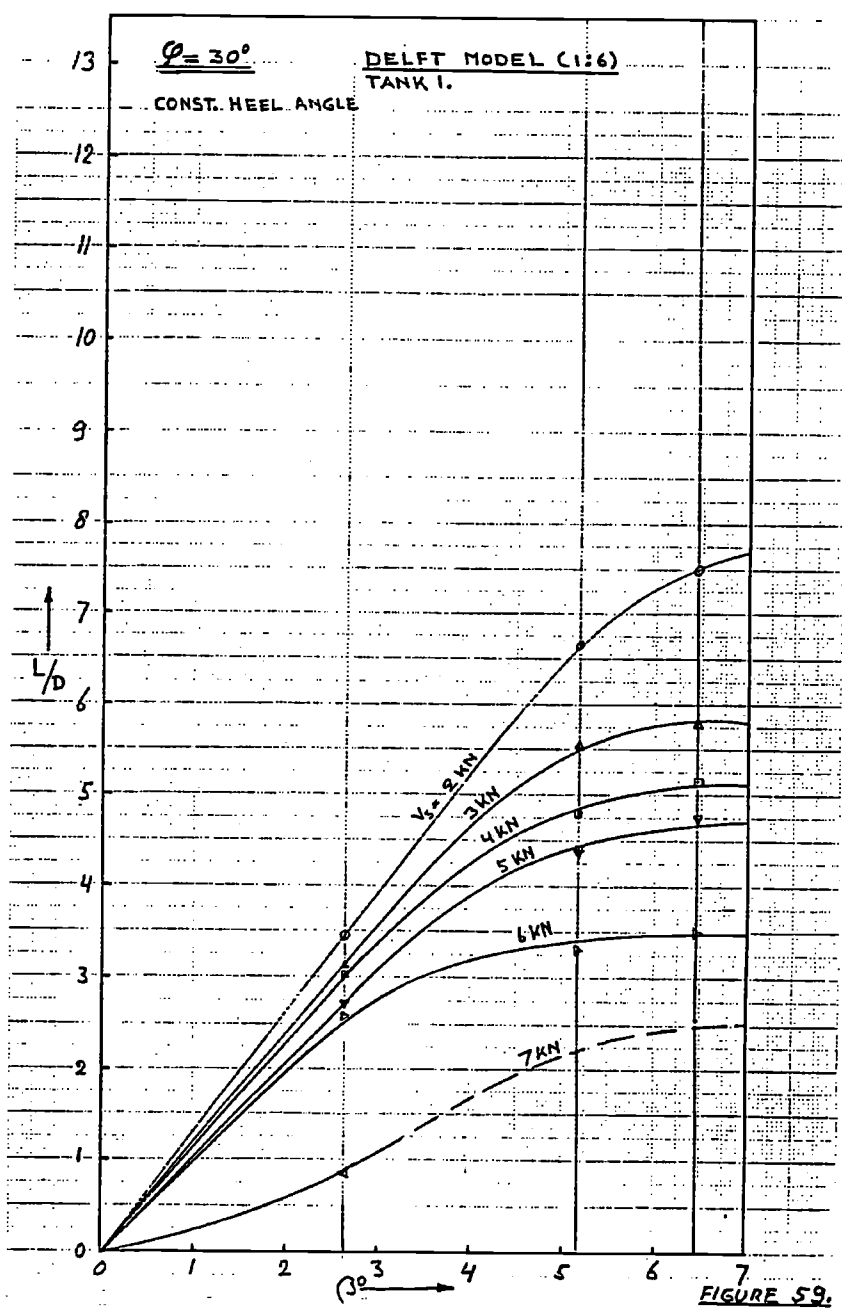
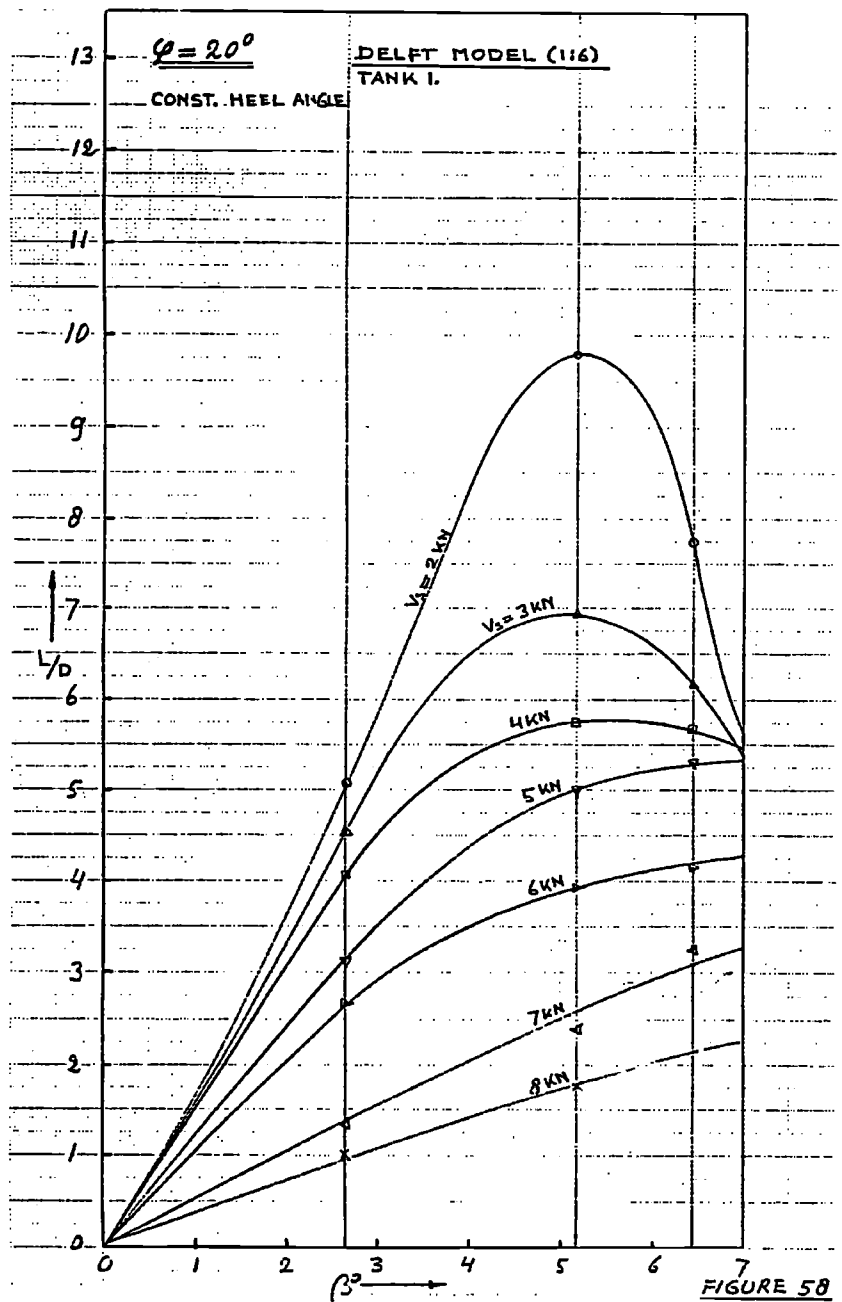
Figures 56 - 59

Constant Heel Angles

Ship - L/D versus  $\beta$

Tank 1





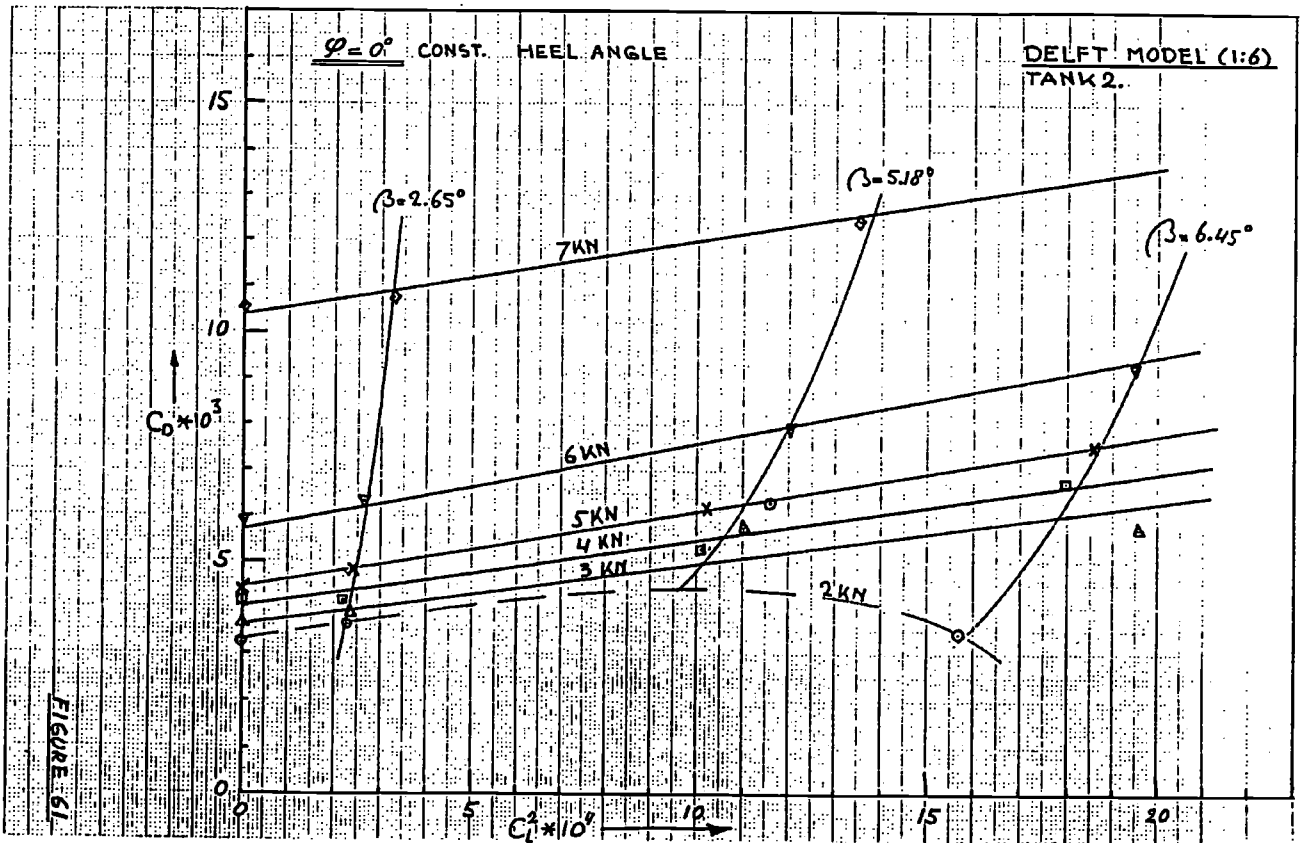
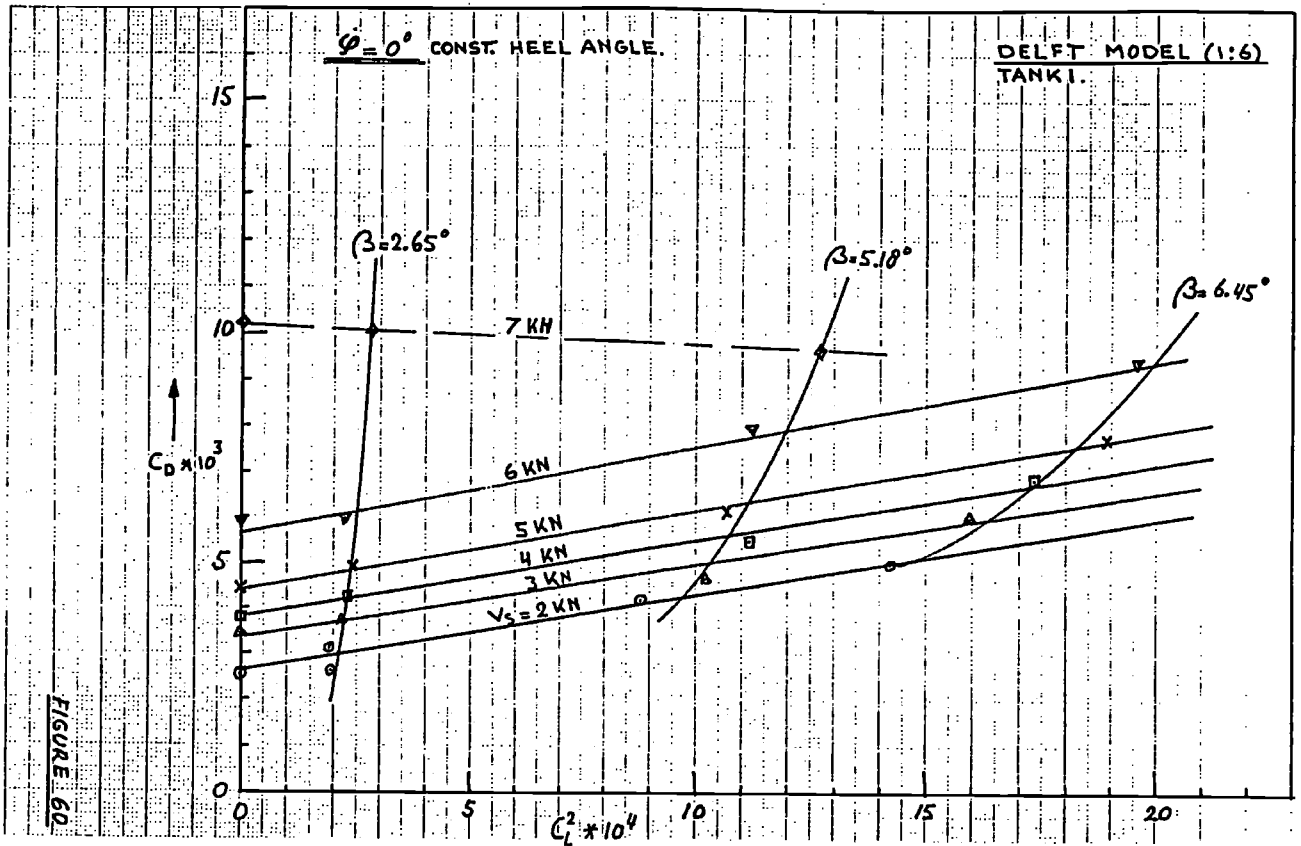
Figures 60 - 67

Constant Heel Angles

Ship  $C_D$  versus  $C_L^2$

Tank 1 and Tank 2





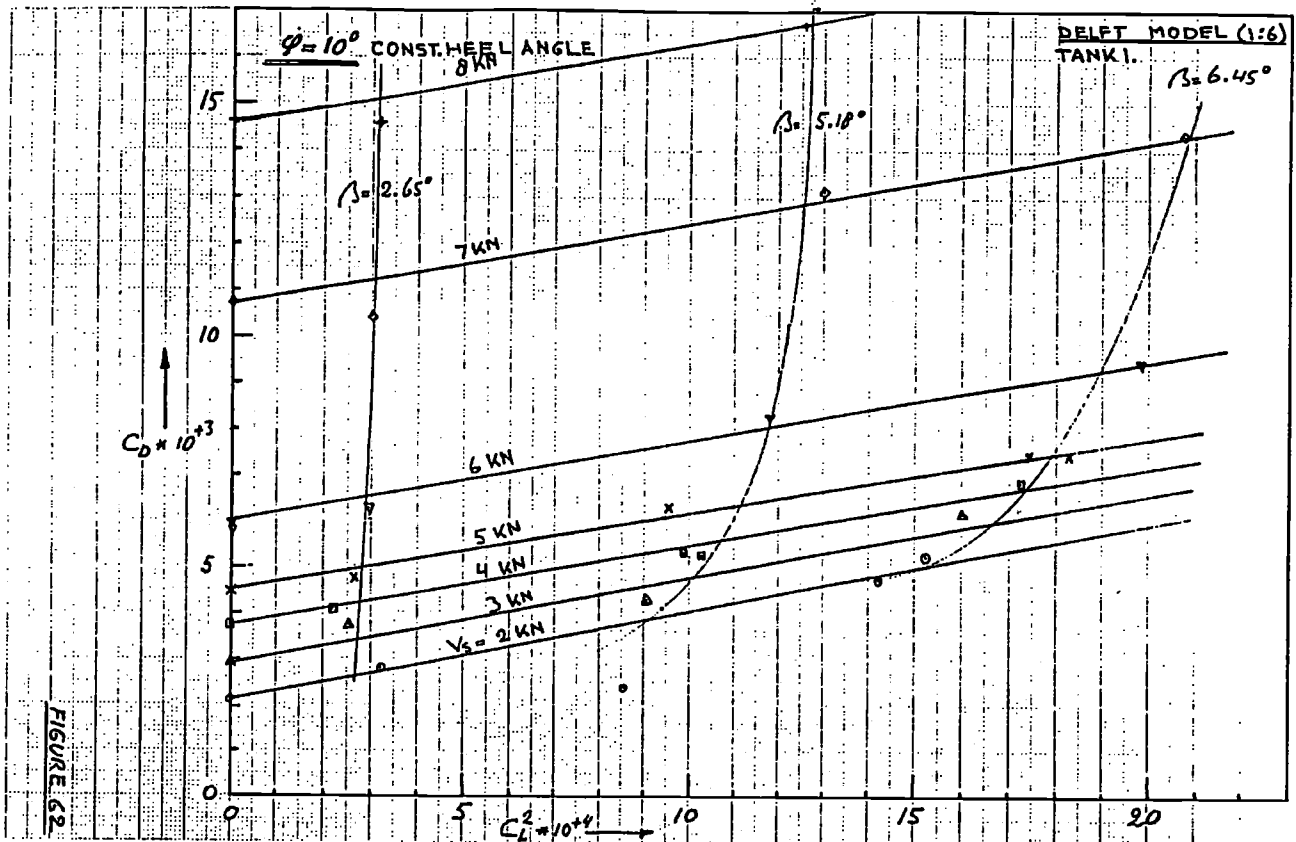


FIGURE 62

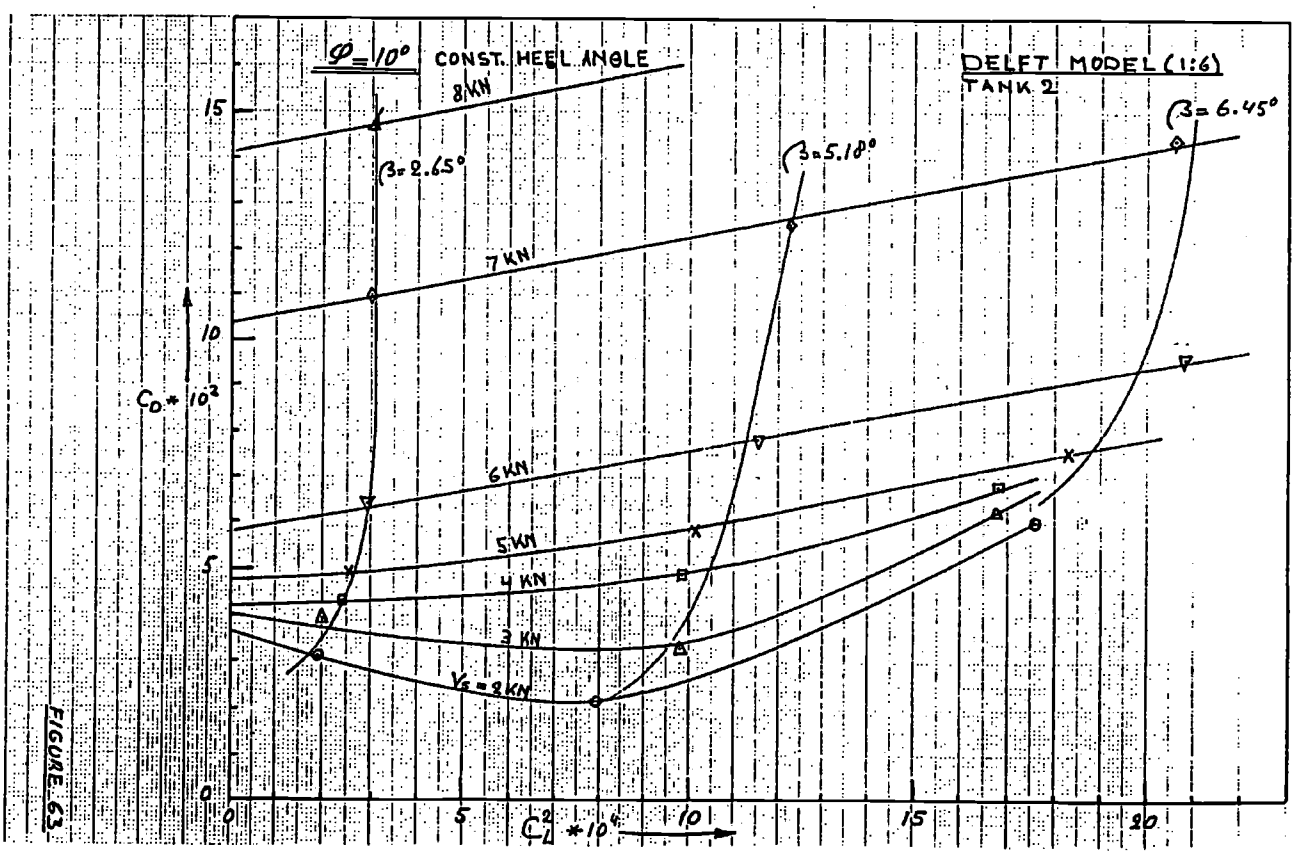


FIGURE 63

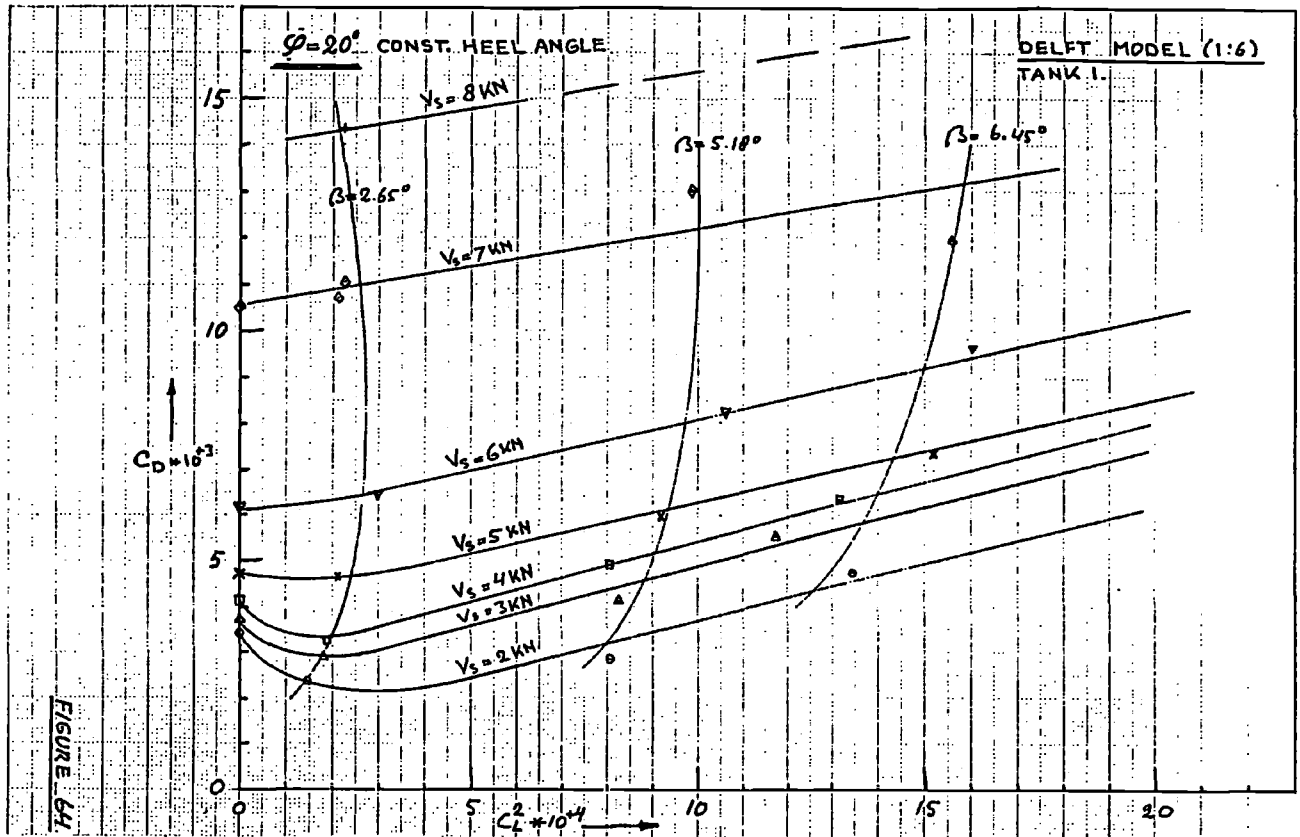


FIGURE 64

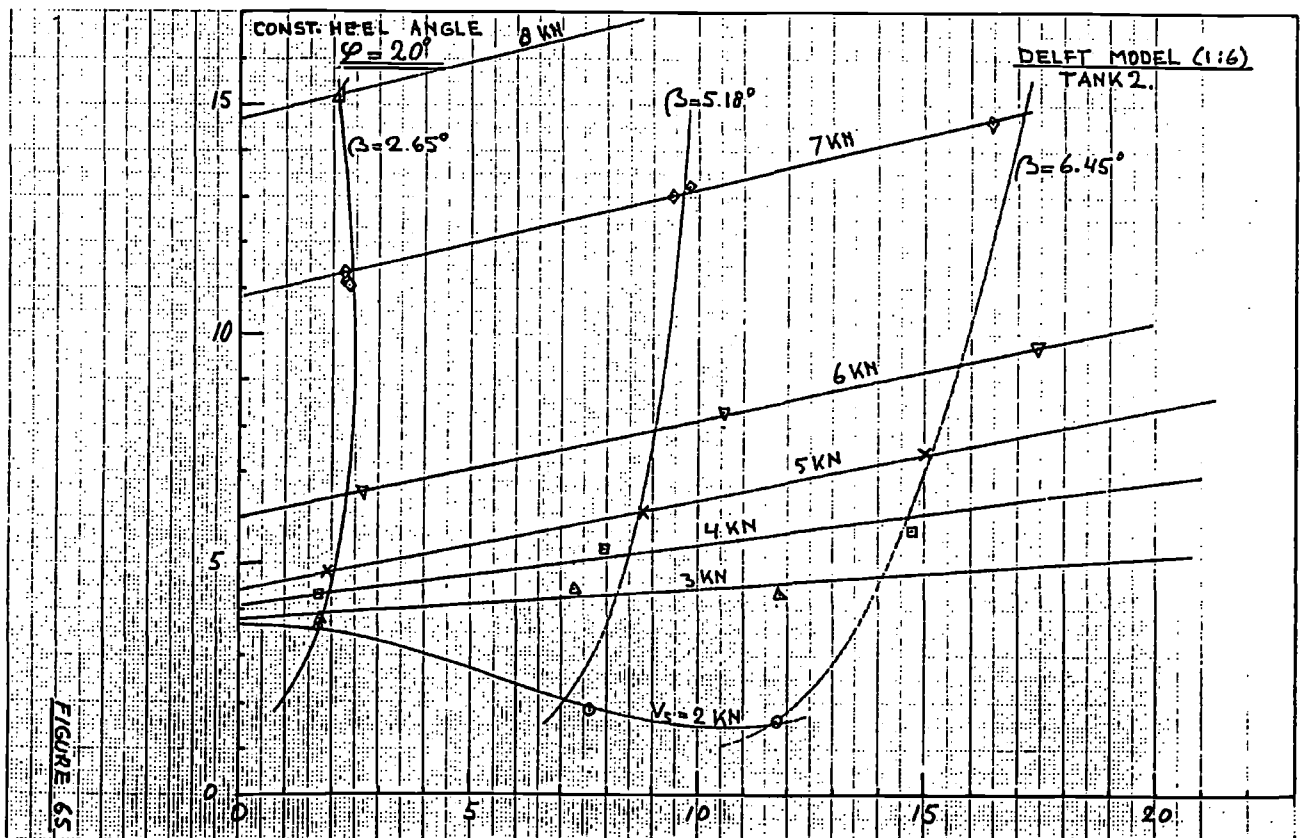
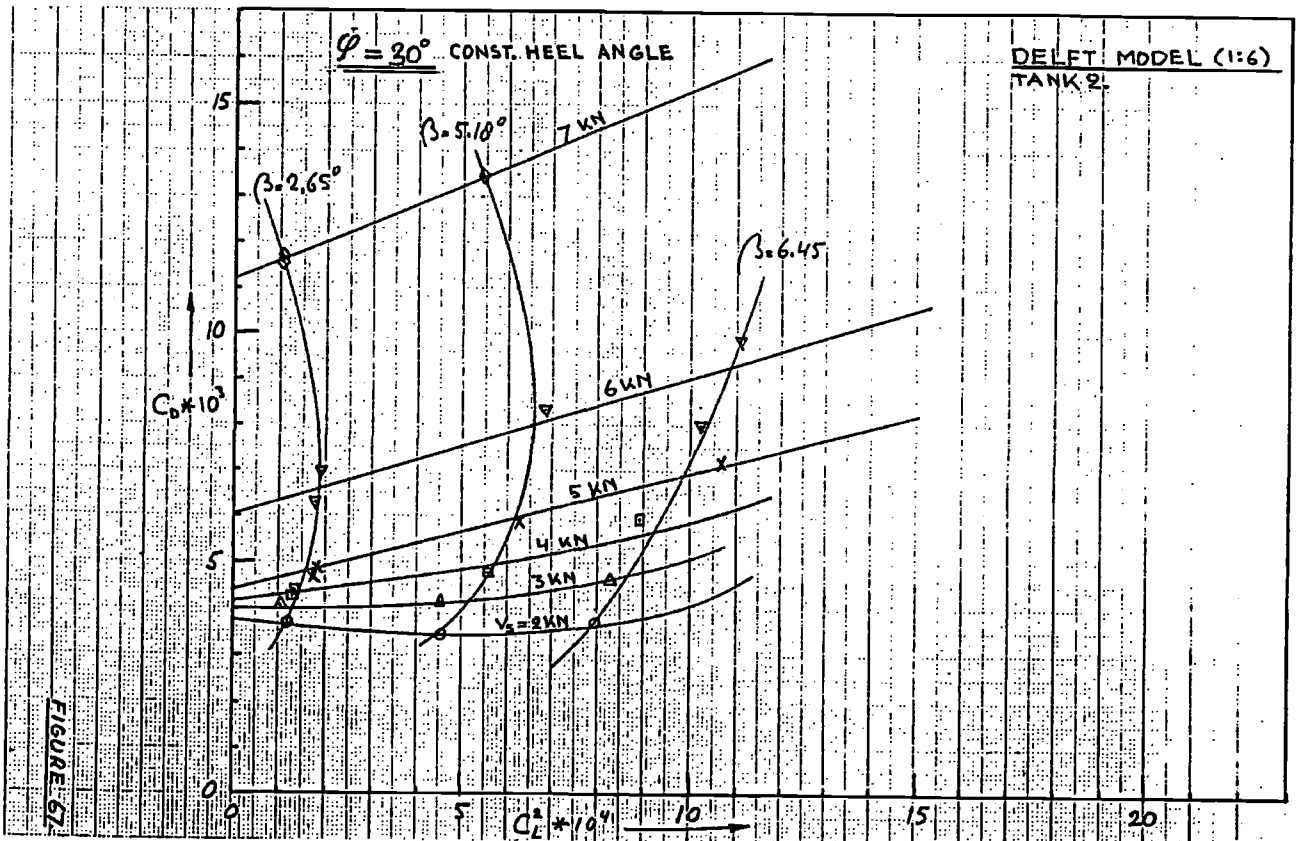
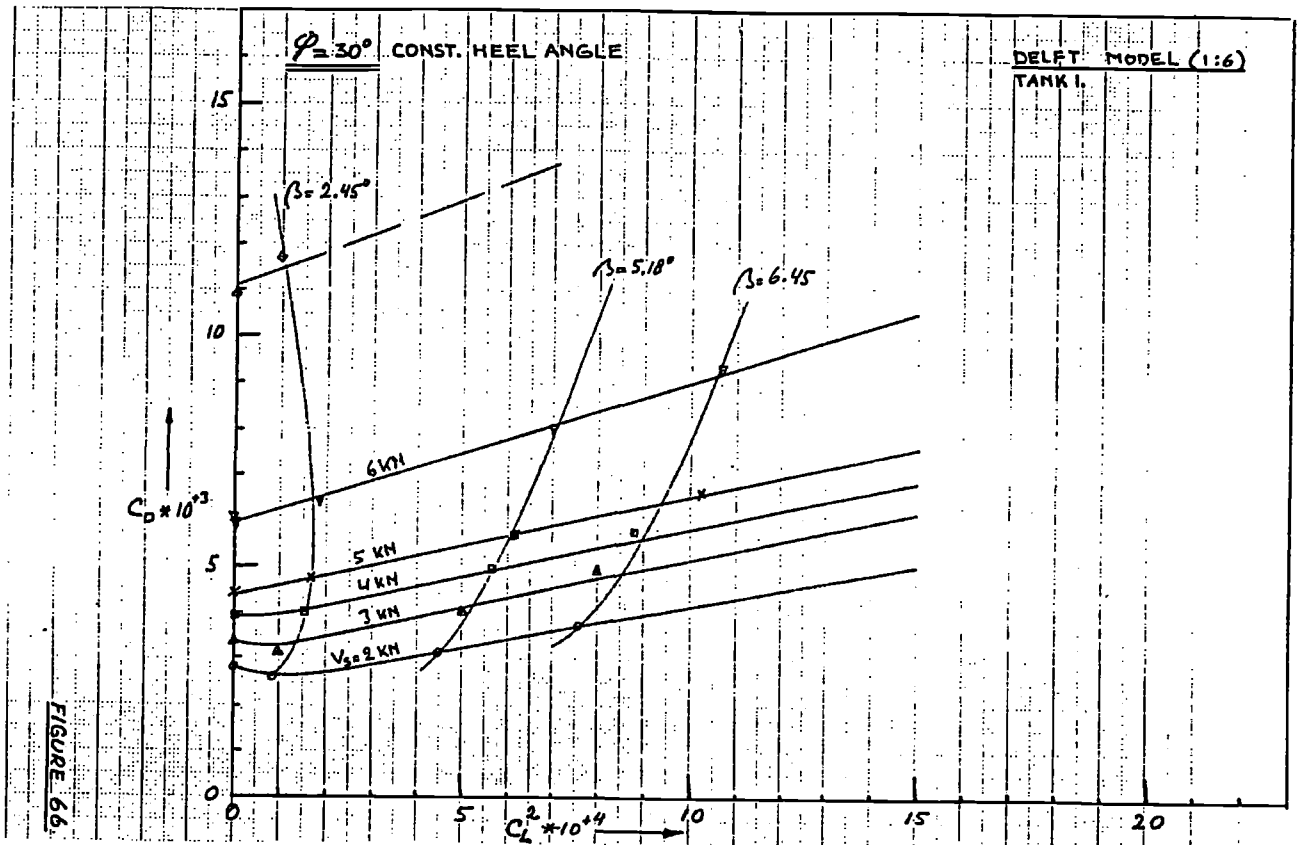


FIGURE 65



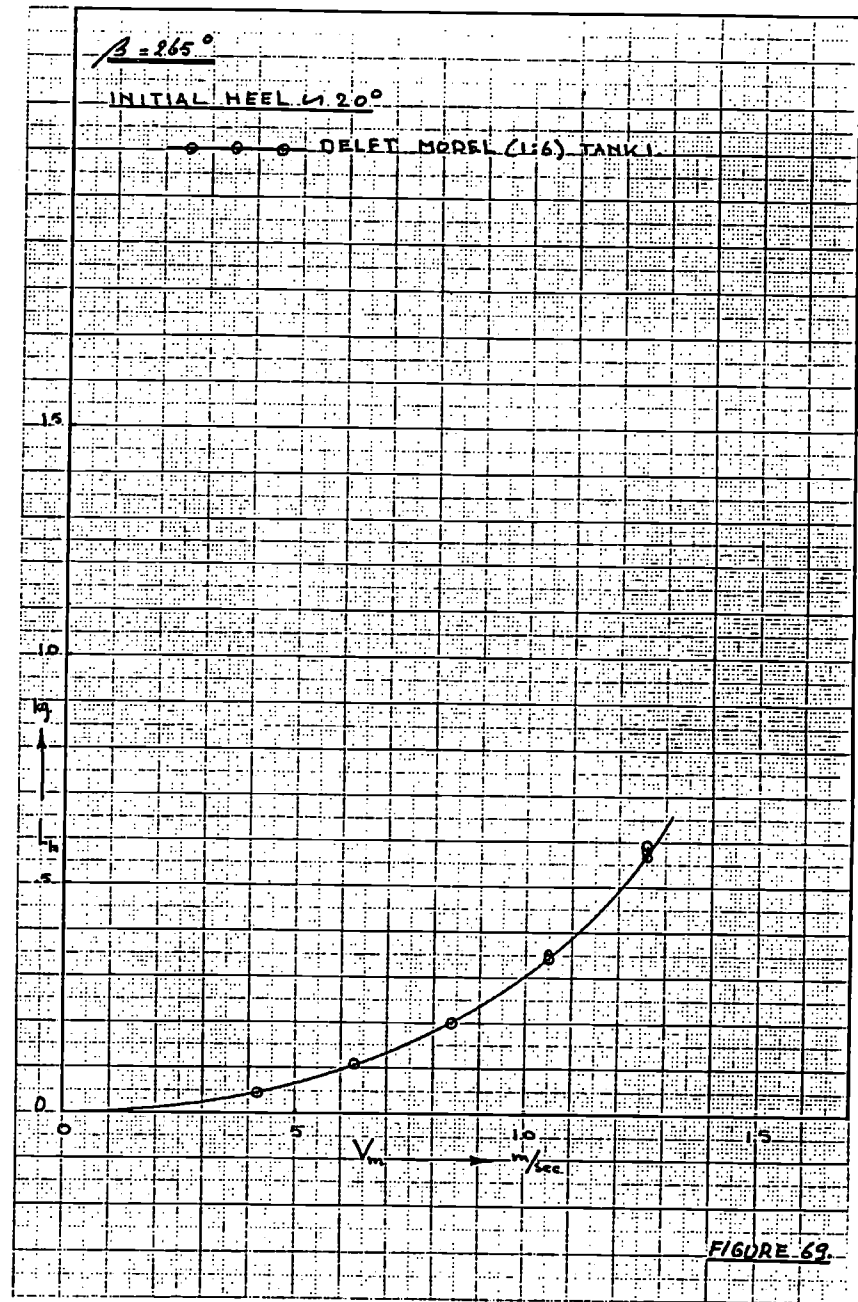
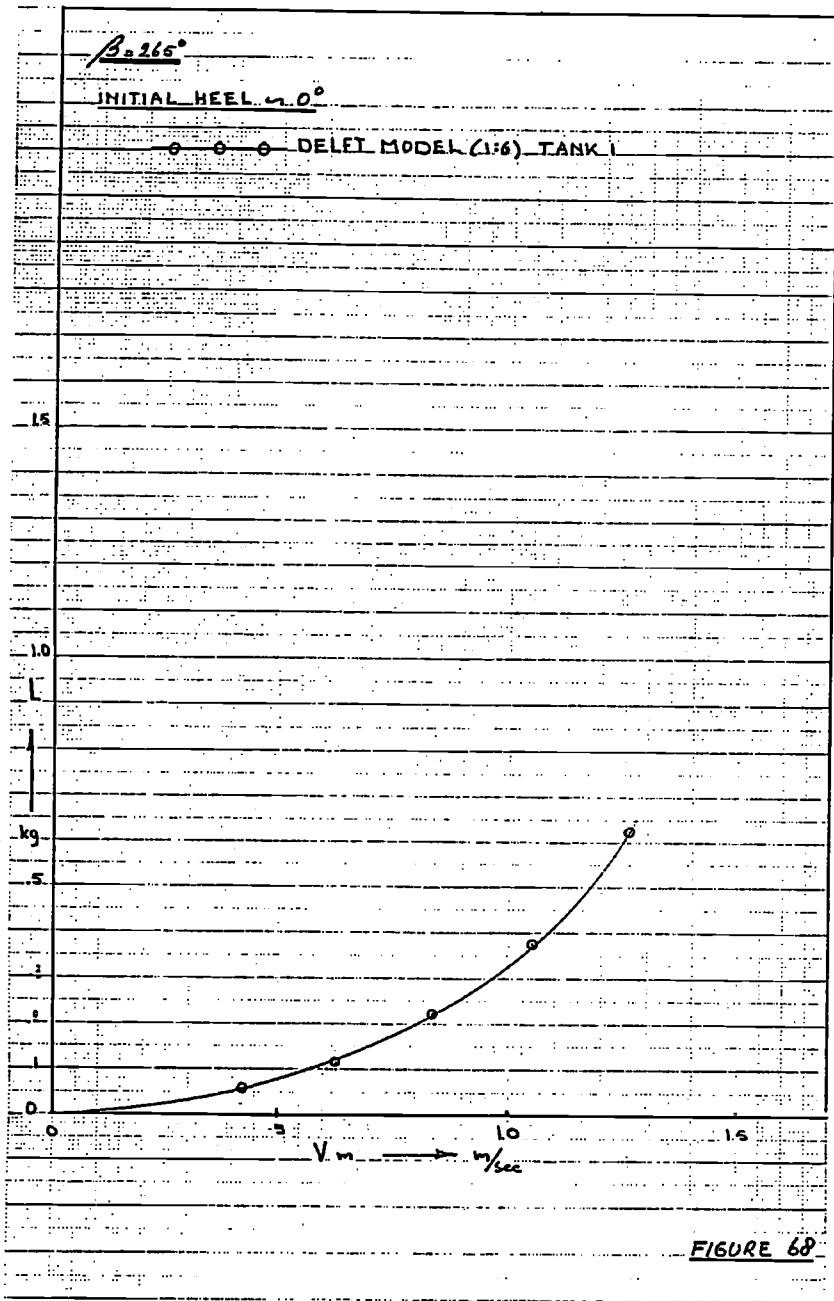
Figures 68 -76

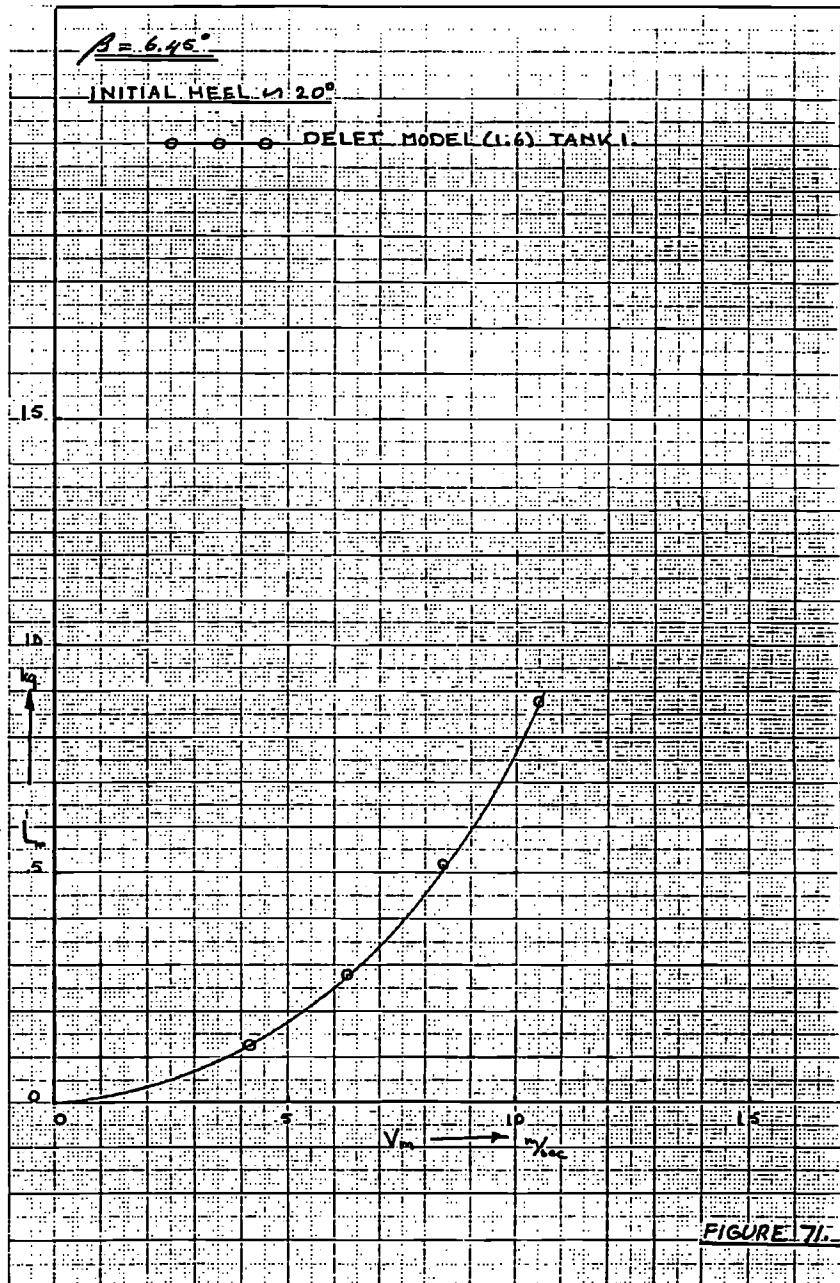
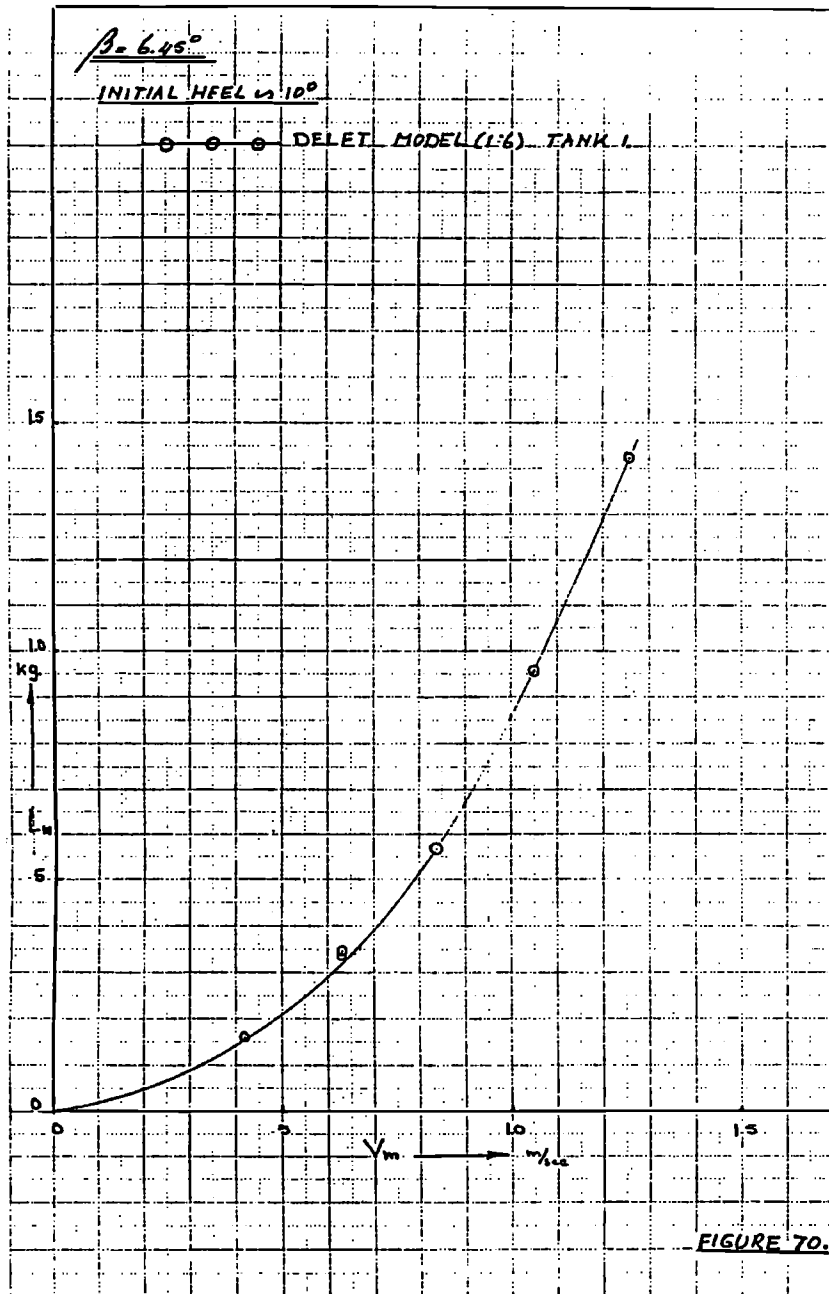
Initial Heel Angles

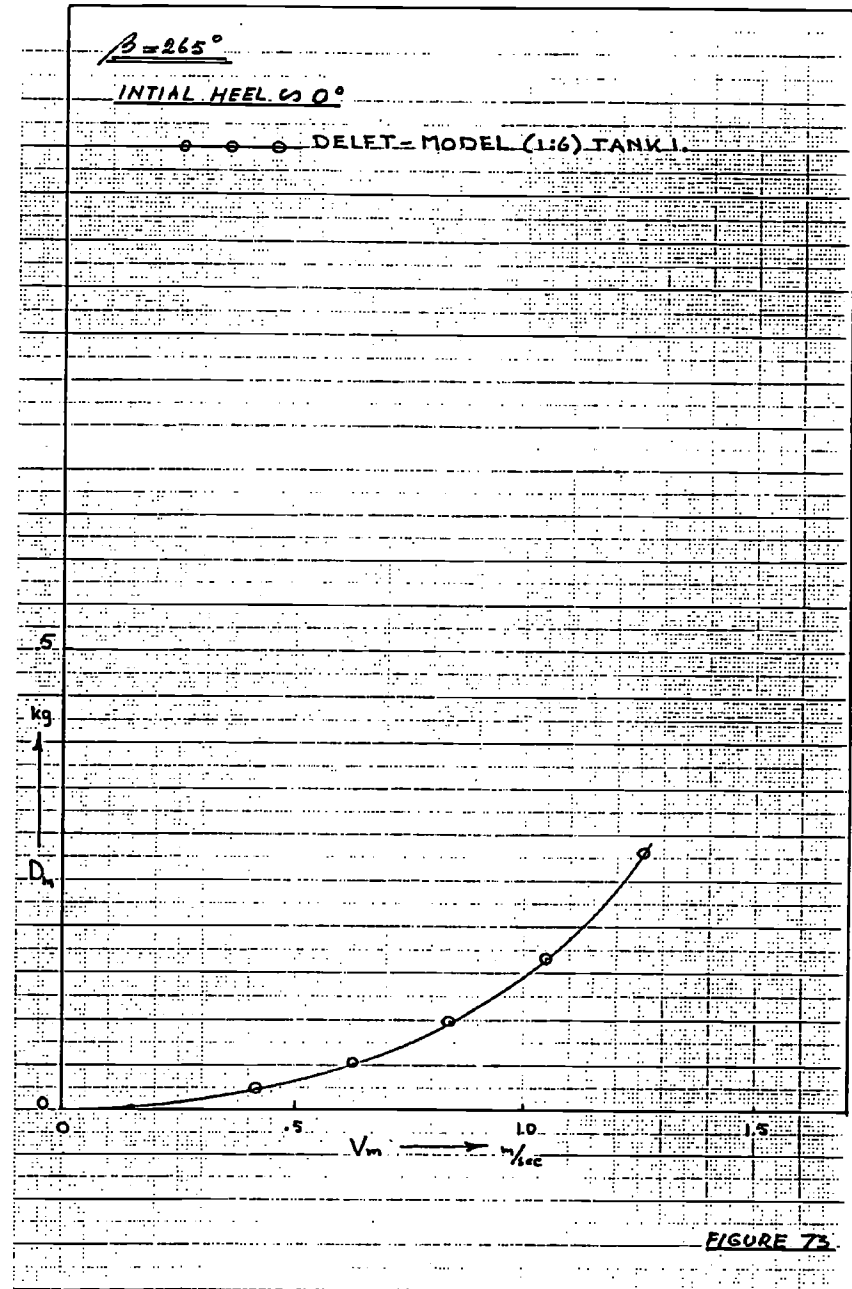
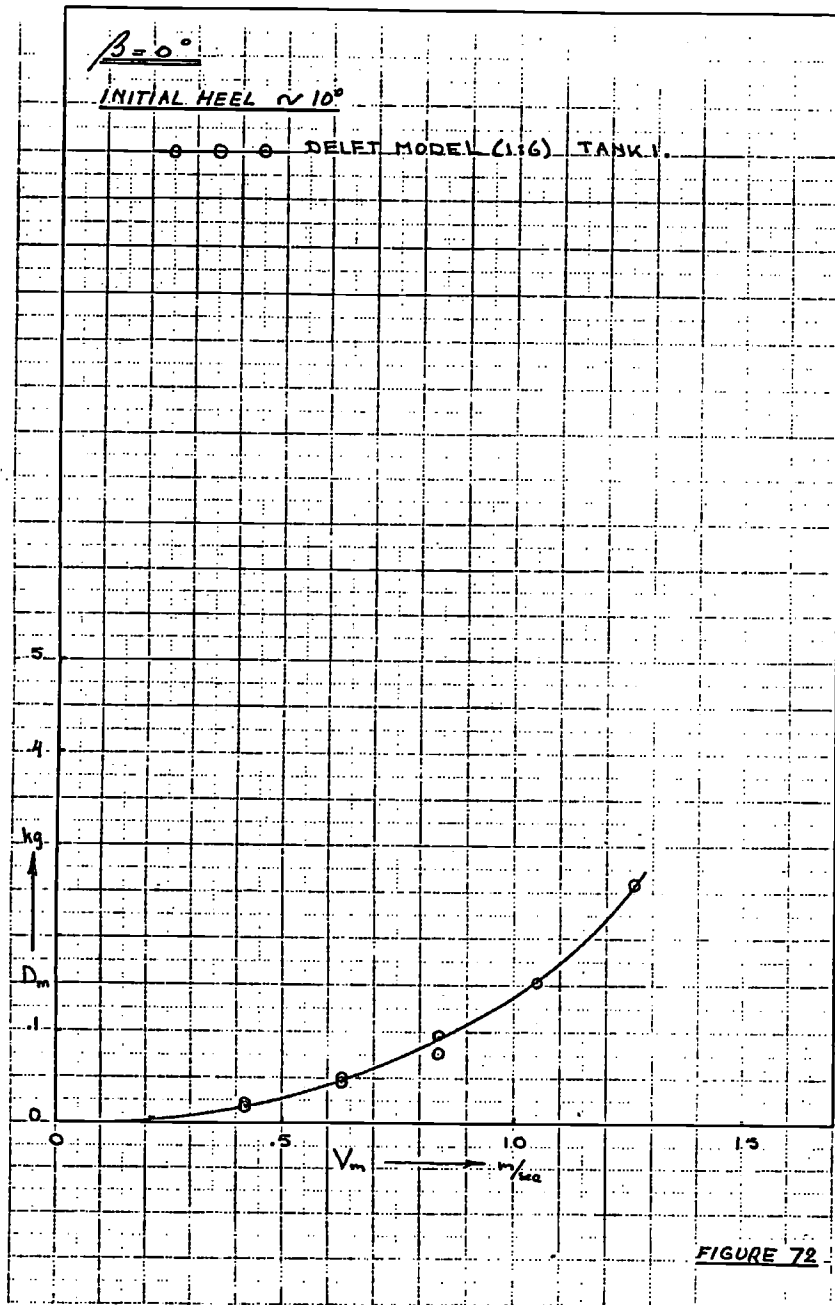
Model Drag versus Speed

Model Lift versus Speed

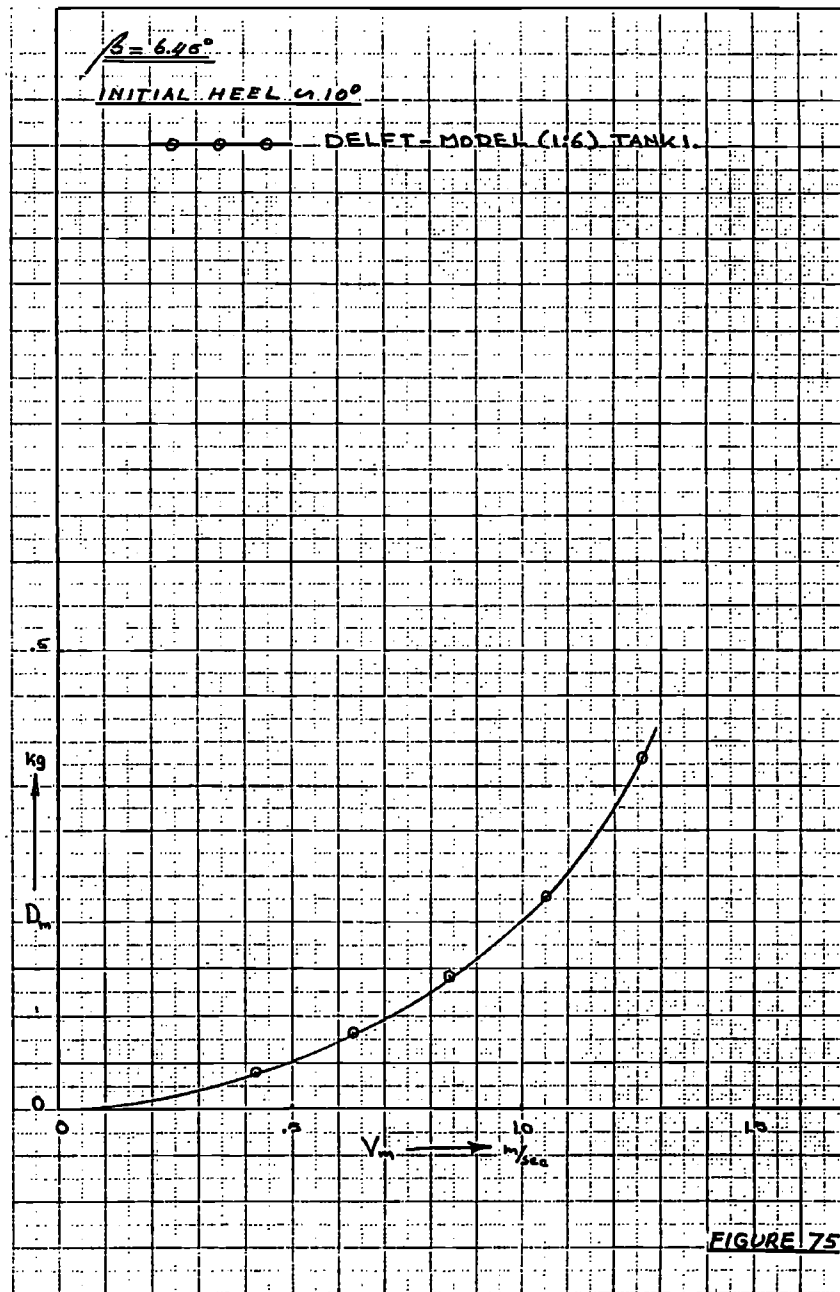
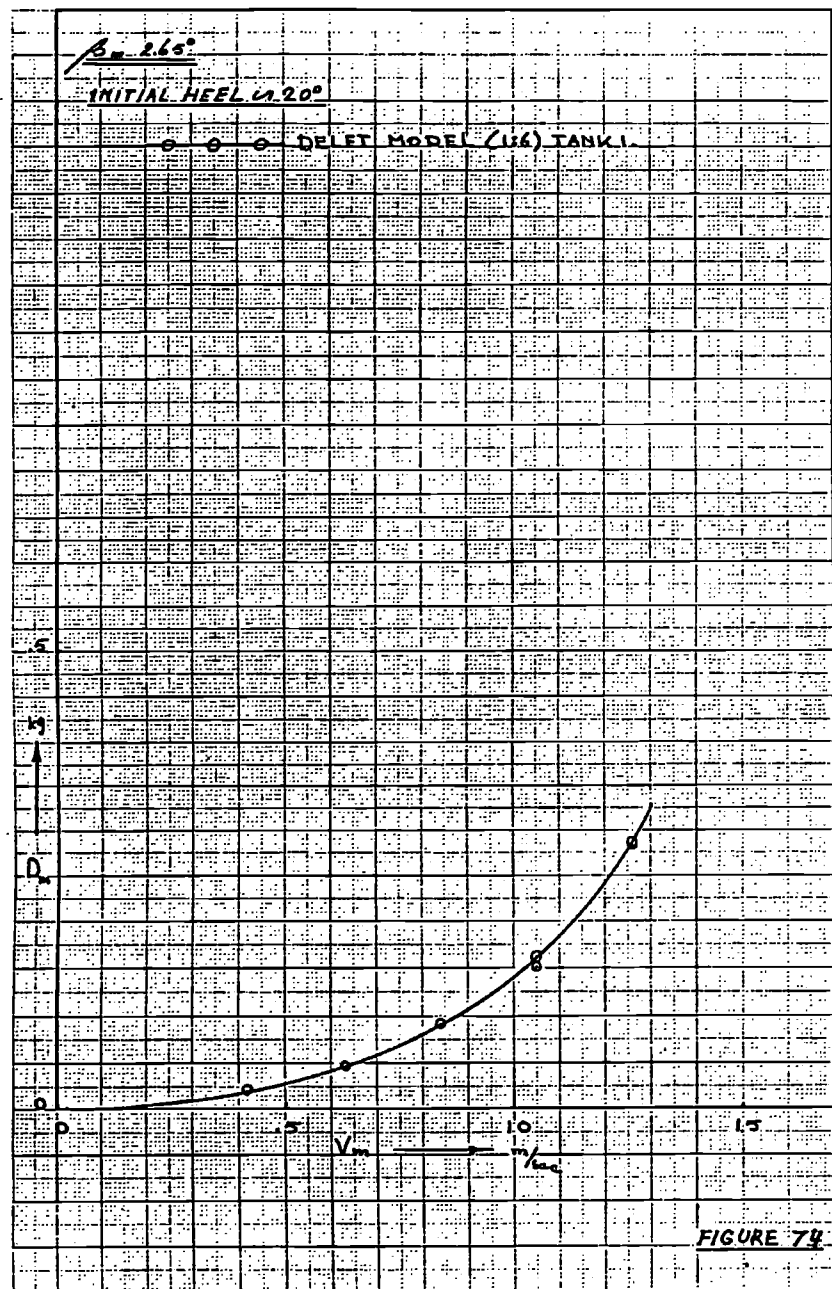
Tank 1











$\beta = 6.45^\circ$

INITIAL HEEL  $\approx 20^\circ$

DELET-MODEL (1:6) TANK 1.

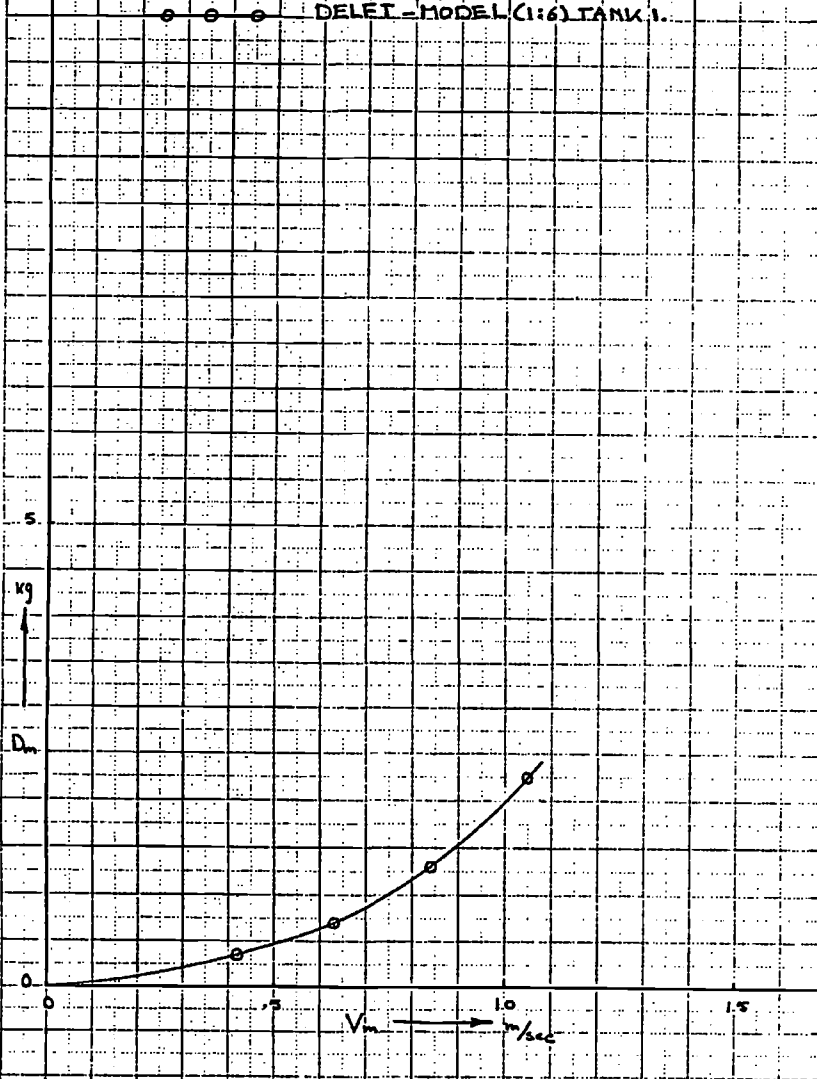


FIGURE 76.

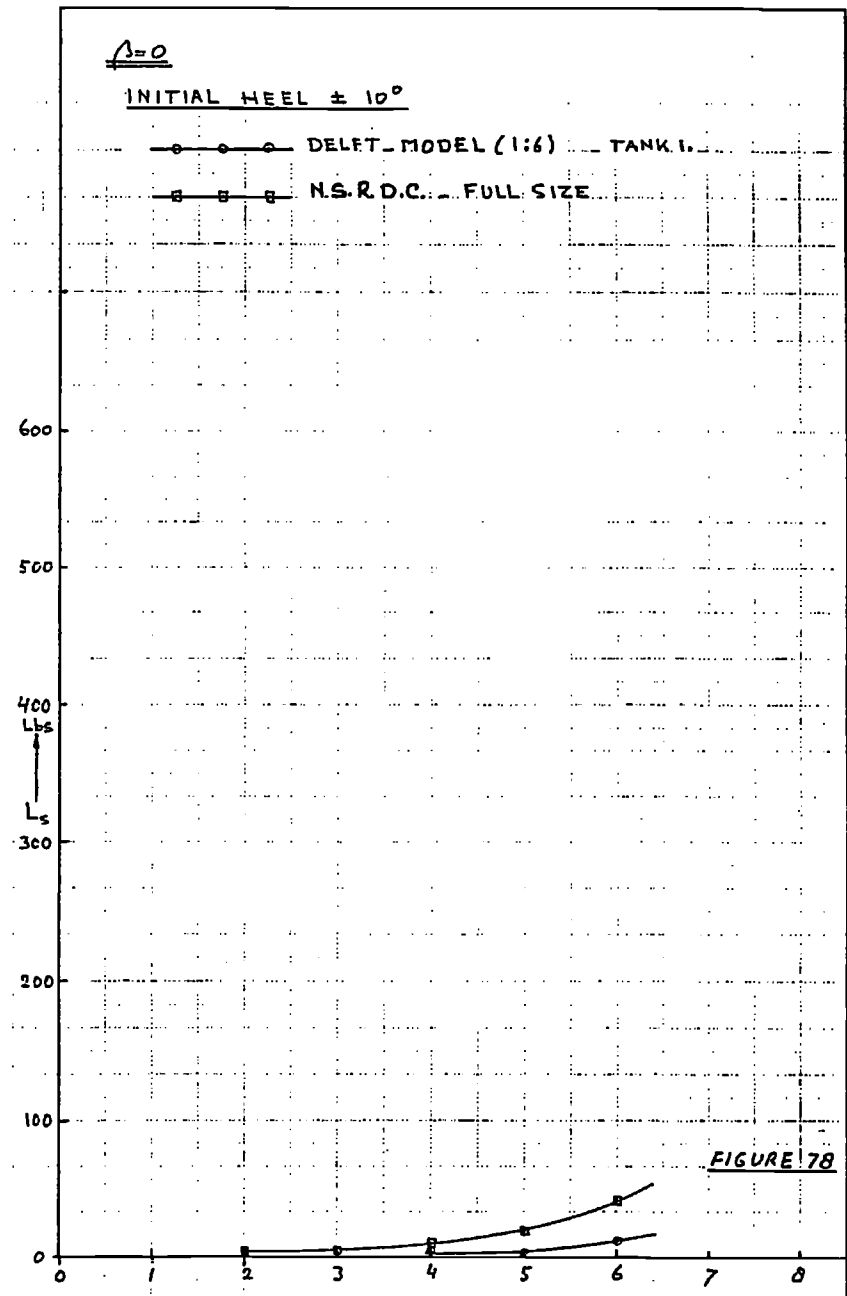
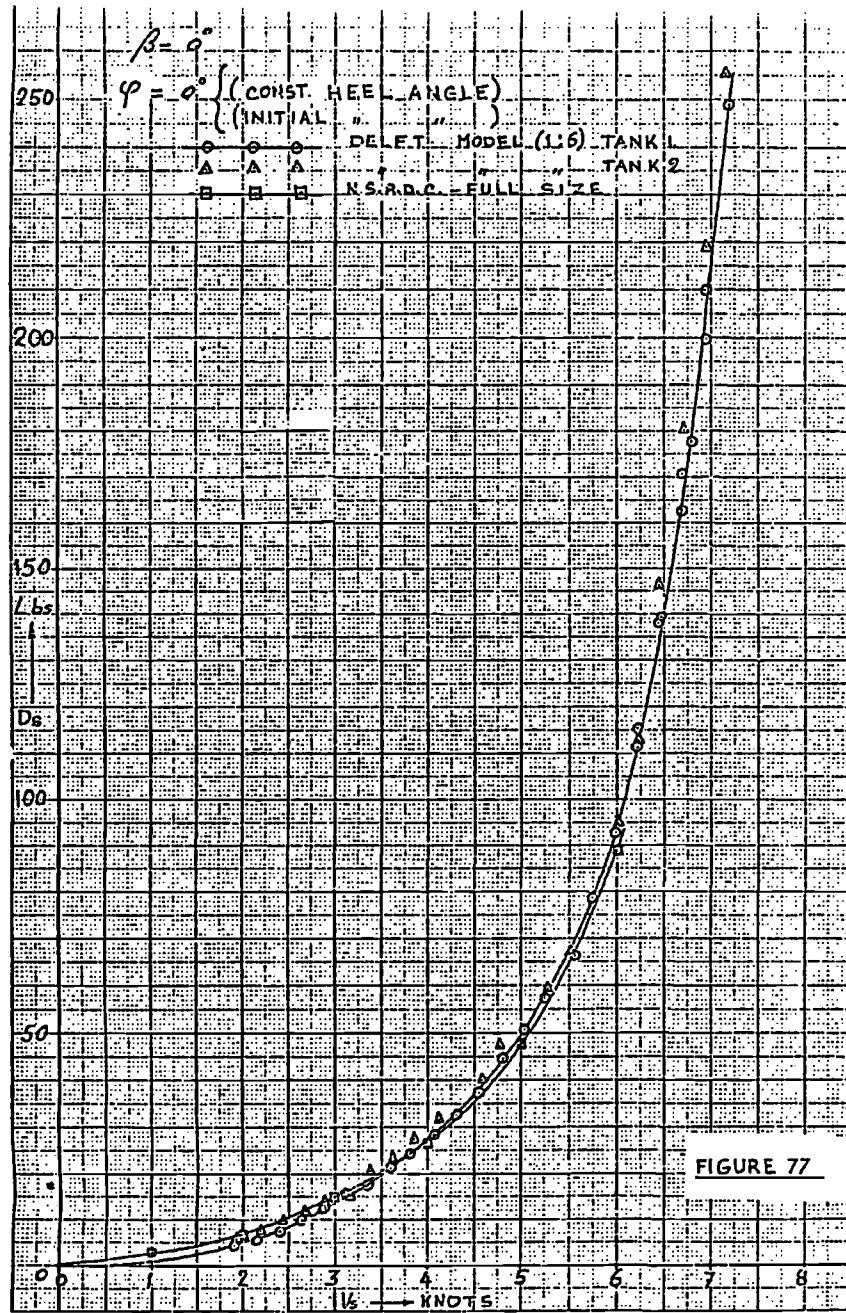
Figures 77 - 87

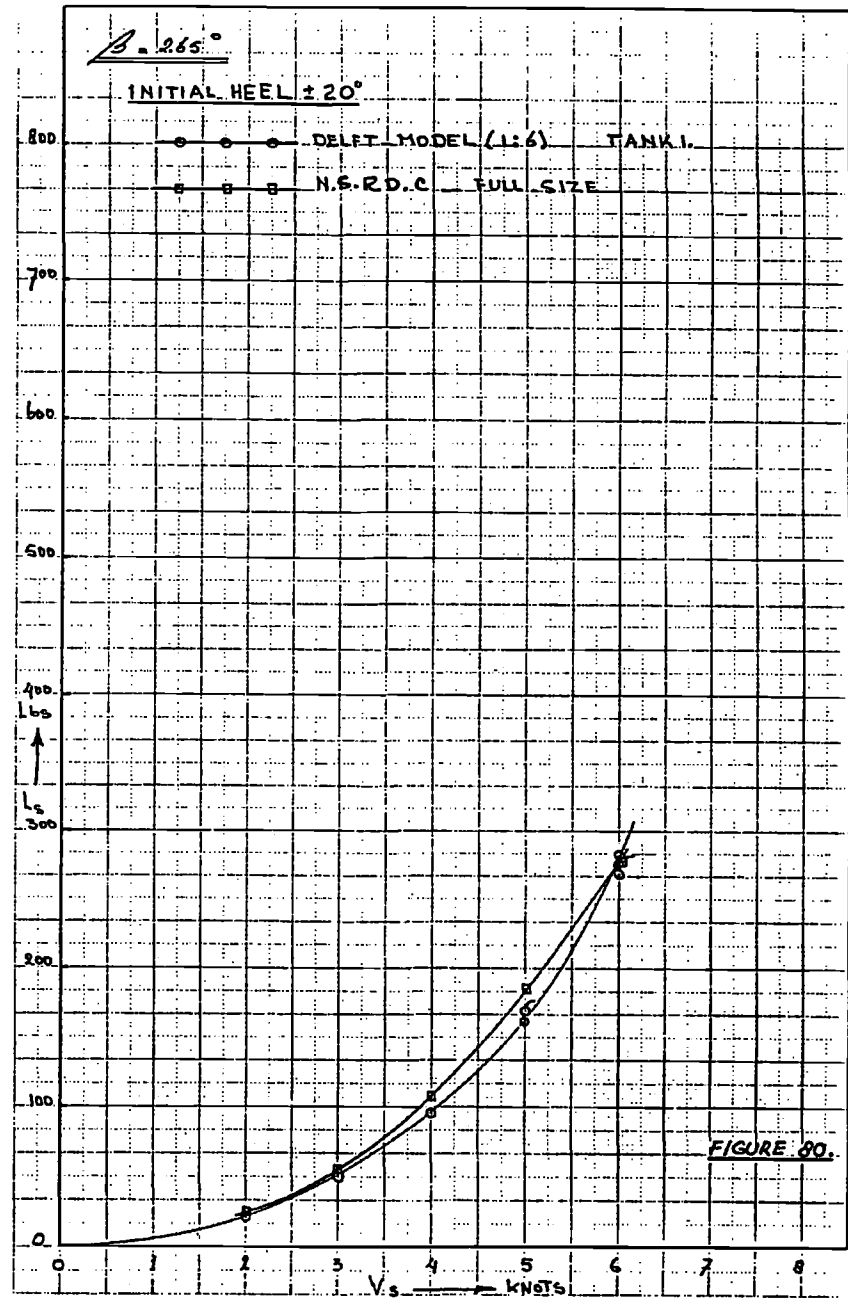
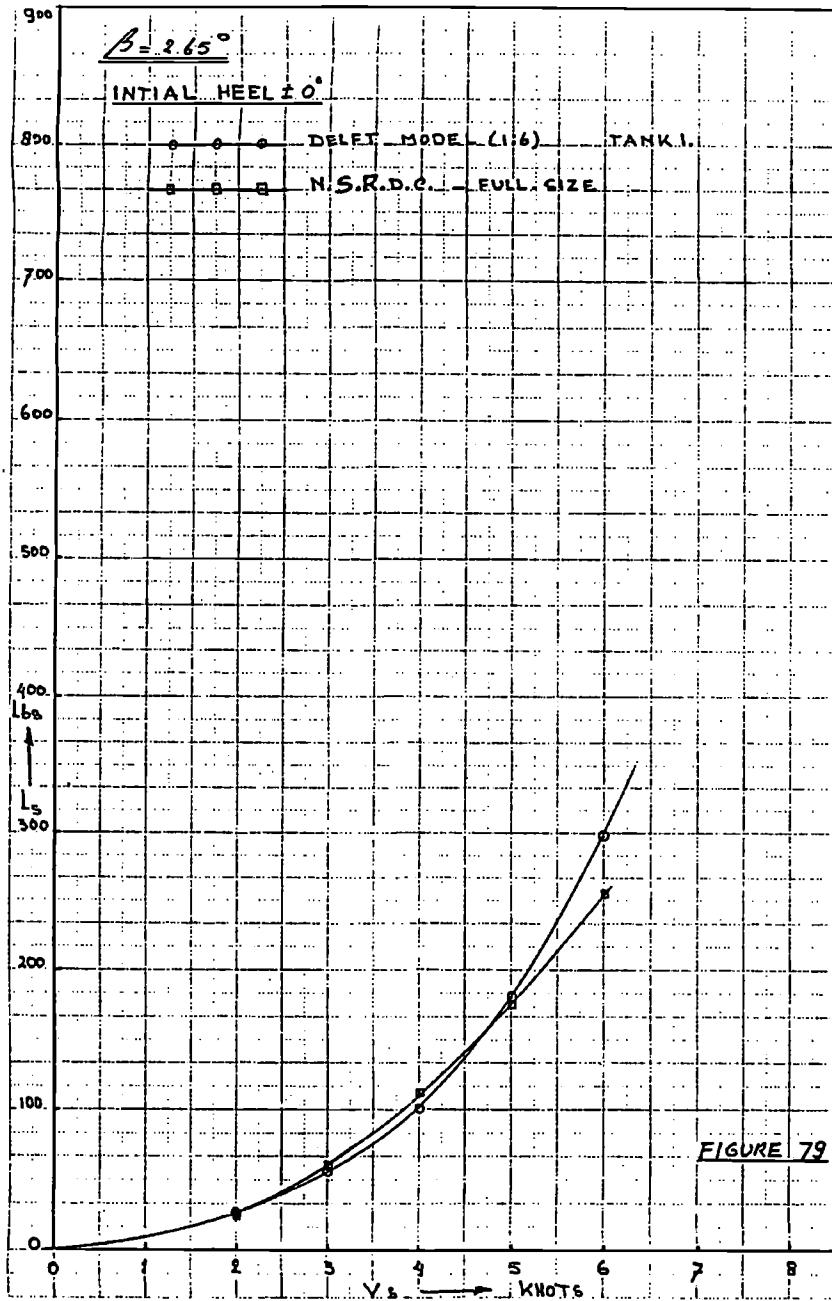
Initial Heel Angles

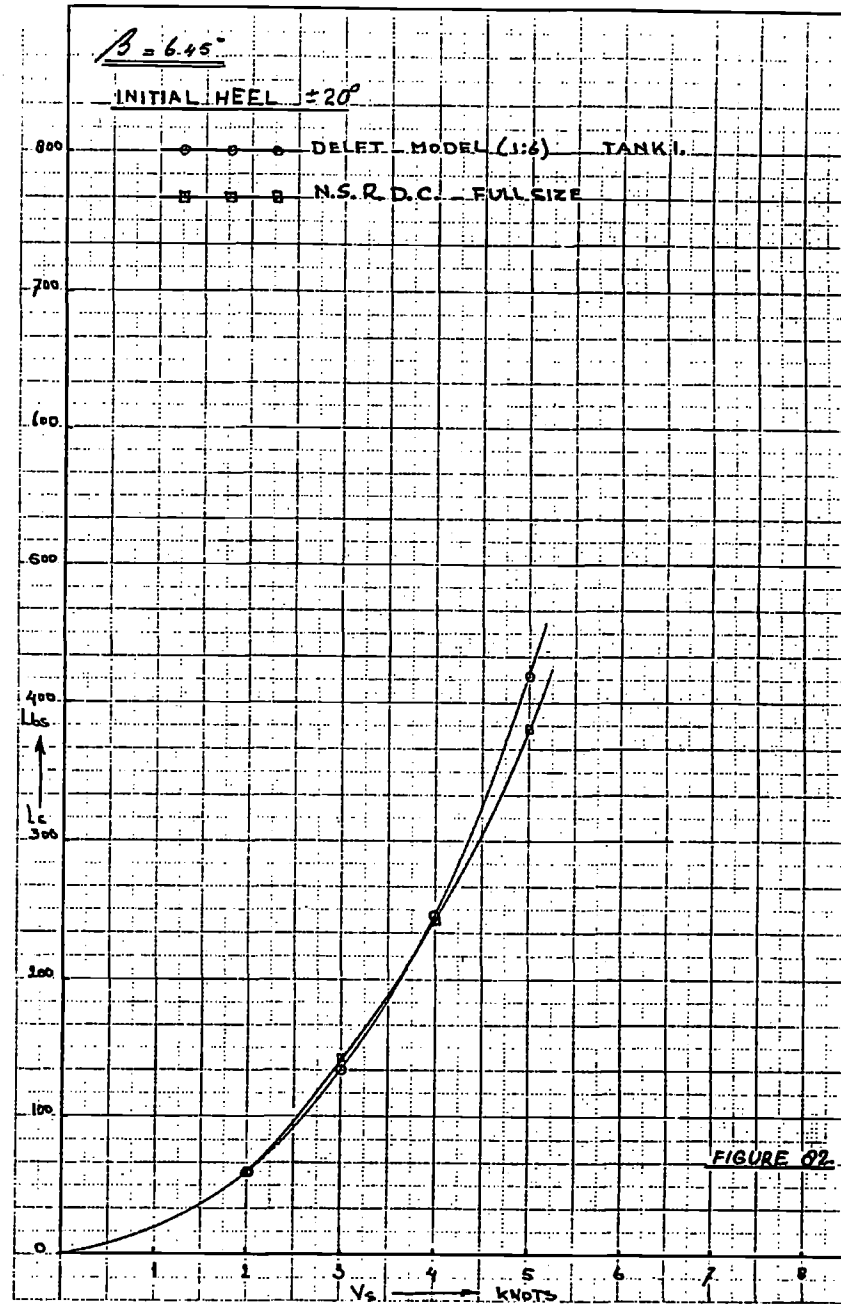
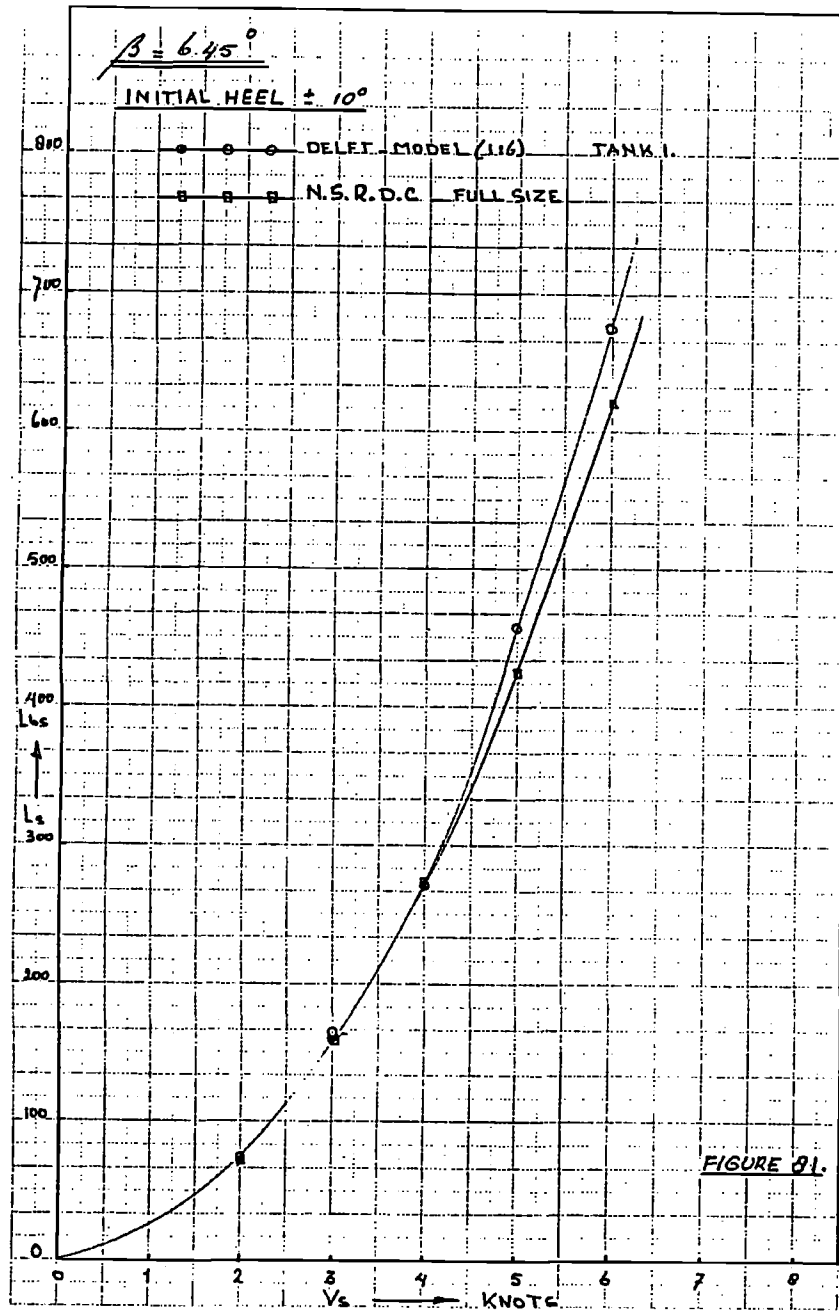
Ship Drag versus Speed

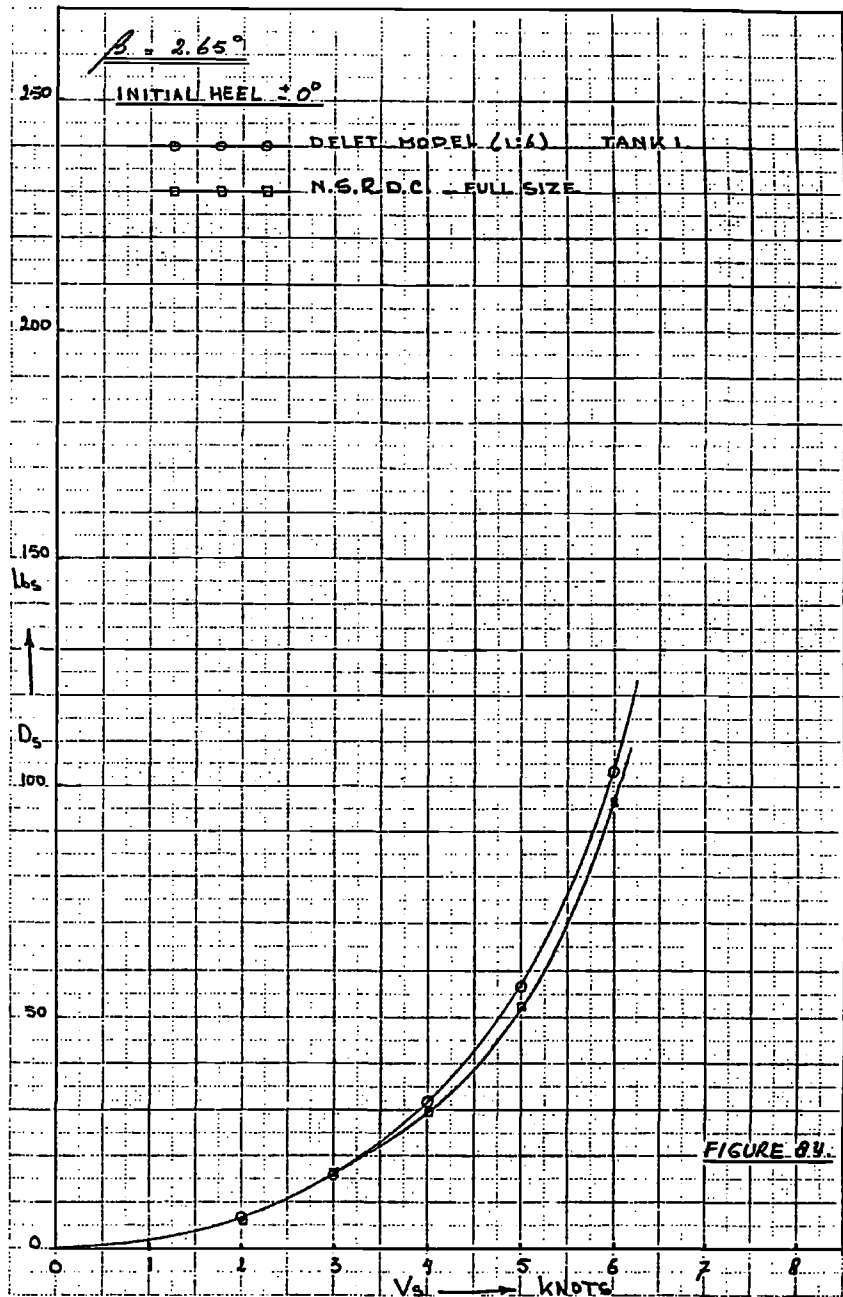
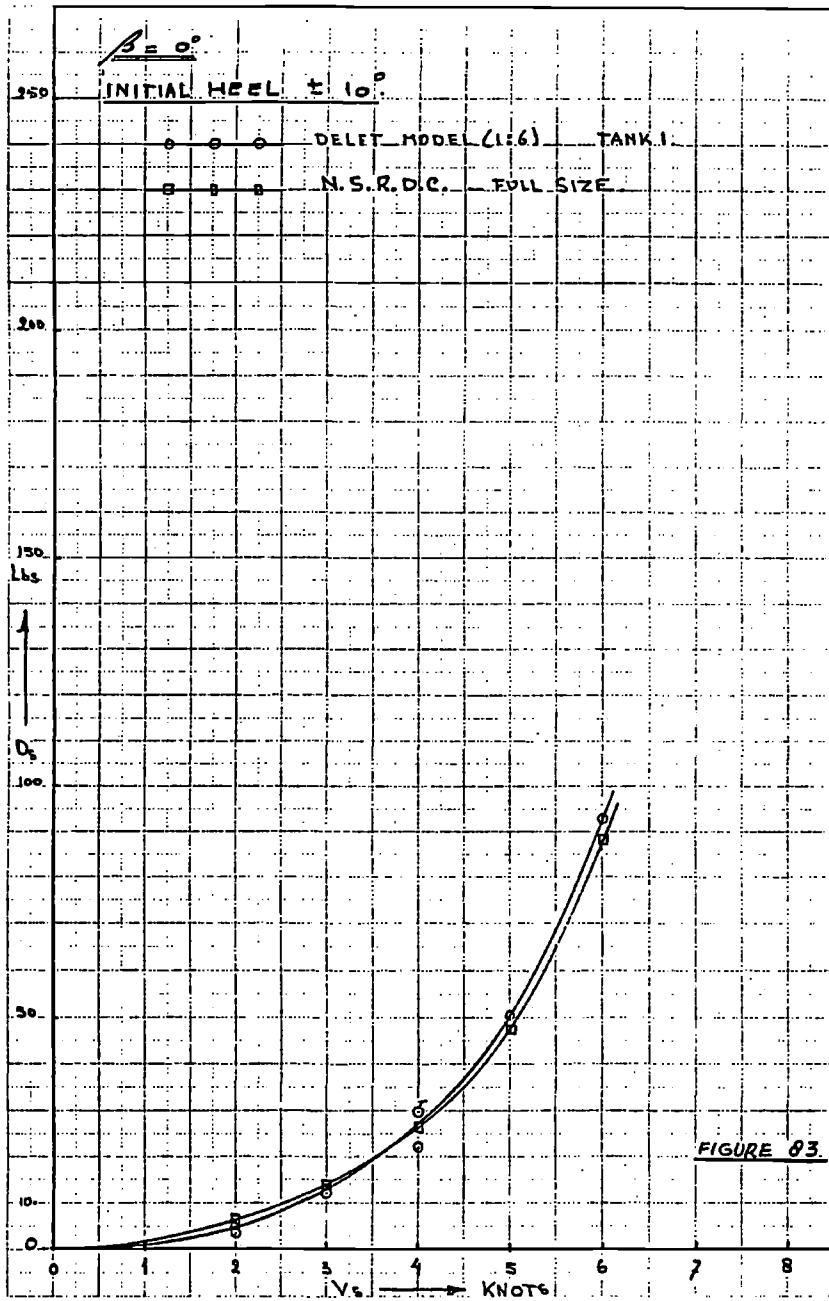
Ship Lift versus Speed

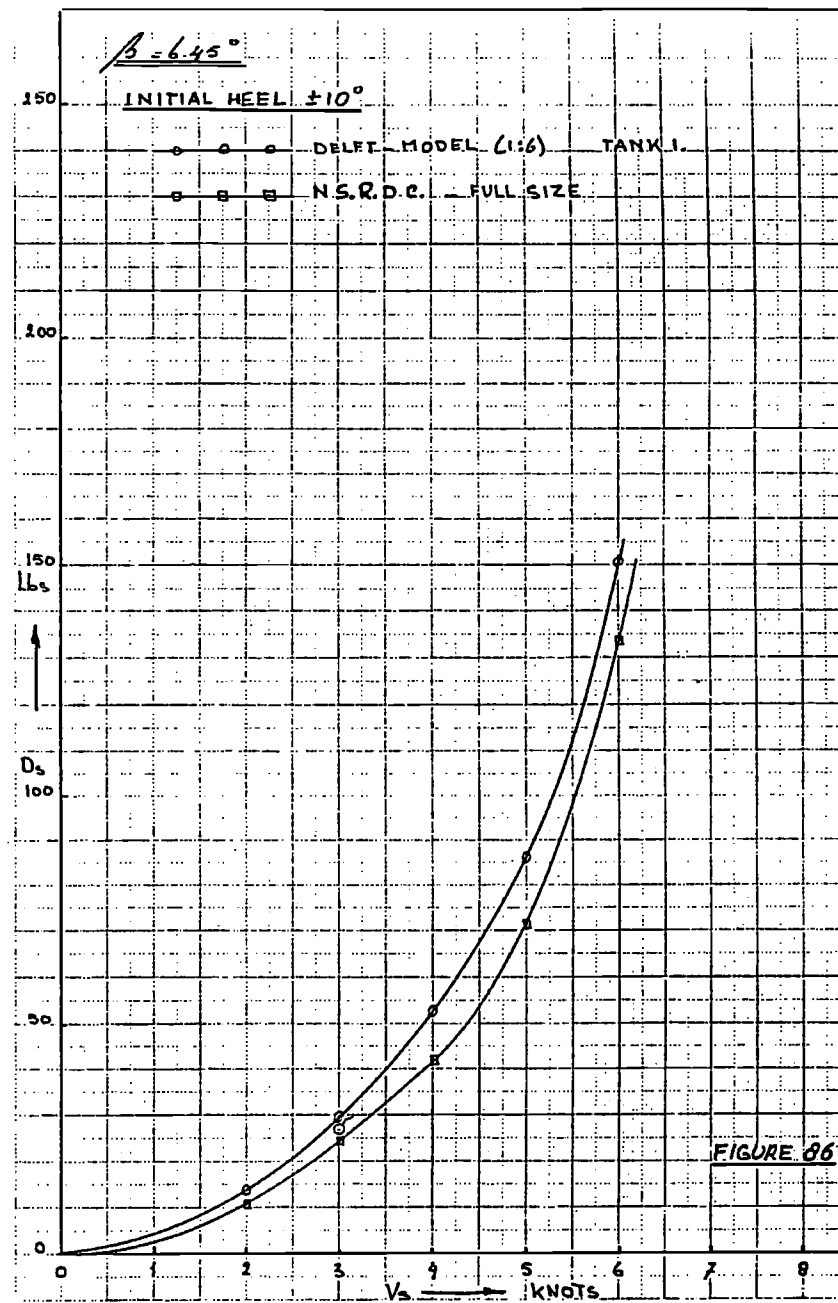
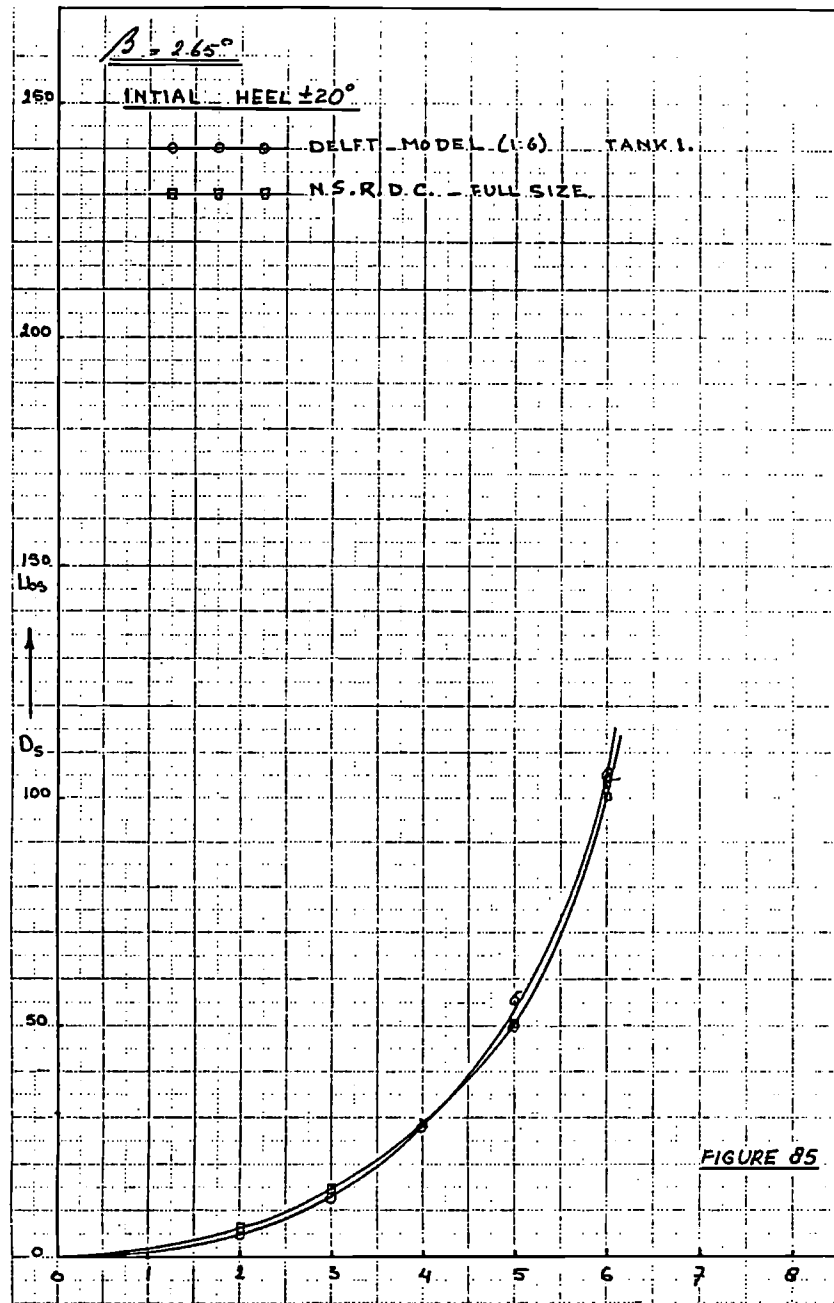
Tank 1



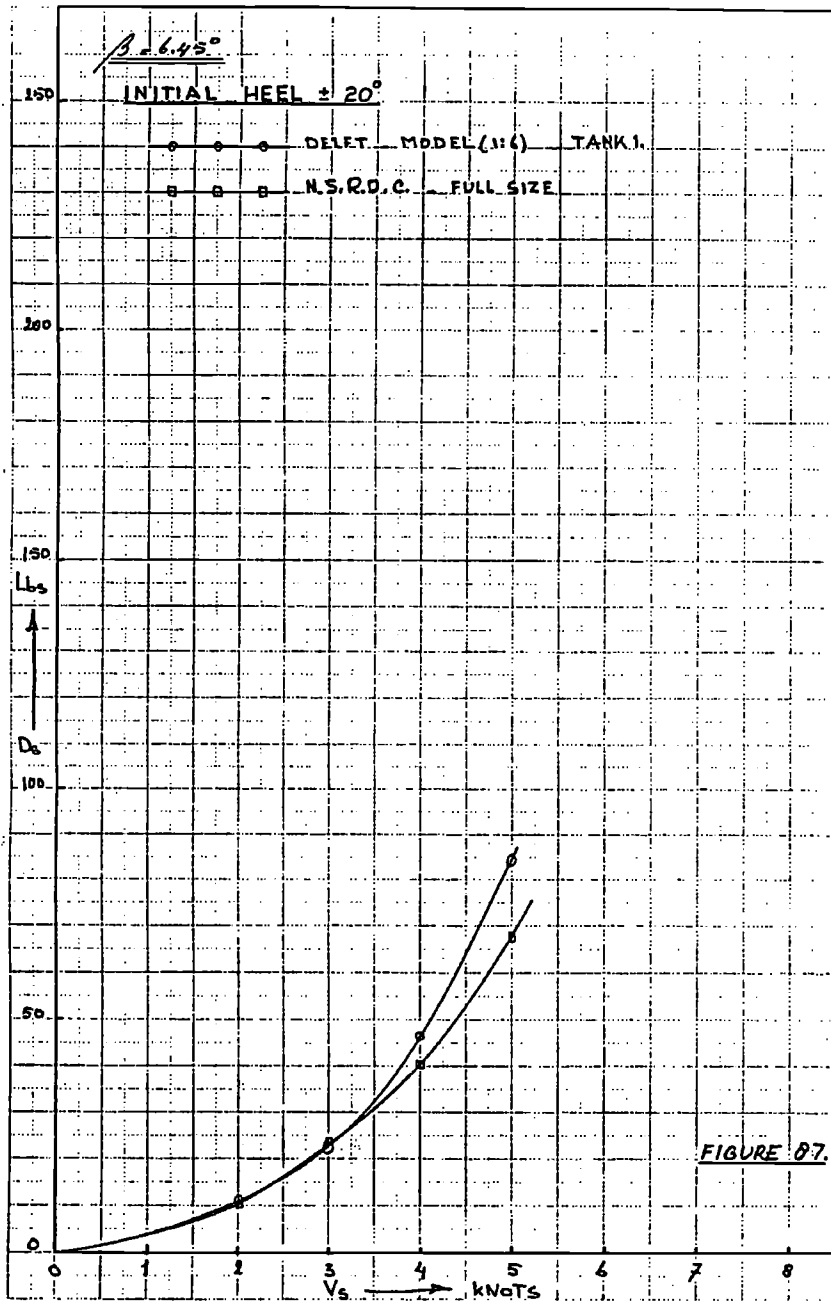












Rapport Nr. 403-P



# LABORATORIUM VOOR SCHEEPSBOUWKUNDE

TECHNISCHE HOGESCHOOL DELFT

THE EFFECTS OF BEAM ON THE HYDRODYNAMIC  
CHARACTERISTICS OF SHIP HULLS

by

J. Gerritsma  
W. Beukelman  
C.C. Glansdorp

Tenth Symposium on Naval Hydrodynamics  
June 24-28, 1974

**TENTH NAVAL HYDRODYNAMICS  
SYMPOSIUM**

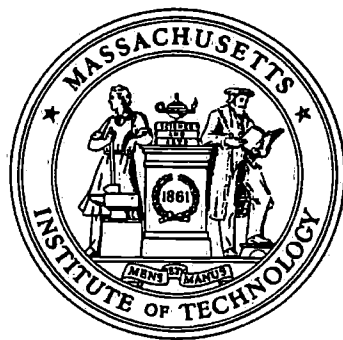
Session I

**TECHNICAL PAPERS**

**Kresge Auditorium**

9:00 am - 12:35 pm

June 24, 1974



# THE EFFECTS OF BEAM ON THE HYDRODYNAMIC CHARACTERISTICS OF SHIP HULLS

J. Gerritsma  
University of Technology  
Mekelweg 2, Delft  
The Netherlands

W. Beukelman  
University of Technology  
Mekelweg 2, Delft  
The Netherlands

C. C. Glansdorp  
University of Technology  
Mekelweg 2, Delft  
The Netherlands

## ABSTRACT

Forced oscillation experiments have been carried out with a systematic ship model family of which the length-beam ratio was ranging from 4 to 20. The experiments also included a thin plate to simulate the case of an infinite length-beam ratio. Vertical and horizontal harmonic motions in calm water have been considered and the corresponding hydrodynamic coefficients have been determined. Moreover the vertical motions and added resistance in waves have been measured. The results are presented in graphical form and are compared with some existing calculation methods.

## NOMENCLATURE

A, B, C, D, E, G	hydrodynamic coefficients of the equations of pitch and heave respectively	$x'$	dimensionless length coordinate in a right hand body fixed coordinate system with centre of gravity in the origin and the starboard side positive
B	ship's beam	$x'_b, y'_b, z'_b$	righthand coordinate system fixed to ship with the origin situated in the ship's waterline and the portside positive
$C_B$	block coefficient	$x'_1$	dimensionless centre connected with the first moment of viscous force distribution
$C_P$	prismatic coefficient	$x'_2$	dimensionless centre connected with the second moment of viscous force distribution
$C^s$	horizontal sectional added mass coefficient	$x'_y$	point of application of total yaw force
$c^s$	wave celerity	$x'_z$	point of application of total sway force
F	total vertical wave force	$y'$	dimensionless hydrodynamic lateral force
$F'$	sectional hydromechanic force	$y'_0$	dimensionless motion amplitude
$F_n$	Froude number	$y_w$	half width of waterline ( $z=0$ )
g	acceleration owing to gravity	z	heave displacement
$I_{yy}$	vertical longitudinal moment of inertia	$\epsilon$	phase angle
$I_{zz}$	dimensionless horizontal moment of inertia	$\lambda$	wave length
$K'$	coefficient of accession to moment of inertia	V	volume of ship's displacement
K	empirical coefficient in the low aspect ratio lift formula	$\omega$	circular wave frequency
$K_{1,2}$	coefficients of accession (long., lat.)	$\omega'$	dimensionless PMM frequency
$k_{yy}$	vertical longitudinal radius of inertia of ship	$\omega_e$	circular frequency of encounter
$k_{zz}$	horizontal longitudinal radius of inertia of ship	$\rho$	density of water
L	ship's length	$\sigma_1$	dimensionless stability root
M	total vertical wave moment; mass of ship	$\sigma_2$	dimensionless stability root
$M'$	dimensionless mass of ship	$\theta$	pitch angle
$m'$	vertical sectional added mass	$\zeta$	instantaneous wave elevation
$N'$	vertical sectional damping coefficient		
$N'_v, N'_v, N'_r, N'_r$	hydrodynamic coefficients of the equations of yaw and sway respectively	Subscripts :	
$Y'_v, Y'_v, Y'_r, Y'_r$		a	amplitude of denoted parameter
$r'$	dimensionless yaw velocity	$F'_\zeta$	wave force with respect to wave elevation
$\dot{r}'$	dimensionless yaw acceleration	$M'_\zeta$	wave moment with respect to wave elevation
T	ship's draught	Superscripts :	
$T^*$	effective draught		sectional values or dimensionless values according to SNAME-nomenclature
$T_e$	period of encounter		
V	forward velocity of ship		
$V_z$	vertical relative velocity with respect to the water		
$v'$	dimensionless sway velocity		
$\dot{v}'$	dimensionless sway acceleration		
$X'_l$	dimensionless longitudinal added mass		

## 1. INTRODUCTION

The calculation of the vertical hydrodynamic forces and moments acting on a ship in seawaves, according to the strip theory, has proved to be a valuable tool. This is also true to a limited extent for horizontal motions, but the experimental verification for low frequency motions, which are of interest for manoeuvring and steering problems, is rather scarce. The detailed comparisons of calculation and experiment for pitch and heave are for the greater part restricted to more or less average hull dimensions, for instance a length-beam ratio of approximately 6 to 8 and block coefficients around .70. Although predictions of vertical motions of extreme ship forms have been quite successful, it has not been known to what extent the strip theory is valid when more extreme hull dimensions are considered. Intuitively one may imagine, that the thinner the ship form, the more the application of the strip method is justified.

For manoeuvring and steering purposes the hydrodynamic coefficients of the equations of motion depend to a larger extent on viscous effects introducing lift phenomena, when compared with vertical motions of a ship in waves. Existing methods to approximate these hydrodynamic forces have a more empirical character. Apart from the length-draught ratio in both cases the length-beam ratio may be regarded as a useful parameter in a comparison of theory and experiment.

The main objective of this paper is to provide extensive experimental data respecting the influence of the length-beam ratio of a systematic ship model family on the hydrodynamic forces on the hull for vertical oscillatory motions in the wave frequency range, as well as for low frequency horizontal motions of interest for steering and manoeuvring.

The experiments cover a large range of length-beam ratio's which includes a very thick ship-form ( $L/B=4$ ) and a very thin ship with  $L/B=20$ . In addition a thin plate has been tested in horizontal motion to simulate an infinitely large length-beam ratio. All of the models have been derived from the standard Sixty Series hull form with  $L/B=7$  and  $C_p = .70$  [1], by multiplying the width by constant factors, to arrive at  $L/B=4, 5.5, 7, 10$  and  $20$ . All models have been made from glass reinforced polyester and have a length of 10 feet. For main particulars see table 1.

## 2. EXPERIMENTAL PROGRAM AND RESULTS

With a vertical Planar Motion Mechanism (PMM) the hydrodynamic coefficients of the heave and pitch equations according to equations (1) of appendix 1 have been measured for Froude numbers  $F_n = .20$  and  $F_n = .30$ . The latter speed is high for all models and large wave making has been observed during the experiments.

Excellent linearity has been found for the considered heave amplitudes which go to 1% of the model length and pitch amplitudes up to 3.5 degrees. For the wave tests wave heights of 2.5 % of the model length have been considered.

The linearity has been proved to be good with  $L/B=4$ .

The non-dimensional mass and damping coefficients as well as the mass and damping cross coupling coefficients are given in figures 1 to 8 in non-dimensional form as a function of the Froude number, the frequency of oscillation and the length-beam ratio.

Figures 9 and 10 give the dimensionless motion amplitudes of heave and pitch and figure 11 gives the added resistance in regular head waves. The motions and the added resistance in waves could not be measured for the  $L/B=20$  model owing to experimental difficulties.

The hydrodynamic coefficients for yaw and sway according to equations (13) of appendix 3 have been measured for three velocities:  $F_n = .15, .20$  and  $.30$ .

A large amplitude PMM has been used; the model frequency range has been between  $\omega = .2(.1) 1.0$ . Strut amplitudes for both modes of motion were respectively 5, 10, 15, 20 and 25 cm; the horizontal distance between the struts being 1 m. A relatively small wave making was observed for the lowest of the three velocities considered, and therefore the experimental results for  $F_n = .15$  have been used for comparing with some calculation methods. Figure 12, 13 and 14 show the coefficients, derived from the force and moment measurements, as a function of  $L/B$ -ratio for the three considered forward speeds. Table 2 gives the numerical values of the various hydrodynamic coefficients.

In figure 15 and 16 the results of the swaying force and swaying moment are presented as a function of speed, frequency,  $L/B$ -ratio and amplitude.

## 3. DISCUSSION OF THE RESULTS

### 3.1. Vertical Motions

First of all the heaving and pitching motions have been calculated with as a basis a formulation of the strip theory as given in appendix 1 and [2]. This formulation has been derived using earlier work by Shintani [3], Söding [4], Semenov-Tjan-Tsansky et al [5], Tasai [6] and affords the same results as given by Salvesen et al [7]. Afterwards the method has been used, which has been formulated principally by Korvin-Kroukovsky and Jacobs [8] and modified by the authors [9]. The results of both methods have been compared with the experimental results.

The added resistance in waves owing to the pitching and heaving motions has been calculated by the method described in appendix 2. The added resistance is determined by calculating the work done by the radiated damping waves, which result from the vertical motions of the ship relative to the water. In [10] this method has been confirmed by experimental results derived from model tests with a fast cargo ship hull form. Further experience included blunt tanker forms, although in some of these cases the agreement has been somewhat less satisfactory at high frequency of encounter.

In the figures 1 to 11 the experimental values are compared with corresponding calculations according to the modified Korvin-Kroukovsky formulation [9] and according to equations (6) and (7). For convenience we will call these the old and the new method respectively. With regard to the coefficients of the equations of motion for heave and pitch the two calculation methods give almost identical results, except for the pitch damping coefficient at low frequencies and for the added mass cross coupling coefficient D for pitch. The differences between the measured added mass and the calculated value are small, even for the very low L/B ratio's. For the added moment of inertia the correlation is still satisfactory, with only few differences for the highest speed and the lowest L/B ratio. The heave damping coefficient is reasonably predicted except for high frequencies where viscous effects, for instance separation of flow, may be important. Both the new and the old method predict the pitch damping rather poorly, particularly at low frequencies. The experimental data do not show a clear preference for one of the two methods. For practical purposes the over-estimation of the pitch damping at low frequencies, according to the new method is not too important in the motion prediction. Considering the absolute magnitude of the damping cross coupling terms the coefficients e and E are very well predicted by both theories for the two considered forward speeds, as well as for all length-beam ratio's. Also the added mass cross coupling coefficient d for heave is reasonably well predicted by both methods, but in the case of the mass cross coupling coefficient D for pitch the experimental points for low frequencies lie between the two predicted curves. For low frequencies the experimental values favour the prediction according to the new method. Heave amplitudes in waves are somewhat over-estimated by the new method. Earlier experience with both methods has shown us a slight preference for the modified Korvin-Kroukovsky and Jacobs method although a desired symmetry in the mass cross coupling coefficients is not fulfilled in their presentation. Moreover added resistance is overestimated by the new method and in this respect it should be remembered that added resistance varies as the squared motion amplitudes. For  $F_n = .20$  the predicted added resistance agrees very well with the measured values, with only minor differences at high frequencies. Even for the very low length-beam ratio's the agreement is satisfactory, considering the more or less extreme hull form and the relatively high forward speed in those cases. For  $F_n = .30$  the correlation between theory and experiment is less. However for all length-beam ratio's, except for L/B=7 this speed is very high, with corresponding high ship waves. Especially for L/B=4 the added resistance at high frequencies is under estimated by the theory.

### 3.2. Horizontal Motions

The coefficients have been determined in a standard graphical way from the in phase and quadrature components of forces and moments measured with the PMM. The accuracy of the coefficients which are displayed in fig. 12, 13 and 14, is probably not high since the relevant forces and moments are small in magnitude. The coefficients indicate a trend in the results and do not pretend to be highly accurate. In table 2 the numerical values of the coefficients are summarized using the dynamic modes of motions. The figures 12, 13 and 14 clearly show the effect of beam, which is not very pronounced for a low Froude number. As could be expected the forward speed affects the results to a certain extent: the thicker the model the more the model generated wave system plays a decisive role in the creation of the resulting hydrodynamic forces and moments. Hu [11] predicted the effect of speed upon the hydrodynamic coefficients, applying sources and doublets in the ship's centerplane and wake and taking into account the boundary conditions on the surface. Comparing the trend of the experimental results and the predicted values with regard to the forward velocity according to Hu, it can be said, that his prediction gives a more pronounced effect of speed. It is interesting to note, that Van Leeuwen's results of his PMM tests [12] with an 8 feet model of the L/B=7 are practically the same as the results presented in this paper, taking a reasonable margin of accuracy into account. In figures 12, 13 and 14 some evidence is produced, that the values of the static and dynamic sway coefficients are approaching each other closely. The condition for straight line stability (this word is used rather than controls fixed stability, since no rudder, propeller nor other hull appendices have been fitted) yields

$$\frac{x'_v}{x'_r} < 1$$

When  $x'_v$  and  $x'_r$  both are positive this condition postulates, that the point of application of the total yaw force is located before the point of application of the sway force. In figure 12, 13 and 14 it may be observed, that for a L/B-ratio exceeding 8 this condition is fulfilled. Since at a L/B-ratio of approximately 20  $Y'_r$  equals the mass  $M', x'_r$  will change sign and becomes extremely negative. In this case the aforementioned criterion is still satisfied, since it is obvious that  $x'_v$  remains positive. In table 2 the stability roots are calculated; the smaller roots are positive for the smaller L/B-ratio's and they are becoming negative for the larger L/B-ratio's. Noteworthy is the difference between the two last columns indicating, that the actually used plate for the experiments has a stable behaviour, but that an imaginary massless plate has an oscillatory stable behaviour. This fact is also found in stability analysis of ships which have large fins or deep keels, like sailing yachts and is caused by the small inertia forces relative to the lift forces [13].

Jacobs [14,15] published a brief account of a simple theory for the calculation of the linear coefficients of the horizontal motion based upon simple hydrodynamic concepts. Apart from an ideal fluid treatment of a wing shaped body in an unbounded flow, resulting in hydrodynamic added masses and added moments of inertia with cross coupling coefficients, a viscous part is included representing the generation of a lift. Therefore, as an example the Jones' low aspect ratio lift formula has been applied. Lift generation depends upon the flow conditions near the trailing edge. As these conditions vary, it seems appropriate to introduce an empirical constant K to take these variations into account, as was suggested by Inoue [16]. This K-constant turns out to be nearly .75 as an average. In appendix 3 a brief account is given of Jacobs' method, which has been chosen for a comparison with the measured results. The total lift, as a result of an inertia distribution and a viscous distribution along the ship length is generated for the greater part in the forebody, which means that the viscous part counter-balances nearly the inertia part in the afterbody [15,17]. The centre of the viscous force distribution therefore lies well aft of the centre of gravity ( $x'_{p1}$ ). The second moment of the viscous force distribution is characterized by  $x'_{p2}$  and obviously this quantity is negative. From the measurements of the relevant quantities the values of K,  $x'_{p1}$  and  $x'_{p2}$  are calculated and they are displayed in Figure 17. They coincide remarkably well with empirical values presented by Inoue and Albring [18]. The coefficient  $Y_1$  can also be used to check the validity of the empirical constants  $K_1, x'_{p1}$ . In figure 12 it may be seen, that there is a satisfactory agreement for the lower Froude number. Apart from considerations regarding the damping coefficients it is obvious, that the added mass, added moment of inertia and the mass cross coupling coefficients are accurately predicted by the simple stripwise integration of sectional values of added mass depending on local fullness and local B/T-values. So called three dimensional corrections have been applied as indicated by Jacobs and others. In order to compare the measured results with other methods available in literature, it has been decided to use the results of Inoue which are principally based upon Bolland's low aspect ratio theory and a number of empirical allowances. Appendix 3 gives a brief account of the used formulae according to Inoue. As can be seen in figure 12 the calculation agrees with the measured results with the exception of  $Y_1$ . Norrbin [19] analysed statistical material and derived regression formulae on the basis of the so called "bis" system of reference. In appendix 3 these regression formulae are "translated" into the nomenclature adopted in this paper. Inspecting the formulae a small effect of the L/B-ratio can be demonstrated, while generally speaking the calculated results using these regression formulae are in close agreement in the normal range of L/B-ratios, as shown in figure 12. Since lift generation is of primary importance in manoeuvring problems and since experimental material about this subject is not extensively published in literature, it has been decided

to give the transverse force and moment in the sway motion for two speeds :  $F_N=.15$  and  $F_N=.30$ , as a function of reduced frequency and amplitude in figures 15 and 16. In a very restricted range full linearity in frequency and amplitude exists. For the higher frequencies linearity is lost to some extent especially in the transverse force and to a smaller extent in the moment. A number of effects are obscuring the results, for instance nonlinearity owing to the cross flow. Also frequency- and amplitude effects are interfering when one tries to interpret the experimental results.

#### 4. REFERENCES

- [1] Todd, F.H.,  
"Some further experiments on single screw merchant ship forms Series 60"  
Transactions of the Society of Naval Architects and Marine Engineers Vol. 61, 1953.
- [2] Gerritsma, J.  
"Some recent advances in the prediction of ship motions and ship resistance in waves"  
International Jubilee Meeting on the occasion of the 40th Anniversary of the Netherlands Ship Model Basin, 1973, Wageningen, The Netherlands.
- [3] Shintani, A.,  
"The New formulae of calculating Pitch and Heave of Ships by the Strip Method"  
Transactions Japan Society of Naval Architects Vol. 124, 1968.
- [4] Söding, H.,  
"Eine Modifikation der Streifenmethode"  
Schiffstechnik Bd.16, Heft 80, 1969, pp 15-18  
Book
- [5] Semenof-Tjan-Tsansky, W.W.,  
Blagowetsjenski, S.N., Golodolin, A.N.,  
"Motions of Ships" (in Russian language)  
Publishing Office Shipbuilding, Leningrad 1969.
- [6] Tasai, F.,  
"Improvements in the theory of ship motions in longitudinal waves"  
Transactions International Towing Tank Conference Rome, 1969, pp. 677.
- [7] Salvesen, N., Tuck, E.O., and Faltinsen, O.  
"Ship motions and Sea Loads"  
Transactions of the Society of Naval Architects and Marine Engineers, Vol. 78, 1970.
- [8] Korvin-Kroukovsky, B.V., and Jacobs, W.R.,  
"Pitching and Heaving Motions of a Ship in regular Waves"  
Transactions of the Society of Naval Architects and Marine Engineers, Vol. 65, 1957
- [9] Gerritsma, J., and Beukelman, W.,  
"Analysis of the modified Strip Theory for the Calculation of Ship Motions and Wave Bending Moments"  
International Shipbuilding Progress, Vol. 14, No. 156, 1967.
- [10] Gerritsma, J. and Beukelman, W.,  
"Analysis of the Resistance Increase in Waves of a fast Cargo Ship"  
International Shipbuilding Progress, Vol. 19, No. 217, 1972.
- [11] Hu, P.N.,  
"Forward Speed Effects on Lateral Stability Derivatives of a Ship"  
DL Report 829, August 1961.

[12] Van Leeuwen, G.,  
 "The lateral Damping and Added Mass of an Oscillating Shipmodel"  
 Shipbuilding Laboratory - University of Technology, Delft, July 1964, Publication no.23.

[13] Gerritsma, J., Glansdorp, C.C., Moeyes, G.,  
 "Still water, Seakeeping and Steering Performance of "Columbia" and "Valiant"  
 Shipbuilding Laboratory, University of Technology, Delft, The Netherlands, report no. 391, March 1974.

[14] Jacobs, W.R.,  
 "Methods of Predicting Course Stability and turning Qualities of Ships"  
 DL Report 945, March 1963.

[15] Jacobs, W.R.,  
 "Estimation of Stability Derivatives and Indices of various Ship Forms and Comparison with Experimental Results".  
 Journal of Ship Research, September 1966, pp. 135-162.

[16] Inoue, S.,  
 "The Determination of Transverse Hydrodynamic Nonlinear Forces by Means of Steady Turning"  
 11th International Towing Tank Conference, Tokyo 1966, pp. 542.

[17] Norrbin, N.H.,  
 "Forces in oblique Turning of a Model of a Cargo-Liner and a Divided Double-Body Geosim"  
 The Swedish State Shipbuilding Experimental Tank, Göteborg, Publication 57.

[18] Albring, W.,  
 "Summary Report of Experimental and Mathematical Methods for the Determination of Coefficients of Turning of Bodies of Revolution"  
 CONLAN 2

[19] Norrbin, N.H.,  
 "Theory and Observations on the use of a Mathematical Model for Ship Manoeuvring in deep and confined Waters"  
 The Swedish State Shipbuilding Experimental Tank, Göteborg, 1971, Publication 68.

[20] Joosen, W.P.A.,  
 "Added Resistance of Ships in Waves"  
 Proceedings of the 6th Symposium on Naval Hydrodynamics, Washington, D.C., 1966 pp. 637.

[21] Resistance in Waves  
 60th Anniversary Series, The Society of Naval Architects of Japan, 1963, Vol. 8 Chapter 5.

[22] Havelock, T.H.,  
 "Notes on the Theory of Heaving and Pitching"  
 Transactions of the Institution of Naval Architects, London 1945.

[23] Clarke, D.,  
 "A Two-Dimensional Strip Method for Surface Ship Hull Derivatives : Comparison of Theory with Experiments on a Segmented Tanker Model"  
 The International Symposium on Directional Stability and Control of Bodies Moving in Water, 17-21 April 1972, London, Paper 8.

5. APPENDIX 1

The equations of motion of heave and pitch

The equations of motion of heave and pitch and their solution are given by :

$$\left. \begin{aligned} (\rho V + a)\ddot{z} + b\dot{z} + cz - d\ddot{\theta} - c\dot{\theta} - g\theta &= F & \text{(heave)} \\ (I_{yy} + A)\ddot{\theta} + B\dot{\theta} + C\theta - D\ddot{z} - E\dot{z} - Gz &= M & \text{(pitch)} \end{aligned} \right\} (1)$$

$$z = z_a \cos(\omega_e t + \epsilon_z) , \theta = \theta_a \cos(\omega_e t + \epsilon_\theta)$$

The various coefficients a-g and A-G are derived from :

$$\rho V \bar{z} \int_L F' dx_b \quad (2)$$

$$I_{yy} \bar{\theta} = - \int_L F' x_b dx_b$$

where F' is the hydromechanical force acting on a cross-section of the ship.

It can be found that :

$$F' = -2\rho g y_w (z - x_b \theta) - \left( \frac{\partial}{\partial t} - V \frac{\partial}{\partial x} \right) (\dot{z} - x_b \dot{\theta} + V\theta - \zeta^*) \left( m \frac{iN'}{\omega_e} \right) \quad (3)$$

The effective wave elevation  $\zeta^*$  is defined as :

$$\zeta^* = \zeta e^{-kT^*} , \text{ where :}$$

$$T^* = - \frac{1}{k} \ln \left( 1 - \frac{k}{y_w} \int_{-T}^0 y_w e^{kz_b} dz_b \right) \quad (4)$$

This expression follows from the integration of the vertical component of the undisturbed incident wave pressure on a cross section contour. The time derivatives of  $\zeta^*$  are used in the calculation of the damping and added mass correction to the "Froude-Kriloff" wave force and moment.

Because harmonic motions only are considered, equation (3) can be written as :

$$\begin{aligned} F' = & -2\rho g y_w (z - x_b \theta - \zeta^*) - m' (\dot{z} - x_b \dot{\theta} + 2V\dot{\theta} - \dot{\zeta}^*) + \\ & + v \frac{dm'}{dx_b} (\dot{z} - x_b \dot{\theta} + V\theta - \zeta^*) - N' (\dot{z} - x_b \dot{\theta} + 2V\theta - \frac{\omega}{\omega_e} \zeta^*) + \\ & + v \frac{dN'}{dx_b} (z - x_b \theta - \frac{V\theta}{\omega_e} - \frac{\omega}{\omega_e} \zeta^*) \end{aligned} \quad (5)$$

Combining equations (2) and (5) one finds :

$$a = \int_L m' dx_b + \left[ \frac{V}{\omega_e^2} \int \frac{dN'}{dx_b} dx_b \right]$$

$$b = \int_L (N' - V \frac{dm'}{dx_b}) dx_b$$

$$c = 2\rho g \int_L y_w dx_b$$

$$d = \int_L m' x_b dx_b + 2 \frac{V}{\omega_e^2} \int_L N' dx_b - \frac{V^2}{\omega_e^2} \int_L \frac{dm'}{dx_b} dx_b + \left[ \frac{V}{\omega_e L} \int \frac{dN'}{dx_b} x_b dx_b \right]$$

$$e = \int_L N' x_b dx_b - 2V \int_L m' dx_b - V \int_L \frac{dm'}{dx_b} x_b dx_b + \left[ \frac{V^2}{\omega_e^2} \int \frac{dN'}{dx_b} dx_b \right]$$

$$g = 2\rho g \int_L y_w x_b dx_b$$

(6a)



$$A = \int_L m' x_b^2 dx_b + 2 \frac{V}{\omega_e} \int_L N' x_b dx_b - \frac{V^2}{\omega_e^2} \int_L \left( \frac{dm'}{dx_b} x_b \right) dx_b + \left[ \frac{V}{\omega_e^2} \int_L \frac{dN'}{dx_b} x_b^2 dx_b \right]$$

$$B = \int_L N' x_b^2 dx_b - 2V \int_L m' x_b dx_b - V \int_L \left( \frac{dm'}{dx_b} x_b^2 \right) dx_b - \left[ \frac{V^2}{\omega_e^2} \int_L \frac{dN'}{dx_b} x_b dx_b \right]$$

$$C = 2\rho g \int_L y_w x_b^2 dx_b$$

$$D = \int_L m' x_b dx_b + \left[ \frac{V}{\omega_e^2} \int_L \frac{dN'}{dx_b} x_b dx_b \right]$$

$$E = \int_L N' x_b dx_b - V \int_L \left( \frac{dm'}{dx_b} x_b \right) dx_b$$

$$G = 2\rho g \int_L y_w x_b dx_b \quad (6b)$$

If  $F = F_a \cos(\omega_e t + \epsilon_{F\zeta})$  and  $M = M_a \cos(\omega_e t + \epsilon_{M\zeta})$  then:

$$\frac{F_a}{\zeta_a} \cos \epsilon_{F\zeta} = 2\rho g \int_L y_w e^{-kT^*} \cos kx_b dx_b + \omega \int_L \left( \frac{\omega}{\omega_e} N' - V \frac{dm'}{dx_b} \right) e^{-kT^*} \frac{\sin kx_b}{\cos kx_b} dx_b + \omega^2 \int_L \left( m' + \left[ \frac{V}{\omega_e} \frac{dN'}{dx_b} \right] \right) e^{-kT^*} \frac{\cos kx_b}{\sin kx_b} dx_b \quad (7a)$$

$$\frac{M_a}{\zeta_a} \cos \epsilon_{M\zeta} = 2\rho g \int_L y_w x_b e^{-kT^*} \cos kx_b dx_b + \omega \int_L \left( \frac{\omega}{\omega_e} N' - V \frac{dm'}{dx_b} \right) x_b e^{-kT^*} \frac{\sin kx_b}{\cos kx_b} dx_b + \omega^2 \int_L \left( m' + \left[ \frac{V}{\omega_e} \frac{dN'}{dx_b} \right] \right) x_b e^{-kT^*} \frac{\cos kx_b}{\sin kx_b} dx_b \quad (7b)$$

For ships where  $N'$  and  $m'$  are zero at the stem and stern the expressions (6) and (7) can be simplified, but this has not been carried through in the corresponding computer program.

When the terms between the brackets are left out from equations (6) and (7) and when  $\frac{\omega}{\omega_e} = 1$  in the coefficients of  $N'$  in (7) the resulting equations of motion are equal to those derived by the modified Korvin-Kroukovsky and Jacobs' results [9].

APPENDIX 2

The Added Resistance in Waves

The added resistance of a ship in waves is a result of the radiated damping waves created by the motions of the ship relative to the water. Joosen [20] showed that for the mean added resistance can be written :

$$R_{AW} = \frac{\omega^3}{2g} (bz_a^2 + B\theta_a^2) \quad (8)$$

This expression was derived by expanding Maruo's expression [21] into an asymptotic series with respect to a slenderness parameter and taking into account only first order terms. His simplified treatment results in an added resistance which is independent of the forward speed. This latter fact is roughly confirmed by experiments [10].

Equation (8) is equivalent to Havelock's equation [22]. Although not consistent with the theory, the frequency of encounter is used by Joosen in (8) when a ship with forward speed is considered. In equation (8) uncoupled motions are considered. In the present work the following procedure is adopted for the calculation of the radiated damping energy  $P$  of the oscillating ship during one period of encounter :

$$P = \int_L \int_0^{T_e} b' V_z^2 dt dx_b \quad (9)$$

where  $b' = N' - V \frac{dm'}{dx_b}$ , the sectional damping coefficient for ship at speed and :

$V_z = \dot{z} - x_b \dot{\theta} + V\theta - \dot{\zeta}^*$ , the vertical relative water velocity at a cross section of the ship. As  $V_z$  is a harmonic function with amplitude  $V_z a$  and a frequency equal to the frequency of encounter  $\omega_e$  we find :

$$P = \frac{\pi}{\omega_e} \int_L b' V_{za}^2 dx_b \quad (10)$$

Following the reasoning given by Maruo in [21] the work being done by the towing force  $R_{AW}$  is given by :

$$P = R_{AW} (V+c) T_e = R_{AW} \cdot \lambda \quad (11)$$

From (10) and (11) it follows that :

$$R_{AW} = \frac{k}{2\omega_e} \int_L b' V_{za}^2 dx_b \quad (12)$$

This expression is almost equal to (8) when the wave elevation  $\zeta$  is small compared with the vertical motions of the ship in addition to a very low forward speed and fore and aft symmetry.

APPENDIX 3

The Equations of Motion of Yaw and Sway

Principally the following account is based upon work by Jacobs [14, 15].

The equations of motion for the bare hull condition are given by :

$$M'(\dot{\psi} + r') = Y'_v \dot{\psi}' + Y'_v v' + Y'_r \dot{r}' + Y'_r r' \quad (\text{sway}) \quad (13)$$

$$I'_{zz} \dot{r}' = N'_v \dot{\psi}' + N'_v v' + N'_r \dot{r}' + N'_r r' \quad (\text{yaw})$$

The hydrodynamic coefficients in (13) can be calculated by assuming a division between an inertia force distribution and a viscous force distribution along the ship's hull. The distribution of the hydrodynamic inertia forces can be found by well-known methods in hydrodynamics of which brief accounts can be found, among others in [19, 23]. Confining ourselves to horizontal motions at a constant forward velocity in an ideal fluid the following expressions for the right-hand sides of (13) are derived :

$$Y'_{id} = Y'_v \dot{\psi}' + X'_u r' + Y'_r \dot{r}' \quad (14)$$

$$N'_{id} = N'_r \dot{r}' + (Y'_v - X'_u) v' + Y'_r (\dot{\psi}' + r')$$

The coefficients appearing in (14) are calculated by the following expressions, assuming that the strip method is applicable together with Lamb's correction coefficients of accession :

$$Y'_v = -\frac{\pi K_2 T^2}{L^3} \int_{-1/2}^{1/2} C_s dx' \quad (15)$$

$$N'_v = -\frac{\pi K_2 T^2}{L^4} \int_{-1/2}^{1/2} C_s x' dx'$$

$$Y'_r = -\frac{\pi K_1 T^2}{L^4} \int_{-1/2}^{1/2} C_s x' dx' = \frac{K_1}{K_2} N'_v$$

$$N'_r = -\frac{\pi K_1 T^2}{L^5} \int_{-1/2}^{1/2} C_s x'^2 dx'$$

$$X'_u = K_1 M'$$

From (14) it is obvious, that for the damping coefficients the following expressions exist in an inviscid fluid :

$$Y'_{v id} = 0$$

$$Y'_{r id} = X'_u \quad (16)$$

$$N'_{v id} = Y'_v - X'_u$$

$$N'_{r id} = Y'_r$$

A ship-shaped low aspect ratio wing in a real fluid develops a circulation around the profile generating a lift owing to the viscosity. This lift can be approximated for moderate speeds by the corrected Jones' low aspect ratio formula, taking into account the action of the water surface by doubling the draught. This formula can also be considered as the integral of the viscous force distribution along the hull. The first and second moments of this distribution yields the remaining damping derivatives :

$$Y'_v \text{ visc} = -K_1 \frac{2T}{L} \frac{T}{L}$$

$$N'_v \text{ visc} = Y'_v r \text{ visc} = -x'_1 p_1 2\pi \frac{KT^2}{L^2} \quad (17)$$

$$N'_r \text{ visc} = -x'_2 p_2 2\pi \frac{KT^2}{L^2}$$

Numerical values of the empirical constants  $K_1$ ,  $x'_1$  and  $x'_2$  are displayed in figure 17. Combining equations (16,17) the total damping coefficients can be listed as follows, assuming that mutual interference between inertia and viscous forces can be neglected :

$$Y'_v = -2K_1 \frac{T^2}{L^2}$$

$$N'_v = Y'_v - X'_u - x'_1 p_1 2K_1 \frac{T^2}{L^2} \quad (18)$$

$$Y'_r = X'_u - x'_1 p_1 2K_1 \frac{T^2}{L^2}$$

$$N'_r = -x'_2 p_2 2K_1 \frac{T^2}{L^2}$$

For the purpose of comparing the results of the experimental coefficients with some existing formulae concerning damping coefficients, the following expressions are appropriate for the even keel condition, following Inoue [16] :

$$Y'_v = -2K_1 \frac{T^2}{L^2}$$

$$N'_v = -2 \frac{T^2}{L^2} \quad (19)$$

$$Y'_r = 2K_1 \frac{T^2}{L^2} (.367 + .42 \frac{T}{L})$$

$$N'_r = -1.08 \frac{T^2}{L^2}$$

Norrbin [19] published data respecting the damping derivatives. His results are given in the form of regression formulae in his non dimensional so called 'bis' system. In the nomenclature adopted in this paper the expressions are given preceded by the corresponding formulae in the 'bis' system.

$$Y''_{uv} = -1.69 \frac{\pi}{2} \frac{LT^2}{v} - 0.04; Y'_v = -1.69 \pi \frac{T^2}{L^2} - 0.08 \frac{B}{L} \frac{C_B T}{L}$$

$$N''_{uv} = -1.28 \frac{\pi}{4} \frac{LT^2}{v} + 0.02; N'_v = -1.28 \frac{\pi}{2} \frac{T^2}{L^2} + 0.04 \frac{B}{L} \frac{C_B T}{L}$$

$$Y''_{ur} = 1.29 \frac{\pi}{4} \frac{LT^2}{v} - 0.18; Y'_r = 1.29 \frac{\pi}{2} \frac{T^2}{L^2} - 0.36 \frac{B}{L} \frac{C_B T}{L}$$

$$N''_{ur} = -1.88 \frac{\pi}{8} \frac{LT^2}{v} + 0.09; N'_r = -1.88 \frac{\pi}{4} \frac{T^2}{L^2} + 0.18 \frac{B}{L} \frac{C_B T}{L}$$

(20)

TABLE 1

		L/B=4.0	L/B=5.5	L/B=7.0	L/B=10.0	L/B=20.0	L/B=∞
$L_{PP}$	m	3.048	.3.048	3.048	3.048	3.048	3.048
LWL	m	3.099	3.099	3.099	3.099	3.099	3.099
B	m	.7620	.5542	.4354	.3048	.1524	.006
T	m	.1742	.1742	.1742	.1742	.1742	.1742
v	m <sup>3</sup>	.2832	.2060	.1618	.1133	.0566	.0032
$A_W$	m <sup>2</sup>	1.8267	1.3342	1.0435	.7331	.3652	-
$I_L$	m <sup>4</sup>	.9737	.7117	.5566	.3909	.1947	-
$C_B$		.70	.70	.70	.70	.70	-
$C_P$		.71	.71	.71	.71	.71	-
LCB before $L_{PP}/2$		.014	.014	.014	.014	.014	-
LCF before $L_{PP}/2$		-.063	-.063	-.063	-.063	-.063	-
$k_{yy}/L_{PP}$		.25	.25	.25	.25	.25	-
M	kgf sec <sup>2</sup> /m	28.859	20.988	16.491	11.544	5.772	7.513
$k_{zz}/L_{PP}$		.267	.268	.230	.229	.229	.275

TABLE 2

$F_n = .15$

L/B	4	5.5	7	10	20	∞	∞*
$M'$	1978	1433	1122	779	379	521	0
$I'_{zz}$	142	103	59	41	20	39	0
$Y'_v$	-1800	-1700	-1600	-1450	-1400	-1500	-1500
$N'_v$	-610	-670	-730	-780	-700	-500	-500
$Y'_v - M'$	-3198	-2703	-2352	-1899	-1559	-1601	-1080
$N'_v$	-120	-50	-40	0	0	+20	+20
$Y'_r - M'$	-1858	-1243	-872	-479	0	0	+521
$N'_r$	-265	-295	-290	-280	-240	-260	-260
$Y'_r$	-110	-90	-60	0	0	0	0
$N'_r - I'_{zz}$	-190	-165	-125	-105	-88	-95	-56
$\sigma'_1$	.538	.304	.200	-.048	-.901	-.935	Re=-2.930
$\sigma'_2$	-2.051	-2.468	-2.955	-3.382	-2.724	-2.739	Im=+1.471

Table 2 to be continued

		$F_n = .20$						
L/B		4	5.5	7	10	20	$\infty$	$\infty^*$
$Y'_V$	} $\cdot 10^5$	-1850	-1760	-1750	-1500	-1400	-1600	-1600
$N'_V$		-650	-720	-790	-800	-700	-450	-450
$Y'_V - M'_V$		-3198	-2543	-2442	-1919	-1559	-1601	-1080
$N'_V$		-180	-70	-50	0	0	0	0
$Y'_R - M'_R$		-1748	-1283	-892	-499	0	0	-521
$N'_R$		-270	-300	-310	-310	-250	-240	-240
$Y'_R$		-120	-60	-60	0	-50	0	0
$N'_R - I'_{ZZ}$		-195	-165	-135	-112	-97	-120	-81
$\sigma'_1$		.548	.369	.170	-.088	-1.064	-.997	Re=-2.222
$\sigma'_2$		-1.929	-2.584	-2.928	-3.461	-2.180	-2.002	Im=+1.458

		$F_n = .30$						
L/B		4	5.5	7	10	20	$\infty$	$\infty^*$
$Y'_V$	} $\cdot 10^5$	-2450	-2300	-2070	-1760	-1450	-1600	-1600
$N'_V$		-700	-840	-900	-980	-860	-500	-500
$Y'_V - M'_V$		-3078	-2603	-2652	-2189	-1599	-1621	-1100
$N'_V$		-160	-100	-20	0	-50	0	0
$Y'_R - M'_R$		-1878	-1303	-1042	-559	-29	0	+521
$N'_R$		-330	-360	-400	-340	-310	-230	-230
$Y'_R$		-180	-100	-100	0	-50	0	0
$N'_R - I'_{ZZ}$		-200	-160	-120	-115	-95	-90	-51
$\sigma'_1$		.387	.225	.090	-.054	-.955	-.985	Re=-2.982
$\sigma'_2$		-2.227	-2.909	-3.879	-3.706	-2.878	-2.558	Im=+1.517

$\infty^*$  plate without mass

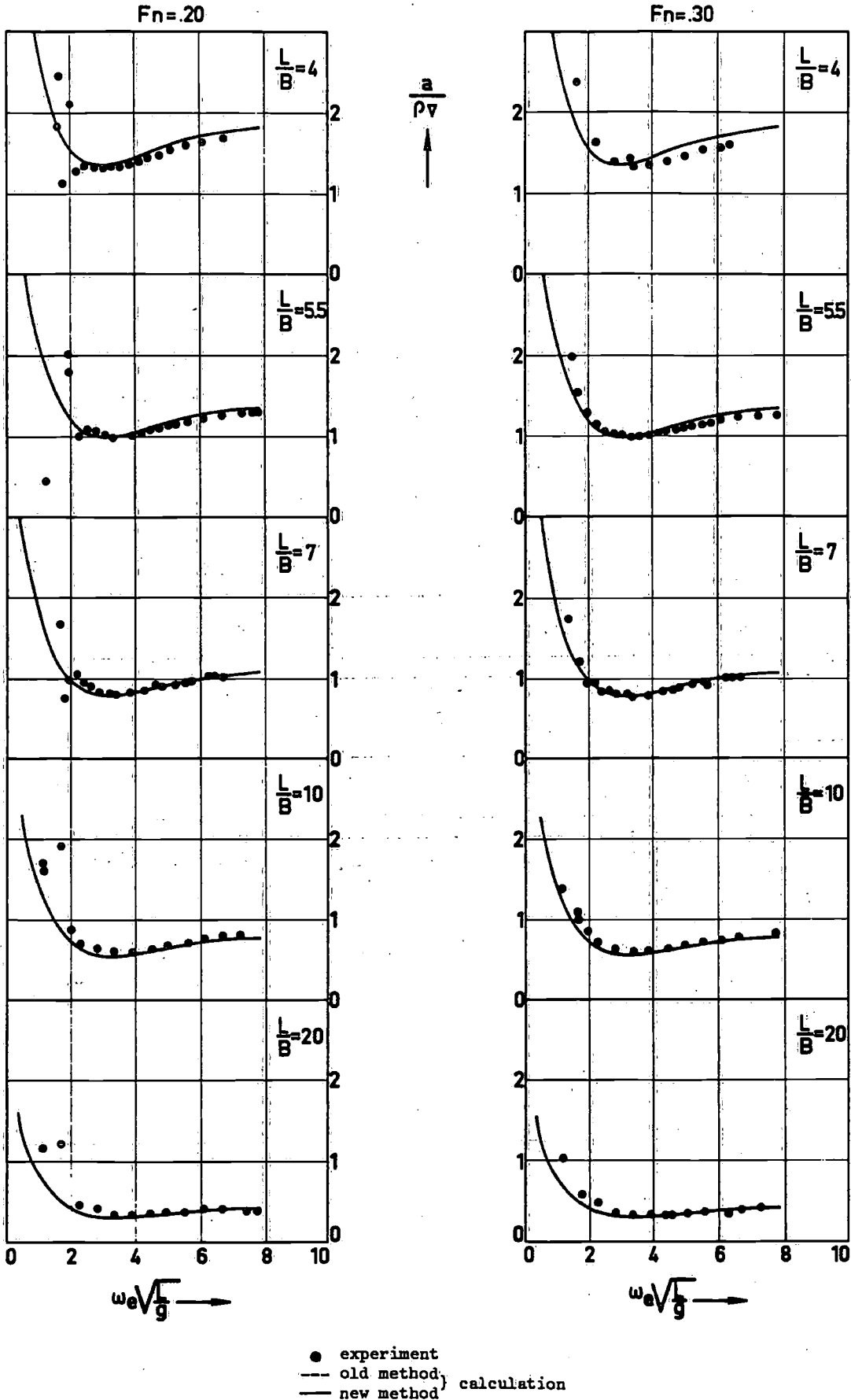


Figure 1: Added mass coefficient for heave

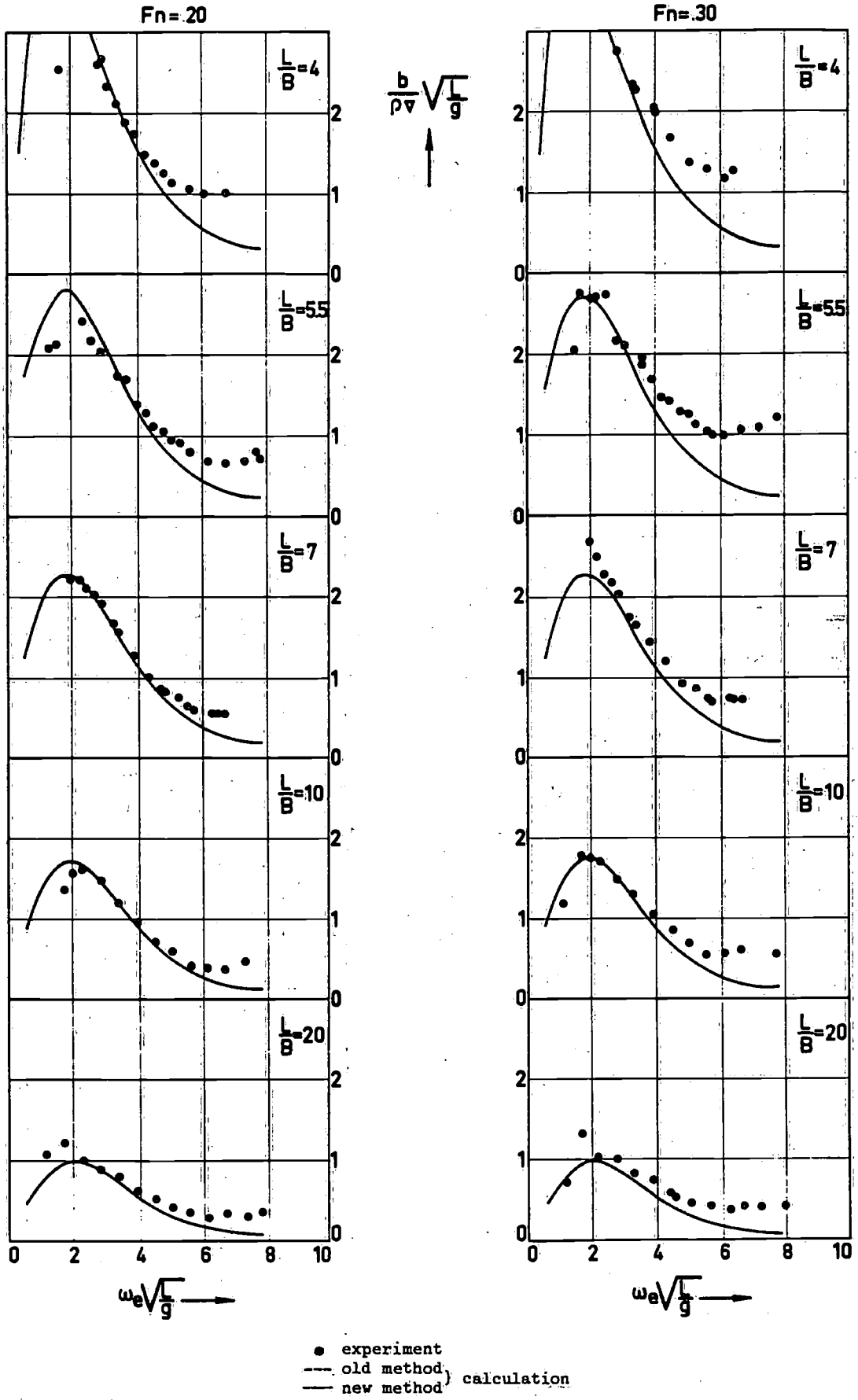


Figure 2 : Heave damping coefficient.

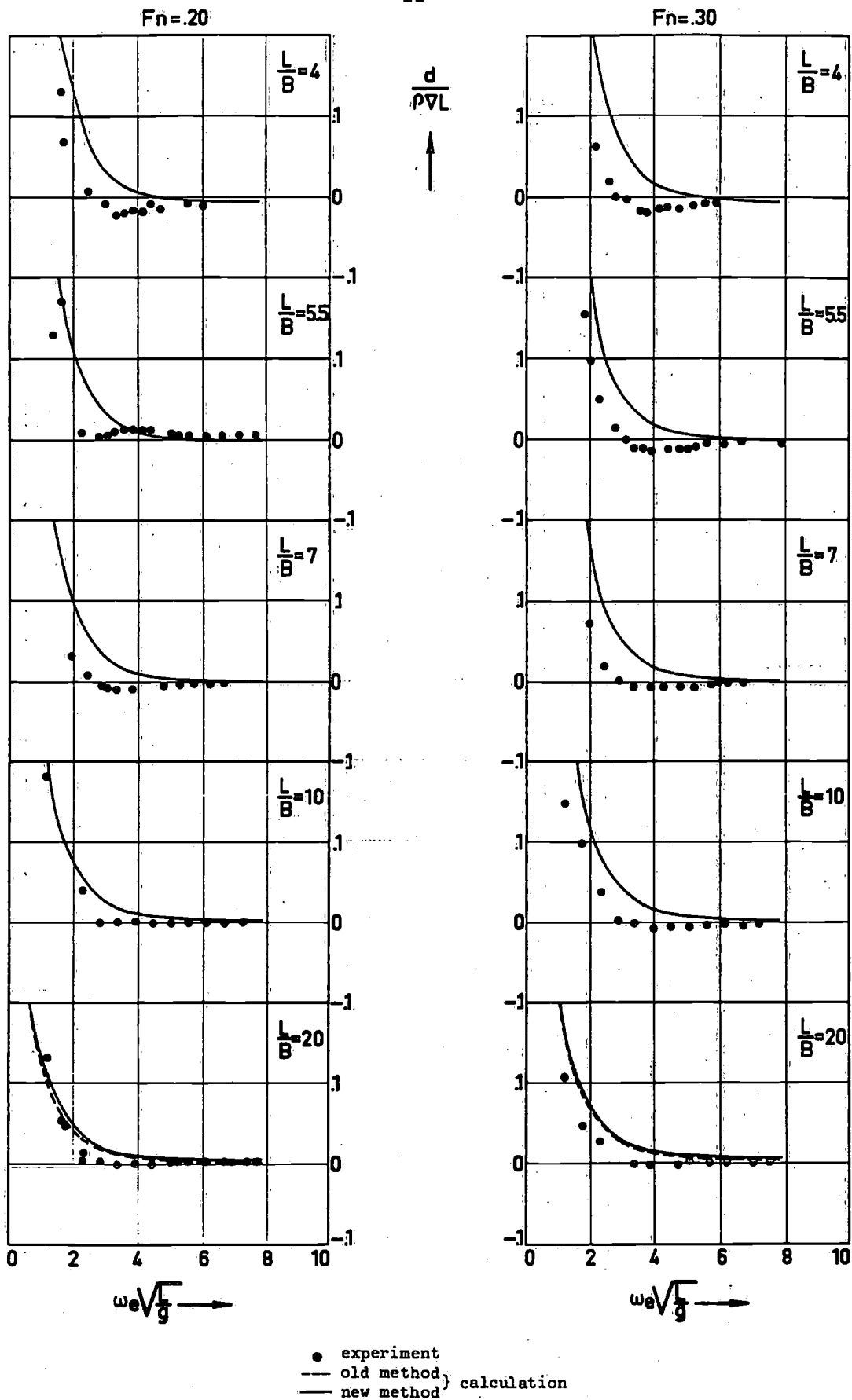
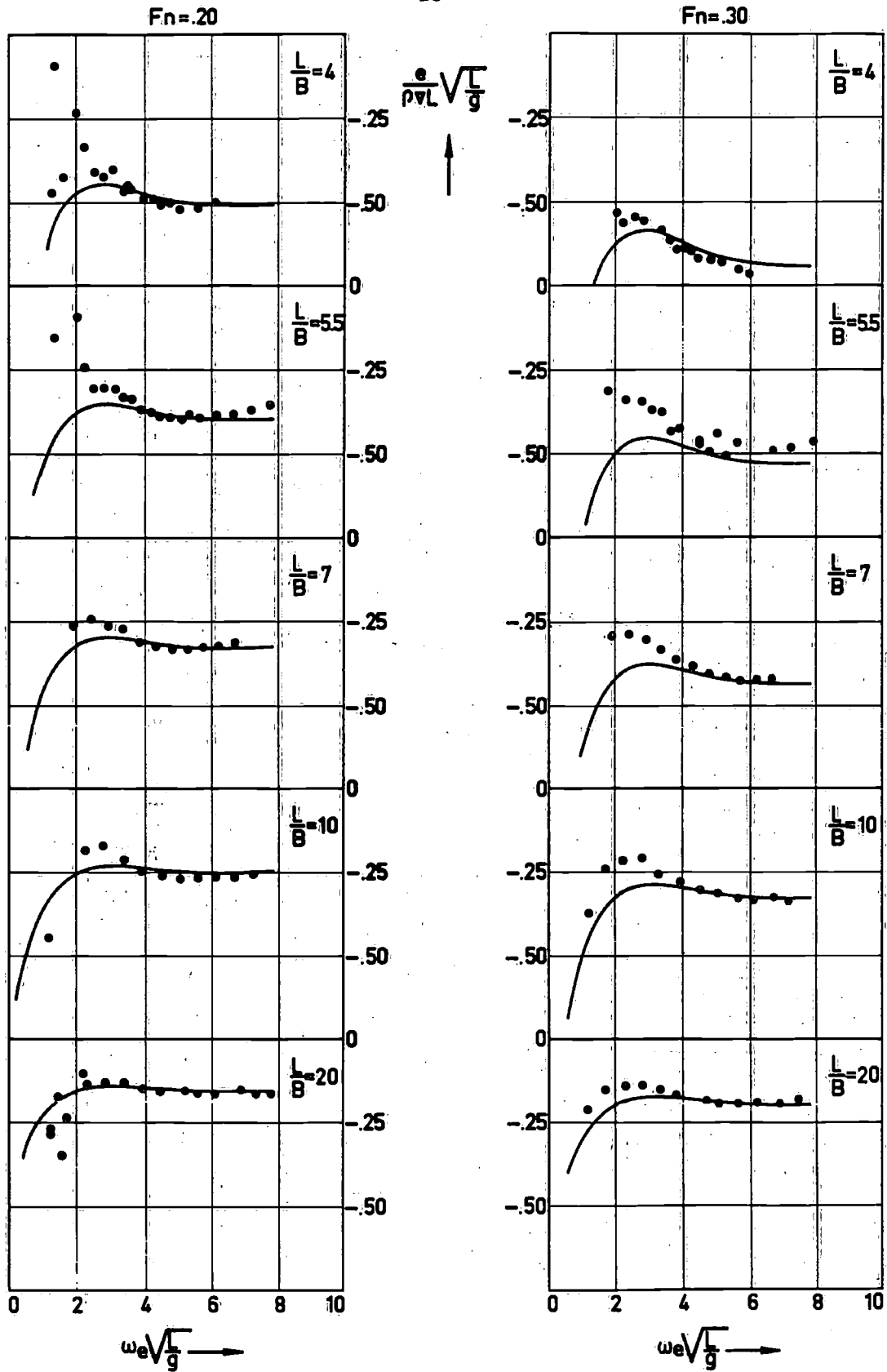


Figure 3 : Added mass cross coupling coefficient for heave



● experiment  
 --- old method } calculation  
 — new method }

Figure 4 : Damping cross coupling coefficient for heave



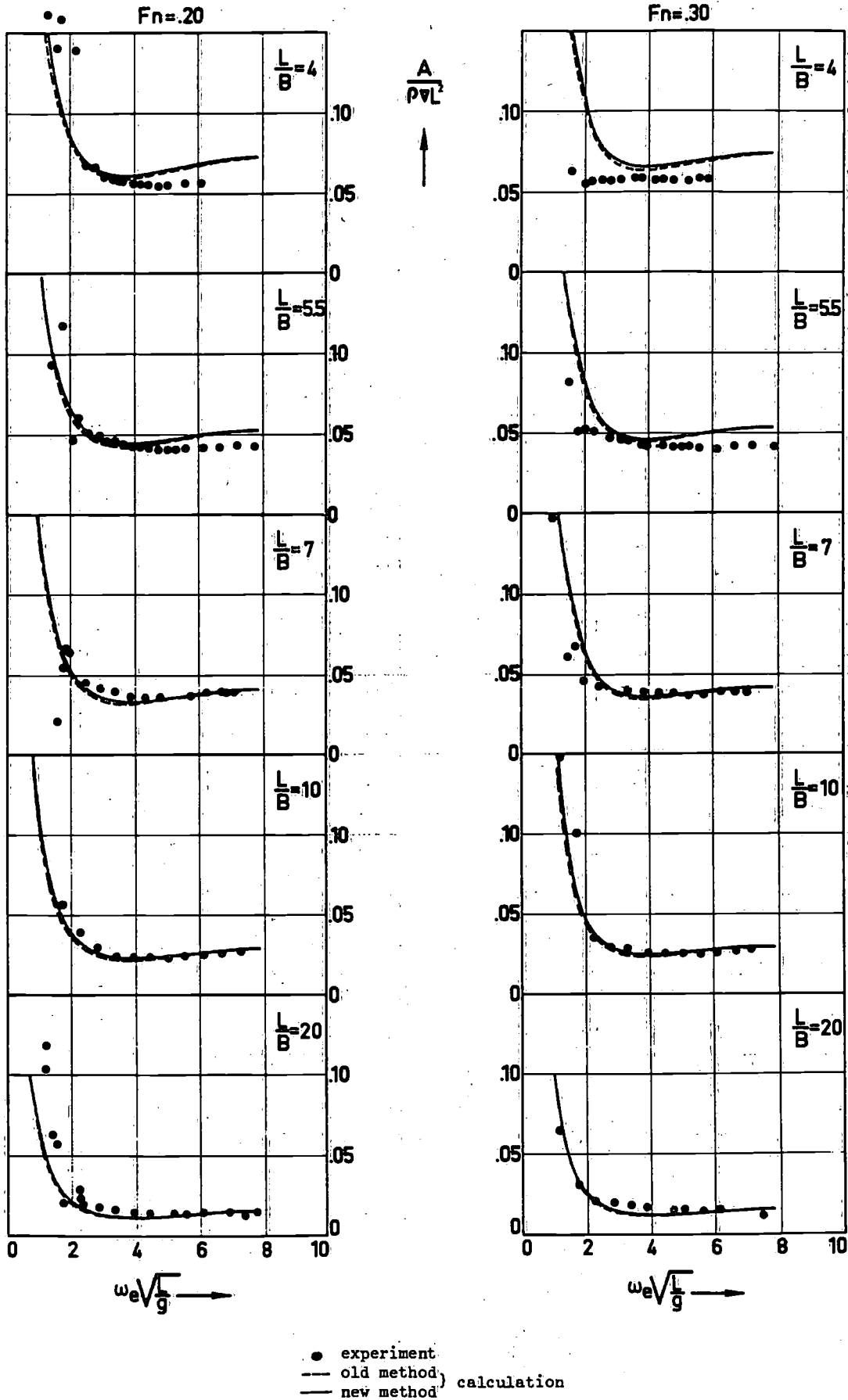


Figure 5 : Coefficient of added mass moment of inertia for pitch

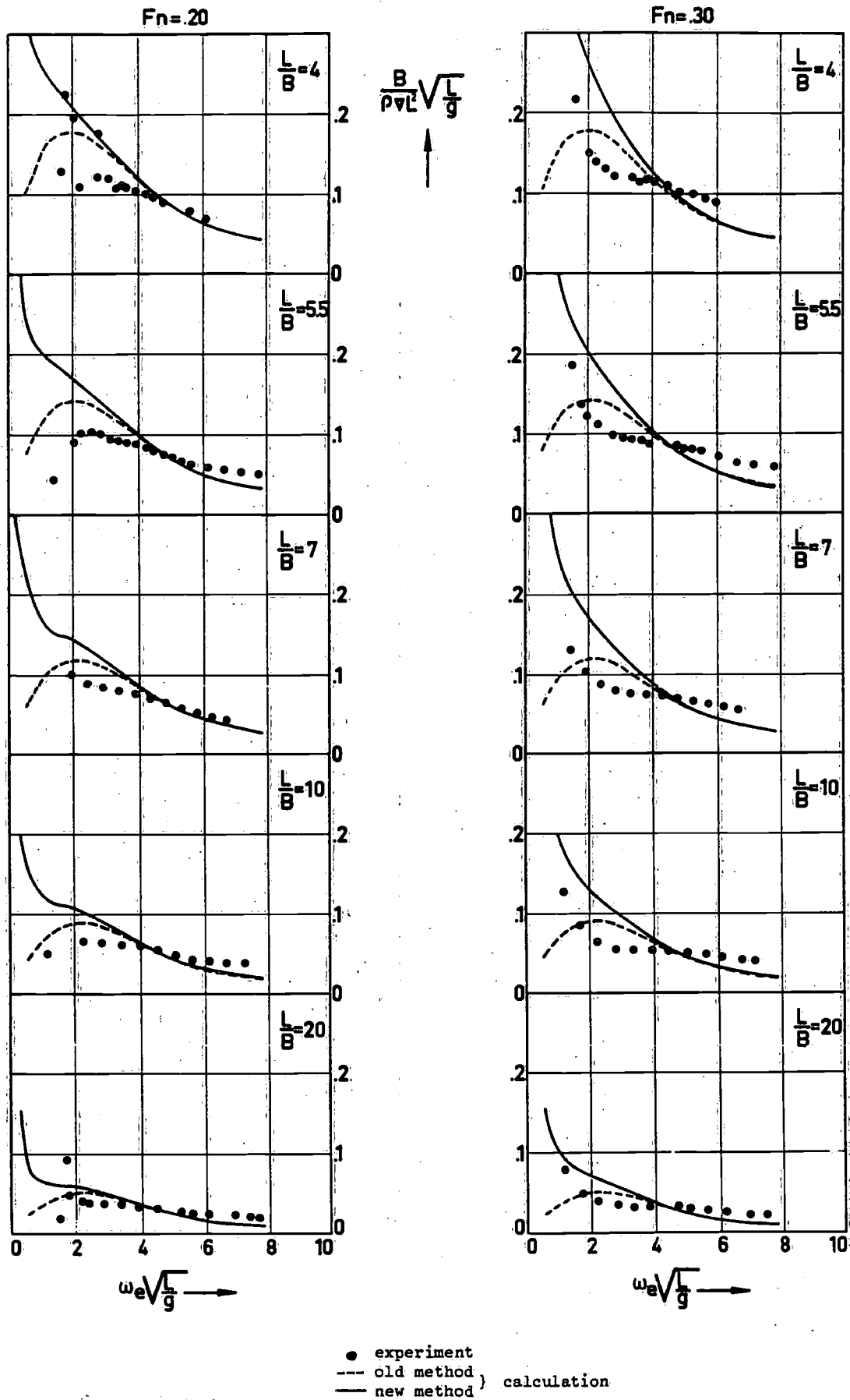


Figure 6 : Pitch damping coefficient

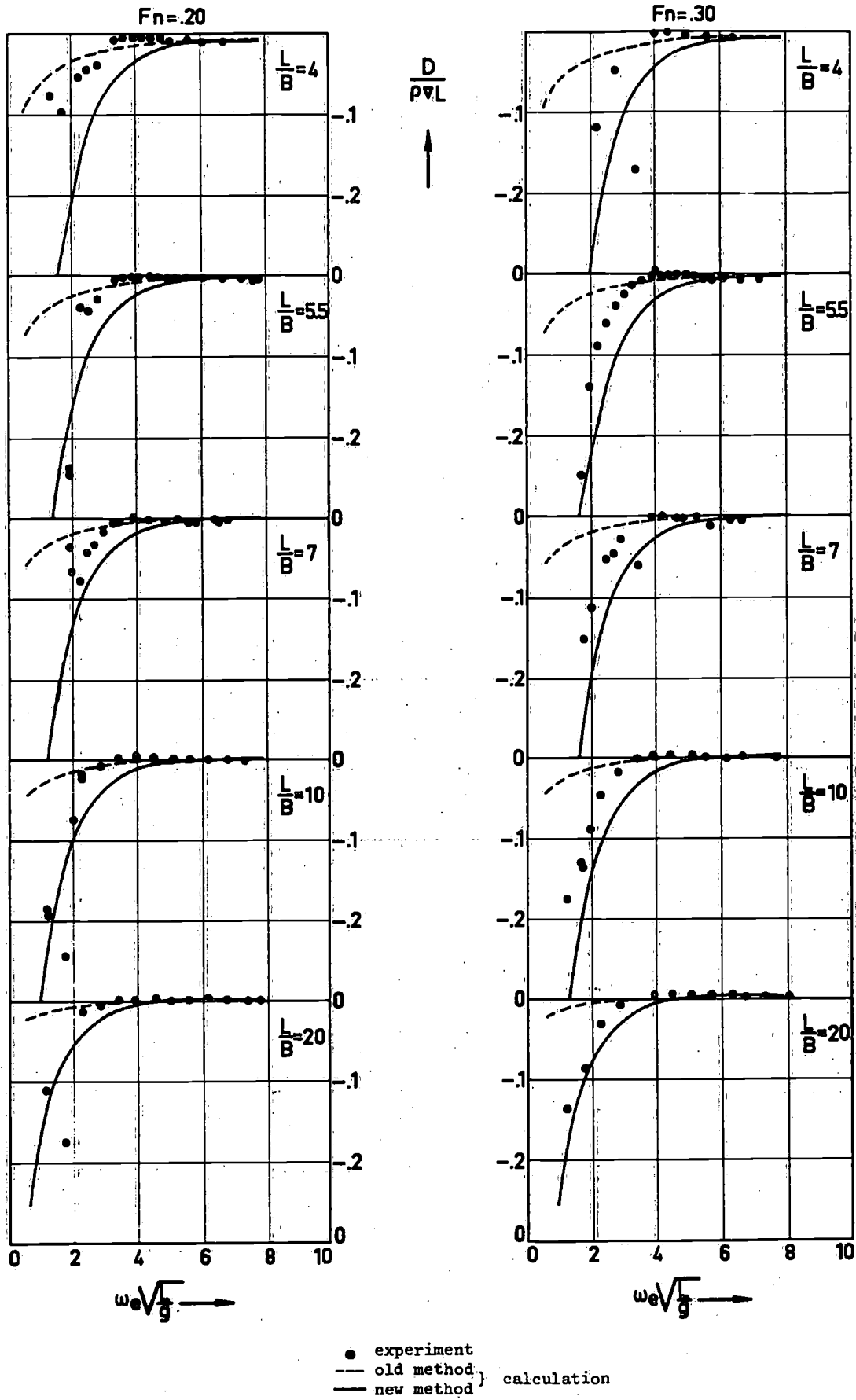


Figure 7 : Added mass cross coupling coefficient for pitch

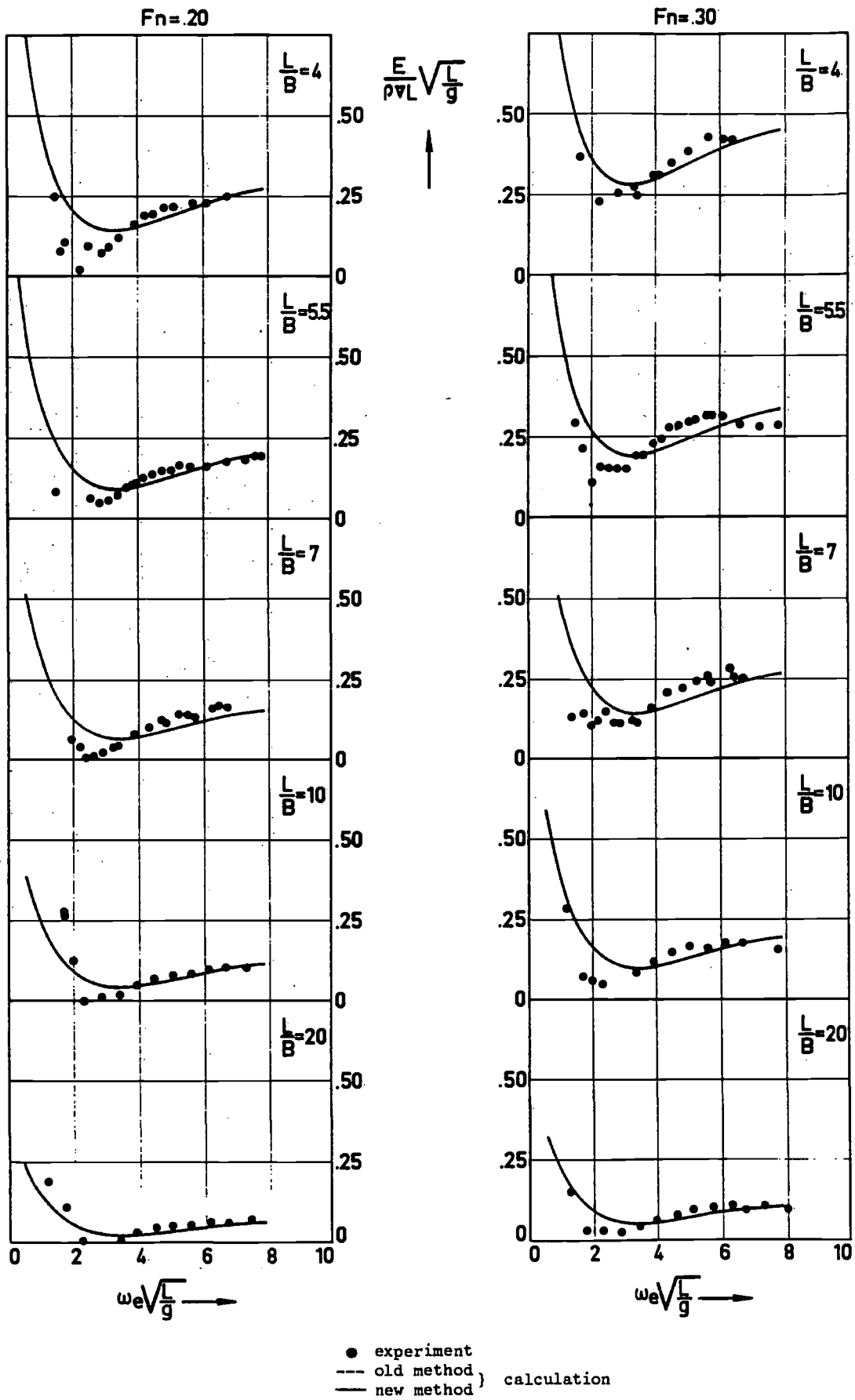


Figure 8 : Pitch damping cross coupling coefficient

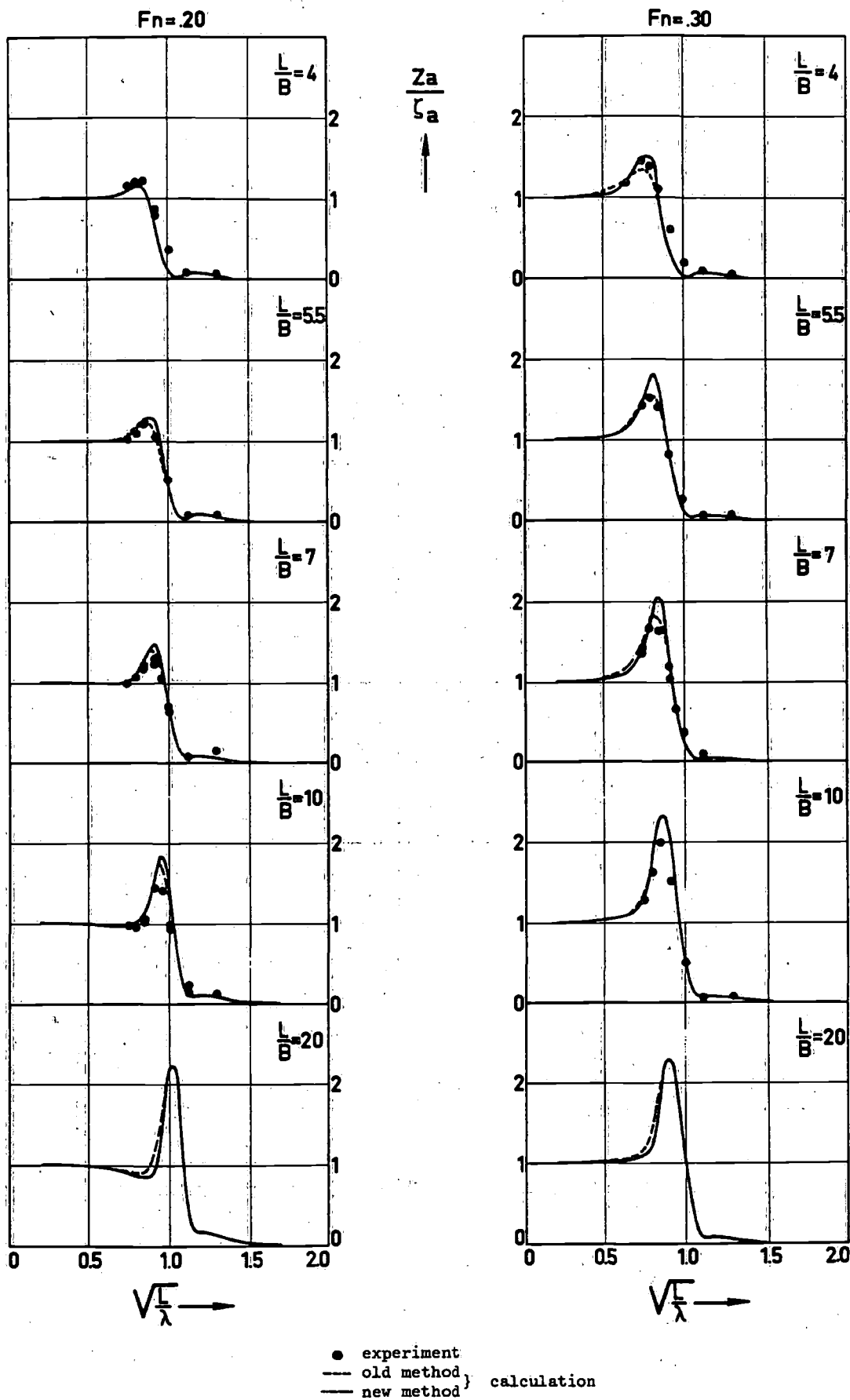


Figure 9 : Heave amplitude in waves

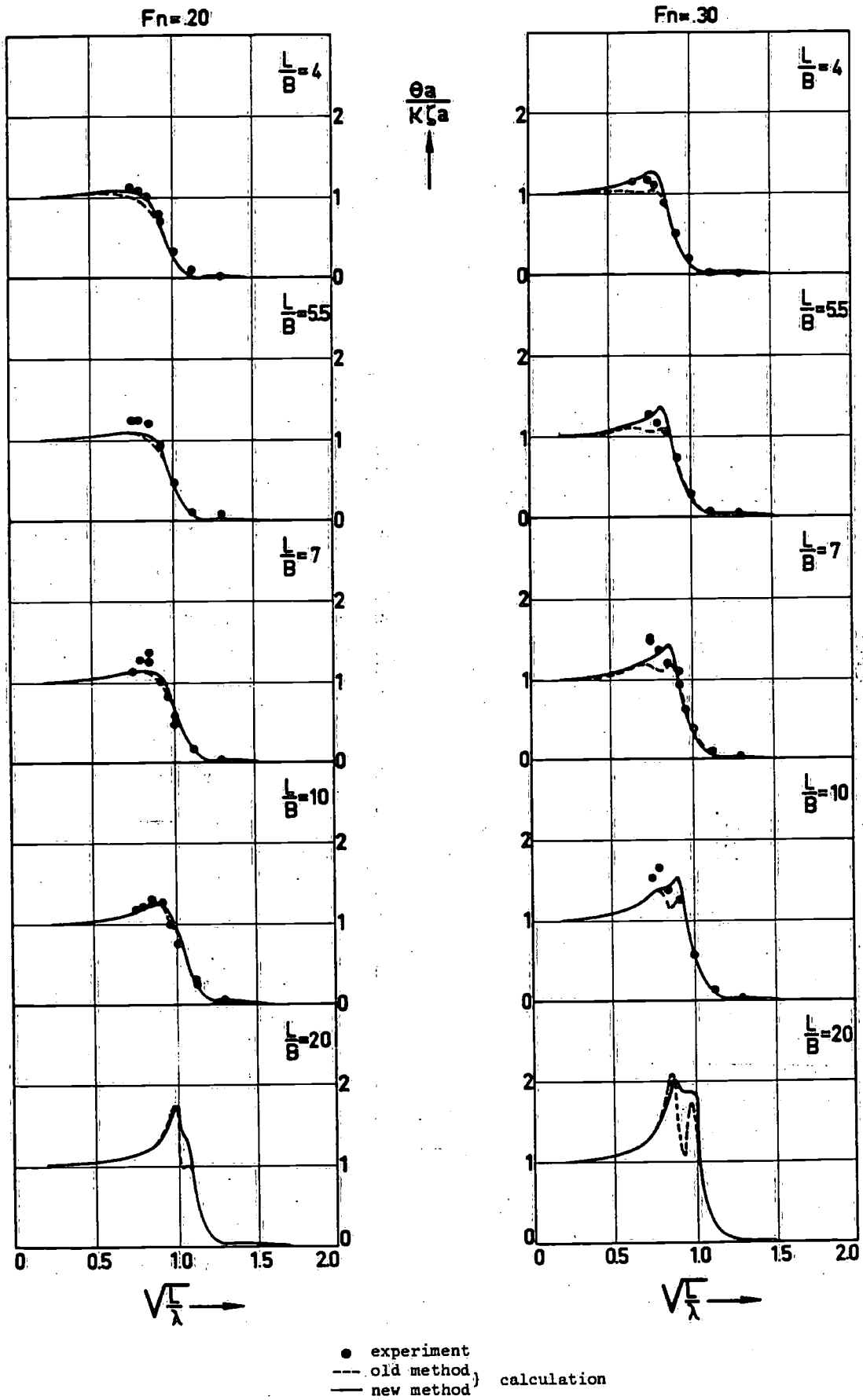


Figure 10 : Pitch amplitude in waves

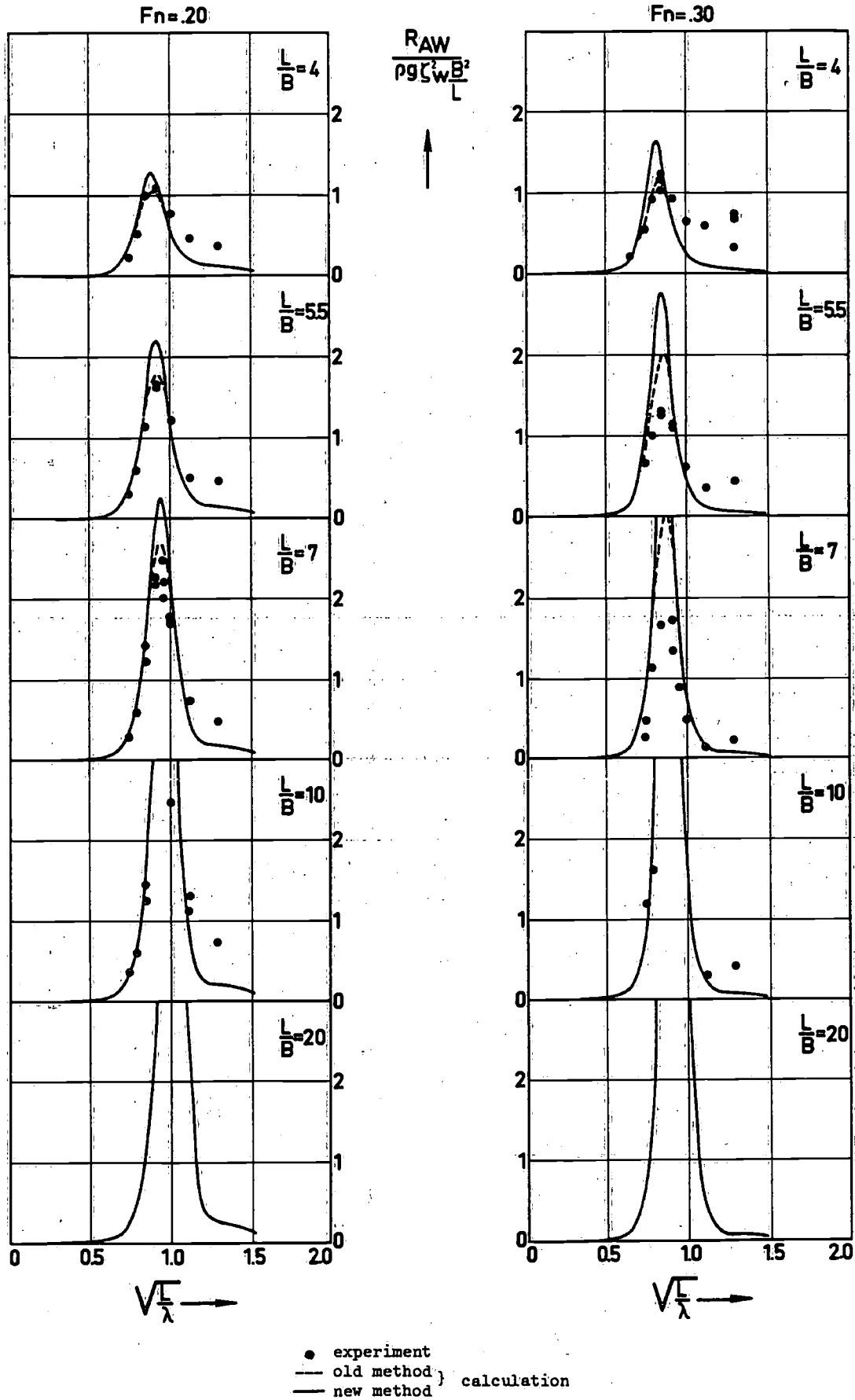


Figure 11 : Added resistance in waves

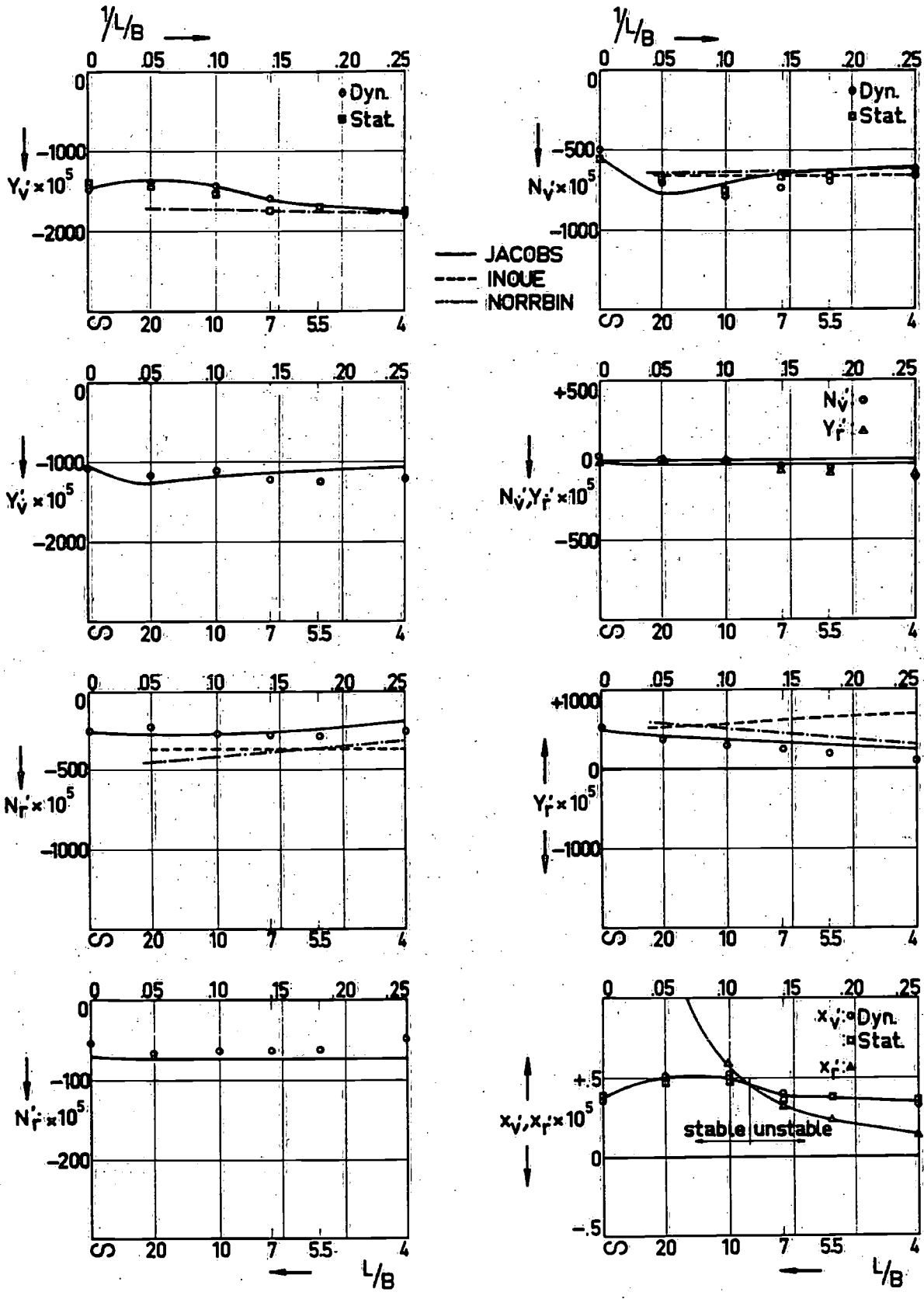


Figure 12 : Hydrodynamic coefficients for  $F_n = 0.15$



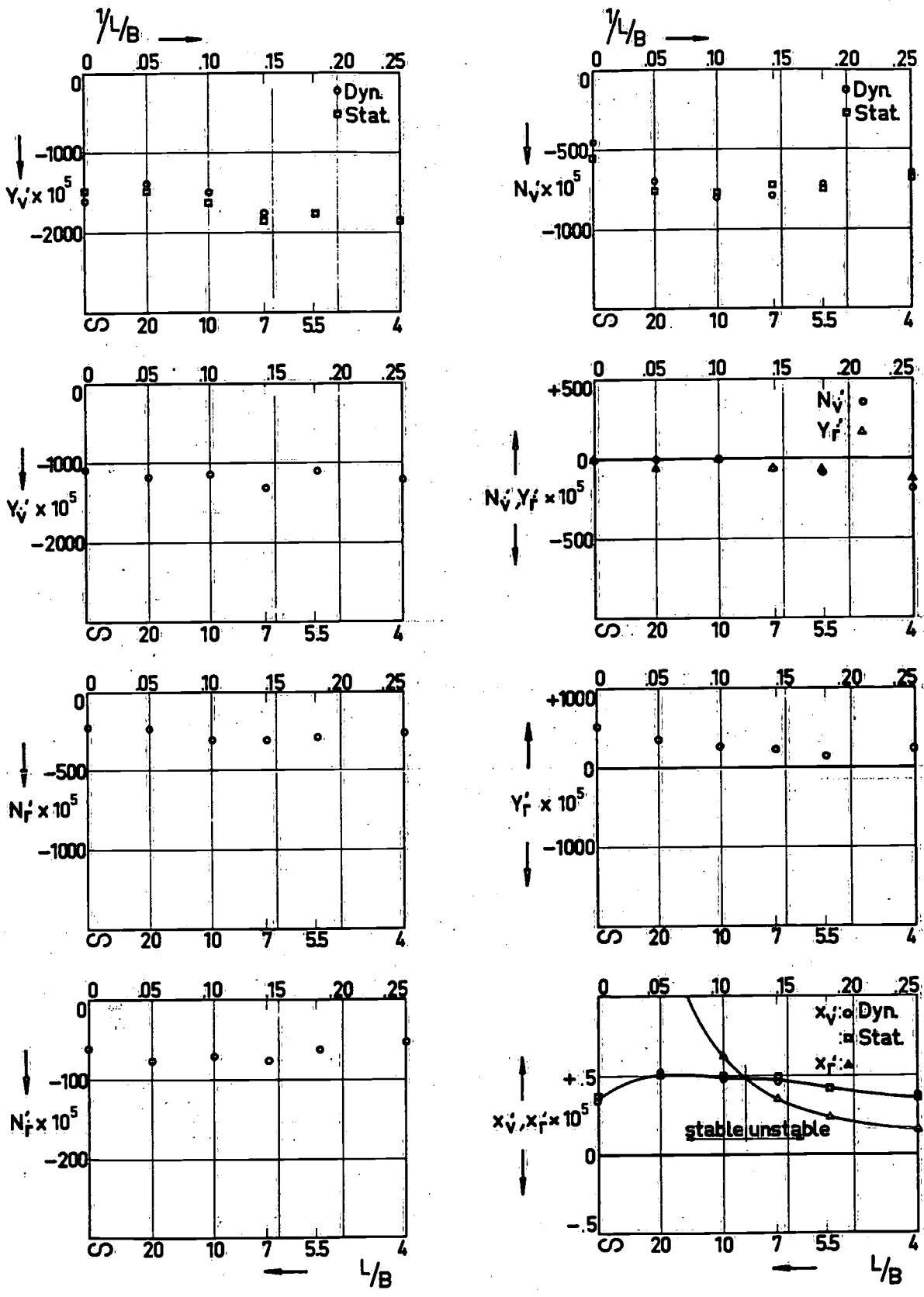


Figure 13 : Hydrodynamic coefficients for  $F_n = .20$

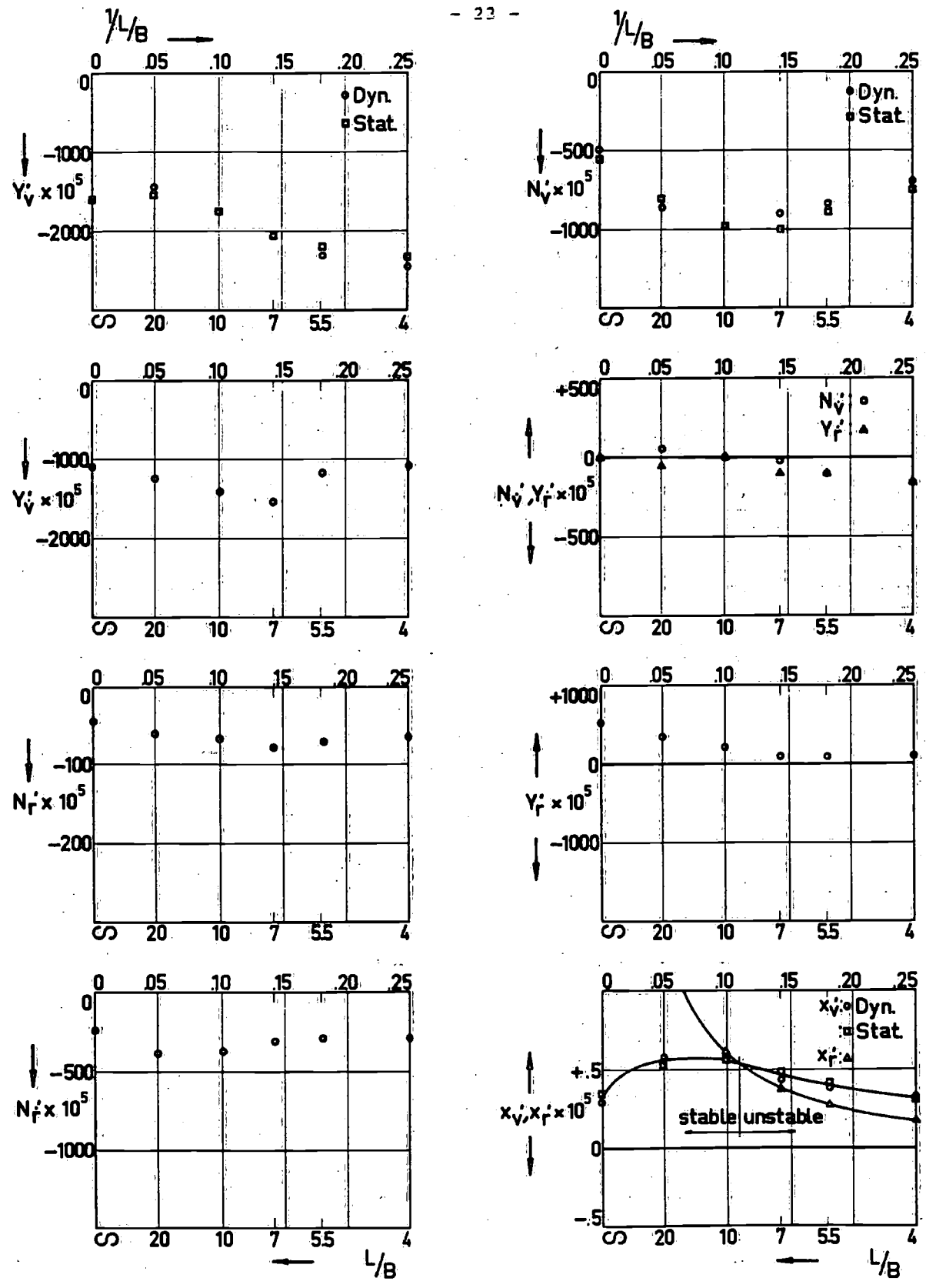


Figure 14 Hydrodynamic coefficients for  $F_n = 0.30$

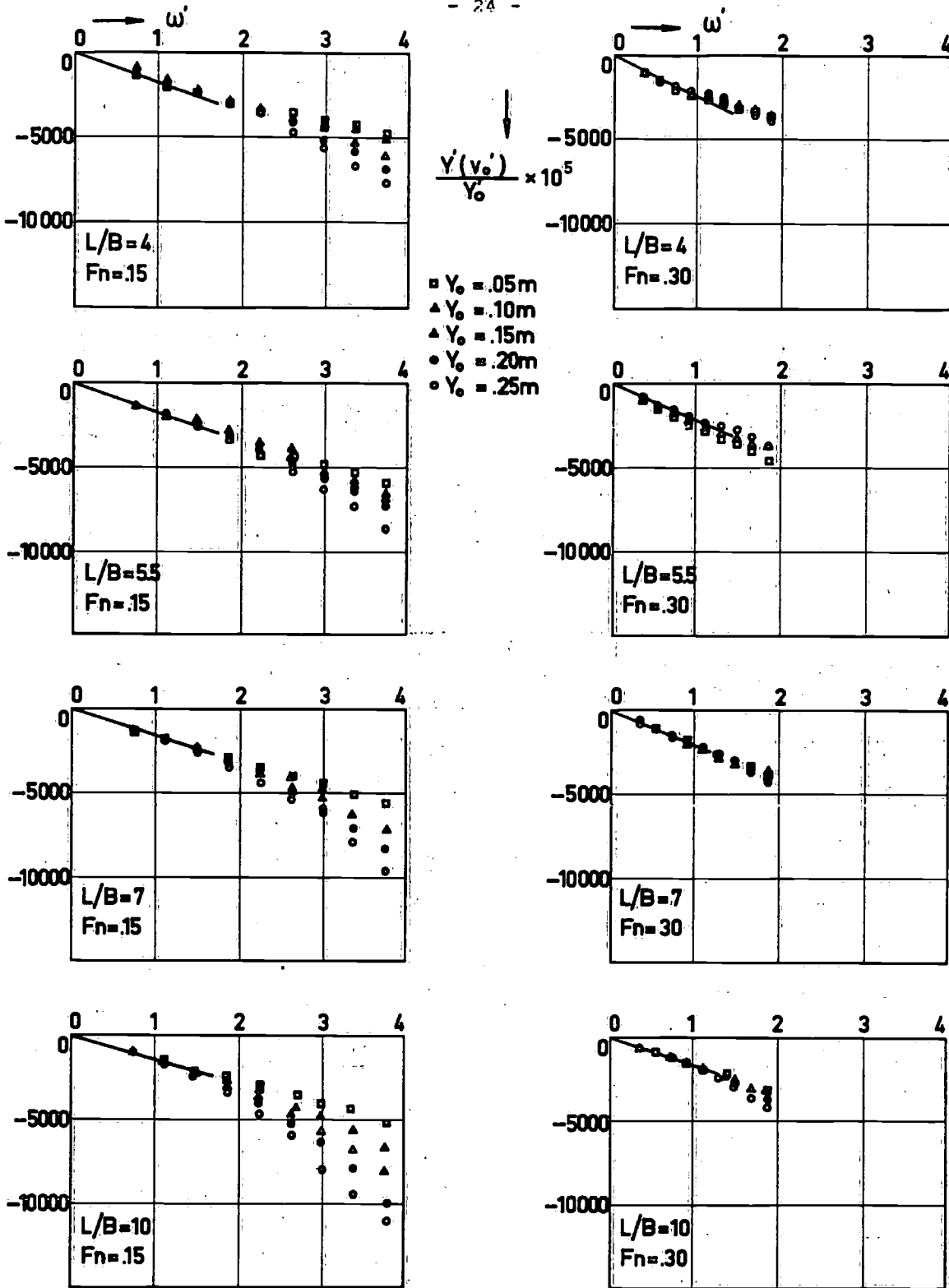


Figure 15 : to be continued

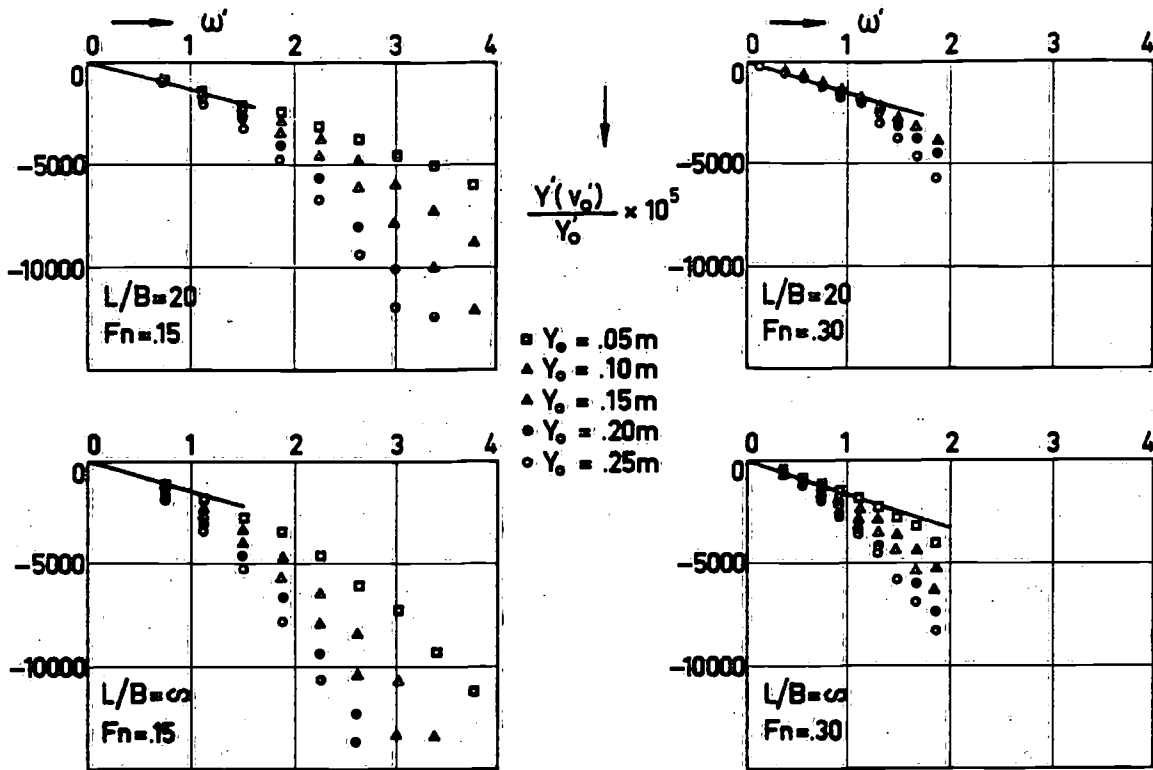


Figure 15 : Sway force for two Froude numbers as function of L/B-ratio

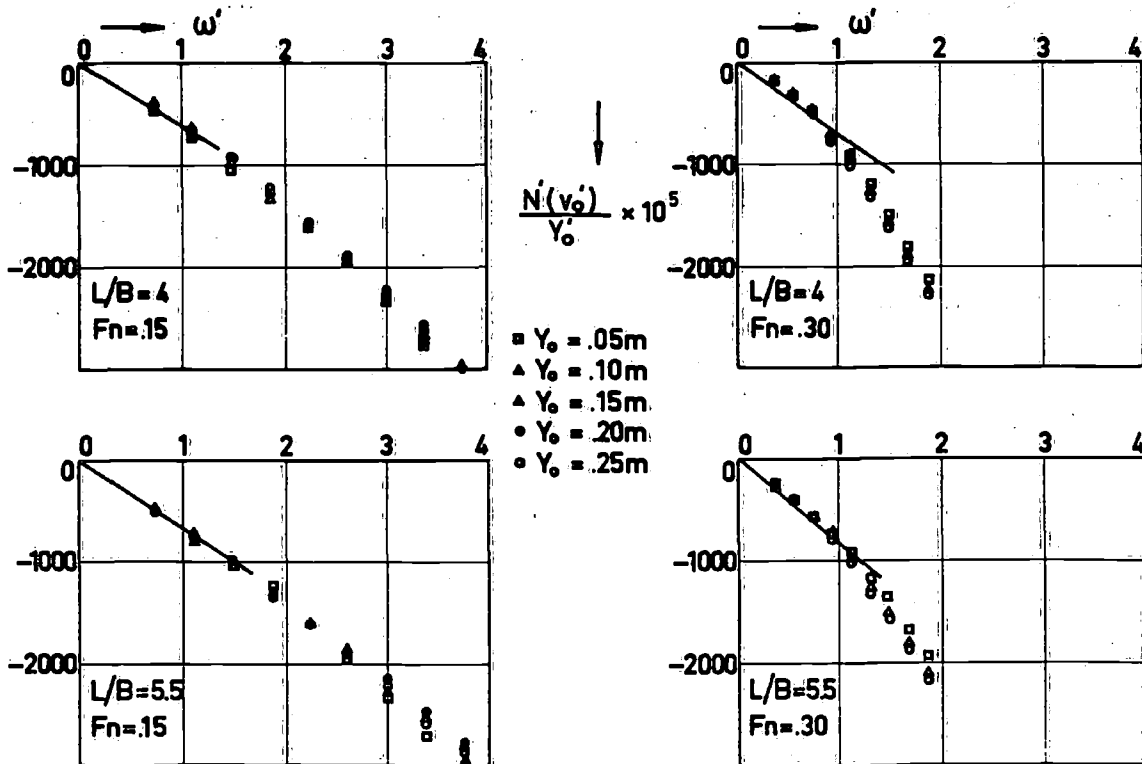


Figure 16 : to be continued

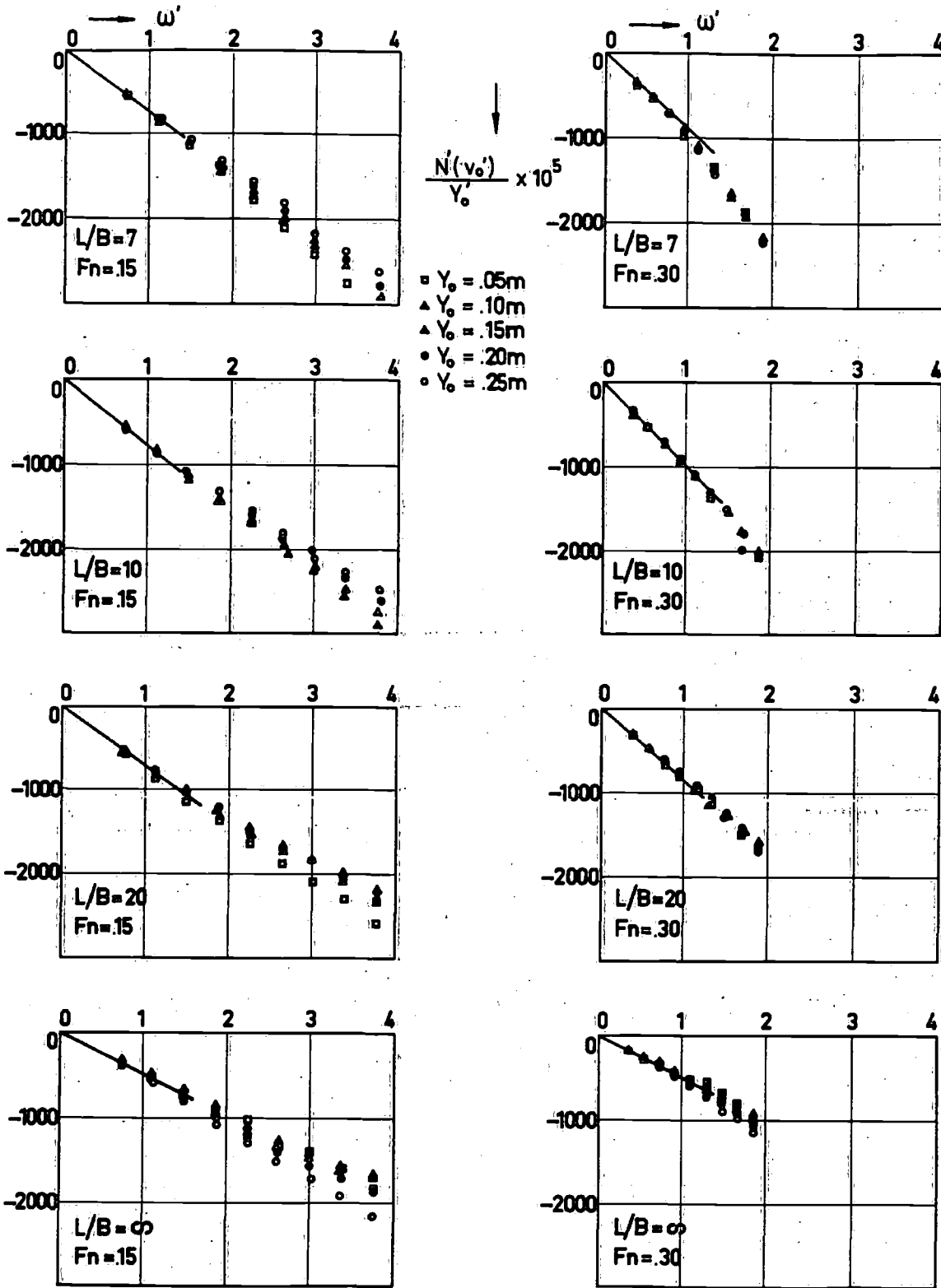


Figure 16 : Sway moment for two Froude numbers as function of L/B-ratio

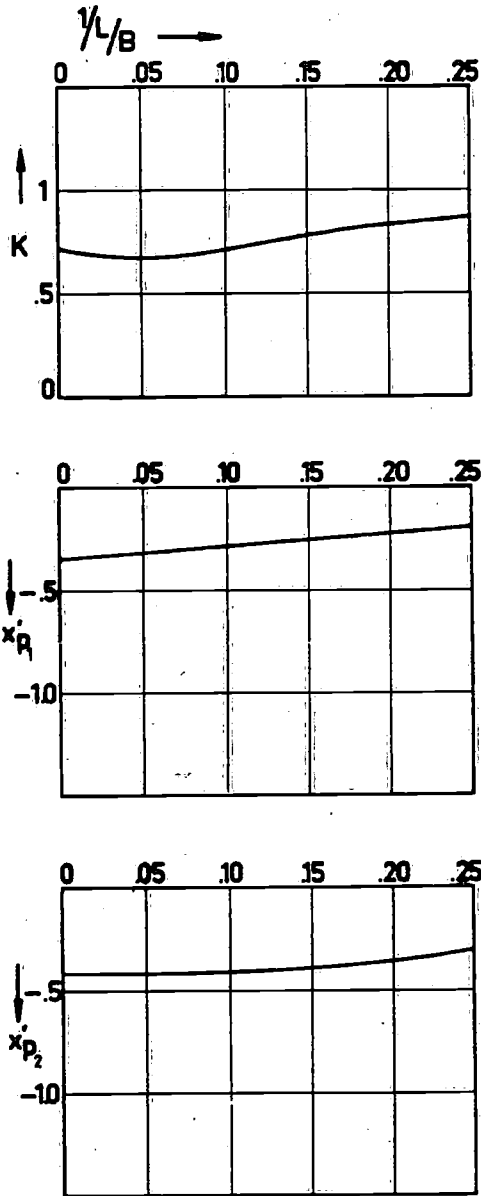


Figure 17 : Empirical coefficients derived from the experiments

Rapport no. 404



# LABORATORIUM VOOR SCHEEPSBOUWKUNDE

TECHNISCHE HOGESCHOOL DELFT

ZEILPRESTATIES VAN DE OCEAN CRUISER 16

door

W. Beukelman

juni 1974

## 1. Uitgevoerde metingen

De Ocean Cruiser 16 is een snel toerjacht voor zeilen op de oceaan. Het jacht is ontworpen door G. Dijkstra, Amsterdam ten behoeve van hemzelf. De prestatieingen zijn met een model van bovengenoemd jacht op de gebruikelijke wijze uitgevoerd in het Laboratorium voor Scheepsbouwkunde. De resultaten van de metingen zijn gegeven in de volgende tabellen en figuren :

### Tabellen :

- I : Belangrijkste gegevens van schip en model
- II : Weerstand recht op en zonder drift
- III : Vergelijking van de weerstand per ton waterverplaatsing van de romp
- IV : Prestaties bij standaard windsnelheden
- V : Zeiloppervlak bij systematisch gevarieerde masthoogte
- VI : Snelheid-voor-de-wind bij variabele masthoogte
- VII : Gezeilde tijd op een standaardbaan
- VIII : Gemeten en berekende dwarskrachtproductie

### Figuren :

- 1. : Vorm testwaterlijn en kromme van spantoppervlakken
- 2. : Snelheid-voor-de-wind
- 3. : Snelheid-in-de-wind
- 4. : Vergelijking dimensieloze snelheid-in-de-wind
- 5. : Snelheid-in-de-wind bij variabele masthoogte en stabiliteit
- 6. : Aangrijpingspunt dwarskracht bij helling nul.



## 2. Resultaten

Recht op varend, zonder drift is de weerstand in kg per ton waterverplaatsing voor snelheden onder  $\frac{+F}{n} = .35$  gunstig ten opzichte van vergelijkbare schepen; boven deze snelheid is de weerstand iets nadeliger. Hieruit blijkt duidelijk de invloed van de lage prismatische coefficient. Waarschijnlijk zou met een kiel van geringere dikte een nog iets gunstiger weerstand te bereiken zijn.

Voor en aan de wind varend blijken de resultaten matig te zijn voor lage windsnelheden tot normaal voor hogere windsnelheden.

Gelet op de gunstige weerstand kan dit wat betreft het varen voor de wind alleen maar veroorzaakt worden door het relatief kleine zeiloppervlak. Hierdoor blijven de prestaties bij lage windsnelheden iets onder die van de vergelijkbare schepen.

De dwarskrachtweerstandsverhouding is matig wat vooral een gevolg kan zijn van de lage aspektverhouding van de kiel. Daardoor zijn de drifthoeken en derhalve ook de weerstand bij aan de wind varen betrekkelijk hoog. De geringere statische stabiliteit ten gevolge van de dikke kiel kan hierbij ook nog een rol spelen.

Dezelfde conclusies gelden ook voor de gezeilde tijden op de standaardbaan.

Uit de snelheid-in-de-wind bij variabele masthoogte en stabiliteit (fig.5) blijkt, dat vergroting van het zeiloppervlak voordelig is.

Merkwaardig is, dat bij lage windsnelheden vermindering van de stabiliteit een overigens gering gunstig effect heeft. Voor de hogere windsnelheden geldt echter het omgekeerde.

Tabel I : Ocean Cruiser 16

: Belangrijkste gegevens van schip en model

symbool	omschrijving	eenheid	schip	model (1)
$L_{OA}$	lengte over alles	m	16.015	1.929
$L_{TWL}$	lengte op testwaterlijn	m	12.800	1.542
$B_{MAX}$	maximum breedte	m	4.124	0.497
$B_{TWL}$	max. breedte op testwaterlijn	m	3.650	0.444
$T_H$	diepgang van de romp	m	0.915	0.110
$T$	diepgang tot onderkant kiel	m	2.360	0.284
$\Delta_H$	deplacement van de romp in zoet water	kg	16942.0	.
$\Delta$	deplacement totaal in zoet water	kg	19451.0	34.018
$LCB_H$	ligging drukkingspunt tov midden testwaterlijn	m	- 0.38	0.046
$L_{TWL} / \Delta_H^{1/3}$	lengte deplacement verhouding (slankheidsgraad)		4.984	.
$B_{TWL} / T_H$	breedte diepgang verhouding		3.989	.
$LCB_H / L_{TWL}$	relatieve ligging drukkingspunt	%	3.96	.
$C_{PH}$	prismatische coefficient		.	.
$S$	totaal nat oppervlak	$m^2$	53.900	0.782
$z_{G_s}$	ligging gewichtszwaartepunt tov waterlijn	m	- 0.538	.
$I$	hoogte voordriehoek	m	19.00	.
$J$	basis voordriehoek	m	6.85	.
$P_e$	effektieve lengte voorlijk grootzeil	m	17.60	.
$E$	lengte onderlijk grootzeil	m	5.07	.
$SA_{eb}$	effektief zeiloppervlak aan-de-wind	$m^2$	99.93	.
$SA_{ed}$	effektief zeiloppervlak voor-de-wind	$m^2$	255.46	.
$z_{CE_e}$	effektief zeilpunt boven testwaterlijn	m	7.99	.
$b$	kielhoogte	m	1.450	.
$\bar{c}$	gemiddelde koorde kiel	m	3.850	.
$a_g$	geometrische aspektverhouding kiel		0.377	.
$\Lambda$	pijlhoek	gr	21.0	.
$\frac{1}{2}\alpha_e$	halve intreehoek waterlijn	gr	19.0	.

(1) Modelschaal: 1 : 8.3

Tabel II : Ocean Cruiser. 16

: Weerstand rechtop en zonder drift.

$v_s$ m/s	$V_s$ kn	$R_{T_s}$ kg	$F_n(1)$	$R_{T_s}/\Delta_H$ kg/ton
1.440	2.80	20.3	0.129	1.20
1.729	3.36	30.4	0.154	1.79
2.017	3.92	42.5	0.180	2.51
2.305	4.48	57.1	0.206	3.37
2.593	5.04	78.5	0.231	4.63
2.737	5.32	89.3	0.244	5.27
2.881	5.60	101.5	0.257	5.99
3.025	5.88	115.3	0.270	6.80
3.169	6.16	130.2	0.283	7.68
3.313	6.44	146.9	0.296	8.67
3.457	6.72	164.2	0.309	9.69
3.601	7.00	183.6	0.321	10.84
3.745	7.28	205.4	0.334	12.12
3.889	7.56	244.3	0.347	14.42
4.033	7.84	292.9	0.360	17.29
4.177	8.12	363.4	0.373	21.45
4.321	8.40	454.3	0.386	26.81
4.466	8.68	553.5	0.399	32.67
4.610	8.96	674.3	0.411	39.80
4.754	9.24	828.8	0.424	48.92
4.898	9.52	1004.9	0.437	59.31
5.042	9.80	1193.9	0.450	70.47
5.186	10.08	1416.3	0.463	83.60
.	.	.	.	.
.	.	.	.	.

$$(1) : F_n = \frac{v_s \text{ (m/s)}}{\sqrt{gL_{TWL}}}$$

Tabel III : Ocean Cruiser 16

: Vergelijking van de weerstand per ton waterverplaatsing  
van de romp.

$F_n$	$R_{Ts} / \Delta_H$ kg / ton		
	$L_{TWL} = 12.80$	model 135 $L_{TWL} = 11.00$	model 132 $L_{TWL} = 14.06$
0.10			0.7
0.15	1.69	1.85	1.8
0.20	3.15	3.46	3.3
0.25	5.58	5.86	5.5
0.30	9.01	8.99	9.2
0.35	15.00	14.66	14.9
0.40	33.42	32.16	29.7
0.45	70.54	67.99	59.0

Tabel IV : Ocean Cruiser 16

: Prestaties bij standaard windsnelheden

wind-snelheid	grootheid	(1)	(2)	(3)	(4)
3.5 m/s	$v_d / \sqrt{gL_{TWL}}$	0.180	0.190	0.179	.
	$v_{mg} / \sqrt{gL_{TWL}}$	0.161	0.170	0.178	.
	$v_s / \sqrt{gL_{TWL}}$	0.211	0.234	0.241	.
	$\phi$	6.4	7.1	8.6	.
	$\beta$	3.6	3.1	2.7	.
7.0 m/s	$v_d / \sqrt{gL_{TWL}}$	0.334	0.350	0.335	.
	$v_{mg} / \sqrt{gL_{TWL}}$	0.246	0.255	0.252	.
	$v_s / \sqrt{gL_{TWL}}$	0.313	0.320	0.319	.
	$\phi$	15.3	17.5	19.6	.
	$\beta$	4.7	4.3	4.1	.
10.0 m/s	$v_d / \sqrt{gL_{TWL}}$	0.402	0.418	0.413	.
	$v_{mg} / \sqrt{gL_{TWL}}$	0.274	0.280	0.273	.
	$v_s / \sqrt{gL_{TWL}}$	0.343	0.345	0.342	.
	$\phi$	23.1	26.0	28.1	.
	$\beta$	6.1	5.7	5.8	.

(1) : Ocean Cruiser

:  $L_{TWL} = 12.80$  m

(2) : Model 135

:  $L_{TWL} = 11.00$  m

(3) : Model 132

:  $L_{TWL} = 14.06$  m

(4) :

:  $L_{TWL} =$  m.

$v_d$  = snelheid-voor-de-wind in m/sec.

$v_{mg}$  = snelheid-in-de-wind in m/sec.

$v_s$  = scheepssnelheid in m/sec. bij zeilen aan-de-wind

$\phi$  = hellingshoek in graden, aan-de-wind

$\beta$  = drifhoek in graden, aan-de-wind

$g$  = versnelling van de zwaartekracht,  $9.81 \text{ m/sec}^2$

$L_{TWL}$  = effectieve lengte testwaterlijn.

Tabel V : Ocean Cruiser. 16

: Zeiloppervlak bij systematisch gevarieerde masthoogte

I m	effektief zeiloppervlak		hoogte effectief zeilpunt boven TWL m
	aan-de-wind m <sup>2</sup>	voor-de-wind m <sup>2</sup>	
17.10	89.6	229.6	7.35
18.05	94.0	242.5	7.66
19.00	99.9	255.5	7.98
19.95	105.1	268.4	8.30
20.90	110.3	281.4	8.62

Tabel VI :

: Snelheid-voor-de-wind bij variabele masthoogte

I m	snelheid-voor-de-wind in m/s		
	$v_{tw}=3.5$ m/s	$v_{tw}=7.0$ m/s	$v_{tw}=10.0$ m/s
17.10	1.97	3.66	4.44
18.05	1.99	3.70	4.47
19.00	2.01	3.74	4.50
19.95	2.03	3.77	4.53
20.90	2.05	3.80	4.56

Tabel VII : Ocean Cruiser 16  
 : Gezeilde tijd op een standaardbaan (1)

schip	L <sub>TWL</sub> m	gezeilde tijd in uur/min/sec.		
		v <sub>tw</sub> = 3.5 m/s	v <sub>tw</sub> = 7.0 m/s	v <sub>tw</sub> = 10.0 m/s
	12.00	5/24/54	3/14/45	2/49/01
	.	1/1	1/1	1/1
model 135	11.00	5/31/00	3/21/14	2/57/05
model 132	14.00	4/54/48	3/02/44	2/39/59

(1) : De baan is 10 mijl lang en wordt heen en terug gevaren. De wind-  
 richting is evenwijdig aan de baan

Tabel VIII : Ocean Cruiser. 16

Gemeten en berekende dwarskrachtproduktie

Bij helling nul :

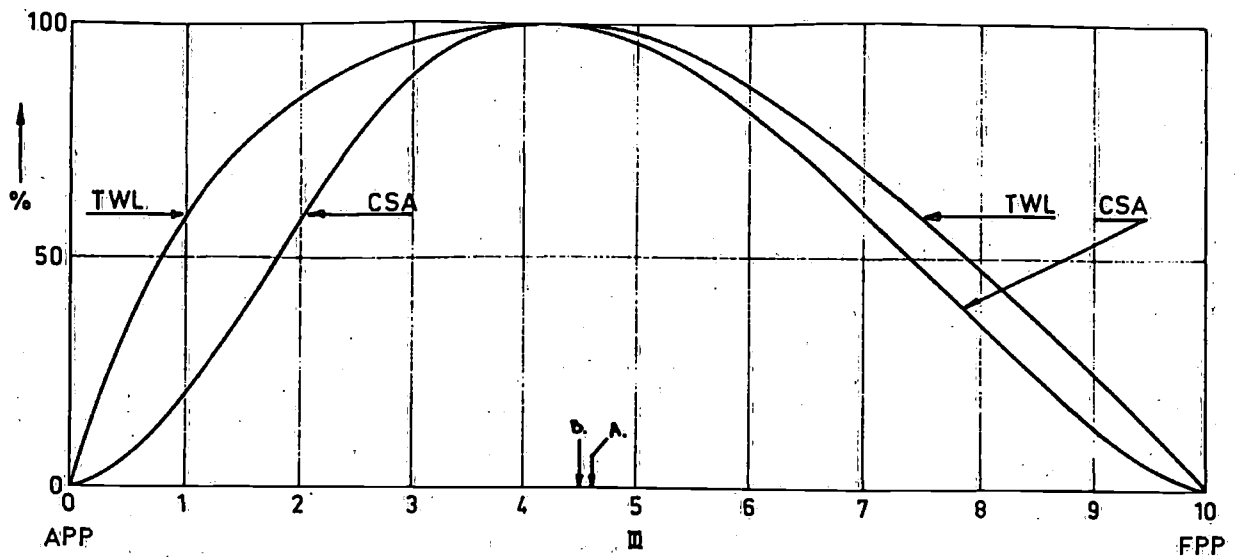
		$F_n = 0.20$ $v_s = 2.24$	$F_n = 0.35$ $v_s = 3.92$
$F_H \cos \phi / (\beta v_s^2)$	berekend	15.0	15.0
$F_H \cos \phi / (\beta v_s^2)$	gemeten	14.7	14.8

Onder helling :

$\phi$ gr	$v_s$ m/s	$F_H \cos \phi / (\beta v_s^2)$ gemeten kg s <sup>2</sup> / graad m <sup>2</sup>	$F_H / (\beta \cos \phi \cdot v_s^2)$ kg s <sup>2</sup> / graad m <sup>2</sup>
10	2.9	14.7	15.1
20	3.7	13.1	14.8
30	4.0	12.0	16.0

N.B. : Hoewel de dwarskrachten gedeeld zijn door  $v_s^2$  blijken de experimentele waarden ook dan nog licht afhankelijk van de snelheid te zijn. Het snelheidsgebied waarin de meting uitgevoerd is, is daarom aangegeven.





- A: ligging drukkingspunt romp in lengte
- B: ligging waterlijnzwortepunt in lengte

Fig. 1: Vorm testwaterlijn en kromme van spontoppervlokken

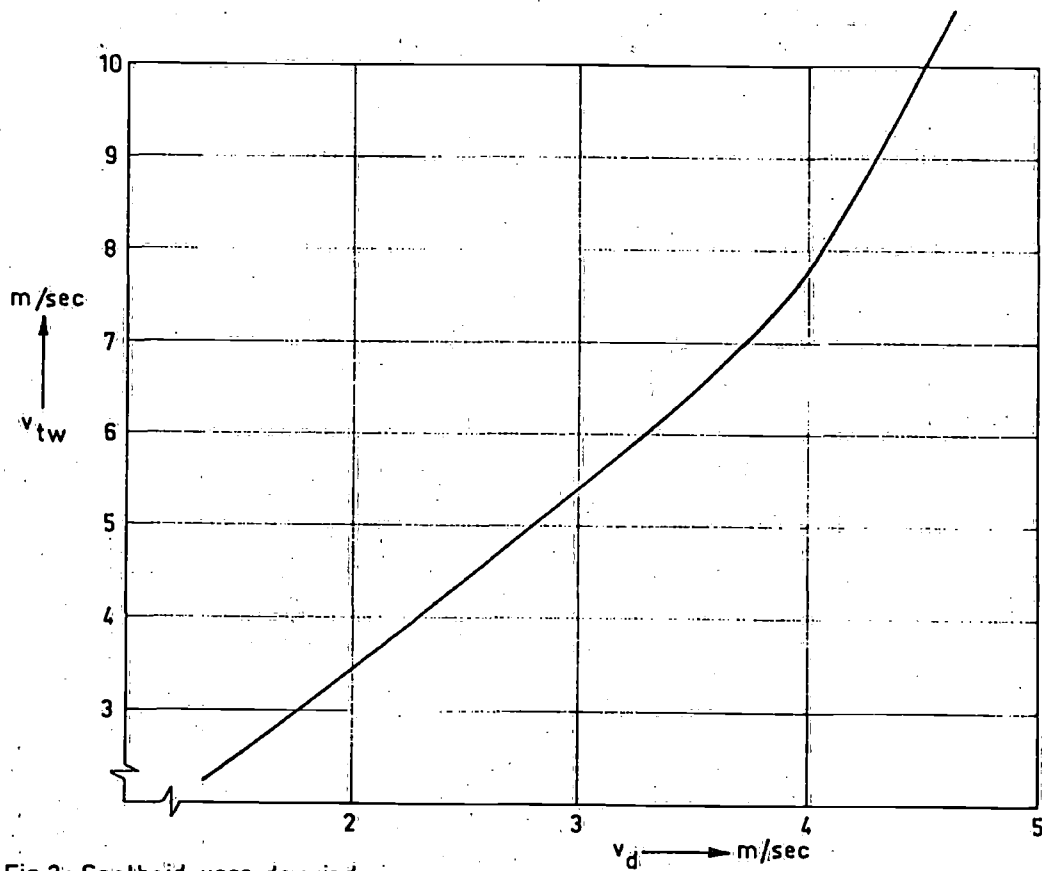


Fig. 2: Snelheid-voor-de-wind

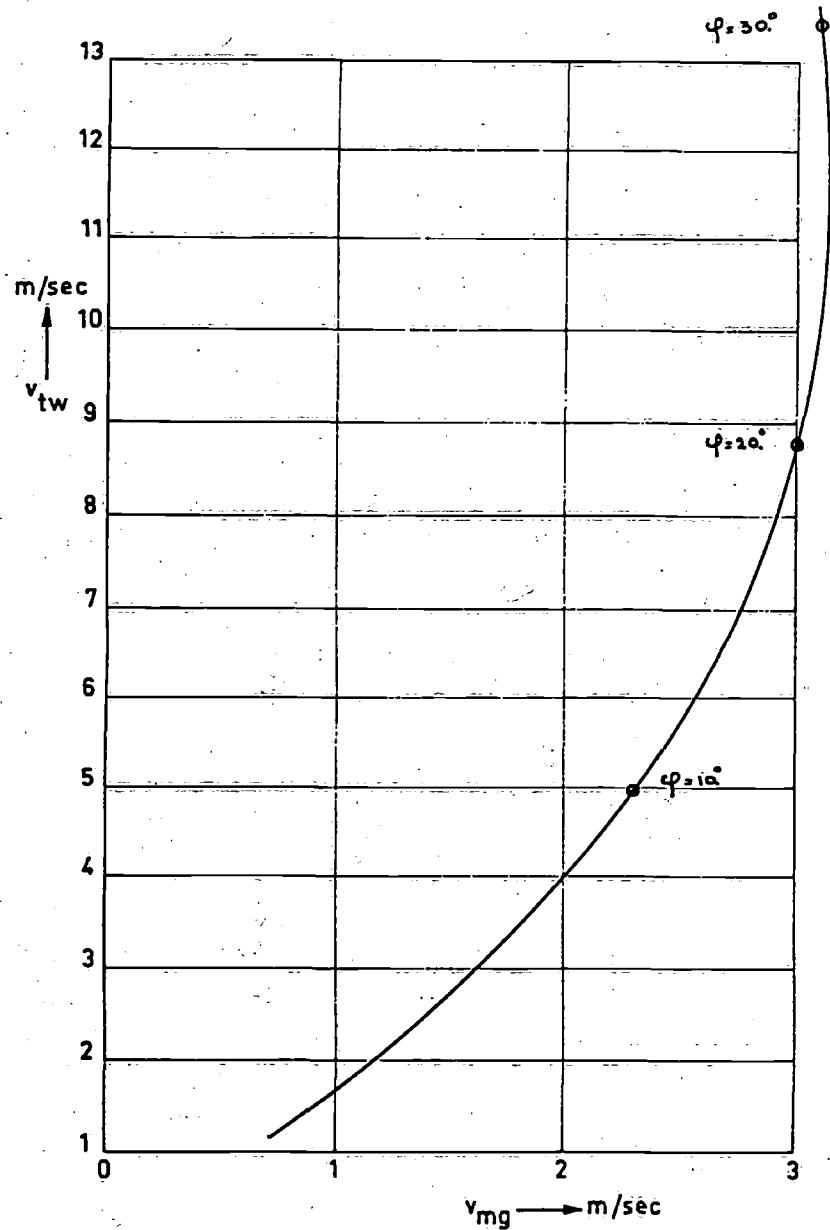


Fig.3: Snelheid-in-de-wind

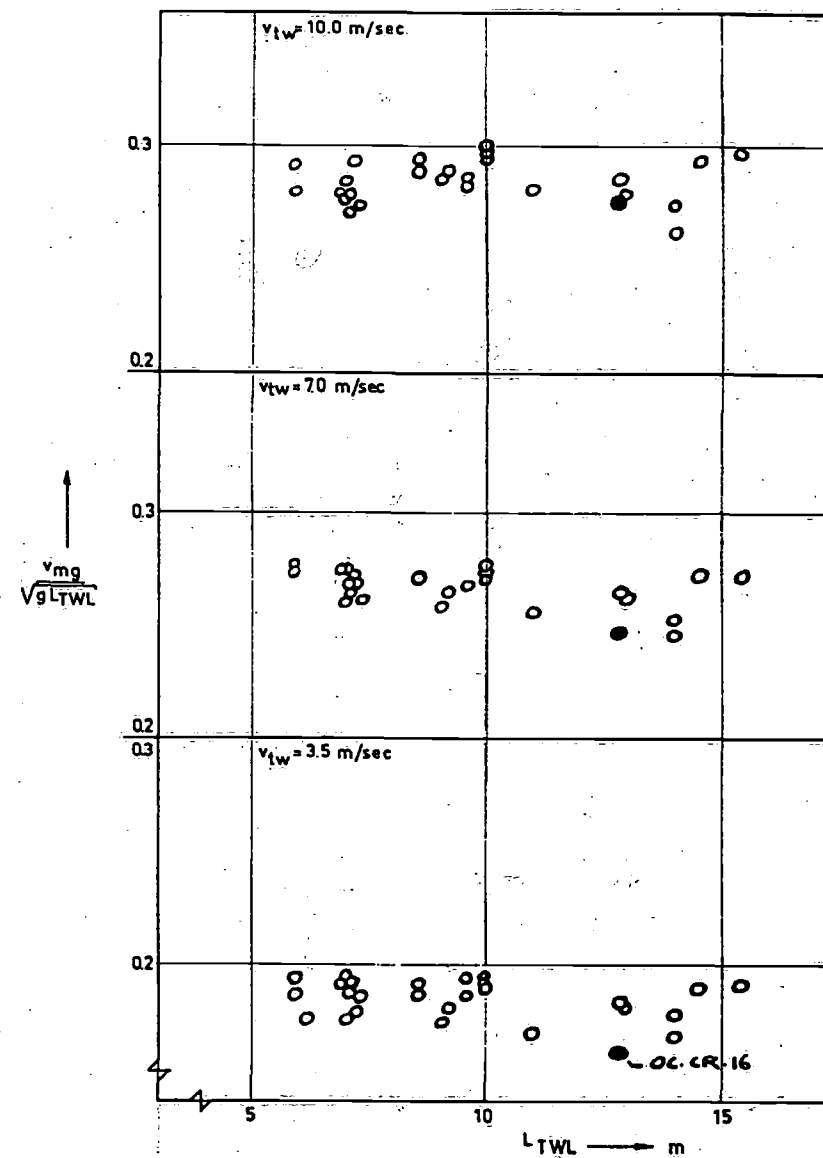
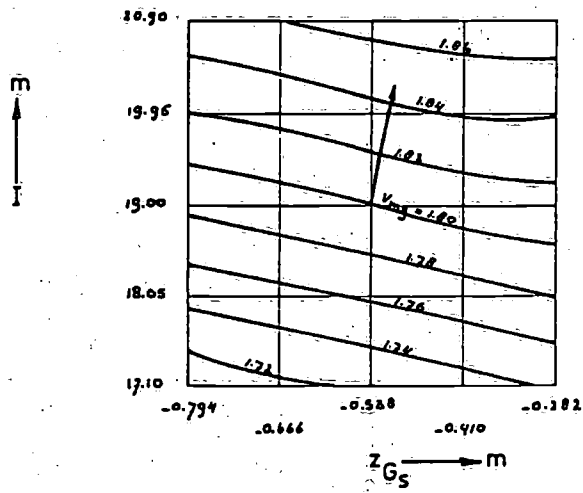
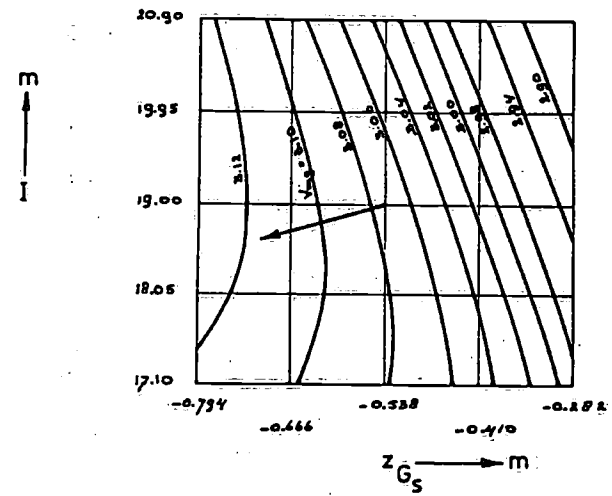


Fig.4: Vergelijking dimensieloze snelheid-in-de-wind.

$v_{tw} = 3.5 \text{ m/sec}$



$v_{tw} = 10.0 \text{ m/sec}$



$v_{tw} = 7.0 \text{ m/sec}$

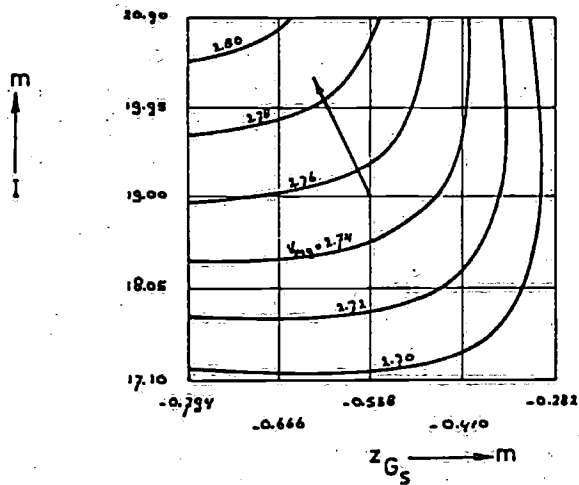
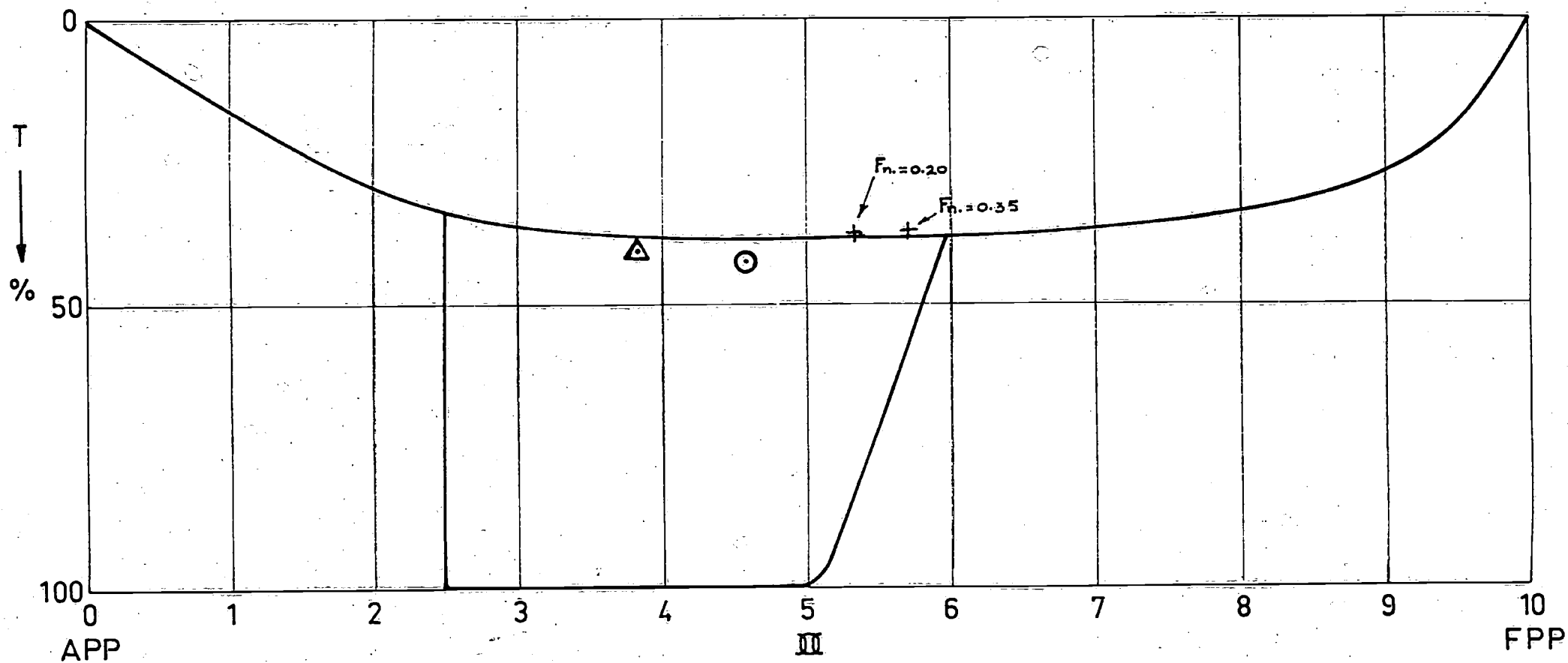


Fig. 5b: Snelheid-in-de-wind bij variabele masthoogte en stabiliteit

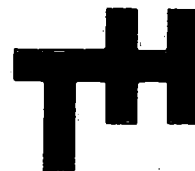
Fig. 5a: Snelheid-in-de-wind bij variabele masthoogte en stabiliteit



- $\odot$  BEREKEND (roer in middenstand)
- $+$  GEMETEN ( " " " )
- $\Delta$  BEREKEND (effektieve invalshoek roer en kiel gelijk)

Fig.6: Aangrijpingspunt dwarskracht bij helling nul.

Report No. 420



# LABORATORIUM VOOR SCHEEPSBOUWKUNDE

TECHNISCHE HOGESCHOOL DELFT

COMPARISON OF SEAKEEPING PREDICTION  
METHODS FOR DIFFERENT SHIPS

by

W. Beukelman

June 1975.

CONTENTS.

1. Summary.
2. Introduction.
3. Ships considered.
4. Calculation procedures.
  - 4.1. Smith effect for bulbous sections.
5. Calculated parameters.
6. Discussion and comparison of results.
7. Conclusions.
8. Nomenclature.
9. References.
10. Tables and Figures.

## 1. SUMMARY.

Four different procedures to determine the added mass and damping have been used to predict the seakeeping performance for different ship-types with an increasing length, block-coefficient and bulb.

Only vertical motions have been considered for the case of head waves.

If the close-fit procedures are accepted as a reference, it appears that besides a MIT bulb-form transformation also and for many cases with slight preference an adaptive Lewis-transformation, suitable for bulbous sections, may be applied for the prediction of seakeeping qualities.

## 2. INTRODUCTION.

For the calculation of added mass and damping of the ship-sections the following procedures have been used:

1. the close-fit mapping method for a good approximation of the cross-section (1,2)
2. an adaptive Lewis-transformation of the cross section to the unit circle with a special application for bulbous sections. For normal Lewis-transformation see (3,4).
3. the Frank close-fit method with a distribution of pulsating sources along the contour of the cross-sections (5,6,11).
4. the MIT bulb-form transformation specially for bulbous sections combined with a normal Lewis-transformation for the other cross-sections (4).

After the calculation of the sectional added mass and damping as denoted above the seakeeping performance in regular and irregular waves has been determined in the same way and according to Korvin-Kroukovky's strip theory as modified by Gerritsma e.a. in (7). It should be remarked, that a version has been used in which no symmetrical terms for the added mass cross coupling coefficients were present. This version is referred to in (8) as the old method.

The following parameters have been determined:

the heaving and pitching motion, the vertical wave bending moment at the midship section, the added resistance or-power in waves, the phenomena of slamming and ship-ping in standard irregular seas.

These calculations have been applied for five ships with different lengths, block-coefficients and bulb-sizes.

It was the intention to show the differences in the final results because of the mentioned methods to determine the sectional added mass and damping.



### 3. SHIPS CONSIDERED.

As denoted before the calculations have been carried out for five ships with increasing length, blockcoefficient and bulb. These ships are the following ones:

1. the well-known Todd 60 series hull form with  $C_B = .70$ .
2. the "S.A. van der Stel", a fast cargo-ship with a small bulb (4.4%) (9)
3. the "Atlantic Crown", a containership with a circular bulb of moderate size (9.5%) (10)
4. the "Davidson A Destroyer" with an extremely bulbous fore-ship (35%) (11)
5. the "Macoma" a tanker with a bulb of 6.9% (12)

For the principal ship data see table 1 and for the offsets see tables 2-6.

It should be remarked, that the MITT-bulbform transformation could only be applied for the "Atlantic Crown" and the "Davidson A Destroyer". The integrated weight-distribution has also been presented in tables 2-6 for the different ships except for the "Atlantic Crown". In this case the integrated weight-distribution was unknown. For the motions of this ship has been made use of an estimated radius of inertia. The block coefficient varied from  $C_B = .540$  until  $C_B = .850$ , while the ship length varied from  $L = 117\text{m}$  until  $L = 310\text{m}$ .

For all ships the full-load condition only has been taken into account.

The calculations have originally been made for two ship speeds, but the tendency proved to be the same for both these speeds, so that in the figures the results for one speed only have been presented.

4. CALCULATION PROCEDURES.

In the close-fit mapping procedure the ship section is conformally mapped to the unit circle and a distribution of multipoles is used for the solution. The mapping is done by the following transformation formula:

$$z = \zeta + \sum_{n=1}^N a_{2n-1} \zeta^{-(2n-1)} \quad (1)$$

where  $N$  = maximum index number of the transformation coefficient.

The number  $N$  used for the ships considered is shown in table 1. The mapping under consideration is rather accurate. A good description of the transformation procedure has been presented by De Jong in (2). The computer results for added mass and damping have proved to agree very well with experimental results (7). For this reason the results of the close-fit procedure are accepted as a reference to check the accuracy more or less of the other methods.

The Lewis-transformation is obtained by using  $N = 2$  for (1) which results into:

$$z = \zeta + \frac{a_1}{\zeta} + \frac{a_3}{\zeta^3} \quad (2)$$

The half-beam to draft ratio and the sectional area coefficient are presented as follows:

$$H_0 = \frac{B}{2T} = \frac{1 + a_1 + a_3}{1 - a_1 + a_3} \quad (3)$$

$$\sigma = \frac{A}{BT} = \frac{\pi}{4} \frac{1 - a_1^2 - 3a_3^2}{(1 + a_3)^2 - a_1^2} \quad (4)$$

From (3) may be derived:

$$a_1 = \frac{H_0 - 1}{H_0 + 1} (a_3 + 1) \quad (5)$$

Substitution of (5) in (4) delivers the following equation:

$$c_1 a_3^2 + c_2 a_3 + c_3 = 0 \quad (6)$$

in which

$$\left. \begin{aligned} c_1 &= \left( 3 + \frac{4\sigma}{\pi} \right) + \left( 1 - \frac{4\sigma}{\pi} \right) \left( \frac{H_0 - 1}{H_0 + 1} \right)^2 \\ c_2 &= 2(c_1 - 3) \\ c_3 &= c_1 - 4 \end{aligned} \right\} \quad (7)$$

The solution of (6) results into:

$$a_3 = \frac{-c_1 + 3 \pm \sqrt{9 - 2c_1}}{c_1} \quad (8)$$

From the discriminant of (8) it is obvious, that the condition holds:

$$c_1 < 4.5 \quad (9)$$

If  $H_0 < 1$  then:

$$0 > \frac{H_0 - 1}{H_0 + 1} > -1 \quad (10)$$

and if  $H_0 > 1$  then:

$$0 < \frac{H_0 - 1}{H_0 + 1} < 1 \quad (11)$$

From (10) and (11) follows:

$$0 < \left( \frac{H_0 - 1}{H_0 + 1} \right)^2 < 1 \quad (12)$$

With (12) it can be shown, that  $c_1$  in (7) is increasing with  $\sigma$  and so the minimum value for  $c_1 = 3$ .

The limits for the coefficient  $c_1$  are

$$3 < c_1 < 4.5 \quad (13)$$

and for  $a_3$ , if only the positive root of (8) is taken into account:

$$.577 > a_3 > -.333 \quad (14)$$

The limits for  $a_1$  are to determine with (5), (10) and (11).

$$\text{if } H_0 < 1 \text{ then } 0 > a_1 > -1.577 \quad (15)$$

$$\text{and if } H_0 > 1 \text{ then } 0 > a_1 > 1.577 \quad (16)$$

The maximum values for the area coefficient may be evaluated for each  $H_0$  with condition (9) and delivers the relation:

$$\sigma < \frac{\pi}{32} \left( 10 + H_0 + \frac{1}{H_0} \right) \quad (17)$$

The minimum value of this range may be obtained by

$\frac{dG}{dH_0} = 0$  which shows, that this minimum value is achieved for  $H_0 = 1$ . and so with (17) the result is

$$\sigma_{MAX} = 1.178 \quad (18)$$

The maximum values for the area coefficient are shown in figure 1 for  $H_0 > 1$  and  $H_0 < 1$ .

Small values of the sectional area coefficient may cause reentrant forms, but this will only occur for very fine sections. This effect on the final results may be neglected or can easily be avoided as denoted in (13,4).

The half-beam of a section should not be too small. For bulbous sections the half-beam should not be smaller than 1% of the maximum half-beam of the ship.

If for a section condition (17) can not be fulfilled the adaptive procedure will be so, that half-beam and area are kept constant, while the draught will be increased to such a value, that condition (17) is satisfied. From this procedure follows the minimum new draught.

$$T = -2.5 B + \sqrt{6B^2 + \frac{16A}{\pi}} \quad (19)$$

For numerical reasons  $T$  should be increased up to  $1.0075T$ .

This procedure as described above is called the adaptive Lewis-transformation and will be specially required for bulbous sections, although the fit is not accurate. Generally speaking the representation of the section by the Lewis-transformation is rather poor, but this fit is not the main-target of the transformation.

It should be noted, that the use of this adaptive Lewis-transformation is restricted to vertical motions only.

The Frank close-fit method is based upon the determination of the velocity potential obtained for a distribution of source singularities over the submerged ship section. The sources which satisfy the linearized free-surface condition and the kinematic boundary condition on the surface of the section-cylinder have to be infinite in number to obtain a continuous source distribution. Frank (5) came to an approximation by using a finite source distribution in such a way, that a constant strength was considered for some straight segments replacing the original section. The hydrodynamic pressures are obtained from the potential by means of the linearized Bernoulli equation. Integration of these pressures over the submerged section-cylinder delivers the hydro-dynamic force. The accuracy of this solution depends on the chosen number of source segments. This number of segments has been denoted in table 1 for the ships considered. The hydrodynamic forces represented as added mass and damping

have been calculated with a computer program described and presented in (6).

The MIT bulb-form transformation developed by Demanche and presented in (4) by Loukakis is just as the Lewis-transformation based on the sectional half-beam to draught ratio and the sectional area coefficient and also characterized as a two-parameter transformation.

The mapping function of the MIT bulb-form is presented as

$$z = \xi + \frac{B\xi}{\xi^2 + A} \quad (20)$$

in which A and B are transformation coefficients.

The half-beam to draught ratio and the sectional area coefficient are related to the coefficients A and B in the next way:

$$H_0 = \frac{1 - A^2 + AB + B}{1 - A^2 + AB - B} \quad (21)$$

$$\sigma = \frac{\pi}{4} \left( 1 + A \frac{1 - H_0^2}{2H_0} \right) \quad (22)$$

The MIT bulb-forms are used in (4) for sections with  $H_0 \leq .6$  and  $\sigma > 1.2$  and claim to afford a rather good fit of the section.

For our calculation of added mass and damping of the bulbous ship sections according to the MIT bulb-form transformation use has been made of the Subroutine Bulb in (4).

The determination of the motions and other parameters have been performed with the same seakeeping computer-program "TRIAL" of the Shipbuilding Laboratory of the Delft University of Technology as described in (14), so that differences in the final results may only arise from differences in the sectional added mass and damping.

#### 4.1. Smith-effect for bulbous sections.

For the calculation of the sectional wave forces and -moments an effective draught  $T^*$  is used in (7) and (8) at which draught these forces and moments are supposed to act. In general this effective draught  $T^*$  may be found for each section by using a sufficient number of waterlines as shown in figure 2 and so it holds, that:

$$\begin{aligned} |\Delta y_0| e^{-kz_0} + |\Delta y_1| e^{-kz_1} + |\Delta y_2| e^{-kz_2} + \dots + |\Delta y_n| e^{-kz_n} \\ (|\Delta y_0| + |\Delta y_1| + |\Delta y_2| + \dots + |\Delta y_n|) e^{-kT^*} \end{aligned} \quad (23)$$

The general expression for each section becomes:

$$e^{-kT^*} = \frac{\sum_0^s |\Delta y_n| e^{-kz_n}}{\sum_0^s |\Delta y_n|} \quad (24)$$

from which the effective draught  $T^*$  may be solved.

If for a section  $y$  is increasing continuously with  $z$ , expression (24) may be written as:

$$e^{-kT^*} = \frac{\int_0^{y_w} e^{-kz} dz}{\int_0^{y_w} dy} \quad (25)$$

After partial integration is obtained:

$$e^{-kT^*} = \left( e^{-kz} y \Big|_0^{y_w} - k \int_0^{y_w} y e^{-kz} dz \right) / \int_0^{y_w} dy$$

If one keeps in mind, that  $z = 0$  for  $y = y_w$  and  $\int_0^{y_w} dy = y_w$ , the result looks as

$$e^{-kT^*} = 1 - \frac{k}{y_w} \int_0^{y_w} y e^{-kz} dz \quad (26)$$

from which follows

$$T^* = -\frac{1}{k} \ln \left( 1 - \frac{k}{y_w} \int_0^{y_w} y e^{-kz} dz \right) \quad (27)$$

This expression for  $T^*$  is analog to the one used in (7), but one should keep in mind, that this expression is only valid for a normal ship section where  $y$  is increasing continuously with  $z$ . For bulbous sections the general expression (24) should be used. It is almost needless to remark, that the described  $T^*$  may be used for vertical wave forces and -moments only.

## 5. CALCULATED PARAMETERS.

First of all the response functions have been calculated for the heaving and pitching motion, the added resistance in waves and the wave bending moment at the midship-section. The last one has not been determined for the "Atlantic Crown" because of the lack of the weight distribution. All these parameters have been plotted on base of the root of the ship-length wavelength ratio  $\sqrt{L/\lambda}$  as follows:

for heave  $z_a/\zeta_a$   
 for pitch  $\theta_a/k\zeta_a$  } in the figures 3 - 7 - 11 - 15 - 19

for the added resistance in waves  $\frac{R_{AW}}{\rho g \zeta_w^2 (B^2/L)}$  in the figures 4 - 8 - 12 - 16 - 20

for the wave bending moment at the midship section  $C_M = \frac{M_{ba}}{\rho g \zeta_a^2 L^2 B}$   
 in the figures 4 - 8 - 16 - 20

in which:  $z_a$  = heave amplitude  
 $\theta_a$  = pitch amplitude  
 $\zeta_a$  = wave amplitude  
 $\zeta_w$  = wave height (twice the wave amplitude)  
 $R_{AW}$  = added resistance in waves.  
 $k = 2\pi/\lambda$  = wave number  
 $\lambda$  = wave length  
 $k\zeta_a$  = maximum wave slope  
 $\rho$  = density of water  
 $g$  = acceleration of gravity  
 $L$  = ship length between perpendiculars  
 $B$  = breadth.

Afterwards the significant values have been determined for the parameters considered in different wave spectra according to the general expression of Pierson - Moskowitz. Moreover the number per hour of shipping and slamming has been calculated. All these parameters have been plotted on base of the significant wave amplitude as follows:

for the significant heave amplitude	$\bar{z}_{a/3}$	}	in the figures 5 - 9 - 13 - 17 - 21
for the significant pitch amplitude	$\bar{\theta}_{a/3}$		
for the increased effective power	$P_{EAW}$		
for the significant wave bending moment amplitude	$\bar{M}_{b a/3}$	}	in figures 6 - 10 - 14 18 - 22
for the number per hour of shipping			
for the number per hour of slamming			

The differences in sectional damping and added mass are neglectable for the greater part of the investigated ships, except for section 20 of the "Atlantic Crown" and section 16 - 20 of the "Davidson A Destroyer". In view of this phenomenon and because of the fact, that the MIT bulb-form transformation could only be applied for both the mentioned ships the sectional damping and added mass have been shown in the next figures for the denoted cases only:

"Atlantic Crown" for  $\omega_E = .87$  ( $\lambda/L = 1.14$ ) the added mass and damping on base of ship-sections in the figures 23 and 24 respectively;  
for section 20 the added mass and damping on base of frequency in the figures 25 and 26 respectively.

"Davidson A. Destroyer" for  $\omega_E = 1.20$  ( $\lambda/L = 1.20$ ) the added mass and damping on base of ship-sections in the figures 27 and 28 respectively;  
for section 16, 17, 18 and 19 the added mass and damping on base of frequency in the figures 29 - 36.



## 6. DISCUSSION AND COMPARISON OF THE RESULTS.

Generally the differences between the results appear to be very small both for the regular and irregular waves. The most sensitive parameters are besides the sectional damping and added mass the resistance increase in waves and the wave bending moment. For the Todd 60 with  $C_B = .70$  and the "S.A. van der Stel" the results are almost identical, which means that for normal ships without or with a small bulb no differences in motions, added resistance and wave bending moment may be expected in consequence of the method considered to determine the sectional added mass and damping i.e. the close-fit mapping method, the Frank close-fit method and the Lewis-form transformation. For the "Atlantic Crown", a ship with a deeply submerged circular bulb of normal size for this type the differences are negligible.

The MIT bulb-form transformation could only be applied for section 20 of this ship and so the small differences in the final results between MIT bulb-form- and the Lewis-transformation can only be caused by the difference in sectional damping and added mass of section 20. See figure 25 and 26.

From these figures it is clear, that the sectional added mass shows rather high values for the adaptive Lewis-transformation in the case of a deeply submerged circular bulb. Nevertheless the influence from this on the motion and resistance parameters is very small and for practical purposes negligible.

The "Davidson A Destroyer" has extreme bulbous sections in the forward part of the ship and the MIT bulb-form transformation could be applied for the sections 16 - 20. A comparison of the results of the methods considered shows, that MIT bulb-form transformation results deviate rather strongly from both the close-fit methods, although for practical use the differences remain yet small.

The differences are mainly caused by too high values for the sectional damping in the case of the MIT bulb-form transformation compared with the results of the other methods. See figure 26 - 36.

The results of the adaptive Lewis-transformation method for sectional damping and added mass are closer to the close-fit methods than those of the MIT bulb-form-transformation. Consequently the same tendency can be shown for the motions, added resistance and wave bending moment in spite of a more correct representation of the section contour in the case of the MIT bulb-form transformation.

## 7. CONCLUSIONS.

For prediction of the seakeeping performance of usual ship types the method of determining sectional added mass and damping is not so important. No significant difference appeared to be for all investigated ship types between the mapping- and Frank close-fit method. If these procedures are considered to be a reference, it has been shown, that for extremely bulbous sections the results of the adaptive Lewis-transformation are closer to this reference than those of the MIT bulb-form transformation with an exception for deeply submerged circular sections.

8. NOMENCLATURE.

A	Sectional area; coefficient of MIT bulb-form transformation.
$a_n$	Transformation coefficient with index number n.
B	Beam of ship; coefficient of MIT bulb-form transformation.
$C_B$	Block coefficient.
$C_M$	Wave bending moment coefficient.
$c_n$	Parameter for Lewis-transformation.
g	Acceleration of gravity.
$H_0$	Half-beam to draught ratio.
k	Wave number.
$k_{yy}$	Longitudinal radius of inertia.
L, $L_{pp}$	Ship length between perpendiculars.
$L_{wl}$	Ship length on the waterline.
$M_{ba}$	Wave bending moment amplitude.
$M_{ba}^{1/3}$	Significant wave bending moment amplitude.
$m'$	Sectional added mass.
N	Maximum index number of the transformation coefficients.
$N'$	Sectional damping.
$P_{EAW}$	Added effective power in waves.
$R_{AW}$	Added resistance in waves.
T	Draught of ship.
$T^*$	Effective draught for Smith-effect.
x, y, z	Right hand coordinate system fixed to ship.
$y_w$	Half width of designed waterline.
z	Heave displacement, mapping function.
$z_a$	Heave amplitude.
$\bar{z}_a^{1/3}$	Significant heave amplitude.
$\lambda$	Wave length.
$\omega$	Circular wave frequency.
$\omega_E$	Circular frequency of encounter.
	Density of water.
$\sigma$	Sectional area coefficient.

$\theta_a$	Pitch amplitude.
$\bar{\theta}_{a1/3}$	Significant pitch amplitude.
$\xi$	Instantaneous wave elevation; denoted reference plane for transformation.
$\xi_a$	Wave amplitude.
$\bar{\xi}_{a1/3}$	Significant wave amplitude.
$\xi_w$	Wave height (twice the wave amplitude).

9. REFERENCES.

1. Porter, W.R.,  
Pressure distribution, added mass and damping coefficients for cylinders oscillating in a free surface.  
University of California, Institute of Engineering Research, Series 82, 1960.
2. Jong, B. de,  
Computation of the hydrodynamic coefficients of oscillating cylinders.
  1. Shipbuilding Laboratory, Delft University of Technology, report 174A.
  2. Netherlands Ship Research Centre TNO, report no. 145<sup>S</sup>, 1973.
3. Tasai, F.,  
On the damping force and added mass of ships heaving and pitching.  
Journal of Zosen Kiokai, 105, July 1959, 47-56, Translated by Wen-ChinLin, edited by W.R. Porter, University of California, Institute of Engineering Research, Berkley, Calif. Series no. 82, issue no. 15, July 1960.
4. Loukakis, Theodore A.,  
Computer aided prediction of seakeeping performance in ship design.  
MIT, report no. 70-3, August 1970.
5. Frank, W.,  
Oscillation of cylinders in or below the free surface of deep fluids.  
NRSDC report 2375, October 1967.
6. Bedel, J.W.; Lee, C.M.,  
Numerical calculation of the added mass and damping coefficients of cylinders oscillating in or below a free surface.  
NRSDC report 3551, March 1971.
7. Gerritsma, J.; Beukelman, W.,  
Analysis of the modified strip theory for the calculation of ship motions and wave bending moments.  
International Shipbuilding Progress, vol.14, no. 156, 1967.

8. Gerritsma, J.; Beukelman, W; Glansdorp, C.Ci,  
The effect of beam on the hydrodynamic characteristics of ship hulls.  
Office of Naval Research 1974.
9. Gerritsma, J., Beukelman, W.,  
Analysis of the resistance increase of a fast cargo ship.  
International Shipbuilding Progress, vol. 19, no. 217, 1972.
10. Beukelman, W., Buitenhek, M.,  
Full scale measurements and predicted seakeeping performance of the container-  
ship "Atlantic Crown".  
International Shipbuilding Progress, vol. 21, no. 243, 1974.
11. Frank, W, Salvesen, N.,  
The Frank close-fit ship-motion computer program.  
NRSDC report no.3289, June 1970.
12. Glansdorp, C.C., Pijfers, J.G.L.,  
The effect of design modifications of the natural course stability of full  
tanker models.  
Shipbuilding Laboratory, Delft University of Technology, report no. 235.
13. Von Kerczek, C., Tuck, E.O.,  
The representation of ship hulls by conformal mapping functions.  
Journal of Ship Research, vol. 13, no. 4, 1969.
14. Beukelman, W., Bijlsma, E.F.,  
Description of a program to calculate the behaviour of a ship in a seaway  
(named: TRIAL)  
Shipbuilding Laboratory, Delft University of Technology, report no. 383.

Table 1      DATA OF SHIPS.

SHIP CHARACTERISTIC (full scale)		Todd 60 $C_B = .70$	"Van de Stel"	"Atlantic Crown"	"Davidson A-Destroyer"	"Macoma"
Length between perpendiculars $L_{pp}$	(m)	121.92	152.50	196.00	116.77	310.00
Length on the waterline $L_{wl}$	(m)	123.96	154.68	203.04	116.77	318.05
Breadth B	(m)	17.42	22.82	28.00	12.45	47.16
Draught T	(m)	6.97	9.14	8.15	4.26	18.90
Volume of displacement	(m <sup>3</sup> )	10324	17910	26061	3345	234994
Blockcoefficient $C_B$		.700	.563	.582	.540	.850
Waterplane area	(m <sup>2</sup> )	1670	2428	3976	1074	13257
Longitudinal moment of inertia of waterplane	(m <sup>4</sup> )	1425054	2816396	8173499	952751	90514506
LCB forward of $L_{pp}/2$	(m)	+ .59	- 1.68	- 1.80	+ 2.01	- 8.74
Centre of effort of waterplane forward of $L_{pp}/2$	(m)	- 2.55	- 4.30	- 5.97	- 10.95	- 6.76
Percentage of bulb		0	4.4	9.5	35.0	6.9
$k_{yy}/L_{pp}$		.2500	.2190	.2556	.2554	.2709
Maximum index number of transformation coefficient for close-fit mapping		19	19	19	31	17
Maximum number of sources segments for Frank close-fit method		9	12	28	21	14
Freeboard at FPP for shipping		5.454	15.000	12.400	5.130	9.100

Table 2.

Todd 60 δ = .70

Ordinate number	Weight from FPP to ordinate ton	Ordinate number	Weight from FPP to ordinate
0	10356.49	11	4635.05
1	10327.17	12	4013.66
2	9958.92	13	3058.83
3	9337.08	14	2558.46
4	8634.07	15	2369.46
5	8071.18	16	1803.61
6	7914.75	17	1068.30
7	7391.27	18	414.76
8	6525.91	19	39.70
9	5783.90	20(FPP)	0
10	5296.57		

T./ORD. no.	0	1	2	3	4	5	6	7	8	9	10
0	0	.154	.517	1.248	2.310	3.572	4.733	5.740	6.451	6.713	6.713
0.581	0	.565	1.550	2.765	4.165	5.515	6.650	7.420	7.915	8.076	8.100
1.161	0	.680	1.895	3.280	4.770	6.190	7.265	7.960	8.375	8.524	8.540
1.742	0	.773	2.129	3.710	5.257	6.674	7.708	8.325	8.595	8.682	8.690
3.484	0	.932	2.734	4.641	6.321	7.558	8.333	8.646	8.708	8.708	8.708
5.226	0	1.428	3.701	5.729	7.184	8.072	8.534	8.708	-	-	-
6.968	.775	3.204	5.347	6.861	7.811	8.368	8.629	8.708	8.708	8.708	8.708

T./ORD. no.	11	12	13	14	15	16	17	18	19	20
0	6.713	6.700	6.304	5.572	4.337	2.934	1.604	.671	.174	0
0.581	8.100	8.100	7.855	7.260	6.335	5.105	3.700	2.330	.895	0
1.161	8.540	8.540	8.310	7.855	7.050	5.880	4.390	2.745	1.195	0
1.742	8.690	8.690	8.551	8.186	7.439	6.292	4.780	3.041	1.373	0
3.484	8.708	8.708	8.656	8.455	7.872	6.774	5.216	3.387	1.541	0
5.226	-	-	8.690	8.534	8.011	6.983	5.459	3.544	1.602	0
6.968	8.708	8.708	8.708	8.577	8.142	7.201	5.703	3.744	1.690	0

Dimensions in meter.



Table 3.

"VAN DE STEL"

Ordinate number	Weight from FPP to ordinate ton	Ordinate number	Weight from FPP to ordinate ton
0	17931.00	11	7104.00
1	17478.25	12	5546.63
2	17287.50	13	4362.50
3	16877.75	14	3695.63
4	16068.00	15	2497.13
5	15313.88	16	1213.75
6	14345.13	17	805.38
7	12899.00	18	491.13
8	11552.63	19	342.88
9	10016.25	20	25.00
10	8512.50		

Dimensions in meter.

T/ORD. no.	0	1	2	3	4	5	6	7	8	9	10
0	0	0	.195	.350	.960	1.940	3.185	4.660	6.205	7.400	7.655
.435	0	0	.515	1.230	2.325	3.750	5.255	6.820	8.160	9.145	9.325
.871	0	0	.700	1.635	2.985	4.590	6.300	7.880	9.135	9.950	10.090
1.304	0	0	.825	1.945	3.440	5.150	6.905	8.505	9.710	10.400	10.510
2.613	0	.060	1.180	2.735	4.600	6.455	8.280	9.715	10.680	11.145	11.225
3.919	0	.125	1.615	3.560	5.615	7.585	9.260	10.445	11.145	11.410	11.410
5.225	0	.145	2.275	4.545	6.655	8.570	10.005	10.900	11.410	-	-
6.531	0	.560	3.225	5.680	7.700	9.365	10.550	11.200	11.410	-	-
7.838	0	1.870	4.510	6.825	8.670	10.025	10.945	11.350	11.410	-	-
9.144	.940	3.475	5.880	7.915	9.470	10.545	11.200	11.395	11.410	11.410	11.410

T /ORD.11 no.	12	13	14	15	16	17	18	19	20
0	6.855	5.450	3.925	2.525	1.905	1.375	.965	.625	.290
.435	8.740	7.645	6.170	4.715	3.510	2.650	1.995	1.515	1.280
.871	9.580	8.615	7.210	5.725	4.335	3.260	2.470	1.915	1.585
1.306	10.045	9.120	7.730	6.265	4.805	3.610	2.715	2.100	1.700
2.613	10.795	9.960	8.750	7.295	5.735	4.265	3.050	2.155	1.560
3.919	11.130	10.440	9.365	7.935	6.310	4.680	3.200	2.040	1.075
5.225	11.265	10.740	9.775	8.425	6.765	5.010	3.345	1.910	.765
6.531	11.320	10.960	10.105	8.850	7.190	5.340	3.500	1.870	.685
7.838	11.370	11.100	10.360	9.205	7.610	5.705	3.750	1.970	.755
9.144	11.410	11.200	10.580	9.520	8.010	6.140	4.160	2.330	.990

Table 4.

"ATLANTIC CROWN"

## No weight distribution

T /ORD. no.	0	1	2	3	4	5	6	7	8	9	10
0	.40	.40	.40	.40	.40	.40	.85	3.90	6.83	8.93	10.00
.388	.41	.40	.44	.81	1.66	3.31	5.48	7.75	9.71	11.06	11.68
.776	.42	.40	.51	1.21	2.62	4.65	6.89	9.01	10.69	11.85	12.35
1.165	.44	.40	.63	1.69	3.55	5.73	7.94	9.89	11.47	12.44	12.79
2.329	.46	.40	1.16	3.12	5.60	7.86	9.98	11.61	12.78	13.43	13.62
3.494	.50	.52	2.03	4.59	7.25	9.51	11.31	12.63	13.48	13.86	13.95
4.659	.52	.97	3.22	6.06	8.72	10.76	12.28	13.31	13.86	14.00	14.00
5.824	.57	1.86	4.74	7.56	9.98	11.73	12.93	13.70	14.00	-	-
6.988	.67	3.37	6.44	9.02	11.07	12.45	13.36	13.89	14.00	-	-
8.153	2.42	5.47	8.21	10.32	11.97	13.04	13.70	13.99	14.00	14.00	14.00

T /ORD. no.	11	12	13	14	15	16	17	18	19	20
0	9.28	7.67	5.62	3.47	1.70	.59	.02	0	0	0
.388	11.14	9.88	8.24	6.22	4.36	2.77	1.46	1.35	1.35	1.35
.776	11.91	10.75	9.16	7.26	5.31	3.57	2.07	1.80	1.80	1.80
1.165	12.38	11.32	9.81	7.96	6.01	4.11	2.48	2.13	2.13	2.13
2.329	13.31	12.45	11.09	9.34	7.34	5.26	3.35	2.50	2.50	2.50
3.494	13.76	13.09	11.89	10.21	8.22	6.10	4.01	2.30	2.30	2.30
4.659	13.96	13.46	12.38	10.82	8.88	6.72	4.54	2.62	1.36	1.36
5.824	14.00	13.67	12.73	11.28	9.39	7.24	4.99	2.97	1.29	.24
6.988	14.00	13.79	13.00	11.65	9.79	7.66	5.39	3.31	1.51	0
8.153	14.00	13.89	13.21	11.95	10.18	8.07	5.81	3.67	1.75	.20

Dimensions in meter.

Table 5.

"DAVIDSON A DESTROYER"

Ordinate number	Weight from FPP to ordinate		ton		Ordinate number	Weight from FPP to ordinate		ton	
0	3447.41				11	1578.60			
1	3355.25				12	1358.66			
2	3259.46				13	1141.72			
3	3139.20				14	932.53			
4	2997.46				15	738.70			
5	2834.24				16	560.23			
6	2649.55				17	397.13			
7	2443.34				18	249.39			
8	2226.41				19	117.01			
9	2009.47				20	0			
10	1792.53								

T/ORD. no.	0	1	2	3	4	5	6	7	8	9	10
0	0	0	0	0	0	0	.13	.13	.54	.81	.81
.203	0	0	0	0	0	0	.39	1.14	1.56	1.89	1.95
.406	0	0	0	0	0	0	.84	1.70	2.13	2.48	2.67
.609	0	0	0	0	0	.19	1.30	2.11	2.61	2.97	3.17
1.217	0	0	0	0	.32	1.71	2.62	3.29	3.74	4.05	4.25
1.826	0	0	0	.57	2.14	3.26	3.80	4.36	4.68	4.88	5.07
2.434	0	0	.93	2.66	3.83	4.54	4.91	5.21	5.43	5.58	5.68
3.043	0	1.38	3.55	4.56	5.06	5.38	5.62	5.82	5.92	6.02	6.06
3.651	2.11	4.20	4.83	5.31	5.56	5.78	5.93	6.09	6.16	6.20	6.20
4.260	3.68	4.44	5.05	5.49	5.72	5.90	6.00	6.11	6.20	6.22	6.22

T/ORD. no.	11	12	13	14	15	16	17	18	19	20
0	.81	.81	.81	.81	.81	.81	.81	.81	.05	0
.203	1.95	1.95	1.95	1.95	1.95	1.95	1.95	1.80	1.41	0
.406	2.67	2.67	2.67	2.67	2.67	2.67	2.62	2.33	1.82	0
.609	3.17	3.17	3.17	3.17	3.17	3.17	3.03	2.69	2.06	0
1.217	4.25	4.25	4.25	4.25	4.25	4.03	3.69	3.22	2.35	0
1.826	5.07	5.01	4.97	4.84	4.62	4.29	3.83	3.23	2.29	0
2.434	5.62	5.45	5.32	5.00	4.56	4.03	3.55	2.82	1.89	0
3.043	5.94	5.72	5.37	4.82	4.27	3.53	2.82	2.05	1.28	0
3.651	6.06	5.79	5.25	4.58	3.90	3.10	2.32	1.59	.93	0
4.260	6.13	5.76	5.20	4.47	3.76	2.92	2.11	1.42	.80	0

Dimensions in meter.

Table 6

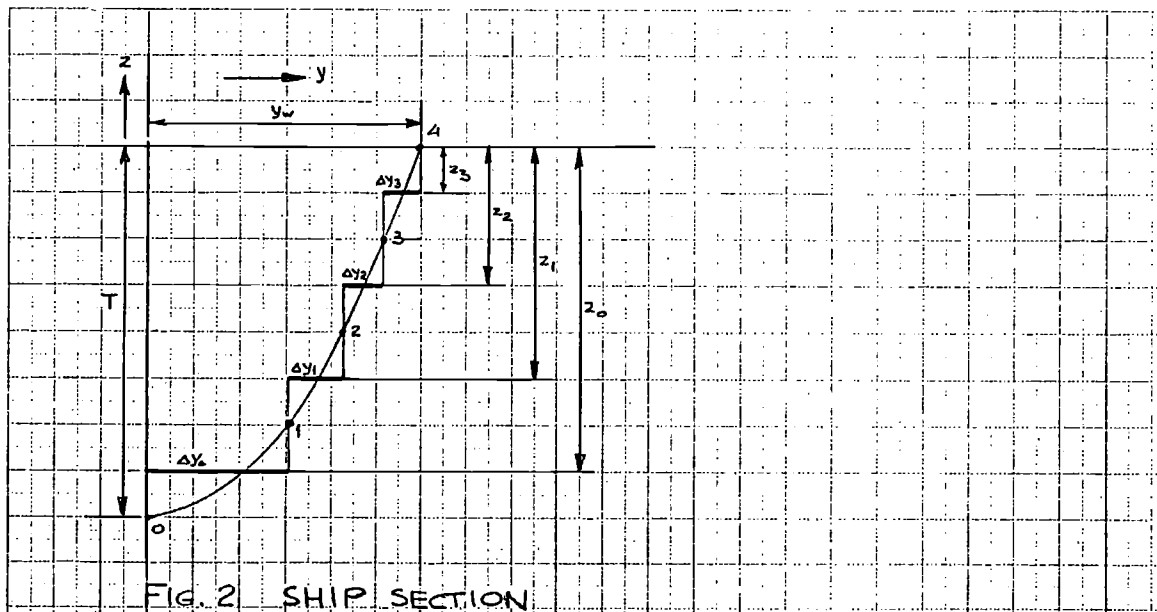
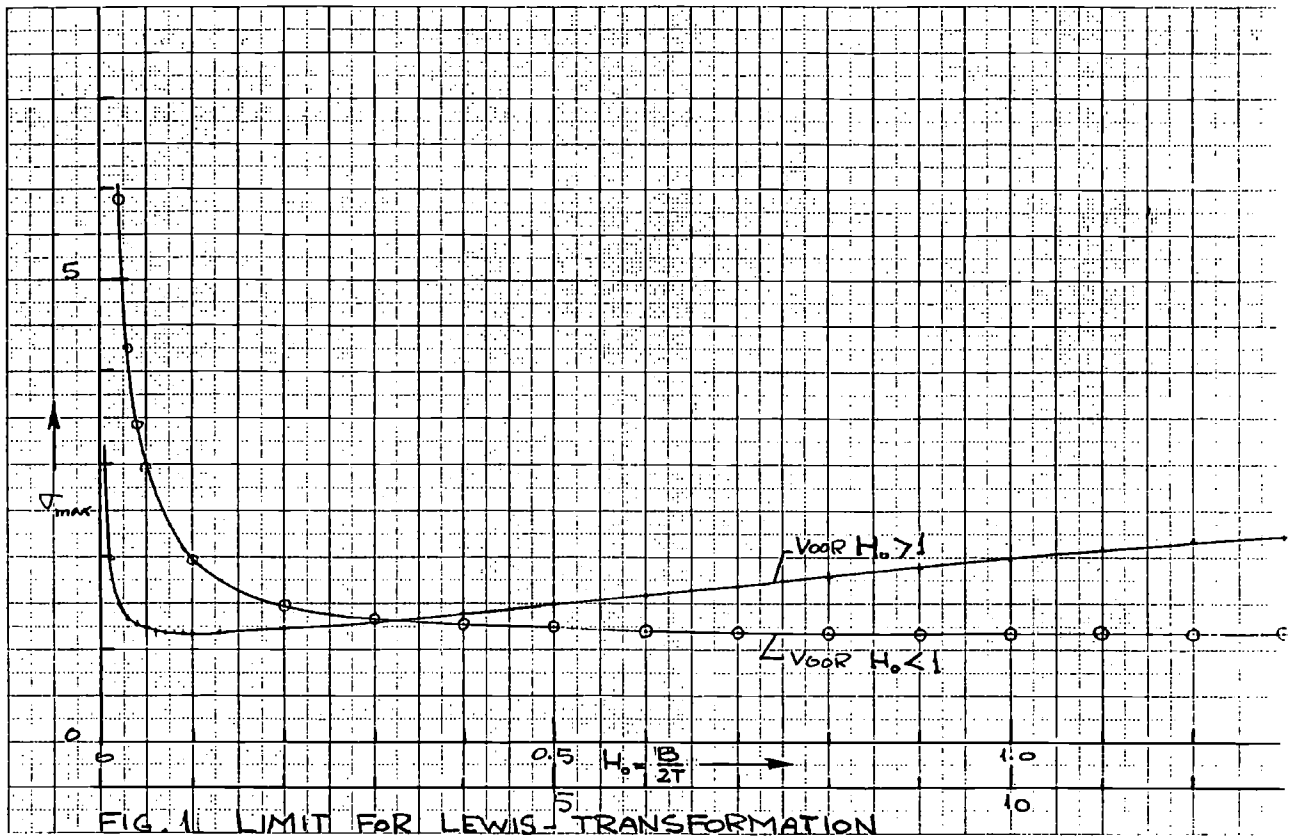
"MACOMA"

Ordinate number	Weight from FPP to ordinate ton	Ordinate number	Weight from FPP to ordinate ton
0	234994	11	112191
1	231094	12	99540
2	223883	13	86889
3	213365	14	74237
4	200749	15	61586
5	188098	16	48935
6	175446	17	36284
7	162795	18	23703
8	150144	19	11589
9	137493	20	0
10	124842		

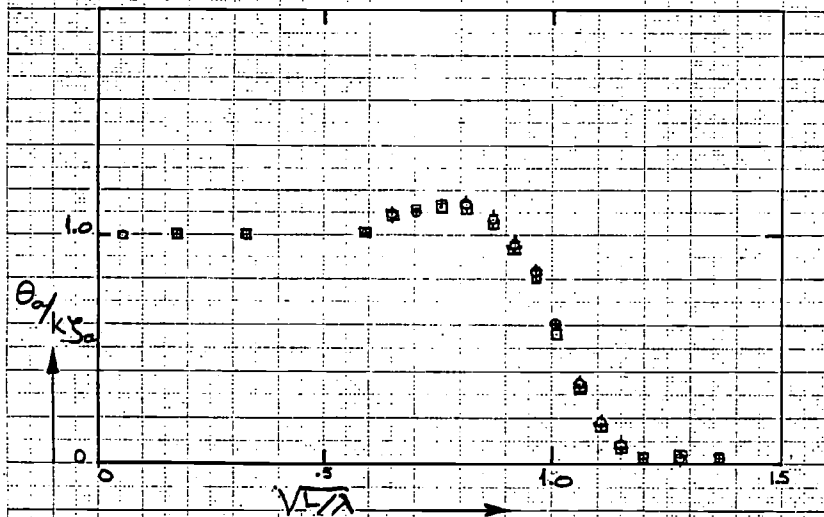
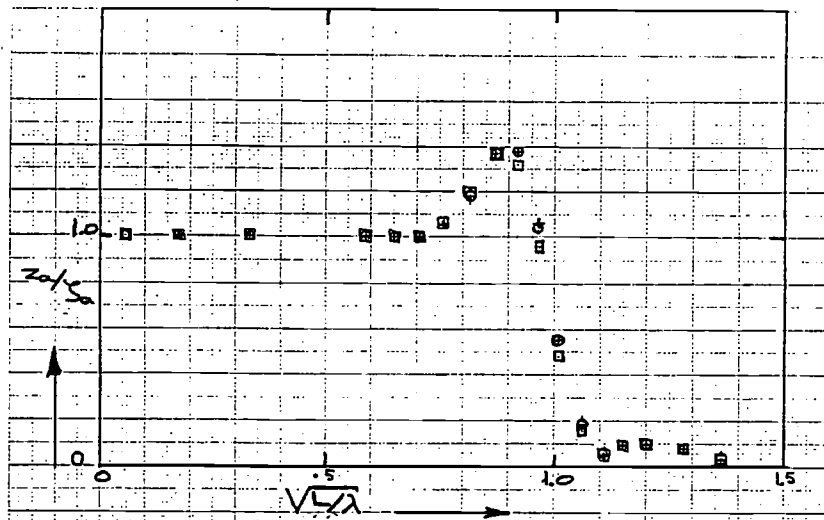
T/ORD. no.	0	1	2	3	4	5	6	7	8	9	10
0.	0	1.10	3.76	7.24	11.38	16.00	20.12	20.55	20.55	20.55	20.55
0.9	0	2.21	6.26	10.94	15.60	19.46	22.10	22.89	22.89	22.89	22.89
1.8	0	2.67	7.43	12.41	17.03	20.58	22.82	23.45	23.45	23.45	23.45
2.700	0	2.98	8.25	13.50	18.09	21.36	23.22	23.58	23.58	23.58	23.58
5.400	0	3.61	10.00	15.81	20.10	22.68	23.58	-	-	-	-
8.100	0	4.31	11.57	17.47	21.32	23.31	-	-	-	-	-
10.800	0	5.60	13.28	18.82	22.13	23.57	-	-	-	-	-
13.500	0	8.26	15.08	19.93	22.68	23.58	-	-	-	-	-
16.200	4.57	11.30	16.78	20.85	23.05	23.58	-	-	-	-	-
18.900	7.14	13.36	18.19	21.52	23.28	23.58	23.58	23.58	23.58	23.58	23.58

T/ORD. no.	11	12	13	14	15	16	17	18	19	20
0	20.55	20.55	20.55	20.55	20.55	20.55	20.40	16.04	7.63	5.26
.900	22.89	22.89	22.89	22.89	22.89	22.89	22.60	18.90	11.05	2.63
1.800	23.45	23.45	23.45	23.45	23.45	23.45	23.16	19.95	12.39	3.37
2.700	23.58	23.58	23.58	23.58	23.58	23.58	23.42	20.59	13.28	3.85
5.400	-	-	-	-	-	-	23.58	21.57	14.79	3.96
8.100	-	-	-	-	-	-	-	21.95	15.40	2.15
10.800	-	-	-	-	-	-	-	22.12	15.60	.48
13.500	-	-	-	-	-	-	-	22.24	15.72	0
16.200	-	-	-	-	-	-	-	22.31	15.92	0
18.900	23.58	23.58	23.58	23.58	23.58	23.58	23.58	22.39	16.29	0

Dimensions in meter.



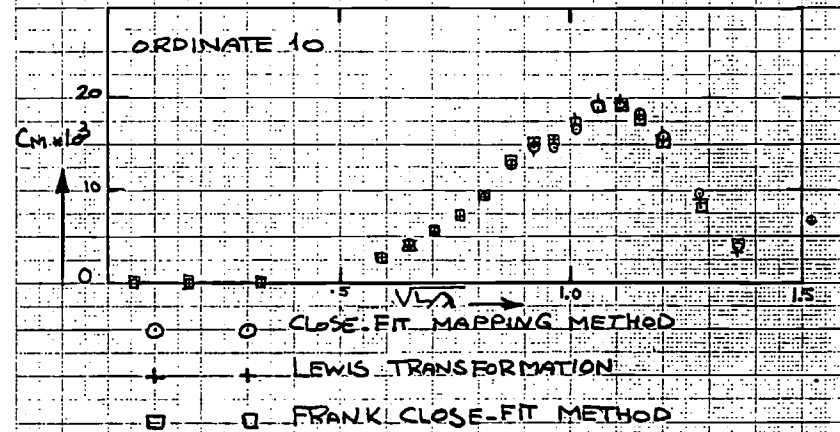
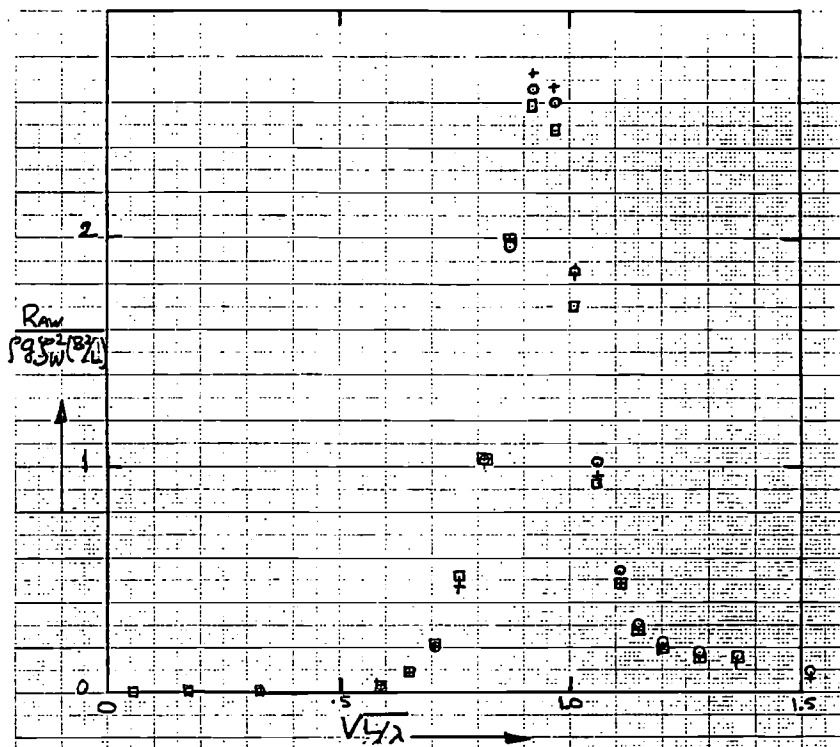
TODD 60  $C_B=0.70$   $F_n=0.20$



- ○ CLOSE-FIT MAPPING METHOD
- + + LEWIS TRANSFORMATION
- □ FRANK CLOSE-FIT METHOD

FIG. 3 RESPONSE FUNCTIONS FOR VERTICAL MOTIONS.

TODD 60  $C_B=0.70$   $F_n=0.20$



- ○ CLOSE-FIT MAPPING METHOD
- + + LEWIS TRANSFORMATION
- □ FRANK CLOSE-FIT METHOD

FIG. 4 RESPONSE FUNCTIONS FOR ADDED RESISTANCE AND WAVE BENDING MOMENT

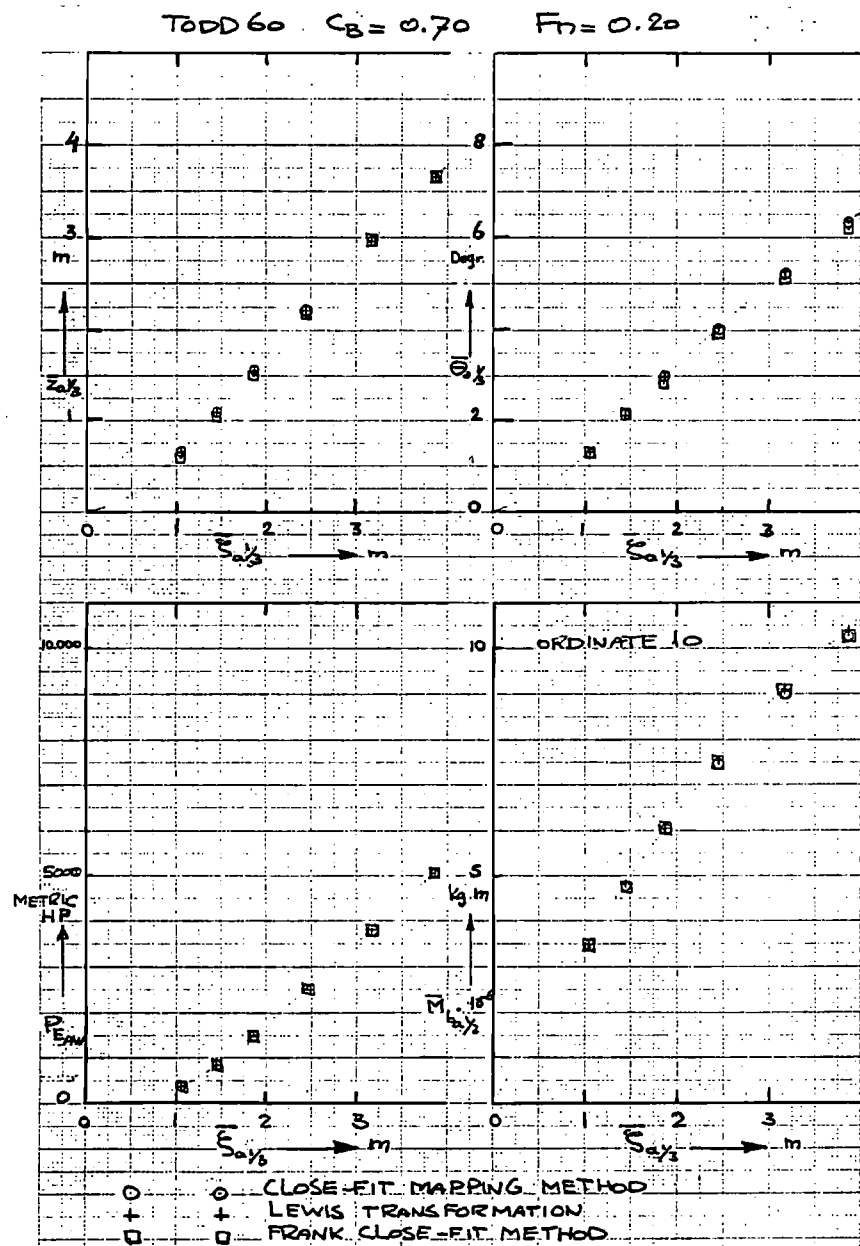


FIG. 5 MOTIONS, ADDED POWER AND WAVE BENDING MOMENT VERSUS SIGNIFICANT WAVE AMPLITUDE

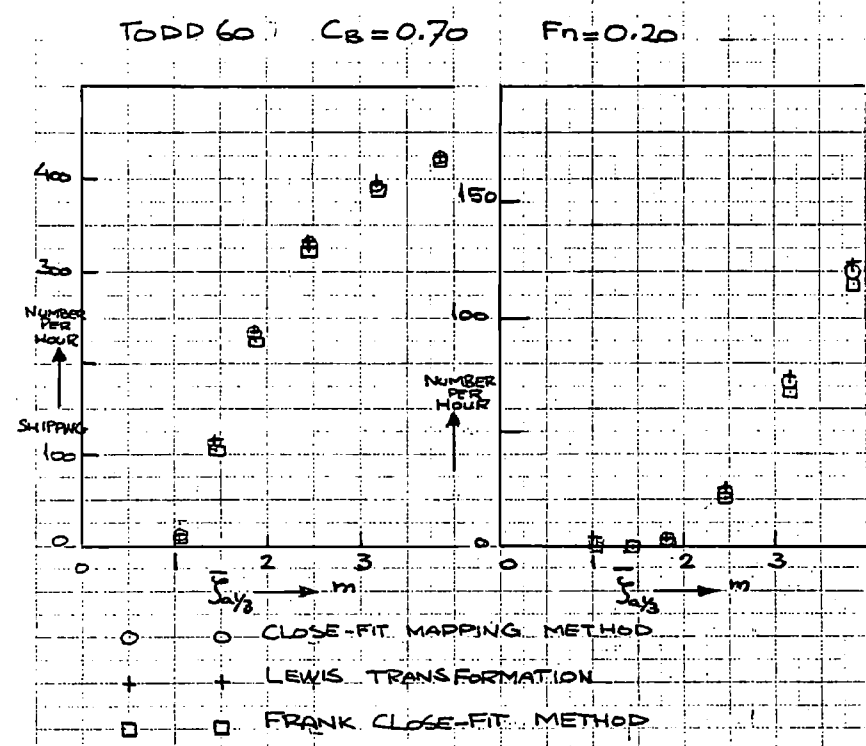
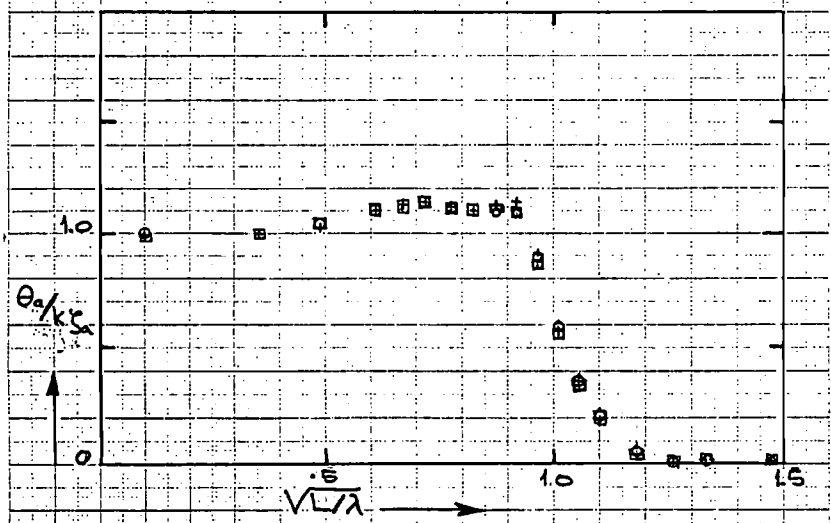
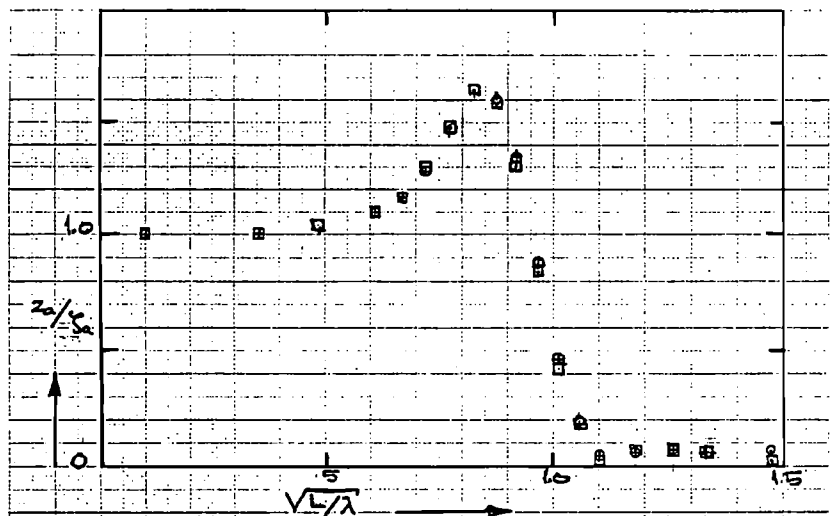


FIG. 6 NUMBER PER HOUR OF SHIPPING AND SLAMMING RELATED TO SIGNIFICANT WAVE AMPLITUDE

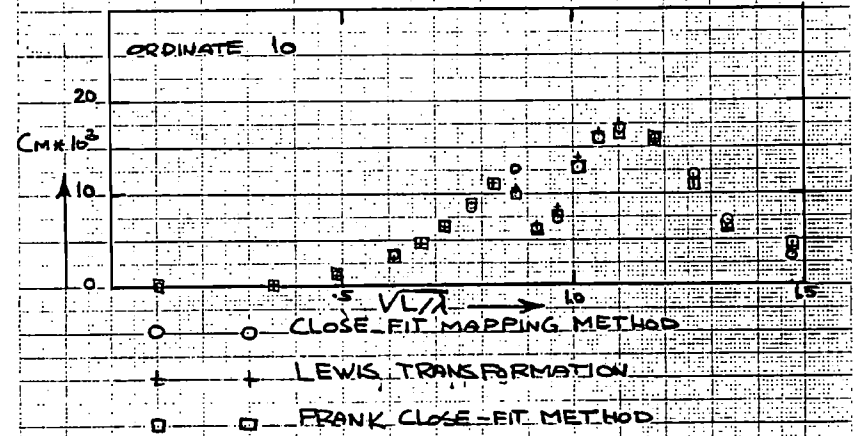
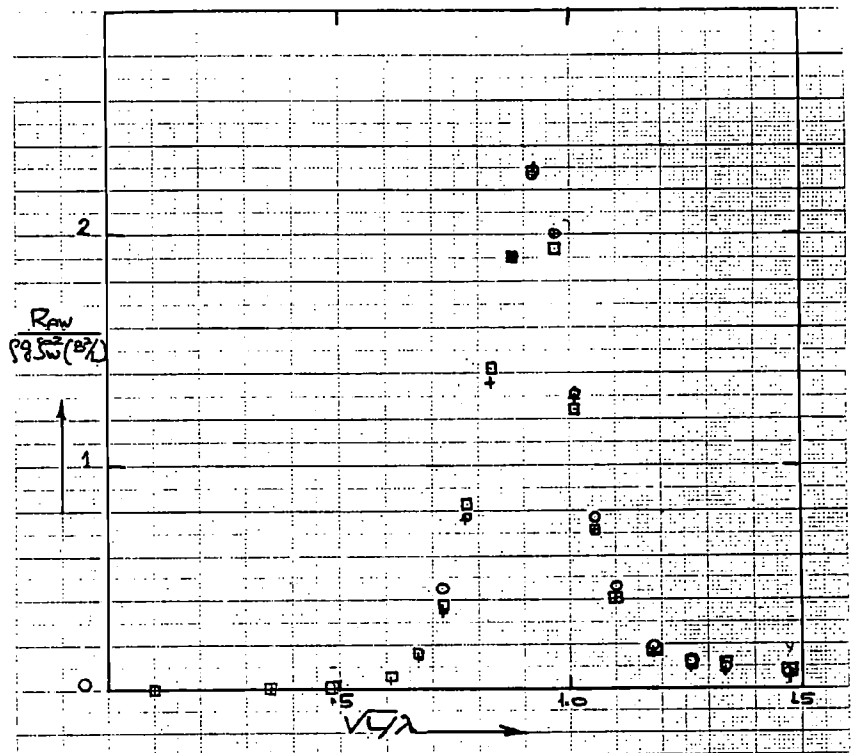
"VAN DER STEL"  $F_n=0.30$



- ○ CLOSE-FIT MAPPING METHOD
- + + LEWIS TRANSFORMATION
- □ FRANK CLOSE-FIT METHOD

FIG. 7 RESPONSE FUNCTIONS FOR VERTICAL MOTIONS

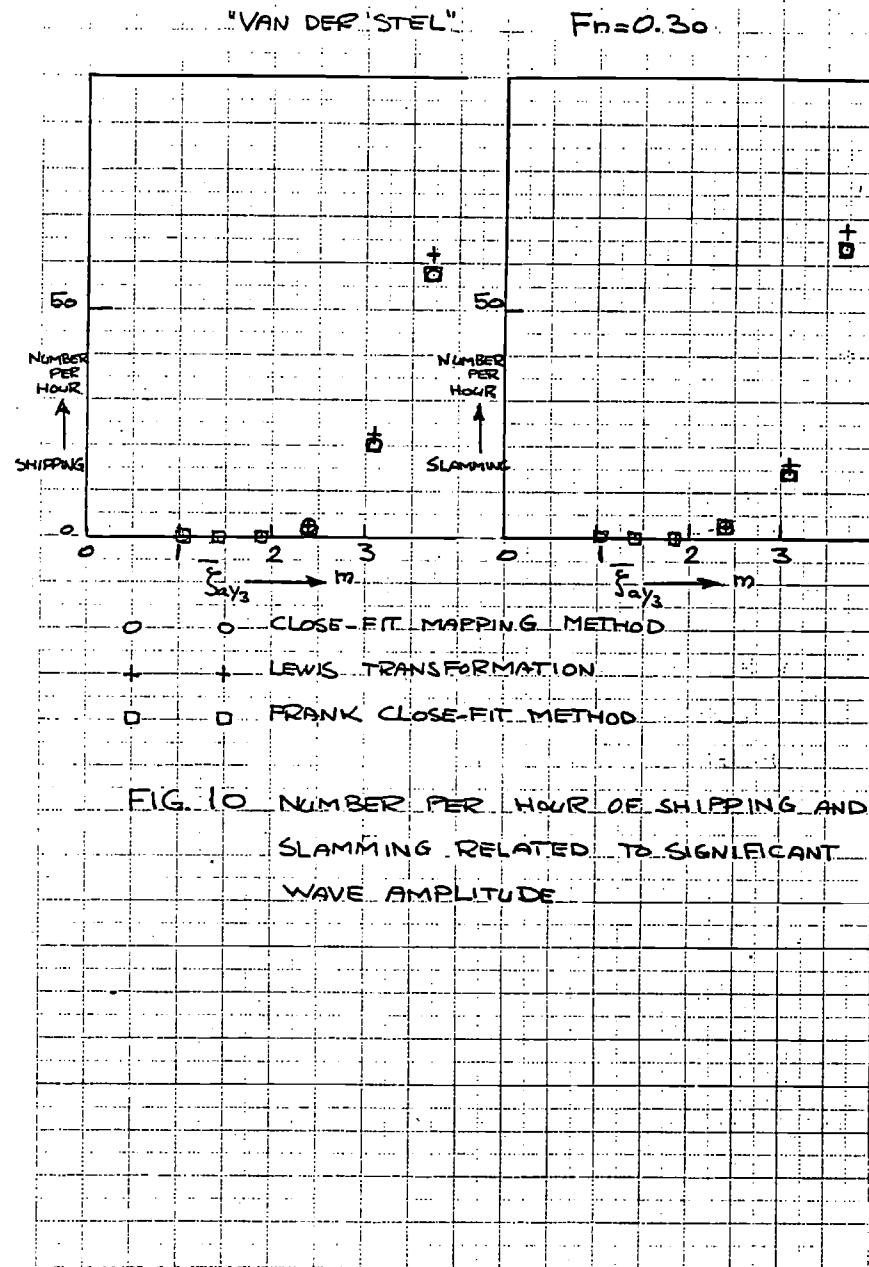
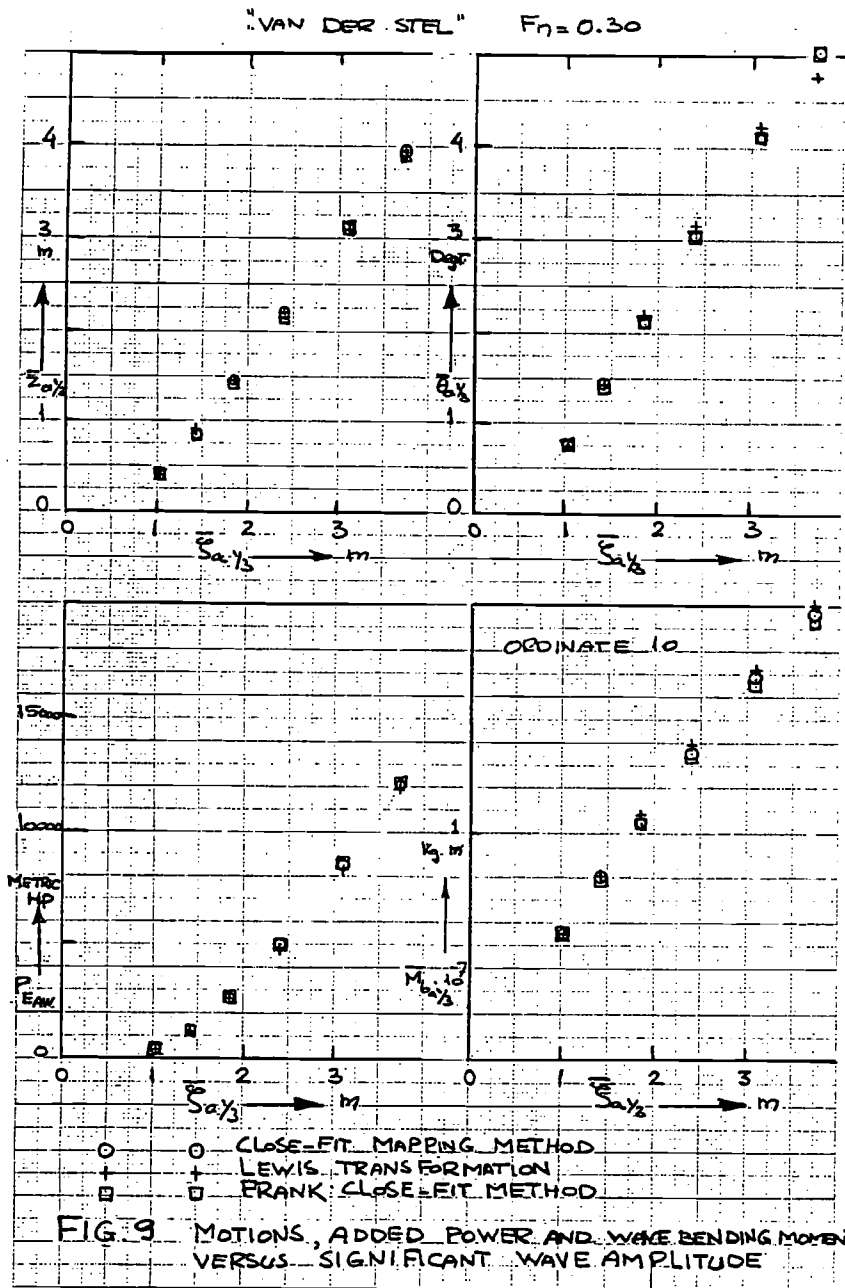
"VAN DER STEL"  $F_n=0.30$



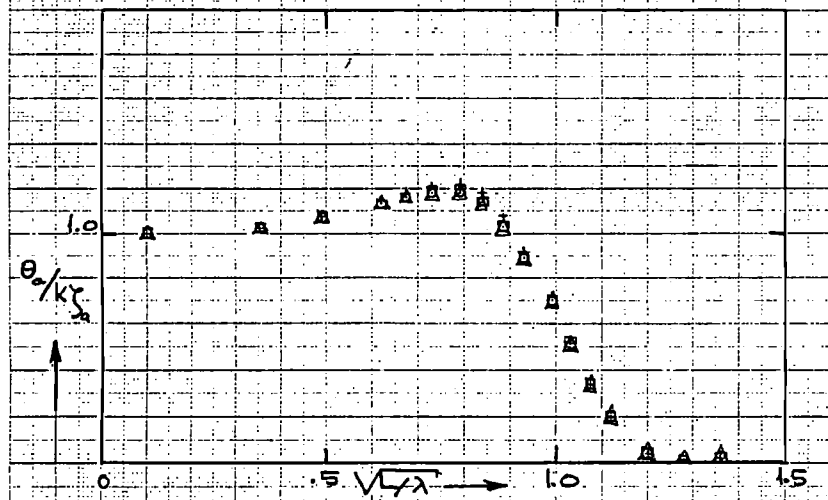
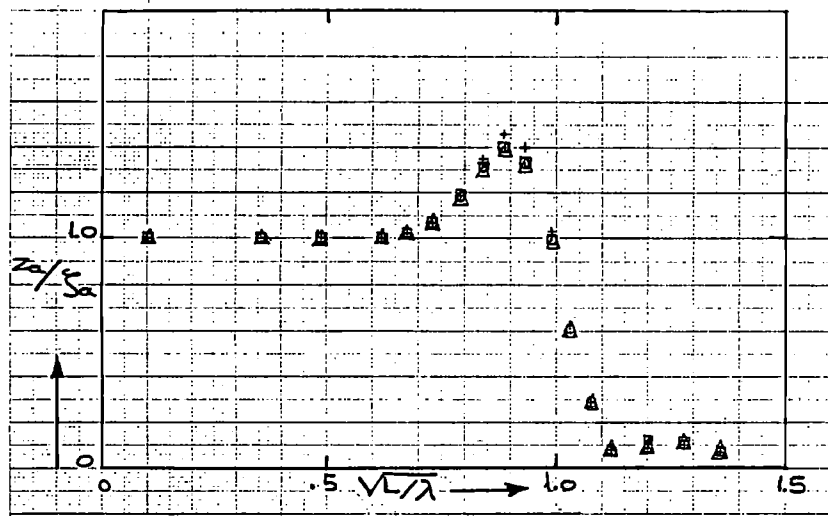
- ○ CLOSE-FIT MAPPING METHOD
- + + LEWIS TRANSFORMATION
- □ FRANK CLOSE-FIT METHOD

FIG. 8 RESPONSE FUNCTIONS FOR ADDED RESISTANCE AND WAVE BENDING MOMENT





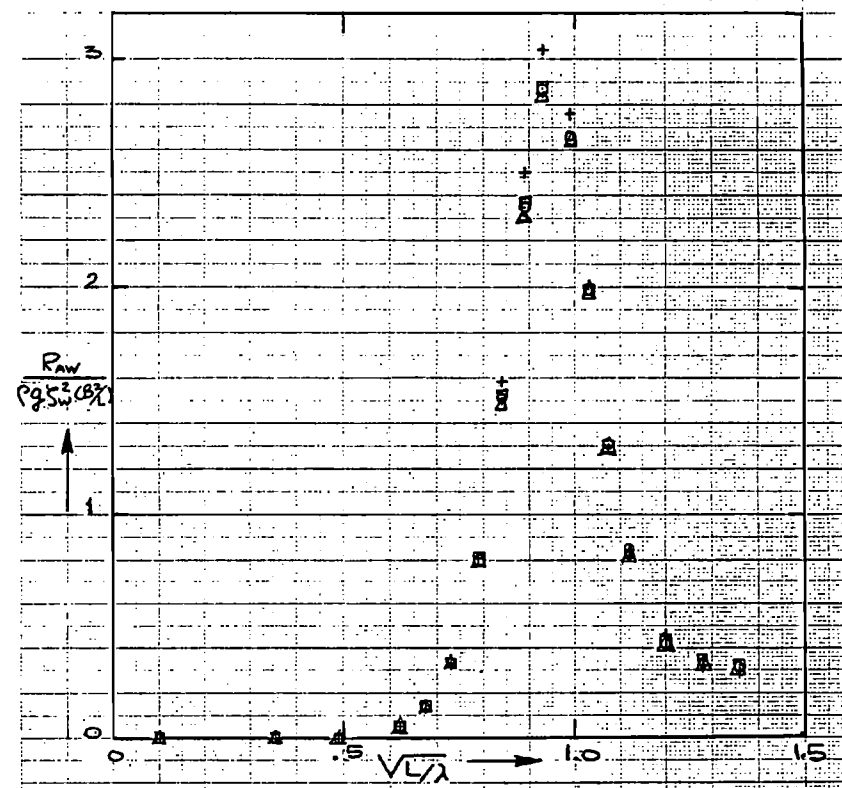
"ATLANTIC CROWN"  $F_n = 0.282$



- ○ CLOSE-FIT MAPPING METHOD
- + + LEWIS TRANSFORMATION
- □ FRANK CLOSE-FIT METHOD
- △ △ M.I.T. BULB FORM TRANSFORMATION

FIG. 11 RESPONSE FUNCTIONS FOR VERTICAL MOTIONS

"ATLANTIC CROWN"  $F_n = 0.282$

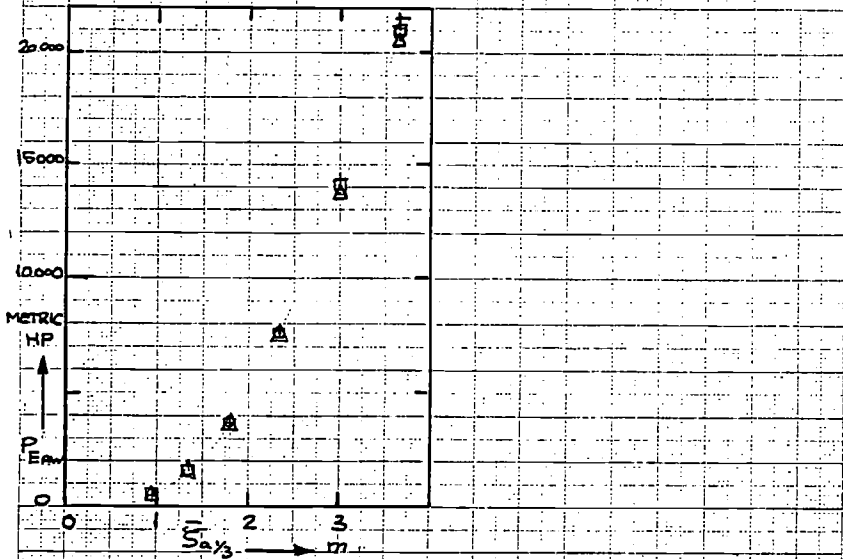
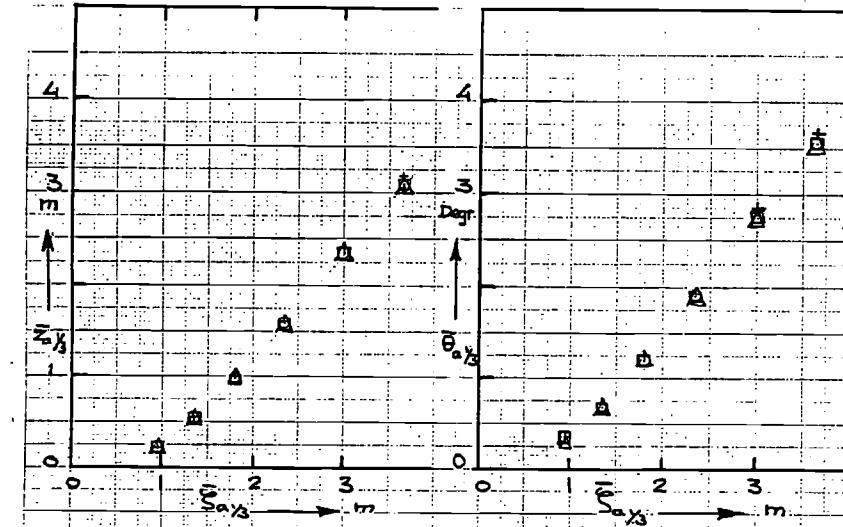


- ○ CLOSE-FIT MAPPING METHOD
- + + LEWIS TRANSFORMATION
- □ FRANK CLOSE-FIT METHOD
- △ △ M.I.T. BULB FORM TRANSFORMATION

FIG. 12 RESPONSE FUNCTION FOR ADDED RESISTANCE

"ATLANTIC CROWN"

$F_n = 0.282$

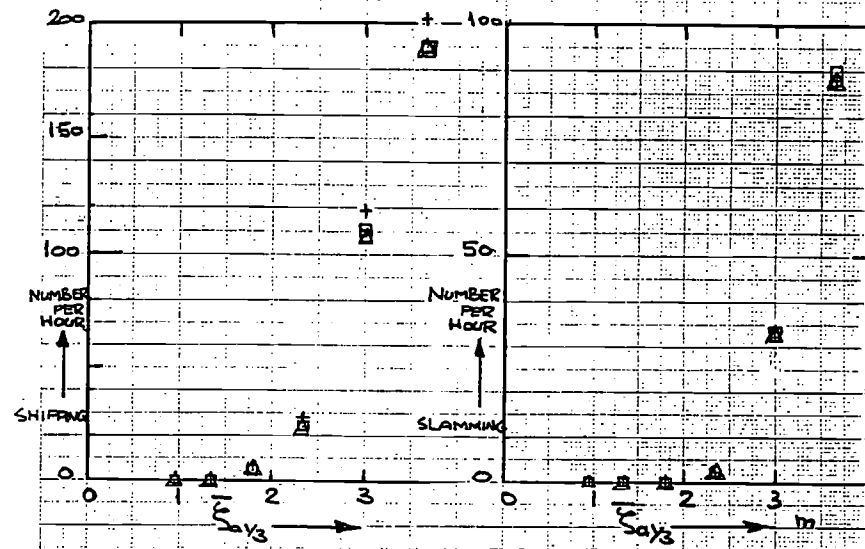


○ ○ CLOSE-FIT MAPPING METHOD      □ □ FRANK CLOSE-FIT METHOD  
 + + LEWIS TRANSFORMATION      △ △ MIT BULB FORM TRANSFORMATION

FIG. 13 MOTIONS AND ADDED POWER VERSUS SIGNIFICANT WAVE AMPLITUDE.

"ATLANTIC CROWN"

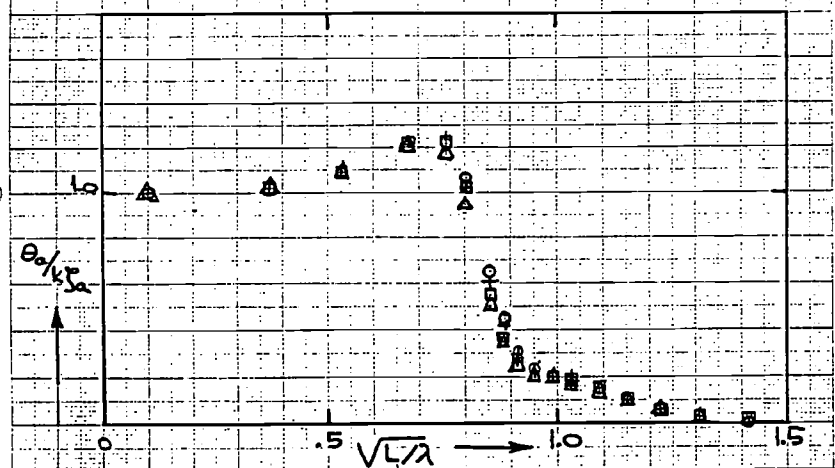
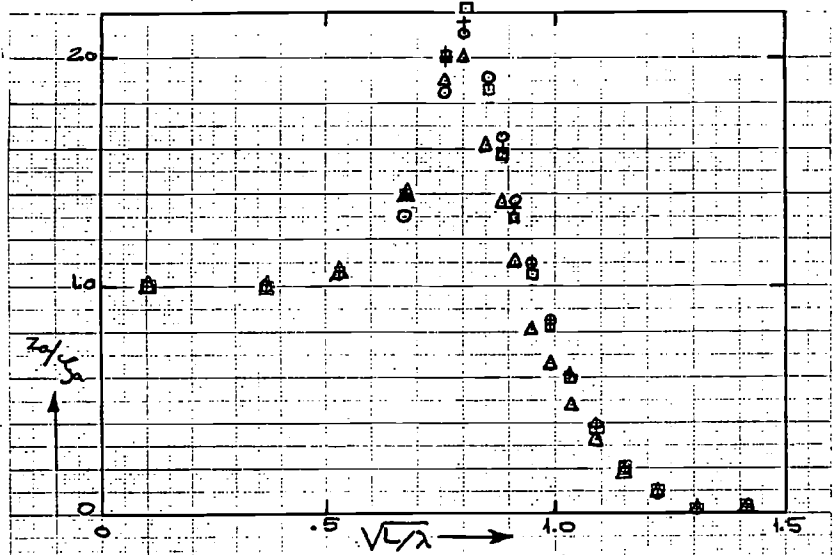
$F_n = 0.282$



○ ○ CLOSE-FIT MAPPING METHOD  
 + + LEWIS TRANSFORMATION  
 □ □ FRANK CLOSE-FIT METHOD  
 △ △ MIT BULB FORM TRANSFORMATION

FIG. 14 NUMBER PER HOUR OF SHIPPING AND SLAMMING RELATED TO SIGNIFICANT WAVE AMPLITUDE

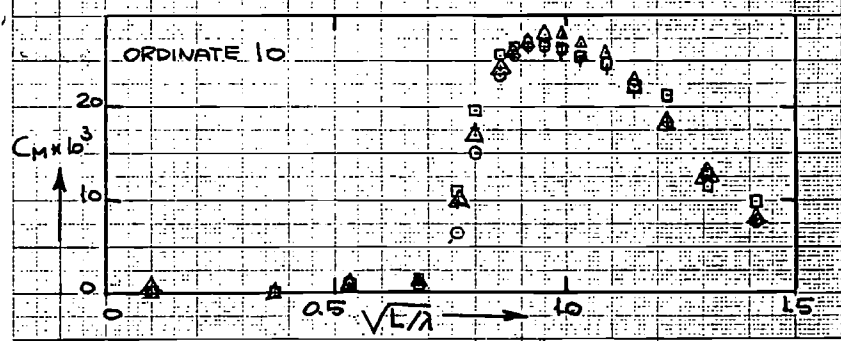
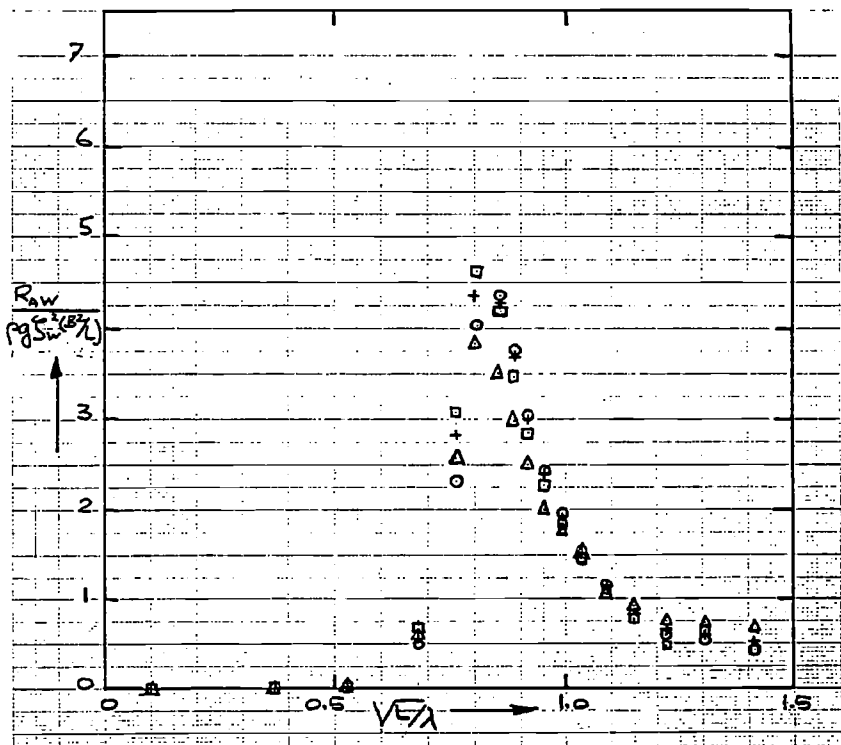
"DAVIDSON A-DESTROYER"  $F_n = 0.35$



- ○ CLOSE-FIT MAPPING METHOD
- + + LEWIS TRANSFORMATION
- □ FRANK CLOSE-FIT METHOD
- △ △ MIT BULB FORM TRANSFORMATION

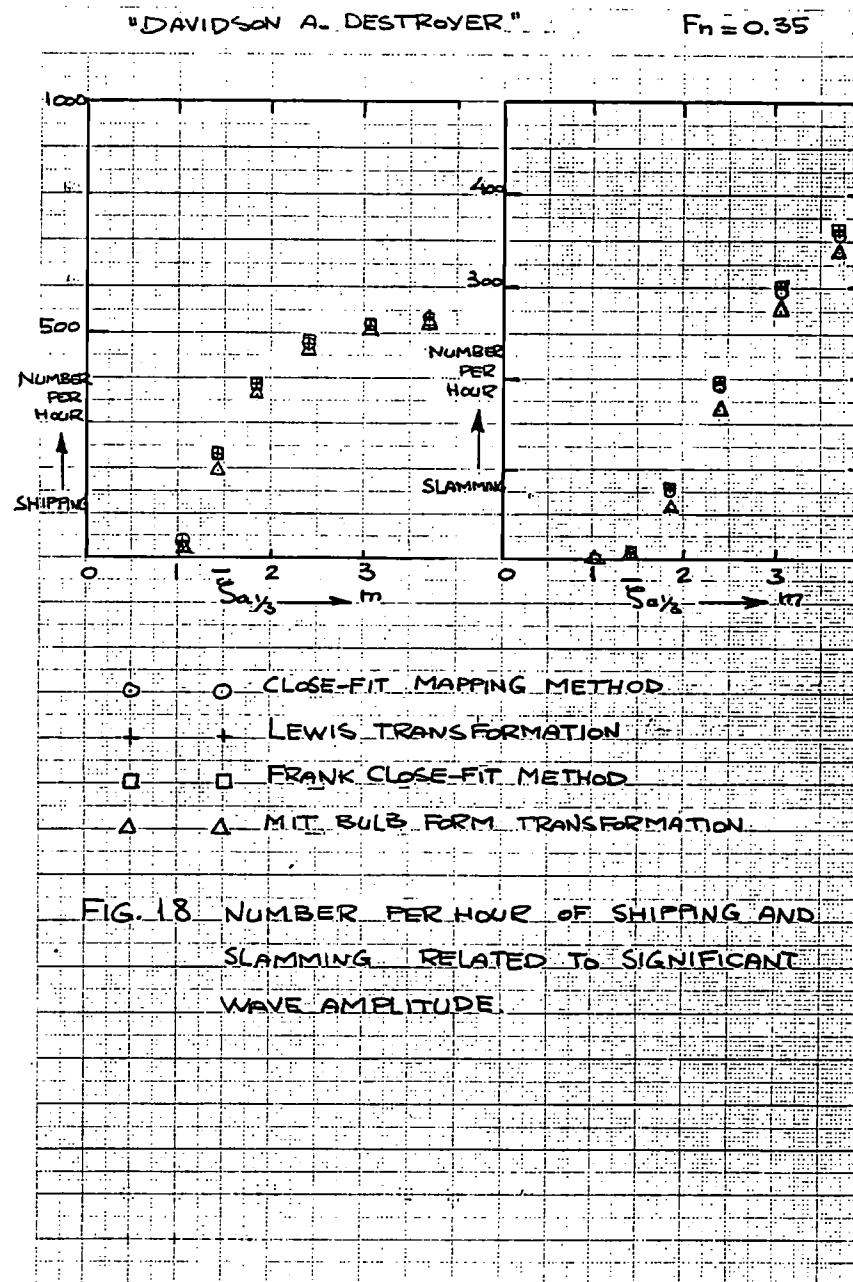
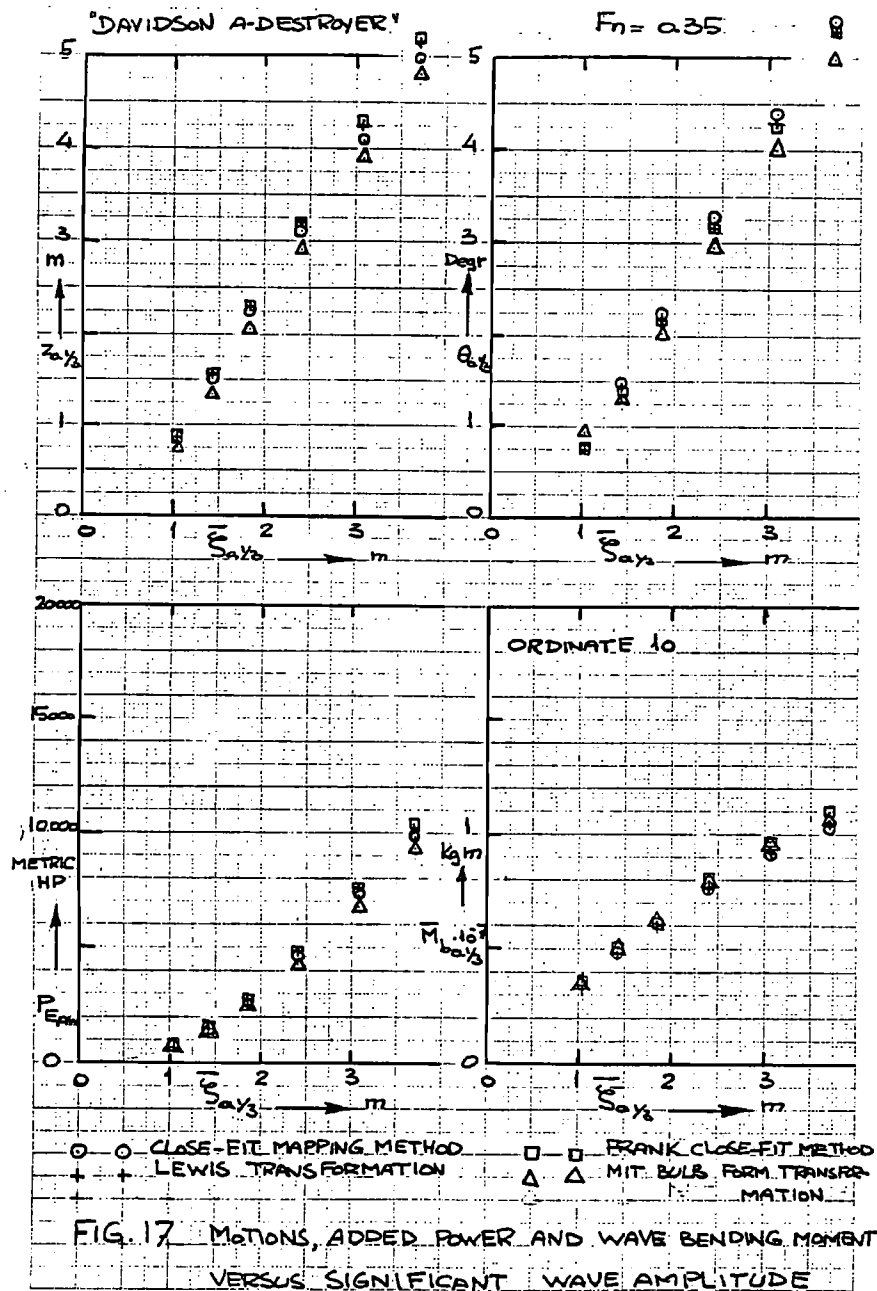
FIG. 15 RESPONSE FUNCTIONS FOR VERTICAL MOTIONS

"DAVIDSON A-DESTROYER"  $F_n = 0.35$

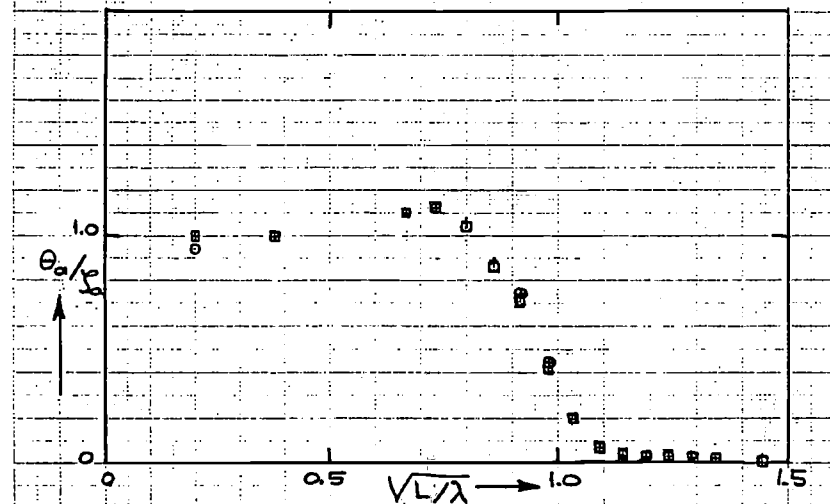
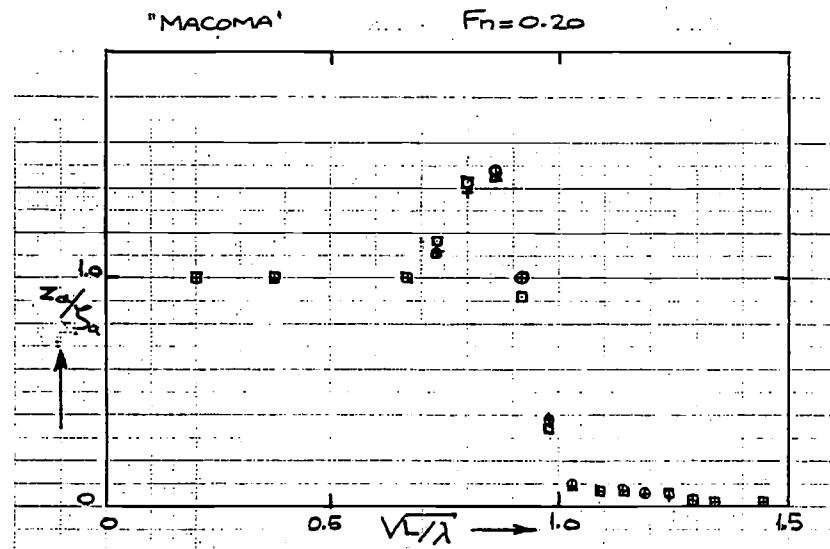


- ○ CLOSE-FIT MAPPING METHOD
- + + LEWIS TRANSFORMATION
- □ FRANK CLOSE-FIT METHOD
- △ △ MIT BULB FORM TRANSFORMATION

FIG. 16 RESPONSE FUNCTIONS FOR ADDED RESISTANCE AND WAVE BENDING MOMENT

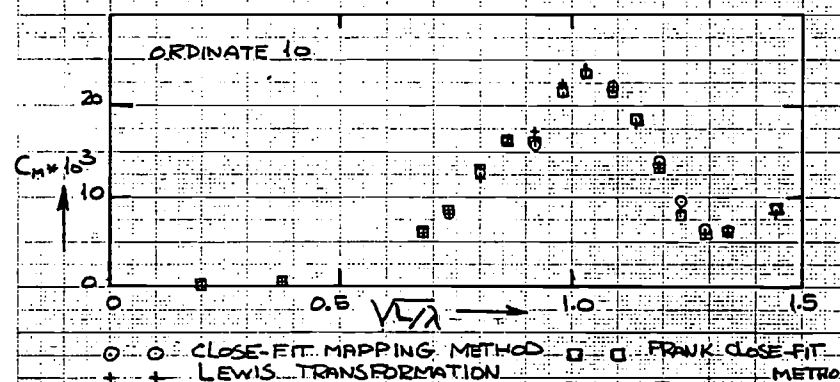
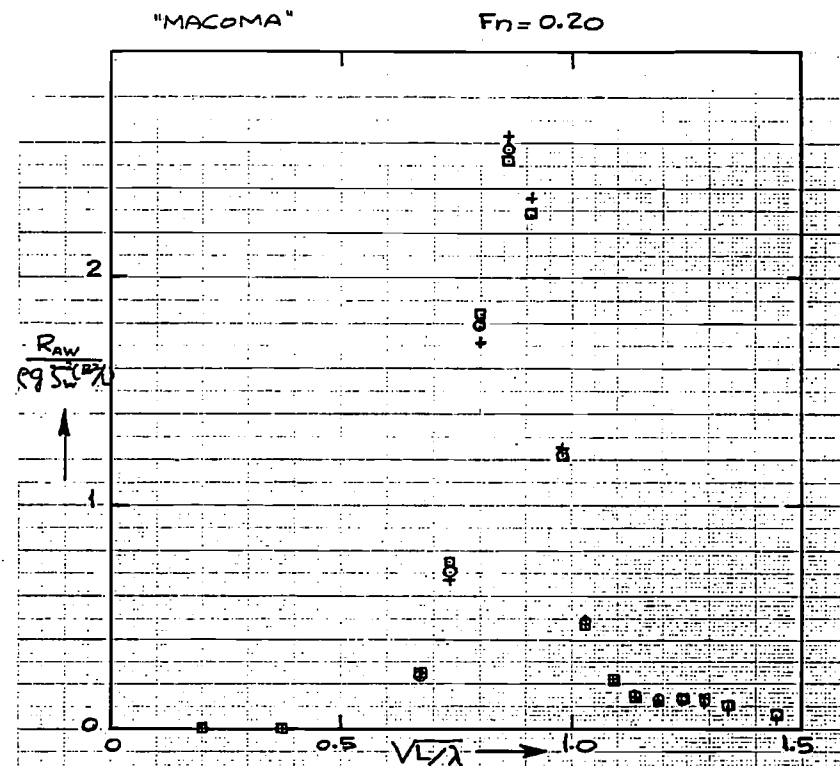


- ○ CLOSE-FIT MAPPING METHOD
- + + LEWIS TRANSFORMATION
- □ FRANK CLOSE-FIT METHOD
- △ △ MIT BULB FORM TRANSFORMATION



○ ○ CLOSE-FIT MAPPING METHOD  
 + + LEWIS TRANSFORMATION  
 □ □ FRANK CLOSE-FIT METHOD

FIG. 19 RESPONSE FUNCTIONS FOR VERTICAL MOTIONS



○ ○ CLOSE-FIT MAPPING METHOD □ □ FRANK CLOSE-FIT METHOD  
 + + LEWIS TRANSFORMATION

FIG. 20 RESPONSE FUNCTIONS FOR ADDED RESISTANCE AND WAVE BENDING MOMENT

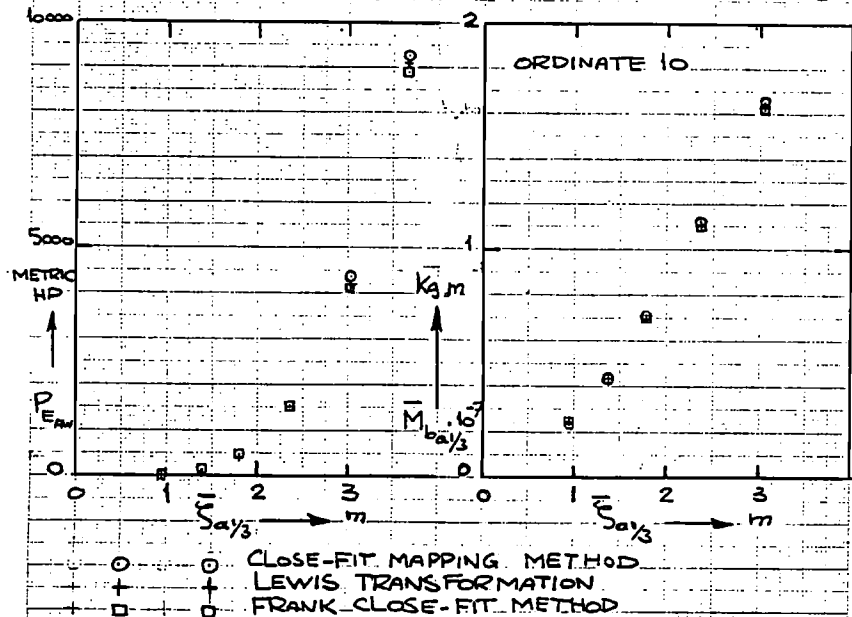
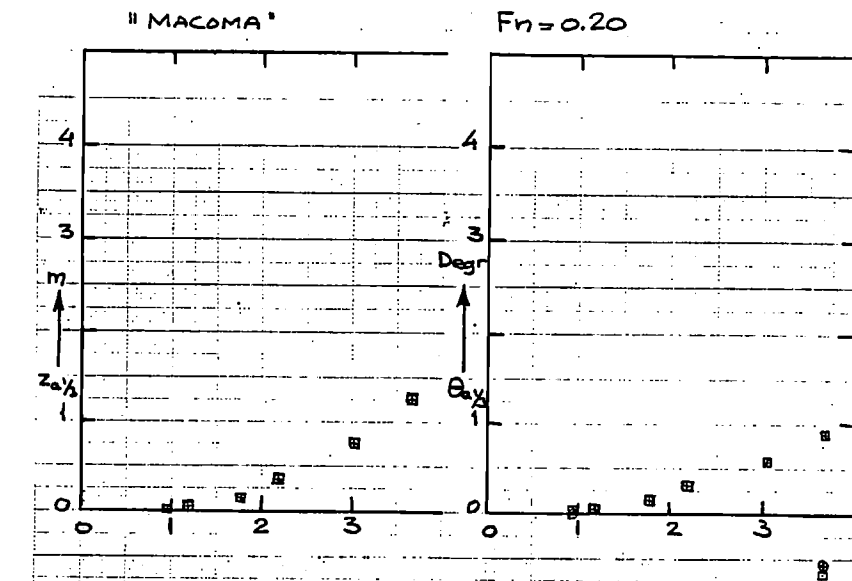
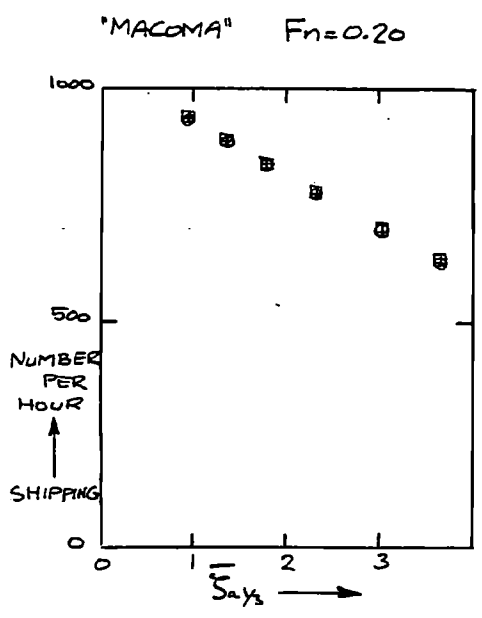


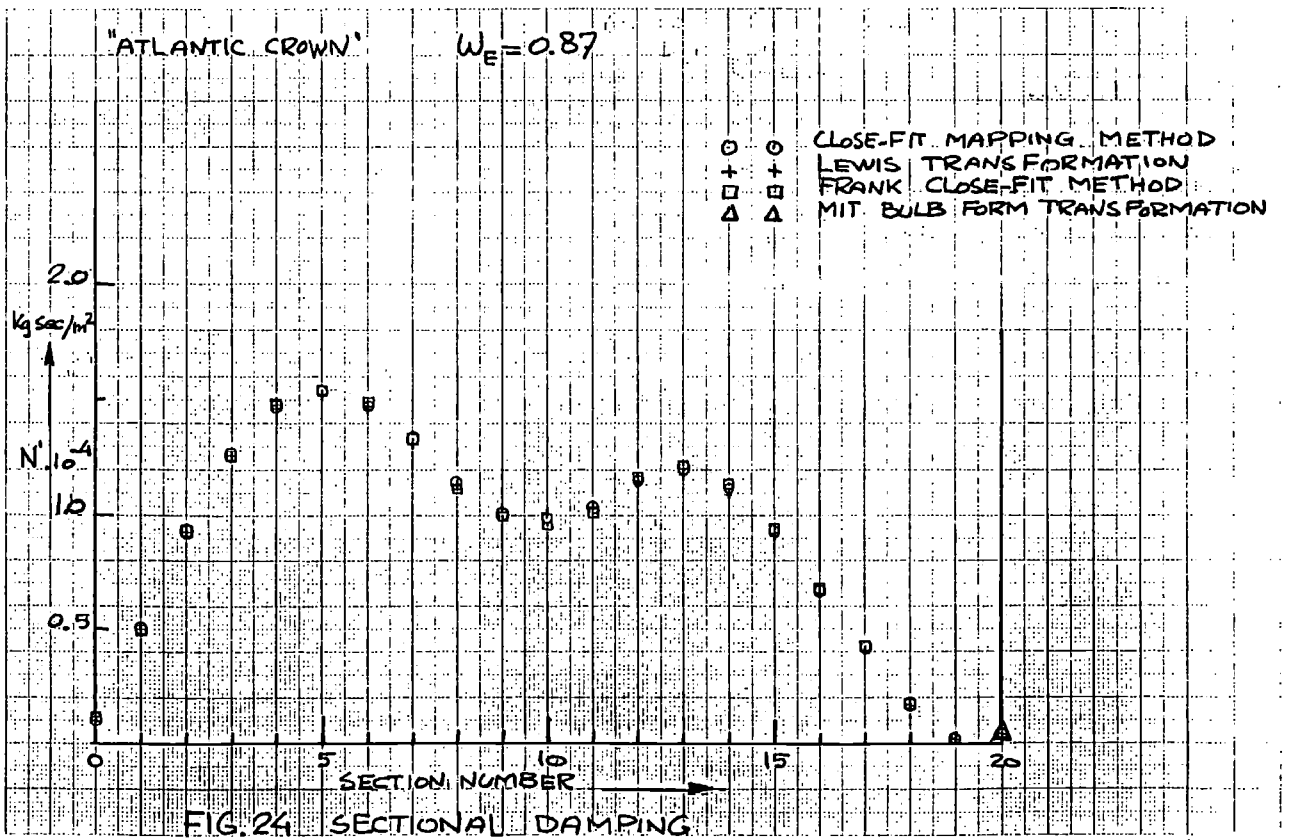
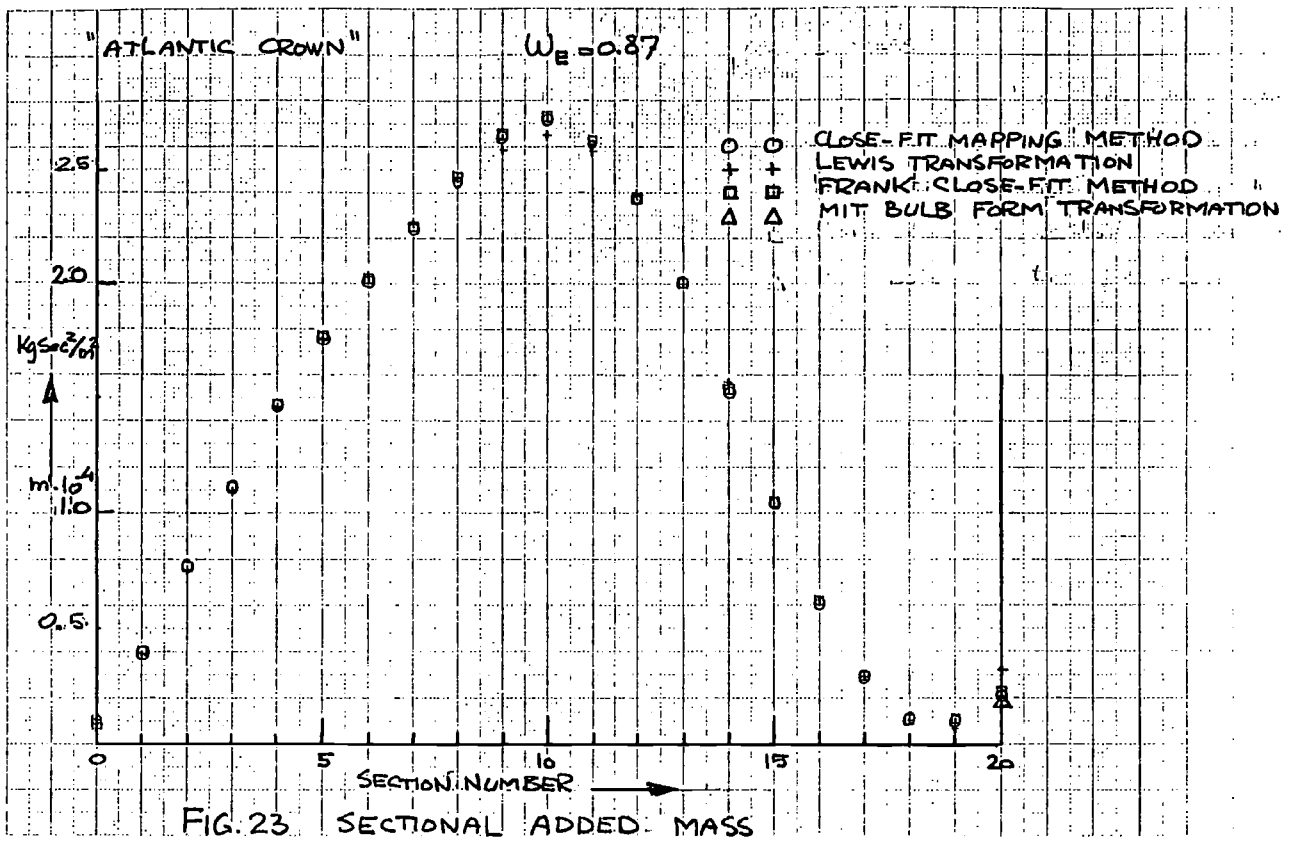
FIG. 21. MOTIONS, ADDED POWER AND WAVE BENDING MOMENT VERSUS SIGNIFICANT WAVE AMPLITUDE



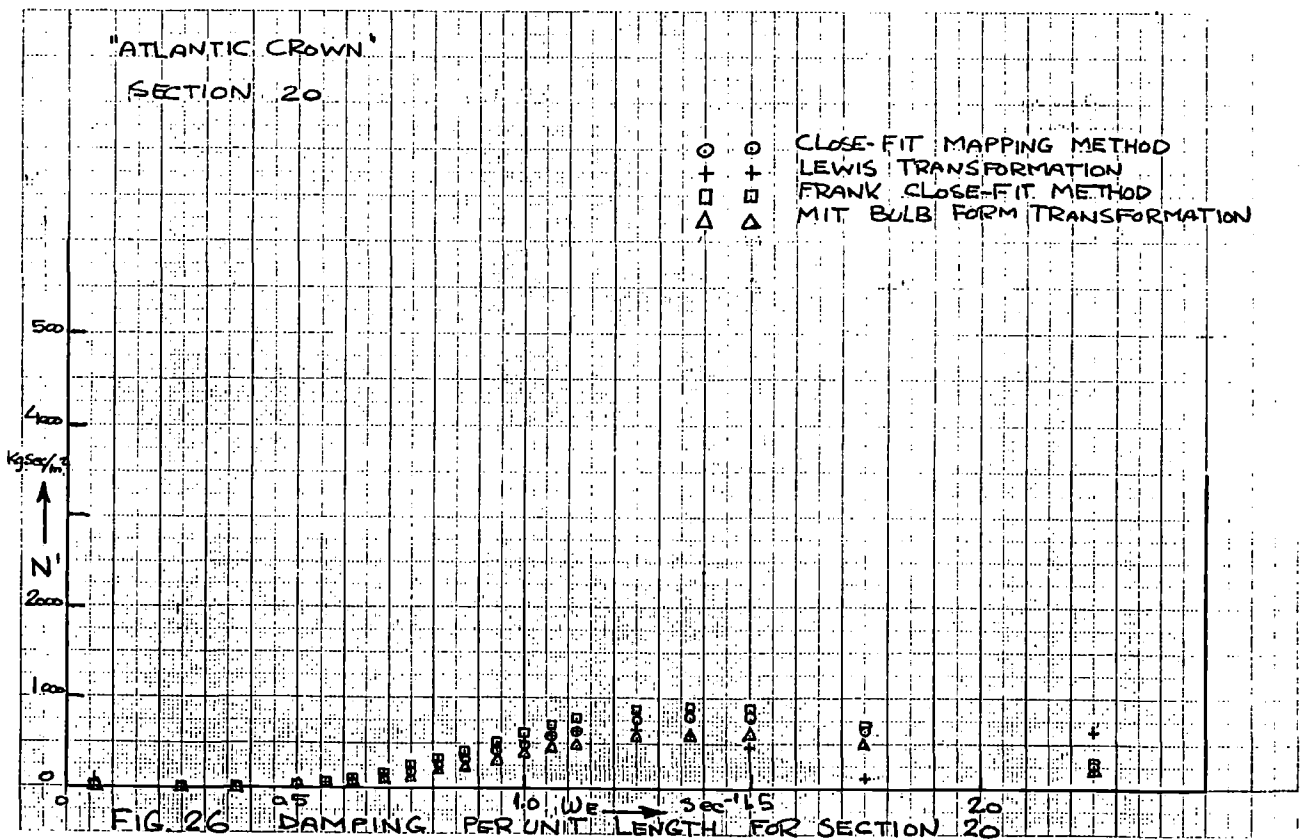
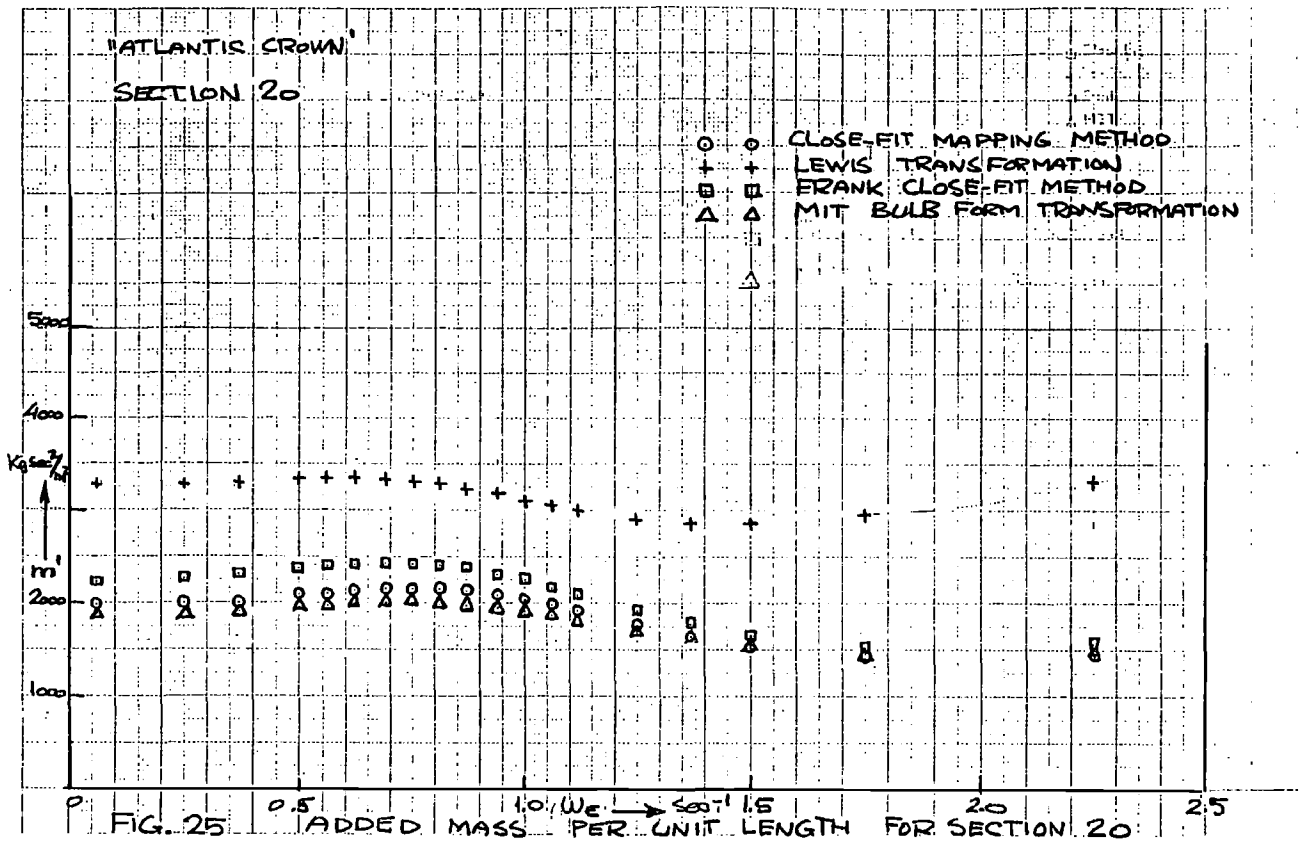
NO SLAMMING

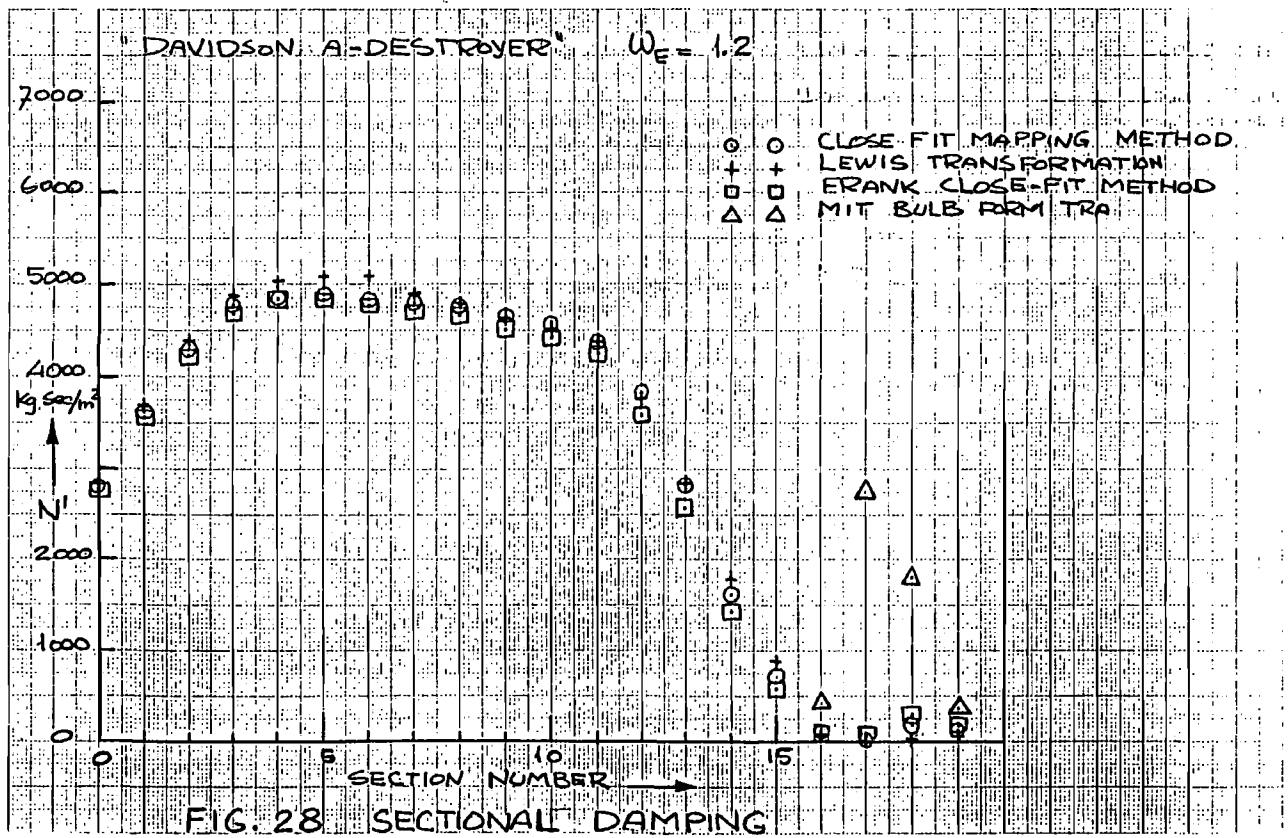
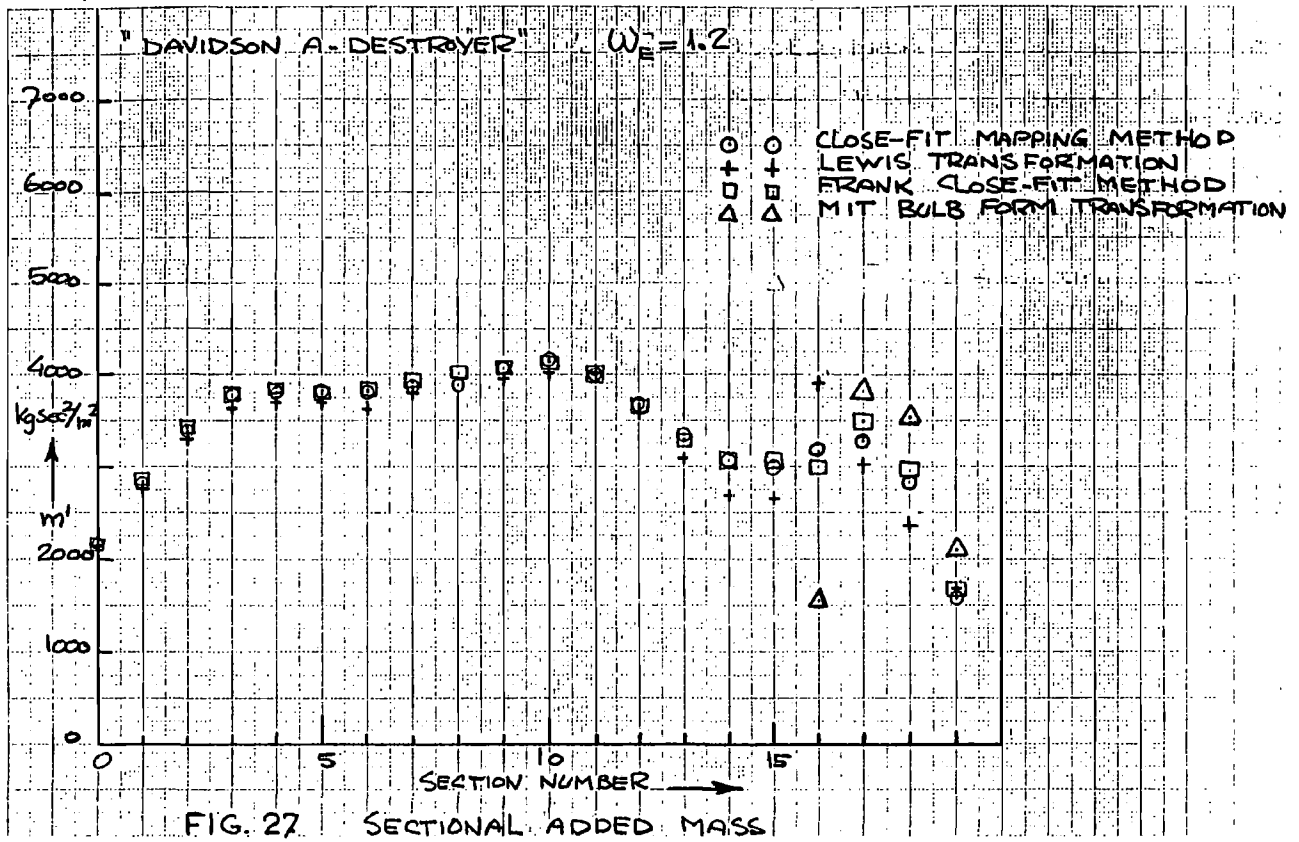
- ○ CLOSE-FIT MAPPING METHOD
- + + LEWIS TRANSFORMATION
- □ FRANK CLOSE-FIT METHOD
- △ △ MIT BULB FORM TRANSFORMATION

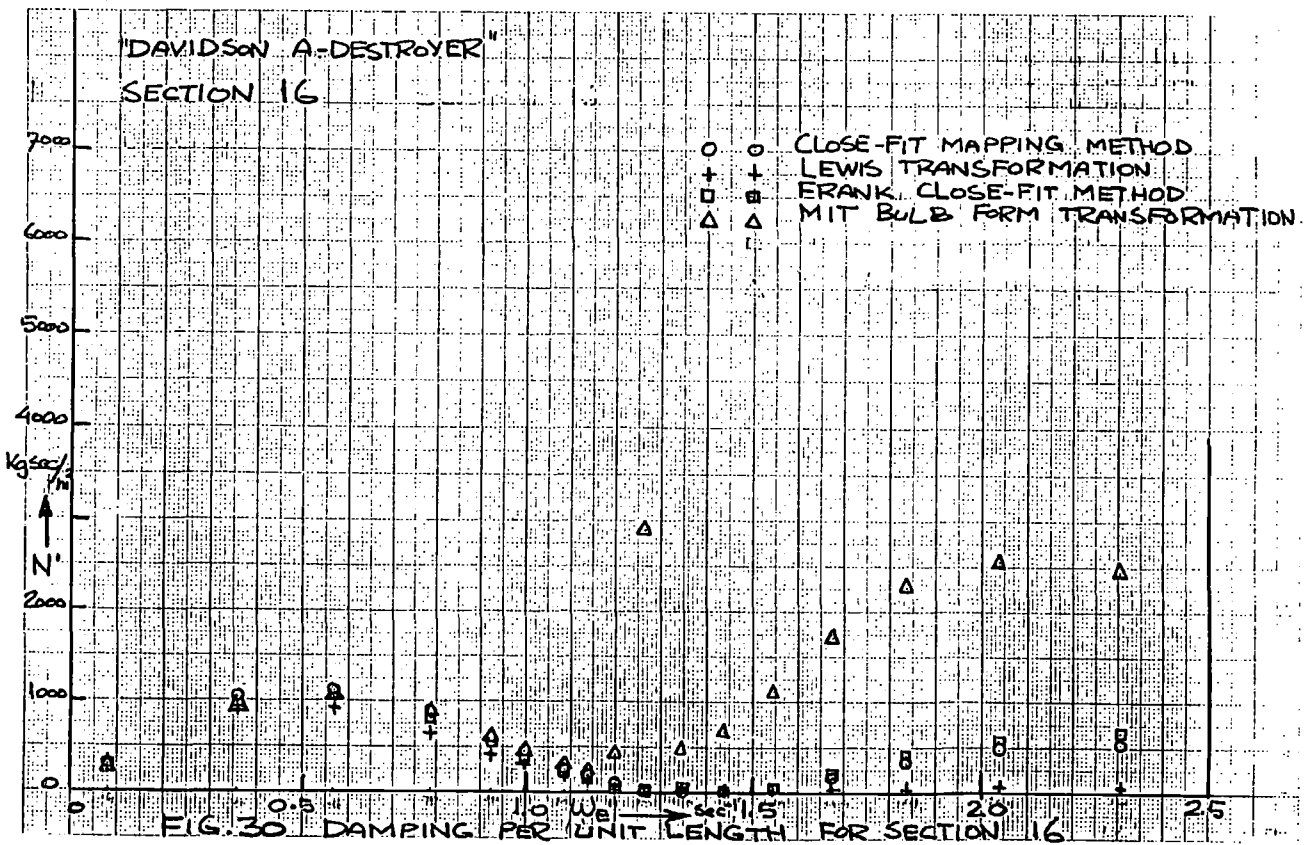
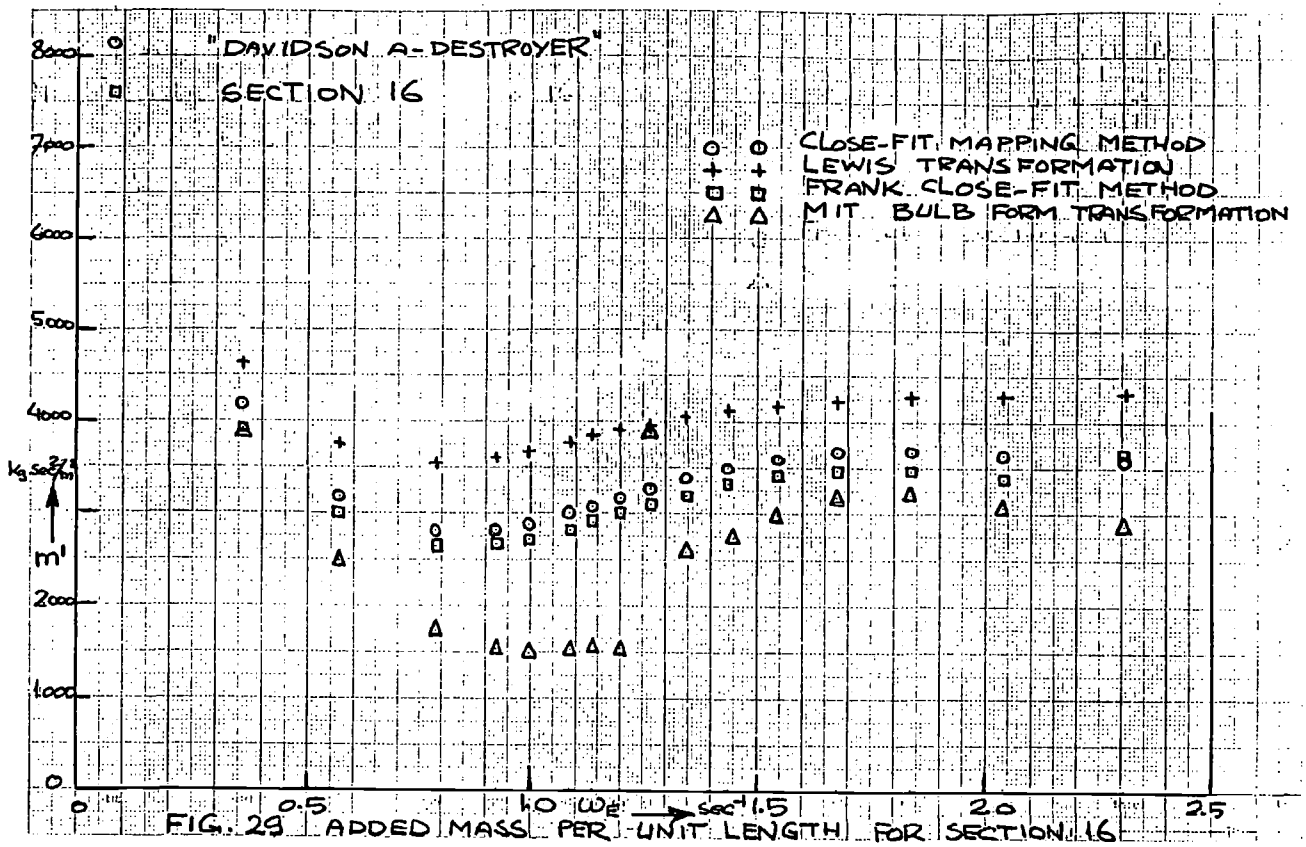
FIG. 22 NUMBER PER HOUR OF SHIPPING RELATED TO SIGNIFICANT WAVE AMPLITUDE

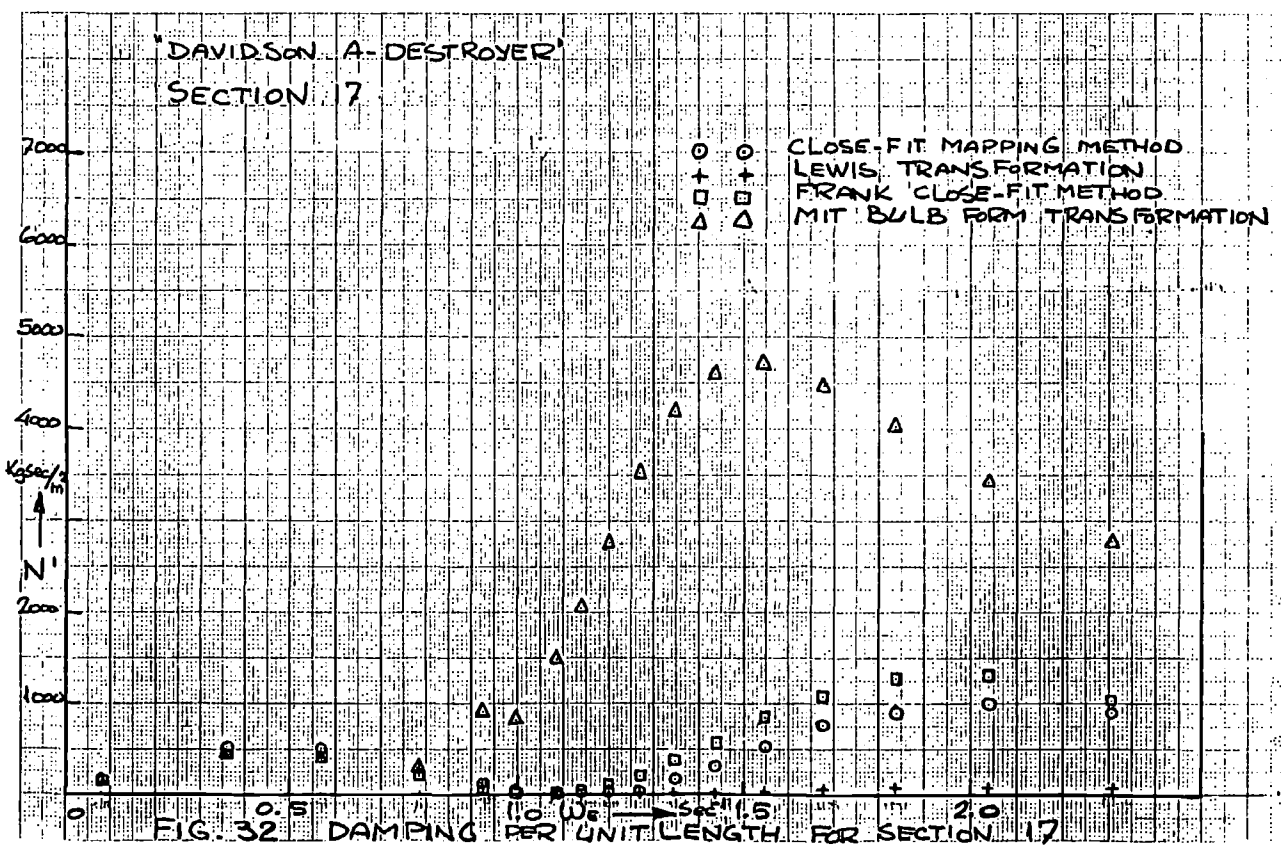
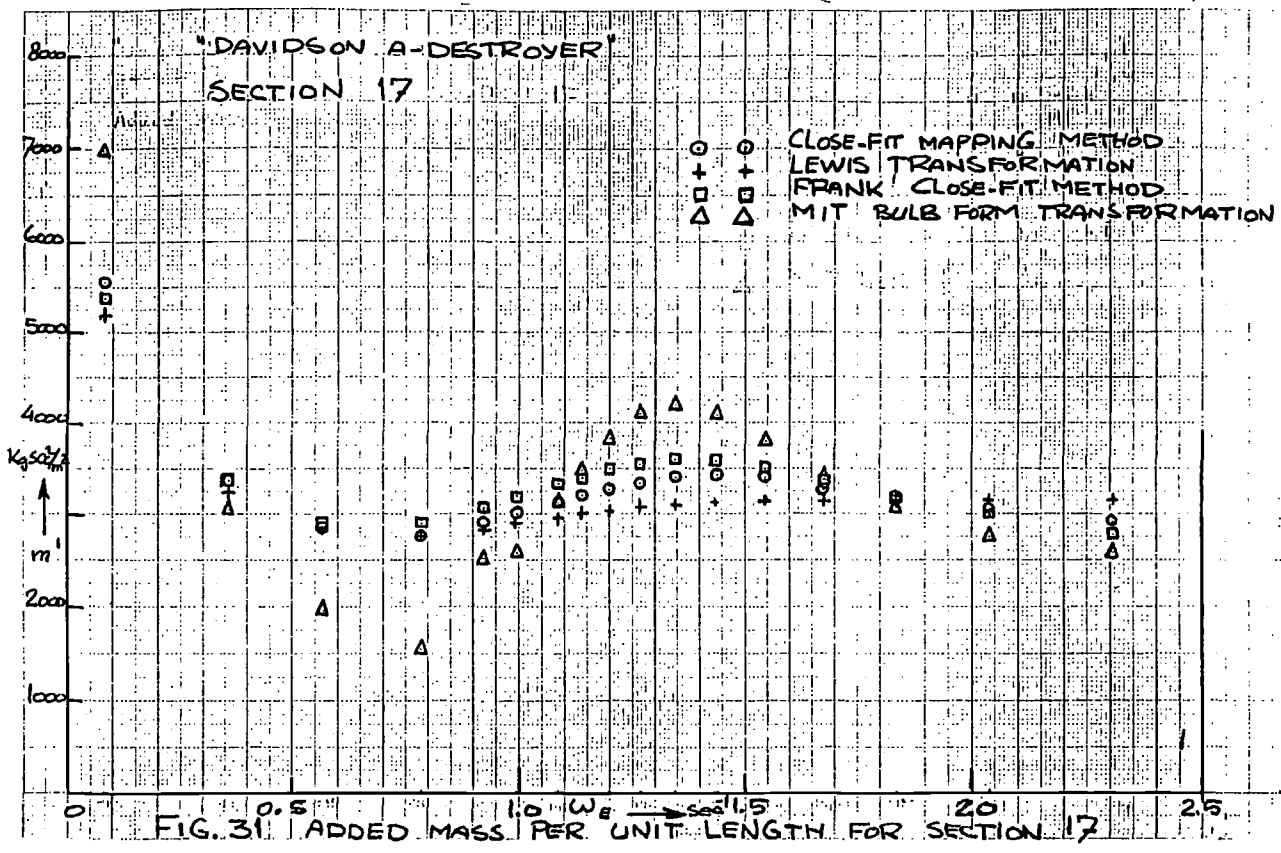


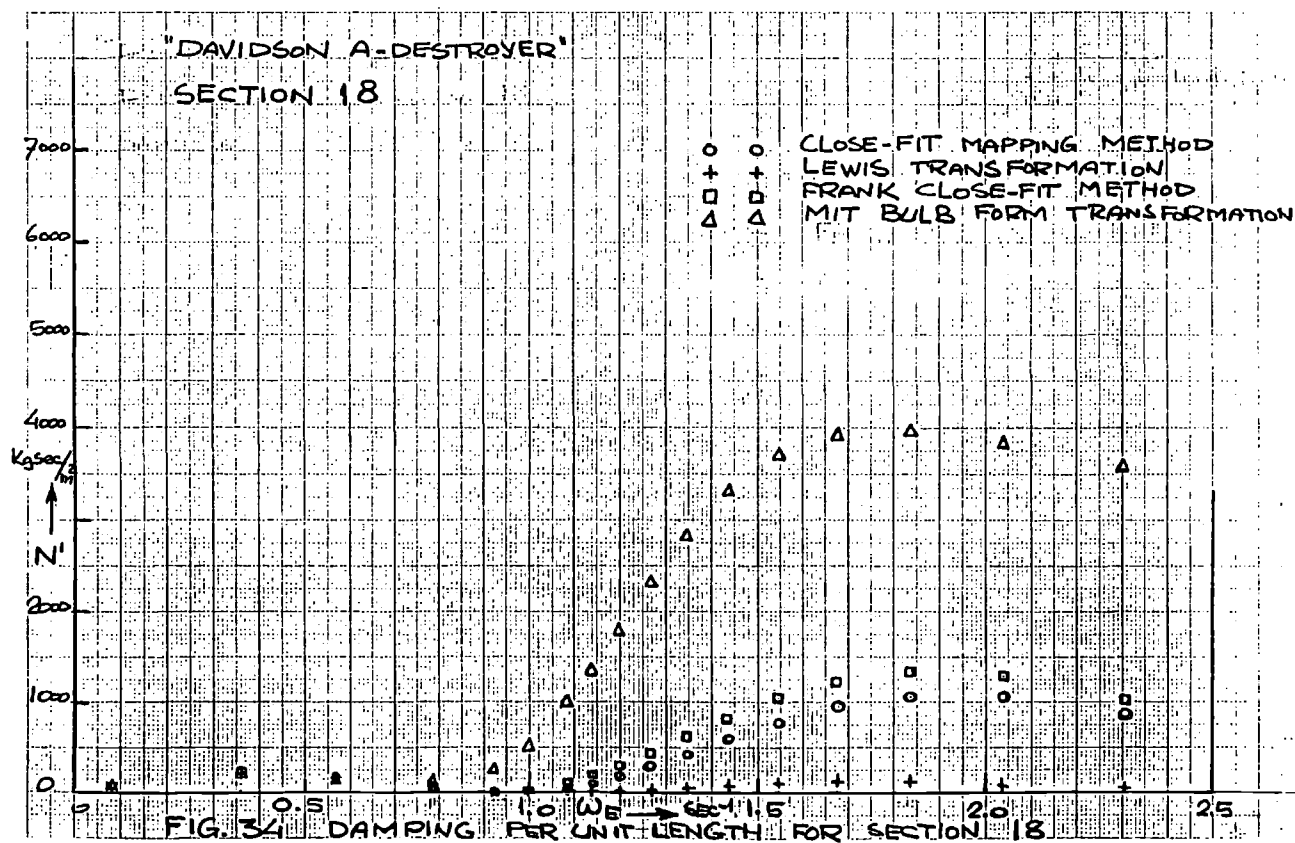
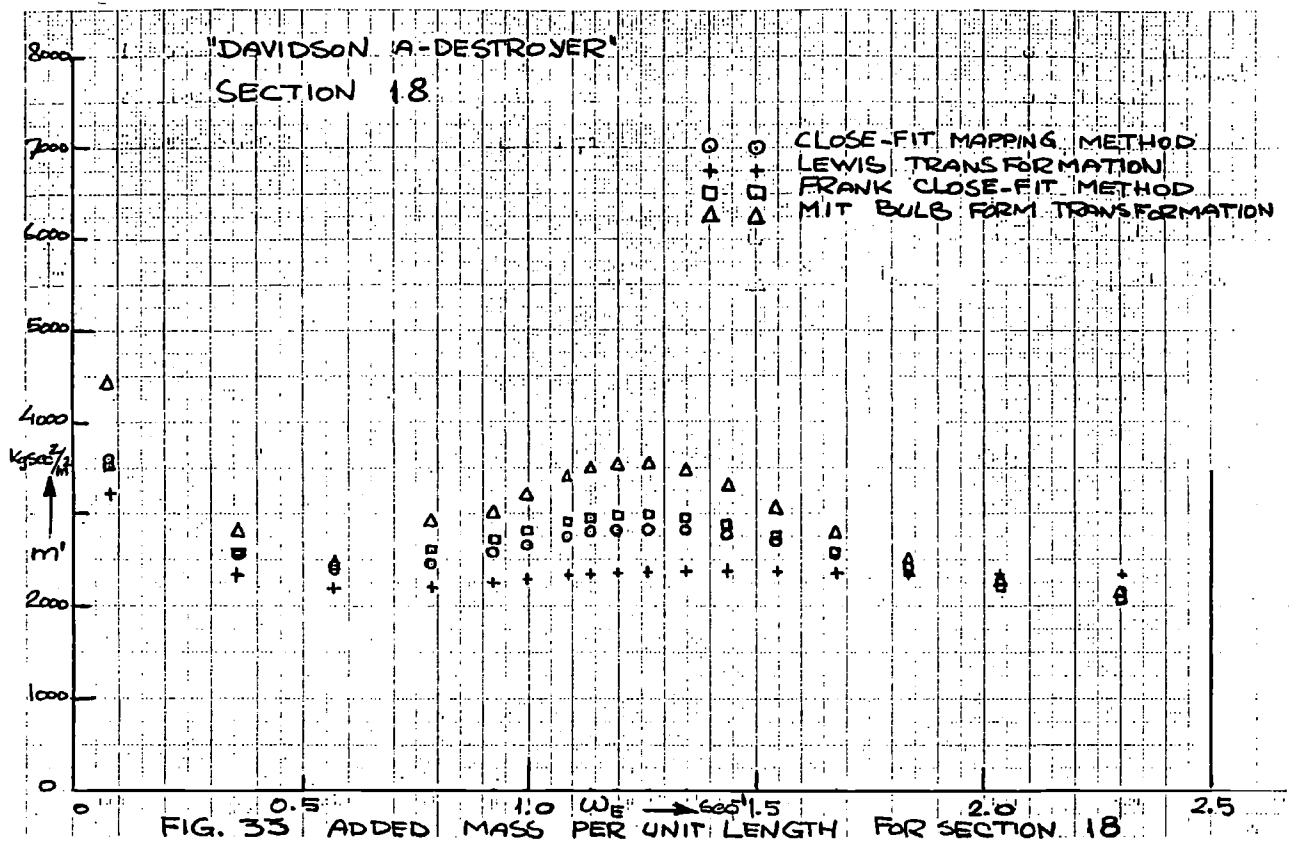




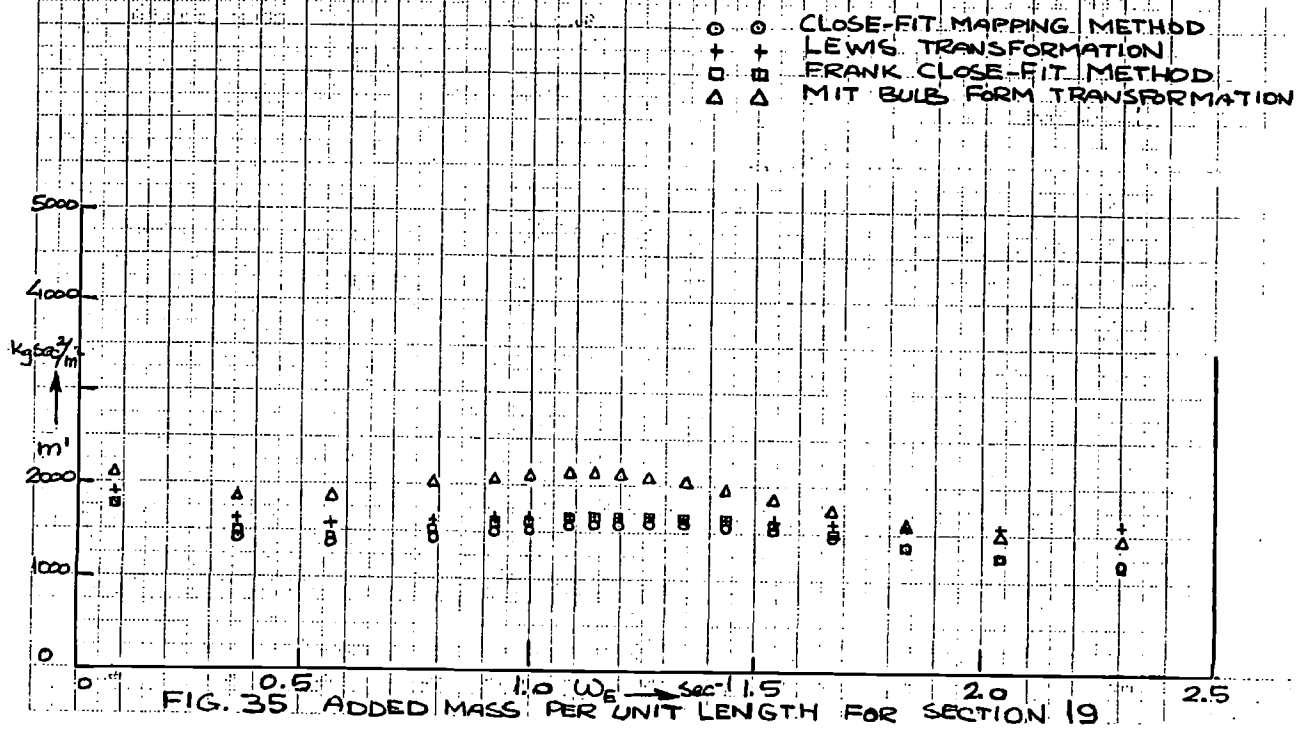




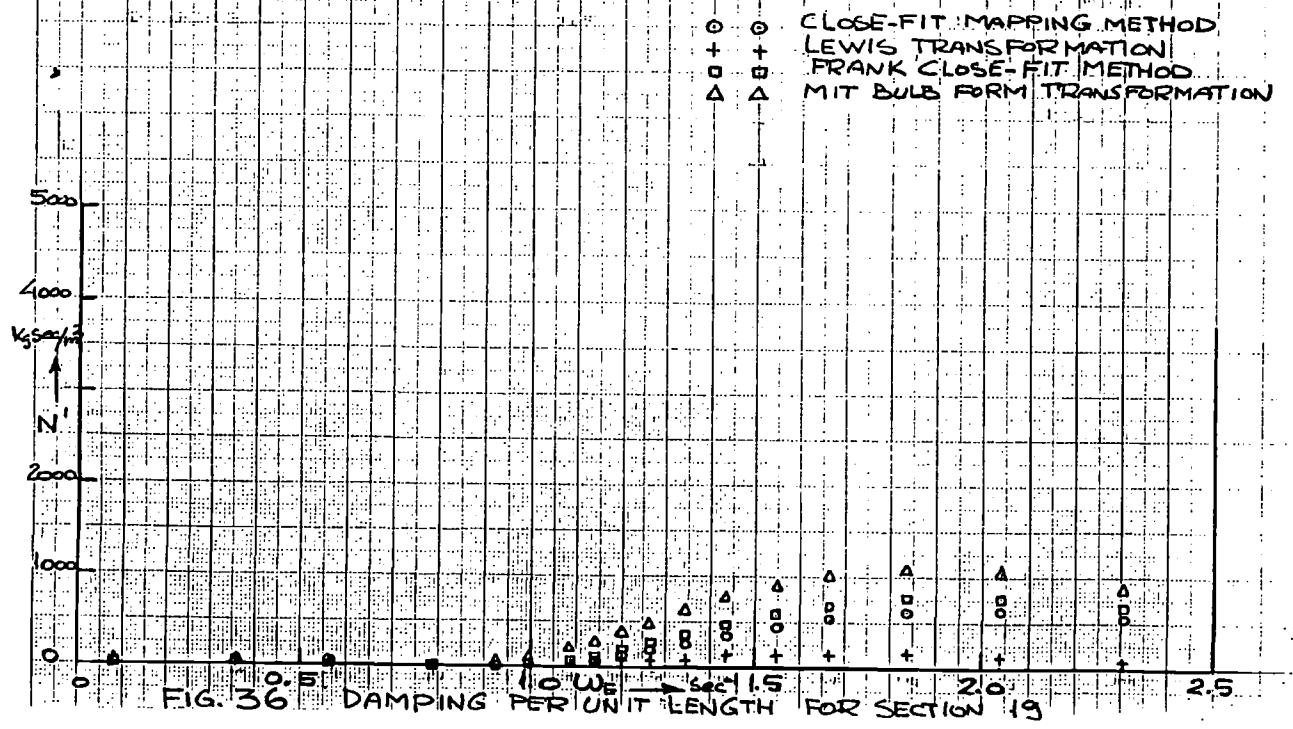




"DAVIDSON A-DESTROYER"  
SECTION 19

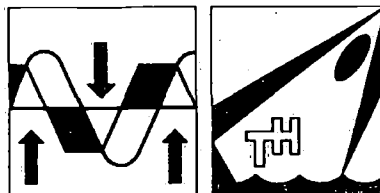


"DAVIDSON A-DESTROYER"  
SECTION 19



TECHNISCHE HOGESCHOOL DELFT  
AFDELING DER SCHEEPSBOUW- EN SCHEEPVAARTKUNDE  
LABORATORIUM VOOR SCHEEPHYDROMECHANICA

Rapport No. 445



THE INFLUENCE OF FIN KEEL SWEEP-BACK  
ON THE PERFORMANCE OF SAILING YACHTS

Symposium Yacht Architecture HISWA 1975

W. Beukelman and J.A. Keuning

**SYMPOSIUM  
YACHT  
ARCHITECTURE  
'75**

november 1975

Delft University of Technology  
Ship Hydromechanics Laboratory  
Mekelweg-2  
Delft 2208  
Netherlands

THE INFLUENCE OF FIN KEEL SWEEP-BACK ON  
THE PERFORMANCE OF SAILING YACHTS

by

W. BEUKELMAN AND J.A. KEUNING

Delft University of Technology  
Shipbuilding Laboratory

ABSTRACT

On a model of a sailing yacht, fin keels with sweep-back angles of 0, 20, 40 and 60 degrees have been investigated to determine the influence of the mentioned parameters on the performance. Two aspect ratios have been considered and for each aspect ratio series, the areas of the keels remained constant.

The performance has been determined from towing test results using the well-known Cimcrack-sail force coefficients.

Results of an analysis with respect to lift and induced drag are presented. Side force measurements in upright and heeled conditions have been compared with "equivalent keel" calculations.

An empirical method is proposed to determine the position of the centre of effort in the horizontal and vertical direction.



## CONTENTS

1. Introduction
2. Experiment
  - 2.1 Ship-, keel- and sail data
  - 2.2 Upright condition
  - 2.3 Heeling condition
3. Performance calculation
4. Analysis of experiments
5. Calculation of side force
6. Discussion
  - 6.1 Induced drag and total resistance for a given lift
    - 6.1.1 Upright condition
    - 6.1.2 Heeling condition
  - 6.2 Induced drag and lift for a given angle of leeway
  - 6.3 Sailing performance
  - 6.4 Calculation of the side force
7. Conclusions
8. Acknowledgement
9. Nomenclature
10. References
11. List of figures.

## 1. INTRODUCTION

Systematic investigations concerning the influence of fin keel sweep-back in connection with sailing performance are scarce. An experimental study was presented by De Saix [1] for sweep-back angles of 0, 25 and 50 degrees and a variation in aspect ratio from 0.5 to 1.52. All keels had the same lateral area and the same taper ratio. Optimum sweep angles, dependent on aspect ratio, had been determined.

Later, routine windward tests had been carried out for these optimum keels from which higher aspect ratio keels appeared to be more favourable.

An experimental and theoretical study on isolated fin keels was carried out by Herreshoff and Kerwin and had been reported in [2]. Lifting surface calculations, according to the concept of an "equivalent keel" had been undertaken to compare the performance of different keel plan forms.

Induced drag was shown to increase by about 1% and lift slope was reduced by about 8% as the sweep angle was increased up to 51°. All of these keels had been investigated in the upright position and the keel-hull interaction had not been taken into account.

Wind tunnel tests carried out by Mac Laverty [3] on a double model of a 5.5 m yacht for keels from 30 - 65° sweep-back showed a decrease in drag with increase of sweep-back for a given side force.

Contrary to this result has been the conclusion of the report of the Advisory Committee for Yacht Research of the University of Southampton [4] which stated, that increase of sweep-back causes an increase of induced drag for a given side force.

For the present investigation performance tests were carried out on a model of the sailing yacht "Spirit 28". Keels had been fitted with sweep-back angles of 0, 20, 40 and 60 degrees for two aspect ratios of 0.94 and 1.20 to determine the influence of these parameters. In addition the experiments were extended to include tests on the bare model-hull with and without rudder. These results were not included in the present report.

The series of experiments consisted of three parts viz.:

1. tests without heel and leeway to determine the upright resistance and to determine downwind performance.

2. tests in the upright condition with leeway to determine side force production and induced drag.
3. test with 10, 20 and 30 degrees heel with leeway to determine heeled side force production and resistance and to calculate close-hauled performance.

The windward performance had been calculated with the normal Gimcrack sail coefficients.

Extended analysis of the experiments had been carried out to find out whether a tendency could be established in the lift and drag induction with respect to sweep-back and aspect ratio.

To a certain extent hull influence had always been included in the results.

The measurements of the side force for both the upright and heeled conditions were compared with the results of calculations according to the "equivalent keel" procedure as presented by Gerritsma in [5, 6]. Some corrections derived from the measurements have been proposed for the calculation of the centre of effort of the side force in horizontal and vertical directions both for the upright and heeled conditions.

## 2. EXPERIMENTS

### 2.1 Ship-, keel- and sail data

The main particulars of the sailing yacht have been presented in table 1 and the hull-form is shown in figure 1.

The keels have been investigated for two geometric aspect ratios viz.:  $a_g = 0.94$  and  $a_g = 1.20$ . The definition of geometric and effective aspect ratio as used in this paper is also presented in figure 1 and in the nomenclature (chapter 9).

For one aspect ratio the keels have had the same lateral area, taper ratio ( $\lambda = 1$ ) and section profile NACA 63<sub>2</sub> - 015 derived from [7].

The keels have been fitted to the hull in such a way that for the aspect ratio  $a_g = 0.94$  the theoretical centre of effort of the effective keel (i.e. the keel extended to the waterline) remained at the same point as shown in figure 1.

With the deeper keels this centre of rotation has been kept at the same position, which means not at the assumed centre of

effort for these keels.

The centre of effort is initially approximated to be on the quarter chord at a distance of 43% of the total draught below the waterline.

The height of the centre of gravity remained the same for all models. The applied sail data have also been presented in table 1.

Table 1.

Ship Data

name : Spirit 28

Model scale 1:4.5

designer : E.G. v.d. Stadt

<u>Description</u>	<u>Symbol</u>	<u>Unit</u>	<u>Quantity</u>
Length over all	LOA	m	8.40
Length on test waterline	LTWL	m	6.90
Maximum breadth	BMAX	m	2.81
Hull draught	TH	m	0.41
Total draught (= effective keel span)	T	m	1.55-1.87
Hull displacement		kg	2547
Total displacement		kg	2719-2763
Length centre of buoyancy of hull before MWL	LCBH	m	-0.29
Hull prismatic coefficient			0.579
Centre of gravity under LTWL		m	0.010
Effective sail area beating		m <sup>2</sup>	27.8
Effective sail area down wind		m <sup>2</sup>	71.1
Effective centre of effort beating above LTWL		m	4.68
Keel span	b <sub>g</sub>	m	1.14-1.46
Keel chord	c <sub>k</sub>	m	1.22
Geometric aspect ratio of keel	a <sub>gk</sub>		0.94-1.20
Keel sweep-back angle	∧ <sub>k</sub>	degree	0-20-40-60
Rudder span	b <sub>gR</sub>	m	1.03
Average rudder chord	c <sub>R</sub>	m	0.45
Geometric aspect ratio of rudder	a <sub>gR</sub>		2.29
Rudder sweep-back angle	∧ <sub>R</sub>	degree	8.25

## 2.2 Upright condition

At first the upright resistance without heel and leeway has been measured for the models with the different keels. For the lower aspect ratio, the differences in this upright resistance appear to be negligible, but for the keels with the higher aspect ratio ( $a_g = 1.20$ ) the resistance has decreased with the increase of sweep-back angle above  $\Lambda_K = 30^\circ$  to  $\Lambda_K = 60^\circ$  by about 5%. The resistance curves are shown in figure 2.

Afterwards the side force and resistance have been determined in the upright position of the model with leeway for two speeds viz.:  $F_n = 0.20$  and  $0.35$ .

The side force is shown in figure 3 for each aspect ratio in relation to the sweep-back angle  $\Lambda$ . The side force is expressed in non dimensional form:

$$Y_\beta = \frac{Y}{\frac{1}{2}\rho V^2 L_{TWL}^2 \beta} \quad (1)$$

in which:

$Y$  =  $F_H \cos \phi$  = hydrodynamic side force

$\rho$  = mass density of water

$V$  = speed

$L_{TWL}$  = length on test waterline

$\beta$  = angle of leeway in radians.

Also in figure 3, the vertical and horizontal position of the centre of effort of the side force for the different keels is shown as actually measured.

These positions have been presented as a percentage of the waterline length with respect to the middle of the test waterline (MWL) (forward is positive) and as a percentage of the maximum draught with respect to the waterline respectively.

For further analysis relative to induced drag and lift see chapter 4.

## 2.3 Heeling condition

For heeling angles of 10, 20 and 30 degrees a minimum number of three angles of leeway and three speeds have been considered to determine the resistance and side force and, finally, the close hauled performance as described in chapter 3.

The side force and the position of the centre of effort in the heeling condition, derived from the measurements, have been shown in figure 4 in the same way as described for the upright position in chapter 2.2.

The results are presented for the conditions in table 2.

Table 2

Heeling angle $\phi$	Speed m/sec
10	1.0
20	1.2
30	1.3

The figures 5 and 6 show the wave pattern of the model with a keel sweep-back angle of 0 and 60 degrees and for heeling angles of 10, 20 and 30 degrees for the cases of normal leeway and without leeway.

For the last condition the model was artificially heeled at the predetermined angle. The photographs are related to the higher aspect ratio series only.

It is obvious from these pictures that the wave amplitude due to heel is strongly dependent on the keel loading and increases significantly with heel, and decreases with sweep-back.

### 3. PERFORMANCE CALCULATION

The performance in running conditions for the ship with different keels, is shown in figure 7.

As the sail area remains constant for the two aspect ratios, it can be seen that the ships with the higher aspect ratio have a lower down-wind performance because of the resistance increase due to the larger lateral keel area. This is to be expected. The difference in speed between both aspect ratios appears to be smaller for keels with corresponding high sweep-back, which is due to the lower upright resistance for the keels with higher aspect ratio and high sweep-back.

The optimum windward performance has been determined from the test results in the usual way with the normal Gimcrack sail coefficients.

When considering the aspect ratio as a constant, figure 8 shows that the speed-made-good is almost the same for all sweep-back angles considered.

There is an exception, however, with strong winds and a high aspect ratio. For this case the keels with high sweep-back angles look attractive.

A disadvantage, however, is the high angle of leeway. The leeway angle appears to increase rather rapidly for the keels with maximum sweep-back angle, as shown in figure 9 for true winds of 3.5, 7 and 10 m/sec.

The speeds-made-good, as a result of the windward performance calculations, are shown in figure 8<sup>b</sup>. This was done on the basis of sweep-angle for the true winds previously mentioned.

#### 4. ANALYSIS OF EXPERIMENTS

For this analysis, induced drag  $D_i$  is characterized by the drag increase above the resistance measured in an upright condition without heel and leeway. It should be remembered, that this upright resistance is not the same for all keels, but reduced for keels with the higher aspect ratio and high sweep-back. This influence is not included in the induced drag, while on the other hand the resistance variation with respect to the upright resistance, is included. This arises from alteration in the wave pattern of hull and keel due to leeway and heel.

The lift and induced drag coefficient are defined as follows:

$$\begin{aligned} c_{Di} &= \frac{D_i}{\frac{1}{2}\rho V^2 A_T} \\ c_L &= \frac{L}{\frac{1}{2}\rho V^2 A_T} \end{aligned} \quad (2)$$

in which:

$L = Y =$  hydrodynamic side force

$A_T =$  the lateral area of the equivalent keel and rudder ( $= b_{eK} c_K + b_{eR} c_R$ ), which means the keel and rudder extended to the waterline.

For the different keels and each aspect ratio, the induced drag coefficient versus the lift coefficient is presented in figure 10 for the upright condition.

Figure 11 shows that for the heeling condition and speed as denoted in table 2 of chapter 2.3.

The lift coefficient versus leeway is shown for the same conditions in fig. 12, 13, 14 and 15.

For a given lift coefficient in the upright condition and for lift force values in the heeling condition near the optimum speed-made-good, the total resistance and induced drag on the basis of sweep-back angle are shown in figure 16 respectively. Also combinations of heeling angle and speed as denoted in table 2 are presented for this case.

## 5. CALCULATION OF SIDE FORCE

Side force calculations have been carried out by means of the "equivalent keel" procedure as introduced by Gerritsma in [5, 6]. The keel and rudder are considered to be extended to the waterline, while the presence of the hull is assumed to be replaced by the extended part of keel and by the extended part of the rudder, if this does not intersect the water surface already. As a resumé, the procedure, including the proposed corrections, is described briefly here-after. To determine the slope of the lift curve use has been made of the expression according to Whicker and Fehlner in [8]:

$$\frac{\partial C_{LK,R}}{\partial \alpha_{K,R}} = \frac{5.7 a_{eK,R}}{1.8 + \cos \Lambda_{K,R} \sqrt{\frac{a_{eK,R}}{\cos^2 \Lambda_{K,R}} + 4}} \quad (3)$$

in which:

- $K,R$  = index for keel or rudder
- $C_{LK,R}$  = lift coefficient
- $\alpha_{K,R}$  = angle of incidence in radians
- $a_{eK,R}$  = effective aspect ratio
- $\Lambda_{K,R}$  = sweep-back angle of quarter chord line.



For keels and for a rudder not intersecting the waterline, the aspect ratio is taken as:

$$a_{eK,R} = \frac{2 b_{eK,R}}{c_{K,R}} \quad (4)$$

with:

$b_{eK,R}$  = span or draught of effective keel or rudder

$c_{K,R}$  = chord length.

If the rudder does intersect the water surface the aspect ratio may be chosen as:

$$a_{eR} = \frac{1.6 b_{eR}}{c_R} \quad (5)$$

For small angles of incidence, the side force of a keel or rudder may be estimated from:

$$L_{K,R} = \frac{1}{2} \rho V_{K,R}^2 A_{K,R} \left( \frac{\partial C_{L_{K,R}}}{\partial \alpha_{K,R}} \right) \alpha_{K,R} \quad (6)$$

in which :

$V_{K,R}$  = water velocity at keel or rudder

$A_{K,R}$  = lateral area of keel or rudder (=  $b_{eK} c_K$  resp.  $b_{eR} c_R$ )

The water velocity at the keel may be set equal to the ship speed, and so

$$V_K = V_s \quad (7)$$

while this velocity at the rudder is estimated as :

$$V_R = 0.8 V_s \quad (8)$$

The angle of incidence for the keel may be put equal to the leeway angle, so :

$$\alpha_K = \beta \quad (9)$$

while the angle of incidence for the rudder after correction for "side-wash" of the keel, can be estimated as :

$$\alpha_R = \left\{ 1 - \frac{1.6 \left( \frac{\partial C_{L_K}}{\partial \alpha_K} \right)}{\pi a_{eK}} \right\} \beta \quad (10)$$

If the situation of the centre of effort for keel and rudder is known, it is possible to determine the situation of the centre of effort for the total side force in horizontal and vertical direction respectively from :

$$x_Y = \frac{L_K x_{YK} + L_R x_{YR}}{L} \quad (11)$$

$$z_Y = \frac{L_K z_{YK} + L_R z_{YR}}{L}$$

in which :

$L = L_K + L_R$  = the total side force

$x_{YK,R}$  = the horizontal distance of the centre of effort of keel or rudder from the middle of the test waterline (positive in forward direction)

$z_{YK,R}$  = the vertical distance of the centre of effort of keel or rudder from the test waterline (positive upwards).

For a spanwise elliptical loading, it is assumed, that the centre of effort is situated on the quarter chord line at 43% of the effective span below the waterline. It appears, however, that particularly for the horizontal direction, the centre of effort, calculated in this way, shows a rather large deviation from the measurements on the model with keel and rudder. This is a consequence of hull and speed influence. A regression analysis has been made from the experimental results and leads to the following preliminary proposals for the horizontal and vertical situation of the centre of effort.

For the keel the vertical distance of the centre of effort as a ratio to the effective span should be chosen on the quarter chord line as :

$$z_{YK}/b_{eK} = 0.50 - \frac{0.1245}{a_{eK}} \quad (12)$$

in which  $a_{gK}$  = the geometric aspect ratio of the keel.

The horizontal distance of the centre of effort, defined off the middle of the testwaterline (MWL) is related to the length of this waterline. Calculated as shown above with  $x'Y/L_{TWL}$  and corrected for speed, hull influence and heeling angle this relative distance may be estimated as:

$$xy/L_{TWL} = x'Y/L_{TWL} + \frac{0.425}{a_{gK}} Fn \cos \Lambda_K (1 - \sin \phi)^2 \quad (13)$$

in which :

$L_{TWL}$  = length on the test waterline

$Fn = \frac{v}{\sqrt{gL_{TWL}}} = \text{Froude number}$

$\Lambda_K$  = sweep-back angle of keel

$\phi$  = heeling angle.

The calculated results are shown in figure 3 and 4 both for the upright and heeled condition and are presented in the same way as described in chapter 2.2. for the experimental results on the understanding that :

$$L=Y=F_H \cos \phi \quad (14)$$

The proposed corrections are only a first step because more extended statistical investigations are needed for different hulls and keels to obtain more reliable results.

## 6. DISCUSSION

To obtain a clear judgement about the test results, the following aspects are taken into consideration :

1. induced drag and total resistance for a given lift
2. induced drag and lift for a given angle of leeway
3. sailing performance
4. calculation of the side force.

For comparison, the results with respect to the total resistance or induced drag and the resulting speeds of the sailing performance, it should be remembered, that the total resistance or induced drag is more sensitive than the speed.

For the upright condition without heel and leeway, it is clear from figure 2 that the differences in resistance are small for the lower aspect ratio, while for the higher aspect ratio the resistance is reduced by about 5% for a sweep-back angle of 0 to 60 degrees. This phenomenon has an important influence on the final results, as will be shown later.

## 6.1. Induced drag and total resistance for a given lift

### 6.1.1. Upright condition

It is evident from the results shown in figure 10, that for the upright condition with leeway, the induced drag is increasing with sweep-back angle for a given side force. This tendency is in agreement with [2] and [4]. The percentage of increase is dependent on the value of the lift force, but generally far more than 1% of that calculated by Herreshoff and Kerwin in [2]. For a certain lift coefficient e.g.  $C_L=0.05$  with respect to the higher aspect ratio, the total drag increases with sweep-back angle of 0 up to 60 degrees by about 6%. For this aspect ratio, especially, one should remember that the upright resistance without leeway reduces by about 5% for a sweep-back angle of 0 to 60 degrees. It should be remarked from figure 10 that increase of induced drag with sweep-back angle is most clearly demonstrated for the higher aspect ratio and the lowest speed in the case of the upright position. Further, the influence of the keel wave may be expected to increase with speed and to decrease with aspect ratio.

### 6.1.2. Heeling condition

The relation between induced drag and sweep-back angle, as found for the upright position, changes a great deal under heel. This may also be caused by the behaviour of the keel wave : the amplitude of this wave increases with heel and decreases with sweep-back angle as remarked in chapter 2.3. This phenomenon appears to be a dominant factor for the induced drag and consequently, for the total resistance.

For the higher aspect ratio and the smallest heeling angle, the tendency is the same as that for the upright position :

induced drag increases with sweepback angle for a given side force.

It is easily understood that for this case the influence of the keel wave is rather small. For the other heeling angles with higher aspect ratio and for all heeling angles with the lower aspect ratio, it is possible to indicate a minimum value of the induced drag with respect to the sweep-back angle for a given side force as shown in figure 16. The same procedure can be used to determine the minimum total resistance relative to sweep-back angle. For the considered lift coefficients, where values have been chosen near those of the optimum speeds-made-good, the minimum total resistance is mostly found at sweep-back angles of 40-50 degrees. It should be emphasized that for the determination of the optimum sweep-back angle on a basis of the minimum total resistance, also the leeway angle should be taken into consideration. The performance calculations in chapter 3 and figure 9 show that the variation in leeway is very small for sweep-back angles of up to 45 degrees which can be regarded favourably.

#### 6.2. Induced drag and lift for a given angle of leeway

Both for the upright and heeled condition, it is clear from the figures 12-15 that induced drag, as well as side force, is decreasing with sweep-back angle for a given angle of leeway. From this relation, it follows that side force production as well as induced drag may be expected to be maximum for a sweep-back angle of zero degree. The reduction of the side force production for a certain angle of leeway is both for the upright and heeled condition clearly shown in figure 3 and 4. It is surprising that for a sweep-back angle of 20 degrees a rather strong reduction of the side force production has been observed, which perhaps might be due to an unfavourable interference of the keel and hull wave.

#### 6.3. Sailing performance

With respect to the results of the performance calculations, it can be shown from figure 7 that the down-wind speed with the lower aspect ratio keel is almost equal for all sweep-back angles, while for the higher aspect ratio keel, the maximum sweep-back angle appears to be the most favourable.

This fact is due to the reduced upright resistance for this case as previously mentioned. The lower speed with the higher aspect ratio in comparison to the lower ratio, is of course caused by the higher frictional resistance due to the larger keel area. The results of the windward performance calculations are shown in figure 8. It is again clear, that the higher aspect ratio keels deliver lower speeds-made-good than the lower aspect ratio keels because of the higher frictional resistance.

Nevertheless, it is noteworthy that for moderate winds, the differences between the speed-made-good values obtained with both aspect ratios, are almost negligible as shown in figure 8 and 9.

This fact might denote that an increase of aspect ratio with equal keel area, within certain limits seems favourable for moderate winds ( $\pm 7$  m/sec).

For strong winds the high sweep-back angle seems to be advantageous, especially, for the higher aspect ratio keel. This gain in speed-made-good is also mainly due to the reduction of the upright resistance for the high sweep-back angle.

It should, however, be kept in mind that the leeway angle, which appears to increase rather significantly by about one degree for the maximum sweep-back angle (figure 9), is not accounted for sufficiently in the usual calculation procedure of the speed-made-good. In practice, it generally holds that the smaller leeway the more a vessel can be sailed close to windward.

#### 6.4. Calculation of the side force

The calculated values of the side force production for each angle of leeway agree very well with the measurements even for the heeling condition as shown in figure 3 and 4. The centre of effort shifts backwards in horizontal direction with the increase of the sweep-back angle and appears to be affected strongly by speed, heeling angle and aspect ratio. For this reason, these parameters are accounted for in the proposed correction. In the vertical direction, the centre of effort remains almost constant and is mainly dependent on the aspect ratio. The proposed correction for the vertical position of the centre of effort is related especially to the upright condition.

The measurements for the heeling condition show a rather large dispersion with again remarkably exceptional values for sweep-back angles of 20 degrees.

The proposed corrections have a preliminary character because they are, probably, related strongly to the hull form considered.

## 7. CONCLUSIONS

The upright resistance has proved to be almost independent of sweep-back angle for an aspect ratio of 0.94, while a reduction of about 5% is found for an aspect ratio of 1.20 at a sweep-back angle of 60 degrees. The tendency that induced drag increases with sweep-back for a given lift in the upright condition, was shown not to be valid under heel. This was caused by the significant influence of the interference of keel and hull wave dependence on sweep-back angle. This important surface influence should not be disregarded for keel design. Under heel, at optimum sailing conditions, the minimum total resistance has been observed at sweep-back angles of 40-50 degrees. Side force production and induced drag decrease with sweep-back if the same angle of leeway is considered. This holds true for both the upright and heeled condition. For 20 degrees sweep-back angle, a strong reduction in side force has been observed. Performance calculations show that leeway proves to be nearly constant with aspect ratio for all angles of sweep-back. An exceptional increase of about one degree has been found for a sweep-back angle of 60 degrees. The leeway angle should be accounted for more satisfactorily in the windward performance calculation. But neglecting this imperfection, the results of the usual windward performance calculation lead to high aspect ratio keels for moderate winds while highly swept back for strong winds. The centre of effort in a horizontal direction shifts backwards with sweep-back angle and is greatly dependent on speed, heeling angle and aspect ratio. The centre of effort in a vertical direction with aspect ratio is rather constant with the exception of 20 degrees sweep-back angle. In conclusion, calculated values according to the "equivalent keel" procedure appear to be in good agreement with the measurements for the side force, whereas the proposed calculation of the position of the centre of effort needs further investigation.

## 8. ACKNOWLEDGEMENT

The authors wish to acknowledge the contribution of Carl R. Witmer and Joel S. Mac. Minn, students at Webb Institute of Naval Architecture, who carried out the performance tests with the lower aspect ratio keels during their stay at Delft.

They are also indebted to A.v.Strien and R. Onnink of the Delft Shipbuilding Laboratory for their assistance in the experiments and analysis.

The authors are indebted to E.G. van de Stadt, who put the design of the "Spirit 28" at their disposal.

Furthermore, they are particularly grateful for numerous discussions with Prof.ir. J. Gerritsma and ir. G. Moeyes of the Delft Shipbuilding Laboratory, who stimulated the present project.

Finally special acknowledgements are made to P. de Heer for the lay-out and manufacture of the graphs and figures.



## 9. NOMENCLATURE

Symbol	description	unit
A	lateral area	m <sup>2</sup>
$A_T = b_{eK}c_K + b_{eR}c_R =$	total lateral area of effective keel and rudder	m <sup>2</sup>
$a_{eK} = b_{eK}/c_K =$	aspect ratio of effective keel i.e. keel extended to the test waterline	
$a_{eR} = b_{eR}/c_R =$	aspect ratio of effective rudder i.e. rudder extended to the test waterline	
$a_{gK} = b_{gK}/c_K =$	geometric aspect ratio of keel	
$a_{gR} = b_{gR}/c_R =$	geometric aspect ratio of rudder	
B	beam	
$b_{eK}$	span of effective keel i.e. keel extended to the test waterline	m
$b_{eR}$	span of effective rudder i.e. rudder extended to the test waterline	m
$b_{gK}$	span of keel from tip chord to root chord at the hull	m
$b_{gR}$	span of rudder until the hull	m
$C_{Di} = \frac{D_i}{\frac{1}{2}\rho V^2 A_T} =$	induced drag coefficient	
C.E.	centre of effort	
$C_L = \frac{L}{\frac{1}{2}\rho V^2 A_T} =$	lift coefficient	
$c_K$	chord of keel	m
$c_R$	chord of rudder	m
$D_i$	induced drag	kg
$F_H$	sail force	kg
$Fn = \frac{V}{\sqrt{gL_{TWE}}} =$	Froude number	
g	acceleration of gravity	m/sec <sup>2</sup>
H	hull as a subscript	
K	keel as a subscript	
L	ship length, lift	m, kg
$LCB_H$	position of centre of buoyancy of hull in length with respect to MWL	

Symbol	description	unit
$L_{OA}$	= length over all	m
$L_{TWL}$	= length on test waterline	m
MWL	= middle of test waterline	
R	= resistance; rudder as a subscript	kg
$R_T$	= total resistance for ship	kg
$R_{T^m}$	= total resistance for model	kg
$T^m$	= draught	m
$V=V_s$	= ship speed	m/sec
$V_D$	= speed down wind or speed in running condition	m/sec
$V_{MG}=V_s \cos(\beta+\beta_{TW})$	= speed-made-good to windward	m/sec
$V_m$	= model speed	m/sec
$V_{TW}$	= true wind speed	m/sec
$x_Y$	= horizontal distance of centre of effort from MWL (positive forward)	m
Y	= hydrodynamic side force	kg
$Y_\beta = \frac{Y}{\frac{1}{2}\rho V_{TW}^2 L_{TW}^2 \beta}$	= dimensionless side force per angle of leeway	
$z_Y$	= vertical distance of centre of effort from the waterline (positive upwards)	m
$\alpha$	= angle of incidence	degrees/radians
$\beta$	= angle of leeway	degrees/radians
$\beta_{TW}$	= angle between course and true wind	degrees
$\lambda$	= taper ratio	
$\phi$	= heeling angle	degrees
$\rho$	= mass density of fluid	kg sec <sup>2</sup> /m <sup>4</sup>
$\Lambda$	= sweep-back angle of quarter chord line	degrees

## 10. REFERENCES

- [1] de Saix, P.  
Yacht keels on experimental study  
Journal "Sail", May 1974
- [2] Herreshoff, H.C. and Kerwin, J.E.  
Sailing yacht keels  
3<sup>rd</sup> HISWA Symposium on Yachts  
Amsterdam, March 1973
- [3] Mac Lavery, K.  
Tests of a 5.5 meter yacht form with various fin sweep-back angles  
University of Southampton, SUYR rep. 17, 1966
- [4] Annual Report of the Advisory Committee for Yacht Research, 1967  
University of Southampton
- [5] Gerritsma, J.  
Course keeping qualities and motions in waves of a sailing yacht  
Proceedings of the third AIAA Symposium on the Aero-hydrodynamics  
of sailing, California 1971
- [6] Symposium onderzoek aan zeiljachten (in Dutch)  
Report no. 350, Shipbuilding Laboratory,  
University of Technology, Delft
- [7] Abbot, I.H. and Doenhoff von, A.E.  
Theory of wing sections  
Dover Book, 1959
- [8] Whicker, L.F. and Fehlner, L.F.  
Free stream characteristics of a family of low aspect ratio  
control surfaces  
DTMB Report 933, May 1958

## 11. LIST OF FIGURES.

- Figure 1 : Hull form and keel configuration.
- Figure 2a : Upright resistance  $a_g = 0.94$ .
- 2b : Upright resistance  $a_g = 1.20$ .
- Figure 3 : Side force production and centre of effort for the upright condition.
- Figure 4 : Side force production and centre of effort for the heeled condition.
- Figure 5 : Photographs of the wave pattern under heel with and without leeway for a sweep-back angle  $\Lambda = 0^\circ$ .
- Figure 6 : Photographs of the wave pattern under heel with and without leeway for a sweep-back angle  $\Lambda = 60^\circ$ .
- Figure 7 : Down-wind performance.
- Figure 8a : Windward performance.
- 8b : Speed-made-good versus sweep-back angle.
- Figure 9 : Leeway at optimum speed-made-good.
- Figure 10a, 10b : Induced drag- versus lift coefficient for the upright condition.
- Figure 11a, 11b, 11c : Induced drag- versus lift coefficient for the heeled condition.
- Figure 12a, 12b : Induced drag- and lift coefficient versus leeway for the upright condition.
- Figure 13 : Induced drag- and lift coefficient versus leeway for  $\phi = 10^\circ$ .
- Figure 14 : Induced drag- and lift coefficient versus leeway for  $\phi = 20^\circ$ .
- Figure 15 : Induced drag- and lift coefficient versus leeway for  $\phi = 30^\circ$ .
- Figure 16a, 16b, 16c : Induced drag and total resistance for a given side force.

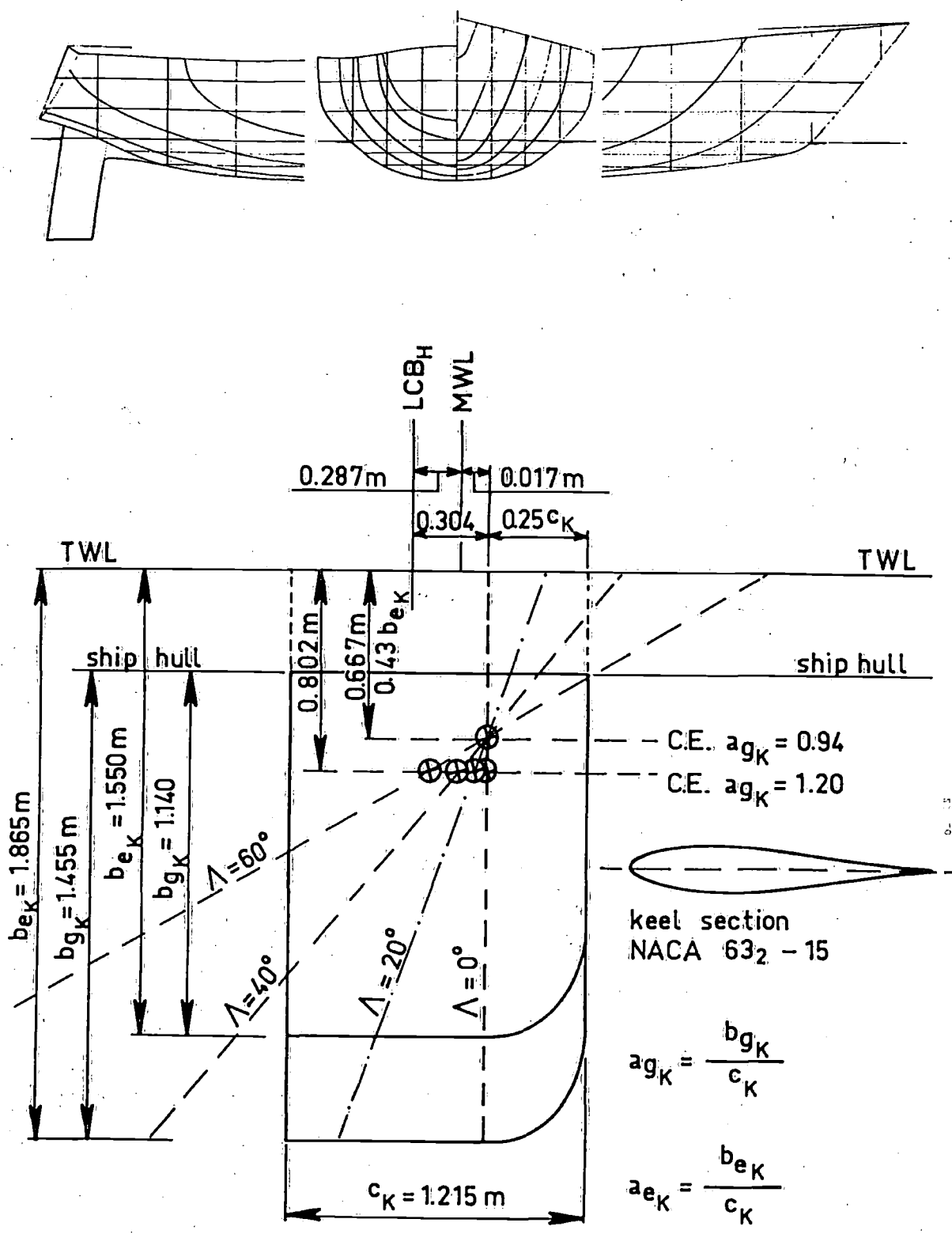


Fig.1: Hull form and keel configuration.

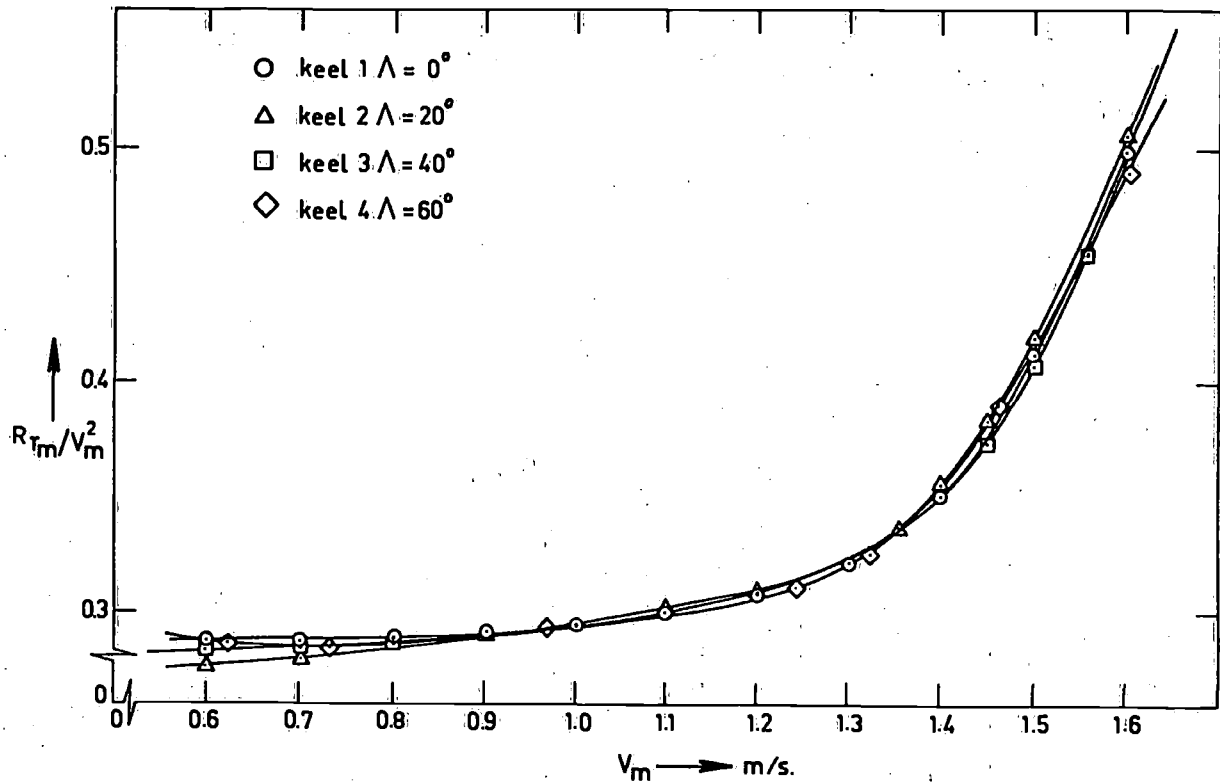


Fig.2a: Upright resistance.  $a_g = 0.94$ .

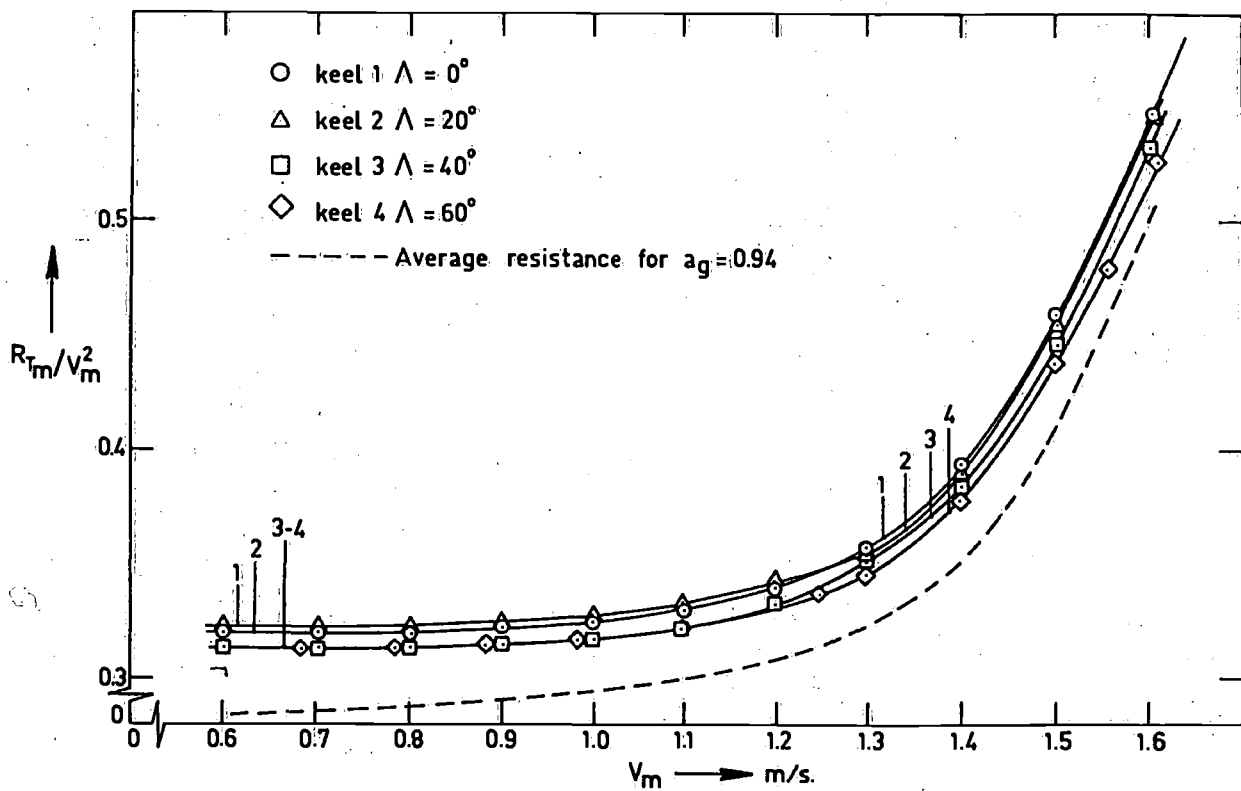


Fig.2b: Upright resistance.  $a_g = 1.20$

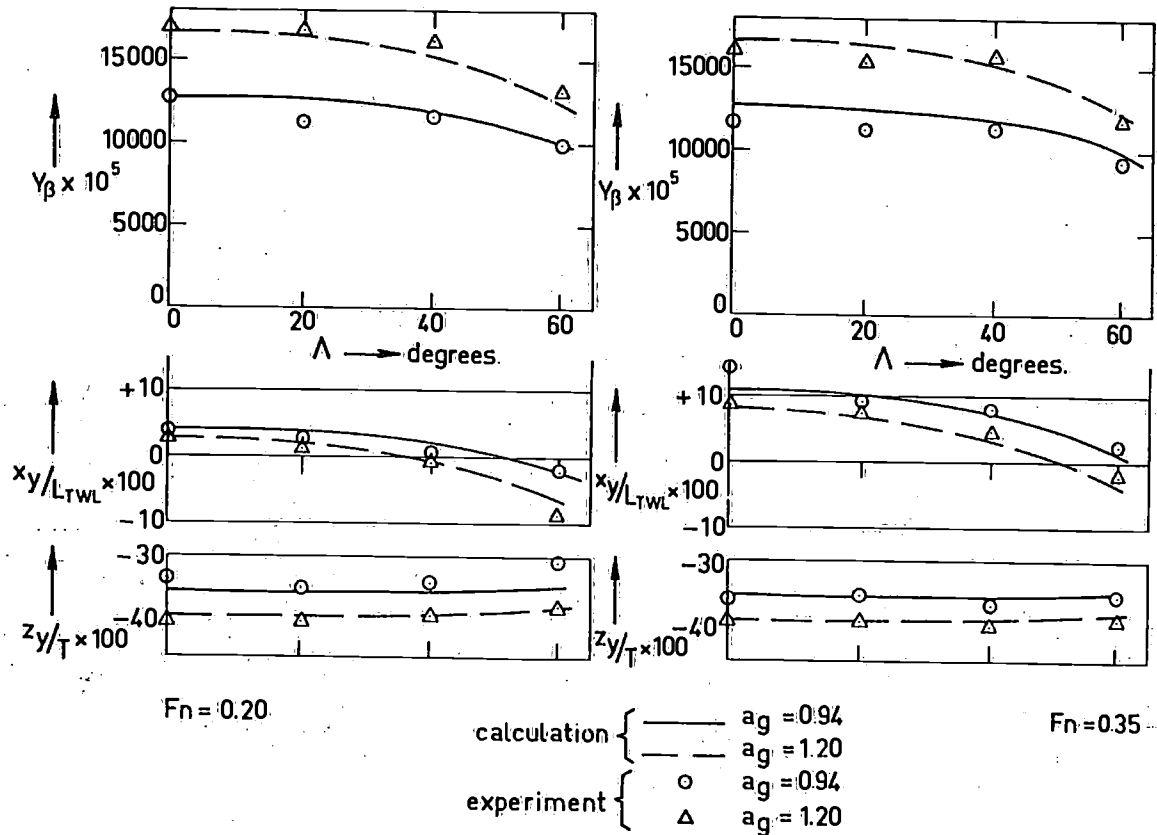


Fig.3: Side force production and centre of effort for the upright condition.

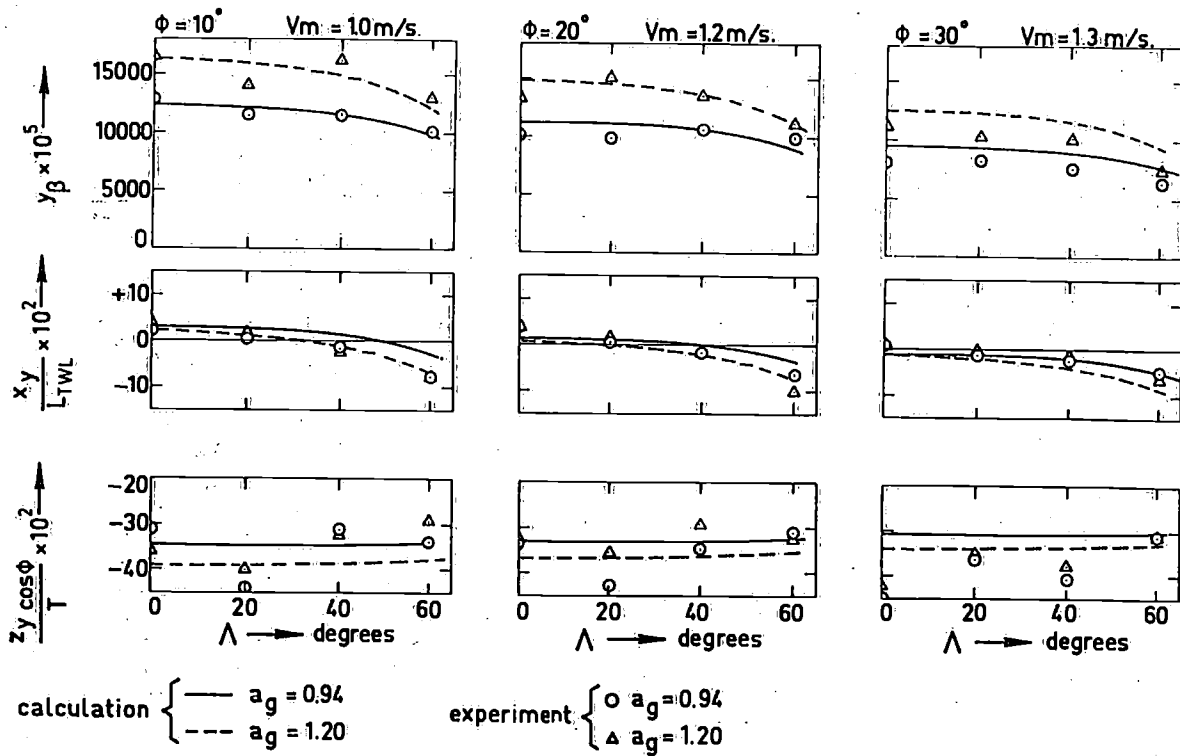


Fig.4: Side force production and centre of effort for the heeled condition.

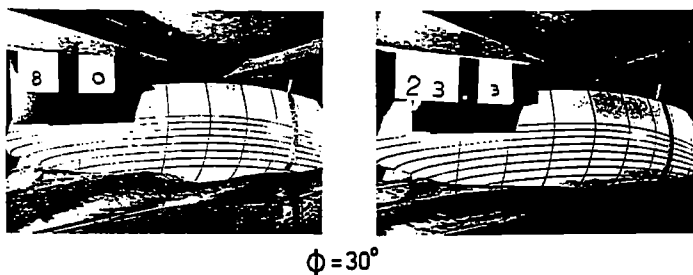
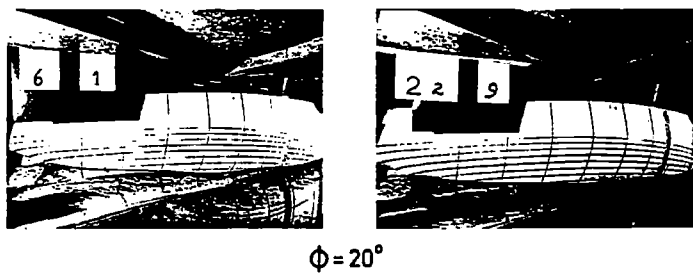
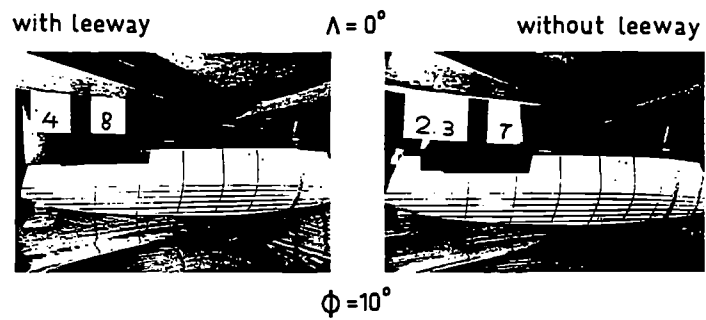


Fig.5: Photographs of the wave pattern under heel with and without leeway for a sweep-back angle  $\Lambda = 0^\circ$ .

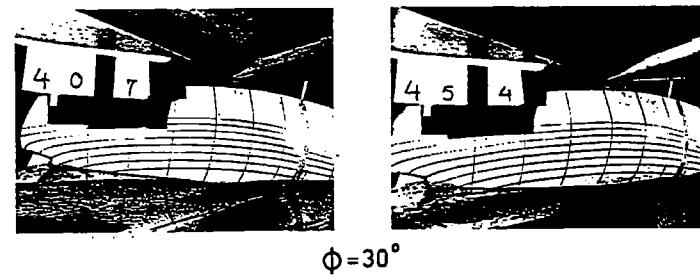
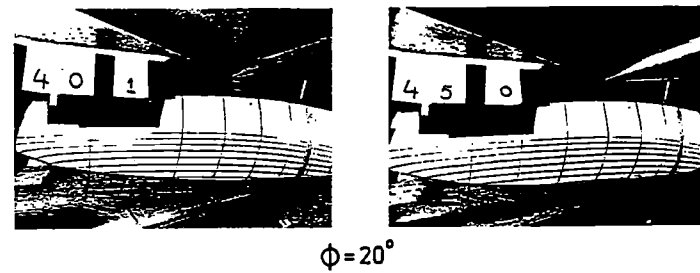
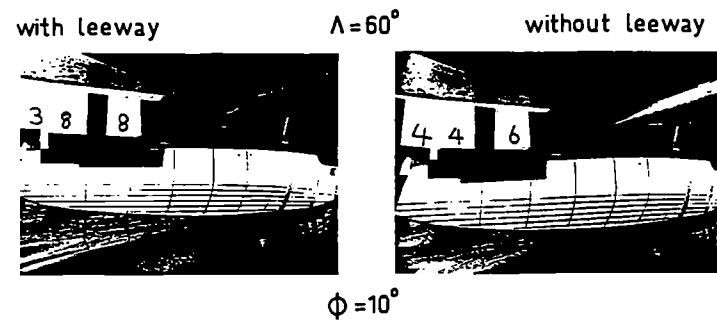


Fig.6: Photographs of the wave pattern under heel with and without leeway for a sweep-back angle  $\Lambda = 60^\circ$ .



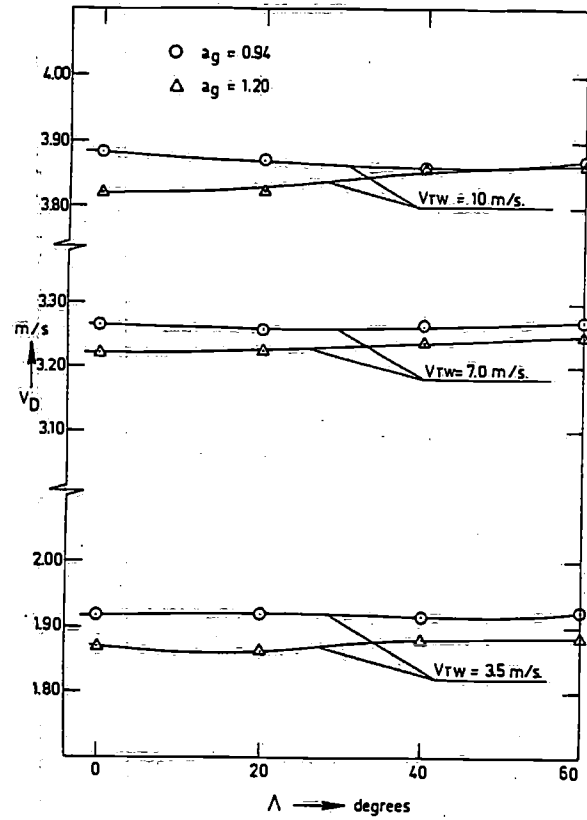


Fig. 7: Down-wind performance.

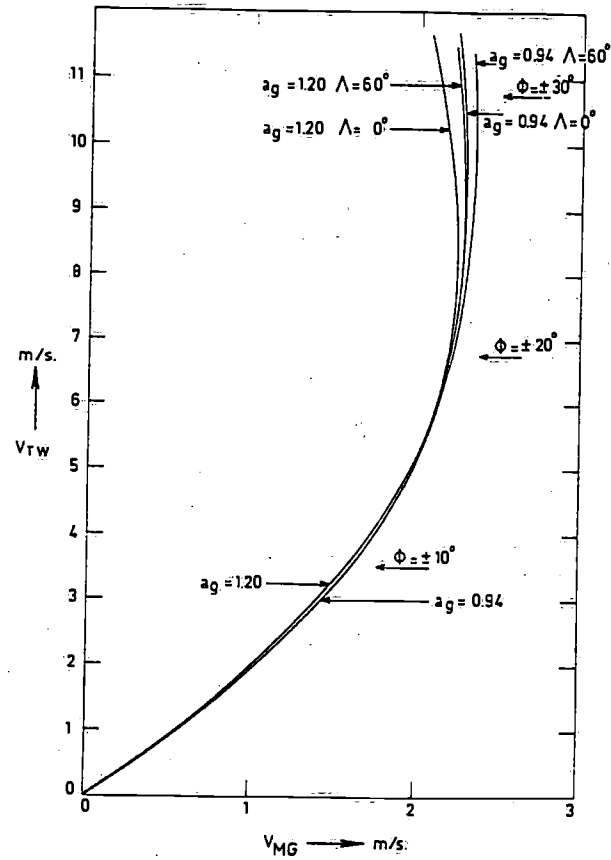


Fig. 8a: Windward performance.

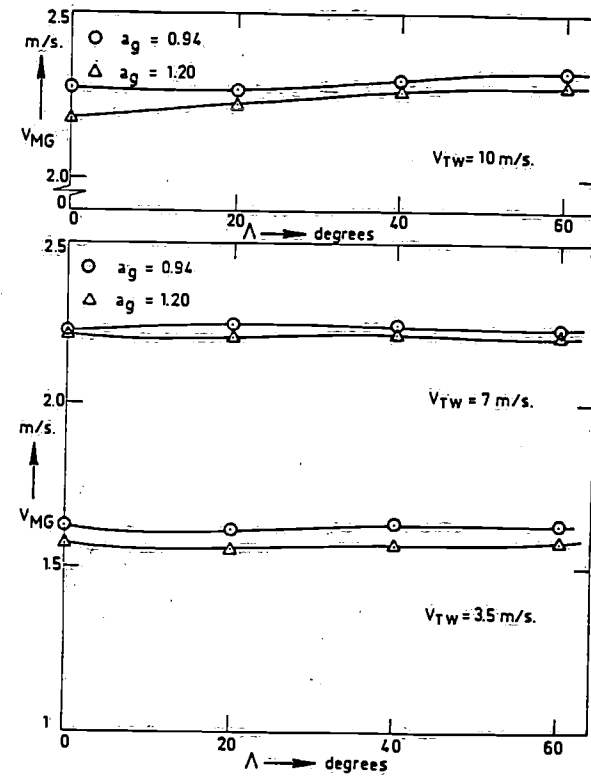


Fig. 8b: Speed-made-good versus sweep-back angle.

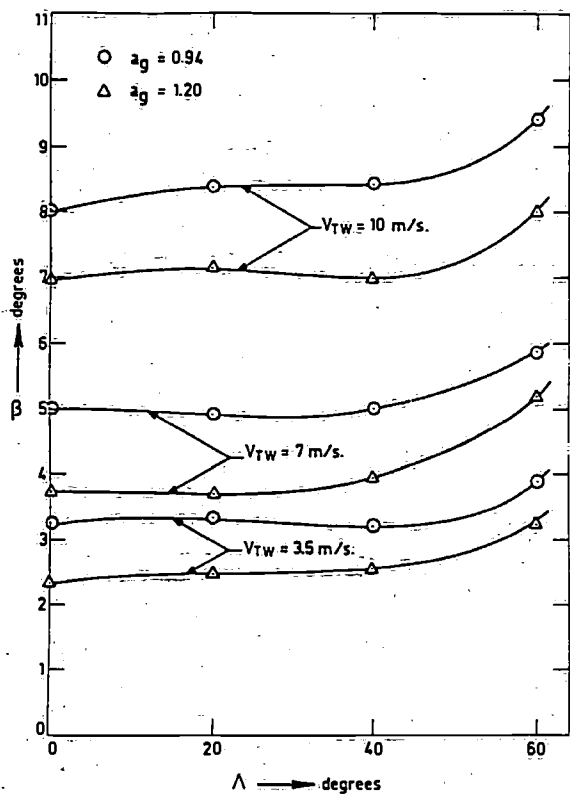


Fig. 9: Leeway at optimum speed-mâdè-good.

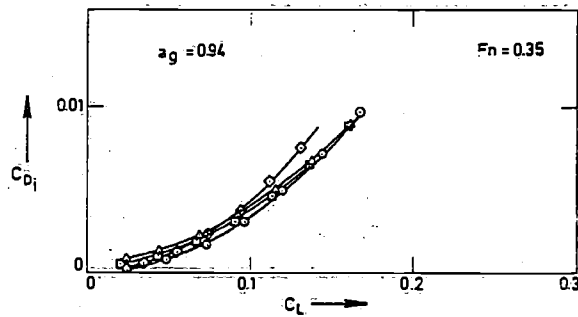
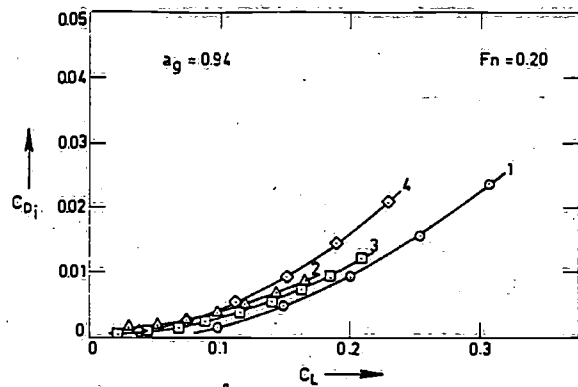


Fig.10a: Induced drag-versus lift coefficient for the upright condition.

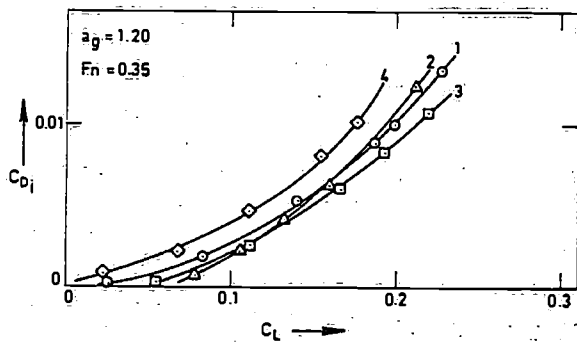
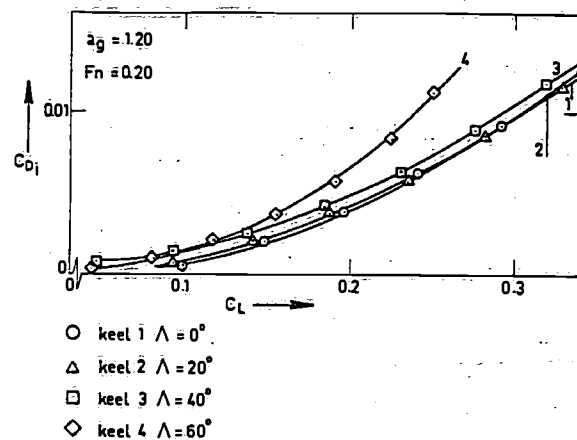


Fig.10b: Induced drag-versus lift coefficient for the upright condition.

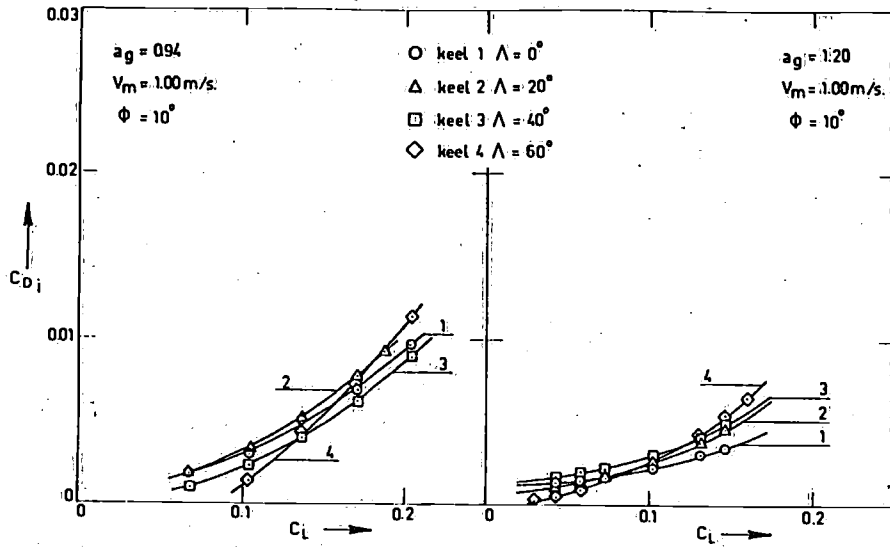


Fig.11a: Induced drag- versus lift coefficient for the heeled condition.

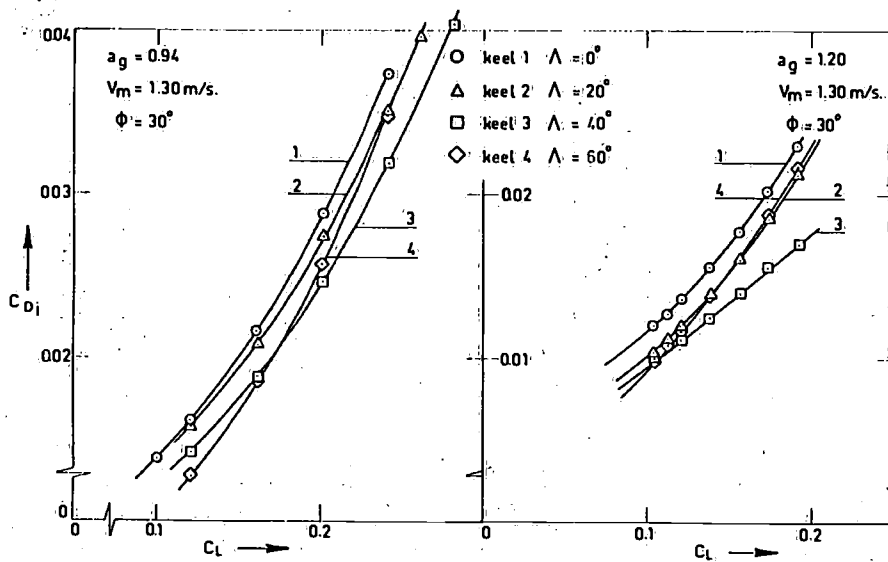


Fig.11c: Induced drag- versus lift coefficient for the heeled condition.

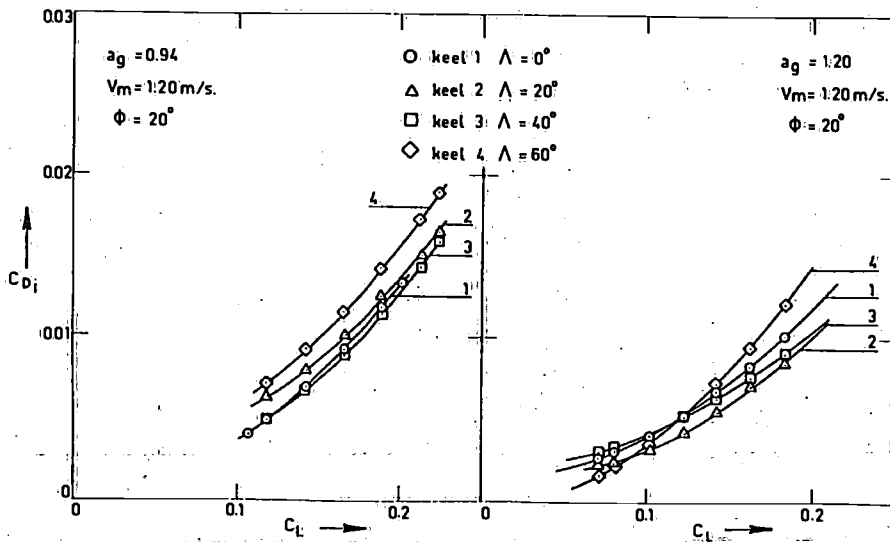


Fig.11b: Induced drag- versus lift coefficient for the heeled condition.

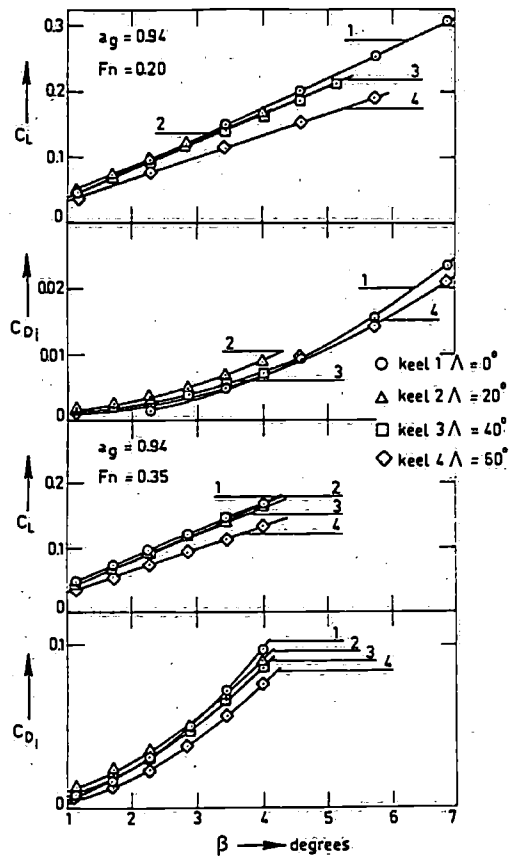


Fig. 12a: Induced drag and lift coefficient versus leeway for the upright condition.

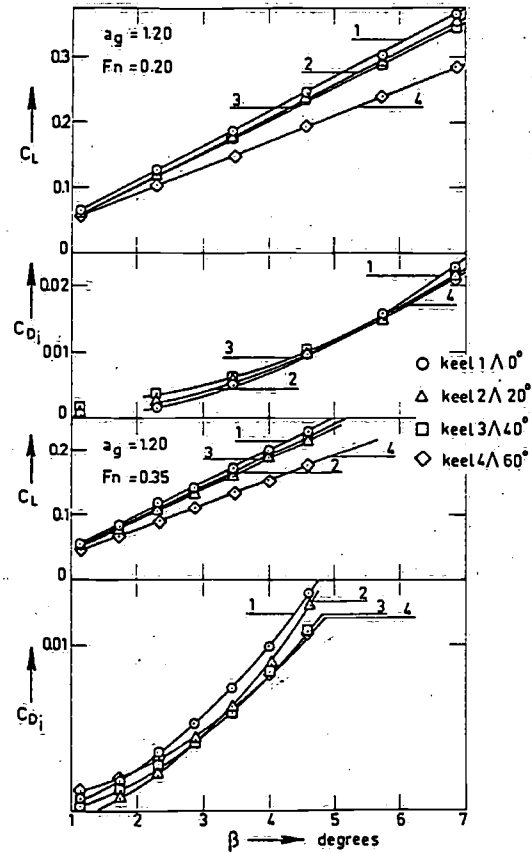


Fig. 12b: Induced drag and lift coefficient versus leeway for the upright condition.

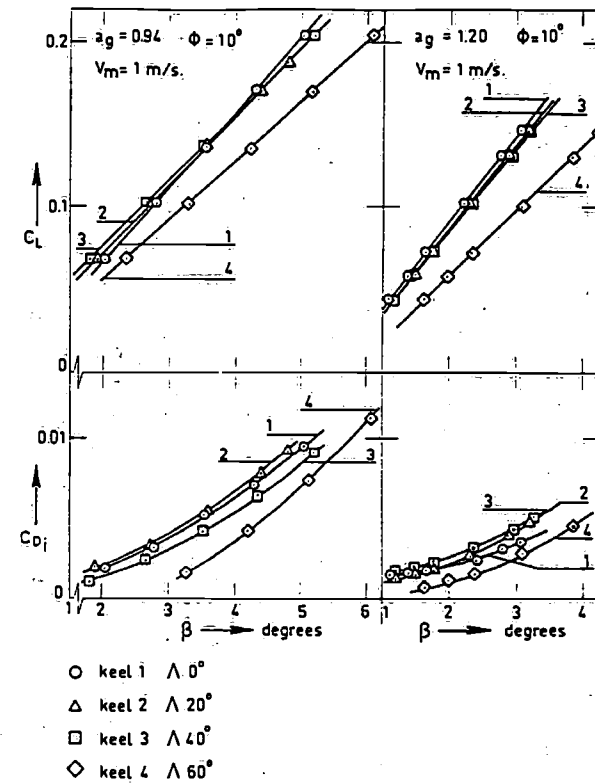


Fig. 13: Induced drag and lift coefficient versus leeway for  $\phi = 10^\circ$ .

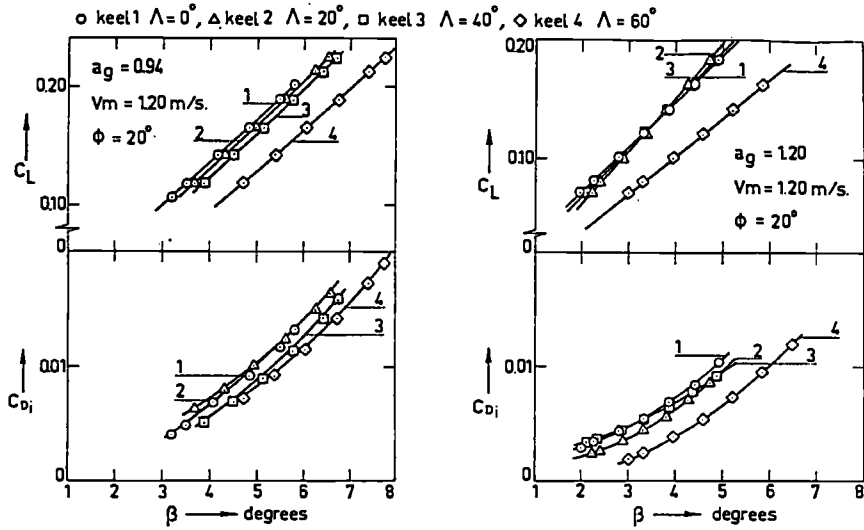


Fig.14: Induced drag - and liftcoefficient versus leeway for  $\phi = 20^\circ$ .

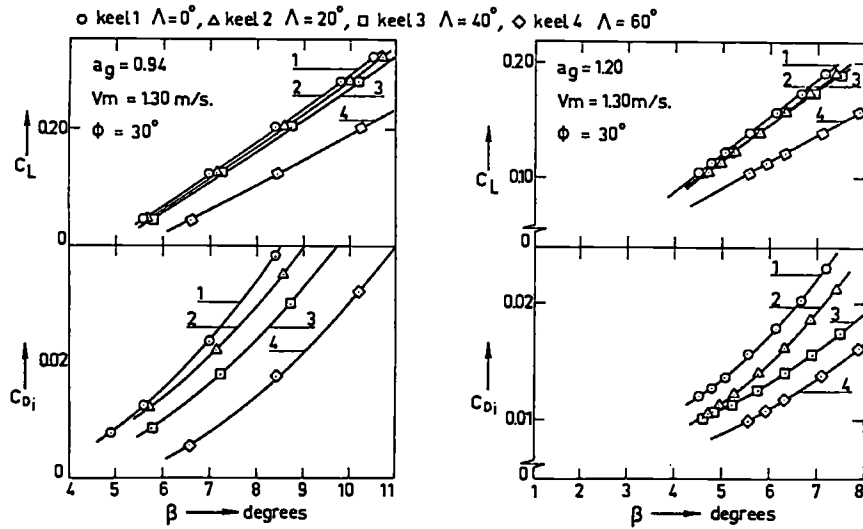


Fig.15: Induced drag - and liftcoefficient versus leeway for  $\phi = 30^\circ$ .

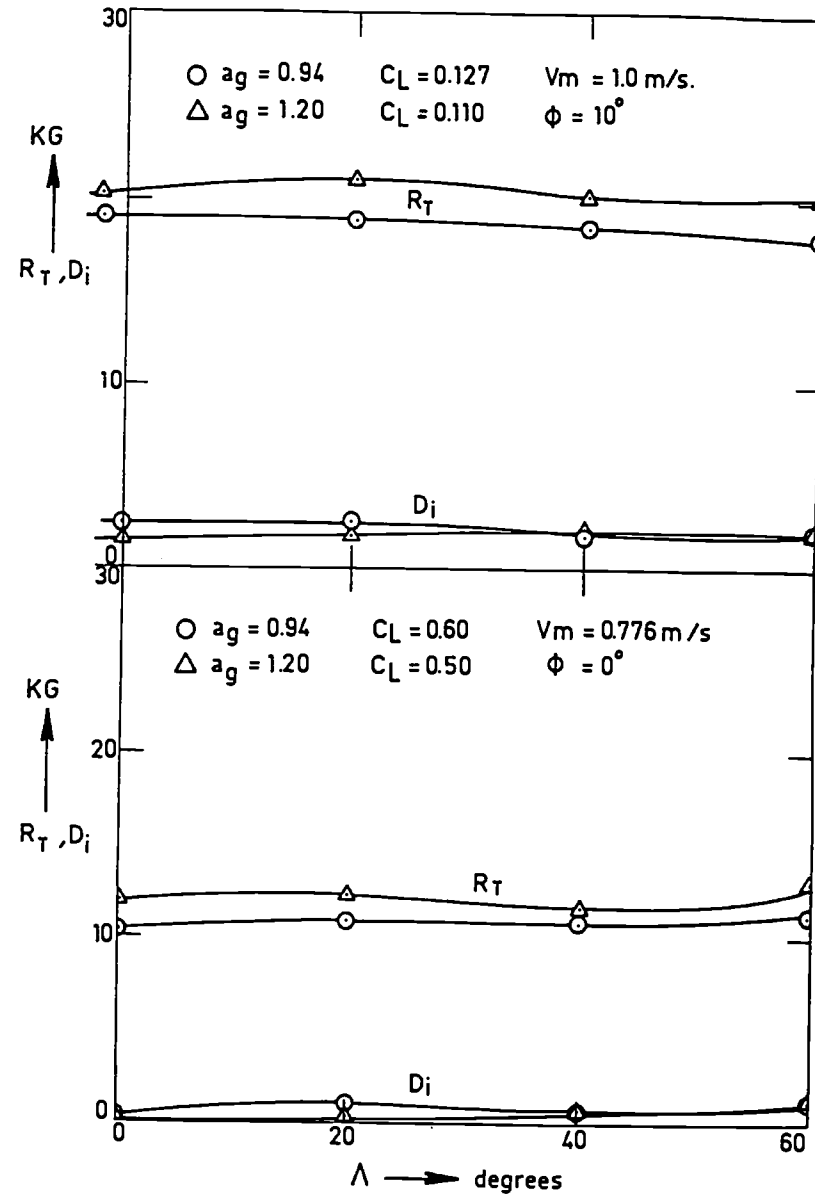


Fig.16a: Induced drag and total resistance for a given sideforce.

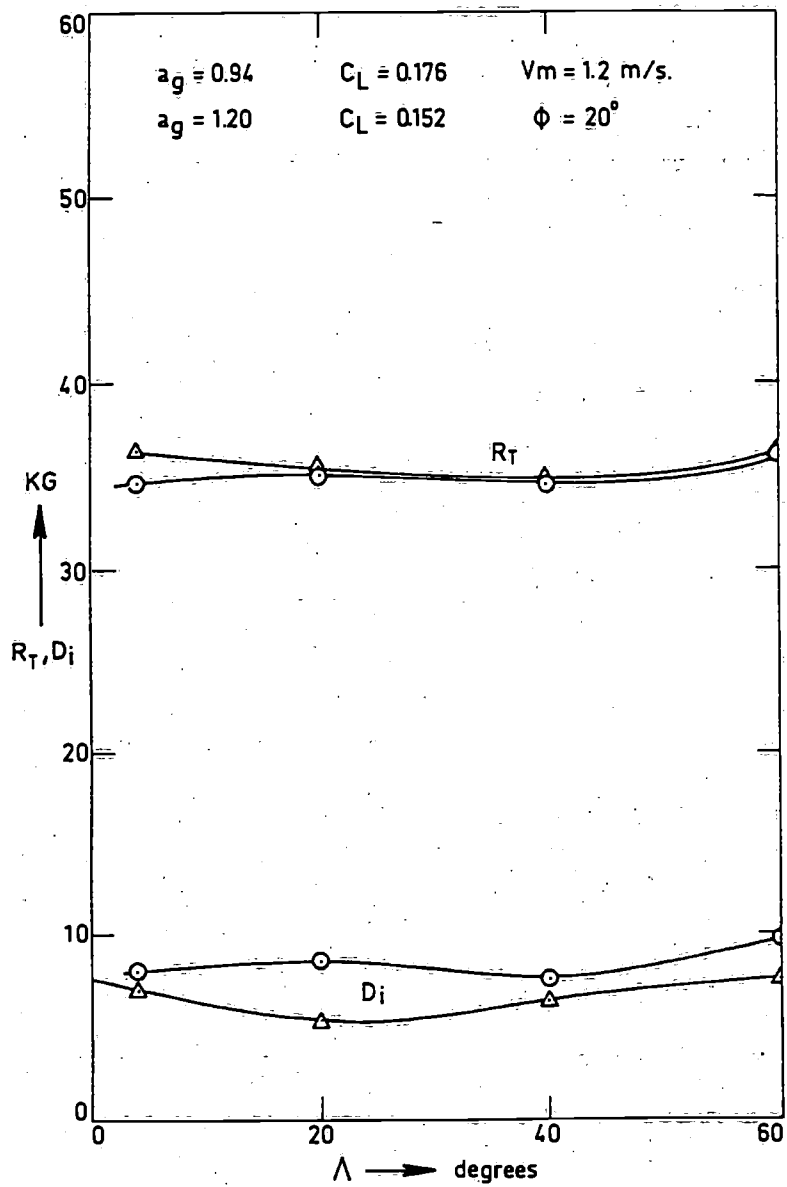


Fig.16b: Induced drag and total resistance for a given sideforce.

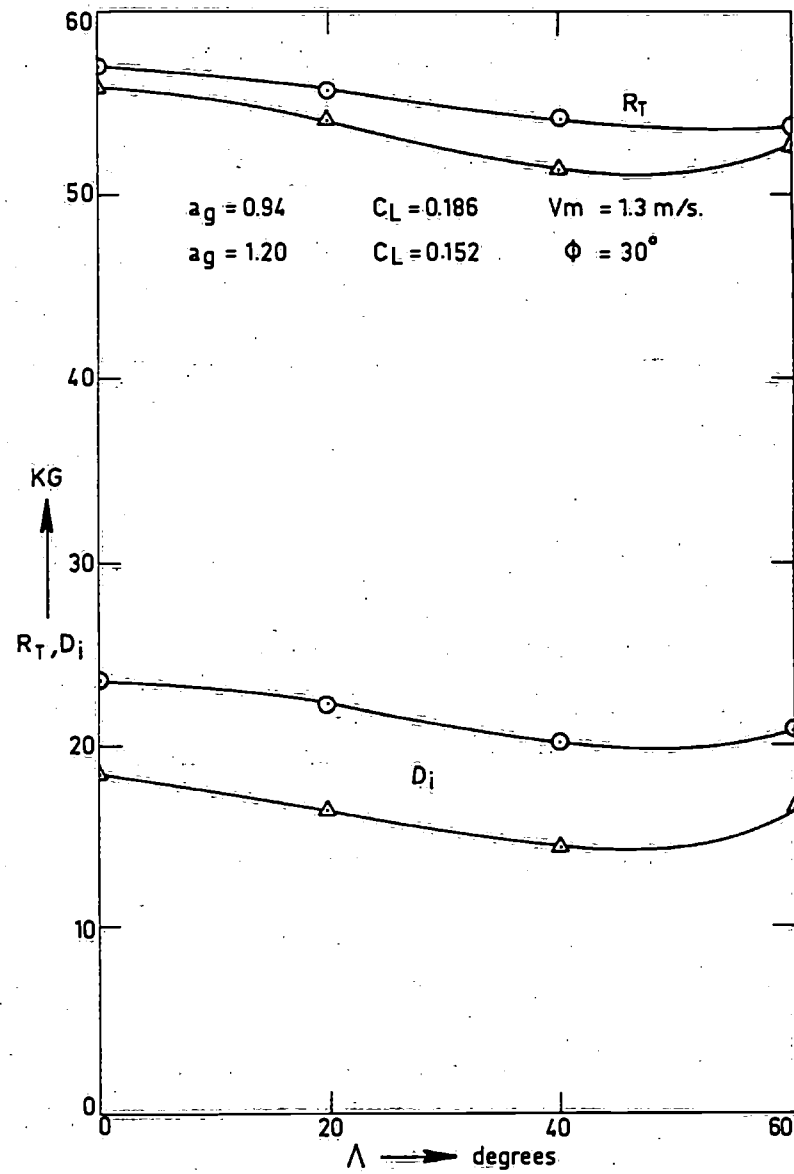
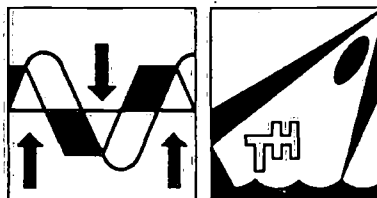


Fig.16c: Induced drag and total resistance for a given sideforce.

**TECHNISCHE HOGESCHOOL DELFT**  
**AFDELING DER SCHEEPSBOUW- EN SCHEEPVAARTKUNDE**  
**LABORATORIUM VOOR SCHEEPHYDROMECHANICA**

Rapport No. 443



**VARIATION OF PARAMETERS DETERMINING SEAKEEPING**

**W. Beukelman and A. Huijser**

**International Shipbuilding Progress, Volume 24**  
**July 1977, No.275.**

**Report No. 443**

**December 1976**

**Ship Hydromechanics Laboratory - Delft.**

**Delft University of Technology**  
**Ship Hydromechanics Laboratory**  
**Mekelweg 2**  
**Delft 2208**  
**Netherlands**

## VARIATION OF PARAMETERS DETERMINING SEAKEEPING

by

W. Beukelman and A. Huijser \*)

### Summary

With the computerprogram "Trial" calculations have been carried out to determine the seakeeping qualities in head waves of systematically varied shipforms.

These ships were derived from the well-known "Todd-60" series.

The following varied parameters show in succession of importance the influence on ship motions etc.: ship-length, speed, forebody section shape, block-coefficient, position of the centre of buoyancy in length, radius of inertia. Pitch especially decreases with ship-length, while heave increases with speed. For V-shaped forebodies the heaving motion is strongly reduced, while there is an advantage in added resistance up to a certain ship length, which depends on speed and sea-condition. Above this length a small profit for U-shaped sections has been established with respect to the added resistance in waves.

### 1. Introduction

The purpose of this investigation is to obtain data about the influence of the variation of different parameters on the behaviour of a ship in a seaway of pure head waves. This insight might be of interest for the designer in an early stage of the design. In former times mostly U-shaped sections were used, but at the present time the choice between U- or V-form sections becomes more and more of interest.

It is the intention to share in this question with respect to the seakeeping qualities of a ship.

The behaviour of a ship in a seaway is determined by:

1. the main ship dimensions, especially the length
2. the ship-speed
3. the ship-form
4. the weight distribution
5. the sea-condition.

Starting from a given seaway it is essential to investigate the influence of each of the mentioned parameters on the behaviour.

For restriction and simplification the influence of the main-dimensions, ship form and -speed is determined for one weight distribution only, while on the other hand the influence of the weight distribution has been investigated for one ship equal in form and main dimensions.

Generally the behaviour of a ship in a seaway may be distinguished in:

1. the ship motions inclusive vertical accelerations
2. the added resistance in waves combined with propulsion and eventually speed reduction
3. the relative motions with included deck wetness and slamming
4. the load of the ship construction.

The propulsion characteristics dependent on the sustained sea-speed for the investigated series of ships will be considered separately in the near future. In this treatise only head waves will be taken into account, while the load of the ship construction has not been taken into consideration. Therefore in this case the following characteristics will be determined:

1. the heaving and pitching motion
2. the added resistance in waves
3. the vertical acceleration at FPP
4. the relative motion at FPP
5. the probability of occurrence of slamming at FPP.

The computer-program "TRIAL" is suitable to calculate the above mentioned characteristics for the required ships and sea-conditions.

In the past several experiments have been carried out to investigate the influence of some of the parameters considered. Lewis [1] published in 1955 results of experiments with two models of the Series Sixty ( $C_B = 0.60$ ) having the same afterbody, while the forebody of the second model was changed into an extreme V-form. With regard to the motions the V-bow was preferred except for very short waves, while on the other hand with respect to the added resistance in waves U-shaped sections showed on advantage for waves smaller than 1.25 times the ship length.

More extended experiments with the Series Sixty ( $C_B = 0.60$ ) were carried out by Swaan and Vossers (1961) [2].

The main variation tested was the forebody section shape. Four models were tested inclusive the original Series Sixty model, which was considered to present U-shaped sections in the forebody. For the other models the section shape in the forebody had been varied until extreme V-form. It was concluded from

\*) Delft University of Technology, Ship Hydromechanics Laboratory, Delft, The Netherlands.



these experiments, that as regards motions, V-shaped sections are advantageous, especially in waves longer than the ship (i.e. for small ships). U-shaped sections, however, appeared to be more favourable as regards wetness, speed loss, bending moments and on some occasions slamming. For long ships, where no advantage was to be expected from using V-shaped sections, a moderate U-form was recommended.

Extended tests are carried out in regular head waves by Bengtsson [3] with four models having a block coefficient  $C_B = 0.675$  and with three models having a blockcoefficient  $C_B = 0.794$ . For each of these model-families the afterbodies were identical, while the forebody section varied from U- to V-form. It appeared that the motions for models with V-shaped forebodies showed minimum amplitudes in an idealized head irregular sea. With respect to resistance and propulsion the models with V-shaped forebody showed advantages in waves longer than the model. For shorter waves and still water the U-shaped sections proved to be more favourable in the model family with  $C_B = 0.794$ , while the trend for the family with  $C_B = 0.675$  was not clear in this respect.

Additional tests performed by Bengtsson [4] with three models ( $C_B = 0.675$ ) at ballast draught generally confirmed the results at the full load draught. Other experiments performed by Swaan [5] showed, that a reduction of motions in head waves can be achieved by a high length-draft ratio, while a low length-draft ratio should be more advantageous with respect to the power increase in waves. Experiments of Swaan and Rijken [6], related to the influence of the longitudinal weight distribution lead to the conclusion, that a decrease of the longitudinal moment of inertia has a favourable effect on the speed loss, but caused an increase of the vertical accelerations of the bow.

Theoretical calculations have been used by Ewing [7] to study the effect of speed, forebody shape, ship length and weight distribution on the ship motions for four models derived from the Series Sixty hull form with  $C_B = 0.70$ . It was concluded from this investigation, that smaller motions were obtained by V-shaped forebody sections, a decrease of the radius of gyration and by moving the LCG aft.

Yourkov varied in his study [8] the forebody sections of each of the Series Sixty models with blockcoefficients  $C_B = 0.60, 0.70$  and  $0.80$  from U- to V-shape. The models with V-shaped forebody appeared to have advantage in heave for all waves while pitch decreased in long waves and increased in short waves. The present study of the authors may be considered to be an extension of the work of Ewing [7] and Yourkov [8] by introducing more ship-form variables in the input and the added resistance in waves in the output.

Furthermore it is valuable to refer to the theoretical evaluation of the seakeeping performance in head waves of 72 hull forms from extended Series Sixty by Loukakis et al in [9]. These results are presented in tabular form as a function of the principal characteristics of the ship, Froude number and seaway.

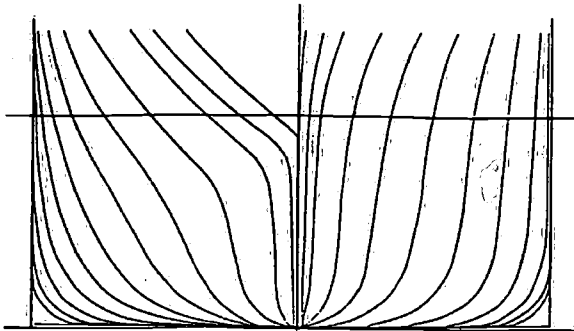
## 2. Shipform-family

To obtain the shipform family for the present investigation use has been made of the series of Yourkov [8]. This means that in principle for each model of the Series Sixty model with blockcoefficient  $C_B = 0.60, 0.70$  and  $0.80$  two forebody sections with UV- and V-form have been designed. The original models of the Series Sixty are considered to have U-shaped sections in the forebody. All nine models had the same length-beam ratio  $L/B = 7$ , length-draught ratio  $L/T = 17.5$  and the same midship-section coefficient  $C_M(\beta) = 0.976$ . For each blockcoefficient the afterbodies were identical as well as the sectional area curve for the whole model and the position of the centre of buoyancy in length (LCB). To obtain the different sectional shapes in the forebody the vertical prismatic coefficient had to be changed. To have a free choice in blockcoefficient, section shape, LCB and to obtain exchangeable fore- and afterbodies, it was necessary to change the midship section and the sections near the midship. The new midship section coefficient became now  $C_M = 0.9814$ . Moreover it was obligatory to add a new afterbody fuller than that of the blockcoefficient  $C_B = 0.80$  and to improve the original lines to be able to maintain for that model the right values of blockcoefficient and LCB.

Afterwards a new computerprogram has been written analog to a system as developed by Versluis [10] for the so called "Guldhammer Shipforms". With the aid of this program it was possible to interpolate between the four afterbody shipforms and the nine forebody shipforms, which were stored in the memory of the program. This interpolation took place on basis of the required blockcoefficient, LCB and sectional shape under the supposition, that the relation between the blockcoefficient of the fore- and afterbody was similar as that given by the "Combination-Diagram" of "Guldhammer" in [10].

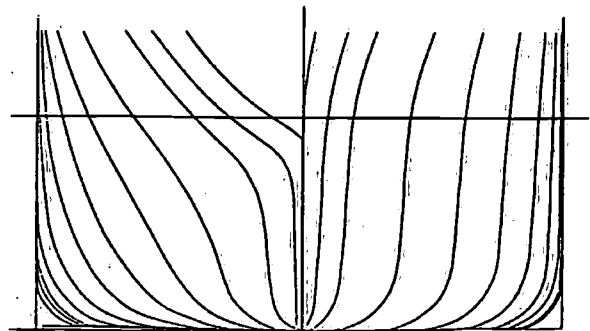
The output of the computer program delivered a body plan as shown in Figure 1 and Figure 2. One should of course keep in mind that for a variation of LCB a slight alteration of the fore- and aftership, according to the trend of respectively the required section shape and the original Series Sixty shape, was necessary.

Figure 1 shows the body plans for  $C_B = 0.60$  (LCB at 2% of L aft L/2) and for  $C_B = 0.70$  (LCB at L/2)



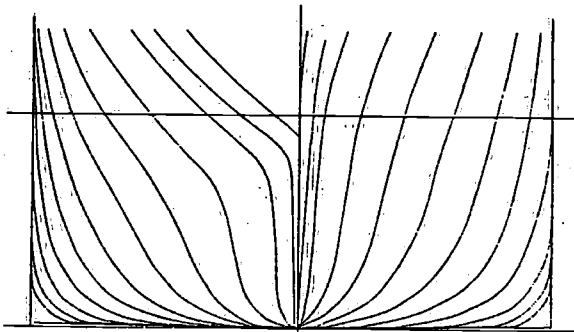
$C_B = 0.6000$   
 $C_{BA} = 0.6400$   
 $C_{BF} = 0.5600$   
 U - shaped sections  
 D1Q3X1 K2S2

$C_{WP} = 0.7047$   
 $C_{VP} = 0.8514$   
 LCB 2%L AFT L/2



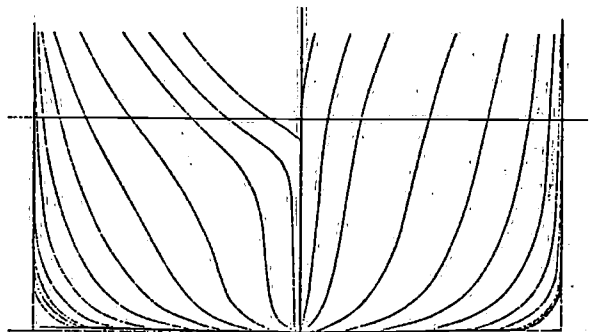
$C_B = 0.7000$   
 $C_{BA} = 0.6990$   
 $C_{BF} = 0.7010$   
 U - shaped sections  
 D2Q2X1 K2S2

$C_{WP} = 0.7848$   
 $C_{VP} = 0.8919$   
 LCB at L/2



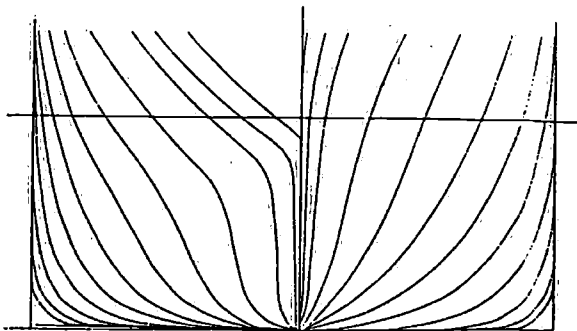
$C_B = 0.6000$   
 $C_{BA} = 0.6400$   
 $C_{BF} = 0.5600$   
 UV - shaped sections  
 D1Q3X2 K2S2

$C_{WP} = 0.7250$   
 $C_{VP} = 0.8276$   
 LCB 2%L AFT L/2



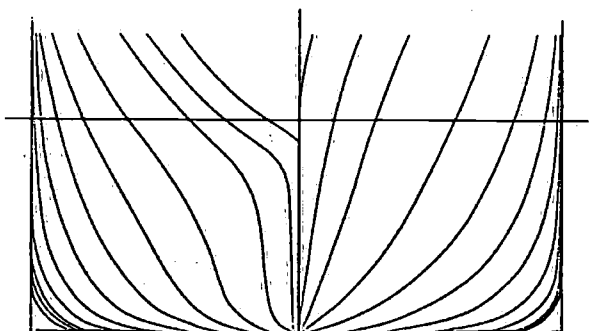
$C_B = 0.7000$   
 $C_{BA} = 0.6990$   
 $C_{BF} = 0.7010$   
 UV - shaped sections  
 D2Q2X2 K2S2

$C_{WP} = 0.8031$   
 $C_{VP} = 0.8716$   
 LCB at L/2



$C_B = 0.6000$   
 $C_{BA} = 0.6400$   
 $C_{BF} = 0.5600$   
 V - shaped sections  
 D1Q3X3 K2S2

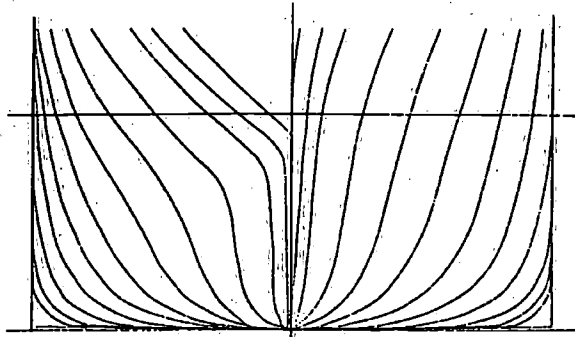
$C_{WP} = 0.7416$   
 $C_{VP} = 0.8091$   
 LCB 2%L AFT L/2



$C_B = 0.7000$   
 $C_{BA} = 0.6990$   
 $C_{BF} = 0.7010$   
 V - shaped sections  
 D2Q2X3 K2S2

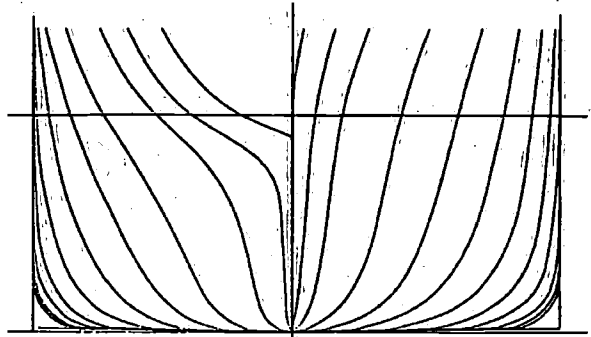
$C_{WP} = 0.8215$   
 $C_{VP} = 0.8521$   
 LCB at L/2

Figure 1. Body plans for  $C_B = 0.60$  and  $0.70$  for different forebody sections.



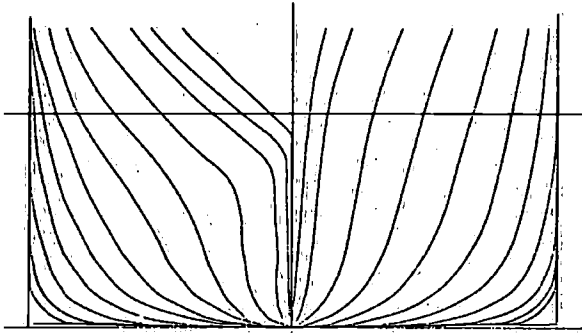
$C_B = 0.6000$   
 $C_{BA} = 0.6180$   
 $C_{BF} = 0.5820$   
 UV-shaped sections  
 D1Q1X2 K2S2

$C_{WP} = 0.7278$   
 $C_{VP} = 0.8244$   
 LCB 1%L AFT L/2



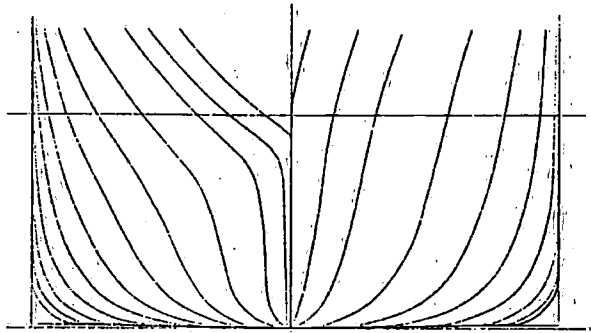
$C_B = 0.7000$   
 $C_{BA} = 0.7410$   
 $C_{BF} = 0.6590$   
 UV-shaped sections  
 D2Q1X2 K2S2

$C_{WP} = 0.8033$   
 $C_{VP} = 0.8714$   
 LCB 2%L AFT L/2



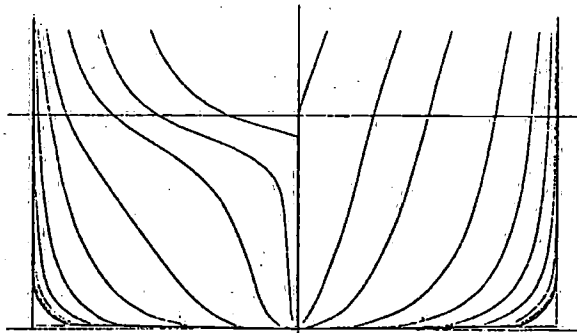
$C_B = 0.6000$   
 $C_{BA} = 0.5975$   
 $C_{BF} = 0.6025$   
 UV-shaped sections  
 D1Q2X2 K2S2

$C_{WP} = 0.7305$   
 $C_{VP} = 0.8214$   
 LCB at L/2



$C_B = 0.7000$   
 $C_{BA} = 0.6550$   
 $C_{BF} = 0.7450$   
 UV-shaped sections  
 D2Q3X2 K2S2

$C_{WP} = 0.8093$   
 $C_{VP} = 0.8649$   
 LCB 2%L BEFORE L/2



$C_B = 0.8000$   
 $C_{BA} = 0.7995$   
 $C_{BF} = 0.8005$   
 UV-shaped sections  
 D3Q2X2 K2S2

$C_{WP} = 0.8923$   
 $C_{VP} = 0.8965$   
 LCB at L/2

Figure 2. Body plans for  $C_B = 0.60, 0.70$  and  $0.80$  with different positions of LCB.

Table 1

Name of parameter	value of parameter	code-number
Blockcoefficient	$C_B = 0.60$	D1
	$C_B = 0.70$	D2
	$C_B = 0.80$	D3
Longitudinal position of centre of buoyancy LCB	LCB at 2% L aft L/2 ( $C_B = 0.70$ ) ( $C_B = 0.60$ )	Q1
	LCB at L/2 ( $C_B = 0.70$ ) ( $C_B = 0.80$ ) ( $C_B = 0.60$ )	Q2
	LCB at 2% L before L/2 ( $C_B = 0.70$ ) LCB at 1% L aft L/2 ( $C_B = 0.60$ )	Q3
Forebody section shape	U-shape	X1
	UV-shape	X2
	V-shape	X3

with the different forebody section shapes. The influence of the displacement of the centre of buoyancy in length has been shown in Figure 2 for  $C_B = 0.60$  and  $0.70$ , while moreover the bodyplan for  $C_B = 0.80$  has been presented in this figure.

### 3. Parameter-variation scheme

It was not useful to calculate the seakeeping behaviour of all ships as designed in the preceding chapter. Such a choice had to be made, that the influence of the principal variation on the behaviour could be clearly shown. As said before the following constant factors will be maintained within the shipform family:

1. the midship section coefficient
2. the length-beam ratio  $L/B = 7$
3. the length-draught ratio  $L/T = 17.50$ .

The form-parameters to be varied are:

1. the blockcoefficient  $C_B$
2. the longitudinal position of the centre of buoyancy, LCB
3. the forebody section shape.

In Table 1 the proposed variation of each of the above mentioned form parameters is shown together with the used code-number.

The position of LCB for  $C_B = 0.60$  which for the Series Sixty is normal at 1.5% L aft L/2, could only reasonably be varied from 1 to 2% aft L/2. For one case the position of LCB at L/2 has been considered, although the section shapes are not smooth.

This irregular shape is due to extrapolation out of the field of the basic ship forms. For this reason it has not been taken into consideration furthermore.

The variation in the position of LCB for  $C_B = 0.70$  is rather wide, especially the aft one.

It was decided to restrict the number of ships as indicated in the added scheme.

Variation scheme of form-parameter

	X1 (U)	X2 (UV)	X3 (V)	
D1	hatched	hatched	hatched	Q1
	hatched	hatched	hatched	Q2
	hatched	hatched	hatched	Q3
D2	hatched	hatched	hatched	Q1
	hatched	hatched	hatched	Q2
	hatched	hatched	hatched	Q3
D3	hatched	hatched	hatched	Q1
	hatched	hatched	hatched	Q2
	hatched	hatched	hatched	Q3

The values of the different geometrical coefficients including the relation vertical prismatic coefficient and forebody section shape as denoted in the variation scheme of form-parameter, are presented in Table 2.

From the scheme of the variation of the form-parameter, it is clear, that special attention has been paid to block coefficient  $C_B = 0.60$  and  $0.70$ . The behaviour of a ship in a seaway is also determined by the main-dimensions. The ratio of ship length-main dimension will be maintained and so the length may be considered to be a scale factor. The ship-length has proved to be one of the most important parameters with respect to seakeeping behaviour. Four ship-length's will be considered. This has been shown in Table 3, which may be seen as a proposed variation of

Table 2

forebody section shape	$C_B$ ( $\delta$ )	$C_{BA}$ ( $\delta_A$ )	$C_{BF}$ ( $\delta_F$ )	$C_{WP}$ ( $\alpha$ )	LCB	$C_{VP}$ ( $x$ )
U	0.6000	0.6400	0.5600	0.7047	2% L aft L/2	0.8514
	-	-	-	-	-	-
	0.6000	0.6180	0.5820	0.7079	1% L aft L/2	0.8477
	-	-	-	-	-	-
	0.7000	0.6990	0.7010	0.7848	at L/2	0.8919
	-	-	-	-	-	-
	-	-	-	-	-	-
UV	0.6000	0.6400	0.5600	0.7250	2% L aft L/2	0.8267
	0.6000	0.5975	0.6025	0.7305	at L/2	0.8214
	0.6000	0.6180	0.5820	0.7278	1% L aft L/2	0.8244
	0.7000	0.7410	0.6590	0.8033	2% L aft L/2	0.8714
	0.7000	0.6990	0.7010	0.8031	at L/2	0.8716
	0.7000	0.6550	0.7450	0.8093	2% L before L/2	0.8649
	-	-	-	-	-	-
0.8000	0.7995	0.8005	0.8923	at L/2	0.8965	
V	0.6000	0.6400	0.5600	0.7416	2% L aft L/2	0.8091
	-	-	-	-	-	-
	0.6000	0.6180	0.5820	0.7447	1% L aft L/2	0.8057
	-	-	-	-	-	-
	0.7000	0.6990	0.7010	0.8215	at L/2	0.8521
	-	-	-	-	-	-
	-	-	-	-	-	-

Table 3  
Variation of scale-parameter

name of parameter	value of parameter	code-number
Length between perpendiculars L	L = 60 m	L1
	L = 120 m	L2
	L = 200 m	L3
	L = 300 m	L4

the scale-parameter together with the related code-numbers.

Variation of ship-length as proposed for all ship-designs was too extensive. New restrictions have been made as denoted in the next parameter-variation scheme together again with the used code-numbers.

It is clear from the parameter variation scheme, that a ship-length of 200 m is chosen as a "central-length".

Parameter variation scheme

	X1(U)	X2(UV)	X3(V)	
D1	/	/	/	Q1
	/	/	/	Q2
	/	/	/	Q3
D2	/	/	/	Q1
	/	/	/	Q2
	/	/	/	Q3
D3	/	/	/	Q1
	/	/	/	Q2
	/	/	/	Q3

This length may also be seen as a critical length while in fully developed seas waves with a length of about 200 m contain the highest energy and therefore the highest amplitude. The "central ship" has been considered to be a ship with a length of 200 m, a blockcoefficient  $C_B = 0.70$ , LCB at midship and is denoted in code-number as: D2Q2X2L3.

The form of the 40 ships as chosen according to the parameter variation scheme has been determined with the computer-program called "Variation Ship-forms". For the most principal shipforms the variation of section shape and the position of the centre of buoyancy in length has been shown in Figure 1 and Figure 2.

As said before in the introduction the seakeeping behaviour is also determined by the weight distribution. The "central" value for the longitudinal radius of inertia is supposed to be  $k_{yy} = 0.25L$ . A variation of the longitudinal radius of inertia has been carried out for the "central-ship" (D2Q2X2L3) only and is denoted in Table 4 together with the code-numbers.

Table 4  
Variation of longitudinal radius of inertia

name of parameter	value of parameter	code-number
Longitudinal radius of inertia $k_{yy}$	$k_{yy} = 0.23 L$	K1
	$k_{yy} = 0.25 L$	K2
	$k_{yy} = 0.27 L$	K3

Table 5  
Variation of sea-condition

name of parameter	value of parameter			code-number	
	Sea-state no.	5	7		9
wave period (sec)	$\tilde{H}_{1/3}$	2.15	2.76	4.85	
cond. 1 $\tilde{T}_1$		5.85	7.02	8.10	S1
cond. 2 $\tilde{T}_2$		6.50	7.80	9.00	S2
cond. 3 $\tilde{T}_3$		7.15	8.58	9.90	S3

Another parameter determining the behaviour of a ship in a sea-way is the sea-condition.

As a "central"-value for the seaway is chosen the average sea-condition in block 6 of the North Atlantic during the month December-February with a relation between significant wave-height ( $\tilde{H}_{1/3}$ ) and average wave-period ( $\tilde{T}$ ) depending on windforce according to the data of Hogben and Lumb [11]. For the distribution of the wave-energy over the wave-frequencies the wave-spectrum according to Pierson-Moskovitz is chosen (ITTC, 1969). A deviation from the average wave-period of 10% up and down has been taken for the variation of the sea-condition. The significant wave-height was kept constant then. The variation of the sea-condition, which has been carried out for the "central-ship" only, is reflected in Table 5.

The "central-ship" may be denoted by the code-number as: D2Q2X2L3K2S2.

The probability of the occurrence of the sea-states as mentioned in Table 5 has been shown in Table 6.

For each ship the behaviour in a seaway is calculated for the following three speeds viz.:

$$Fn = 0.15, 0.20, 0.25.$$

The total number of cases to be computed with program "TRIAL" is now 44. A review of the different variations has been given below (the varied parameters are underlined>:

Table 6  
Probability of the occurrence of sea-states

Windforce			probability of occurrence
sea-state (Beaufort)	windspeeds at 10 m above surface (for landstation)		North Atlantic Block 6 Dec.-Febr.
scale	knots	m/sec.	%
5	17-21	8.0 - 10.7	32.5
7	28-33	13.9 - 17.1	23.5
9	41-47	20.8 - 24.4	5.5

Variation of forebody section shape and length

$C_B = 0.60$		
D1Q1X1L1K2S2	D1Q1X2L1K2S2	D1Q1X3L1K2S2
D1Q1X1L2K2S2	D1Q1X2L2K2S2	D1Q1X3L2K2S2
D1Q1X1L3K2S2	D1Q1X2L3K2S2	D1Q1X3L3K2S2
D1Q1X1L4K2S2	D1Q1X2L4K2S2	D1Q1X3L4K2S2
D1Q2X1L1K2S2	D1Q2X2L1K2S2	D1Q2X3L1K2S2
D1Q2X1L2K2S2	D1Q2X2L2K2S2	D1Q2X3L2K2S2
D1Q2X1L3K2S2	D1Q2X2L3K2S2	D1Q2X3L3K2S2
D1Q2X1L4K2S2	D1Q2X2L4K2S2	D1Q2X3L4K2S2
$C_B = 0.70$		
D2Q2X1L1K2S2	D2Q2X2L1K2S2	D2Q2X3L1K2S2
D2Q2X1L2K2S2	D2Q2X2L2K2S2	D2Q2X3L2K2S2
D2Q2X1L3K2S2	D2Q2X2L3K2S2	D2Q2X3L3K2S2
D2Q2X1L4K2S2	D2Q2X2L4K2S2	D2Q2X3L4K2S2

Variation of LCB

$C_B = 0.60$	$C_B = 0.70$
D1Q1X2L3K2S2	D2Q1X2L3K2S2
D1Q2X2L3K2S2	D2Q2X2L3K2S2
D1Q3X2L3K2S2	D2Q3X2L3K2S2

Variation of blockcoefficient

D1Q2X2L3K2S2
D2Q2X2L3K2S2
D3Q2X2L3K2S2

Variation of longitudinal radius of inertia

D2Q2X2L3K1S2
D2Q2X2L3K2S2
D2Q2X2L3K3S2

Variation of seacondition

D2Q2X2L3K2S1
D2Q2X2L3K2S2
D2Q2X2L3K2S3

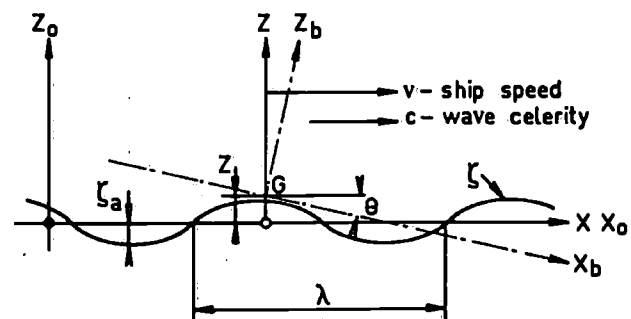
4. Calculations

All calculations for seakeeping have been carried out with the aid of the computerprogram "TRIAL" of the Ship Hydromechanics Laboratory of the Delft University of Technology, of which an earlier version has been described in [12]. With the program "TRIAL" it is possible to calculate vertical motions (heave and pitch), relative motions, vertical accelerations, shearing forces, bending moments and added resistance in head waves.

The calculations of the ship motions are based on the linear strip theory of Korvin-Kroukovsky as modified by Gerritsma and Beukelman in [13].

For all sections use has been made of the Lewis-transformation to determine sectional added mass and damping. Three right hand coordinate systems are used throughout all calculations in the program, from which the first one ( $x_o, y_o, z_o$ ) is fixed in space, the second ( $x_b, y_b, z_b$ ) and third system ( $x, y, z$ ) are moving along with the ship, while the third system ( $x, y, z$ ) has the x-axis in the same direction as the first system ( $x_o, y_o, z_o$ ).

The origin of the second and third coordinate system is situated in length at the centre of buoyancy. The positive x-axis is in the direction of the bow and the positive z-axis is pointing upwards. This is shown in Figure 3.



wave -  $\zeta = \zeta_a \cos(kx_o \cos \mu - \omega t)$  in  $x_o, y_o, z_o$   
 $\zeta = \zeta_a \cos(\omega_e t)$  in  $x, y, z, x=0$   
 heave -  $z = z_a \cos(\omega_e t + \epsilon_z \zeta)$   
 pitch -  $\theta = \theta_a \cos(\omega_e t + \epsilon_\theta \zeta)$   
 $\omega_e = \omega - \frac{\omega^2}{g} v \cos \mu$

Figure 3. Symbols and definitions.

4.1. Regular waves

The wave elevation with respect to the coordinate system fixed in space is given as:

$\zeta = \zeta_a \cos(kx_o + \omega t)$  (1)

in which:

- $\xi_a$  = wave amplitude  
 $k = 2\pi/\lambda = \omega^2/g$  = wave number  
 $\lambda$  = wave length  
 $g$  = acceleration of gravity  
 $\omega$  = circular wave frequency.

For the calculation of the heaving and pitching motions the following well known equations are used:

$$(a + \rho \nabla) \ddot{z} + b \dot{z} + cz - d \ddot{\theta} - e \dot{\theta} - g \theta = F_a \cos(\omega_e t + \epsilon_{F_f})$$

(heave)

$$(A + k_{yy}^2 \rho \nabla) \ddot{\theta} + B \dot{\theta} + C \theta - D \ddot{z} - E \dot{z} - G z = M_a \cos(\omega_e t + \epsilon_{M_f})$$

(pitch) (2)

with the hydrodynamic coefficients  $a, b, c, d, e, g, A, B, C, D, E, G$ , according to [13].

- $F_a$  = wave force with phase angle  $\epsilon_{F_f}$   
 $M_a$  = wave moment with phase angle  $\epsilon_{M_f}$   
 $k_{yy}$  = longitudinal radius of inertia of the ship  
 $\omega_e$  = wave frequency of encounter  
 $\nabla$  = volume of displacement  
 $\rho$  = density of water.

The ship motions (2) are defined by:

$$z = z_a \cos(\omega_e t + \epsilon_{z_f}) \quad \text{for heave} \quad (3)$$

$$\theta = \theta_a \cos(\omega_e t + \epsilon_{\theta_f}) \quad \text{for pitch}$$

in which  $\epsilon_{z_f}$  and  $\epsilon_{\theta_f}$  are respectively the phase angle of the heaving and pitching motion with respect to the wave motion at the origin of the coordinate system.

The absolute motions for the sections are given by:

$$v = z - x_b \theta \quad (4)$$

while the relative motions with respect to the water surface are determined by:

$$s = \xi - z + x_b \theta \quad (5)$$

The vertical absolute sectional velocity and acceleration are found by determining the time derivative of (4) in succession as follows:

$$\dot{v} = \dot{z} - x_b \dot{\theta} \quad (6)$$

$$a_v = \ddot{v} = \ddot{z} - x_b \ddot{\theta}$$

The relative velocity and acceleration are similarly found from (5):

The added resistance in waves has been calculated according to the method presented in [14], [15] and [16].

The expression for this resistance increase in waves reads as follows:

$$R_{AW} = \frac{-k \cos \mu}{2\omega_e} \int b' v_{za}^2 dx_b \quad (7)$$

in which:

- $\mu$  = direction of wave travel  
 $V_{za}$  = the amplitude of the vertical relative water velocity for each section:  $V_z = \dot{z} - x_b \dot{\theta} + V \theta - \dot{\xi}^*$   
 $\xi^*$  = the effective vertical wave displacement for a cross section  
 $b'$  = sectional damping at speed.

The response functions for all above mentioned parameters have been determined for 22 different wave-lengths.

#### 4.2. Irregular waves

The prediction of the seakeeping performance in a seaway is based on the response operators determined for the regular waves from which the irregular sea is supposed to be composed. Spectral techniques are used for the determination of the behaviour of a ship in a seaway as described in [12] and [17]. The irregular sea is considered to be a fully developed seaway according to the formulation of Pierson and Moskowitz with significant wave heights  $\tilde{H}_{1/3}$  and average wave periods  $\tilde{T}$  as denoted in Table 5.

The formula for this wave spectrum as recommended by the 12th ITTC may be written in a form suitable for direct application as follows:

$$S_f(\omega) = \frac{691}{\tilde{T}^4 \omega^5} \left( \frac{\tilde{H}_{1/3}}{2} \right)^2 \exp\left( \frac{-691}{\tilde{T}^4 \omega^4} \right) \text{m}^2/\text{rad}/\text{sec}. \quad (8)$$

For all variations and sea-states mentioned in Table 1-5 the next behaviour parameters have been determined:

- the significant heave amplitude  $\tilde{z}_{a1/3}$
- the significant pitch amplitude  $\tilde{\theta}_{a1/3}$
- the significant vertical acceleration amplitude at the FPP:  $\tilde{a}_{va1/3}$
- the mean added resistance  $\bar{R}_{AW}$
- the probability of occurrence of slamming at the FPP:  $P[\text{SLAMMING}]$
- for all ships with  $C_B = 0.70$  the freeboard at the FPP has been determined for which the probability of shipping  $P[\text{SHIPPING}] = 5\%$ , while for ships with  $C_B = 0.60$  this freeboard has been calculated for all sections.

The calculations of the freeboards have been performed without taking into account the influence of the bow wave and the dynamic swell-up.

The criteria to determine these phenomena as presented by Tasaki [18] are partly valid for the ships considered and for this reason they are totally omitted. Moreover it appeared from recent investigations [19], that the crest of the bow wave varies remarkably in height and longitudinal position with the ship speed.



5. Discussions of the results

The computed results mostly confirm the conclusions of the former investigators as mentioned in the introduction.

Some exceptions may be established, especially with respect to the choice between U- or V-shaped sections in the forebody.

For this choice another one is very important viz. which aspect should be considered: the motions or the resistance. To make this choice one should keep in mind that the ratio ship-length/wave-length is important. For very small- and very long waves the motions may be neglected.

For long waves the still water resistance is dominant, while for small waves both the still water- and added resistance in waves should be taken into account. Herewith one should take into consideration the phenomenon that in many cases the still water resistance for U-shaped sections is lower than for V-shaped sections.

For a good review and discussion of the results it is convenient to treat separately the influence of the various parameters on the behaviour of the ship in a seaway. Generally speaking it is obvious from all figures, that the motions, added resistance, accelerations etc., increase with a higher sea-state. Speed influence will be treated separately as well as in combination with each of the parameters considered.

5.1. Influence of speed

The computed results show in Figures 4,5 and 6 that the heaving motion significantly increases with speed. For the highest sea-state considered the influence of speed on heave appeared to be maximum for  $L = 120$  m, but may be neglected above  $L = 200$  m. From the Figures 4,5 and 6 it is also clear, that there is a small increase of pitch with speed up to a certain length, which depends on sea-state, section shape and block-coefficient. This length decreases with sea-state, block-coefficient and an increase of the prismatic coefficient. The added resistance in waves grows with the ship speed up to a certain length dependent on sea-state. After this length the situation is just reversed.

For sea-state 9 this ship-length  $L = \pm 200$  m and for sea-state 5  $L = \pm 150$  m. The vertical acceleration, the relative motion and slamming at FPP increase with speed, however the rate of increase decreases with length and may be neglected above  $L = 200$  m. See Figures 4,5 and 6.

5.2. Influence of forebody section shape

From Figures 4 and 5 it is evident, that the heaving motion strongly increases with the prismatic coefficient,

so with more U-shaped sections in the forebody, while pitch appears to be almost indifferent for the forebody section shape. As shown in Figures 4 and 5 it appears, that the added resistance in waves increases with more U-shaped sections up to a certain length which depends on sea-state and speed. After this length the situation has been reversed and so V-shaped sections are unfavourable then. The length for which this reversion occurs increases with sea-state and decreases

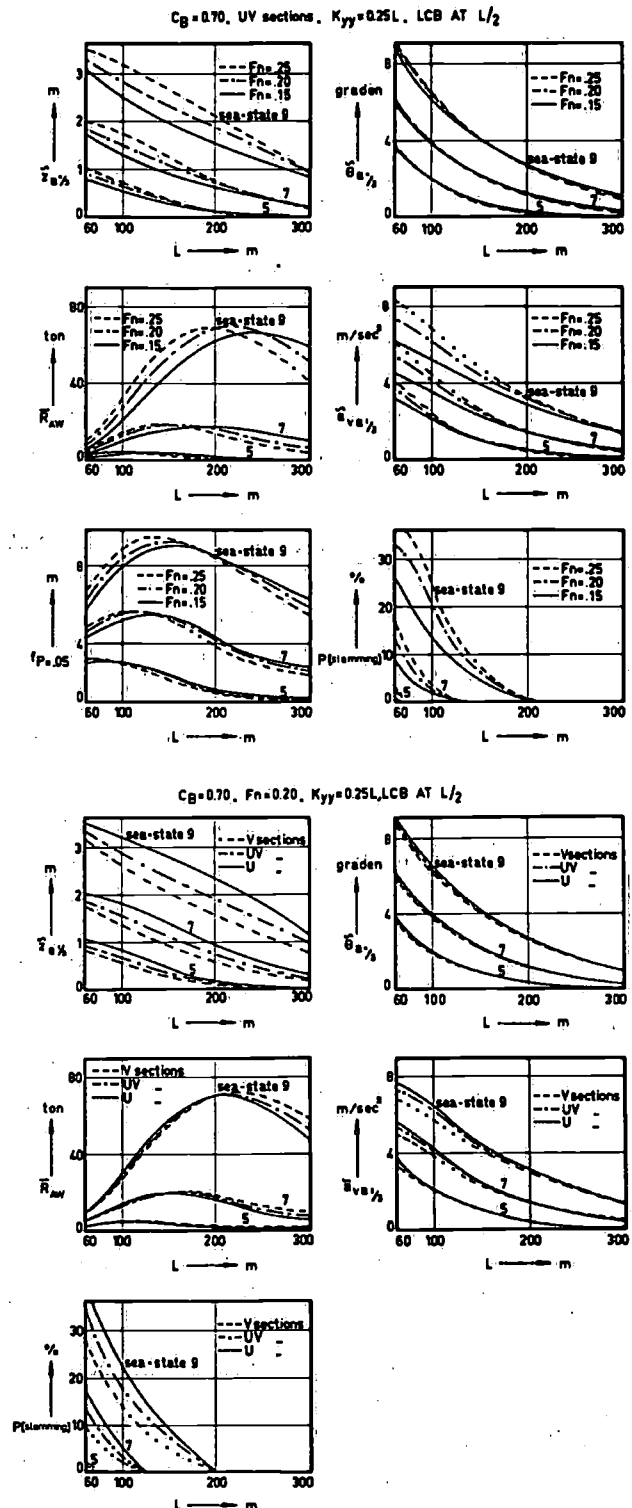


Figure 4. Ship behaviour as a function of length and related to speed and section shape for  $C_B = 0.70$ .

with speed and blockcoefficient. For sea-state 9 this length amounts about 200 m at  $F_n = 0.15$  and about 130 m at  $F_n = 0.25$ .

The vertical acceleration at FPP increases with more U-shaped sections in the forebody as shown in Figures 4 and 5, but this influence may be neglected above a length of 200 m for an average sea-state and speed.

Slamming at FPP increases rather strongly with the prismatic coefficient, but has almost disappeared for a

ship length  $L = 200$  m at sea-state 9 and  $L = 120$  m at sea-state 7. See Figures 4 and 5. The relative motion at FPP for  $C_B = 0.60$  also increases with the prismatic coefficient and achieves a maximum value which depends on sea-state and speed. The upper limit is about  $L = 120$  m. After this length the influence of the forebody section shape reduces.

5.3. Influence of ship length

Heave, and pitch motions are reduced significantly if the ship length increases as Figures 4, 5 and 6 show.

The added resistance in waves increases with ship-length up to a certain value which is related to sea-state, speed and blockcoefficient. This length increases with sea-state, a reduction in speed and blockcoefficient as shown in Figures 4 and 5. For an average speed this length may be established at  $L = 210$  m in the case of sea-state 9 and at  $L = 160$  m for a sea-state 7.

The vertical acceleration at FPP shows a strong reduction with ship-length in Figures 4, 5. The same phenomena can be established for slamming as shown in Figures 4, 5, 6. Above  $L = 200$  m for sea-state 9 and above  $L = 120$  m for sea-state 7 the probability on slamming may be neglected. The relative motion shows an increase with ship-length up to a certain length, which depends on sea-state and speed.

For an average speed and sea-state this length appears to be about 120 m. In Figure 7 the freeboard for which the probability of shipping is 5% ( $f_p = .05$ ) has been presented as a percentage of the ship length for

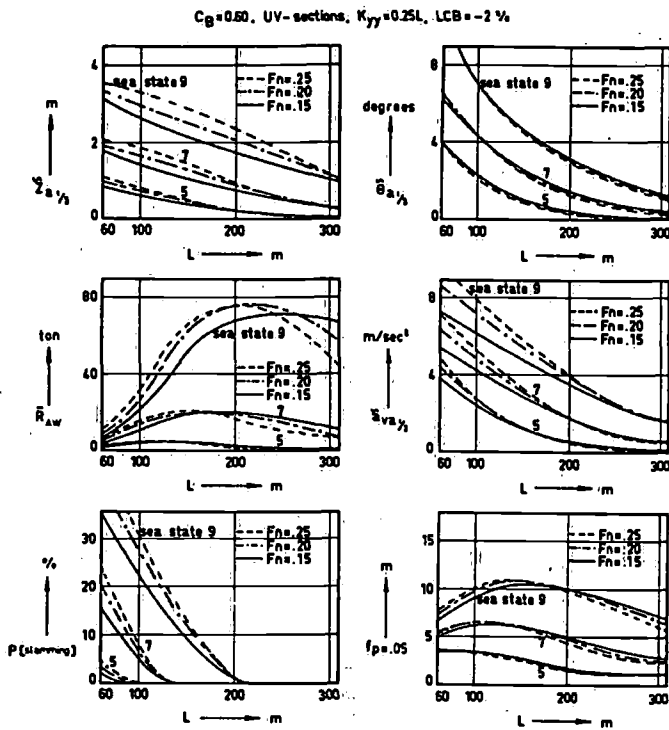


Figure 5. Ship behaviour as a function of length and related to speed and section shape for  $C_B = 0.60$ .

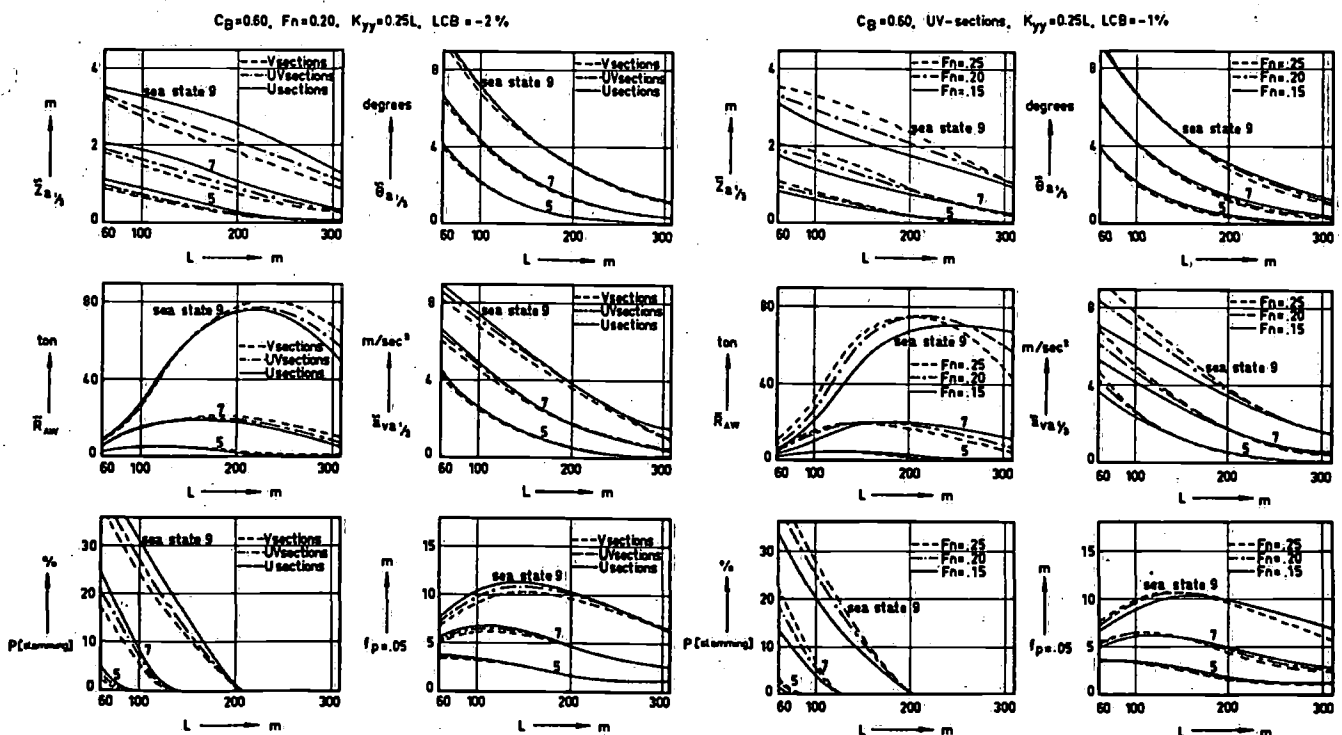


Figure 6. Ship behaviour as a function of length and related to speed for  $C_B = 0.60$  and  $LCB$  at  $1\%L$  aft  $L/2$ .

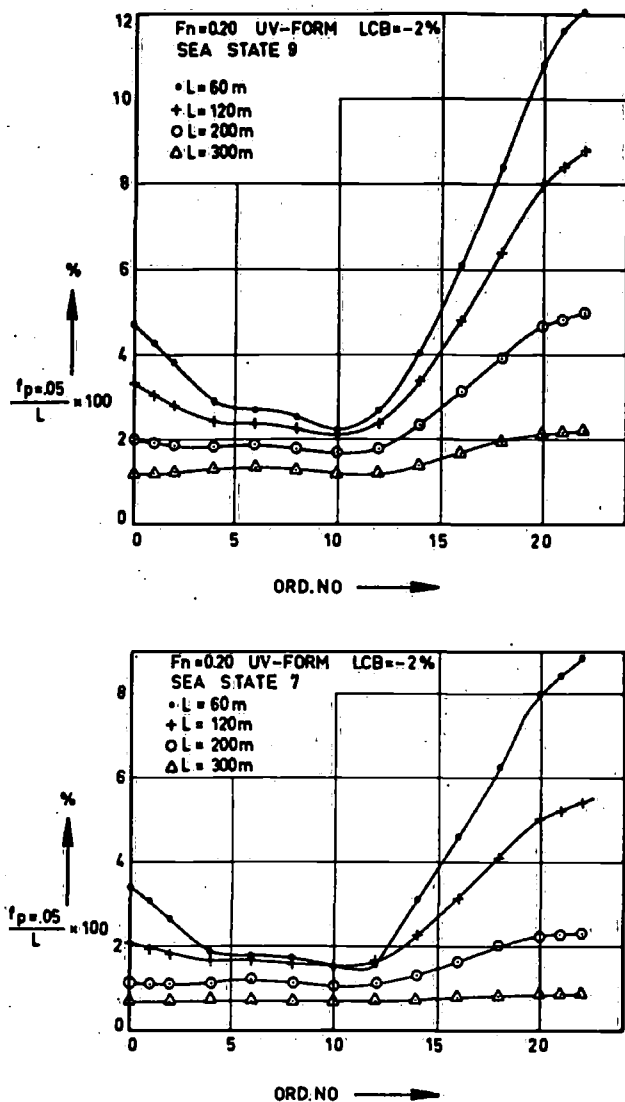


Figure 7. Ratio of freeboard with probability of shipping of 5% and ship length.

the sections of different ships with blockcoefficient  $C_B = 0.60$ .

This freeboard is especially restricted to  $F_n = 0.20$ , UV-forebody sections, sea-state 7 and 9.

It is clearly shown in this Figure, that the longest ship needs the smallest freeboard in relation to the ship-length especially for the sections forward of section 12.

#### 5.4. Influence of the centre of buoyancy in length

Moving forward of LCB for blockcoefficient  $C_B = 0.70$  results in a small increase of pitch, vertical acceleration, relative motion and slamming at FPP. See Figure 8. From Figures 5 and 6 it is clear, that for blockcoefficient  $C_B = 0.60$  the situation of the centre of buoyancy in length has no significant influence on the motions, added resistance in waves, accelerations and slamming at FPP.

#### 5.5. Influence of blockcoefficient

From Figure 8 it can be seen, that an increase of the blockcoefficient causes a rather strong reduction of the motions, acceleration, added resistance and slamming. It should be remarked, that the rate of reduction is almost independent of the speeds considered.

#### 5.6. Influence of the weight distribution

Increase of the radius of inertia results in somewhat higher heaving motions (negligible for sea-state 5) and pitching motions for the lowest speed and highest sea-state only. See Figure 9. For  $F_n = 0.20$  the influence of the radius of inertia on pitch may be neglected, while for  $F_n = 0.25$  a small decrease in pitch with the increase of the radius of inertia could be established. The vertical acceleration is almost independent of the radius of inertia. Only for the lowest speed and the highest sea-state a small increase of the vertical acceleration at FPP with the radius of inertia is evident from Figure 8. For the highest sea-state only an increase of the added resistance in waves with the radius of inertia has become clear. The probability on slamming grows with the longitudinal radius of inertia, while the relative motions increase with this radius at the highest speed only.

#### 5.7. Influence of the average wave period

A variation of the sea-condition as denoted in Table 4 shows in Figure 9 that all motions, added resistance, vertical acceleration at FPP, etc. increase rather significantly with the average wave-period.

For a high sea-state in combination with a low ship speed only a maximum value of the added resistance could be observed at a wave period of 1.05 times the average wave period.

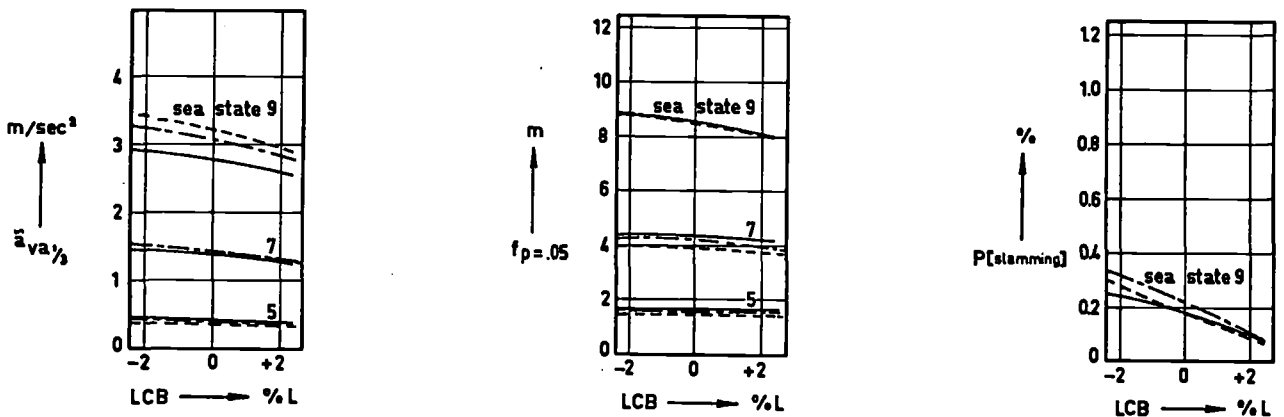
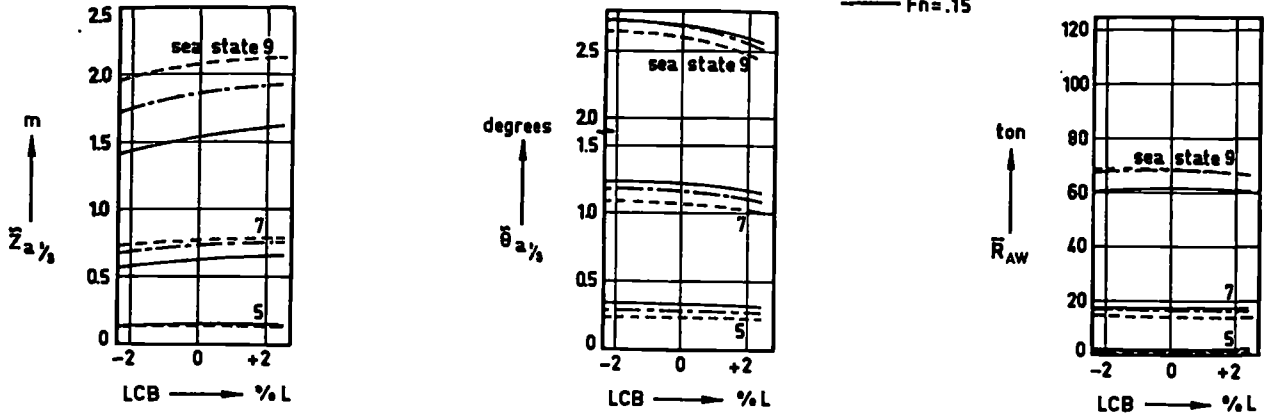
## 6. Conclusions and recommendations

From the preceding parametric-study the following conclusions and recommendations may be derived:

1. From all parameters investigated the *ship-length* approves to have the greatest influence on the motions (especially on pitch), acceleration, added resistance, slamming etc. With increase of the ship length the motions, accelerations and slamming decrease significantly up to about  $L = 200$  m for sea-state 5 and  $L = 300$  m for sea-state 7. Added resistance increases with length up to a certain value dependent on sea-state, speed and blockcoefficient. A longer ship requires a smaller ratio of freeboard and ship-length.

$L=200\text{m}$ ,  $C_B=0.70$ , UV sections,  $K_{yy}=0.25L$ ,

---  $F_n=0.25$   
 - - -  $F_n=0.20$   
 —  $F_n=0.15$



$L=200\text{m}$ , UV sections,  $K_{yy}=0.25L$ , LCB AT  $L/2$ ,

---  $F_n=0.25$   
 - - -  $F_n=0.20$   
 —  $F_n=0.15$

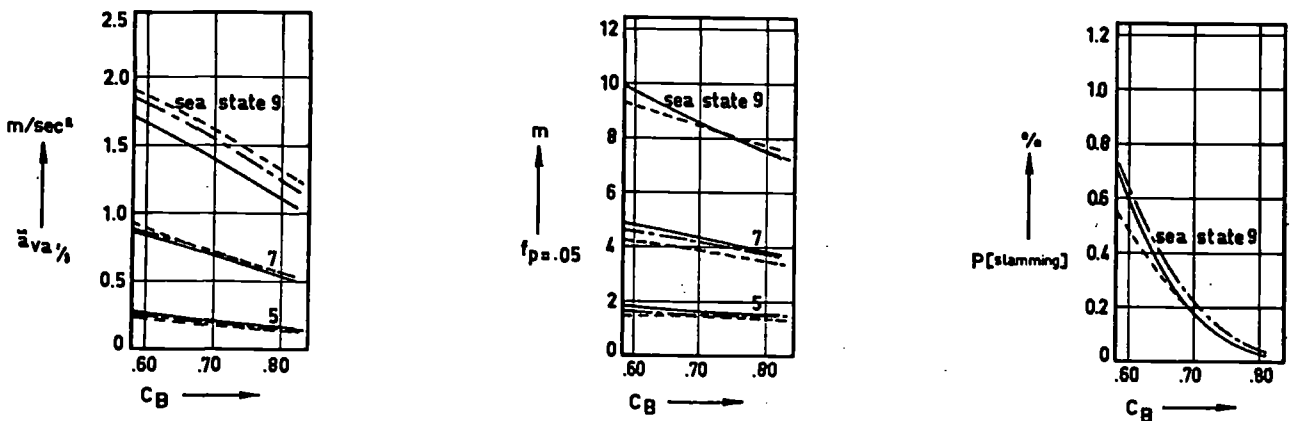
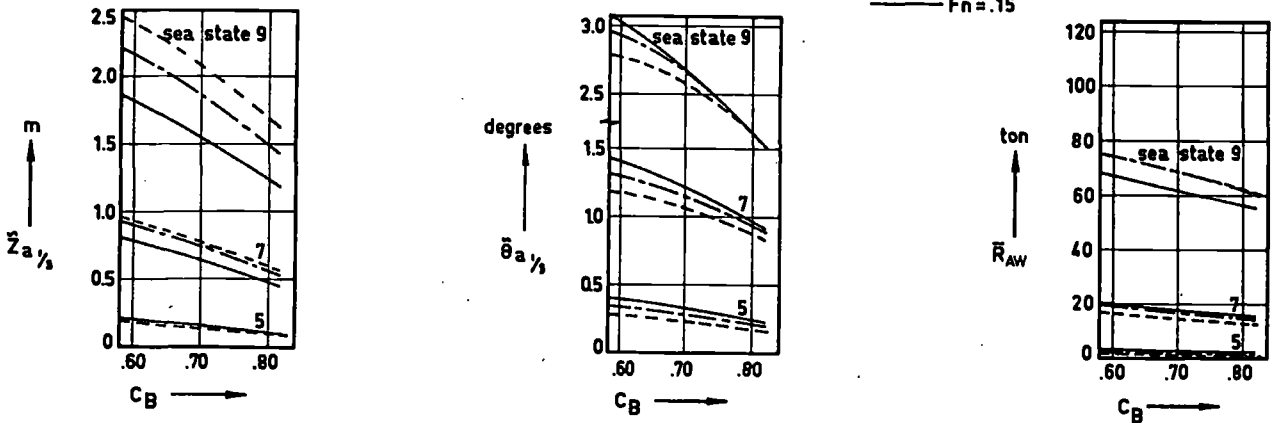
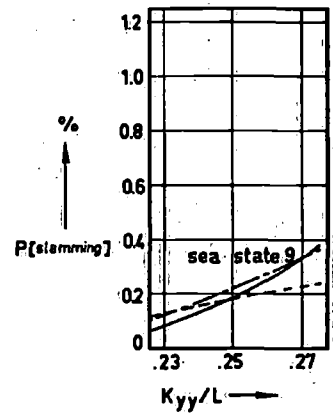
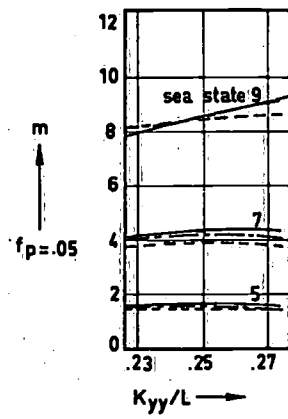
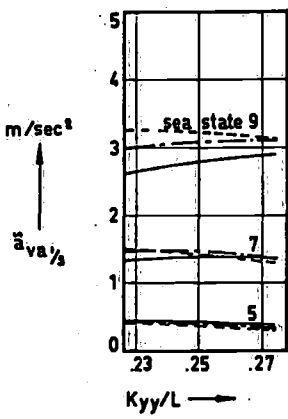
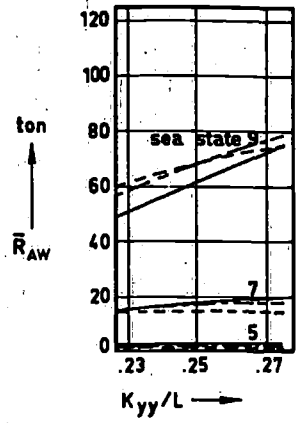
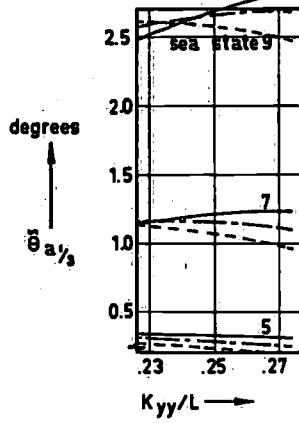
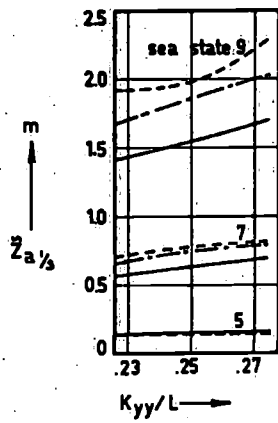


Figure 8. Influence of LCB and  $C_B$  on ship behaviour.

L=200m,  $C_B = 0.70$ , UVsections, LCB AT L/2,

--- Fn=.25  
 - - - Fn=.20  
 ——— Fn=.15



L=200m,  $C_B = 0.70$ , UVsections,  $K_{yy} = 0.25L$ , LCB AT L/2,

--- Fn=.25  
 - - - Fn=.20  
 ——— Fn=.15

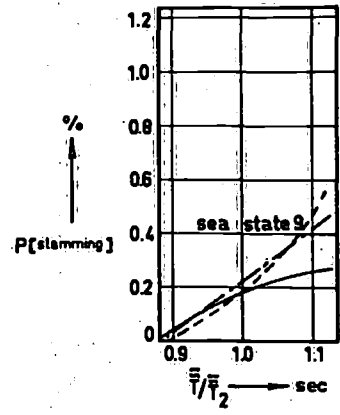
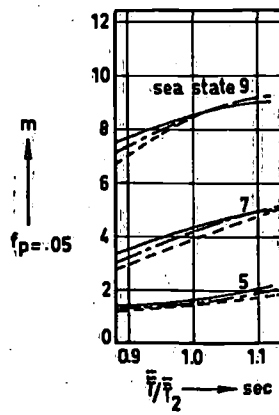
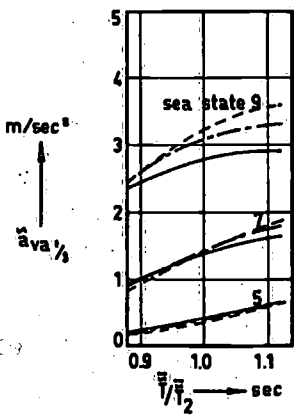
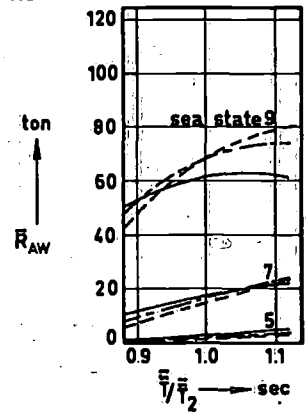
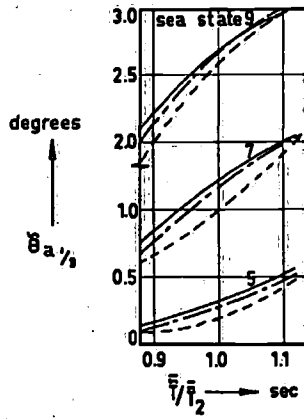
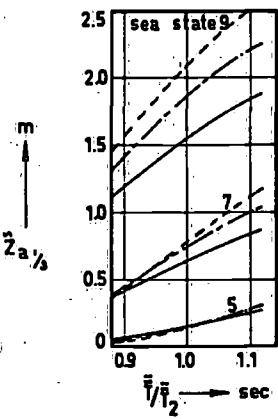


Figure 9. Influence of weight distribution and average wave period on ship behaviour.

2. The *ship-speed* appears to be a second factor of importance to influence ship motions, accelerations, added resistance, slamming etc.

The heaving motions strongly increase with speed (maximum for  $L = \pm 120$  m), while pitch appears to be almost indifferent for speed.

The added resistance in waves increases with speed up to a certain ship-length dependent on sea-state.

3. The *forebody section shape* should be mentioned as the third factor of importance to influence ship motions etc.

V-shaped forebody sections, so a lower prismatic coefficient, result in a reduction of heave, added resistance, vertical accelerations, slamming and relative motions. However, above a ship length of about 200 m U-shaped forebody sections are preferable with respect to the added resistance in waves. The influence of the forebody section shape on pitch is very small.

4. The *block-coefficient* is the next factor of importance to influence the motions. An increase of the blockcoefficient causes a rather strong reduction of the motions, accelerations, added resistance, relative motions and slamming.

5. The situation of the *centre of buoyancy in length* LCB and the *radius of inertia* are factors of minor importance to influence the ship motions. Only for the higher blockcoefficients such a shift in LCB is possible, that moving aft of LCB results in a small decrease of pitch, vertical acceleration, relative motion and slamming. Added resistance is hardly influenced by a shift of LCB.

The radius of inertia mainly influences the heaving motion. Heave, added resistance and slamming increase with the radius of inertia, while vertical acceleration and relative motion are almost indifferent for variation of the radius of inertia. Pitch is rather speed-dependent in this respect.

6. Care should be taken in using an average *wave-period* for comparison of the behaviour of different ships in a seaway.

All motions, added resistance, slamming etc. increase rather significantly with the wave period.

## 7. Acknowledgement

The authors wish to acknowledge the valuable contribution and criticism of Prof.ir. J. Gerritsma and ir. J.M.J. Journée.

They are also especially indebted to Mr. A. Versluis for his efforts to design the hull-forms investigated.

Furthermore they are particularly grateful to Mrs. E. Langstraat for typing the manuscript and to Mr. P.W. de Heer for the lay-out and preparation of the graphs and figures.

## 8. List of symbols

a,b,c,d,e,g	coefficients of the equations of motion
A,B,C,D,E,G	for heave and pitch
$a_v$	vertical absolute sectional acceleration
$a_{va}$	amplitude of vertical absolute sectional acceleration
B	breadth of the ship
$b'$	sectional damping for ship on speed
$C_B, \delta$	blockcoefficient
$C_{BA}, \delta_A$	blockcoefficient of afterbody
$C_{BF}, \delta_F$	blockcoefficient of forebody
$C_M, \beta$	midship section coefficient
$C_{VP}, X$	vertical prismatic coefficient
$C_{WP}, \alpha$	waterplane area coefficient
D	denotation for blockcoefficient in parameter-variation scheme
$F_a$	wave force amplitude
FPP	fore perpendicular
f	freeboard
$F_n$	Froude number
$g$	acceleration of gravity
$\bar{H}_{1/3}$	significant wave height
K	denotation for longitudinal radius of inertia in parameter-variation scheme
$k=2\pi/\lambda$	wave number
$k_{yy}$	longitudinal radius of inertia
L, $L_{pp}$	length between perpendiculars
LCB	position of the centre of buoyancy in length
$M_a$	wave moment amplitude
P	probability of occurrence
Q	denotation for LCB in parameter-variation scheme
$R_{AW}$	added resistance in waves
S	denotation for sea-condition in parameter-variation scheme
$S_f$	wave spectrum
s	relative motion with respect to the water surface
$\bar{T}$	average wave period
V	forward speed of ship
v	vertical absolute sectional motion
$v_z$	vertical relative velocity
$v_{za}$	amplitude of the vertical relative water velocity
X	denotation for forebody section shape in parameter-variation scheme.
x,y,z	right hand coordinate system fixed to ship
$x_b, y_b, z_b$	heave displacement
z	heave amplitude
$z_a$	waterplane area coefficient
$\alpha, C_{WP}$	midship section coefficient
$\beta, C_M$	vertical prismatic coefficient
$\chi, C_{VP}$	block coefficient
$\delta, C_B$	

$\delta_A, C_{BA}$	blockcoefficient of afterbody
$\delta_F, C_{BF}$	blockcoefficient of forebody
$\epsilon$	phase angle between the motions, forces, moments and the waves
$\lambda$	wave length
$\mu$	direction of wave travel (head waves = $180^\circ$ )
$V$	volume of displacement
$\omega$	circular wave frequency
$\omega_e$	circular wave frequency of encounter
$\rho$	density of water
$\theta$	pitch angle
$\theta_a$	pitch amplitude
$\zeta$	instantaneous wave elevation
$\zeta_a$	wave amplitude

### 9. References

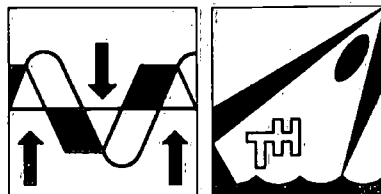
- Lewis, E.V., "Ship speeds in irregular seas", SNAME 1955.
- Swaan, W.A., Vossers, G., "The effect of forebody shape on ship behaviour in waves", International Shipbuilding Progress, 1961, Vol. 8, No. 83.
- Bengtsson, B.G., "Influence of V and U shaped forebody sections on motion and propulsion of ships in waves", Swedish State Shipbuilding Experimental Tank; 1962, No. 49.
- Bengtsson, B.G., "Influence of V and U shaped forebody sections on motions and propulsion of ships in waves at ballast draught", Swedish State Shipbuilding Experimental Tank, 1962, No. 56.
- Swaan, W.A., "The influence of principal dimensions on ship behaviour in irregular waves", International Shipbuilding Progress, June 1961, Vol. 8, No. 82.
- Swaan, W.A., Rijken, H., "Speed loss at sea as a function of longitudinal weight distribution", International Shipbuilding Progress, 1964, Vol. 11, No. 115.
- Ewing, J.A., "The effect of speed, forebody shape and weight distribution on ship motions", TRINA, 1967, Vol. 109.
- Yourkov, N., "Vertical motions of ships with different form of forebody", Delft University of Technology, Ship Hydromechanics Laboratory, Report No. 316.
- Loukakis, Th.A. and Chryssotomides, Chr., "Seakeeping standard series for cruiser-stern ships", SNAME, 1975.
- Versluis, A., "Scheepsvorm- en carèneberekening van een gedeelte van de Guldhammer serie voor Container- en Roroscepen" (in Dutch), Delft University of Technology, Ship Hydromechanics Laboratory, Report No. 408.
- Hogben, N., Lumb, F.E., Book: "Ocean wave Statistics", London HMSO, 1967, (for NPL).
- Beukelman, W., Bijlsma, E.F., "Description of a program to calculate the behaviour of a ship in a seaway" (named TRIAL), Delft University of Technology, Ship Hydromechanics Laboratory, Report No. 383.
- Gerritsma, J., Beukelman, W., "Analysis of the modified striptheory for the calculation of ship motions and wave bending moments", International Shipbuilding Progress, 1967, Vol. 14, No. 156.
- Gerritsma, J., Beukelman, W., "Analysis of the resistance increase in waves of a fast cargo ship", International Shipbuilding Progress, 1972, Vol. 19, No. 217; 13th ITTC 1972, Vol. 2, p. 902-917.
- Gerritsma, J., Beukelman, W., Glansdorp, C.C., "The effects of beam on the hydrodynamic characteristics of ship hulls", Tenth Symposium Naval Hydrodynamics, 1974.
- Beukelman, W., Buitenhok, M., "Full scale measurements and predicted seakeeping performance of the container ship 'Atlantic Crown' ", International Shipbuilding Progress, 1974, Vol. 21, No. 243.
- Gerritsma, J., "Behaviour of a ship in a seaway", International Shipbuilding Progress, 1966, Vol. 13, No. 143.
- Tasaki, R., "On shipment of water in head waves", 10th ITTC, London, 1963.
- Journée, J.M.J., "Motions, resistance and propulsion of a ship in longitudinal regular waves", Delft University of Technology, Ship Hydromechanics Laboratory, Report No. 428.





TECHNISCHE HOGESCHOOL DELFT  
AFDELING DER SCHEEPSBOUW- EN SCHEEPVAARTKUNDE  
LABORATORIUM VOOR SCHEEPSHYDROMECHANICA

Rapport No. 449-M



HANDLEIDING VOOR HET GEBRUIK VAN HET  
SCHEEPSBEWEGINGEN-PROGRAMMA VOOR  
6 GRADEN VAN VRIJHEID.

W. Beukelman

April 1977

Delft University of Technology  
Ship Hydromechanics Laboratory  
Mekelweg 2  
Delft 2208  
Netherlands

## INHOUD

### Algemeen.

#### 1. Beschrijving van SM16 (LOMO 1).

##### 1.1. Algemeen.

##### 1.2. Invoeraanwijzingen.

##### 1.3. Kaartinvoer SM16 (LOMO 1).

##### 1.4. Kaart- en programma-uitvoer SM16 (LOMO 1).

#### 2. Beschrijving van SM02.

##### 2.1. Algemeen.

##### 2.2. Kaartinvoer SM02.

##### 2.3. Kaart- en programma-uitvoer van SM02

###### 2.3.1. Kaartuitvoer van SM02.

###### 2.3.2. Programma-uitvoer van SM02.

#### 3. Beschrijving van SM03.

##### 3.1. Algemeen.

##### 3.2. Kaartinvoer SM03.

##### 3.3. Kaart- en programma-uitvoer van SM03.

###### 3.3.1. Kaartuitvoer SM03.

###### 3.3.2. Programma-uitvoer van SM03.

#### 4. Beschrijving van SM04.

##### 4.1. Algemeen.

##### 4.2. Kaartinvoer SM04

##### 4.3. Programma-uitvoer van SM04.

#### 5. Aanbevelingen.

#### 6. Referenties.

Algemeen.

De eerste versie van het scheepsbewegingen-programma voor 6 graden van vrijheid is ontwikkeld door het Laboratorium voor Scheepsbouwkunde van de Technische Hogeschool te Delft.

Dit vond plaats in het kader van het promotiewerk van dr.ir. J. Vugts [1]. Het programma was oorspronkelijk geschreven in ALGOL 60.

Daarna zijn door ir. R. Wahab en ir. J.H. Vink wijzigingen aangebracht in de theorie met betrekking tot de golfkrachten en -momenten [2].

Hiervoor werd ook een nieuw programma opgezet onder de naam "LOMO".

Het eerstgenoemde programma (genaamd "SM" naar Ship Motions) werd in "FORTRAN"-taal door ir. J.G.L. Pijfers van TNO - IWECO ter beschikking gesteld van het Laboratorium voor Scheepshydronechanica.

Hierin werden wijzigingen aangebracht o.a. in de integratie-procedure van de hydrodynamische afgeleiden, de golfkrachten en -momenten.

Voor dit programma is deze handleiding bedoeld.

De instructies zijn gedeeltelijk ontleend aan de handleiding voor het scheepsbewegingen programma "LOMO" en aan de ervaringen met het ITTC-project voor Scheepsbewegingen in 1976.

Voor het berekenen van de bewegingen van een schip in zeegang met zes graden van vrijheid dienen achtereenvolgens de volgende vier programma's gebruikt te worden:

1. SM16 (LOMO 1) voor het bepalen van de transformatie-coëfficiënten van de verschillende secties.
2. SM02 voor het bepalen van de hydrodynamische coëfficiënten per sectie afhankelijk van de ontmoetingsfrequentie
3. SM03 voor het bepalen van de response-functies in regelmatige golven.
4. SM04 voor het bepalen van de significante waarden van de bewegingen in een golfspectrum.

Voor elk van de bovengenoemde programma's zal een beschrijving worden gegeven van de kaartinvoer en de uitvoer van kaarten en programma.

Voor de kaartin- en-uitvoer geeft I een geheel getal (integer) aan en FL een getal met drijvende komma (floating point).

## 1. Beschrijving van SMI6 (LOMO 1)

### 1.1. Algemeen

De voornaamste invoer-parameters zijn de spantcoördinaten. Indien gewenst en wanneer het mogelijk is, wordt een conforme transformatie voor iedere sectie uitgevoerd waardoor de spantvorm benaderd wordt. Als de methode van de conforme transformatie niet gewenst wordt of niet mogelijk blijkt te zijn, worden de coördinaten alleen getransformeerd naar een ander assenstelsel, zodanig dat de methode van Frank [3] kan worden toegepast. De eerste methode, genoemd de "close fit" methode, is geschikt voor de meeste spantvormen [4]. Voor bulbvormige spanten moet toch een bepaalde breedte op de waterlijn ingevoerd worden, bijv. 0.01 van de maximale scheepsbreedte, om de "close fit" methode volgens Ursell te kunnen toepassen.

Met de methode van Frank kan elke spantvorm worden behandeld, zelfs een volledig ondergedompeld spant. Er is evenwel een belangrijk nadeel bij deze methode. Bij vollere spanten, ongeveer over 0.25 L tot 0.75 L, treedt resonantie op bij sommige frequenties. Deze resonantie betreft het vloeistofoppervlak, dat binnen de contour van het spant is gelegen. Er zijn aanwijzingen, dat dit nadeel kan worden ondervangen door het spant van boven af te sluiten, maar dit is nog niet onderzocht. Het verdient derhalve de voorkeur om zoveel mogelijk gebruik te maken van de "close fit" methode.

### 1.2. Invoeraanwijzingen.

1. Bij de invoer mag de dwarsscheepse y-coördinaat nooit de waarde nul hebben, maar bijv.  $10^{-5}$ . Op de waterlijn moet deze breedte minstens  $0.01 \times$  de maximale scheepsbreedte zijn.
2. Horizontale delen moeten een zeer kleine helling krijgen, zodat y steeds afneemt. Deze helling kan zeer klein genomen worden bijv.  $10^{-6} : 1$ .
3. De afwijking van het benaderingspolynoom, waarmee de transformatie voor de "close fit" methode wordt uitgevoerd ten opzichte van het werkelijke spant mag niet groter zijn dan een op te geven waarde

$$\sum_n \{ (x_b - x)^2 + (y_b - y) \} < \epsilon$$

De waarde van  $\epsilon$  wordt per spant ingelezen en toegekend aan EPSLL.  
De rekentijd voor het transformeren hangt af van de opgegeven

waarde voor EPSLL.

Een normale waarde is

$$\text{EPSLL} = \text{eps}' * \text{diepgang} * \frac{1}{2} \text{ breedte} * \text{gemiddeld aantal meetpunten per sectie}$$

$$\text{waarbij eps}' = 0.005 \text{ à } 0.0001$$

4. Wanneer de voorste ordinaat alleen een punt is t.p.v. de waterlijn, dan moet voor dit spant een zeer kleine cirkel worden ingevoerd met een straal van bijv.  $10^{-5}$  m.

### 1.3. Kaartinvoer SM16 (LOMO 1).

#### Kaart no. 1

kol 1-80

Titel, die boven elke pagina van de uitvoer wordt afgedrukt.

#### kaart no. 2

kol 1-5, I,

N01 = ordinaat nummer van de eerste van een serie gelijkvormige ordinaten.

kol 6-10, I,

N02 = ordinaat nummer van de laatste van een serie gelijkvormige ordinaten.

N.B. Als er geen parallel middenschip is, moeten ordinaat nummers worden opgegeven boven het nummer van het aantal beschouwde ordinaten, de eerste lager dan de tweede.

#### kaart no. 3

kol 1-5, I,

NN = aantal spanten (min. 1, max. 31)

#### kaart no. 4

kol 1-10, FL,

FACT = faktor voor omzetten van invoercoördinaten in meters. (=1. als invoer in meters plaats vindt).

kol 11-20, FL,

SCALE = schaal waarop de ordinaten geplot moeten worden. (op dit ogenblik werkt het plot-programma niet).

Vanaf hier wordt de volgende invoer per spant herhaald:

#### kaart no. 5

kol 1-5-, I,

II = keuze variabele

II = 0 als methode Frank wordt gewenst.

II ≠ 0 als "close fit" methode gewenst wordt.

In dat geval geeft II tevens aan hoe-

veel transf. coëfficiënten minimaal moeten worden berekend. Indien conforme transformatie niet mogelijk blijkt te zijn, wordt automatisch de methode van Frank gehanteerd.

- kol 6-10, I, MM = aantal coördinaten paren, max. 46.
- kol 11-15, I, NUM = ordinaat nummer, achteraan beginnend met 0
- kol 21-30, I, ESPLL = toegelaten afwijking bij transformatie.  
Zie de invoeraanwijzingen onder 1.2.  
Voor II = 0 een willekeurig getal nemen.
- kol 31-40, I, RKANT = 1.0 wanneer de ordinaat rechts geplot moet worden.  
= -1.0 wanneer de ordinaat links geplot moet worden.
- kol 44-45, I, MAXB = volgnummer van het coördinatenpaar waarvoor de max. breedte van de ordinaat optreedt.
- kol 49-50, I, MD = 1 als ordinaat ondergedompeld is.  
= 2 als ordinaat een waterlijn bezit.
- kol 51-60, FL, DEP = diepte van bovenste punt ordinaat onder de waterlijn in dezelfde maat als gebruikt voor in te lezen coördinaten van de ordinaat, als MD = 1; als MD = 2, dan DEP = 0; als II ≠ 0, dan MD = 2 en DEP = 0; als MD = 1 en DEP ≠ 0, dan wordt de methode van Frank toegepast ook al is II ≠ 0.

kaart no. 6 a,b,c etc.

- |                |       |   |
|----------------|-------|---|
| kol 1-10, FL,  | X (1) | } Coördinaten van punten op de omtrek van het spant. Als er meer dan 4 coördinaatparen zijn, worden volgkaarten (no. 6 <sup>b</sup> , 6 <sup>c</sup> , 6 <sup>d</sup> , etc.) gebruikt met dezelfde indeling.<br>Max. 46 coördinaatparen.<br>X wordt gemeten vanuit hart schip<br>Y wordt gemeten vanaf het laatste punt van de ordinaat. |
| kol 11-20, FL, | Y (1) |   |
| kol 21-30, FL, | X (2) |   |
| kol 31-40, FL, | Y (2) |   |
| kol 41-50, FL, | X (3) |   |
| kol 51-60, FL, | Y (3) |   |
| kol 61-70, FL, | X (4) |   |
| kol 71-80, FL, | Y (4) |   |

Het eerste punt moet het bovenste punt van de ordinaat zijn en de volgende punten langs het contour naar beneden toe. Het laatste punt is het kielpunt.

kaart no. 7

kol 1-2, I,

III = aantal hoekintervallen (theta)

voor berekening van het getransformeerde spant.

Max. 31 en groter dan 0.

Voor kleine spanten in voor- en achterschip bijv. III = 5 of 4 en voor de overige spanten III = 10 - 17.

Voor alleen verticale bewegingen (stampen en dompen) III = 5 of 4

kol 11-12, I,

MMM = aantal multipolen. Max. 30.

$MMM \leq III - 1$ .

Als  $II = 0$  dan kunnen III en MMM willekeurige waarden bezitten.

kaart no. 8

kol 1-10

X0 = langsscheepse positie van de ordinaat t.o.v. L/2 in meters.

1.4. Kaart- en programma-uitvoer SM16 (LOM01)

De kaartuitvoer van SM16 kan niet direct gebruikt worden voor de invoer van programma SMO2 en wordt daarom hier niet verder beschreven. Wel is er aansluiting op eenzelfde programma SM15 (LOMO 2) met daaropvolgend SM14 (LOMO 3). Een beschrijving hiervan is weergegeven in de instructies van ir. R. Wahab. De programmautvoer bevat voor elke sectie o.a.:

1. de titel als weergegeven op invoerkaart no.1
2. het oorspronkelijke en nieuwe sectienummer (het nieuwe sectienummer begint van achteren af met 0)
3. het halve sectie-oppervlak, de halve breedte op de waterlijn, de diepgang
4. de Lewis-coëfficiënt  $a_1$  en  $a_3$
5. de totale afwijking EPSLL van het oorspronkelijke ordinaat (zie 1.2. onder 3)
6. de hoeken theta waarvoor het getransformeerde spant is berekend met de afwijkingen DELTA-X en DELTA-Y van het oorspronkelijke ordinaat, de nieuwe en oude x en y-ordinaten
7. de nieuwe x- en y-ordinaten voor hoeken theta met intervallen van 2.5 graden
8. de transformatie-coëfficiënten A1, A3, A5 etc.
9. de gebruikte schaalfactor.

## 2. Beschrijving van SM02.

### 2.1. Algemeen

Voor verschillende in te voeren ontmoetingsfrequenties worden de hydrodynamische coëfficiënten per sectie berekend.

Hierbij wordt de scheepssnelheid gelijk aan nul verondersteld, zodat de ontmoetingsfrequentie gelijkgesteld kan worden aan de golffrequentie. In feite worden de hydrodynamische coëfficiënten bepaald voor een reeks regelmatige golven met een ingevoerde golfhoogte.

De kaartinvoer van dit programma wordt gebruikt voor de invoer van programma SM03.

### 2.2. Kaartinvoer SM02.

#### kaart no. 1

kol 1-80

Titel, die boven elke pagina van de uitvoer wordt afgedrukt.

#### kaart no. 2

kol 1-10, I,

IJJ = aantal ordinaten

kol 11-20, I,

RR = aantal frequenties, max. 15

kol 21-30

BOOL = normaal 1, anders moeten dimensieloze ontmoetingsfrequenties, als  $\omega \sqrt{B/2g}$  worden ingelezen. (Zie kaart no. 3)

#### kaart no. 3 a,b

kol 1-10, FL, OMEGA (1)

Ontmoetingsfrequenties.

kol 11-20, FL, OMEGA (2)

Max. 15.

kol 21-30, FL, OMEGA (3)

Indien er meer dan 8 frequenties zijn, de rest op vervolgkaart no. 3 b plaatsen.

kol 31-40, FL, OMEGA (4)

kol 71-80, FL, OMEGA (8)

#### kaart no. 4

kol 1-10, I,

BOOL 1 = normaal 0, anders wordt voor GOLF de max. golfhelling ingelezen.

kol 11-20, FL,

GOLF = golfamplitude in m als BOOL 1 = 0, anders max. golfhelling in rad.

kol 21-30, FL,

RHO = dichtheid van het water (voor zee-water  $104.5 \text{ kg sec}^2/\text{m}^4$ )

kol 31-40, FL,

G = versnelling van de zwaartekracht (=  $9.81 \text{ m/sec}^2$ ).



kaart no. 5

kol 1-10, I,	II = aantal hoekintervallen van het getransformeerde spant, meestal 8, 9 of 10
kol 11-20, I,	MM = aantal multipolen, normaal 7,8 of 9
	$MM \leq II - 1.$

Vanaf hier wordt de volgende invoer telkens per spant herhaald:

kaart no. 6 (Zie programma uitvoer SM16 onder 1.4.)

kol 1-5, I,	J = ordinaat nummer
kol 6-10, I,	NN = aantal transformatie coëfficiënten - 1.
kol 11-22, FL,	B = <u>halve</u> breedte op de waterlijn van het getransformeerde spant (New -x)
kol 23-34, FL,	D = diepgang van de sectie
kol 35-46, FL,	OPP= oppervlak van de <u>halve</u> sectie.

kaart no. 7 a,b. (Zie programma uitvoer SM16 onder 1.4.)

kol 1-15, FL,	Transformatie coëfficiënt, A1
kol 16-30, FL,	Transformatie coëfficiënt, A3
kol 31-45, FL,	Transformatie coëfficiënt, A5
kol 46-60, FL,	Transformatie coëfficiënt, A7
kol 61-75, FL,	Transformatie coëfficiënt, A9

Indien er meer dan 5 transformatie coëfficiënten zijn, deze plaatsen op kaart 7 b,c met dezelfde indeling als kaart no.7a, daarna afsluiten met:

kol no., zie boven, FL,XPL=halve breedte op de waterlijn van het getransformeerde spant (New -x)

2.3. Kaart- en programmavitvoer van SM02.

De kaartuitvoer van SM02 kan direct gebruikt worden als gedeeltelijke invoer van programma SM03.

2.3.1. Kaartuitvoer SM02.

Deze kaartuitvoer bevat achtereenvolgens eerst voor iedere sectie:

kaart no. 1

kol 1-4, I,	NUM = kaartnummer
kol 5-8, I,	J = sectienummer
kol 9-20, FL,	XO = o.o
kol 21-32, FL,	OPP = oppervlak van de gehele sectie
kol 33-44, FL,	B = halve waterlijn breedte van de sectie
kol 45-56, FL,	OB = ligging van het drukkingspunt t.o.v. de waterlijn

daarna per sectie en per ontmoetingsfrequentie:

kaart no. 2

kol 1-3, I,	NUM 1 = kaartnummer
kol 4-14, FL,	O(R) = frequentie
kol 15-25, FL,	AYY(R) = toegevoegde massa bij verzetten
kol 26-36, FL,	BYY(R) = demping bij verzetten
kol 37-47, FL,	AZZ(R) = toegevoegde massa bij dompen
kol 48-58, FL,	BZZ(R) = demping bij dompen
kol 59-69, FL,	ARR(R) = toegevoegde massa bij slingeren
kol 70-80, FL,	BRR(R) = demping bij slingeren

kaart no. 3

kol 1-3, I,	NUM 2 = kaartnummer
kol 4-14, FL,	AROLLY(R) = massa-koppeling van verzetten in slingeren
kol 15-25, FL,	BROOLLY(R) = dempings-koppeling van verzetten in slingeren
kol 26-36, FL,	TTSTER(R) = effectieve diepgang van de sectie
kol 37-47, FL,	DRIFTF(R) = driftkracht
kol 48-58, FL,	EPSZ(R) = faseverschil van dompen
kol 59-69, FL,	EPSY(R) = faseverschil van verzetten
kol 70-80, FL,	EPSRLL(R) = faseverschil van slingeren

} met golf

2.3.2. Programmauitvoer van SM02.

De programmauitvoer bevat voor elke sectie op:

pagina 1 :

1. de titel als weergegeven op invoerkaart no. 1
2. sectienummer en andere gegevens van de sectie
3. de transformatie coëfficiënten
4. het statisch moment t.o.v. de waterlijn, het oppervlak van de getransformeerde sectie, de ligging van het zwaartepunt t.o.v. de waterlijn

pagina 2 en

eventueel 3 :

1. de titel als weergegeven op invoerkaart no. 1
2. de ingevoerde frequenties, ook dimensieloos  $\omega\sqrt{\frac{B}{2g}}$   
waarin:  
B = breedte schip  
g = versnelling zwaartekracht

pagina 3 en

eventueel 4 :

1. de titel als weergegeven op invoerkaart no. 1
2. voor de ingevoerde frequenties de absolute en procentuele fouten in dompen, stampen en slingeren

3. voor de ingevoerde frequenties worden de verschillende golfkarakteristieken evenals de effectieve diepgang  $T^*$  opgegeven.

pagina 4 en

eventueel 5 :

1. de titel als weergegeven op invoerkaart no. 1
2. voor de ingevoerde frequenties worden voor het dompen (heave) o.a. de toegevoegde massa (AZZ), de demping (BZZ) en de fasehoek (EPSZ) bepaald
3. voor de ingevoerde frequenties worden o.a. de golfgegevens bepaald evenals de golfkracht (ZZA) en fasehoek (EPSZZ) volgens de diffractie- en relatieve bewegingsmethode.
4. de toegevoegde massa (AZZ) voor een oneindig hoge frequentie.

pagina 5 en

eventueel 6 :

1. de titel als weergegeven op invoerkaart no. 1
2. voor de ingevoerde frequenties worden voor het verzetten (sway) o.a. bepaald:  
de toegevoegde massa (AYY)  
de demping (BYY)  
de massa-koppeling van verzetten in slingeren (AROLLY)  
de dempings-koppeling van verzetten in slingeren (BROLLY)
3. voor de ingevoerde frequenties worden o.a. de golfgegevens bepaald evenals de golfkracht (YYA) en fasehoek (EPSYZ) volgens de diffractie- en relatieve bewegingsmethode.
4. voor de ingevoerde frequenties de driftkracht (DRIFTF)

pagina 6 en

eventueel 7 :

1. de titel als weergegeven op invoerkaart no. 1
2. voor de ingevoerde frequenties worden voor het slingeren (roll) o.a. bepaald:  
de toegevoegde massa (ARR)  
de demping (BRR)  
de massa-koppeling van slingeren in verzetten (AYROLL)  
de dempings-koppeling van slingeren in verzetten (BYROLL)
3. voor de ingevoerde frequenties worden o.a. de golfgegevens bepaald evenals het golfmoment (KKA) en fasehoek (EPSRZ) volgens de diffractie- en relatieve bewegingsmethode.

### 3. Beschrijving van SM03.

#### 3.1. Algemeen

Voor de in het programma SM02 ingevoerde frequenties worden voor één of meer snelheden eerst de hydrodynamische coëfficiënten voor het gehele schip bepaald. Daarna worden golfkrachten en -momenten berekend. Vervolgens worden de bewegingen en de daarbij behorende response functies berekend en tenslotte worden voor bepaalde punten aan boord van het schip de relatieve bewegingen berekend.

De kaartuitvoer van dit programma kan worden gebruikt als een gedeelte van de kaartinvoer van programma SM04.

#### 3.2. Kaartinvoer SM03.

##### Kaart no. 1

kol 1-80                      Titel, die boven elke pagina van de uitvoer wordt afgedrukt.

##### kaart no. 2

kol 1-10, FL,	LL = lengte tussen de loodlijnen
kol 11-20, FL,	BB = max. breedte
kol 21-30, FL,	TTV = diepgang voor
kol 31-40, FL,	TTA = diepgang achter
kol 41-50, FL,	BKH = hoogte van kimkiel
kol 51-60, FL,	BKL = lengte kimkiel

##### kaart no. 3

kol 1-10, FL,	XGG = lengteligging van het zwaartepunt (achter -, voor +)
kol 11-20, FL,	ZGG = vert. afstand van G t.o.v. WL (onder -, boven +)

##### kaart no. 4

kol 1-20, FL,	IIX = massa-traagheidsmoment t.o.v. x-as
kol 21-40, FL,	IYY = massa-traagheidsmoment t.o.v. y-as
kol 41-60, FL,	IIZ = massa-traagheidsmoment t.o.v. z-as
kol 61-80, FL,	IIXZ = massa-traagheidsproduct

##### kaart no. 5

kol 1-10, FL,	RHO = dichtheid van het water in $\text{kg sec}^2/\text{m}^4$ (voor zeewater = 104.5 en zoetwater = 101.9)
kol 11-20, FL,	G = versnelling van de zwaartekracht

kaart no. 6

kol 1-2, I,

kol 11-12, I,

kol 21-22, I,

kol 31-32, I,

kol 41-42, I,

kol 51-52, I,

kol 61-62, I,

JJ = aantal secties (max. 31)

DJJ = aantal secties, dat midscheeps aan elkaar gelijk is (minimaal 1)

RR = aantal ontmoetingsfrequenties (Max. 15)

MM = aantal golfhoeken (max. 7); kopgolven =  $180^{\circ}$

VV = aantal (stroom) snelheden (max. 6)

SS = aantal punten waarvoor relatieve bewegingen en versnellingen berekend worden (max. 7)

IBE = aantal stroomhoeken (max.5)

kaart no. 7

kol 1-10, FL,

kol 11-20, FL,

kol 61-70, FL,

MUGR= golfhoek in graden ( $0^{\circ}$  = achteropkomend,  $180^{\circ}$  = kopgolven)

kaart no. 8

kol 1-10, FL,

kol 11-20, FL,

kol 61-70, FL,

FR = (stroom)snelheden in knopen

kaart no. 9

kol 1-10, FL,

kol 11-20, FL,

kol 61-70, FL,

DJJ = nummer(s) van secties

die aan elkaar gelijk zijn. Zijn er geen secties aan elkaar gelijk dan -100 opgeven.

kaart no. 10

kol 1-4, I,

kol 5-8, I,

kol 57-60, I,

BETA= stroomhoeken in graden

(voor schip zonder koers- en gierhoek: 0)

kaart no. 11 a,b---g

kol 1-10, FL,

kol 11-20, FL,

kol 21-30, FL,

XP(S) }  
YP(S) = }  
ZP(S) } ordinaten van punten waarvoor relatieve bewegingen en versnellingen worden berekend. Voor elk punt één kaart. + = vóór, SB en boven G

kaart no. 12

kol 1, I,

kol 11-20, FL,

BOOLG = 0 indien wordt gerekend met opgegeven golfamplitude, anders met golfhelling

GOLF = golfamplitude in m als BOOLG = 0, anders max. golfhelling in radialen.

kaart no. 13

kol 1, I,

DELTA P = 0 indien geen visceuze massa wordt  
ingevoerd, anders -1

kaart no. 14 a,b

kol 1-10, FL,

DELP44 = totale extra massa per frequentie (max. 15)  
indien DELTA P = -1, anders vervalt kaart  
14 a,b

kol 71-80, FL,

kaart no. 15

kol 1, I,

DELTA Q = 0 indien geen visceuze demping wordt  
ingevoerd, anders -1

kaart no. 16 a,b

kol 1-10, FL,

DELQ44 = totale extra demping per frequentie  
(max. 15) indien DELTA Q = -1, anders  
vervalt kaart 16 a,b

kol 71-80, FL,

N.B. Aangeraden wordt geen extra visceuze massa of demping in te voeren als  
klimkiel in rekening wordt gebracht.

kaart no. 17

kol 1,6,11,--56, I,

BOOLP = 1 voor volledige uitvoer, anders ge-  
deeltelijk (indien kol 26-56 = 0 worden  
alleen de hydrodynamische coëfficiënten  
uitgevoerd; indien kol 16 = 1 kaartuit-  
voer)

kaart no. 18 a,----f

kol 1-12, FL,

HRR = krachten op eventuele ankerlijnen

kol 13-24, FL,

kol 61-72, FL,

kaart no. 19 a,b,c

kol 1-10, FL,

XO = langscheepse positie van de ordinaten

kol 11-20, FL,

t.o.v. L/2 in meters (achter = negatief)

kol 71-80, FL,

Hierna komt de kaartuitvoer van SM02 als weergegeven onder 2.3.1.

3.3. Kaart- en programmuitvoer van SM03.

De kaartuitvoer van SM03 kan direct gebruikt worden als gedeeltelijke invoer  
van programma SM04.

3.3.1. Kaartuitvoer SM03.

De kaartuitvoer bestaat achtereenvolgens uit:

kaart no. 1

kol 1-80

Titel, die boven elke pagina van de uitvoer wordt afgedrukt als weergegeven op kaart no.1 van de invoer van SM03 onder 3.2.

kaart no. 2

is gelijk aan kaart no. 2 van de invoer van SM03 onder 3.2.

kaart no. 3

kol 1-12, FL,

ZGG = verticale afstand van zwaartepunt (G)  
t.o.v. WL (onder -, boven +)

kaart no. 4

kol 1-5, I,

IBE = aantal stroomhoeken (max. 5)

kol 6-10, I,

VV = aantal (stroom)snelheden

kol 11-15, I,

MM = aantal golfhoeken (max. 7)

kol 16-20, I,

RR = aantal ontmoetingsfrequenties (max. 15)

kaart no. 5

kol 1-4, I,

NUM(2) = kaartnummer

kol 6-17, FL,

FR = snelheid volgens getal van Froude

kol 18-29, FL,

BETA = stroomhoek(en) in graden (voor schip zonder koers- en gierhoek o.o.)

kol 30-41, FL,

MU = golfhoek in radialen (0 voor achteropkomende golven)

Daarna voor elke snelheid, elke stroomhoek en elke frequentie de volgende 3 kaarten:

kaart no. 6

kol 1-4, I,

NUM(2) = kaartnummer

kol 6-17, FL,

XA = amplitude van de schrikbeweging

kol 18-29, FL,

YA = amplitude van de verzetbeweging

kol 30-41, FL,

ZA = amplitude van de dompbeweging

kol 42-53, FL,

PHIA = amplitude van de slingerbeweging in radialen

kol 54-65, FL,

THA = amplitude van de stampbeweging in radialen

kol 66-77, FL,

PSIA = amplitude van de gierbeweging in radialen

kaart no. 7

kol 1-4, I,	NUM(2) = kaartnummer
kol 6-17, FL,	EPSXZ = fasehoek van de schrikbeweging in graden
kol 18-29, FL,	EPSYZ = fasehoek van de verzetbeweging in graden
kol 30-41, FL.	EPSZZ = fasehoek van de dompbeweging in graden
kol 42-53, FL,	EPSPHIZ = fasehoek van de slingerbeweging in graden
kol 54-65, FL,	EPSTHZ = fasehoek van de stampbeweging in graden
kol 66-77, FL,	EPSPSIZ = fasehoek van de gierbeweging in graden

kaart no.8

kol 1-4, I,	NUM(2) = kaartnummer
kol 6-17, FL,	DRFO = driftkracht
kol 18-29, FL,	DRMO = driftmoment
kol 30-41, FL,	OMEGA = golffrequentie
kol 42-53, FL,	OMEGAE = ontmoetingsfrequentie

3.3.2. Programmauitvoer van SM03

Indien er max. 15 frequenties en 1 stroomhoek worden beschouwd, geven de eerste 13 pagina's de kaartuitvoer van SM02 als volgt weer:

Per sectie wordt eerst afgedrukt:

sectienummer

XO = afstand van de sectie t.o.v. L/2 (vóór positief)

OPP = sectie-oppervlak

$\frac{1}{2}B$  = halve breedte van de sectie op de W.L.

OB = de ligging van het drukkingspunt t.o.v. de waterlijn

Daarna worden per sectie, frequentie en stroomhoek de volgende gegevens afgedrukt:

NUM	= frequentienummer
AYY(R)	= toegevoegde massa bij verzetten
BYY(R)	= demping bij verzetten
AZZ(R)	= toegevoegde massa bij dompen
BZZ(R)	= demping bij dompen
ARR(R)	= toegevoegde massa bij slingeren
BRR(R)	= demping bij slingeren



AROLLY(R) = massa-koppeling van verzetten in slingeren  
BROLLY(R) = dempings-koppeling van verzetten in slingeren  
TTSTER(R) = effectieve diepgang van de sectie  
DRIFTF(R) = driftkracht  
EPSZ(R) = faseverschil in graden van dompen  
EPSY(R) = faseverschil in graden van verzetten  
EPSR(R) = faseverschil in graden van slingeren

} met  
golf

Na het afdrucken van de kaartuitvoer van SM02 volgen de resultaten van SM03, als volgt:

pagina 1 : 1. de titel als weergegeven op invoerkaart 1.  
2. de algemene scheepsgegevens  
3. de hydrostatische coëfficiënten

pagina 2 : 1. de titel als weergegeven op invoerkaart 1  
2. de hydrodynamische coëfficiënten voor schrikken, dompen en stampen per ontmoetingsfrequentie  
3. de dimensieloze hydrodynamische coëfficiënten voor schrikken, dompen en stampen per ontmoetingsfrequentie

pagina 3

en 4 : 1. de titel als weergegeven op invoerkaart 1  
2. de hydrodynamische coëfficiënten voor verzetten, slingeren en gieren per ontmoetingsfrequentie  
3. de dimensieloze hydrodynamische coëfficiënten voor verzetten, slingeren, en gieren per ontmoetingsfrequentie

pagina 5 : 1. de titel als weergegeven op invoerkaart 1  
2. per ontmoetingsfrequentie voor de ingevoerde snelheid de algemene golfgegevens.

pagina 6 : 1. de titel als weergegeven op invoerkaart 1  
2. per ontmoetingsfrequentie de golfkrachten voor het schrikken (XXA) met bijbehorende fasehoek (EPSXZ)

pagina 7 : 1. de titel als weergegeven op invoerkaart 1  
2. per ontmoetingsfrequentie de golfkrachten en -momenten voor resp. het dompen (ZZA) en het stampen (MMA) met bijbehorende fasehoek (EPSZZ resp. EPSMZ)

pagina 8 : 1. de titel als weergegeven op invoerkaart 1  
2. per ontmoetingsfrequentie de golfkrachten en -momenten voor resp. het verzetten (YAA) en het gieren (NNA) met bijbehorende fasehoek (EPSYZ resp. EPSNZ).

pagina 9 : 1. de titel als weergegeven op invoerkaart 1  
2. per ontmoetingsfrequentie de golfmomenten voor het slingeren (KKA) met bijbehorende fasehoek (EPSKZ)

pagina 10 : 1. de titel als weergegeven op invoerkaart 1  
2. per ontmoetingsfrequentie de driftkracht en het driftmoment op het vastgehouden schip

pagina 11 : 1. de titel als weergegeven op invoerkaart 1  
2. per ontmoetingsfrequentie de schrikamplitude (XA) en fase (EPSXZ) en de driftkracht en het driftmoment op het vrij oscillerende schip

pagina 12 : 1. de titel als weergegeven op invoerkaart 1  
2. per ontmoetingsfrequentie de domp- en stampamplitude (resp. ZA en THA) met bijbehorende fasehoeken (resp. EPSZZ en EPSTHZ)

pagina 13 : 1. de titel als weergegeven op invoerkaart 1  
2. per ontmoetingsfrequentie de verzet- en gieramplitude (resp. YA en PSZA) met bijbehorende fasehoeken (EPSYZ en EPSPSIZ)

pagina 14 : 1. de titel als weergegeven op invoerkaart 1  
2. per ontmoetingsfrequentie de slingeramplitude (PHIA) met bijbehorende fasehoek (EPSPHIZ).

De volgende pagina's geven voor elk punt P waarvoor de relatieve bewegingen en de versnellingen berekend moeten worden het volgende weer:

pagina 15a: 1. de titel als weergegeven op invoerkaart 1  
2. de positie van het punt P  
3. per ontmoetingsfrequentie:  
a. de verplaatsingen van het punt P in X, Y en Z richting  
b. de verticale relatieve snelheid van het punt P t.o.v. het wateroppervlak  
c. de versnellingen van het punt P in X,Y en Z richting

pagina 16a: 1. de titel als weergegeven op invoerkaart 1  
2. de positie van het punt P  
3. per ontmoetingsfrequentie de fasehoeken behorende bij de verplaatsingen van het punt P in X, Y en Z richting en bij de verticale relatieve snelheid van dat punt.

4. Beschrijving van SM04.

4.1. Algemeen

Met behulp van de in programma SM03 berekende responsefuncties worden voor bepaalde in te voeren golfspectra de gemiddelde en significante waarden van de bewegingen berekend [5].

De kaartuitvoer van programma SM03 kan als een gedeelte van de kaartinvoer van programma SM04 worden gebruikt.

4.2. Kaartinvoer SM04.

Deze invoer bestaat uit de volgende kaarten:

kaart no. 1

- kol 1-10, I,           SS = aantal punten waarvoor de relatieve bewegingen en versnellingen berekend dienen te worden
- kol 11-20, I,         KK = aantal golfspectra, dat ingevoerd wordt

Hierna voor elk in te voeren golfspectrum de volgende gegevens op:

kaart no. 2 a,b,c---

- kol 1-10, FL,         HSIGN(K) = de significante golfhoogte
  - kol 11-20, FL,       TAV(K)    = de gemiddelde golfperiode
  - kol 21-30, I,         MET(K)   = methode waarop de spectrale dichtheid volgens Pierson - Moskowitz bepaald wordt
- 1 = met  $\frac{\sigma}{T} = 2 \frac{m0}{m1}$
- 2 = met  $\frac{\sigma}{T} = 2 \sqrt{\frac{m0}{m2}}$
- 3 = als alleen de significante golfhoogte ingevoerd wordt

Hierna volgt voor elk punt P waarvoor de relatieve beweging en de versnellingen berekend wordt:

kaart no. 3a, b,c,

- kol 1-10, FL,         XP(S) = ordinaat in langsrichting van punt P (voor G = +)
- kol 11-20, FL,       YP(S) = idem voor de ordinaat in dwarsrichting (SB = +)
- kol 21-30, FL,       ZP(S) = idem voor de ordinaat in hoogte (boven G = +)

Tenslotte volgt de kaartuitvoer van programma SM02, als weergegeven onder 3.3.1.

#### 4.3. Programmauitvoer van SM04.

De programmauitvoer van SM04 bestaat uit de volgende pagina's:

- pagina 1 : 1. titel als weergegeven op invoerkaart 1 van SM03  
2. snelheid volgens Froude, stroom- en golfrichting  
3. scheepslengte, -breedte, diepgang vóór en achter en de waterverplaatsing  
4. de X- en Z-ordinaat van de punten P, waarvoor de relatieve beweging en de versnellingen berekend worden.

Voor elk golfspectrum volgt nu:

- pagina 2 : 1. titel als weergegeven op invoerkaart 1 van SM03  
2. snelheid volgens Froude, stroom- en golfrichting  
3. per ontmoetingsfrequentie de spectrale dichtheid van:  
XX - het schrikken  
YY - het verzetten  
ZZ - het dompen  
PHI - het slingeren  
THA - het stampen  
PSI - het gieren

- pagina 3 : 1. titel als weergegeven op invoerkaart 1 van SM03  
2. snelheid volgens Froude, stroom- en golfrichting  
3. per ontmoetingsfrequentie de spectrale dichtheid van:  
ZTA - de golfhoogte  
DFLS- de driftkracht  
DMLS- het driftmoment  
YPI - de verzetbeweging van punt P1  
ZPI - de dompbeweging van punt P1  
SPI - de relatieve beweging t.o.v. het wateroppervlak van punt P1.

Volgende pagina's bevatten de spectrale dichtheid per ontmoetingsfrequentie van de verzet-, domp- en relatieve beweging van punt 1,2 etc.

Daarna volgt voor elk golfspectrum:

pagina 4

- of 5 : 1. titel als weergegeven op invoerkaart 1 van SM03  
2. snelheid volgens Froude, stroom- en golfrichting  
3. de significante golfhoogte en gemiddelde periode van het beschouwde golfspectrum  
4. daarna volgen voor de bewegingen en krachten per kanaal:

M0 }  
M1 } momenten van het spectrum  
M2 }

$4 * \text{SQRT} M_0$  = de significante golfhoogte

$2 \pi * R T M_0 / M_2$  = de gemiddelde golfperiode

$2 \pi M_0 / M_1$  = de gemiddelde golfperiode

Hierbij geeft kanaal:

- 1 - het schrikken
- 2 - het verzetten
- 3 - het dompen
- 4 - het slingeren
- 5 - het stampen
- 6 - het gieren
- 7 - de absolute horizontale beweging van punt 1
- 8 - de absolute verticale beweging van punt 1
- 9 - de relatieve beweging t.o.v. het wateroppervlak van punt 1
- 10 - de absolute horizontale beweging van punt 2  
etc.

De laatste drie kanalen geven de driftkracht, het driftmoment en de golfhoogte.

## 5. Aanbevelingen

Met betrekking tot een verdere ontwikkeling van het beschreven scheepsbewegingen-programma voor 6 graden van vrijheid worden de volgende aanbevelingen van belang geacht:

1. De slingerdemping van zowel schip als kimkielen beter te bepalen mede door vergelijking met gemeten resultaten.
2. Voor het berekenen van de schrikbeweging dient een andere methode opgesteld en ingevoerd te worden. Vergelijking met metingen is ook hiervoor belangrijk, vooral in achteropkomende golven.
3. De golfkrachten en -momenten als weergegeven in [2] dienen gecontroleerd te worden.
4. Het kan van belang zijn om het "LOMO"-programma te activeren en de resultaten te vergelijken met het "SM"-programma. Het "LOMO"-programma geeft

als extra de buigende momenten en dwarskrachten in verticale en horizontale richting.

5. Vooral voor achteropkomende golven dient het aantal frequenties opgevoerd te worden boven het huidige aantal van 15.
6. De kaartuitvoer van SM03 voor achteropkomende golven zal zodanig moeten zijn, dat het gehele golfspectrum bestreken wordt
7. De kaartuitvoer van SM-16 (LOM01) dient geschikt gemaakt te worden voor invoer van SM02.
8. Het gedeelte van het programma van SM16 (LOM0 1), dat de getransformeerde spanten plöt, zal verbeterd moeten worden.
9. De in SM16 ingebouwde methode van Frank dient voor verschillende spantvormen gecontroleerd te worden.
10. Het is van belang de driftkrachten en toegevoegde weerstand zoals die in het programma berekend wordt te controleren en voor 0 en 180<sup>o</sup> te vergelijken met de resultaten van "TRIAL" [ 6 ].
11. In de toekomst moet het mogelijk zijn om ook andere spectra (bijv. ook gemeten golfspectra) in te voeren.

## 6. Referenties

### 1. Vugts, J.H.,

Hydrodynamic Forces and Ship Motions in oblique waves.  
Netherlands Ship Research Centre TNO,  
Report no. 150 S, December 1971.

### 2. Wahab, R and J.H. Vink

Wave induced motions and loads on ships in oblique waves.  
Netherlands Ship Research Centre TNO,  
Report no. 193 S, May, 1974.

### 3. Frank, W.,

Oscillation of cylinders in or below the free surface of deep fluids.  
NRSDC report 2375, October 1967.

4. De Jong, B.,

Computation of the hydrodynamic coefficients of oscillating cylinders.  
Netherlands Ship Research Centre TNO,  
Report no. 145 S, June 1973.

5. Gerritsma, J.,

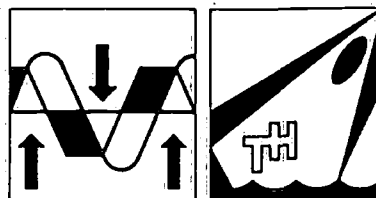
Behaviour of a ship in a seaway.  
Netherlands Ship Research Centre TNO,  
Report no. 84 S, May 1966.  
ISP, vol.13, no. 143, 1966.

6. Beukelman, W. and E.F. Bijlsma

Description of a program to calculate the behaviour of a ship in a  
seaway (named : TRIAL)  
Shipbuilding Laboratory,  
Delft University of Technology, report no. 383

**TECHNISCHE HOGESCHOOL DELFT**  
**AFDELING DER SCHEEPSBOUW- EN SCHEEPVAARTKUNDE**  
**LABORATORIUM VOOR SCHEEPHYDROMECHANICA**

**Rapport No. 479**



**BOTTOM IMPACT PRESSURES DUE TO FORCED OSCILLATION**

**W. Beukelman**

**International Shipbuilding Progress, Volume 27**  
**May 1980, No.309.**

**Report No. 479**

**Februari 1979**

**Ship Hydromechanics Laboratory - Delft.**

**Delft University of Technology**  
**Ship Hydromechanics Laboratory**  
**Mekelweg 2**  
**Delft 2208**  
**Netherlands**



# BOTTOM IMPACT PRESSURES DUE TO FORCED OSCILLATION\*

by

W. Beukelman\*\*

## Abstract

Forced oscillation tests about the water surface have been carried out with a segmented ship model to measure slamming pressures on two segments.

A calculation procedure based on a two-dimensional approach has been proposed.

These analytical results, together with those of other theories have been compared with the measurements.

The results of the proposed calculation method proved to be rather satisfactory.

## 1. Introduction

The literature about tests and theories on slamming is rather extensive.

In most of the experiments, the object was to find a relation between the vertical impact velocity and the maximum slam pressure [1, 2, 3, 4, 5, 6]. A general form for this relation is presented by Margaret Ochi and José Bonilla-Norat in [3] as

$$p = kv^n$$

where:

$p$  = the impact pressure

$v$  = the impact velocity

$k$  and  $n$  are constants.

Experimentally, these authors found that the pressure is proportional to the square of the velocity at impact and that the proportionality constant  $k$  is dependent on the section shape. Others like Takezawa et al., M.K. Ochi, L.E. Motter [1, 2, 7] used a similar relation,

$$p = \frac{1}{2}\rho k_1 v^2$$

and established experimentally the coefficient  $k_1$  of the impact pressure dependent on the position considered as a flat bottom or stem front. For the pressure distribution on the surface of a wedge-shaped body the authors used the well-known formula of Wagner [8].

Remarkable model test results, together with theoretical results, are presented by P. Kaplan et al [9] for the case of bow slamming of SES craft in waves.

Most frequently used up to now is the procedure introduced by Tick [10] and Ochi [4] with respect to bottom impact slamming. After some evaluations, Ochi et al [4, 11] stated two conditions required for bottom impact slamming to occur viz.:

- a. bow (fore foot) emergence
- b. a certain magnitude of relative velocity between wave and ship bow.

The critical relative velocity below which slamming does not occur is called the 'threshold velocity', denoted by  $v^*$ .

Ochi showed by tests on a Mariner model that the threshold velocity is nearly constant with an average of 12 fps for a ship of 520 ft length. Aertssen [12] advised that the threshold value should be 50 percent greater for the Mariner, that is 18 fps. Mostly the threshold velocity according to Ochi is accepted with an appropriate Froude scaling law for ships of different lengths.

To analyse the problem experimentally a series of drop tests with a flat plate [13, 14] or a wedge [7, 15, 16, 17] have been executed. Very often, the behaviour of the air layer between the falling body and the water surface has been taken into consideration [13, 18, 19, 20].

Chuang [21] showed that the effect of this compressible air causes a remarkable reduction of the acoustic pressure, which is frequently assumed.

Mathematical models have been developed to describe the cushioning effect of the air between the descending body and the water surface for instance by Verhagen [13] and Greenberg [20]. The predictions of Verhagen showed good agreement with experimental results. It is, however, rather complicated to apply these theories to the real problem of ship bottom impact because no account is taken of forward speed or of the three-dimensional flow caused by changes in the shape of the sections.

Model experiments in waves or full scale observations may statistically deliver rather good and useful results [1, 2, 3, 4, 6, 12, 22], but do not give a deeper insight in the phenomena slamming. This might be very important for establishment of design criteria.

Several authors have tried to formulate mathematical models describing slamming [13, 20, 22, 23, 24, 25, 26, 27].

The great majority of them accepted the rate of change of the momentum of the hull's added mass as the main cause of the arise of slamming forces. In this way they

\*) Report 479 P.

\*\*\*) Delft University of Technology, Ship Hydromechanics Laboratory, Delft, The Netherlands.

found, that the maximum slamming pressure is indeed proportional to the squared relative vertical impact velocity.

To calculate the hydrodynamic impact force, Kaplan [24] made use of the well-known strip method, however, with a different way of treatment of the forward speed influence.

Kaplan [24], Ochi [6] and Lewison [22] also stated that the slamming pressure is proportional to the rate of change of the added mass with depth.

Stavovy and Chuang [26] determined slamming pressures for fast ships by a method based on the Wagner impact theory, the Chuang cone impact theory and experiments.

They stated that slamming pressures acting normal to the hull bottom may be separated into two components.

1. the *impact pressure* due to the normal component to the water surface of the relative velocity between the impact surface and the wave.
2. the *planing pressure* due to the tangential component to the water surface of the relative velocity between the impact surface and the wave.

The planing pressure is usually small compared to the impact pressure.

In the present work it was the intention to investigate mainly bottom impact slamming. To know more exactly the relationship between the vertical impact velocity and slamming pressure a choice had been made for experiments with a model forced oscillated in still water.

The bottom in which several pressure gauges were mounted was situated at or near the watersurface.

The measurements of the maximum slamming pressure have been compared with the results of some of the discussed methods and with the results of a proposed calculation procedure.

## 2. Description of the experiments

The oscillation tests were carried out with a glass fibre reinforced polyester ship model of the Todd Series 60,  $C_B = 0.70$  parent hull form. The same model has been used in the past for experiments described in [28]. The main particulars of the model are summarized in Table 1. The model consisted of seven separate segments connected to a continuous strong box girder above the model, see Figure 1.

For pure heaving without an angle between the bottom and the water surface three pressure gauges A, B and C were placed in the middle segment (no. 4) and three, D, E and F in segment no. 6 after the forward one, as denoted in Figure 1.

Table 1  
Main particulars of ship model

Length between perpendiculars ( $L_{pp}$ )	2.258 m
Breadth ( $B$ )	0.322 m
Draught (design) ( $T$ )	0.129 m
Draught (used for test condition) ( $T'$ )	0.040 m
Volume of displacement (design)	0.0657 m <sup>3</sup>
Volume of displacement (test condition)	0.0181 m <sup>3</sup>
Block coefficient (design) ( $C_B$ )	0.700
LCB forward of $L_{pp}/2$ (design)	0.011 m
LCB forward of $L_{pp}/2$ (test condition)	0.035 m

For pitching and heaving with an angle between the bottom and the watersurface, all six pressure gauges were mounted in segment no. 6. See also Figure 1. Each of the segments with the pressure gauges was connected to the box girder above the model by means of a force dynamometer. This provided a rough check

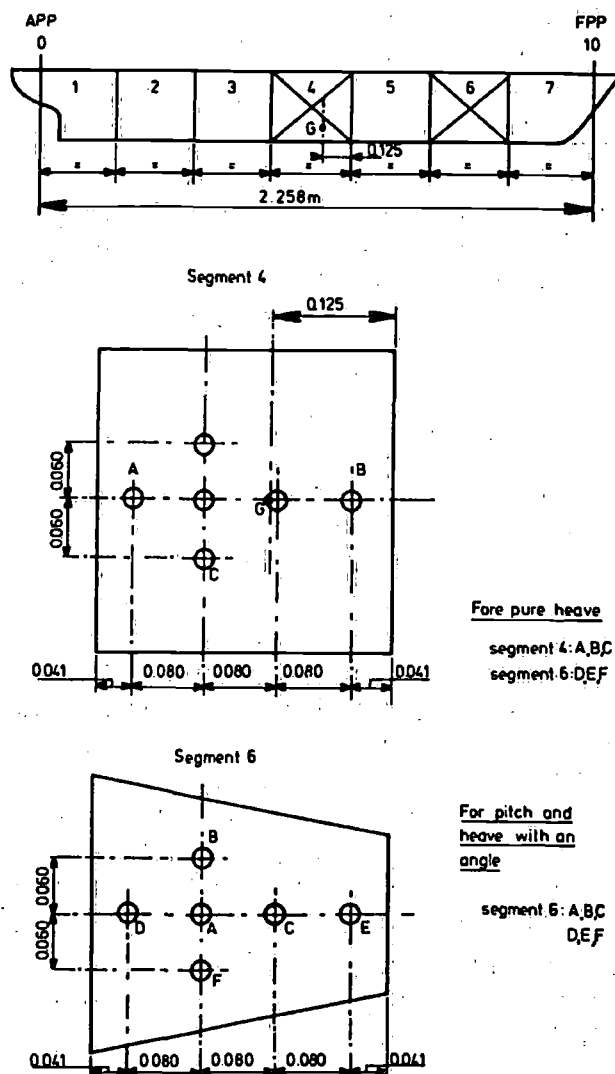


Figure 1. Place of pressure gauges in the segments for the different modes of oscillation.